Elizabeth Campbell Manning

Enhancement of the tube-jack non-destructive test method for historical structural masonry diagnosis

October 2016

Elizabeth Campbell Manning   Enhancement of the tube-jack non-destructive test method for historical structural masonry diagnosisese

UMinho | 2016

Universidade do Minho
Escola de Engenharia

Elizabeth Campbell Manning

Enhancement of the tube-jack non-destructive
test method for historical structural masonry
diagnosis

Tese de Doutoramento
Engenharia Civil - Estruturas

Trabalho efectuado sob a orientação do
Professor Doutor Luís F. Ramos
e coorientação do
Professor Doutor Francisco M. Fernandes

October 2016

STATEMENT OF INTEGRITY

I hereby declare having conducted my thesis with integrity. I confirm that I have not used plagiarism or any form of falsification of results in the process of the thesis elaboration.

I further declare that I have fully acknowledged the Code of Ethical Conduct of the University of Minho.

University of Minho, 27/10/2016

Full name: Elizabeth Campbell Manning

Signature: _____

ACKNOWLEDGEMENTS

ABSTRACT

Non-destructive testing techniques provide a means to obtain important characteristics of historical structural masonry without, or with minimal, damage to irreplaceable materials. Flat-jack testing is a non-destructive test method that is traditionally used to determine the state of stress in masonry and deformable characteristics of unreinforced historical structural masonry. However, difficulty in interpreting the results of flat-jack tests in irregular masonry and the necessity to cut through historical masonry units during testing in irregular masonry has led to the need for an alternative method. Tube-jack testing is being developed at the University of Minho, as an alternative to flat-jack testing, that can be performed on traditional Portuguese masonry that contains large units and irregular mortar joints. The development of the tube-jack test method from a theory into a functioning test system is the aim of this thesis.

Basic tube-jack prototypes were developed into a complete tube-jack test system that could be tested in masonry. The system was tested in three masonry walls, constructed with granite units and cement-lime mortar and with three different typologies, in the laboratory and compared with traditional flat-jack tests performed in the same specimens. Laboratory tests showed that the tube-jack test system was able to apply pressure to the masonry and perform complete tests. When compared with the flat-jack test method, the tube-jack test was more suited for large unit masonry with low strength mortar than the flat-jack was.

Successful completion of the laboratory tests led to a numerical analysis phase where each of the tests was simulated and the effects of pressurizing the masonry in each test were analyzed. Important findings were made through these tests and numerical analyses, such as; performing the tests too close to each other or too close to edges of the walls affects the results, the Young's modulus results depend on the percentage of mortar over which measuring devices measure, and the change in stress between two lines of tube-jacks or two flat-jacks, in the double tube-jack and flat-jack tests, is less than the change in pressure applied to the masonry. Final testing of the tube-jack system in-situ on a historical masonry structure showed that the developed system and the procedural lessons learned resulted in a test method that could estimate the state of stress and deformability characteristics of the masonry with as much accuracy as the flat-jack test but will less damage to the historical masonry.

The tube-jack test method is a promising enhanced non-destructive test method that, through further research and development, will likely be able to provide an alternative to flat-jack testing for irregular and large unit masonry diagnosis.

RESUMO

As técnicas de ensaios não-destrutivos são um meio de fornecer importantes características estruturais das construções históricas em alvenaria, sem ou com um mínimo de dano induzido. O ensaio com macacos planos (*Flat-jacks*) é um método ligeiramente destrutivo, tradicionalmente usado para determinar o estado de tensão em paredes em alvenaria e a sua deformabilidade. No entanto, a dificuldade em interpretar os resultados destes ensaios quando são executados em alvenaria irregular, com grandes unidades e com a necessidade de cortar unidades, face à dificuldade de encontrar juntas regulares horizontais, levou à necessidade de desenvolver um método alternativo que superasse essas dificuldades. O ensaio com os *Tube-jacks*, método que está a ser desenvolvido na Universidade do Minho, apresenta-se como uma alternativa para o ensaio com os *Flat-jacks*. Com um princípio de funcionamento semelhante, os *Tube-jacks* foram propostos para serem uma alternativa mais prática em paredes de alvenaria tradicional Portuguesa, formadas por grandes unidades e juntas de argamassa irregulares.

O desenvolvimento do método de ensaio com os *Tube-jacks*, desde os seus princípios teóricos, até à sua aplicação prática, foi o principal objetivo da presente tese. Para tal, foram desenvolvidos vários protótipos do sistema que foram testados em laboratório em três paredes de alvenaria à escala 1:2, construídas com unidades de granito e argamassa à base de cal com pequenas percentagens de cimento, sob três tipologias diferentes. Nas mesmas paredes foram comparados com os resultados com os dos tradicionais *Flat-jacks*. Os ensaios em laboratório demonstraram que o sistema com os *Tube-jacks* foi capaz de aplicar pressão na alvenaria e de realizar ensaios semelhantes aos dos *Flat-jacks*. Quando comparado com o método tradicional, os *Tube-jacks* foram mais adequados para paredes de alvenaria com grandes unidades e argamassas com reduzida rigidez.

Após os ensaios em laboratório foi realizada uma extensiva análise numérica, onde cada ensaio foi simulado para analisar a eficiência do método. Conjugando os resultados experimentais com os numéricos, importantes conclusões fora retiradas, tais como: a realização dos ensaios muito próximos uns dos outros ou muito perto dos bordos das paredes afetam os resultados; o módulo de elasticidade estimado com os métodos depende da percentagem de argamassa sobre a qual é medido a deformabilidade da parede; e a alteração do estado de tensão induzido na parede entre duas linhas de *Tube-jacks* ou de *Flat-jacks* é menor do que a variação desejada da pressão a aplicar na alvenaria. Posteriormente, o ensaio de *Tube-jacks* foi validado *in situ* numa construção histórica, permitindo demonstrar que o sistema desenvolvido e os procedimentos aprendidos durante as etapas anteriores poderão ser utilizados para estimar o estado de tensão e a deformabilidade em paredes de alvenaria com uma precisão da mesma ordem de grandeza que o ensaio com *Flat-jacks*, embora induzindo menos dano na construção histórica.

O ensaio com *Tube-jacks* é um método de ensaio não destrutivo que, através de investigação complementar e desenvolvimentos futuros, será uma alternativa fiável aos ensaios com *Flat-jacks* para o diagnóstico de paredes de alvenaria de pedra com grandes unidades e juntas irregulares.

Enhancement of the tube-jack non-destructive test method for historical structural masonry diagnosis

X

TABLE OF CONTENTS

1.   INTRODUCTION

1.1   Motivation

Historical structures exist throughout the world. They are valuable assets to the societies in which they are present and are worthy of protection and conservation. Structural assessments are often necessary in order to ensure their safety and preservation. To perform a structural analysis of a historical structure it is often necessary to determine mechanical characteristics of the materials and structure. Many historical structures have very few records of their construction procedures, details, and material properties. In addition, damages and changes to the structure have occurred over time, some of them hard to detect or trace. Thus, alternative methods must be used to determine the current mechanical characteristics of the structure and its materials.

Several methods can be used to obtain structural and material characteristics necessary for analysis of the structure including: (a) estimation using previously gathered knowledge about the structure, its materials, building techniques, and comparison to similar structures; (b) construction of replicas of the structure for laboratory tests; (c) laboratory tests on materials taken from the structure or whole sections of the structure; and (d) non-destructive or minor-destructive tests on the structure. Estimation of the properties of the structure can be difficult given the variability in construction practices and procedures, even between buildings of the same era and typology. Estimations can lead to large errors in analyses or the necessity to be overly conservative in evaluations. Conservative engineering can lead to unnecessary interventions that are irreversible and damage the historic materials of the structure. Construction of replicas, or similar specimens for laboratory testing, can be expensive and time consuming. Given the historical nature of the structures being analyzed and the desire to preserve as much as possible of these irreplaceable materials, it is preferable, if not required, to avoid invasive and destructive procedures. This usually eliminates the possibility of doing laboratory tests or field tests on large portions of the structure. Thus, non-destructive or minor-destructive tests on the structure are usually the preferable method for determining the necessary structural and material characteristics for analysis of the structure, even if the method's results can only give qualitative information.

Non-destructive testing or minor-destructive testing of masonry structures is a relatively recent field of research with studies dating back only about three and a half decades. In the 1980s, there was an increase in interest in the area of preservation and restoration of historical buildings and monuments, which lead to the development of new non-destructive testing techniques and the adaptation of methods, previously used to investigate concrete structures or geological formations, for use on masonry structures [1]. A vast number of techniques have been developed, to varying degrees, in the following decades to investigate a variety of aspects of historical structures including: typology, damage state, material identification, mechanical characteristics, seismic behavior, and others.

One non-destructive testing, or minor-destructive, technique that can be used to determine the mechanical characteristics of masonry, is the flat-jack test method. The flat-jack test method, previously used in the field of rock mechanics and developed in the 1980s for use on masonry structures [1], involves cutting slots in the masonry, inserting flat jacking devices, pressurizing the jacks, and recording the movements of the masonry to determine the local stress state and

deformability characteristics of the masonry [2], [3]. While this method produces reasonably accurate results, many issues and obstacles have been encountered in the years of performing and studying this test including, but not limited to, the slightly destructive nature of the test and difficulty in interpretation of the results when it is used on irregular masonry structures [4].

Traditional masonry in the northern part of Portugal, where this thesis work was conducted, is composed of large granite stones and soft mortar [5]. Some masonry is very regular with horizontal mortar joints and rectangular units and some is irregular in typology with misaligned mortar joints and rough stones of varying sizes and shapes. Traditional flat-jack tests are usually performed on masonry with units much smaller than those found in traditional Portuguese masonry. Thus, the question arises whether flat-jack testing can accurately determine the stress state and material properties of this type of masonry. In addition, flat-jack testing can result in damage to the masonry units in this type of masonry when irregular mortar joints require the slots to be cut through the stones.

In order to prevent damage to the historic masonry in Portugal and still obtain the required masonry characteristics for analysis, an enhanced method termed, "Tube-Jack Testing", which relies on some of the same principles as the flat-jack test, is being developed at the University of Minho. Initial studies on the concept and theory of this method showed that it has the potential to provide the same amount or more information about the mechanical properties of regular and irregular masonry as the flat-jack test, but with less damage [6]. The development of the tube-jack test method from a theory to a functioning test system is the focus of this thesis.

1.2   Objectives

The aim of this thesis is to enhance the tube-jack non-destructive test method to provide a method that is less damaging to historic structures and will provide more confident, efficient, and accurate information about the characteristics of the structural masonry. In this thesis, the tube-jack test method is developed from the initial stages of conception and theory through prototype development, laboratory testing in various masonry specimens and typologies, in depth numerical analysis, to final in-situ testing on a historic structure. The following are objectives for the enhancement of the tube-jack test method:

- Development of a tube-jack device and test method that can be used to determine the stress state and deformability characteristics of a masonry wall;

- Demonstration that this tube-jack system works through laboratory testing in various masonry specimens with different typologies and through numerical modeling;

- Apply the tube-jack technique with in-situ testing on a historic structure for final proof of the concept.

Throughout the development of both the tube-jack test method, the results from each test are compared with the accepted and standardized flat-jack method and with other non-destructive test methods. The goal for the final result is a more efficient and accurate test method that can be used as an alternative to flat-jack testing, that produces minimal damage and accurate results for the masonry characteristics.

1.3   Organization of the thesis

The thesis is divided into nine chapters, which clearly outline the procedure for the development and testing of the tube-jack test method. The organization of the chapters is as follows:

➢ Chapter 1: Introduction

In this chapter an introduction to the field of structural analysis of historical structures and non-destructive testing, is given. Motivation for the thesis research and the objectives of the work are outlined.

➢ Chapter 2: Overview of Non-destructive Testing Techniques for Historic Masonry

This chapter provides a background into the variety of non-destructive test methods that are available and most widely used to investigate historical structures. A focus is placed on the flat-jack and tube-jack test methods.

➢ Chapter 3: Tube-jack System Development

The development of the tube-jack system from a theory into a physical system that can apply pressure to the masonry is presented in this chapter.

➢ Chapter 4: Mechanical Characterization of the Masonry

The design, construction, and mechanical characterization of three masonry walls of different typologies are presented in this chapter. These walls were constructed for testing the developed tube-jack test system.

➢ Chapter 5: Tube-jack Testing in Laboratory Walls

This chapter presents the tube-jack and flat-jack testing performed in the three masonry walls in the laboratory.

➢ Chapter 6: Numerical Analysis

The numerical analysis of the tube-jack and flat-jack tests performed in the laboratory is presented in this chapter, along with in-depth analysis of how the masonry is affected by these tests.

➢ Chapter 7: In-situ Testing – San Francisco Convent

The results of the in-situ single and double tube-jack and flat-jack tests at the San Francisco Convent are presented in this chapter.

➢ Chapter 8: Conclusions and Future Work

Final conclusions from each of the phases of the thesis are presented. Ideas are provided for future research based on questions and hypotheses presented throughout the thesis.

2. OVERVIEW OF NON-DESTRUCTIVE TESTING TECHNIQUES FOR HISTORIC MASONRY

2.1 Introduction

Non-destructive testing encompasses all testing techniques that can be performed on a structure to determine more information about that structure without causing destruction of the structure. These tests can range in the amount of damage that they cause on a structure from absolutely no damage to a minimal amount of damage that can be easily repaired, minor destructive tests. Minor destructive tests will be included in this review in order to comment on the broad range of testing techniques that can be applied to historical masonry.

Growth and development in the science of non-destructive testing (NDT) began as a result of its use on modern structures to ensure the quality and performance of modern engineering materials. It was not until the late 1970s that NDTs were considered for study and use on historical structures. This was due to the different nature of historical building materials, heterogeneous and anisotropic wood and masonry for the historical materials versus homogeneous metals and concrete for the modern materials. Starting in 1978 with Susan Hum-Hartley's review of available NDT methods and her proposal for their use in investigation of historical structures [7], reviews of NDT methods currently in use and those needing further study were the most common publications concerning NDT development and continued to be published throughout the 1980s and into the 1990s [8]. The promotion of NDT techniques as a means of preserving historical structures began as articles stated, "Masonry tests requiring only basic equipment and simple techniques provide essential structural data without disfiguring historic buildings" [9]. Methodologies and procedures for investigating historical structures using these NDT techniques were being developed in the 1990's, such as comprehensive assessment criteria by the Applied Technology Council in the United States [9], although only recently has a complete methodology been presented.

Binda and Cardani [10] proposed a general procedure for investigation and testing and a template for masonry quality evaluation. The first stage of the procedure is an onsite survey of the structure and its damages. Masonry typologies and representative sections are identified for planning of the NDTs. Cracks and other damages are observed and recorded. The second phase is the NDT. These tests allow for the collection of quantitative and qualitative data about the structure and an obtainment of a higher level of knowledge about the structure for better analysis and safety assessment.

There is a large variety of NDTs that have been proposed and/or performed on historic structures. Some were used in the past but found too destructive, expensive or inefficient, and new test methods continue to be developed today. Due to the vastness of the topic not all of the NDTs will be discussed in this review, but rather, just the most important, the most prevalent, and those pertaining to the determination of the mechanical characteristics.

NDT techniques can be categorized into five groups: mechanical tests, wave tests, sampling, dynamic tests, and monitoring. These groups are based on several characteristics, including: the type of properties they are intended to investigate, whether they are minor destructive or completely non-destructive, the properties they can evaluate, and whether they give qualitative or quantitative information. Table 2-1 shows the categorization of the NDTs.

Table 2-1 Non-Destructive Testing Techniques

	Technique	Area of Investigation	Non or Minor Destructive	Evaluated Property	Qualitative or Quantitative
Mechanical Tests	In-place Shear Test/ (Push) test	Mechanical	Minor	Bed joint shear strength	Quantitative
	Bond wrench test	Mechanical	Minor	Bond strength	Quantitative
	In-situ Stress Test/ Single Flat-Jack Test	Mechanical	Minor	Local Compressive Stress	Quantitative
	In-situ Deformability Test/ Double flat-jack test	Mechanical	Minor	Masonry Young's Modulus Masonry Compressive Strength	Quantitative
	Borehole dilatometer test	Mechanical	Minor	Masonry Young's Modulus	Quantitative
	Hardness Test	Mechanical	Minor	Mortar Compressive Strength	Quantitative
Wave Transmission Tests	Sonic Pulse Velocity Test	Typological Mechanical	Non	Consistency of the Masonry Masonry Young's Modulus	Qualitative Quantitative
	Sonic Tomography	Typological	Non	Consistency of the Masonry	Qualitative
	Impact-Echo	Typological	Non	Consistency of the Masonry	Qualitative
	Ultrasonic Velocity Test	Typological Mechanical	Non	Consistency of the Masonry Masonry Young's Modulus	Qualitative Quantitative
	Ground Penetrating Radar	Typological	Non	Consistency of the Masonry	Qualitative
	Thermographic Analysis	Typological	Non	Consistency of the Masonry	Qualitative
	Radiography	Typological	Non	Consistency of the Masonry	Qualitative
Sampling	Core Drilling	Typological Mechanical Chemical	Minor	Internal Material Identification Bonding Number of wythes Chemical Characteristics Physical Characteristics Mechanical characteristics Foundation Materials Internal Cracks	Qualitative and Quantitative
Dynamic Tests	Dynamic Identification	Dynamic	Non	Overall structural behavior	Qualitative Quantitative
Monitoring	Monitoring	Static and Dynamic	Non	Overall structural behavior Crack propagation Stress distribution	Qualitative Quantitative

6

2.1.2   Mechanical Tests

The mechanical tests are in situ techniques that have been developed to determine the mechanical behavior of masonry without the necessity of removing specimens from the structure for laboratory testing. These methods give quantitative values for the properties they are evaluating. The drawback to these tests is that these tests produce a varying degree of damage to the masonry, ranging from a minimal amount to substantial damage.

Shear Test

The in-situ shear test or push test, developed to measure the bed joint shear strength, was presented by Kingsley and Schuller et. al. [11], [9]. The bed joint shear strength parameter can be used in assessing the masonry's shear strength for seismic hazard analysis. The Uniform Building Code (UBC) Standard 21-6 [12] presents the procedure and requirements for the test; however, according to Schuller et. al. ASTM was also developing standards for this test in 1995. The in-place shear test was designed using tests on clay brick masonry in Southern California and thus may not be useable on other types of masonry [9]. It consists of the removal of one masonry unit and the head joint on either side of a chosen test unit, horizontal displacement of the test unit using a hydraulic jack, and the recording of the horizontal force required to cause the initial movement of the test unit [11]. The test can also employ flat-jacks placed in joints above and below the test unit to control the normal stress across the shear surfaces of the test unit (see Figure 2-1). By conducting the test at several stress levels, the residual angle of friction of the bed joint can be obtained.
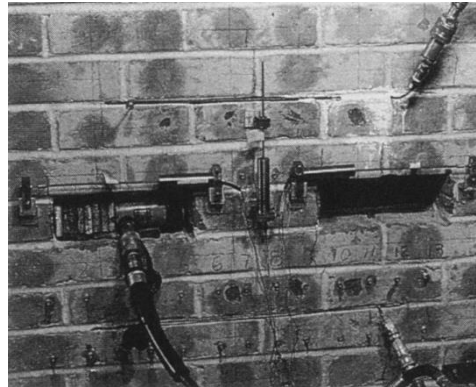
Figure 2-1 In-place shear test using flat-jacks to control the normal stress on the shear planes of the test unit [9]

Bond Wrench Test

The bond wrench test can be used to determine the bond strength between the units and the mortar. In 1980 Hughes and Zsembury developed the bond wrench test. It basically consists of clamping a long lever to a masonry unit, applying load to the other end of the lever, and recording the load at which the bond fails [8]. Simple linear elastic calculations are performed to resolve the forces on the test unit and determine the flexural tensile strength of the joint. Disadvantages to the test are that the equipment for in-situ bond testing must be custom designed and fabricated to fit the masonry typology being tested, only regular masonry typologies can be tested and at least two units below the test unit must be removed to make space for the bond wrench. The masonry can be repaired following the test by replacing the units and grouting them in [9]. There are standards for this test in the USA (ASTM C 1072-86) and in Australia (SAA 1988) [8]. A photo of the test being performed is shown in Figure 2-2.

Figure 2-2 Bond wrench test being performed to determine the flexural bond strength [9]

Flat-jack Test

Single and double flat-jack tests are used to determine the local compressive stress in the masonry and the deformability characteristics of the masonry. These tests will be the focus of section 2.2 and thus will not be discussed further here.

Borehole Dilatometer Test

The borehole dilatometer test was developed to measure the local elastic modulus or Young's modulus of the masonry. The test is performed by drilling a cylindrical core in the masonry; inserting a special probe, about 25 cm long, that applies uniform hydrostatic pressure on the borehole surface; and measuring the resulting deformation to calculate the modulus of elasticity, see Figure 2-3. Since the single probe is only 25 cm long, the pressure applied to the masonry is very local producing only local deformability results. However, the method can be applied multiple times and at various depths within the masonry. This method has been used in assessing the grouting strengthening of the Tower of Pisa with positive results [1].
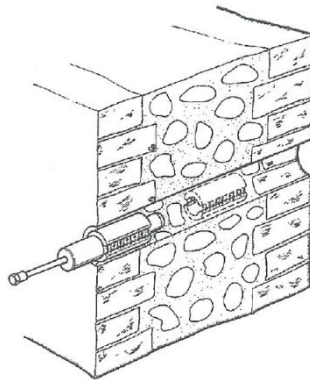
Figure 2-3 Schematic of a borehole dilatometer test [1]

Hardness Test

The final test of the mechanical tests group is the hardness test. The purpose of this test is to indirectly determine the compressive strength of the masonry materials through a correlation with the measured hardness of the materials. The hardness test is much less destructive than the other mechanical tests and often involves making only a very small hole or dent in the material. Various methods have been used to determine the hardness of the materials.

8

The traditional method of determining the hardness of a material in the field was scratching the surface of the material with handy objects such as a knife, screwdriver, or keys. In 1989 Pume [8] suggested a method by which a hand drill, instrumented with a percussion and impact counter, with an 8 mm diameter drill bit was used to penetrate the material by 10 successive impacts at 150 N force and the depth of the penetration measured. An empirical formula was used to relate the depth of penetration to the compressive strength. Pume also suggested that, instead of a drill, a 4 mm diameter cylindrical indentor could be used to impact the surface of the material with one Joule of energy. The number of impacts to drive the indentor 5 mm into the material is then related to the compressive strength.

Similar to Pume's work, in 1989 Chagneau and Levasseur [13] developed a method called the 'dynamostratigraphic method' to measure the mechanical properties of construction materials by measuring the force required to drill into the materials at a fixed rate. Gucci and Moretti [14] introduced their own drilling method in 1989 called the 'PNT-G' technique and Gucci and Barsotti [15] further developed and presented it in 1995. The PNT-G method is based on measuring the amount of energy required to drill a small cavity in a mortar layer and correlating that energy to the mortar compressive strength. However, this method was only valid for mortar having sand aggregate and a compressive strength below 4 MPa.

In 1991 Van Der Klugt developed the Schmidt pendulum hammer for use on masonry [8]. This test has been shown to correlate reasonably with the compressive strength of masonry prisms. However, quantitative determination of a masonry compressive strength requires relation to a series of prism compressive tests. The test measures the height at which a small mass rebounds, inside a small hammer, from the surface of the masonry. This rebound is an indication of the material hardness. Hammers with different energy levels are used on different material types [9].

2.1.3   Wave Transmission Tests

The second group of NDTs is the wave transmission tests. These tests consist of measuring waves that have passed through or have been emitted by the masonry. Wave transmission tests can be completely non-destructive. The purpose of these tests is usually to study the typology or geometry of the masonry including the identification of cracks, voids, anomalies, and changes in materials. Mechanical characteristics can sometimes be obtained but the analysis of the wave data may be difficult and correlative laboratory tests may be required. Each wave transmission test uses either different wave types or different transmitter and receiver positioning to obtain diverse results.
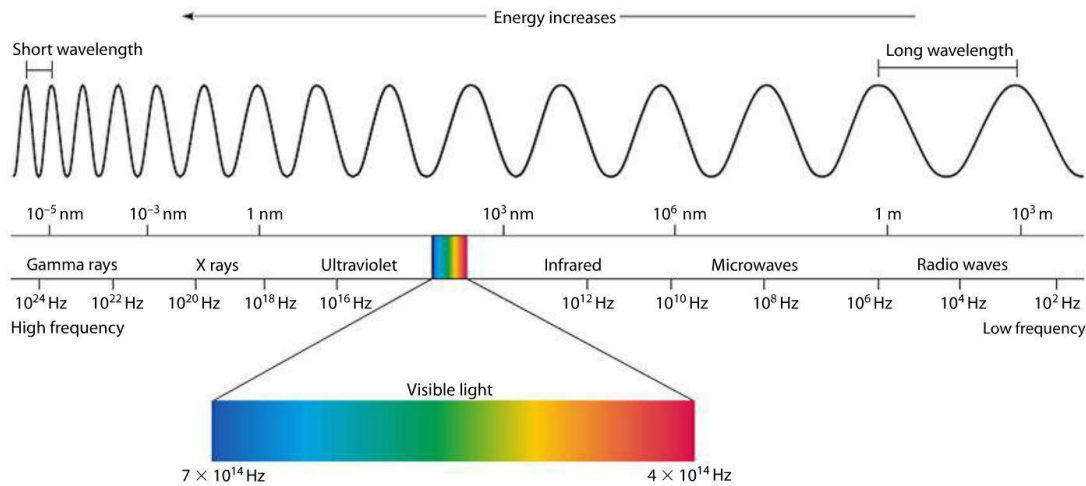
Figure 2-4 Electromagnetic Spectrum [16]

Waves can be categorized based on their ability to be transmitted through a vacuum. Electromagnetic waves are capable of transmitting their energy through a vacuum. They are produced by the vibration of charged particles [17]. The variation of the wavelength of electromagnetic waves produces the electromagnetic spectrum (Figure 2-4).

Mechanical waves, on the other hand, cannot be transmitted through a vacuum and must have a medium for transmission. Acoustic waves form the subset of mechanical waves that are most often used for NDTs. The acoustic, or sound spectrum, can be divided into four ranges: Infrasonic from 1 Hz to 20 Hz; sonic from 20 Hz to 20 kHz; ultrasonic from 20 kHz to 2 GHz and hypersonic beyond 2 GHz (Figure 2-5).
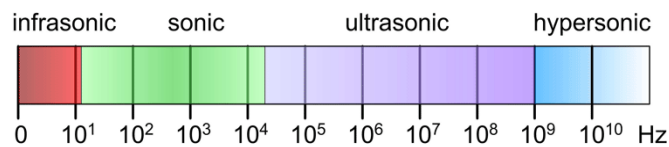
Figure 2-5 Acoustic spectrum of mechanical waves [18]

Sonic Tests

The first four NDTs shown in the wave transmission test group in Table 2-1 all use mechanical waves. Sonic testing is the most widely used mechanical wave transmission NDT. It has been applied to concrete and masonry since 1938 ([19] via [20]). Sonic pulse velocity tests and sonic tomography testing are conducted by transmitting a mechanical wave through the masonry using a hammer and receiving the wave with a sensor at another location on the masonry (Figure 2-6). Analysis of both the transmitted wave and received wave, the time taken to travel through the masonry allow for various conclusions to be made about the consistency of the masonry and possibly even the mechanical characteristics to be estimated.
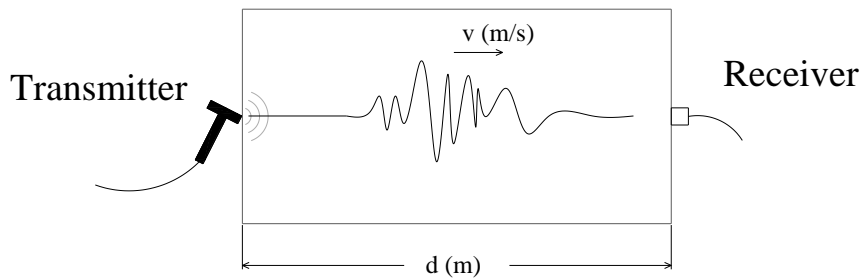
Figure 2-6 Basic concept of a sonic test

In order to better understand the reasons for the numerous configurations and data analyses that can be used with this test, some of the basics of wave motion through masonry materials are explained here.

There are two families of waves: body waves and surface waves. Body waves travel outward in all directions from their origin. There are two types of body waves: compression waves and shear waves. Compression waves are able to travel through solid and liquid material by alternating pulses of contraction and expansion of the material particles in the direction of wave travel. These waves propagate the fastest and therefore are also called Primary waves (P-waves). Shear waves travel through solids by deforming or translating the particles of the material perpendicular to the direction of wave travel. Since liquids have no shear stiffness, they cannot transmit shear waves. Because shear waves propagate slower than compression waves, they are termed Secondary waves (S-waves). Visual representations of P and S-waves are shown in Figure 2-7.
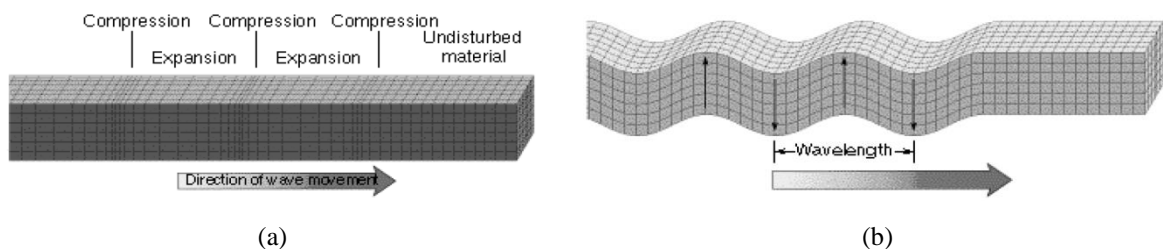
Figure 2-7 Body waves: (a) Compression waves (P-waves); and (b) Shear waves (S-waves)

The other family of waves consists of the surface waves. These waves result from the interaction of the Body waves with the surface of the material. Surface waves can be of two types: Love waves and Rayleigh waves. Love waves are shear waves in the horizontal plane. The magnitude of the horizontal translation of the material decreases with increasing depth. Rayleigh waves (R-waves) are produced by the interaction of both types of body waves, P-waves and vertical S-waves, on the surface of the material. The combination of vertical motion with compressional motion of the particles produces a small rotation of the particles. Similar to the Love waves, the motions of the particles in a Rayleigh wave diminish with increasing distance from the surface. In terms of wave speed, surface waves travel slower than body waves and Rayleigh waves travel slower than Love waves. Visual representations of Love waves and Rayleigh waves are shown in Figure 2-7.

(a)   (b)
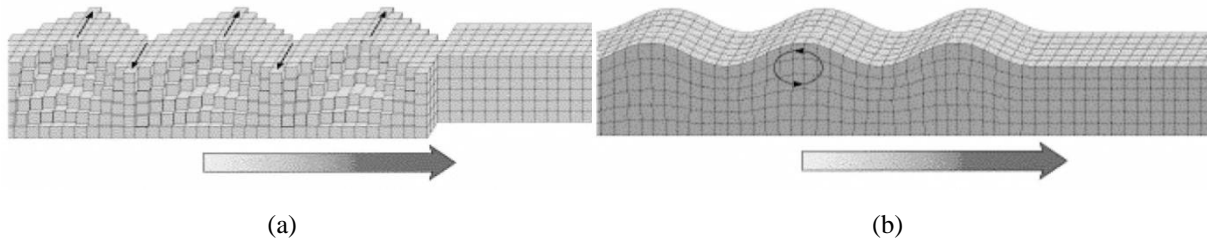
Figure 2-8 Surface waves: (a) Love waves; and (b) Rayleigh waves (R-waves)

By recording the motions of the material in different directions over time, the different wave forms can be identified. An example of wave motion from an earthquake is shown in Figure 2-9, where each of the types of waves is identified.
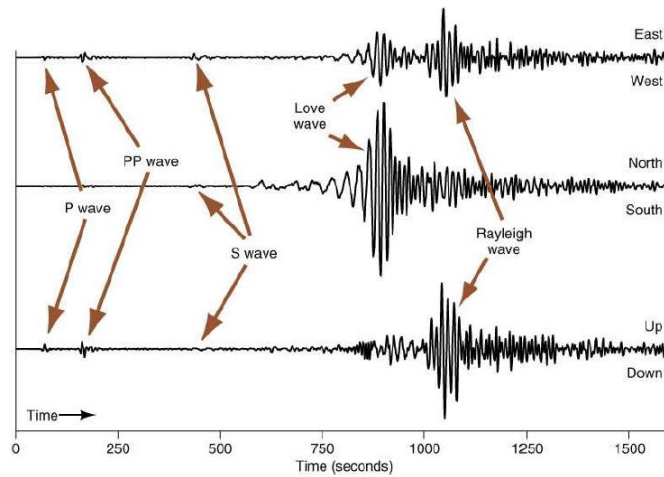
Figure 2-9 Wave forms identified in a seismic wave example

While the relative velocities of the different wave types can help to identify them, the precise velocity, energy and wavelength of each wave is determined by the physical and mechanical properties of the materials through which it passes. It follows then that studying the changes in a wave's signal as it passes through a material can provide information about the material's properties. Several studies have used the wave energies and frequencies to make correlations with the material properties [9]. However, since wave velocity is the quickest and easiest property to distinguish, it is used most often in sonic testing. The velocity of a wave traveling through a material, V, can be calculated simply dividing the distance a wave travels, d, by the time, t, it takes to travel that distance, as shown in Figure 2-6 and Eq. (1).

$$V = \frac{d}{t} \tag{1}$$

P-waves have the highest velocity and can be precisely measured both adjacent to an impact source of the wave on the same surface and through the material. R-waves have a distinguishably higher magnitude and energy [21] and can be recorded on the same surface as the initiation of the wave. In addition, the relationship between the P-waves and R-waves allows for the estimation of mechanical properties of the material.

For isotropic, elastic, homogeneous, and infinite materials, there are derived relationships between the wave velocity and the Poisson ratio, modulus of elasticity, and density of the material. Eq. (2) shows the relationship for P-waves [20].

12

$$V_p = \sqrt{\frac{E(1-v)}{\rho(1+v)(1-2v)}} \qquad (2)$$

where V_p is the velocity of the P-wave; E is the modulus of elasticity; v is the Poisson ratio; and ρ is the density of the material. The relationship for the R-waves is shown in Eqs. (3) [20].

$$V_r = \frac{0.87 + 1.12v}{1+v} \sqrt{\frac{E}{\rho} \frac{1}{2(1+v)}} \qquad (3)$$

where V_r is the velocity of the R-wave and all of the other variables remain the same as in Eq. (2). The relationship between the P-wave and R-wave can be described analytically by Eq. (4) assuming that the material is homogeneous, elastic, and semi-finite [20]. With this equation, if the velocities of the P-waves and R-waves are known, the Poisson ratio can be determined.

$$\frac{V_p}{V_r} = \sqrt{\frac{2(1-v)}{(1-2v)} \cdot \frac{(1+v)^2}{(0.87+1.12v)^2}} \qquad (4)$$

Masonry does not satisfy the required assumptions in order to use Eqs. (2), (3), and (4). Thus, these equations can only be used to estimate the modulus of elasticity and the Poisson ratio.

Sonic pulse velocity testing uses various configurations of transmitters and receivers to record the mechanical waves as they are induced in the material and after they have passed through the material. The three configurations, Direct, Semi-direct and Indirect, are shown in Figure 2-10.
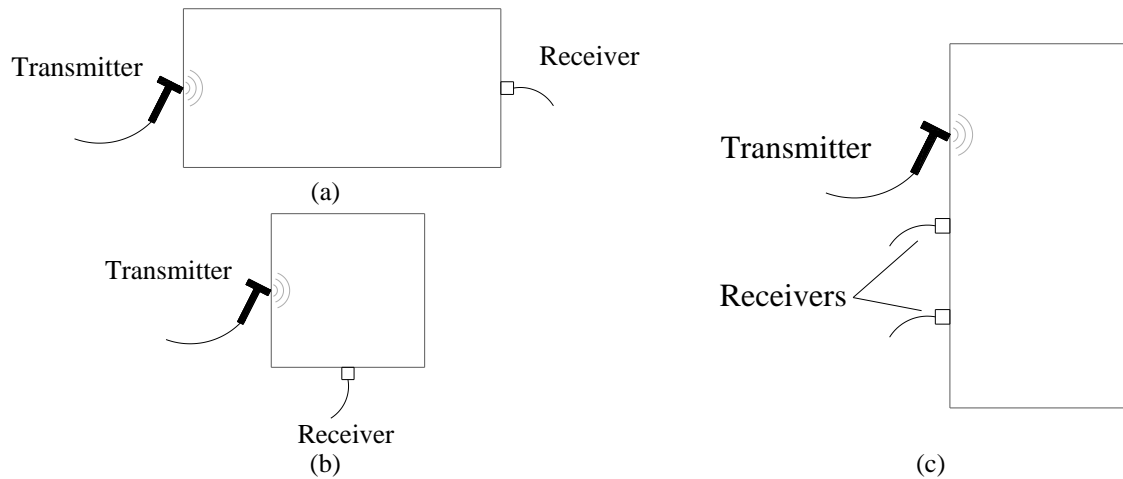
Figure 2-10 Sonic Pulse Velocity Test Configurations: (a) Direct; (b) Semi-direct; and (c) Indirect

Selection of a specific configuration depends on the type of information about the material that is desired and the accessibility of the surfaces of the masonry. In the direct test configuration, the sonic waves that pass directly through the material are measured, allowing the observation of the P-waves and S-waves. Similarly, the P-waves and S-waves can be recorded using the semi-direct configuration. If the indirect configuration is used where the receivers are on the same surface as the transmitter, all of the wave forms can be observed. However, the receiver sensors must be sensitive to the P-wave compression waves being transmitted perpendicularly to the sensor's application. Therefore, the most efficient way to determine the P-wave velocity

is to use the direct configuration and the only way to determine the R-wave velocity for estimation of the Poisson ratio and Young's modulus is by using the indirect method. In historic structures it can be difficult or impossible to gain access to both sides of the masonry, thus semi-direct and indirect tests are common configurations used, and sometimes the only ones possible.

Studying the morphology or the shapes and arrangements of units, mortar, and voids, is the most common reason for performing sonic testing on historical masonry. The variation of wave velocity can be due to the density of the materials within the masonry. It can be possible to distinguish between units or stones with different densities by comparing the velocities of sonic waves passing through those units or stones. In a study by Binda, et al. [22], the researchers were able to distinguish different types of stones in testing the pillars of the collapsed cathedral of Noto. Vasconcelos [5] found in her study of granites with ultrasonic pulse velocity tests that the wave speed was affected by the porosity and density of the granite. Higher ultrasonic velocities were found in granites with higher dry densities.

Mortar usually has a different density than the units. Thus, it can be possible to distinguish where there are more mortar joints or larger areas of mortar versus units. Miranda [20] studied the effects of both dry joints and mortar joints on the propagation of sonic waves through the masonry. He found that waves that must pass through dry joints or mortar have lower velocities than would be expected based on the sonic velocities of the individual constituent materials. The joints cause the dispersion of the waves increasing their travel time through the masonry and calculated velocity. This idea has been used in determining if there are multiple leaves or wythes of masonry in a masonry wall or column and if the inner wythe contains rubble masonry with a higher proportion of mortar or inhomogeneous material. Several studies, such as those by Da Porto, et al. [23], Binda, et al. [24], and Colla, et al. [25], have identified inner wythes of rubble masonry or backfill material by observing lower sonic velocity values in these areas.

One way of studying the morphology of an area of masonry is to compare the results of direct sonic tests in several points in the area. An objective comparison of direct sonic pulse velocity tests performed on an area of masonry can be obtained by creating a grid of points on the masonry surface and testing each point [9]. The velocities found at each point are then plotted in a contour plot showing the variation of the velocity over the surface of the masonry as presented by Anzani, et al. [26] in their study of historic masonry towers, see Figure 2-11. The contour plot shows areas of low velocity corresponding to low density material and low quality masonry.

(a) (b)
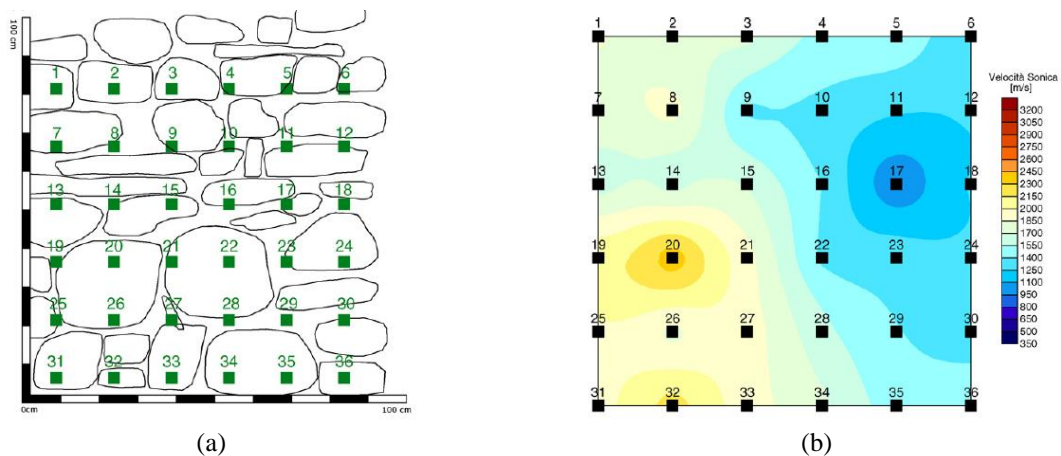
Figure 2-11 Direct sonic pulse velocity tests performed in a grid: (a) locations of the grid points on the masonry; and (b) contour plot showing the wave velocities [26]

Where there are low velocities, in comparison to the other points, there may be something impeding the transmission of the wave. Usually the presence of air voids impedes the transmission of the wave. Schuller at al. [9] reported this method can be used to detect flaws and voids in the masonry larger than 10 cm (4 inches) in diameter. They also used the amplitude and frequency of the wave signals to produce a contour plot describing the quality of the masonry.

Direct sonic tests in the grid format can also be applied in the same locations as flat-jack tests in order to compare the results. It could be expected that higher quality masonry with high strength units, few voids, and a high modulus of elasticity found using a double flat-jack test; would also have high velocity values in comparison to masonry with a poor quality, many voids, and a low modulus of elasticity. Indeed, Binda and Cardani found that sonic test results were in agreement with double flat-jack test results [10].

Impact Eco and Ultrasonic Tests

Where arrangements of the transmitters and receivers often require access to both sides of the masonry element for sonic pulse velocity tests and sonic tomography tests, impact echo testing only requires access to one face of the masonry being tested. The test is performed by using a small hammer to generate a stress wave and holding an accelerometer or piezoelectric transducer against the masonry surface next to the hammer to record multiple internal reflections of the stress wave (Figure 2-12). The waveform is analyzed in the frequency domain to obtain information about the internal features of the masonry. The test can be used in two ways: 1) wall thickness or the depth to internal discontinuities can be determined if the characteristic velocity of sonic waves in the masonry is known; 2) general masonry quality can be determined by calculating the velocity of the waves if the wall thickness is known [9].
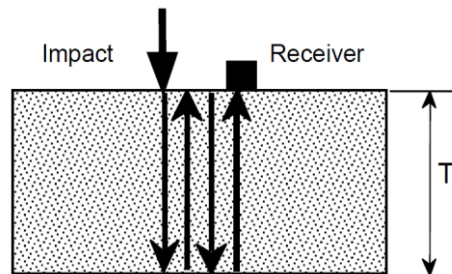
Figure 2-12 Basic setup for an Impact-Eco test [27]

Sonic pulse velocity, sonic tomography, and impact-eco tests all use mechanical waves in the sonic frequency range produced by hitting the masonry with a hammer. Ultrasonic tests are performed by using higher frequency waves in the ultrasonic range. To produce the higher frequency waves an electronic transmitter, placed on the surface of the masonry, emits an ultrasonic wave that is received by a receptor (Figure 2-13). This equipment, specially made for this test, automatically calculates the wave velocity when the distance, between the transmitter and receiver, is input.
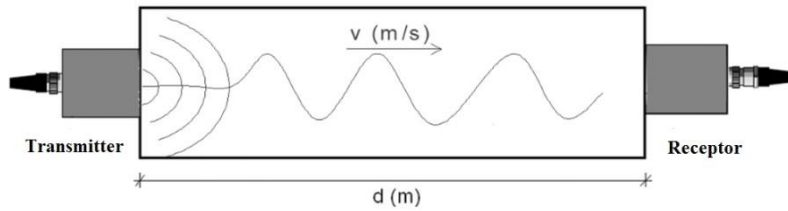
Figure 2-13 Ultrasonic test setup [20]

In the late 1970s ultrasonic tests were being developed for the determination of density and dimensions of masonry elements. At this time it was suggested that this test could also be used to detect hidden structural details, location of voids, faults, and cracks [7]. The main focus of the test, as in the other wave tests, was in determining the typology or geometric characteristics of the masonry. One disadvantage to using ultrasonic waves is that the transducers must be directly coupled to the material surface [7]. Small defects or roughness of the surface can affect the results because the short wavelength of the signal prevents it from passing through voids between the surface and the receiver. This precision detection is both an advantage and disadvantage for the test because defects as small as 2.5-5.0 cm (1-2 inches) can be precisely located and sized but only if the material is homogeneous and has only a small number of these anomalies. Heterogeneity of the material, or large voids, result in rapid wave attenuation, prevention of the waves from passing through the material, and pour quality results [9]. Variation in ultrasonic values can reveal valuable information about the consistency of the materials. As an example, ultrasonic tests were used on a study of the stones in the Cathedral of Noto, in Italy. The variation in the ultrasonic tests showed the void rich nature of the travertine stone allowing for its identification and distinction from the other more consistent calcarenite stone [22].

Meaningful quantitative results can be obtained but only through correlation with a reference material previously tested for its mechanical characteristics [7]. Various studies have been performed in the past to determine if ultrasonic velocities can be correlated with the compressive strength or modulus of elasticity of the material. Penelis et al. [8] conducted tests in 1983 and found that there was a low correlation between ultrasonic tests and core compression tests. However, there was a good correlation with the dynamic modulus of elasticity. Schuller et al. [9] also reported that there are poor correlations between velocity and compressive strength or other material properties.

Ground Penetrating Radar

The ground penetrating radar (GPR) test uses, instead, electromagnetic waves in the frequency range of 10 MHz to 3 GHz. The equipment is specifically designed for this test and can be quite expensive. An antenna emits a flux of waves in very short impulses, 0.5 to 5 μs, at a high rate. The waves reflect when they encounter materials with different dielectric constants and are received by the same or a different antenna. The time of the reflections allows for the determination of the distance to the change in material. Thus, internal defects in the masonry such as damp areas, cavities, metal, cracks, and joints, can be located [8]. GPR tomography has also been performed by holding the transmitter on one side of the masonry and moving the receiver across the masonry on the other side [24]. There are several drawbacks to the GPR method. The readings have a very high sensitivity making them difficult to interpret [8]. With high frequencies, the depth of penetration into the material is limited. A high moisture content of the material can influence or even prevent the attainment of clear results [24]. Nevertheless,

GPR testing has shown good correlations with sonic tests in several studies and can be used to complement or confirm the sonic test results [24], [28].

Thermography

The shorter wavelength infrared waves can also be used, in the NDT method known as thermography, to detect typological characteristics or constituent material differences. Invisible radiant energy is emitted from materials based on their thermal properties and surface temperature. Special equipment can be used to visually record the variations in infrared waves emanating from the materials. Since different materials emit different amounts of infrared radiation, the technique can potentially detect changes in material, defects and voids [7]. Images of the thermography testing can be compared to other tests, such as the GPR test, as a confirmation of their results [29], see Figure 2-14. Thermography can be performed passively by collecting the natural thermal radiation from the material surface or actively by applying a heat source to the material for a certain length of time and then recording the thermal radiation during cooling [8]. Disadvantages to this technique are that the penetration depth is only a few centimeters [8], so the inner details of thick sections are not possible to detect, and the technique is sensitive to the environmental conditions including the presence of water in the material [7].

(a)   (b)
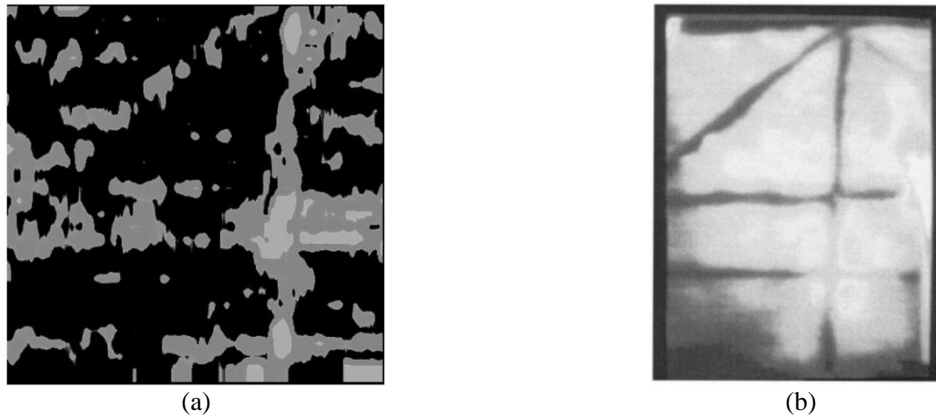
Figure 2-14 Comparison of two electromagnetic wave tests: (a) GPR; and (b) Thermography [29]

Radiography

Electromagnetic waves with extremely short wavelength such as x-rays and gamma rays can also be used to detect internal discontinuities in masonry materials. In the late 1970's radiography using these types of waves was being suggested as a potential NDT. In this method, the intensity of the radiation passing through the material is modified by the thickness and density of the material. A film or Geiger counter is used to record the variation of the radiation on the opposite side of the material from the application. This technique could show cracks, voids, density variations between the constituent materials, and the presence of foreign objects. However, the method has not been used much because of the health hazard of being exposed to radiation and the expense of the technique [7].

2.1.4 Sampling Tests

One minor destructive method that can yield a large amount of information about the materials used in historical structures is core drilling. Cores of the masonry materials can be tested in a variety of controlled laboratory tests to determine chemical, physical, mechanical, and bonding characteristics of the materials. Drilling cores in the masonry provides not only samples to be tested in the laboratory but also a means of gaining access to the interior of the masonry

structure. Once the core is drilled, a video camera can be inserted into the hole to survey the interior of the element, identify different materials, locate voids, and determine the dimensions of the masonry wythes [8]. An example of this borescopy technique is shown in Figure 2-15. If the cores are extracted in the same locations as other NDTs are performed the results can be compared. Core drilling can confirm the presence of voids and material interfaces observed previously in sonic tests, radar tests, and thermographic tests. Masonry cores have also been compared to sonic tomography results where it was found that solid brickwork and loose or poor material in the core corresponded to different sonic velocities [28].
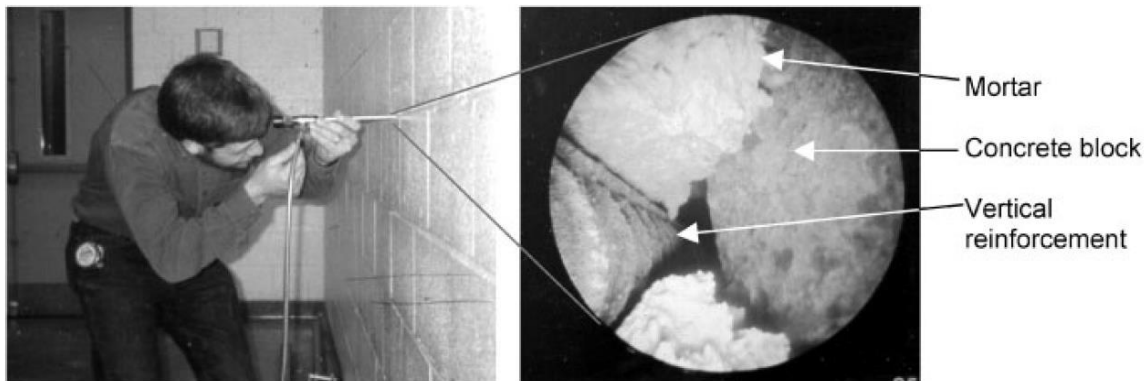
Figure 2-15 Borescope investigation in a small core of a reinforced masonry [29]

2.1.5   Dynamic Tests

Dynamic tests are the only completely non-destructive NDTs capable of providing information about the structural behavior of the entire structure. Through these tests the dynamic behavior of the structure can be observed. This provides invaluable information for assessing the behavior and safety levels of the structure when seismic loads are applied. Dynamic identification is most closely associated with the seismic behavior of the structure. It is performed by attaching accelerometers or other types of sensors to various positions on the structure, recording the vibrations, and using these vibrations to calculate natural frequencies and mode shapes of the structure [8]. The dynamic identification test can be performed using the natural motion of the structure, called ambient vibration, caused by the wind, ground motion, and other sources of vibration, or the structure can be excited with a forced external vibration [1].

2.1.6   Monitoring

Several different techniques and tests can be used to monitor an historical structure based on the type of information that is required. Rossi [1] describes several of the methods used in Italy to monitor the behavior of old structures: crack widths to determine the rate of movement of sections of the structure, tilting and horizontal movements of vertical structures using pendulums, relative horizontal movements using base extensometers, rotation using clinometers, and temperature using thermometers. Movements of the structure can also be monitored using accelerometers or other sensors that are left in place for long periods of time. These are attached to data acquisition systems that either record movements at fixed time intervals or when the acceleration exceeds a certain level signaling the occurrence of a seismic event [30].

2.2   Flat-Jack Testing

In the field of inspection and diagnosis, flat-jack testing is known as a relatively non-destructive technique among the various types of tests that can be performed on a masonry structure [2], [31]. This is because usually only a small amount of material must be temporarily removed for the placement of the jacks. The minor destructive nature of the test is one of the key reasons why this test has been adapted for use on historical structures. It produces important information about the structure without causing a large amount of damage to the irreplaceable historical structure. The primary goal of conducting an in-situ flat-jack test is to determine the local state of stress in the masonry and the existing deformability characteristics of the masonry. Thus, this test is usually performed on structural elements such as walls and columns.

The flat-jack method was first used in the field of geomechanics. Advancements were made to the method in the 1960's by LNEC, the National Civil Engineering Laboratory, in Lisbon Portugal [32]. In the early 1980's the method was adapted for masonry by Italian researcher Paolo Rossi and first used for testing brick masonry [4]. Since that time, the method has become standardized and widely used for analysis of historical masonry structures. In the United States standards were developed by ASTM in 1991 and, in Europe, RILEM standards were introduced in 1990. The standards include:

- ASTM C 1196-91 In-situ Compressive Stress within Solid Unit Masonry Estimated Using Flat-jack Measurements;
- ASTM C 1197-91 In-situ Measurement of Masonry Deformability Properties Using the Flat-jack Method;
- RILEM standard LUM.D.2 ;
- RILEM standard LUM.D.3.

The ASTM standards used in this work were versions 1196-04 [31] and 1197-04 [33]. The RILEM recommendations used and referenced in this work were MDT.D.4 [2] and MDT.D.5 [3].

The flat-jack device used for masonry tests consists of two metal plates welded on the edges to form a thin envelope or bladder. There are inlet and outlet ports welded into one side of the jack to allow the insertion of oil or water, which allow inflation and pressurization of the jack. Different sized and shaped flat-jacks can be made to fit the type of masonry to be studied and the method of preparation of the slot (Figure 2-16). In general, the flat-jacks should fit the size and shape of the formed slot. For instance, rectangular flat-jacks should be used when stitch drilling is the method of producing the slot or when the deformability is to be determined, while, circular or semi-circular flat-jacks should be used when the slot is created using a circular saw [34]. The length of the jacks should be longer than one unit in the masonry to be tested and as wide as the thickness of the outer masonry leaf. The A, B, and R dimensions shown in Figure 2-16 are specified in the ASTM and RILEM recommendations. Larger jacks would be able to induce stress over a larger portion of the masonry and possibly produce results more representative of the masonry, however, the devices must be designed to be easily inserted and removed from the masonry and to produce the least amount of damage to the historical structure.
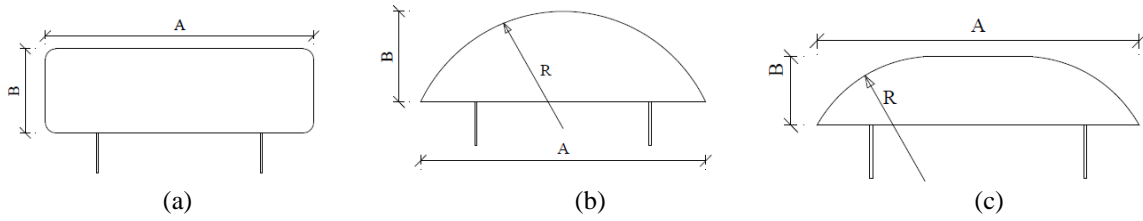
Figure 2-16 Typical Flat-jack device designs; (a) rectangular, (b) circular, and (c) semi-circular [31]

2.2.1   Single Flat-jack Test

The test relies on the principle that a relaxation of stresses will occur above and below the location where a slot is opened in the masonry. This will cause the closing of the slot. If a jack is placed in the slot and inflated to return the wall to its original position, the pressure in the jack can be correlated with the stress in the wall. The phases of the test are shown in Figure 2-17. The arrows above the wall sections indicate load from masonry above.
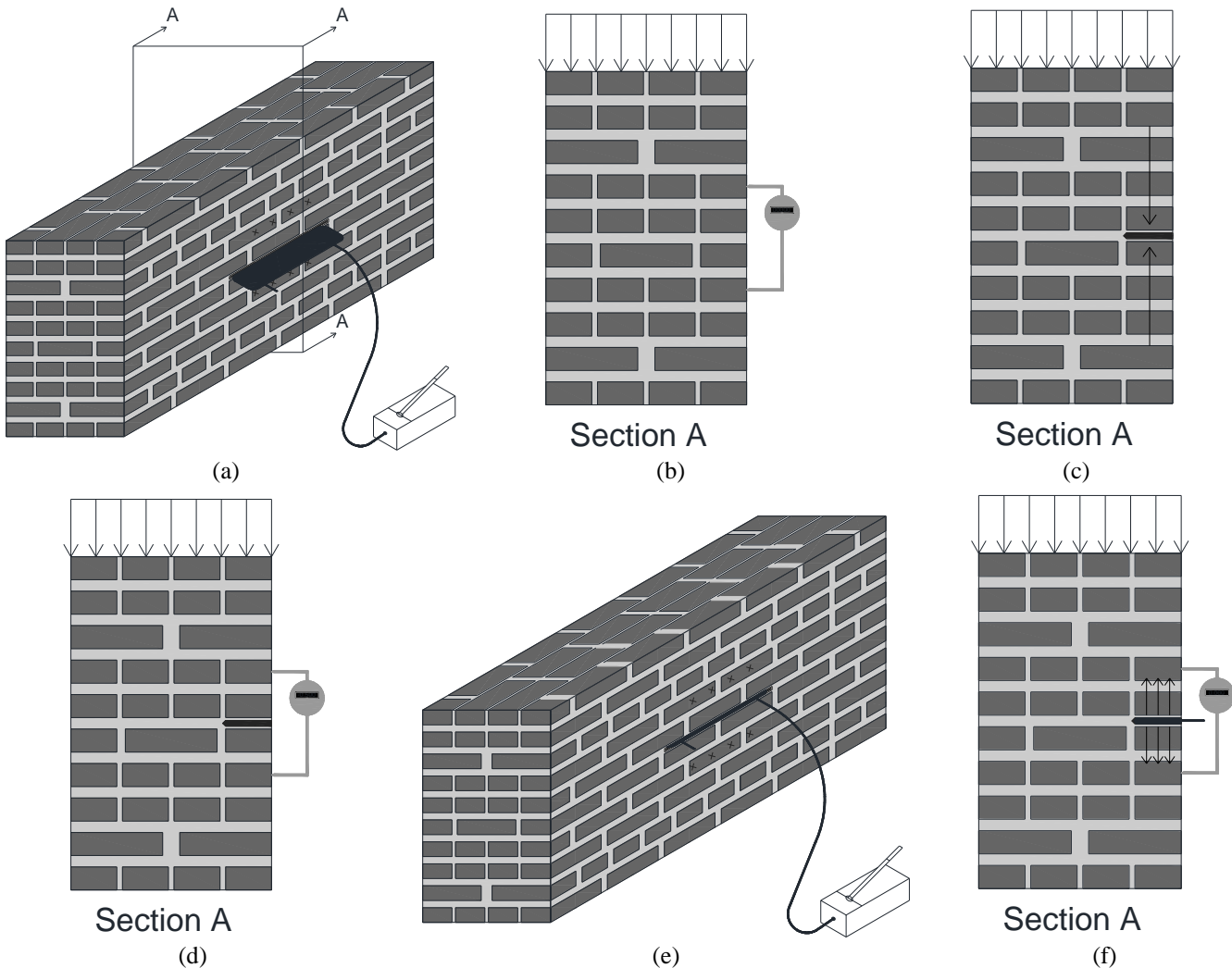
Figure 2-17 Phases of the Single Flat-Jack test: (a) Determining the location for the slot and applying gage points; (b) measuring the initial distance between the reference points; (c) cutting the slot (d) measuring the relative displacement of the gage points due to cutting the slot; (e) inserting the flat-jack and seating it in the slot; and (f) pressurizing the flat-jack until the relative displacements are restored to zero or the distance between the gage points is the same as it was before the slot was created [34]

The procedure for the test is as follows. The location of the slot is selected and marked. If a double flat-jack test was to be performed, following the single flat-jack test, space is left above the slot for the second slot of the double flat-jack test. Reference, or gage, points are secured to the surface of the masonry above and below the location where the single flat-jack slot will be created. The positions of the gage points are shown in Figure 2-17a as X's on the wall. Linear Variable Displacement Transducer (LVDT) holders can also be secured to the masonry for placement after the insertion of the jack. An example of an LVDT and gage points mounted to the wall is shown in Figure 2-18c. The initial distance between the gage points is measured using a demountable mechanical strain gage or DEMEC (Figure 2-17b). A typical analog DEMEC is shown in Figure 2-18a. Next the slot is cut. Due to the removal of the material in the slot, the masonry around the slot relaxes and there is a slight closing of the slot, shown by the arrows in Figure 2-17c. To record this displacement, the distance between the gage points, is measured again (Figure 2-17d). The flat-jack is inserted into the slot (Figure 2-17e) and, if they are being used, LVDTs are positioned over the slot for a continuous record of displacement.
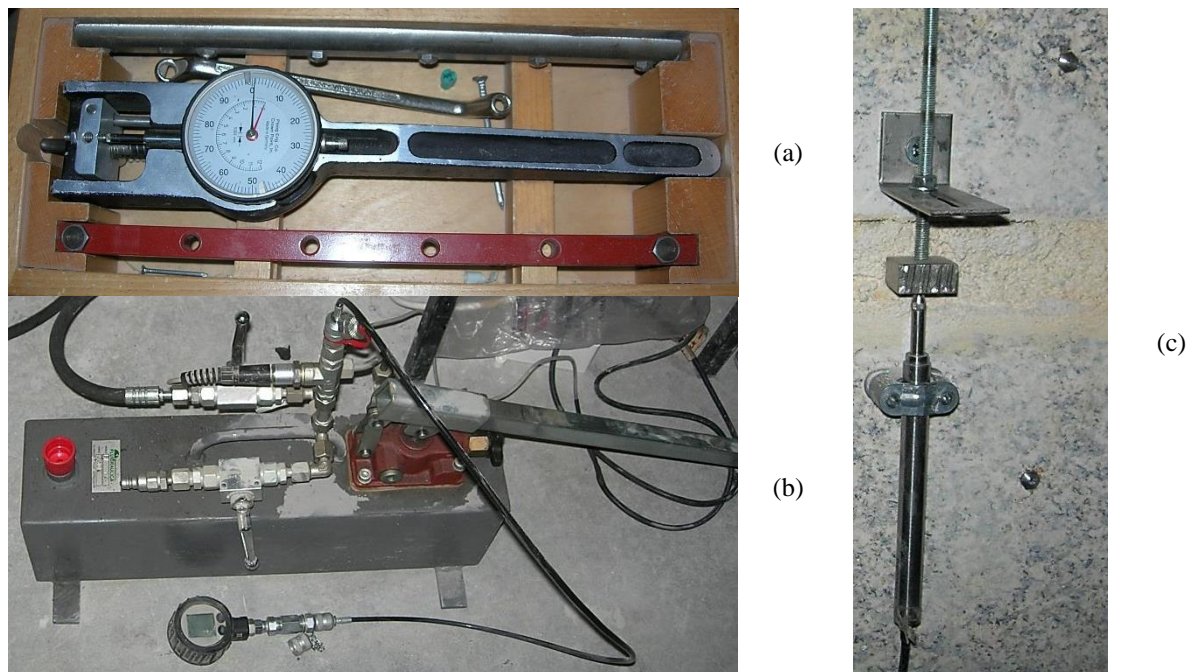
Figure 2-18 Equipment used in flat-jack testing: (a) demountable mechanical strain gage (DEMEC); (b) hydraulic pump; and (c) linear variable displacement transducers (LVDTs) and gage points

The flat-jack is connected to an oil pressure pump with a gage to measure the pressure in the system. A typical hydraulic hand pump is shown in Figure 2-18b. The flat-jack is initially inflated and the pressure held constant in order to seat the jack or allow it to fill the slot. Once the jack is seated in the slot, the pressure in the jack is increased and the displacement of the LVDTs observed. When it is certain that the distance between the gage points has returned to the initial distance before the slot was cut, the test is concluded (Figure 2-17f). The pressure at this point, is called the canceling pressure or restoring pressure. The restoring pressure can be related to the compressive stress in the masonry normal to the slot. Due to the stiffness of the flat-jack, that resists expansion when pressurized, and due to the jack not being able to completely fill the surface area of the slot, the pressure in the flat-jack is larger than the local compressive stress. The relation, including these factors, is described by Eq. (5).

$$\sigma_m = K_m K_a p \tag{5}$$

where: σ_m is the local state of stress in the masonry, K_m is the jack calibration factor, K_a is the area correction factor, and p is the jack pressure required to restore the original opening dimensions as determined by the measuring devices, within an allowable tolerance. The jack calibration factor is determined in the laboratory during the calibration of each individual flat-jack [31]. The area correction factor is the ratio of the surface area of the flat-jack to the surface area of the slot.

Several assumptions are made when performing this test including [34]:

- The state of stress in the masonry is uniform and compressive;
- The masonry around the slot is homogeneous;
- The masonry will deform symmetrically;
- The stress applied to the masonry by the flat-jack is uniform;
- The masonry deforms elastically.

Since not all of these conditions may be true for the tested masonry, sources or error are introduced. Early on in the use of flat-jack testing, a method was developed to improve the contact area between the flat-jack and the slot. Kingsley and Noland [35] showed that shims could be used for uneven masonry surfaces to improve the uniformity of the applied pressure and reduce the deformation of the jack. Shims could be made of flat pieces of metal or an additional flat-jack could be used as a shim. Single and multiple piece shims were incorporated into the standards. Despite the use of shims, stress distribution for typical stainless steel flat-jacks is not uniform over its surface. Gregorczyk and Lourenço [34] showed that a more uniform stress distribution can be obtained with a rubber jack. Laboratory testing by Gregorczyk and Lourenço in a regular masonry wall with a steel flat-jack produced typical single flat-jack test results as shown in Figure 2-19.
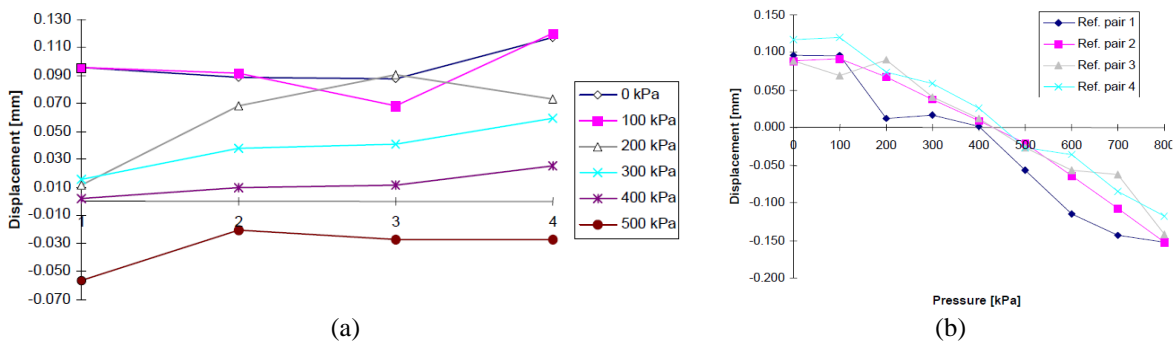
Figure 2-19 Typical single flat-jack test results: (a) Displacements of reference point pairs 1-4 at various pressure levels; and (b) Influence of pressure increase on the displacement of reference point pairs [34]

2.2.2 Double Flat-jack Test

The double flat-jack test is a minor destructive test performed on masonry to observe the stress-strain behavior. With the stress-strain behavior, the modulus of elasticity, poison ratio and sometimes the compressive strength can be estimated. The principle of the test is the same as a laboratory compression test except that it is performed in-situ with flat-jack devices. Two slots are cut in the masonry, preferably in the mortar joints, to vertically isolate a masonry "specimen" in the larger masonry element. The masonry between the two slots is assumed to be unloaded after the slots are cut. Flat-jacks are inserted in the slots and pressurized to

compress the specimen. The lateral and longitudinal deformations of the masonry are measured using gage points and a digital extensometer or LVDTs. The general test setup is shown in Figure 2-20a. Typical locations for vertical sets of gage points are marked with X's on the wall.

(a)   (b)
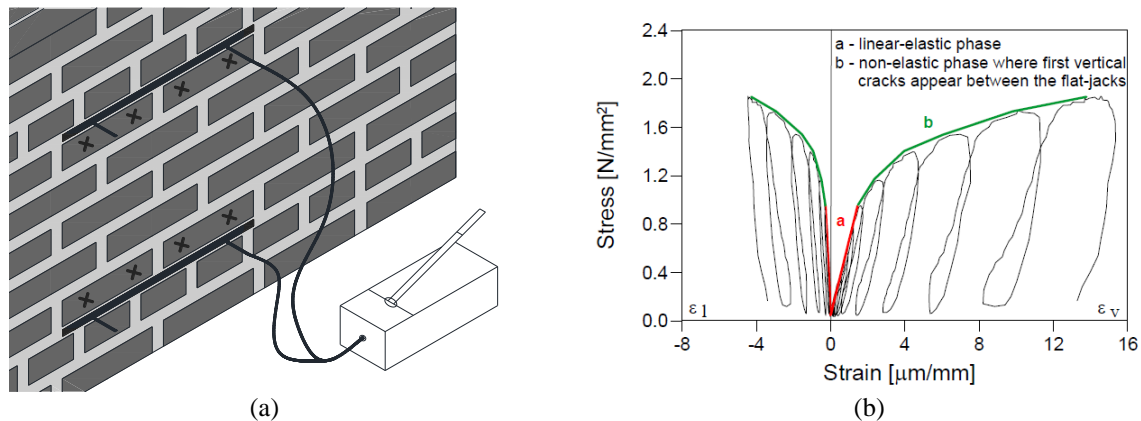
Figure 2-20 Double flat-jack test: (a) setup; and (b) sample results indicating linear and nonlinear phases [36]

The following procedure is used. The test is usually performed in the same location as the single flat-jack test in order to use the slot already prepared for the single flat-jack test. After the single flat-jack test has been concluded, a second slot location is determined above the first slot and opened using the same sawing or drilling method. The second flat-jack is inserted into the slot. The LVDTs are removed from over the first flat-jack and are placed vertically and horizontally between the two flat-jacks. The distances between the LVDT connection points are measured for later calculation of the strains. The flat-jacks are pressurized and the pressure held constant in order to seat the jacks in the slots. After the jacks have inflated to fit the slots, the pressure is increased and decreased in cycles, performing a compressive test on the masonry "specimen". The displacements of the LVDTs are recorded and the strains calculated. If some additional damage is permitted in the area of the test, the test can be continued into the nonlinear phase to estimate the compressive strength of the masonry. However, the test can only continue within the pressure limits of the flat-jacks. An example of test results including both the linear and nonlinear phases is shown in Figure 2-20b. The test is concluded when the stress induced by the jacks on the masonry surrounding the test "specimen" reaches its compressive limit and the masonry above the top jack begins to crack and break apart, indicating failure of the masonry.

Several assumptions are made when performing this test including [34]:

- The masonry between the flat-jacks is homogeneous;
- The stress applied to the masonry by the flat-jacks is uniform;
- The state of stress in the test specimen between the jacks is uniaxial;
- Lateral effects from the masonry being connected horizontally are neglected.

While the flat-jack test method was originally developed for regular brick masonry, the equipment was further adapted by Binda, Modena, Baronio, and Abbaneo in 1997 [37] for heterogeneous or irregular masonry. Calibration of this adaptation with comparison compression tests showed regularity of the results, repeatability, and applicability of the test. However, further studies have shown that when the stress level is low, the material is weak, or the material is non-homogeneous, the results can be unreliable [4].

Finally, double flat-jack testing has been used to monitor the effect of grout injection [37]. By performing double flat-jack tests both before and after injecting the grout, it can be

determined if the necessary increase in Young's Modulus of the masonry has been obtained, indicating the success of the grouting intervention.

2.2.3   Difficulties with Flat-Jack Testing

Several difficulties have been found in using the flat-jack testing method with irregular masonry walls. It can be difficult to follow the standards when placing measuring devices and gage points due to the irregularity of the units and mortar joints [38]. The distances over which the devices measure may have to be different from each other in order to attach them to the units Figure 2-21a. The effect of the different measuring distances will be examined in the numerical modeling portion of this thesis. The surface of the masonry may also be irregular as units protrude from the surface Figure 2-21b. This can also pose problems for attaching measuring devices and aligning them in the directions to be measured. Measuring device attachment to gritty, sandy, or soft units can also be difficult. Several methods of attachment including gluing, screwing in inserts or both may need to be tested to see what method works best for a particular unit type.

Besides being problematic for placing measuring devices, irregular masonry can cause issues in determining the appropriate locations for the flat-jacks. Stress can be concentrated where there are larger and stiffer units. Thus, placement of the jacks will affect both the single and double flat-jack tests. Large unit masonry poses a particular problem because the flat-jacks may be shorter than the units (Figure 2-21c). Thus, only one or two units could be being tested, not the masonry as a whole.

| (a) | (b) | (c) |
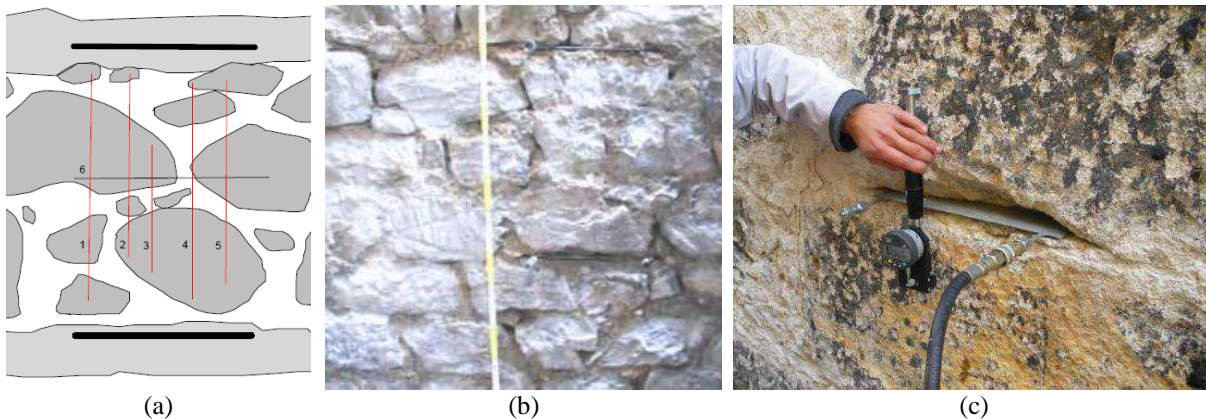
Figure 2-21 Challenges due to irregular masonry: (a) different measuring distances [4]; (b) units protruding from the surface of the masonry [36]; and (c) units larger than the length of flat-jack [20]

When the flat-jack test is performed, a cutting device, such as a saw, makes a thin slit in the masonry element into which the flat-jack is inserted. Because of the length of normal sized flat-jacks (400 mm), the stress distribution along the slit is non-uniform, with high stress peaks near the edges of the slit. This non-uniform stress distribution could influence the accuracy of the flat-jack test results.

The slot is usually cut in a horizontal mortar joint of a masonry element. Many masonry structures are built with stone pieces of various shapes and sizes. The randomness of the stone units results in an irregular construction pattern with mortar joints that are not in horizontal lines (Figure 2-22a). Consequently, sawing slots for the flat-jacks, even in the most horizontal portions of the joints, will require destruction of some units as seen in Figure 2-22b and c. Due to these damages, additional repair to the masonry in the tested area will be required once the testing is concluded. Furthermore, utilization of heavy equipment to cut the slot for the flat-jack

24

can be cumbersome. This may result in the slot thickness being too small or non-uniform (Figure 2-22d), the necessity to make multiple cuts, change the saw blade to attain a suitable opening to install the jack, or to fix the saw machine to the wall [4]; all of which can be time consuming and labor intensive.

(a)   (b)   (c)

(d)
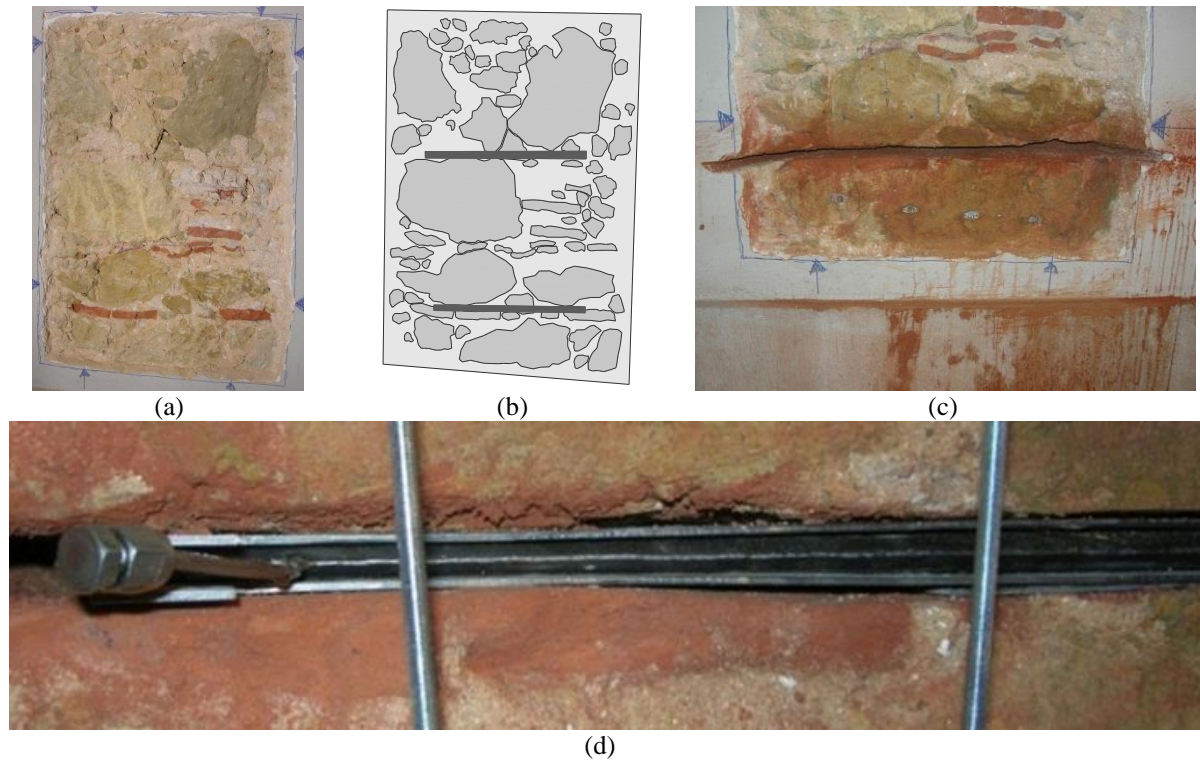
Figure 2-22 Flat-jack Test Difficulties: (a) Irregular masonry of a Historical structure in Lisbon, Portugal; (b) schematic drawing showing locations for flat-jack slots; (c) Damage to surrounding units from saw cutting; and (d) Variable thickness of the flat-jack slot from multiple saw cuts

Variable thickness of the flat-jack slot can lead to a non-uniform application of pressure by the flat-jack on the masonry. Applied pressure variations coupled with irregular distribution of stones and mortar can lead to asymmetric results and the inability to fully recover the initial reference point distances making result interpretation difficult [4]. Two other difficulties, reported by Binda and Tiraboschi [4], include low reliability of the test when the load over the masonry is low and unreliable interpretation of the results when the material is weak or non-homogeneous. In their test case shown in Figure 2-23, the irregular configuration of the stone units resulted in an uneven stress distribution during the double flat-jack test, which resulted in an apparent higher stiffness at LVDTs 1-3 than at LVDT4.
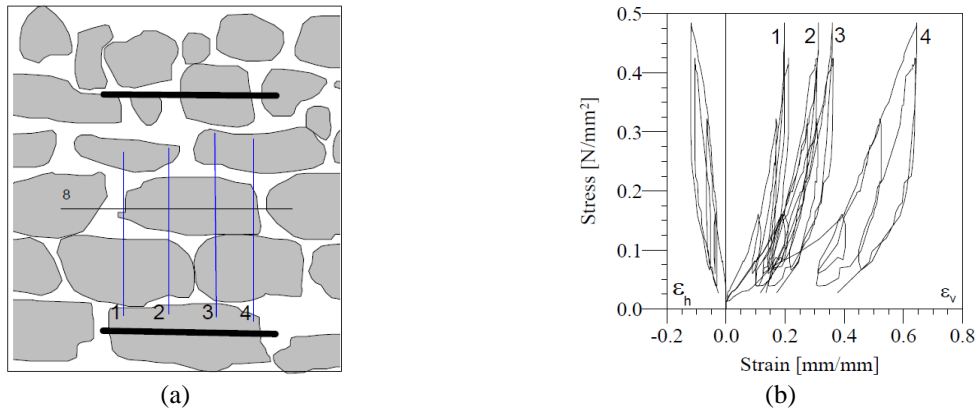
Figure 2-23 Uneven stress distribution during double flat-jack test presented by Binda and Tiraboschi: (a) test set-up in relation to stones, and (b) stress-strain results [4]

There can also be difficulties when applying the double flat-jack test in masonry in low stress state conditions [36]. Due to equilibrium of forces, if the pressure applied by the upper jack reaches a level greater than the stress state in the masonry, the jack will start to push the masonry upwards and cracking in the masonry above could appear. An example of the results obtained and cracking is shown in Figure 2-24. The stress levels in the masonry tested as part of this thesis work were very low and this likely contributed to the poor results presented later in the thesis.
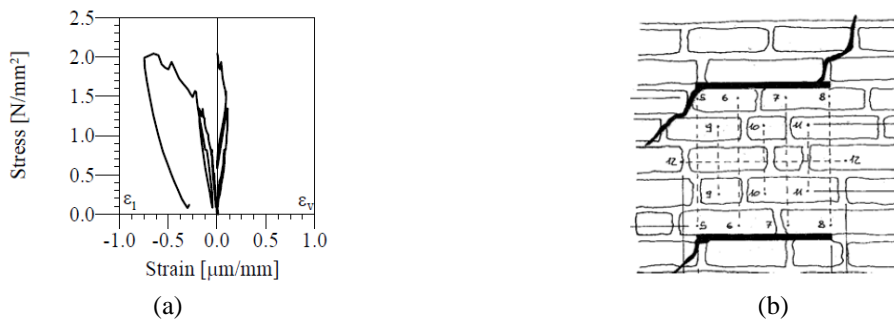
Figure 2-24 Double flat-jack test example in low stress state conditions: (a) stress versus strain results; and (b) cracking above and below the jacks [36]

It can even be difficult to analyze the results of the single and double flat-jack tests. In the single flat-jack test, in most cases the results of the individual LVDTs or measurement lines will be different from each other. This is because the center of the slot deforms more than the edges as shown in Figure 2-25a. Measurement lines 2 and 3 will see more relative displacement from opening the slot than lines 1 and 4. When restoring the relative displacements with the flat-jack pressurization it is unlikely that all lines will be restored at the same pressure [36].

In double flat-jack tests the determination of the elastic modulus can be difficult due to the nonlinearity of the masonry. The initial elastic phase of the test can be difficult to measure due to the adjustment of the jacks in the slots and adjustment and locking of the units as they are initially compressed. Two methods are given by ASTM and RILEM, the tangent modulus and the secant modulus [3] and [33]. The tangent modulus of elasticity, E_t, is the slope of the envelope of the stress versus strain curve and is given by Eq. (6)

$$E_t = df_m/de_m \qquad (6)$$

where df_m is the increment of stress and de_m is the increment of strain at a certain stress level. An example of the tangent modulus method being applied to results is shown in Figure 2-25b. The secant modulus, E_s, is the slope to a point on the stress versus strain curve from the point of zero stress and strain and it is given by Eq. (7)

$$E_s = f_m/e_m \tag{7}$$

where f_m is the cumulative stress and e_m is the cumulative strain increment from zero. Since the point where the modulus is measured from is left up to the operator this method can be subjective. Another common method is to use the tangent modulus during the linear portion of the loading or unloading phase of the pressurization cycles. This is shown in Figure 2-25c.
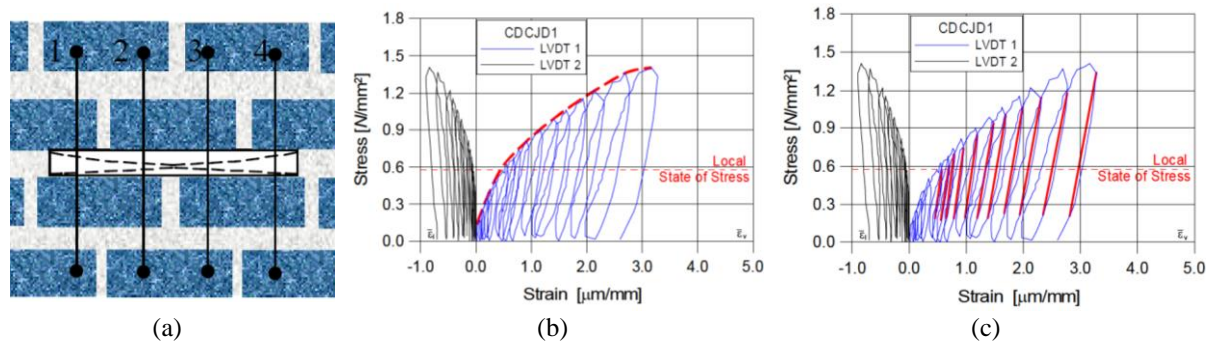
Figure 2-25 Difficulties in analyzing results: (a) variation of stress and displacement along the slot [38] and; (b) tangent elastic modulus envelope [36] versus; (c) tangent elastic modulus during unloading phases [36]

In order to solve these problems with flat-jack testing or create new methods for determining the required structural characteristics, several techniques have been presented in the past. In 1983 a simple flat-jack device used to determine the Young's modulus in concrete was patented in Japan [39]. This device could also be used on masonry but it had the same issues as previously described by the flat-jack and also did not solve the issue of damaging masonry units during a test on irregular masonry.

Single cylindrical jacks have also been used, usually to determine the two-dimensional stress field in rock masses [40] and [41]. A 1996 Italian patent refers to a cylindrical jack that can be used to determine the modulus of elasticity of the masonry [42]. The method uses a diamond coring machine to make the first hole in the masonry. This device consists of a tube with a rigid layer and flexible layer. Oil or another substance is pumped into the flexible layer. The deformation of the masonry between the two layers is measured to determine the modulus of elasticity. In this method the coring and drilling must be done in the stone units and the test is localized to the cored material. Thus, this technique does not solve the issue of protecting the masonry units and is too localized to determine the modulus of elasticity of the composite masonry material. More recently, another version of the cylindrical jack, called the dilatometer (see Figure 2-26), has been used for measuring stresses in masonry [43]. However, no previous solution has used multiple cylindrical jacks.

Figure 2-26 Dilatometer testing: (a) dilatometer; and (b) dilatometer inserted in drilled hole and oil pump for applying pressure

2.3   Tube-Jack Testing

In an effort to develop methods that are less destructive to the historical structure and which can provide more reliable and accurate information about the characteristics of the structure, an enhanced method termed "Tube-Jack Testing" is under development at the University of Minho [44]. This method uses a line of individual cylindrically shaped jacks to pressurize the masonry instead of flat-jacks. The method relies on the same principles as the widely used flat-jack test method [2] to determine the local state of stress in a masonry element, the modulus of elasticity, an estimation of the Poisson's ratio, and, whenever is possible, the masonry compressive strength.

2.3.1   System Description

Tube-jacks are cylindrical jacks made from a flexible tubing material. The tube-jacks have metal fittings at each end. One side is closed and the other can be connected to a hose for fluid insertion (Figure 2-27a). The tube-jack system consists of a series of tube-jacks, forming an equivalent flat-jack, which is connected to a pump via connection bars and hoses (Figure 2-27b). Replacing the flat-jack with a series of tube-jacks allows the holes to be drilled along misaligned mortar joints in irregular masonry, leading to less damage to the historical structure during the test. The assumption is that the line of tube-jacks will perform similarly to a large flat-jack, an equivalent flat-jack. The flexibility of this system allows the length of the line of tube-jacks to be varied by changing the number of tube-jacks used in the test. Thus, masonry with large stones, which could not be easily and accurately tested with the fixed size flat-jacks, can be tested with the tube-jack system.

LVDTs are attached to the masonry surface to measure the relative displacement of the masonry throughout the test; including drilling, stress redistribution, tube-jack insertion, and pressurization phases (see Figure 2-27c). A data acquisition system and computer are used to record the pressure in the tube-jack system and the LVDT data throughout the test. Since the tube-jacks are discontinuous along the equivalent flat-jack line, the LVDTs can be placed between the tube-jacks and used throughout the test. Continuous data collection is one more advantage over the traditional flat-jack test, which requires removal of the measuring devices during creation of the slots.

28
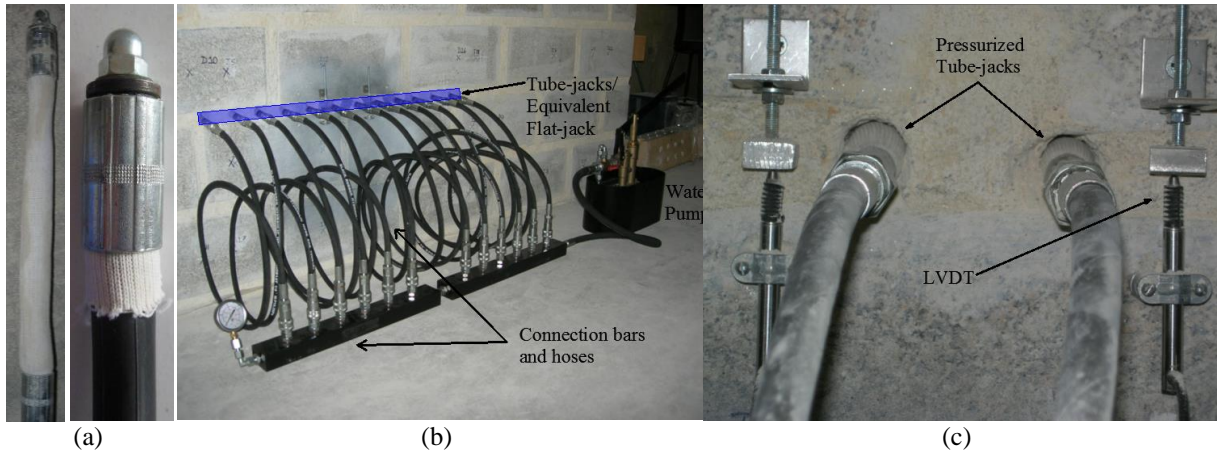
Figure 2-27 Tube-jack test system components including: (a) single tube-jack; (b) tube-jacks forming an equivalent flat-jack, connection bars and hoses, water pump; and (c) pressurized tube-jacks and LVDTs

The set-up of the tube-jack system is slightly different depending on the aim of the test. If the aim of the test is to determine the state of stress in the masonry, a single line of tube-jacks will be used and the LVDTs will be placed at regular intervals between the tube-jacks as shown in Figure 2-27. This type of test will be referred to as a "Single Tube-Jack Test." If the aim of the test is to determine the deformability characteristics of the masonry, then two approximately parallel lines of tube-jacks, two equivalent flat-jacks, will be used as shown in Figure 2-28. The LVDTs for this configuration will be placed between the two lines of equivalent flat-jacks. This test set-up will be referred to as a "Double Tube-Jack Test."
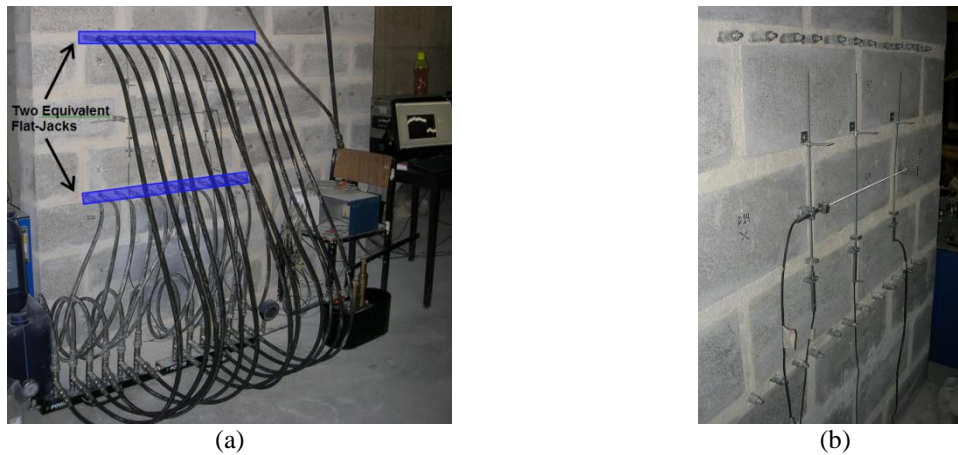
Figure 2-28 Double tube-jack test system set-up: (a) tube-jack lines forming two equivalent flat-jacks; and (b) LVDTs located between the lines of tube-jacks, as seen from the back of the wall

2.3.2 Theory

The tube-jack test method is very similar to that presented in existing standards and recommendations for the flat-jack method [2], [31]. However, instead of creating a slot in the masonry and inserting a flat-jack, several holes are drilled in the line of the mortar joint and tube-jacks are inserted into these holes. The basic procedure used in the single tube-jack test to determine the local state of stress of the masonry is as follows. The location of an approximately linear masonry joint, perpendicular to the assumed direction of compressive stress in the masonry, is determined and marked on the wall. LVDTs are attached to the masonry units so that they measure over the masonry joint to be tested. Acquisition of data from these LVDTs is started and, if the wall is in a steady state of stress, the relative displacements of the LVDTs should read zero. Holes are drilled in the masonry joint. Removal of this material induces a

stress relaxation around the holes and their subsequent closing. The LVDTs should record relative displacements due to the movement of the masonry around the holes. Tube-jacks are placed in the holes and inflated to fill the holes. The line of tube-jacks forms the equivalent flat-jack. The pressure in the tubes is increased to exert pressure on the surrounding masonry. When the relative displacement of the masonry is reduced to zero, or the masonry returns to its original position before the drilling of the holes, the pressure in the tube-jacks can be used to estimate the state of stress in the masonry.

The procedure for the double tube-jack test, used to determine the mechanical characteristics of the masonry such as the Young's modulus and the Poisson ratio, requires a second line of tube-jacks forming a second equivalent flat-jack. An approximately linear mortar joint is identified above the mortar joint used for the single tube-jack test. This second joint should be at least two courses above the first line and should be as long as the first line. LVDTs or other measuring devices are attached to the masonry so that they will measure the masonry between the two equivalent flat-jacks. A similar set-up for the measuring devices can be used as is suggested in the standards and recommendations for the double flat-jack test. An example set-up was shown in Figure 2-28. Next the holes are drilled in the second mortar joint. The two lines of holes separate a masonry specimen between them. Tube-jacks are inserted in both lines of holes. The tube-jacks are attached to the same pressure pump and gage so that the entire system has the same internal pressure. The tube-jacks are pressurized in cycles, applying pressure to the separated masonry specimen. After adjustments to the internal pressure to determine the pressure applied on the masonry, these pressure values can be plotted versus the recorded relative displacements and strains to estimate the Young's modulus and Poisson ratio of the masonry.

The determination of how much pressure the tube-jacks apply to the masonry is more complex than for the flat-jacks because of the cylindrical shape of the holes and tube-jacks. Consider a tube situated along axis z as shown in Figure 2-29a. The tube has an inner radius a and an outer radius b. The initial thickness of the tube wall is $t_i = b - a$ when no pressures are exerted on the tube. The Young's modulus, E, and Poisson ratio, v, must be known for the tube material for this calculation. The tube is subject to internal water pressure p_w and external masonry pressure p_m as shown in Figure 2-29b. Due to these pressures, the tube will deform radially so that the new inner radius is c and the outer radius is d. The unknowns that must be determined are the external masonry pressure, p_m, and the deformed inner radius of the tube, c, required for calculation of p_m.

(a)   (b)   (c)
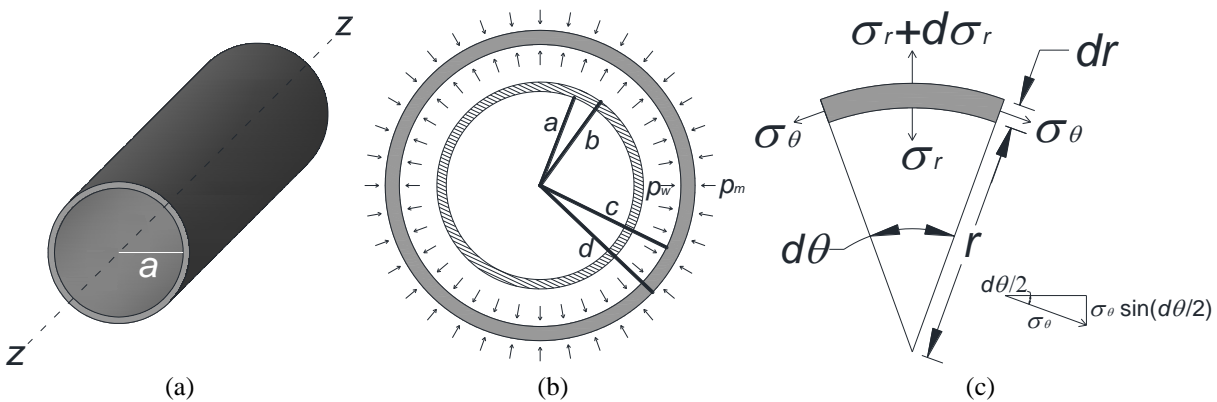
Figure 2-29 Calculation of the pressure applied to the masonry: (a) tube before pressures are exerted on it; (b) sections of the original unstressed tube (dashed) and deformed tube under pressures pw and pm; and (c) small element within the thickness of the tube

In the deformed tube, the radial pressure through the wall of the tube will vary between p_w and p_m. Consider a small element within the thickness of the tube as shown in Figure 2-29c. This element is located at radius r and has a thickness dr and length dz along the axis of the tube. The radial dimension of the element is $rd\theta$ at radius r. Since the pressure varies through the thickness of the tube there is a radial stress σ_r at radius r on the element. A slightly different stress $\sigma_r+d\sigma_r$ would act at the other edge of the element at radius $r+dr$. To satisfy equilibrium, the stress difference results in a tangential or hoop stress σ_θ [45]. By circular symmetry, the stresses σ_θ and σ_r are functions only of r. Thus, there are no shear stresses in the tube. Considering equilibrium of forces in the radial direction gives Eq. (8).

$$(\sigma_r + d\sigma_r)(r + dr)d\theta dl - \sigma_r r d\theta dl - 2\sigma_\theta dr dl \sin(d\theta/2) = 0 \tag{8}$$

Neglecting higher order terms and noting that at small values of θ, $\sin(d\theta/2) = d\theta/2$, Eq. (8) can be reduced to Eq. (9):

$$r\frac{d\sigma_r}{dr} + \sigma_r - \sigma_\theta = 0 \tag{9}$$

Eq. (9) can be integrated since σ_r and σ_θ and both functions of the radial position r. Before performing the integration consider the axial strain ε_z, in the direction of the axis of the tube. According to Hooke's Law this axial strain can be expressed as:

$$\varepsilon_z = \frac{\sigma_z - \nu(\sigma_r + \sigma_\theta)}{E} \tag{10}$$

where σ_z is the axial stress in the tube. The tube that we are considering has closed ends resulting in an axial stress uniformly distributed over the thickness of the tube in regions away from the ends of the tube. Hence, ε_z, σ_z, E, and ν are considered constants. These constants can be combined into one constant, $2C_1$. Eq. (10) is arranged to get Eq. (11)

$$(\sigma_r + \sigma_\theta) = \frac{\sigma_z - E\varepsilon_z}{\nu} = 2C_1 \tag{11}$$

Substituting and arranged Eq. (11), $\sigma_\theta = 2C_1 - \sigma_r$, into Eq. (9), results in Eq. (12)

$$r\frac{d\sigma_r}{dr} + 2\sigma_r - 2C_1 = 0 \tag{12}$$

Multiplying all terms in Eq. (12) by r and rearranging gives Eq. (13):

$$r^2\frac{d\sigma_r}{dr} + 2r\sigma_r = 2rC_1 \tag{13}$$

Consider the derivative of a product of functions u and w with respect to dr:

$$\frac{d}{dr}(uw) = u\frac{dw}{dr} + w\frac{du}{dr} \tag{14}$$

If the function $u = r^2$ and the function $w = \sigma_r$ then the following Equations, Eqs. (15) and (16), are true:

$$\frac{d}{dr}(r^2\sigma_r) = r^2\frac{d\sigma_r}{dr} + 2r\sigma_r \tag{15}$$

$$\frac{d}{dr}(r^2\sigma_r) = 2C_1 r \tag{16}$$

Integrating Eq. (16) yields:

$$r^2\sigma_r = C_1 r^2 + C_2 \tag{17}$$

where C_2 is a constant of integration. Rearranging Eq. (17) to solve for σ_r and applying Eq. (11) to solve for σ_θ results in Eqs. (18) and (19).

$$\sigma_r = C_1 + \frac{C_2}{r^2} \tag{18}$$

$$\sigma_\theta = C_1 - \frac{C_2}{r^2} \tag{19}$$

Boundary conditions can be used to determine the constants C_1 and C_2. The known boundary conditions are the radial pressures applied to the tube at the inner and outer radii of the deformed tube. The negative sign for each of the pressures corresponds to applying a compressive radial stress on the element. The boundary conditions are expressed as:

$\sigma_r = -p_w$ at $r = c$
$\sigma_r = -p_m$ at $r = d$

Using these boundary conditions in Eqs. (18) and (19) and solving for C_1 and C_2 results in Eqs. (20) and (21).

$$C_1 = \frac{p_m c^2 - p_w d^2}{c^2 - d^2} \tag{20}$$

$$C_2 = \frac{c^2 d^2 (p_w - p_m)}{c^2 - d^2} \tag{21}$$

Therefore, the final equations for the radial stress and tangential stress in an element at radius r within the thickness of the tube are given in Eqs. (22) and (23). These equations are known as Lamé's equations [45].

$$\sigma_r = \frac{p_m c^2 - p_w d^2}{c^2 - d^2} + \frac{c^2 d^2 (p_w - p_m)}{c^2 - d^2}\frac{1}{r^2} \tag{22}$$

$$\sigma_\theta = \frac{p_m c^2 - p_w d^2}{c^2 - d^2} - \frac{c^2 d^2 (p_w - p_m)}{c^2 - d^2}\frac{1}{r^2} \tag{23}$$

Consider the axial stress in the tube, σ_z. In the case of the tube-jack, the bolt inside the tube-jack resists the longitudinal expansion of the tube. Thus, the axial stress in the tube away from the ends of the tube may be assumed as zero. Therefore, Hooke's Law for the tangential stress in the tube becomes:

$$\sigma_\theta = E\varepsilon_\theta + \nu\sigma_r \tag{24}$$

Inserting Eqs. (22) and (23) into Eq. (24) yields Eq. (25).

$$\left(\frac{p_m c^2 - p_w d^2}{c^2 - d^2} - \frac{c^2 d^2 (p_w - p_m)}{c^2 - d^2}\frac{1}{r^2}\right)$$
$$= E\varepsilon_\theta + \nu\left(\frac{p_m c^2 - p_w d^2}{c^2 - d^2} + \frac{c^2 d^2 (p_w - p_m)}{c^2 - d^2}\frac{1}{r^2}\right) \tag{25}$$

At radius $r = d$, the exterior of the cylinder, $\sigma_r = -p_m$ and Eq. (25) becomes Eq. (26).

$$\left(\frac{p_m c^2 - p_w d^2}{c^2 - d^2} - \frac{c^2 (p_w - p_m)}{c^2 - d^2}\right) = E\varepsilon_\theta - \nu p_m \tag{26}$$

This equation can be rearranged to solve for the external masonry pressure, p_m, as shown in Eq. (27).

$$p_m = \frac{E\varepsilon_\theta (c^2 - d^2) + 2p_w c^2}{c^2 + d^2 + \nu(c^2 - d^2)} \tag{27}$$

The tangential strain, ε_θ, at radius $r = d$ depends on the stressed and unstressed circumference of the tube:

$$\varepsilon_\theta = \frac{2\pi d - 2\pi b}{2\pi b} = \frac{2\pi(d - b)}{2\pi b} = \frac{d - b}{b} \tag{28}$$

The radial strain, ε_r, can be determined based on the initial thickness, t_i, and final thickness, $t_f = d - c$, of the tube:

$$\varepsilon_r = \frac{t_f - t_i}{t_i} = \frac{(d - c) - (b - a)}{(b - a)} \tag{29}$$

Inserting Eq. (28) and Eq. (29) into the equation for the Poisson ratio gives Eq. (30).

$$\nu = -\frac{\varepsilon_r}{\varepsilon_\theta} = \frac{b\big(-(d - c) + (b - a)\big)}{(b - a)(d - b)} \tag{30}$$

Eq. (30) can be solved for the unknown inner radius of the deformed tube, c, as shown in Eq. (31).

$$c = \frac{\nu(d - b)(b - a)}{b} + a - b + d \tag{31}$$

Finally, Eqs. (28) and (31) can be inserted into Eq. (27) to find the external masonry pressure in terms of only the known values established at the beginning of this derivation, shown in Eq. (32).

$$p_m = \frac{E\left(\frac{d-b}{b}\right)\left(\left(\frac{\nu(d-b)(b-a)}{b} + a - b + d\right)^2 - d^2\right) + 2p_w\left(\frac{\nu(d-b)(b-a)}{b} + a - b + d\right)^2}{\left(\frac{\nu(d-b)(b-a)}{b} + a - b + d\right)^2 + d^2 + \nu\left(\left(\frac{\nu(d-b)(b-a)}{b} + a - b + d\right)^2 - d^2\right)} \quad (32)$$

According to Newton's third law, the external masonry pressure on the tube is equal in value and opposite in direction to the pressure the tube applies on the masonry, so the variable p_m will be used for this quantity as well.

The water pump applies equal pressure to all of the tube-jacks during the pressurization. The line of tube-jacks forms an equivalent flat-jack that applies pressure to the masonry mostly perpendicular to the line of the tube-jacks (see Figure 2-27 and Figure 2-28). One particular advantage of this system is that the application of the pressure at discrete intervals at each of the holes, instead of continuously as a single flat-jack does, allows the holes to be drilled and the tube-jacks inserted into nonlinear mortar joints. The non-linearity of the equivalent flat-jacks could change the direction of the applied pressure from that calculated in the equations above. The effects of placing the tube-jacks in a non-linear arrangement were not thoroughly examined in this thesis work. Further research should be done to see how much effect deviations of the tube-jacks will have on the applied pressure. Thus, this system has the potential for application in irregular masonry typologies. In addition, the flexibility of this system allows the length of the line of tube-jacks to be varied by changing the number of tube-jacks used in the test. Masonry with large stones, which could not be accurately tested with the fixed size flat-jacks, could be tested with the tube-jack system by increasing the number of tube-jacks and the length of the "equivalent flat-jack".

An estimation of the local state of stress within the masonry can be accomplished with the results from the single tube-jack test and a formula similar to the one used for flat-jack testing [2] and [31], which is presented in Eq. (33).

$$\sigma_m = k_a p_m \quad (33)$$

where: σ_m is the local state of stress in the masonry, k_a is the area correction factor, and p_m is the pressure applied to the masonry at the point when the average relative displacements are restored to zero, i.e., the state before the holes were drilled. In this work the area correction factor has been multiplied by the pressure applied to the masonry to obtain the "applied pressure," $p_{Applied}$. Thus, at the point when the average relative displacements are restored, the $p_{Applied}$ gives an estimate of the local state of stress in the masonry. Note that in Eq. (33) there is no jack calibration factor, as there is in the flat-jack test equation. This is because the properties of the tube material are taken into consideration in the calculation of the applied pressure. The area correction factor for single tube-jack tests using only one line of tube-jacks can be determined using Eq. (34).

$$k_a = \frac{A_T}{A_H} \quad (34)$$

where: A_T is the total surface area of tube-jacks in contact with and applying pressure to the masonry projected on a plane through the centroid of the tube-jacks, and A_H is the total cross-sectional area of the holes drilled in the masonry. As the flexible tubing material expands, it conforms to the contours of the hole and completely fills the circumference of the hole. Thus,

the value of A_T can be estimated by multiplying the length of the tubing material by the diameter of the hole and multiplying that value by the number of tube-jacks. The value of A_H can be calculated by multiplying the diameter by the length of each hole and then summing those values. A diagram of these cross-sectional areas is shown in Figure 2-30. This cross-section is taken through the centroid of the tube-jacks and assumes that all of the holes are in a straight joint.
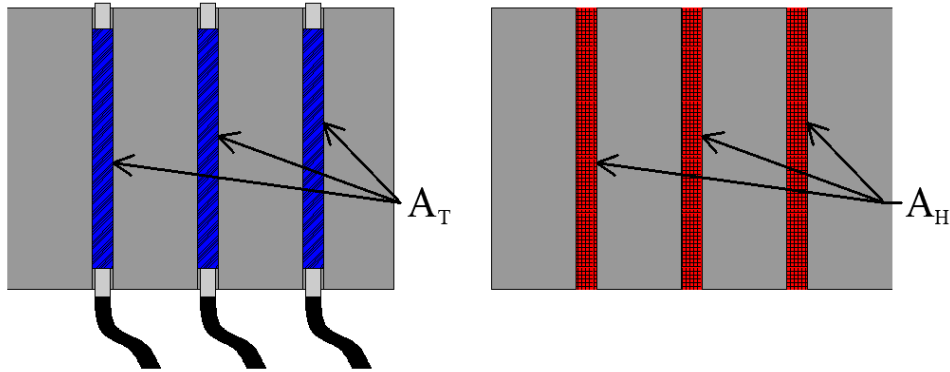
Figure 2-30 Cross-section of masonry during a single tube-jack test showing the cross-sectional area of the tube-jacks that is applying pressure to the masonry, A_T, and the cross-sectional area of the drilled holes, A_H

The area correction factor for the double tube-jack tests is determined differently and is described by Eq. (35).

$$k_a = \frac{Average(A_{T1}, A_{T2})}{A_S} \tag{35}$$

where: A_{T1} is the total surface area of the tube-jacks in the lower equivalent flat-jack that are applying pressure to the masonry projected on a plane through the centroid of the tube-jacks, A_{T2} is the total surface area of the tube-jacks in the upper equivalent flat-jack that are applying pressure to the masonry projected on a plane through the centroid of the tube-jacks, and A_S is the total cross-sectional area of the specimen between the two equivalent flat-jacks. A_{T1} and A_{T2} are determined in the same way that A_T was determined for the single tube-jack test. A_S can be calculated by multiplying the average length of the equivalent flat-jacks by the average depth of the wall.

2.3.3   Previous Development

The technique was first proposed by Ramos and Sharafi [46]. In these first studies several limitations of the traditional flat-jack test method were identified including the difficulty in using the saw to cut slots in the masonry and unwanted damage of masonry units in irregularly constructed masonry when joints are not aligned. It was shown that through the proposed tube-jack testing these limitations could be overcome by positioning the tube-jacks in locations along the mortar joint regardless of whether that joint is linear and by using a simple hand drill to create the holes for the tube-jacks. A comparison of the flat-jack test and the tube-jack test was conducted with a Finite Element model of a homogeneous wall. The results showed that the tube-jack test produced a more even stress distribution in the wall and obtained a reasonably accurate estimation of the compressive stress in the wall, thus providing a numerical validation of the method.

2.4   Conclusions

This chapter presented an overview of non-destructive test methods used to diagnose and analyze historical masonry. The many techniques discussed were categorized as mechanical tests, wave transmission tests, sampling tests, dynamic tests, and monitoring. Some tests can provide quantitative results while others provide only qualitative results about the properties of the masonry. Some are completely non-destructive, while others are considered minor-destructive or semi-destructive, requiring some repair to the masonry after testing. The focus of the chapter was in introducing the flat-jack and tube-jack tests, as these were also the focus of this thesis.

The flat-jack test method is a well-established method used to determine both the local state of stress in the masonry and also the deformability characteristics of the masonry. ASTM and RILEM standards and recommendations provide engineers with a basic understanding and procedure for the test. Numerous published resources also provide examples of how these tests have been applied to historical masonry structures. However, these applications have also revealed that issues still exist with this technique, especially when testing irregular masonry, masonry with thick mortar joints, masonry under low stress states, and masonry with units larger than typical flat-jack lengths. Difficulties have also been found in creating the slots for the flat-jack tests, applying measuring devices to irregular masonry, and in interpreting the results. Some alternative methods have been proposed by others but with little success.

The tube-jack test method is being developed at the University of Minho as an alternative to flat-jack testing. The development and testing of this method is the focus of this thesis. In this chapter the system was described, the theory behind the test was presented, and contributions from previous researchers acknowledged. It is the hope that this method will be able to solve some of the issues that the flat-jack test method faces. For example, drilling holes in mortar should create more uniform openings as compared with flat-jack slots and with less effort on the part of the operator. This method will also allow the measurement of the movement of the masonry during the drilling process, possibly reducing errors from removing and replacing measuring devices. The method also makes it possible to test the entire depth of the masonry, by drilling holes and using tube-jacks that cross the entire thickness of the wall, as opposed to testing only the exterior face of the masonry, as in the flat-jack tests. Along with measuring deeper, the test can also use a larger or small number of tube-jacks to extend the length of the test so that masonry with larger units can be tested. Finally, less damage is caused to the masonry because holes are drilled only in the mortar joints, regardless of the linearity of the joints, as in the case of irregular masonry typologies.

3. TUBE-JACK SYSTEM DEVELOPMENT

3.1 Introduction

At the beginning of this thesis work, the tube-jack test method was only an idea. The idea had been tested using computer modeling but it had not yet been made physical [46]. In order to prove the theory of the tube-jack test method, the system would need to be built and tested in a historic masonry structure. Thus, the first step in obtaining this goal was to physically develop the tube-jack system and test it in a controlled laboratory environment.

The initial design of the tube-jack system was based on the adaptation of the flat-jack test system to fit the theoretical idea. From that point onward, the development of the tube-jack system was based on the results and analysis of a progression of laboratory tests. After each test, results were analyzed, modifications to the system were made, and new tests devised to test the improved system.

This chapter starts with an explanation of how the tube-jack system was adapted from the flat-jack system and the creation of an initial set of goals for development of the system. Following this, the designs for prototypes are presented. The prototypes were tested for the first time in a small two-block masonry specimen. Questions about how the specimen was reacting to the drilling and how the tube-jacks were applying stress to the specimen were explored in a numerical model of the test. These tests revealed that confinement of the tubing material was required. This led to the development of knitted fibrous structures, or tube socks, for this purpose. Inflation tests of the tube-jacks were developed to test the confinement of the tube-jacks by the tube socks and are presented following the characterization of the tube socks. The rubber tubing material characterization is also presented at this point. The testing of the complete system in two larger walls concludes the development tests presented in this chapter. Results from these final tests led to the change in pressurization fluid from air to water. The final section presents the complete water pressure system that was used for the tube-jack testing throughout the rest of the thesis work.

3.2 Adaptation of the Flat-jack Test System and Development Goals

The tube-jack test is based on the same principles as the flat-jack test and is very similar in setup. Thus, some of the same components used in the flat-jack test method were used in the tube-jack test system or gave a basis for how to develop applicable parts. Putting together a system that combined applicable parts from the flat-jack test with several tube-jacks led to some goals for the development of the system.

Three main goals were established for the initial development. The first goal for the prototype development was to determine the best fluid for inflating and pressurizing the tube-jacks. Flat-jack testing traditionally uses oil for inflating and pressurizing the jacks, although some systems have also used water. Oil can cause damage to the masonry and is difficult to remove after the test is complete. Water is cleaner than oil but it is best not to add moisture to the masonry if it can be avoided. Thus, compressed air was chosen as the fluid for inflation and pressurization of the tube-jacks in the initial tests. The initial air pressure system included an air compressor, non-inflatable plastic hoses and quick release connectors, and an air pressure gage for measuring the pressure in the system throughout the test.

Numerical modeling in previous studies [46] indicated that the amount of initial relative displacement from drilling cylindrical holes in the masonry would be much smaller than in the case of flat-jacks. Thus, the second goal for the initial development was to determine the relative displacement magnitude caused by drilling the holes and the ability of various measurement devices to accurately record this relative displacement. It was believed that the displacements would be too small to be measured with a demountable mechanical strain gage, which is often used in flat-jack test. Thus, two measuring devices were used on the initial tests; high-precision LVDTs and a low-cost solution based on optical measurements with a handheld microscope. The possibility of using low-cost devices for tube jack testing may contribute to widening the scope of application for this technique.

Collecting the data and analyzing it during and after the testing can be performed using similar equipment to that used in flat-jack testing. A data acquisition system was used that could read output from the displacement measuring devices and the pressure within the tube-jack system. A flat-jack test computer program was modified to show the real-time measurements being taken and produce graphs for further analysis.

The one remaining component to the tube-jack system is the tube-jack. This is the component that requires the most attention and development. The third goal was to determine the type of tube material that would be both flexible and tough enough to inflate to the size of the holes and pressurize the masonry without bursting. The tube material selected would also need to allow multiple inflations without residual deformations or damage.

3.3 *Prototype Design*

Tube-jack prototypes were constructed based on the design shown in Figure 3-1a. One goal for the design of the tube-jack system was to make the system easy and efficient to use so that in-situ testing difficulties and the testing time are reduced. With this goal in mind, the initial system was designed with plastic connection tubes that could be cut to whatever lengths were necessary and plastic connectors with quick releases. The plastic connectors allowed tube-jacks to be added to the system to create a longer equivalent flat-jack or removed and replaced if they burst during a test.
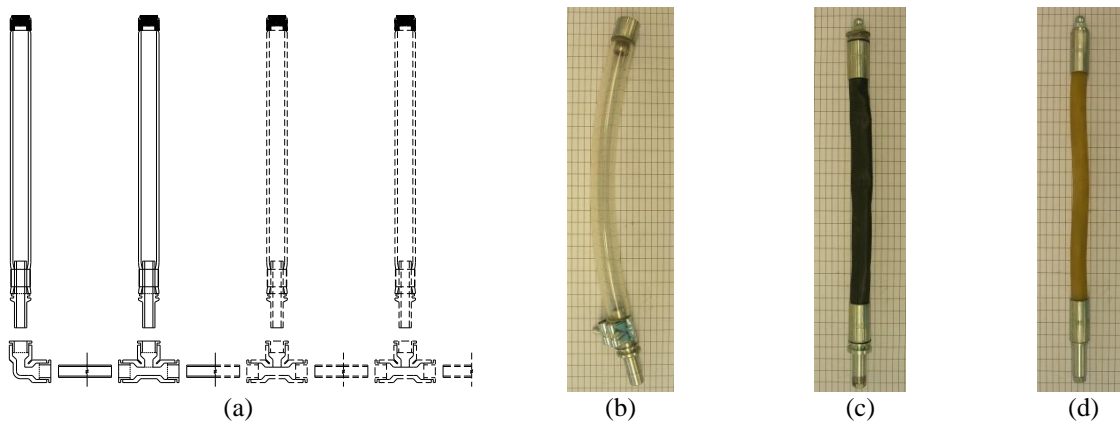
Figure 3-1 Tube-jack Prototypes: (a) Tube-jack basic design; (b) PVC tube-jacks; (c) rubber tube-jacks; and (d) latex tube-jacks

The tube-jack design consisted of a length of inflatable tubing with two metal ends clamping the ends of the tubing material. One metal end was closed off so that no fluid could pass through.

The other metal end allowed fluid to enter the tube-jack from the plastic connectors and connection tubes. Three types of tubing were used for the tube-jack prototypes: clear PVC, black rubber, and latex (see Figure 3-1b, c, and d, respectively). The diameters and thicknesses of each of the types of tubes are presented in Table 3–1.

Table 3–1 Dimensions of the tested tubing materials

Tubing Material	Material Thickness	Tube Diameter
	[mm]	[mm]
PVC	2.5	20
Rubber	0.83	14
Latex	1.8	12

The length of each of the tube-jacks was set at approximately 20 cm to match the thickness of the specimens designed for laboratory test throughout this thesis work. However, due to the different materials, the metal end fittings were of different designs for each of the prototypes. Thus, the lengths of the inflatable portions of the tubing were different for each prototype. These lengths were measured and taken into account when determining the area correction factor for each tube-jack test, as described in section 2.3.2. To ensure the stability of the tube-jack when inserting it into the hole and to prevent longitudinal expansion of the tube, a steel threaded rod with 6 mm diameter was included in the center of the rubber and latex tube-jacks.

3.4 Two-block Single Tube-Jack Tests

3.4.1 Test Specimen and Procedure

A simple two-block specimen was designed and constructed in order to test the tube-jack testing technique. The specimen consisted of two granite blocks with dimensions of 20 cm wide by 20 cm thick by 150 cm tall with a 3 cm thick mortar joint between them. The granite stones had a modulus of elasticity equal to 52.2 GPa, a Poisson ratio of 0.23, and a mass density of 2660 kg/m^3. The mortar consisted of a cement, lime, and sand mixture (1:3:16 ratio), which had a compressive strength of 1.26 MPa at 28 days. These materials were used in another work and details on the characterization of the material properties can be found in [5] and [47] for the granite and the mortar, respectively.

The two-block specimen was compressed vertically between a hydraulic hand jack and a load cell, which recorded loading throughout the test, to obtain a stress level of 0.4 MPa at the level of the mortar. Metal plates and a lower granite block were used to distribute the load. Holes for the tube-jacks were located at mid-height of the joint, horizontally centered, and had a center-to-center spacing of 75.0 mm. Two measurement techniques were used to measure the differential displacements during the test: LVDTs and a microscope imaging system. The initial test setup is shown in Figure 3-2, where the location of the LVDT and the microscope are displayed (both anchored to the top and bottom granite blocks). One LVDT was placed on the front and one on the back of the specimen. The microscope was positioned at the front. The LVDT had a total range of ±2.5 mm, and together with a 16 bit data acquisition system allowed measurements with resolution smaller than one micrometer.

The microscope-based measurement system was composed of a graduated sliding ruler, with each extremity fixed to each granite block. The microscope was held in front of the ruler

according to Figure 3-2c, thus detecting the relative displacement between the two parts of the sliding ruler. The microscope was a VEHO VMS-004D, with a magnification power of 400× and a native capturing resolution of 640 × 480 pixels. At the maximum magnification (~400×), the field of measurement is about 1.00×0.75 mm, meaning that each pixel corresponds to approximately 1.6 micrometers. To improve the sharpness of image measurement, at the area where the displacements were measured on the sliding ruler, a SIM chip from a mobile phone was placed at each ruler. The use of SIM chips was necessary due to the unevenness of the lines marked in the rulers, which were not sharp enough for the intended level of measurement precision. Also, due to the known thickness of the markers in the SIM, it was possible to apply calibration procedures at every measurement. Further details on the implementation and measurements using the microscope-based system can be found in [48].
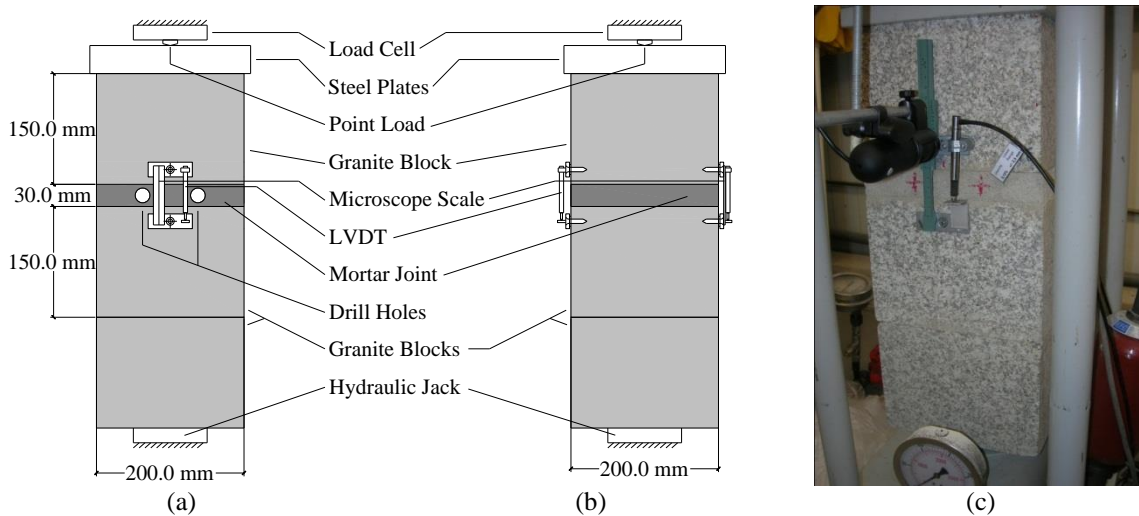
Figure 3-2 Two-block tube-jack test specimen and differential displacement measurement systems: (a) Front face; (b) Back face; and (c) photo of the test specimen

3.4.2   Experimental Results and Discussion

To begin the tests, measurements were taken by the LVDTs and the microscope measurement system and then the two holes were marked on the mortar joint and drilled completely through the thickness of the joint (Figure 3-3a). The diameter of the drill bit used for drilling was 20 mm. This drill bit created holes slightly larger than 20 mm and large enough to insert the tube-jacks. Drilling the two holes in the mortar joint between the two granite blocks caused the two blocks to move together. Negative relative displacements recorded and presented for all of the measuring devices in this thesis represent a contraction of the masonry or a movement together. Positive relative displacements represent an expansion of the masonry or a movement apart. Figure 3-4 b shows the relative displacement of LVDTs 1 and 2 during the pressurization of the tube-jacks. The relative displacement shown at zero pressure is the relative displacement due to drilling the holes in the specimen. The difference in relative displacement between the front and back of the specimen, approximately 0.7 micrometers, was significant considering the average relative displacement of −1.8 micrometers. Thus, it was hypothesized that the specimen might have bent during the hole drilling.

(a) (b)
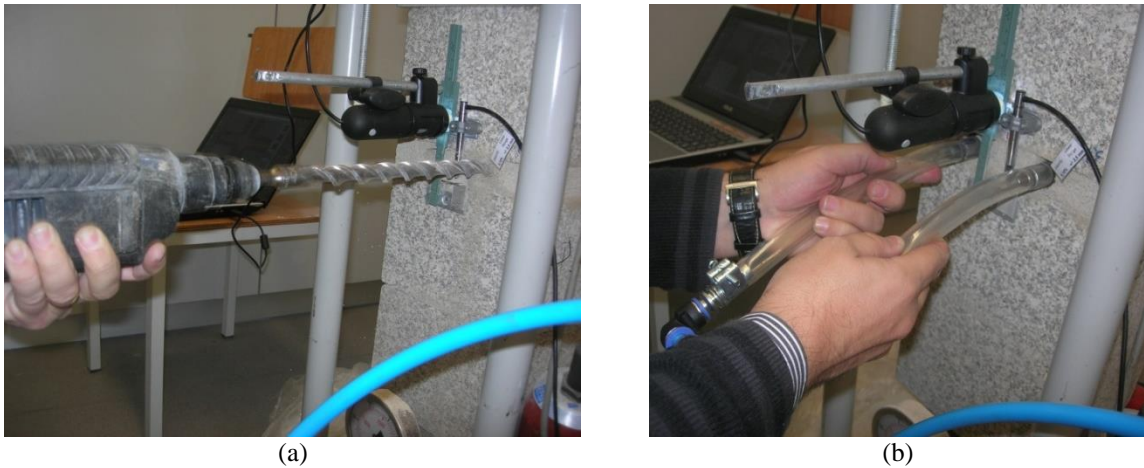
Figure 3-3 PVC tube-jack test: (a) drilling holes in the mortar joint; and (b) inserting the PVC tube-jacks

The first tube-jack prototype tested was the PVC tube-jack. Following the drilling, the PVC tube-jacks were inserted into the holes and pressurized (Figure 3-3b). Air pressurization for this test was as simple as turning the valve on the pressure gage to control the pressure, as shown in Figure 3-4 a. The air pressure was measured and recorded with a pressure transducer connected to the data acquisition system.

The results of the pressurizing the PVC tube-jacks in the holes are shown in Figure 3-4 b. The length of the inflatable portion of the PVC tubing was the same as the depth of the specimen, resulting in no area correction factor being applied to the results. Because these initial tests were performed at the beginning of the thesis work, the tube-jack test theory had not yet been developed as shown in section 2.3.2. Therefore, the pressure presented in these initial results is the air pressure recorded by the pressure transducer without correction factors applied.

(a) (b)
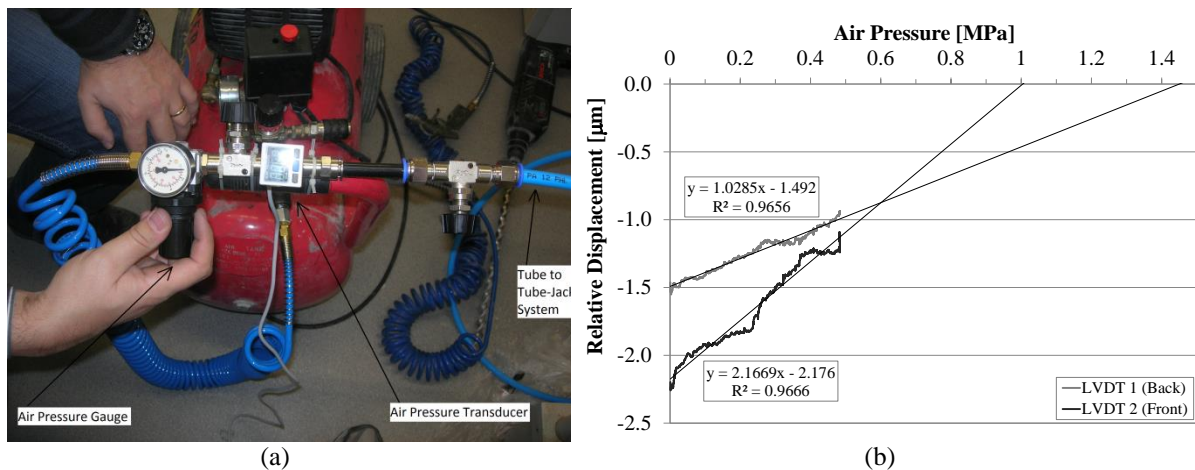
Figure 3-4 PVC Tube-jack test pressurization: (a) photo of the air pressurization system; and (b) pressure versus relative displacement results

The positive trend in the relative displacements as the air pressure was increased indicates that the PVC tube-jacks were successful in expanding to the size of the drilled holes and pressurizing the masonry. However the increase in relative displacement was at a low rate, suggesting the inflexibility of the PVC material. The maximum air pressure allowed by the air compressor system was reached before the relative displacement was returned to zero. The estimated pressure required to restore the displacement to zero was greater than 1.3 MPa, much larger

than the induced stress in the masonry, 0.4 MPa. Due to the inflexibility of the PVC tube-jacks, this type of tubing wasn't used for further testing.

The microscope imaging system was used to check the relative displacements found using the LVDTs. A good correlation was found between the two systems (Figure 3-5) considering the level of resolution allowed by the microscope (i.e. approximately 1.6 micrometers). However, in view of the microscope's resolution, the level of precision was not considered adequate for this application or other applications that involve displacements smaller than 10 micrometers.
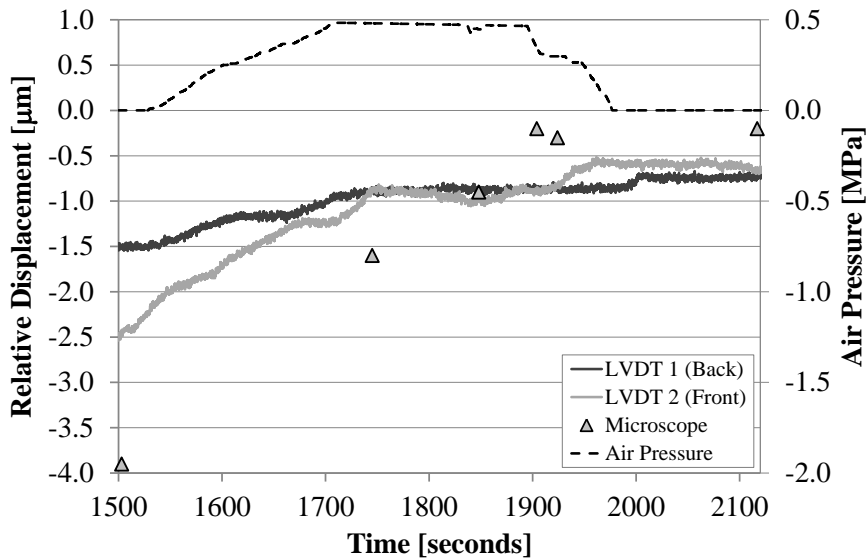
Figure 3-5 Comparison between the LVDT measurements, the microscope measurements and the air pressure during the pressurization

An issue related to the accuracy of the LVDT measurements was also encountered during this test. The LVDTs were fixed to the center plates via hot glue shortly before the test was conducted. It was found that the LVDT most recently fixed to the plates was observed to be moving even when no pressure was being applied by the tube-jacks to the masonry, as shown in Figure 3-5 . This movement was caused by creep in the mounting glue. In tests where larger displacements are recorded, this movement would not be noticeable. Since the measured displacements are so small in the tube-jack test, this creep has an impact on the accuracy of the results. Thus, it was determined that either the LVDT devices must be attached further in advance with the glue or they must be attached in another way.

A second trial was performed with the rubber tube-jack prototypes. Additional LVDTs were used in this second test on the edges of the specimen (Figure 3-6). The purpose of these LVDTs was to determine if the specimen was bending during the test, as was hypothesized in the PVC tube-jack test. The LVDTs were attached either to the fastening plate as in the previous test or directly to the granite stones using hot glue. The LVDTs were attached one day in advance to ensure that they were well secured to the specimen and no creep would occur in the glue. This strategy produced more reliable LVDT measurements with no observable creep movements during the test.
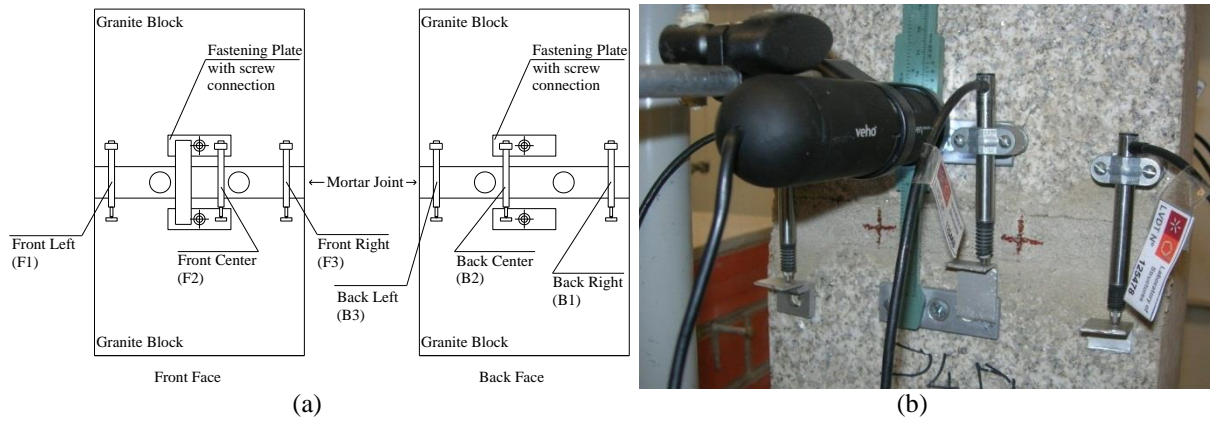
Figure 3-6 Second trial setup: (a) Schematic of LVDT locations; and (b) front view of the specimen with the measurement devices

The relative displacement of the masonry, as recorded by the LVDTs, during the drilling of the two holes is shown in Figure 3-7 . During the drilling of each of the holes, the pressure from the drill caused bending in the specimen, positive relative displacements on the back of the specimen and negative relative displacements on the front of the specimen. This can be most clearly seen during the drilling of the right hole. After the drilling was complete, only the LVDTs on the back center and back right side of the specimen show negative displacement or a closing of the joint, indicating the stress level was not equal over the horizontal cross-section of the specimen. Due to these issues, it was concluded that further testing would need to be done on larger specimens.
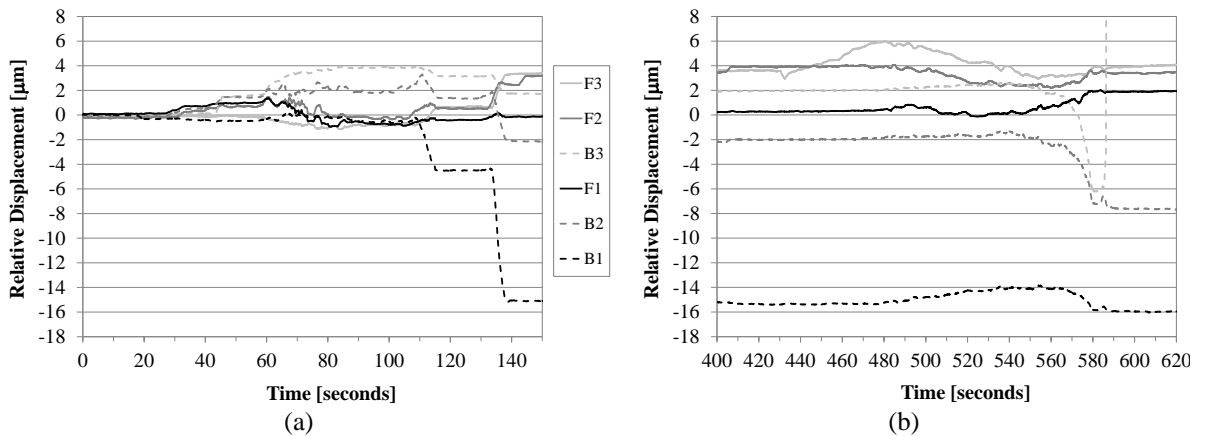
Figure 3-7 Relative displacement during drilling for the rubber tube-jack test: (a) left hole; and (b) right hole

Because the specimen was only the width of one granite unit, there was no horizontal confinement of the mortar in the joint. Therefore, when the drill broke through to the back of the specimen during drilling of the second hole, the pressure from the drill caused two chunks of mortar to break free from the mortar layer at the back of the specimen, one chunk in between the holes and a second at the back left side. The chunk on the back left side hit LVDT B3 so that it was no longer useful (Figure 3-8 a). The missing mortar on the back left side of the mortar joint had an impact on the pressurization of the rubber tube-jacks during the test. The test was cut short when one of the tubes burst at a pressure of just 0.282 MPa due to the lack of confinement in this location (Figure 3-8 b).

(a)   (b)

Figure 3-8 Second trial issues: (a) mortar breaking out on the back of the specimen; and (b) lack of confinement of the tube-jack leading to rupture

The overall movement of the specimen was observed by averaging the measurements recorded from five of the LVDTs, LVDT B3 was not considered. The continued observation of the behavior of the specimen throughout each of the phases of the test is shown in Figure 3-9 a. Measuring the movement of the masonry is not be possible with LVDTs during a flat-jack test since measuring devices must be removed from the surface of the masonry during the creation of the flat-jack slot. Therefore, this continuous measurement is a significant advantage of tube-jack testing.
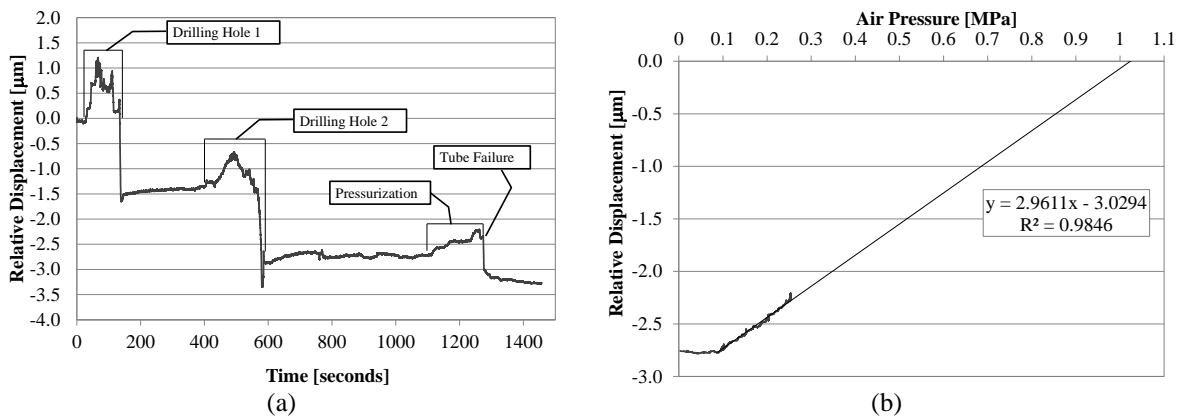
Figure 3-9 Average relative displacement: (a) throughout the stages of the test; and (b) versus air pressure

The results of the relative displacement versus the air pressure are presented in Figure 3-9 b. As in the PVC tube-jack test, no correction factors were applied in this test and the air pressure presented is the pressure recorded directly from the pressure transducer. The rubber tube-jacks performed slightly better than the PVC tube-jacks. The rubber tube-jacks inflated to the size of the holes with less than 0.1 MPa of pressure and had a higher rate of displacement recovery, as pressure was increased. However, the rubber tube-jacks were also unable to return the displacements to zero. It was estimated that an air pressure of approximately 1.0 MPa would be required to return the displacements to zero.

Two conclusions were drawn from these results. First, in order to have a more uniform distribution of loads and a more representative specimen, a larger masonry specimen (a wall) would be necessary for the prototype tests. It was decided not to repeat the test with other tubing materials in the same type of specimen. Second, if the rubber tube-jacks are confined in some way to prevent them from bursting, where voids are present in the masonry, this tube-jack prototype might be successful. Additional details and findings from the initial prototype trials can be found elsewhere [49].

3.4.3 Numerical Model Construction

A numerical model of the two-block test specimen was constructed in the Finite Element Modeling program DIANA [50]. The purpose of the model was to analyze several aspects of the initial tube-jack tests, to get an idea if this two-block test was representative of a larger masonry specimen test, and to analyze the horizontal confinement of the mortar joint. A two dimensional model was constructed with the dimensions described previously in section 3.4.1. The base of the bottom block was fixed in both the horizontal and vertical directions, while all other edges were left free to move (Figure 3-10 a). A vertical pressure load of 0.40 MPa was applied along the top surface of the top block. A radial pressure load was applied in an outward direction on the faces of the elements surrounding the tube-jack hole elements. Four sided plane stress elements with eight nodes were used to mesh the model. The material properties used for the granite blocks were the same as presented in section 3.4.1 and all material properties were kept linear in the analysis. The mortar was considered to have a modulus of elasticity equal to 1 GPa, a Poisson ratio equal to 0.20 and a mass density equal to 1800 kg/m^3. Reference points above and below the tube-jacks were selected to record the displacements throughout each step of the analysis (Figure 3-10 b).
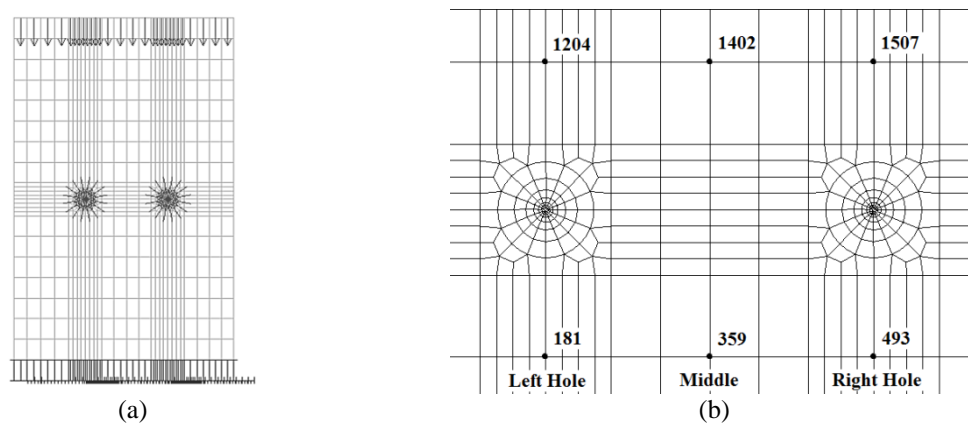
Figure 3-10 Two-Block Specimen Model: (a) Loads and boundary conditions; and (b) Reference Points

To observe the different stages of the tube-jack test, a phased analysis was conducted. The four phases were: (1) after applying the vertical and gravitational loads, (2) after removing the elements constituting the first (left) tube-jack hole which represented the point in time when the hole had been completely drilled, (3) after removing the elements of the second (right) tube-jack hole, and (4) after introducing a radial pressure load to the edges of the elements surrounding the tube-jack hole elements, which represents the pressurization of the tube-jacks.

3.4.4 Numerical Model Analysis and Discussion

Several aspects of the tube-jack test in the two-block specimen were examined in the numerical analysis. The first aspect was the influence of drilling one hole before the other as opposed to drilling both holes at the same time. This was studied by observing the results in the second phase versus the third phase of the analysis. Bending of the specimen was observed after the left hole elements were removed in the second phase and that side of the specimen settled under the applied loads (Figure 3-11 a).

(a)   (b)
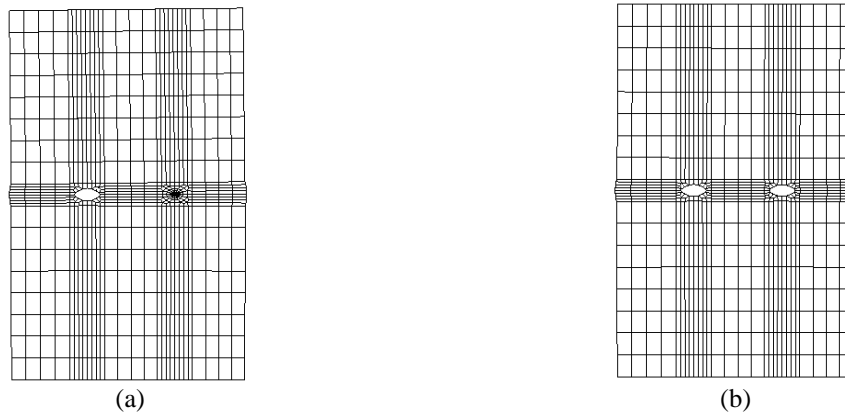
Figure 3-11 Deformed shapes after drilling (deformation factor equal to 800): (a) left hole; and (b) both holes.

The bending of the specimen after drilling the first hole is similar to the bending behavior observed in the experimental results. The difference occurs when the second hole is drilled. In the experimental specimen, the settlement on the right side of the specimen did not equal that of the left side, as it did in the numerical simulation (Figure 3-11 b). This could be because, after the first settlement, the experimental specimen could have shifted causing a redistribution of stresses and an eccentricity in the loading. The experimental results also indicated a bending of the specimen from front to back during the drilling process. A three dimensional model, out of the scope of this work, would be required to study the front to back bending of the specimen.

The initial displacements, or reduction in distance between the reference points above and below the mortar joint, can also be compared to the relative displacements found in the experimental testing. The initial displacements of the reference points were −2.86 μm over the center line of the left hole, −2.85 μm at the center line between the two holes, and −3.02 μm at the center line of the right hole. These displacements are very close to the initial displacements found in the experimental tests, which were between −1.50 and −3.00 μm for the first test (Figure 3-4 b) and an average of about −2.75 μm for the second test (Figure 3-9 b).

The next aspect of the test studied was the pressurization of the holes. In the numerical model, the pressure load was applied on all of the surfaces of the holes equally. Thus, the area correction factor for the model is considered to be equal to one, the same as in the initial tests. Since the numerical model does not model the tubing material inside the holes, the radial pressure applied to the edges of the holes represents the pressure applied by the tube-jack on the masonry. The pressure presented in the initial test results was the air pressure inside of the tube-jack system. Therefore, it was difficult to directly compare the air pressure results from the experimental tests with the pressure applied in the numerical models. Considering that the tubing material will resist the inflation of the tube, the air pressure will be higher than the pressure applied by the tube-jacks on the masonry at the point where the relative displacements caused by drilling the holes have been restored to zero.

Ideally, the pressure applied by the tube-jacks on the masonry that restores the masonry to its original position, the restoring pressure, is the estimated state of stress in the masonry for that tube-jack test. In this simple numerical model, the restoring pressure, or the estimated state of stress, should equal the pressure applied to the top of the specimen, if the weights of the materials are not considered in the model. The numerical results showed that the pressure applied by the tube-jacks on the masonry that was required to restore the specimen to its original position, as defined by the distances between the reference points, was very near to the applied vertical load. However, it did not exactly equal this vertical load and was influenced by the

location of the reference points. The restoring pressure, about 0.39 MPa (see Figure 3-12), was slightly less than the applied load for the middle reference line. Even though the difference between the restoring pressure and the applied pressure is only 0.01 MPa and is unlikely to be observable in experimental results, the causes for the difference were explored further.
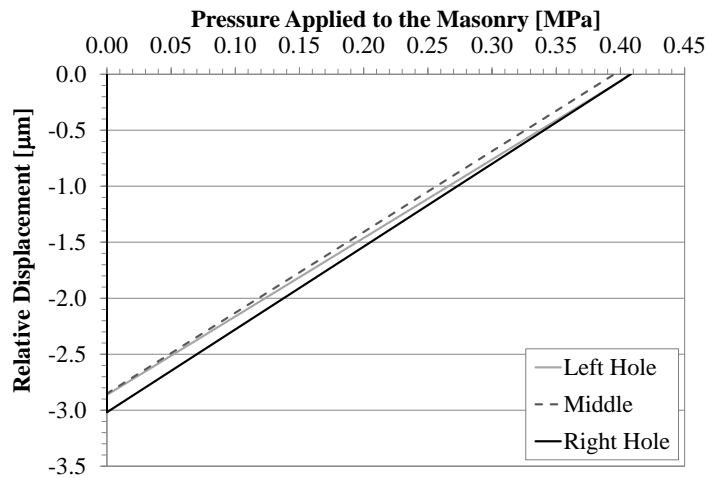
Figure 3-12 Relative displacements of reference points at the centerline of the left and right holes and midway between the holes during pressurization in the two-block finite element model

Horizontal stresses in the specimen were found to be the main contributing factor in the discrepancy. When the specimen was loaded vertically, the granite stones and the mortar expanded horizontally by different amounts due to differences in their Young's Modulus values and Poisson coefficients. The friction and bond between the granite and the mortar prevented the mortar from expanding at the interface; however the edges of the mortar layer were able to expand outward. Since the mortar in the center of the specimen was unable to expand, horizontal compression stresses occur (Figure 3-13 a) leading to a biaxial compression state within the mortar. When the holes were drilled in the mortar layer, stresses were relieved resulting in the closing of the holes both vertically and horizontally (Figure 3-13 b). Vertical stresses remained much higher than the horizontal stress, so the vertical deformation was much larger than the horizontal deformation.

(a)   (b)
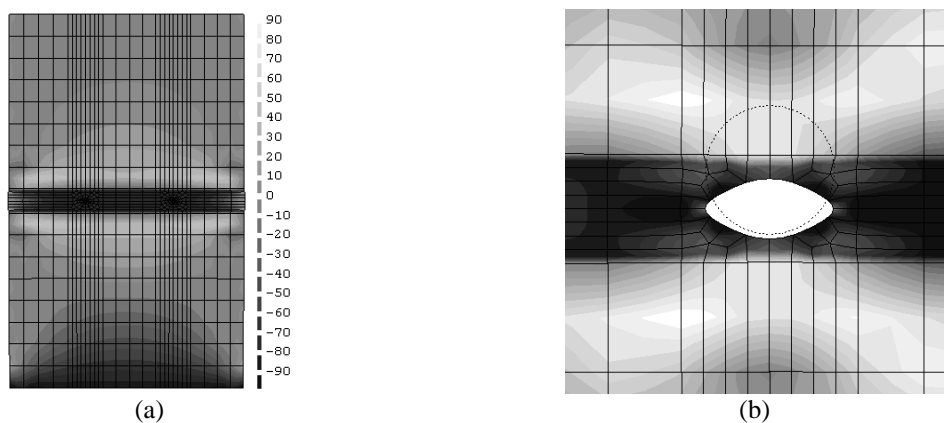
Figure 3-13 Horizontal stresses (kPa) in the two-block specimen: (a) under vertical load; and (b) surrounding the holes after drilling (deformation magnification factor equal to 800)

When the tube-jacks were inserted into the holes and pressurized, the horizontal pressure applied was equal to the vertical pressure. Since the horizontal closing of the holes was much smaller than the vertical closing, the horizontal relative displacements were recovered much sooner than the vertical relative displacements. Once the horizontal relative displacements were

restored, further pressurization of the tubes created larger horizontal compression stresses in the middle of the mortar joint and horizontal tensile stresses in the mortar above and below the hole (Figure 3-14). Since the horizontal expansion of the mortar was confined by the shear stresses between the mortar and granite, the only way for compression stresses to be relieved was in vertical expansion of the mortar layer. Hence, the horizontal compression of the mortar produced vertical expansion of the masonry in addition to the vertical expansion caused by the vertical pressure on the holes. Thus, the pressure required to restore the vertical relative displacements between the holes is slightly less than the stress state in the masonry.
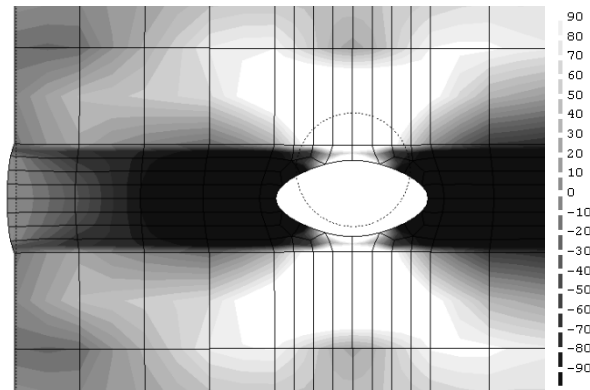
Figure 3-14 Horizontal stresses (kPa) around the left hole when applied vertical pressure in the hole equals the vertical stress applied to the top of the two-block specimen (deformation magnification factor equal to 800)

Given the influence of horizontal stresses on the required restoring pressure, the confinement of the specimen was studied. In larger masonry specimens, the masonry surrounding the test area will create a horizontal confinement, which limits the horizontal expansion of the masonry during the pressurization. The lack of confinement was evident in the rubber tube-jack test when the drill was able to break apart some of the mortar and when pressurization of the tube-jack further expelled this mortar (Figure 3-8). To see the influence of confinement in the numerical analysis additional boundary conditions were created so that the horizontal edges of the specimen could not move horizontally. The result was a decrease in the restoring pressure, 0.39 MPa, by 1.3%. Using this confined specimen to predict the behavior of a larger masonry specimen, an estimated factor of about 1.04 should be applied to the tube-jack pressure in order to obtain the actual stress level in the wall. Since this value is so close to one, it is acceptable to neglect it. Additional modeling of the tube-jack tests performed in the laboratory walls was performed in a later phase of this thesis work and is presented in Chapter 6.
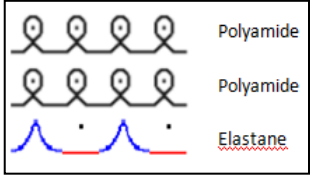
3.5   *Tubular Knitted Fibrous Structures*

One of the conclusions of the initial tube-jack prototype tests in the two-block specimen was that the tubing of the tube-jacks needs to be confined in some way so that when it expands within the masonry it does not burst. One possible solution to the tube confinement issue is a tubular knitted fibrous structure placed over the length of the tube section of the tube-jack. Three types of tubular knitted fabrics were produced, tested and analyzed. One of the desired characteristics for the tube-jack, and a goal for their development, is unchanging elastic properties after multiple uses. Thus, the cyclic tensile behavior of the tubular knitted fabrics needed to be tested. The characterization of the tubular knitted fabrics and the results of the tensile tests are presented in the following subsections.

3.5.1 Characterization of Tubular Knitted Fabrics

Knitted fibrous structures, designated by labels L1, L3 and L4, were produced using 95% polyamide (ground structure) and 5% polyamide covered elastane yarns (inlays) in a single jersey pattern [51]. Table 3–2 presents the dimensional properties of the three types of tubular knitted fibrous structures produced.

Table 3–2: Characteristics of the produced jersey fabrics

Sample	Tube knitted fabrics		L1	L3	L4	
Pattern				Jersey		
Yarns	Elastane yarn	Core Elastane (dtex)		285		
		Cover Polyamide		44/13		
	Polyamide microfiber (Den)			70/68x2		
Dimensional Properties	Loop length (cm)		0,47	0,48	0,47	
	Cover factor (K)		9,0	8,5	8,7	

3.5.2 Cyclic Tensile Behaviour of Tubular Knitted Fibrous Structures

The tensile behavior of the tubular fibrous fabrics has been evaluated under cyclic testing using a HOUSFIELD H10KS universal testing machine. Tests were conducted in the course wise direction, according to the NP EN ISO 13934-2 standard, using the Grab method. The cyclic tests were conducted by performing 10 cycles up to 25 mm in elongation. Figure 3-15 shows the test set-up and the results obtained. The results show that the knitted fibrous structures selected for this application are able to recover the deformations provided by the load applied. In this way, these materials might be used several times without losing their elastic performance, fitting the requirement of the application.

(a)   (b)   (c)
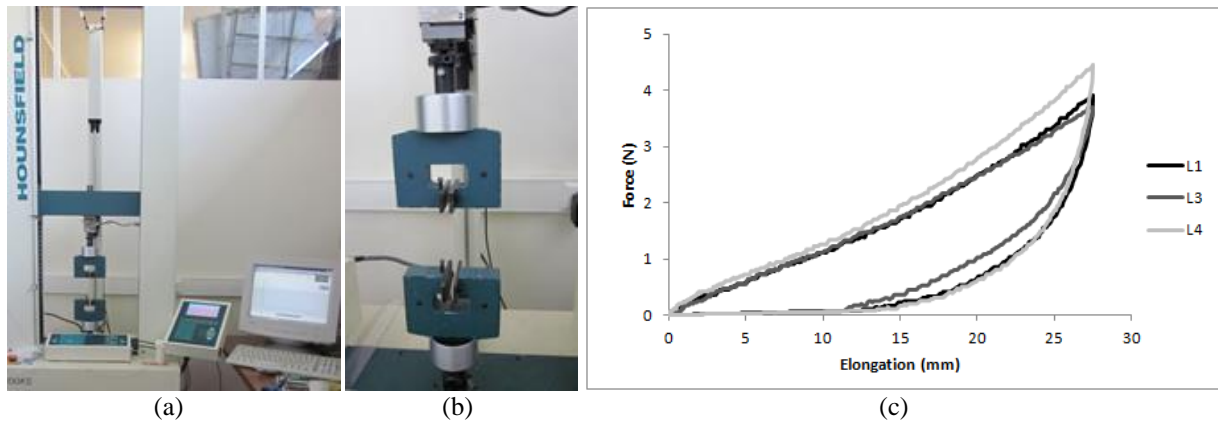
Figure 3-15 Tubular knitted fibrous structure cyclic testing: (a) complete test setup; (b) grips used for testing; and (c) test results for the 1st cycle

3.6 Tube Inflation Tests

Performing two-block specimen tests and complete tube-jack tests requires a significant amount of time and preparation constructing the specimens, setting up the test and placing the measuring devices, performing the test and analyzing the data. In addition, only one test can be performed in each test specimen. Thus, to test the various tube-jack prototypes numerous times and analyze the inflation process without requiring numerous specimens, inflation tests were performed. Confined tests were performed inside a clear pipe to see how the tube inflated to fill

the pipe. Unconfined tests were performed to see how the tubing material and knitted fibrous structure deformed when unconfined.

3.6.1   Clear Pipe Inflation Tests

A simple test was devised to see how the tube-jacks were inflating inside the holes in the masonry. The tube-jacks were inserted into a clear pipe with a diameter of 22 mm (slightly larger than the tube-jack diameters) and then slowly inflated and deflated. This test was performed with both the rubber and latex tube-jacks to determine if these materials would be adequate for further tube-jack tests. The PVC tube-jacks were not tested because of the poor results obtained when testing them in the two-block specimen.

During the inflation test, the tube-jacks were inflated in increments of 0.025 MPa to observe the behavior of the tube-jack tube's expansion to the size of the clear tube, the contact area between the tube-jack and the clear pipe, and the maximum pressure. In both the rubber and latex tube-jack inflation tests the tubes expanded to completely fill the inner diameter of the clear tube with no gaps or voids (Figure 3-16 a and b). The tubes proceeded to apply pressure on the clear tube and were able to reach an internal air pressure of 0.6 MPa without bursting (air compressor maximum pressure). Near the ends of the tubes, the tube material was seen to expand out over the metal fittings (Figure 3-16 c). This was more evident in the latex tube-jack and was a result of the latex material's greater longitudinal expansion. This means that the ends of the tubes are potential areas for rupture and strengthening of these areas may be necessary. These simple tests showed that if the tube-jacks could be adequately confined, while still allowing small radial expansions, they could be used to apply pressure to the inside of the drilled holes in the masonry joint and perform the jacking task for which they are intended.

(a)

(b)   (c)
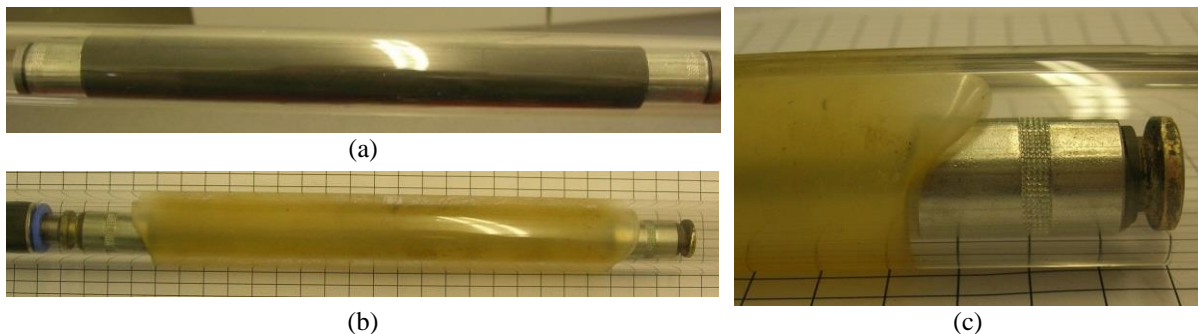
Figure 3-16 Clear Tube Inflation Tests: (a) rubber tube-jack; (b) latex tube-jack; and (c) longitudinal expansion over end fittings

3.6.2   Unconfined Inflation Tests with the Tubular Knitted Fabrics

Three phases of unconfined inflation tests of the tube-jacks using the tubular knitted fabrics were performed. In each phase, the design of the tubular knitted fabric and the tube-jack as a whole was refined and improved based on the qualitative and quantitative results of the inflation tests.

In the first phase, the objective was to determine qualitatively what type of fabric should be used for the tubular knitted fabrics. Two fabrics were tested, a black fabric and a white fabric. The tubular knitted fabric was simply slipped over the tubing material of the tube-jack, similar to the way a sock is put on. Therefore, "socks" or "tube socks" were used as shortened terms for the tubular knitted fibrous structures throughout the rest of the thesis work. The tube-jacks were inflated with air using the same air pressure system used in the two-block single tube-jack

tests in section 3.4 in intervals of 0.025 MPa. Photos were taken of the specimen at each pressure interval. In order to compare the size of the tube between pressure intervals and between different tests, a grid, with lines spaced 5 mm vertically and 10 mm horizontally, was placed behind the tube-jack.

The black sock was tested on both the rubber tube-jack and latex tube-jack. In the test with the rubber tube-jack, the maximum air pressure obtained was only 0.2 MPa when the tube ruptured. The portion of the black sock that was over the tubing stretched out during the test and was not restored to its original shape and elasticity after the test. It was also observed that the rubber tubing expanded the most at the end of the tube, expanding over the metal end fitting, which is where the rupture occurred (Figure 3-17 a and b).

| (a) | (b) |
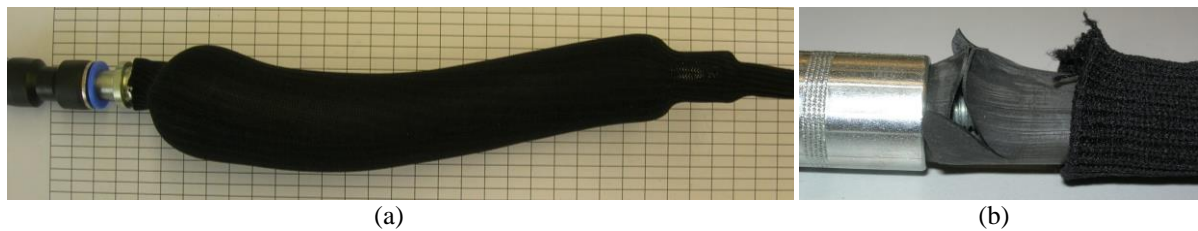
Figure 3-17 Phase one unconfined inflation test with the rubber tube-jack and black sock: (a) deformation of the tube-jack and sock during the test; and (b) rupture of the rubber near the metal end fitting

When the latex tube-jack was inflated inside another black sock, the maximum pressure obtained was only slightly higher than with the rubber tube-jack, 0.25 MPa. The sock again stretched out and was no longer usable. The sock allowed for too much expansion of the latex tube, allowing the latex tube to twist as it tried to elongate as shown in Figure 3-18 a. The latex tube also ruptured near the metal end fitting (Figure 3-18 b).Due to the issues with the black sock stretching out after each use and allowing too much expansion of the tubes, use of the black sock was discontinued and no analysis of its characteristics were performed.

| (a) | (b) |
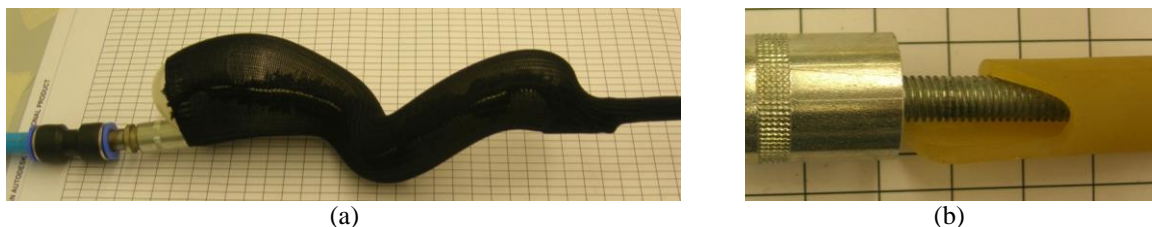
Figure 3-18 Phase one unconfined inflation test with the latex tube-jack and black sock: (a) deformation of the tube and sock during the test; and (b) rupture of the latex near the metal end fitting

The final test of this first phase of unconfined inflation tests was using the rubber tube-jack with the white sock. The white sock was able to control the inflation of the rubber tube better than the black sock, as shown in the photo of the tube-jack at the maximum pressure in Figure 3-19 a. The maximum pressure obtained with this test was the highest yet, 0.3 MPa. The tube-jack failed by the rubber pulling out from the metal end fitting (Figure 3-19 b). It was decided that this type of fabric would be used for the next phases of testing and the characterization of the fabric was undertaken as previously presented in section 3.5.
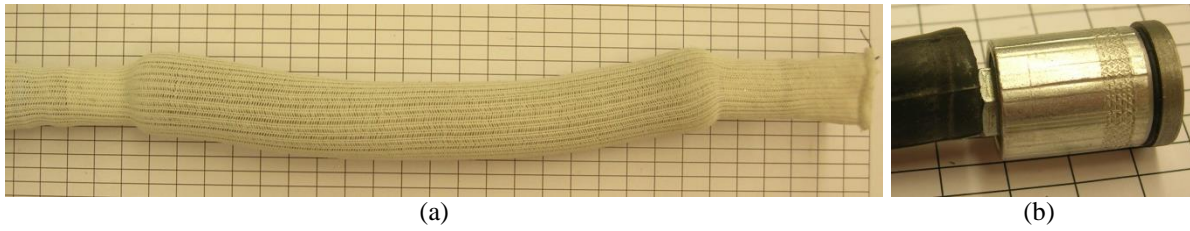
Figure 3-19 Phase one unconfined inflation test with the rubber tube-jack and white sock: (a) deformation of the tube and sock during the test; and (b) failure mode of the tube-jack

The objective of the second phase of unconfined inflation tests was to determine the best size, in terms of circumference, for the tube sock. In addition to the size, this phase also started to examine which of the three fabrics characterized in section 3.5 would work the best. The tests in this phase were performed in the same way as the tests in the first phase, except that some tests were not performed to failure and the tube-jack and sock combination was tested a second time. Based on the grid placed behind the specimens, the photos were scaled and several measurements were made along the length of each specimen to determine the maximum diameters for each test. The location of the failure along the length of the tube and the material observed to have failed first were also recorded. The results of the second phase of unconfined inflation tests are presented in Table 3–3.

Table 3–3 Results of the second phase of unconfined inflation tests

Tube Type	Sock Size [cm]	Fabric	Usage	Max Diameter [mm]	Max Pressure [Mpa]	Failure location	Failure
Latex	5	L1	1	30	0.600	none	none
Latex	5	L1	2	30	0.575	center	sock
Latex	6	L4	1	35	0.500	none	none
Rubber	5	L3	1	41	0.400	end	tube
Rubber	6	L3	1	41	0.250	end	tube and sock
Rubber	6	L1	1	38	0.425	none	none
Rubber	6	L1	2	40	0.425	end	tube

The results of the second phase of unconfined inflation tests show that in the tests of the latex tube-jacks, the smaller sock with a 5 cm circumference was able to obtain the highest maximum pressure before rupture. In the tests of the rubber tube-jacks, the 5 cm sock with fabric L3 obtained nearly as high of a maximum pressure as the 6 cm sock with fabric L1. Therefore, for the next phase of testing, it was decided that the socks should be made with a circumference of 5 cm. The failures of the tube-jacks during this phase of testing showed that, most of the time, the sock would not confine the tubing material at the ends of the tube-jack and it would expand over the metal end fittings causing it to rupture in this location before the failure of the sock.

To confine the ends of the tubing as well as the center of the tube, the tube socks were incorporated into the design of the tube-jack prototypes for the third phase of unconfined inflation tests. Socks were clamped with the tubing material inside the metal end fittings. The three fabric types and two tubing materials (rubber and latex) were tested in this phase. One prototype was made for each combination of fabric sock and tubing material, resulting in six total specimens. In this phase of testing, all of the inflation tests were performed until failure. The results of the inflation tests are shown in Table 3–4.

Table 3–4 Results of the third phase of unconfined inflation tests

Tube Type	Fabric	Max Diameter [mm]	Max Pressure [MPa]	Failure Location	Failure
Rubber	L1	35.7	0.550	right middle	sock
Rubber	L3	36.0	0.550	left middle	sock
Rubber	L4	39.5	0.525	left middle	sock
Latex	L1	35.4	0.575	right middle	sock
Latex	L3	38.8	0.600	left middle	sock
Latex	L4	38.0	0.595	right middle	sock

In comparing the latex tube-jack inflation results with the rubber tube-jack inflation results, the latex tube-jacks were able to sustain higher pressures before bursting. The rubber tube-jacks were able to reach pressures of at least 0.525 MPa, an improvement of at least 0.1 MPa from tests in the second round of testing. The latex tube-jacks were able to reach pressures of at least 0.575 MPa, as high as or higher than in previous tests. All of the specimens' maximum diameters were between 35 and 40 mm with no notable difference between the rubber tube-jacks and the latex tube-jacks. Smaller maximum diameters were observed in the tests with fabric L1. However, a smaller maximum diameter did not necessarily result in a higher maximum pressure. No correlation between the fabric type and the maximum pressure could be made based on the results.

The incorporation of the sock into the end fittings was successful in confining the tube material at the ends of the tube-jack and preventing it from longitudinally expanding over the ends of the fittings (Figure 3-20 a). The locations of the failures occurred closer to the center of the tube because the ends of the tube-jack were not overstressed by longitudinal expansion (Figure 3-20 b). As can be seen by the observed failure type, the failure was always caused by the failure of the fabric sock first. Following the failure of the sock, the tubing material was no longer confined and expanded through the hole in the sock until it also failed. Failure of the fabric sock led to almost immediate failure of the tube.

(a)   (b)
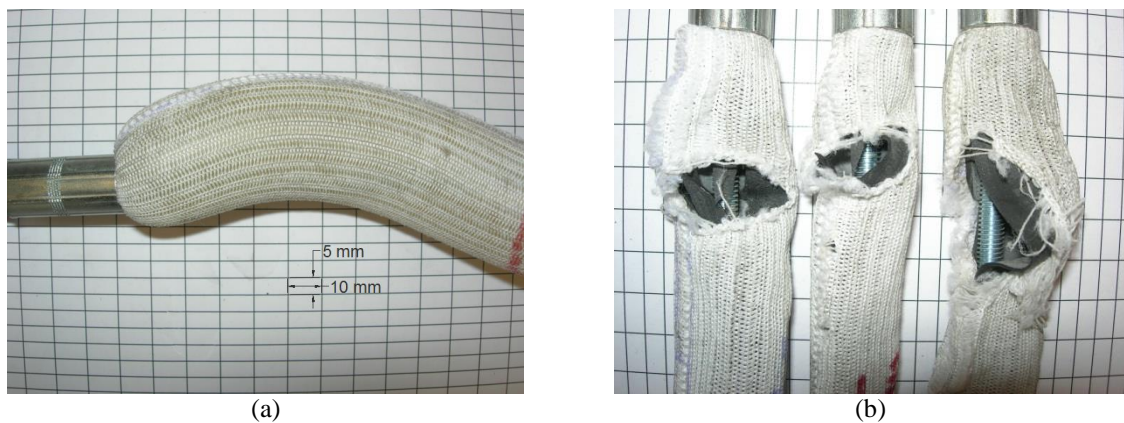
Figure 3-20 Phase 3 Tube knitted fabrics Tests: (a) Tube knitted fabrics prevention of longitudinal expansion of metal end fittings; and (b) Tube knitted fabrics failure locations for rubber tube-jacks

To more closely study the rate of expansion of the tube-jacks throughout the inflation process, photos taken during the tests were analyzed. Four points were identified along the length of the tube and the diameter measured at each of these points. The average of these diameters was used to develop curves for the pressure versus diameter relationship, shown in Figure 3-21 .
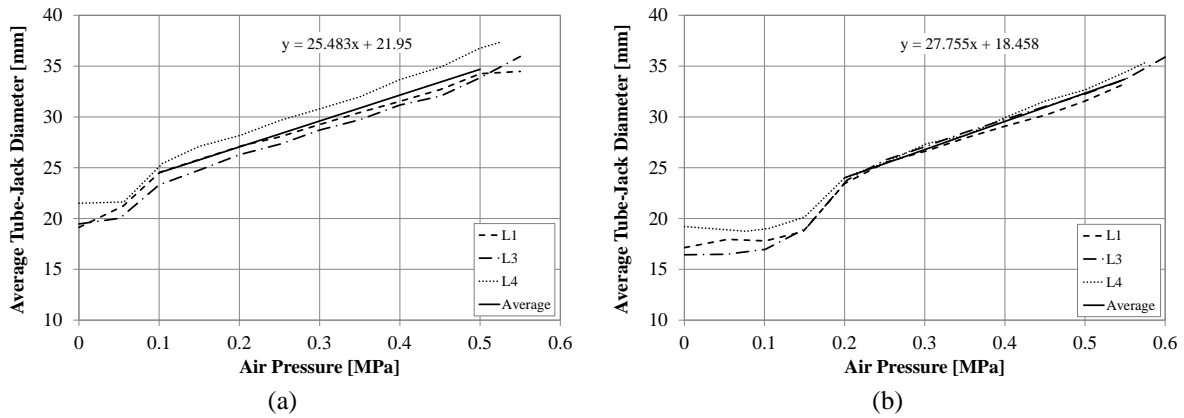
Figure 3-21 Tubular knitted fabrics test: Inflation diameter versus pressure relationship for the (a) rubber tube-jacks; and (b) latex tube-jacks

The first observation from these results is that there seems to be three phases of inflation. In the first phase, the diameter of the tube does not change much. In this pressure range, air is filling the tube and starting to induce pressure on the walls of the tube. There is a distinct point marking the beginning of the second phase where the pressure causes the tube walls to start to deform. This point is different for the two materials: between 0.05 and 0.10 MPa for the rubber tube (Figure 3-21 a) and between 0.15 and 0.20 MPa for the latex tube (Figure 3-21 b). The lower pressure required to inflate the rubber tube-jack and begin its expansion is an advantage of using the rubber over the latex. The rubber tube will inflate to the size of the hole in the masonry at a lower pressure and begin pressurizing the masonry at a lower pressure. This will lead to a lower maximum internal air pressure required to restore the relative displacements in the tube-jack test. In this second phase of inflation, only the tubing material is expanding and the fabric sock has not yet been engaged. Thus, if the tube-jack inflates to the size of the hole within this pressure range, the calculation of the pressure applied to the masonry, as described in section 2.3.2, will only depend on the material properties of the tubing material and not on the combined properties of the tube and sock together.

A second point, where the slope of the graph changes again, can be considered the beginning of the third phase. This point is at approximately 0.1 MPa for the rubber tube-jack and approximately 0.2 MPa for the latex tube-jack. During the third phase of inflation, the tubing has started to engage the fabric sock and the two are working together. The inflation rates in the third phase, for both the rubber and latex tubes, appear to be linear. This is an optimistic finding because it predicts the linear inflation and pressure application to the masonry in an actual tube-jack test.

The average diameters for the three fabric types were averaged for this phase of the inflation test. A linear trend line was fit to the average data and the equations are shown on the graphs in Figure 3-23 a and b. The rate of inflation of the rubber tube-jacks is slightly lower than the latex tube-jacks. The higher inflation rate of the latex tube-jack is an advantage of using the latex for the tube-jacks because it means that less of the air pressure will be used in inflating the tube-jack and more of the air pressure will be used to pressurize the surrounding masonry.

Since the rubber tube-jack has the advantage of having a lower inflation pressure and the latex tube-jack has the advantage of a higher inflation rate once the sock is engaged, the determination of which material is better suited for the tube-jack system was deferred to after further testing of tube-jacks in a larger masonry wall. In addition, the elasticity of the sock used

seems to have little impact on the inflation rate. Therefore, any of the three fabrics could be used for further construction of the tube-jack prototypes.

3.7 Tube-Jack Rubber Material Characterization

During the initial development of the tube-jack system, it was assumed incorrectly that after filling the tube-jack to the size of the hole, all of the additional pressure applied beyond that point was being applied to the masonry. With this understanding of the system, all of the laboratory testing of the tube-jack tests was carried out.

In the analysis following the laboratory testing, it was discovered that the initial assumption about the amount of pressure being applied to the masonry was incorrect. At that time the derivation of the equation for the pressure applied to the masonry was developed, as shown in section 2.3.2. That derivation shows that the elasticity of the tube-jack affects the pressure applied to the masonry. As explained in section 3.6.2 and shown in Figure 3-21 , if the size of the hole is less than approximately 25 mm in diameter then the tube sock will not affect the pressure applied to the masonry. Only the tubing material contributes to the elasticity of the tube-jack in this range of tube diameters. Thus, it is important to know the material properties of the tubing material.

During the laboratory testing, as is described in the following chapters, it was determined that the rubber tubing material was the best for the tube-jack system. Thus, the tests described in this section were only performed on the rubber tubing and not on the latex tubing.

To determine the elastic modulus of the rubber tubing, tensile tests were performed following ASTM standard D412-98a "Standard Test Methods for Vulcanized Rubber and Thermoplastic Elastomers - Tension" [52]. Five rubber dumbbell specimens, labeled R1-R5, were cut from the rubber tubing using the standard dies. The same test machine used for the tests on the fabric socks, as shown in Figure 3-15 , was used for these tests. A photo of specimen R5 during the test is shown in Figure 3-22 a. The results for all of the tests are shown in Figure 3-22 b. It is difficult to distinguish between the results of each of the specimens because they followed nearly the same stress-strain curve.
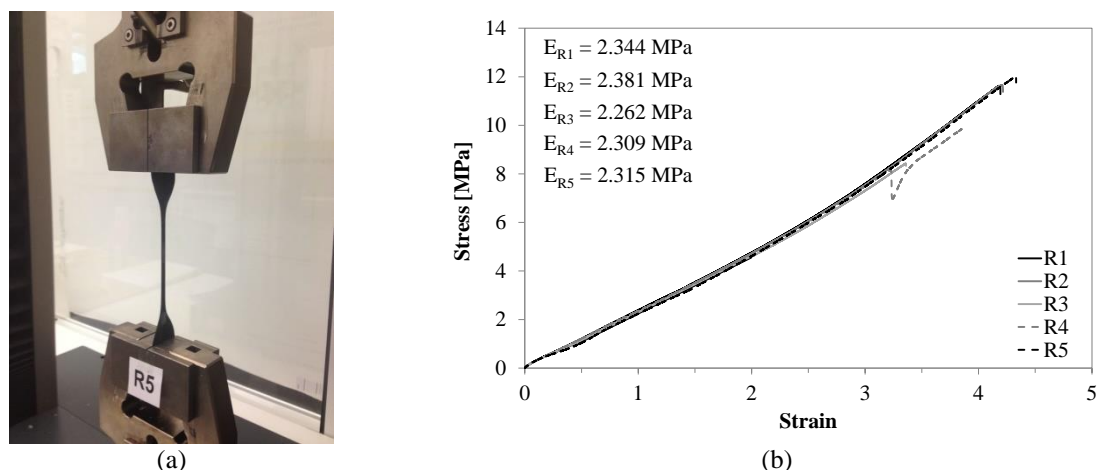
Figure 3-22 Tensile testing of the rubber tubing material: (a) specimen R5 during the tensile test; and (b) results of all of the tensile tests on the rubber

These results show the rubber to be approximately linear elastic. However, at a strain of approximately 2.5, the slope of the stress-strain lines change slightly. It was expected that the

size of the holes in the masonry would not be greater than 40 mm in diameter, which corresponds to a tube-jack perimeter of 126 mm. Given the initial rubber tube perimeter of 45 mm, the maximum strain for a perimeter of 126 mm is less than 2. Thus, trend lines were fit to the linear portion of the data, between strains of 0.5 and 2, to estimate the elastic modulus of the material. The results are shown in Figure 3-22 b. The average elastic modulus of the rubber was 2.32 MPa with a standard deviation of 0.044 MPa (COV = 1.91%). A Poisson's ratio of 0.499 was assumed for the rubber based on literature review [53].

3.8   First Complete Single Tube-Jack Tests

Two initial single tube-jack tests were performed in masonry walls constructed in the structures laboratory (LEST) at the University of Minho. The purpose of these first complete tube-jack tests was to determine if the tube-jack system was working properly and to fix any issues with the system, test set-up and procedure.

3.8.1   Rubble masonry wall tube-jack test

The first test was performed in an irregular rubble masonry wall. This wall had been constructed for a different research program and the tube-jack tests were performed after the research originally intended for this wall had been completed. The purpose of this test was to determine if the newly designed tube-jacks with confining tube socks could be inflated within holes in the masonry without bursting. The masonry wall was loaded from above using hydraulic jacks as shown in Figure 3-23 a. Initially, ten holes were drilled in the masonry with eight LVDTs positioned on the front surface of the wall to measure the vertical relative displacement. Three rubber tube-jacks were pressurized inside the three central holes. Following the first pressurization with three tube-jacks, a second pressurization was carried out using all ten tube-jacks.
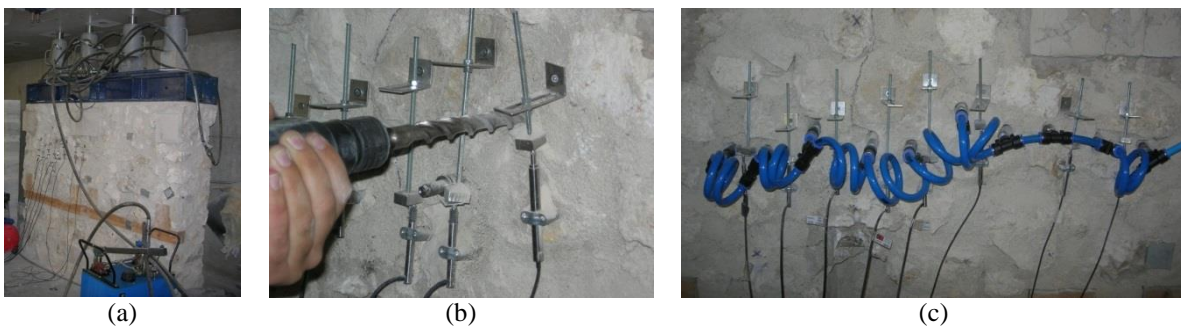
Figure 3-23 Tube-jack test on an irregular masonry wall: (a) large irregular wall loaded in compression; (b) drilling the holes; (c) insertion of the tube-jacks and pressurization

The following observations were drawn from the setup and drilling portion of the first single tube-jack test:

- It was most convenient to place the LVDTs below the holes and the stands above so that the cables didn't need to be held up during the test;

- Caution had to be taken during drilling so as not to touch the LVDTs (Figure 3-23 b). If the LVDTs are touched, the data has to be analyzed closely after the test is complete. Due to the high precision and sensitivity of the LVDTs, the slightest touch can cause the measurement value to jump. If the movement is out of the range of movement typically being observed by the other LVDTs and it happens nearly instantaneously, it

can be identified as an error due to a touch and the data can be corrected. Figure 3-24 a shows an example of a jump in the LVDT measurement during this first test which was due to touching the LVDT. If the movements of the LVDT due to a touch are within the same range as the movement of the wall or happen over a period of several seconds, it can be difficult to distinguish them from the movement of the wall and the data from that LVDT might not be usable for the test;

- Drilling produced vibration in the wall and dust that fell on the LVDTs and stands. The vibrations could be seen in the LVDT data recorded during this first test and are shown in Figure 3-24 b. It was not determined if the dust that fell on the LVDTs and stands affected the LVDT results. In the analysis of the data, the vibrations and noise was reduced by creating a moving average of the data and systematically reducing the number of data points.
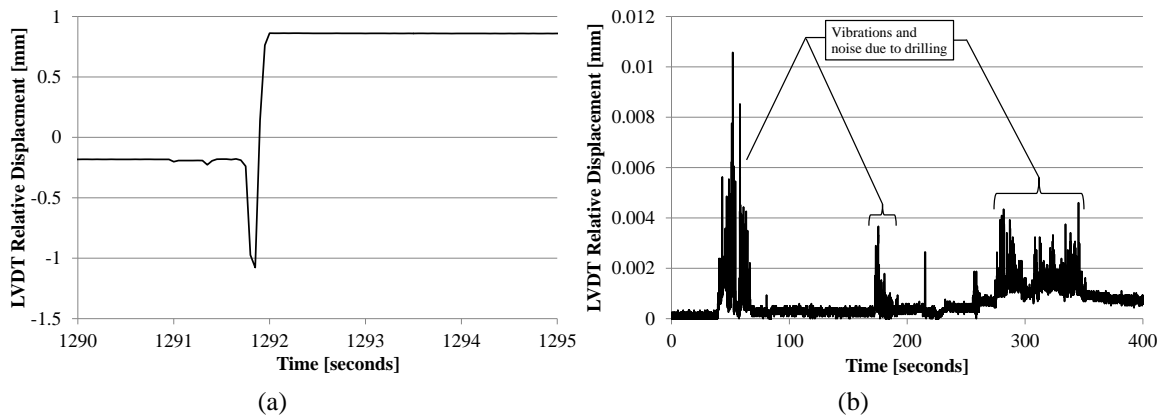
Figure 3-24 Difficulties found in the analysis of the data: (a) jumps in the LVDT data due to something touching the LVDT during the drilling; (b) vibrations and noise recorded by the LVDTs during the drilling

The following observations were made for the insertion and inflation of the tube-jacks in the holes during the first test:

- Following the drilling, the tube-jacks were easy to insert into the holes. However, the connection tubes were difficult to arrange so that they did not touch the LVDTs, see Figure 3-23 c;

- The tube-jacks inflated to fill the circumference of the drilled holes as shown in Figure 3-25 a;

- After inflation, the tube-jacks applied pressure to the masonry as evidenced by positive relative displacement of the LVDTs during pressurization, as shown in Figure 3-25 b;

- The tube-jacks and confining fabric were not damaged during pressurization up to an internal air pressure of 0.5 MPa. The tube-jacks following the tube-jack test are shown in Figure 3-25 c. Therefore, the tube-jacks can be used for more than one pressurization.

(a)   (b)   (c)
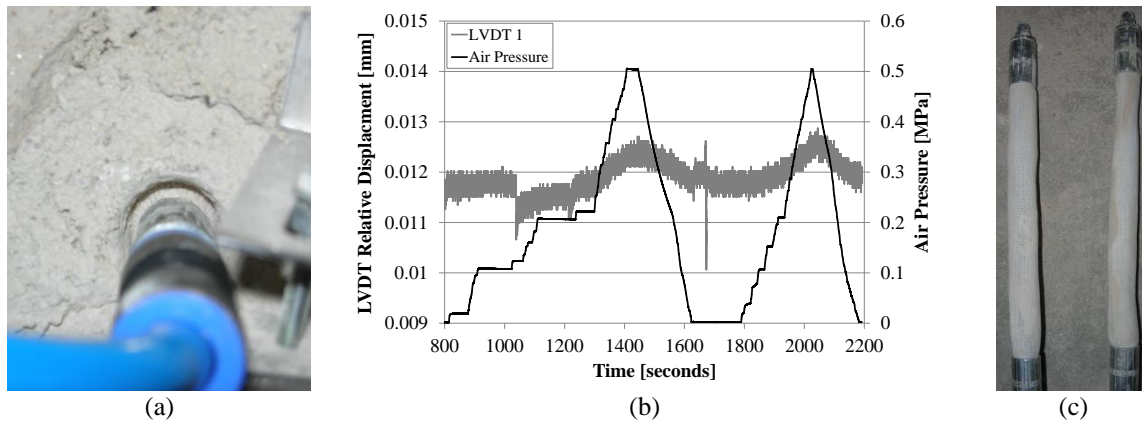
Figure 3-25 Observations from inflating the tube-jacks in the holes: (a) tube-jack inflated to the size of the hole (b) increases and decreases in the relative displacement of LVDT 1 as the tube-jacks are pressurized and depressurized; (c) condition of the tube-jacks after the test

3.8.2   Regular masonry wall tube-jack test

The second complete tube-jack test was performed in a granite block wall made with cement-lime mortar with a regular typology. This second wall was specially built for this test program and the construction will be described in more detail in Chapter 4. A schematic for the test set-up, including 8 LVDTs and 12 holes, is shown in Figure 3-26 . The number of holes was increased to 12 so that the length of the equivalent flat-jack would be the width of two granite blocks. Two LVDTs were placed on the back of the wall to see if both sides of the wall were moving uniformly as the holes were drilled through the thickness of the wall and the tube-jacks were pressurized. The wall was loaded in a similar manner to the irregular wall used for the first test. Two hydraulic jacks were pressurized above a steel profile that distributed the load to the wall. The stress level in the wall was approximately 0.2 MPa.
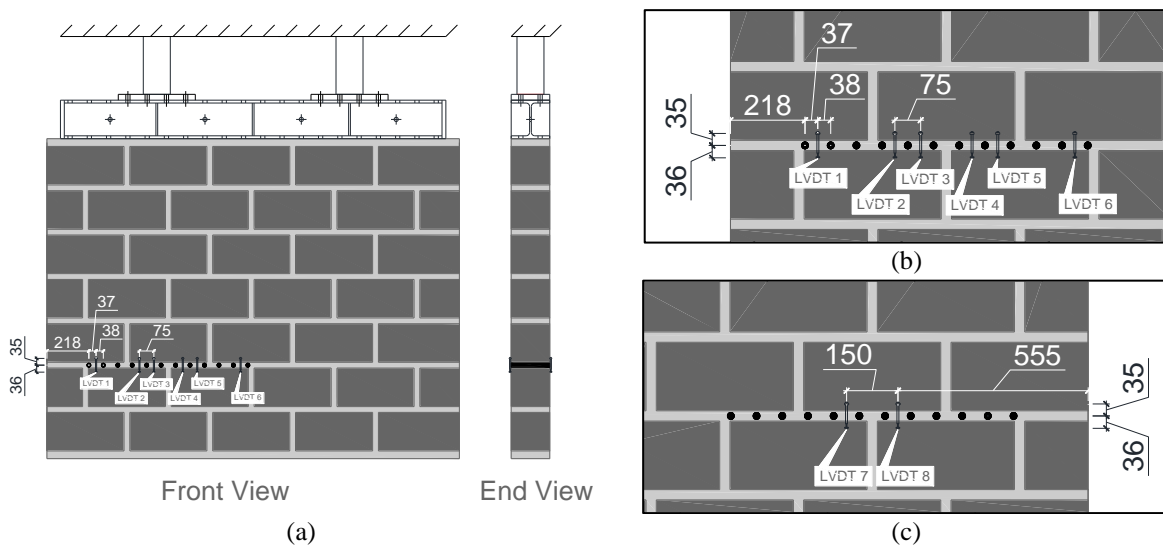
Figure 3-26 Schematic of the Tube-Jack test set-up: (a) Front and End view of the wall; (b) close-up of the LVDT and hole positions on the front of the wall; and (c) close-up of the LVDT positions on the back of the wall (Dimensions in mm)

The procedure for the test was the same as in the first tube-jack test. In this test, the first pressurization was performed with all 12 LVDTs placed in the holes. Photos of the set-up, drilling the holes, and tube-jacks inserted in the holes are shown in Figure 3-27 .

(a)   (b)   (c)
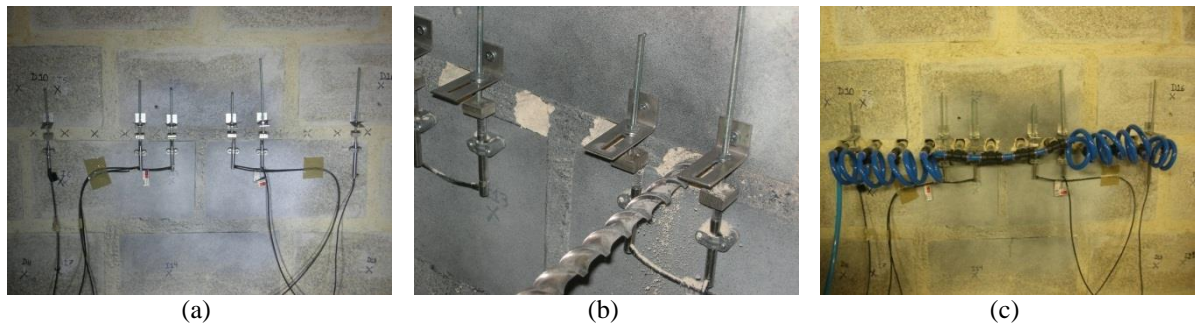
Figure 3-27 Preparation for the tube-jack test: (a) Spray painting the central test area for image correlation measurements; (b) drilling process; and (c) insertion of the tube-jacks

The LVDT measurements were recorded throughout the test, including during the drilling of the holes and during the four pressurization cycles. Initial analysis of the LVDT relative displacements in Figure 3-28 shows that the magnitude of displacement recorded by the LVDTs on the back of the wall (LVDTs 7-8) was not the same as on the front of the wall (LVDTs 1-6).
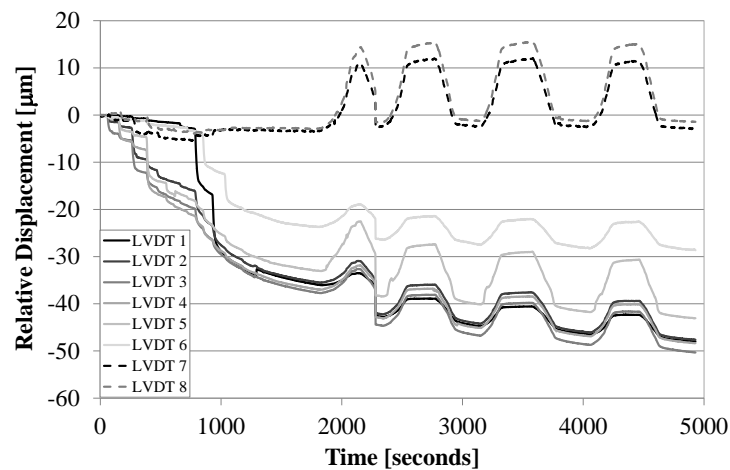
Figure 3-28 LVDT relative displacements throughout the tube-jack test

Since the test was being performed through the entire thickness of the wall, the goal was to determine the movement of that area of the wall overall. However, simply averaging all of the results would give preference to the side of the wall where there are more LVDTs. Therefore, the results of the test were analyzed in three ways: averaging the center two LVDTs on the front and back of the wall, giving the same weight to the two back LVDTs as to the six front LVDTs, and doing an average of all of the LVDTs equally. The results of these three methods are shown in Figure 3-29 .

The LVDTs on the front of the wall showed more negative relative displacements during the hole drilling than the LVDTs on the back of the wall. This is evident in the average of all of the LVDTs because the front LVDTs have a greater influence than the back LVDTs in this average. When the back LVDTs are given as much weight as the front LVDTs, then negative relative displacement is reduced, as shown by the top curve in the graph. The middle curve is perhaps the most representative of the actual movement of the wall because it considers two LVDTs from the front and back of the wall in the same positions. However, these LVDTs are just in the center of the equivalent flat-jack and the movement of the whole test area can't be discerned from only these four. In conclusion, it is best to have the same number of LVDTs on both sides

of the wall to have a representative average, in the case that the wall does not move uniformly on both sides.
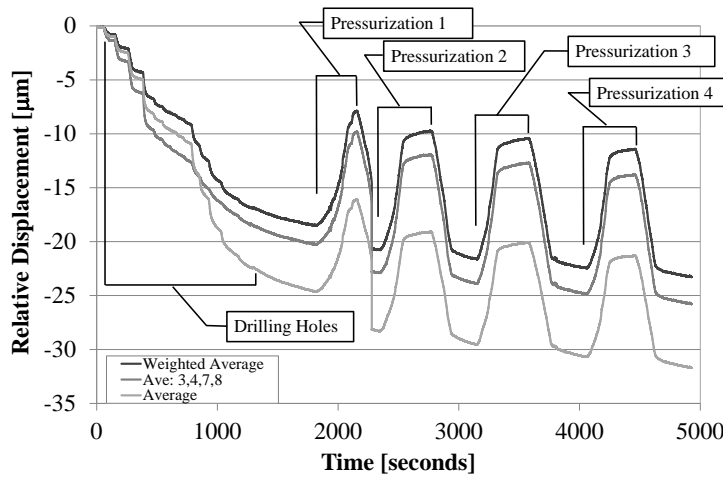
Figure 3-29 Average relative displacements of the LVDTs throughout the phases of the tube-jack test

Another important observation from this test was that the masonry continued to move together (negative relative displacements) even after the drilling of the holes was complete. One likely reason for this movement was that this wall was still curing and drying due to the damp conditions in the laboratory. Another possible reason is that the load distribution within the wall was still adjusting after drilling the holes and that a longer period of time needs to be allowed for load redistribution before pressurization is started. This will be observed during testing throughout this work.

During the pressurization cycles, the tube-jacks were pressurized to a maximum of 0.525 MPa. The air pressurization system was not able to supply enough pressure to the masonry via the tube-jacks to restore the wall to its position before drilling the holes. The quick release connections for the tubes were not tight enough to prevent air from leaking and air had to be constantly added to the system.

The following four conclusions were drawn from the observations of the second complete single tube-jack test:

- The movements of the front and back of the wall were not uniform, despite the relative homogeneity of the masonry arrangement and test setup;

- An equal number of LVDTs or other measuring devices should be used on both sides of the wall;

- More time needs to be given for load redistribution within the wall after drilling the holes;

- A new pressurization system is required that can obtain higher pressures without leaking.

3.9   Water Pressure System

A water pressure system was developed to solve the issues found with the air pressure system during the single tube-jack tests presented in the previous section. Water was chosen over oil because it would be cleaner than oil if a rupture in the system were to occur. There were three main requirements for the water pressure system. The first was that it could obtain higher gage pressures than the air pressure system. The second was that it would not leak during the pressurization. The third was that the hoses connecting the tube-jacks to the pressure system would not interfere with the LVDTs between the holes.

The system developed consisted of a water pressure hand pump, a water pressure gage, connection hoses, steel connection strips, and tube-jacks. The complete system and its components were shown in Figures 21 and 22, for both the single tube-jack test setup and the double tube-jack test setup, in section 2.3.1 where the tube-jack system was initially described. The water pressure hand pump (see Figure 3-30 a) was able to apply pressure to the system as high as the user was capable of pumping. The highest internal water pressure reached during testing was approximately 1.0 MPa. The hand pump had a release valve that allowed water to be drained from the system. Instead of an air pressure gage, the water pressure gage and transducer shown in Figure 3-30 b was installed between the pump and the steel connection strips. This pressure transducer was connected to the data acquisition system, as shown in Figure 3-30 a, so that the pressure could be recorded throughout the tests. All of the connection hoses used in this system, such as the one connecting the hand pump to the water pressure gage in Figure 3-30 a, were able to withstand high water pressures with no expansion.

<div align="center">(a)   (b)</div>
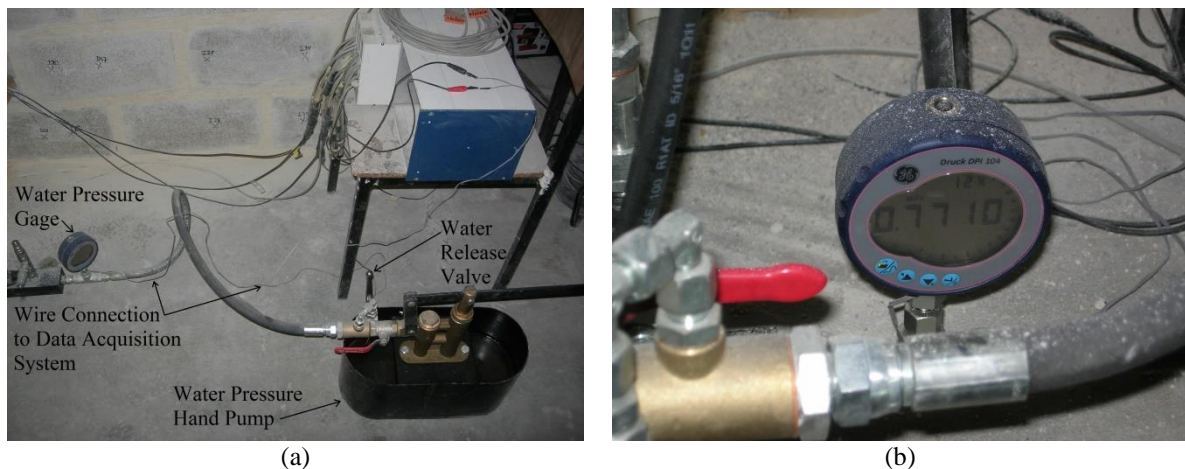
Figure 3-30 Water pressure system components: (a) water pressure hand pump, water pressure gage, and transducer connection to the data acquisition system; and (b) close-up of the water pressure gage

The two steel connection strips each had twelve ports for connecting tube-jacks via connection hoses, as shown in Figure 3-31a. Thus, using both connection strips, a single tube-jack test using twelve tube-jacks or a double tube-jack test using two lines of twelve tube-jacks could be performed. The tube-jacks themselves were not changed in the switch from air pressure to water pressure. To ensure that all of the air in the tube-jacks had been expelled prior to testing, several cycles of pumping water into the system and then releasing the water and excess air were performed before each test. The pressure during this procedure was kept very low so as not to rupture the tube-jacks. During these cycles, any defective and leaking tube-jacks, such as the one shown in Figure 3-31b, could be discovered and replaced before starting the pressurization of the tube-jacks in the masonry.

(a)   (b)
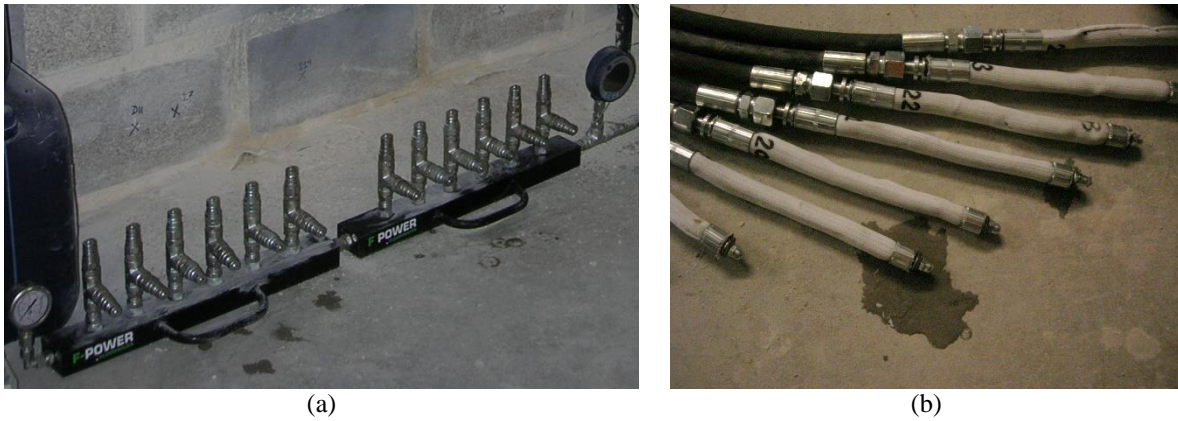
Figure 3-31 Water pressure system components: (a) steel connection strips with quick release connection ports; and (b) leaking tube-jack discovered during the initial filling of the tube-jacks with water

A couple of different connections were used to connect the components of the system together and prevent water from leaking. Connections between the hand pump and the connection hose and between the connection hose and the steel connection strip were screw connections that could be secured tightly with wrenches. The connections between the connection hoses and the tube-jacks were also screw connections. The connection between the tube-jack connection hoses and the connection strip were quick release connections that allowed the tube-jacks to be quickly removed and replaced if necessary during a tube-jack test.

By using individual connection hoses to connect each of the tube-jacks to a central connection strip, the hoses could come directly out of the wall and down to the connection strip, as shown in the photo of a double tube-jack test in Figure 3-32 a. This meant that no hoses were crossing over the LVDTs between the tube-jacks, as shown in Figure 3-32 b, reducing the likelihood of the hoses interfering with or touching the LVDTs during the test. Connecting the hoses to a central connection strip also made it easier to add or replace tube-jacks during the test without affecting the other tube-jacks.

(a)   (b)
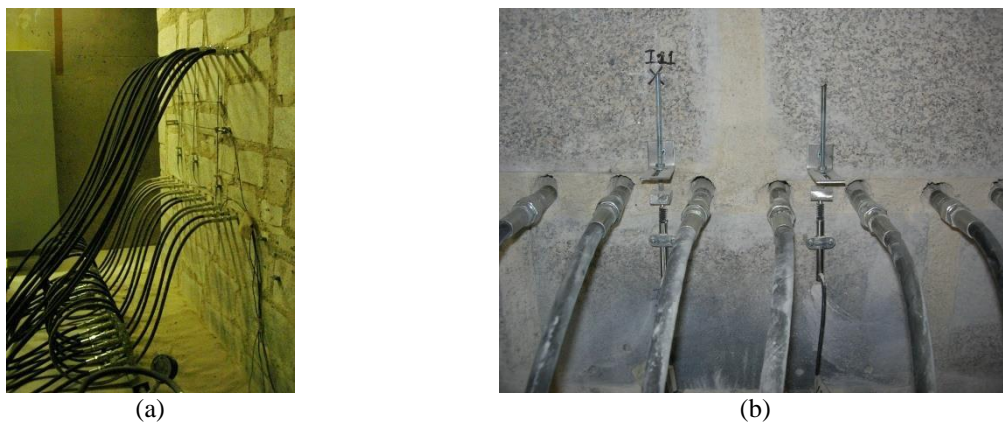
Figure 3-32 Water pressure system components: (a) connection hoses coming straight out from the wall and down to the connection strip; and (b) connection hoses not interfering with the LVDTs

This water pressure system was used in all of the laboratory and in-situ tube-jack testing performed during this thesis work. The results of the tube-jack tests are presented in the following chapters.

3.10   Conclusions

This chapter presented the development of the tube-jack system throughout this thesis work. Initially, three tube-jack prototypes were built with different tubing materials including PVC, latex, and rubber. Through testing in a small two-block specimen it was discovered that the PVC material was not flexible enough for the application and that the rubber and latex tubing material must be confined so that the tubing does not rupture at low pressures. Through numerical analysis of the two-block test, it was learned that the horizontal pressure applied to the masonry by the tube-jacks has an impact on the test and that larger masonry wall specimens would be required to test the tube-jack system.

In preparation for testing the tube-jack prototypes in larger masonry walls, a series of inflation tests was conducted with the latex and rubber tube-jack prototypes to improve the design. Tubular knitted fibrous structures, tube socks, were characterized using cyclic tests and were incorporated into the design of the tube-jacks to help confine the tubing material and prevent it from rupturing. Final inflation tests of the improved design showed three phases of inflation and pressurization for the tube-jacks; filling the tube-jack with fluid, inflation of the tubing material only, and expansion of the tubing and sock together. For tube-jack tests where the inflation is within the second phase, the characterization of the tubing material is required. Thus, the tensile testing of the rubber tubing was presented.

The first tube-jack tests in masonry walls showed that the newly designed tube-jacks, with socks incorporated, could inflate to the size of the drilled holes and pressurize the masonry without being damaged during the test. However, the connections in the air pressure system were constantly leaking and loosing pressure and it was difficult to keep the tubing from one tube-jack to another from hitting the LVDTs. Thus, the final development was to change to a water pressure system, where a higher pressure could be applied to the tube-jacks, connection hoses from the tube-jacks would come straight down to a connection strip avoiding the LVDTs and leaks could be easily identified and fixed.

The tube-jack system developed through this phase of the thesis work was adequate for the next phases of the thesis, testing in laboratory masonry walls, numerical modeling and in-situ. However, through the analysis of the results in those phases, imperfections were found in the system. Therefore, the development presented in this chapter is only a start to the development of the tube-jack system and further work beyond the scope of this thesis should be performed.

4.   MECHANICAL CHARACTERIZATION OF THE MASONRY

4.1   Introduction

It was found during the tube-jack system development that the two-block masonry specimens were too small for testing the tube-jack system. Larger walls would be necessary for both the tube-jack tests. Thus, large masonry walls and small wallets were constructed in the Structural laboratory at University of Minho (LEST). The masonry test specimens were designed to be representative of masonry currently found in traditional masonry structures in northern Portugal. This was to provide a similar masonry typology and testing situation in the laboratory as would occur in the field, so that when final tests were conducted in-situ, minimal changes would need to be made. The following subsections of this chapter describe the typical masonry typologies found in Portugal, the design and construction of the single leaf masonry walls and wallets, and the mechanical characterization of the constituent materials and small masonry wallets.

4.2   Traditional Portuguese masonry typologies

Masonry typologies vary throughout the country, and the world, depending on the materials used, the skills of the masons, cultural traditions, and period of construction. Several studies have been made in Portugal detailing the typologies of existing masonry structures [54]. In this subsection of Chapter 4, four studies are briefly described, one focusing on masonry in the town of Tentúgal in the center of Portugal by Lorenço et al. [55], one on masonry in Northern Portugal by Vasconcelos [5], and two on masonry in Porto by Mota [56] and Almeida [57]. For each of these studies, the masonry typology, dimensions, and materials are described in as much detail as was provided in the original studies. This information was the basis for the design of the masonry walls used in this work, which is presented in section 4.3.

4.2.1   Walls of Tentúgal

Masonry in the town of Tentúgal, Portugal, near Coimbra, was described in a typological study by Lorenço et al. [55]. According to the study, the masonry in the area was made of irregularly shaped Ançã stone with medium-sized stones between 15 cm and 25 cm in length. The joints had a thickness of 2 cm or greater and consisted of a low strength mortar made of clay and lime. Overall, the walls had thicknesses from 45 cm to 90 cm but 62.5% were between 47.5 and 55 cm. The walls that were up to 70 cm thick were single leaf masonry construction, while larger width walls had two leaves, either with connectivity between the leaves or without. Figure 4-1 shows the outlines of the stones in four typical cross-sections. Nearly 40% of the material in the wall cross-sections was mortar.
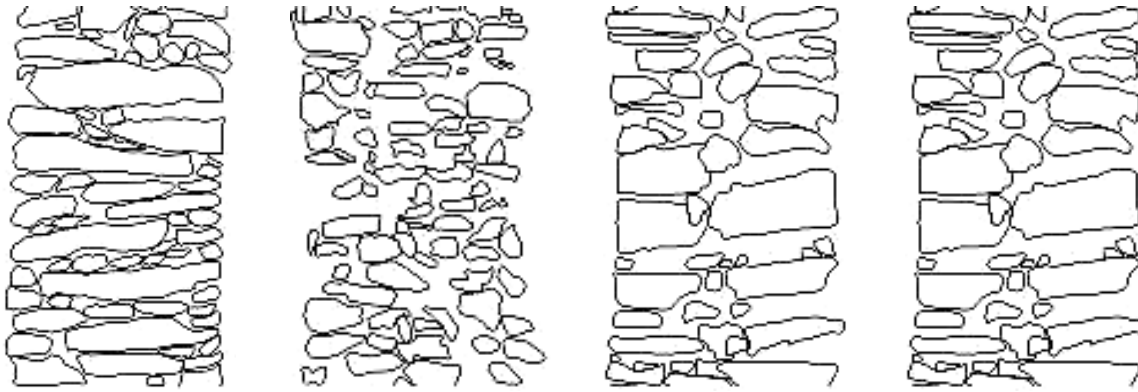
Figure 4-1 Typical cross-section typologies for masonry in Tentúgal [55]

The laying pattern for the stones was typically irregular with no alignment of the mortar joints. The pattern used in 87.5% of the walls investigated in this study is shown in Figure 4-2.

Figure 4-2 Irregular typology of the masonry in Tentúgal [55]

4.2.2   Walls in Northern Portugal

In a study performed by Vasconcelos [5], granite masonry walls, constructed to be representative of ancient masonry structures in Northern Portugal, were tested. Two mica, medium-coarsed granite, considered representative of granite material used in ancient masonry structures in Northern Portugal, was used in the study. The mortar used was a ready-mix called "Albaria Structturale" supplied by Bettor-MBT Company. This mixture consisted of hydrated lime and natural aggregates with a granulometric range between 0.1 mm and 0.2 mm. The mortar compressive strength at 7 days was 3.0 N/mm^2, which was considered by Vasconcelos to be close to the mortar strength found in historic buildings.

Three different masonry patterns were used in Vasconcelos's study (Figure 4-3). The first wall type used sawn stones with dry joints. The other two patterns have more irregular shaped stones and were considered to be characteristic of traditional vernacular and monumental ancient structures. The hand cut stones in the second pattern were similar in shape but of varying sizes. The rubble masonry wall had variable shape and size stones arranged randomly. Both of these irregular walls were constructed with the low strength mortar described previously. The size of the individual stone units is not specifically stated for the wall specimens, however, the dimensions can be estimated to be around 15 cm to 20 cm both vertically and horizontally based on the provided patterns and dimensions (Figure 4-3).
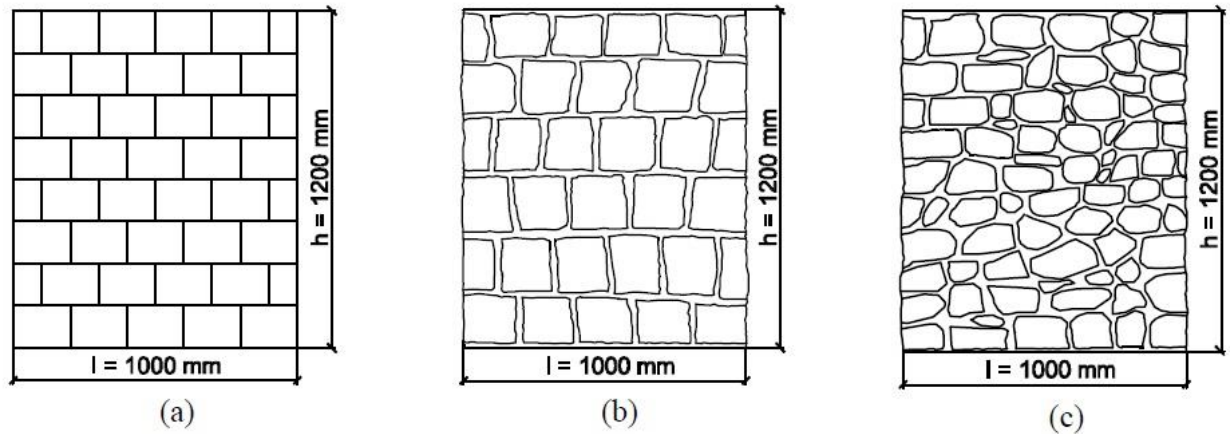
Figure 4-3 Masonry wall specimens tested by Vasconcelos: (a) Regular masonry with dry joints; (b) Hand cut stone masonry with linear joints; and (c) Rubble masonry [5]

The dimensions of the tested walls were 1.0 m wide by 1.2 m high by 0.2 m deep. The dimensions for the walls and units were considered to have an approximate scale of 1:3 in reference to typical single leaf walls found in Northern Portugal.

4.2.3   Walls in Porto

A study was carried out at the University of Porto focused on developing a data-base of geometry and construction techniques for traditional masonry walls [56]. Walls in old buildings located in and around Porto were visually inspected and in situ testing was carried out. The majority of the masonry investigated contained granite units. Stone sizes were characterized into four groups based on their diagonal dimension: large stones with dimensions greater than 80 cm, medium stones with dimensions between 50 cm and 80 cm, small stones with dimensions between 10 cm and 50 cm and tiny stones with dimensions less than 10 cm.

The first masonry section investigated (A1) consisted of stones ranging in size from 23 cm to 91 cm with the majority being medium to large stones with dimensions from 53 cm to 91 cm. Most stones were rectangular in shape and some linearity in the horizontal joints could be seen (Figure 4-4a). Joints were 1 cm or less in thickness and were made with a cream colored lime and clay mortar. A second section of masonry (A2) was examined in the same structure (Figure 4-4b). This masonry had a similar pattern with slightly smaller units having small to medium sizes in a range from 38 cm to 73 cm.
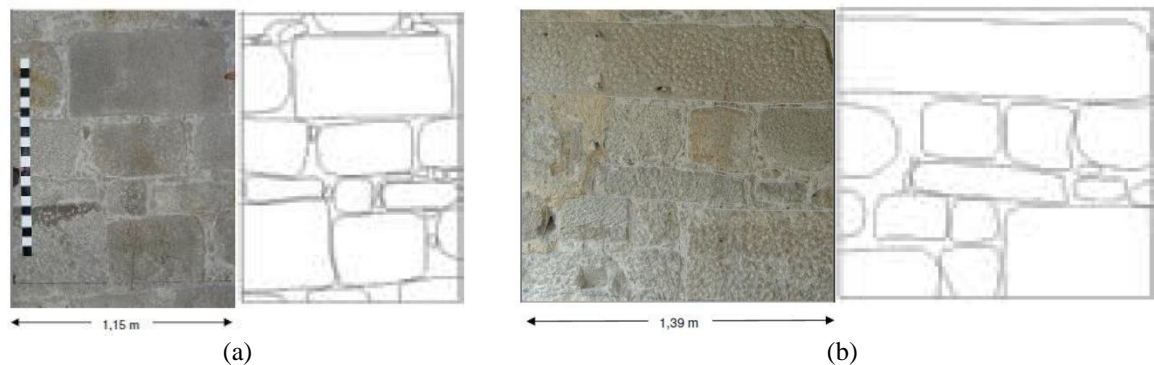
Figure 4-4 Granite masonry typology in traditional building in Porto: (a) A1; and (b) A2 [56]

In another structure in Porto the granite masonry was found to be more irregular. This masonry contained stones that were more irregular in shape and small in size, having dimensions between 10 cm to 50 cm. In one area studied on this building (C), the stones were arranged without any linearity in horizontal joints (Figure 4-5a). In this area, the masonry did not have as much mortar between the stones as in the other locations. In contrast, in another area of the same building (D3), where very irregular or rubble masonry was found, mortar between the stones was much thicker and was partially covering parts of the stone surfaces (Figure 4-5b). The stones in this area were classified as small and very small, having dimensions between 15 cm and 37 cm.

(a)   (b)
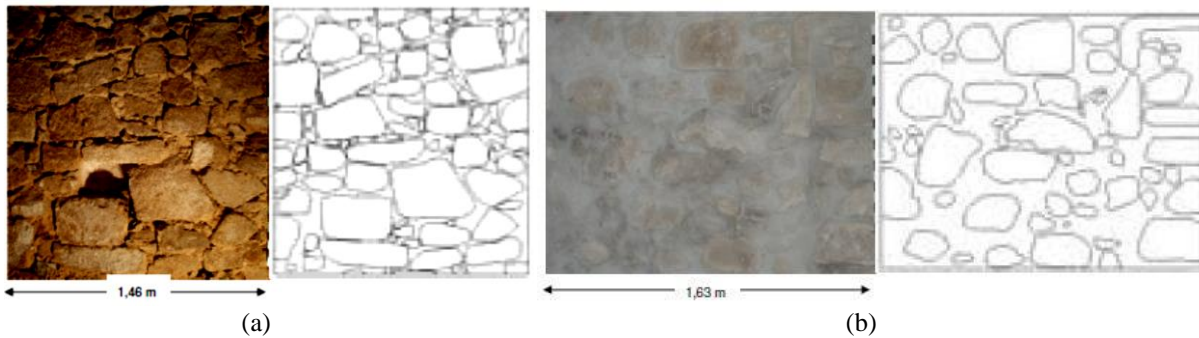
Figure 4-5 Granite masonry typology in a traditional building in Porto: (a) C; and (b) D3 [56]

In another study by Almeida et al. [57], a typical masonry structure built in 1916 for industrial purposes was used as a case study. Image processing was used to identify outlines of individual stones in single leaf wall sections. The masonry pattern found was semi-irregular with medium to large stones making up most of the wall and clear horizontal alignment of the stones. The stones themselves were roughly hewn, sometimes irregular in shape, and of varying sizes. Elevations and cross-sections are shown in Figure 4-6.
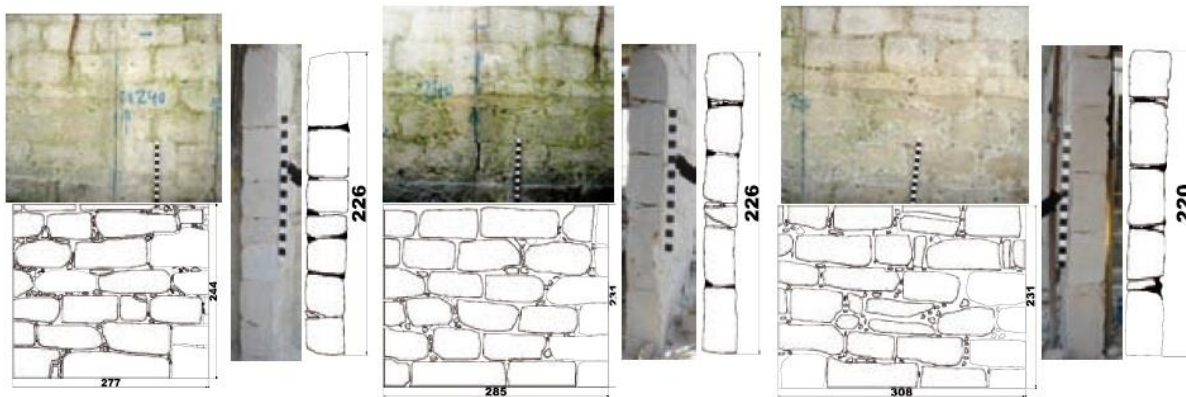
Figure 4-6 Elevations and cross-sections of walls surveyed in Porto [57]

The rectangular yellow granite stones ranged from 50 cm to 90 cm diagonally. Small stone wedges and occasionally brick pieces were fit between the large stones where space allowed in the mortar joints. The joints ranged in thickness from 0.5 cm to 2 cm and consisted of a cream colored brittle mortar. The cross-section of the wall was 30 cm thick. The study noted that it was evident that during construction mortar was placed on the borders or edges of the main stone pieces, without completely filling the interior of the wall, resulting in voids and cavities in the center of the masonry.

Similar single leaf walls were examined on another floor of the same structure. These walls had thicknesses of 40 cm and 50 cm.

In the study's material characterization tests, it was found that the granite stones had a compressive strength of 61 MPa and a Young's Modulus of 26 GPa. The mortar was found to consist of lime and sand with a ratio of 1:3 [57].

4.3   Single leaf masonry wall design and construction

Three single leaf masonry walls were designed and constructed for testing the tube-jack prototypes. The design goal for these walls was to be representative of traditional structural masonry found in Northern Portugal. Thus, the design was based on the studies presented in the previous subsection. The three walls were constructed of granite units from a local quarry in Northern Portugal and cement-lime mortar. The dimensions of the walls were approximately 2 meters long by 1.6 meters high by 0.2 meters deep. These dimensions produced a wall that had a scale of 1:2 compared to single leaf walls found in Northern Portugal.

The granite unit size was based on the possible density and weight of the granite. The density of granite stones can range between about 2450 kg/m^3 and 2700 kg/m^3 depending on the type of granite and the water content [5]. If the density of the stone is at the higher end of the range, a stone with dimensions 0.8 m by 0.4 m by 0.4 m, a normal size for large stones units for traditional Portuguese masonry, could weigh 345.6 kg. However, if the stone dimensions were limited to a maximum of 0.4 m by 0.2 m by 0.2 m, half of each dimension and one eighth of the volume, then the weight would be just 43.2 kg, allowing the wall to be built by hand without the need for machinery to lift and place the units. Hence, the latter dimensions were chosen. Based on the size ranges defined in the study by the University of Porto [56], the unit size chosen would be characterized as small.

Since the dimensions of the wall and the granite units were designed to be approximately half of the normal dimensions for typical traditional masonry found in the Northern Portugal, it would be logical to design the mortar joints to also be half of their typical dimensions. However, this would make the joints much too narrow to perform the tube-jack tests. The tube-jacks, as developed and presented in Chapter 3, require a hole with a minimum diameter of 2 cm. To ensure there was tolerance for variability in construction and drilling, the joints were designed to have a minimum thickness of 3 cm.

Each masonry wall was designed to have a different masonry typology to reflect the diversity of the masonry typologies described in the studies presented in the previous subsection of this chapter. The first wall constructed and tested was a regular masonry wall with rectangular units having maximum dimensions of 0.4 m by 0.2 m by 0.2 m, linear horizontal joints, and vertical head joints. The surface of each unit was very smooth. This masonry typology could be representative of a modern granite masonry wall, but was mainly constructed to be the most regular and predictable wall. The geometry and construction are shown in Figure 4-7.
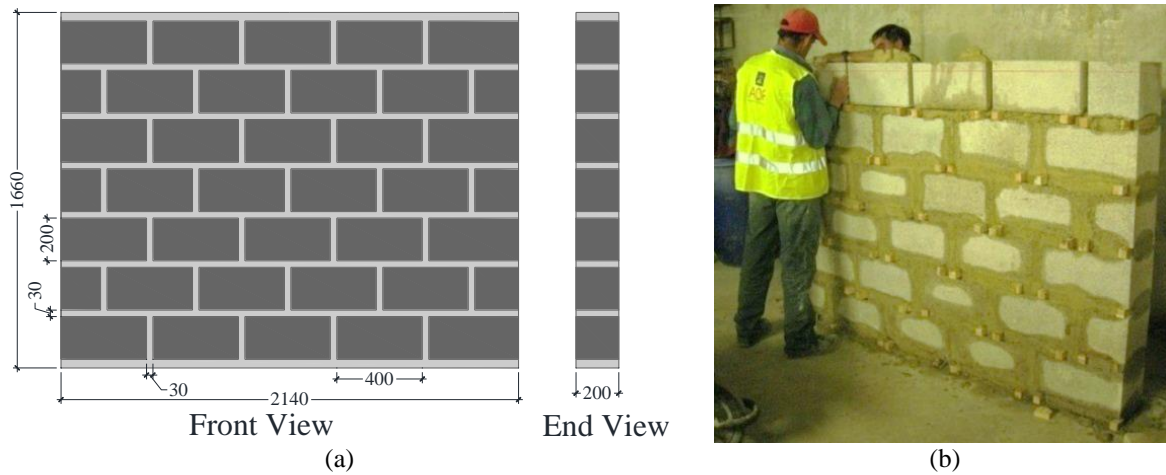
Figure 4-7 Regular granite masonry wall: (a) schematic design (dimensions in mm); and (b) construction

A second wall was constructed with a semi-irregular typology. This wall had irregularly shaped stones with smaller filler stones and roughly linear horizontal joints. This pattern is similar to granite masonries found in some structures in Porto as seen in Figure 4-4. Most of the faces of the units were very smooth and others slightly rough from cutting with a circular saw. The maximum dimensions of the units were the same as the regular masonry wall. The geometry and construction of the semi-irregular wall are shown in Figure 4-8.
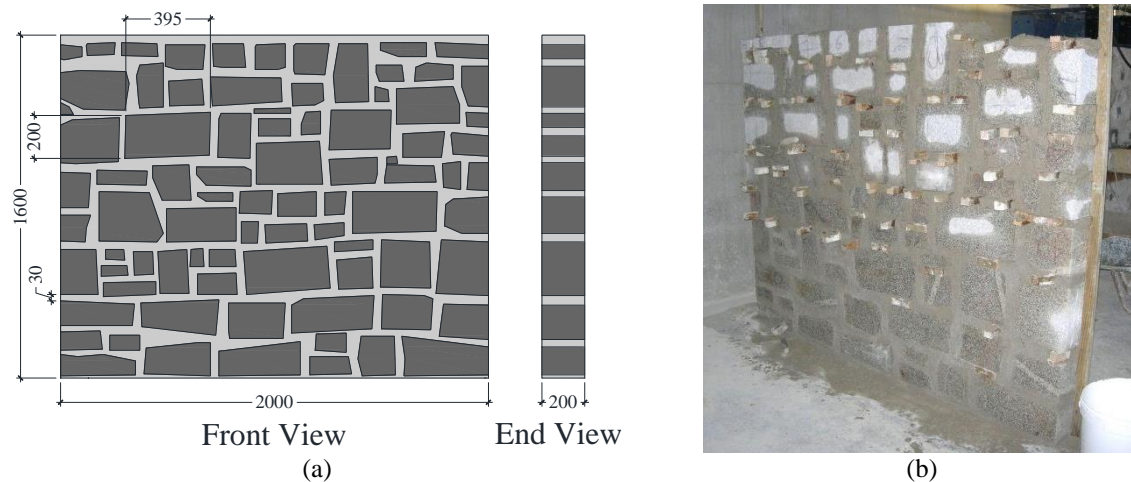
Figure 4-8 Semi-Irregular masonry wall: (a) schematic design (dimensions in mm); and (b) construction

The final wall was constructed with an irregular or rubble masonry typology. The granite stone units were irregularly shaped and the surfaces in their naturally rough state. The maximum dimensions for the granite units were the same as for the regular and semi-irregular masonry walls. There was little linearity in the joints. This wall was similar in typology to granite walls found in Porto, as shown in Figure 4-5. The semi-irregular and irregular walls provided masonry specimens where the ability of the tube-jack system to function in non-linear joints could be tested. The irregular wall geometry and construction are shown in Figure 4-9.
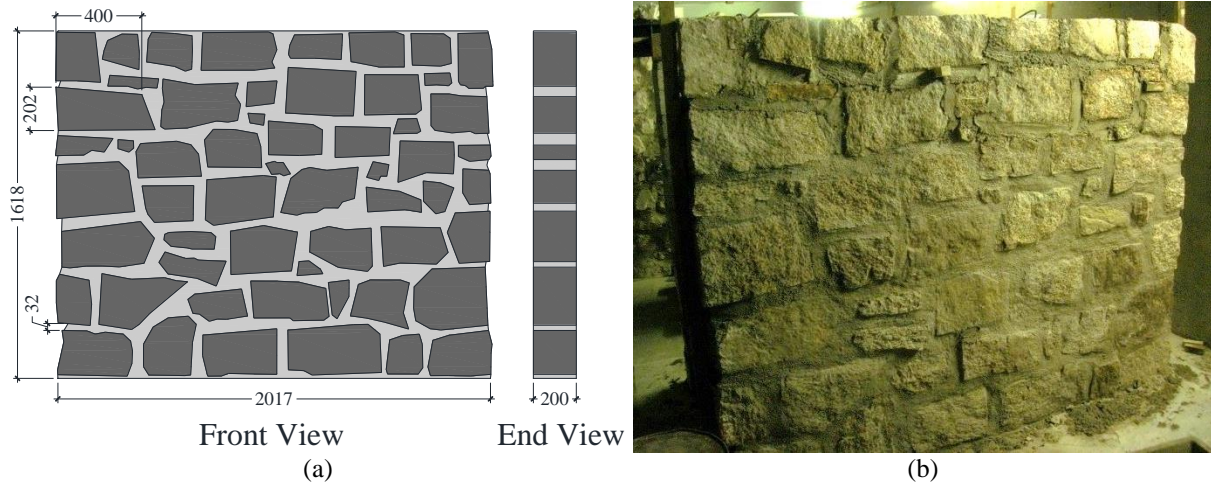
Figure 4-9 Irregular masonry wall: (a) schematic design (dimensions in mm); and (b) construction

All three of the masonry walls were built at the Structural Lab at the University of Minho (LEST). A private construction company was hired to build the walls according to the design described here. The granite units were delivered to the laboratory already cut to size but the mortar was mixed on site by the workers. The regular wall was constructed with a very low strength mortar consisting of: 8 parts slaked lime, 1 part Portland cement, 2 parts yellow clay, 20 parts sand, and 4 parts fine sand. This mortar composition equates to a binder to aggregate ratio of approximately 1:2.9. The semi-irregular and irregular walls were constructed after the testing of the regular masonry wall had been completed, approximately one year later. During the testing of the regular masonry wall, as described in the following sections and chapters, that the mortar in the regular wall was very weak and that a slightly stronger mortar would be better for further testing in the semi-irregular and irregular walls. Thus, when the semi-irregular and irregular walls were constructed, the mortar mix was revised to increase its strength.

To ensure the mortar joints were thick enough during the construction of the walls, wood blocks were used to ensure the spacing of the joints and to hold the units in place. These blocks were later removed and the holes filled with mortar. The construction of the regular and semi-irregular walls took two days and the irregular wall took three days. Following the construction, the walls were allowed to cure in the laboratory without any additional wetting. The regular wall was cured for 50 days before it was loaded and testing was performed. The semi-irregular and irregular walls were cured for over three months before they were loaded and used for testing.

4.4   Granite Cylinders

Granite cylinders were cored from the same stock of granite blocks used for building the masonry walls. These cores were tested to determine the granite material properties. The tests performed are described in the following subsections.

4.4.1   Specimens

Fifteen granite cylinders were cored from four granite blocks. The cylinders were cut and rectified to approximately 150 mm in height (Figure 4-10). They were dried at 100 ºC for 6 hours and then placed in the same curing environment as the masonry wallets. The cylinders were labeled RG1 through RG15. Each of the cylinders was weighed and dimensions were taken at quarter points. The cylinders had an average diameter of 73.25 mm. From these

measurements, the densities were calculated. The average density of the granite cylinders was 2614 kg/m^3 with a standard deviation of 37 kg/m^3 and coefficient of variation of 1.41%. This density is at the higher end of the density range for granites (see section 4.3). Additional information can be found in Appendix A, Table A-1.

(a)   (b)   (c)
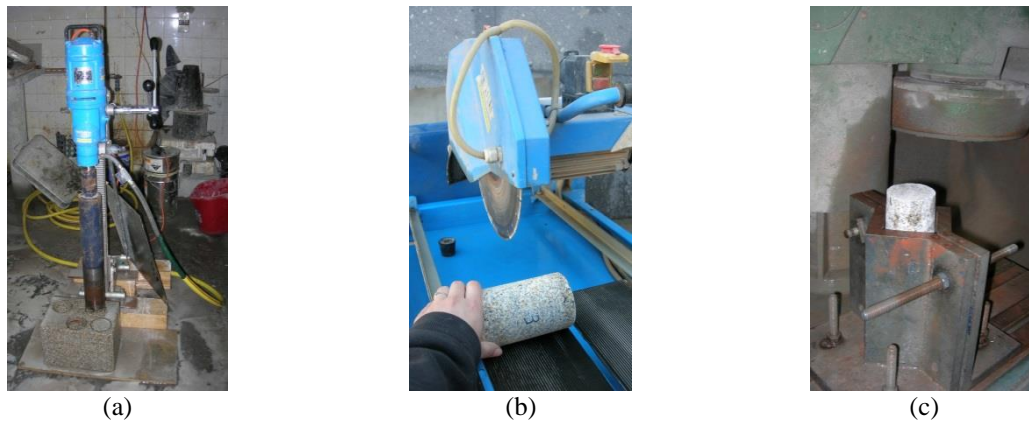
Figure 4-10. Cylinder preparation: (a) granite coring; (b) sawing granite cores to the correct height; and (c) rectifying the granite cylinder ends

4.4.2   Ultrasonic Pulse Velocity

Before the granite cylinders were tested to determine their mechanical characteristics, ultrasonic tests were performed on the first seven specimens. The Pundit Lab ultrasonic testing equipment by Proceq was used for these and other ultrasonic tests performed throughout this work [58]. The test equipment has two transmitters/receivers that must be coupled with the material via a couplant. The user supplies the distance that the wave will pass through the material. In this test, the transmitter and receiver were placed on the ends of the cylinders so that the wave would pass through the length of the cylinder. Once the transmitter and receiver are in place, the machine transmits several waves through the material and calculates the average wave velocity. The test set-up is shown in Figure 4-11.

(a)   (b)

Figure 4-11. Ultrasonic pulse velocity testing of granite cylinders: (a) test equipment and set-up; and (b) performing a test on specimen RG2

Three readings were taken for each of the cylinders and then averaged to get the ultrasonic velocity for each specimen. The average results for each specimen are shown in Table A-2 in Appendix A. The readings ranged from 2500 m/s up to 3000 m/s. The average ultrasonic velocity for the seven granite cylinders was 2682 m/s with a standard deviation of 174 m/s and a coefficient of variation of approximately 6.5%.

4.4.3   Young's Modulus Tests

The granite cylinders were tested in uniaxial compression to determine the Young's modulus of the material. These tests were carried out in a very stiff frame containing a high capacity load cell and closed-loop control system, located at the University of Minho Structural Laboratory (Figure 4-12a).

The set-up for the Young's Modulus test is shown in (Figure 4-12b). The specimen was placed in the center of the test machine on top of a greased spherically seated steel plate to prevent load eccentricities. Steel plates were used beneath the spherically seated plate to raise the specimen up to the level of the actuator. Two aluminum rings were placed at one third and two thirds of the height of the specimen. Three LVDTs where placed at third points around the circumference and secured to the top ring so they could measure the displacement of the middle third of the specimen throughout the test.

The Young's Modulus test was performed by applying a 10 kN preload to the specimen and then loading and unloading the specimen four or five times. An iterative process was used to determine the optimal maximum load and loading rate for the test, however, these variables did not seem to significantly affect the test results. The maximum load ranged from 100 kN to 150 kN and the loading rate ranged from 3 kN/s to 5 kN/s. For each of the tests, trend lines were fit to the reloading curves (see the results from specimen RG15 in Figure 4-12c). The average slope of the trend lines was determined to be the Young's modulus of the specimen (see Table A-2 in Appendix A for individual test results). The average Young's modulus for all of the specimens was approximately 30 GPa with a standard deviation of 4.7 GPa and a coefficient of variation of approximately 15.7%.
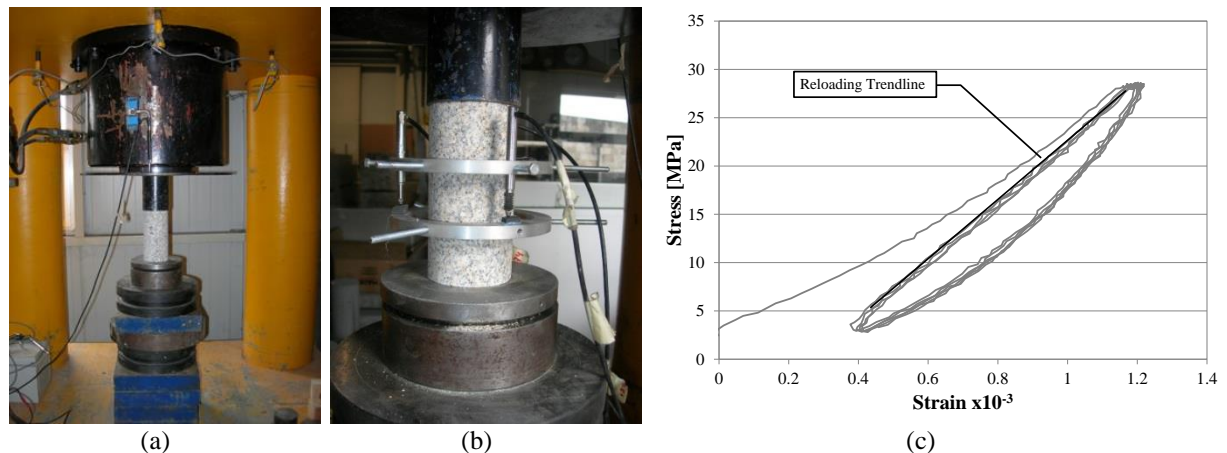
Figure 4-12. Granite cylinder Young's Modulus tests: (a) test frame and specimen support; (b) LVDT set-up; and (c) typical test results – results for specimen RG15 are shown

4.4.4   Compression Tests

The same testing apparatus was used for the compression tests as for the Young's modulus tests. The test set-up was also the same, except that the aluminum rings and LVDTs were not used for measuring the displacement of the middle third of the specimen. Instead, a cylindrical metal grate was placed around the specimen to prevent any small pieces of granite from leaving the test area in case the specimen had a brittle failure. Vertical displacement control and a test speed of 5 μm/s were used for the compression tests. Two typical failure mechanisms for the granite cylinders are shown in Figure 4-13a and b. The results from all of the compression tests are graphed in Figure 4-13c. The values of the compressive strength for each of the test

73

specimens can be found in Table A-2 in Appendix A. The average compressive strength of the granite was 65 MPa with a standard deviation of 12 MPa and a coefficient of variation of approximately 18.5%.
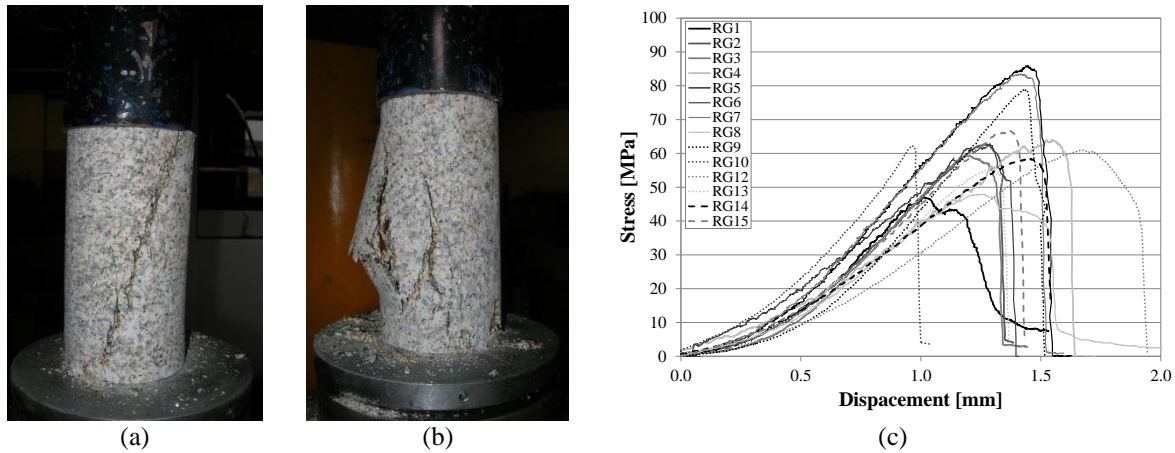
Figure 4-13. Granite cylinder tests: (a) Shear failure mechanism of granite cylinder; (b) cone failure mechanism of granite cylinder; and (c) compression test results from all granite cylinders

4.5   Mortar Cylinders

Mortar cylinders were cast during the construction of the three large masonry walls in the laboratory. These mortar cylinders were later tested to determine the mechanical properties of the mortar used in the masonry walls. The following subsections describe the preparation of the specimens, the Young's modulus and compression test procedure and test results.

4.5.1   Specimen casting and preparation

Mortar cylinders were cast throughout the construction of the three large walls. At least one mortar cylinder was cast from each batch of mortar for the walls. The mortar was cast in cylindrical PVC tubes approximately 70 mm in diameter and 150 mm long, capped at the bottom and open at the top (Figure 4-14a). The mortar specimens were cured in the ambient air temperature and humidity of the laboratory (Figure 4-14b), the same curing conditions as for the masonry walls. The specimens were removed from the PVC tubes approximately two weeks after casting (Figure 4-14c). The mortar cylinders cast from the mortar used in the regular wall construction were cured for a total of 47 days before testing. The mortar cylinders cast from the mortar used in the semi-irregular and irregular wall construction were cured for over three months before testing.

Two days before testing, the mortar cylinders were prepared for the tests. The cylinders cast during the construction of the regular masonry wall were labeled R1 through R20. The cylinders cast during the semi-irregular and irregular wall construction were labeled S1 through S23. Each of the cylinders was weighed and dimensions were taken at quarter points. The average density of the regular wall mortar, specimens R1-R20, was 1735 kg/m^3 with a standard deviation of 40 kg/m^3 and coefficient of variation of 2.31%. The cylinders cast from the mortar used to build the semi-irregular and irregular walls were measured with the cement capping layer already applied, as described below. The average density of the semi-irregular and irregular wall mortar, specimens S1-S23, was 1794 kg/m^3 with a standard deviation of 69 kg/m^3 and coefficient of variation of 3.84%. The measurements of all of the mortar cylinder specimens can be found in Appendix B.

74

A fine cement capping layer was added to the top and bottom of each specimen (Figure 4-14d). This quick hardening cement corrected any irregularities in the surface of the mortar cylinders and ensured good contact with the platens in the test set-up and smooth transfer of the load during testing.

| (a) | (b) | (c) | (d) |
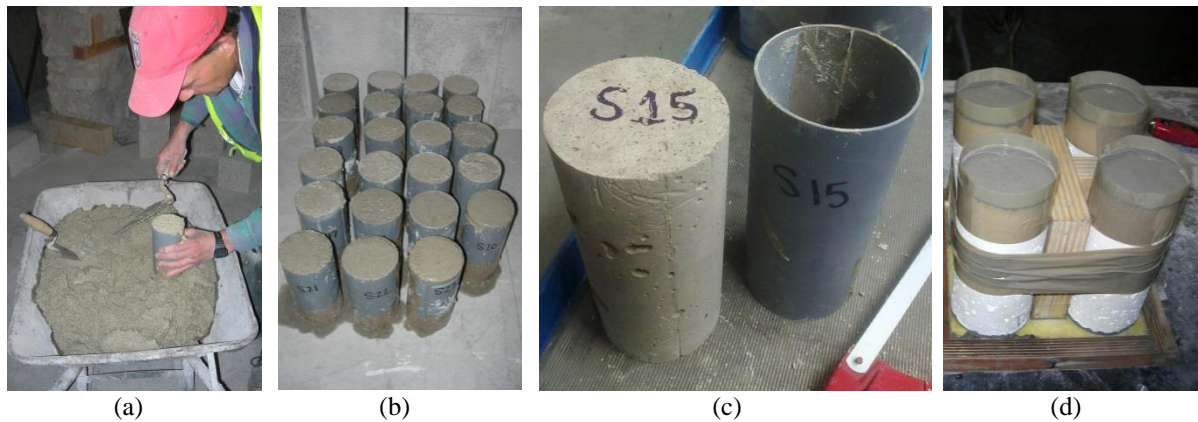
Figure 4-14. Preparation of the mortar cylinder specimens: (a) casting during masonry wall construction; (b) curing; (c) removal from PVC cylinders; and (d) capping ends with a fine cement paste

4.5.2   Mortar Cylinder Compression Tests

The mortar cylinders were tested in uniaxial compression to determine the Young's modulus and compressive strength of the mortar. The test setup and procedure were based on ASTM standards C39/C39M [59] and C469 [60]. Since the mortar was expected to be very weak, it was decided that specimens would not be loaded and unloaded in cycles, but loaded only once. Also due to the weakness of the material, the LVDTs could not be attached directly or via rings as was done in the testing of the granite cylinders. The pressure from tightening the pins on the rings would have caused the specimen to break. Thus, the LVDTs were secured in a stand at the base of the specimen and measured the displacement of the whole length of the specimen. Three LVDTs were placed at third points around the circumference of the specimen. The loading rate was 2 µm/s and was controlled by an additional external LVDT. The test set-up is shown in Figure 4-15a.

Each mortar cylinder was compressed to failure. The typical failure cracking can be seen in Figure 4-15b. The average displacements of the three LVDTs were used to calculate the specimen's strain throughout the test. A typical stress-strain curve is shown in Figure 4-15c. To determine the chord elastic modulus as described in the standard [60], a linear trend line was fit to the linear portion of stress-strain curve. In numerous cases there was a non-linear portion of the test as the specimen adjusted to the initial loading. Therefore, the linear portion of the stress-strain curve was not always in the same range. To accommodate this variability from one test specimen to another, the trend line was fit to a set percentage of the loading curve, 35%, but the range for this percentage varied between 5% and 60% of the ultimate strength of the specimen, depending on the most linear portion of the curve. An example is shown in Figure 4-15c, where the trend line is from 5% to 40% of the ultimate strength.
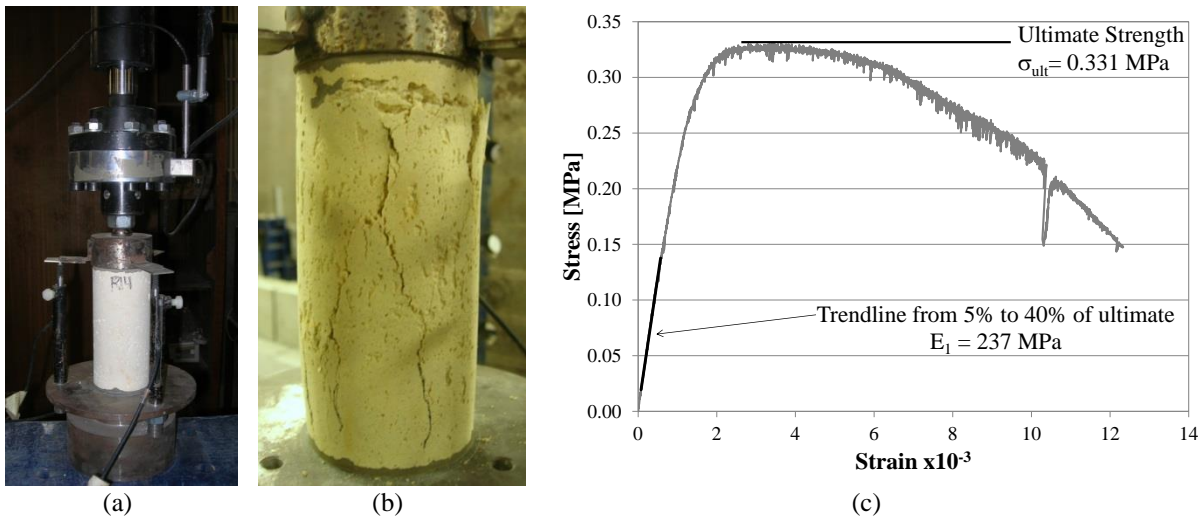
Figure 4-15. Compression testing of mortar cylinders: (a) test set-up; (b) vertical cracking failure mechanism; and (c) typical stress-strain curve showing ultimate strength and trendline used to determine Young's modulus – results for specimen R8 are shown

The results of the compression tests on the mortar cylinders are shown in Figure 4-16. Note the scale of the compressive stress for each graph. The average ultimate strength of the regular wall mortar was 0.327 MPa with a standard deviation of 0.034 MPa and a coefficient of variation of 10.32%. The average ultimate strength of the semi-irregular and irregular wall mortar was 3.08 MPa with a standard deviation of 0.50 MPa and a coefficient of variation of 16.30%. The average Young's modulus of the regular wall mortar was 260 MPa with a standard deviation of 73 MPa and a coefficient of variation of 28%. The average Young's modulus of the semi-irregular and irregular wall mortar was 1017 MPa with a standard deviation of 337 MPa and a coefficient of variation of 33%.
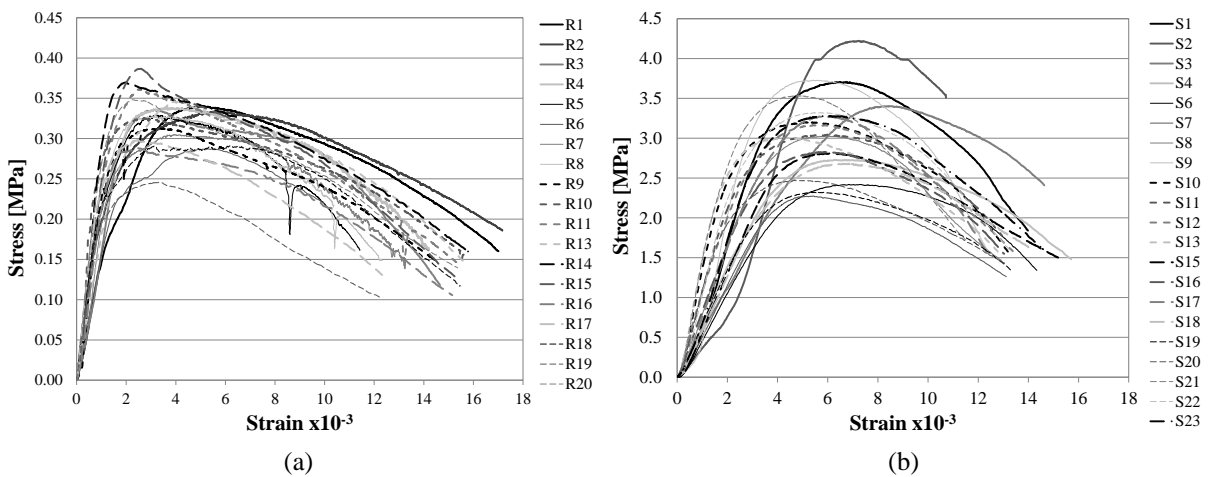
Figure 4-16. Mortar cylinder compression test results: (a) regular masonry wall cylinders; and (b) semi-irregular and irregular wall masonry cylinders

The mortar used to build the semi-irregular and irregular walls was almost ten times stronger and about four times stiffer than the mortar used for the regular wall. As described in the design of the masonry walls in section 4.3, the mortar composition was adjusted to be slightly stiffer and stronger for the semi-irregular and irregular walls. However, it was not intended that they would be this much stiffer and stronger. The difference in material properties had an impact on the properties of the masonry, as shown in the tests on the masonry wallets in the next section, and on the tube-jack and flat-jack tests performed in the walls, as presented in the next chapter.

4.6   *Masonry Wallets*

The mechanical properties and behavior of masonry under compressive loads is different from the individual mortar and granite components. Therefore, these material properties must be determined by testing the masonry as a whole. The large size of the single leaf masonry walls poses issues such as controlling the loading of the wall uniformly in time and obtaining a high compressive stress. For these reasons, small masonry wallet specimens, representative of the three masonry typologies used in the single leaf masonry walls, were constructed. Three masonry specimens were made for each of the three typologies, resulting in nine total small masonry wallets. These wallets were tested in compression to determine their deformability characteristics and estimate their compressive strength. This section presents the design and construction of the specimens, the test set-up and procedure, and results of the Young's modulus and compressive strength tests.

4.6.1   Design and construction

In designing the small masonry specimens, previous works were considered. The uniaxial compressive behavior of masonry can be determined using several different types of specimens. Lourenço [61] describes two tests commonly used, the stacked bond prism and the RILEM test specimen (Figure 4-17). Lourenço noted that according to Mann and Betzler [62], it is unclear what differences there are in the obtained masonry strength between the two test methods. The RILEM test specimen is a more realistic representation of the masonry typology but it also requires a larger, more expensive test specimen.
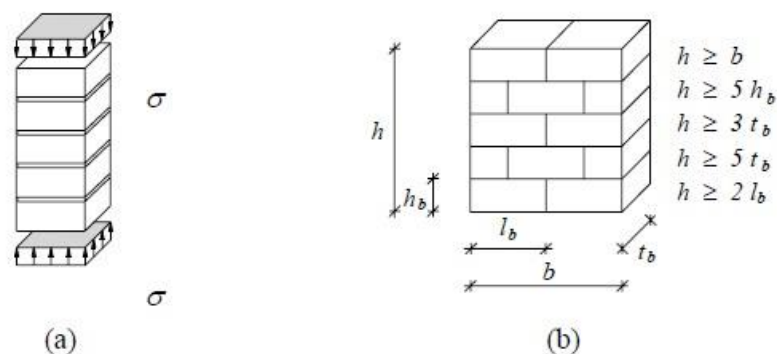
Figure 4-17 Uniaxial Compressive Strength Test Specimens for Masonry: (a) Stacked bond prism; and (b) RILEM specimen [61]

Oliveira [63] did tests on dry stack stone prisms and brick masonry prisms according to RILEM recommendations from 1994. Vasconcelos [5] cited the European Standard's recommendations [64] regarding the preferred geometry of the masonry specimen for compressive testing. This standard recommends wallets that include at least one head joint in the central course of masonry. Vasconcelos found that the technical limitations of the actuators available in the laboratory prevented the use of this standard and stacked prisms of granite were used instead [5]. The stacked prisms tested by Vasconcelos had a height to length ratio of three in accordance with the ASTM E447 (1992) standard. Three cubic stones with sides of 15 cm in length were placed on top of each other with mortar joints of 1 cm. The maximum compressive strength of the specimen consisting of granite blocks and mortar was found to be 37.0 N/mm^2 in this study.

Wallets were chosen for this thesis work to ensure that the typology of the small masonry specimens was representative of the larger single leaf walls. In similarity to Vasconcelos's

findings, these larger wallet specimens were too large to test until failure due to laboratory test machine limitations. However, the compressive strength of the masonry was not of high value for this study since the main objectives were to study the non-destructive or minor destructive tests on the masonry in its elastic range. Hence, the specimens were designed based on the European Standard for compression testing of masonry wallets [64]. Due to the large granite units and thick joints in this masonry, the European Standard could not be strictly adhered to. The design and dimensions of the regular masonry wallets are shown in Figure 4-18a.
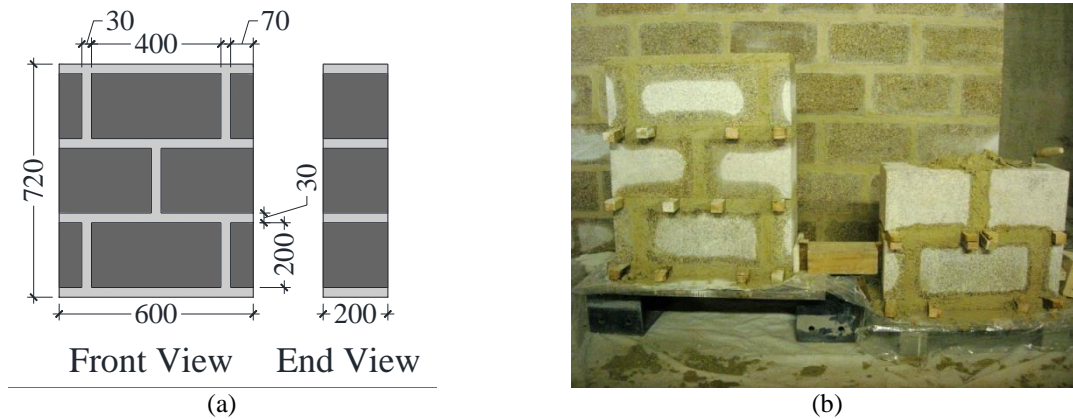
Figure 4-18 Regular masonry wallets: (a) design (dimensions in mm); and (b) construction

Construction of the small masonry wallets was done during the construction of the larger walls of the same typology. The wallets were made with the same mortar and granite units as used for the larger walls of the same typology. Each of the small wallets was built on a steel plate supported on blocks so that it could easily be moved and positioned under the actuator in the reaction frame for testing (see Figure 4-18b). The specimens were labeled after completion, RS1 through RS3 for the regular wallets, SS1 through SS3 for the semi-irregular wallets, and IS1 through IS3 for the irregular wallets.

While the geometry of the regular masonry wallets was almost exactly the same for each wallet, the variabilities in construction resulted in slightly different geometries for each semi-irregular wallet. The geometries and construction of the three semi-irregular wallets are shown in Figure 4-19.
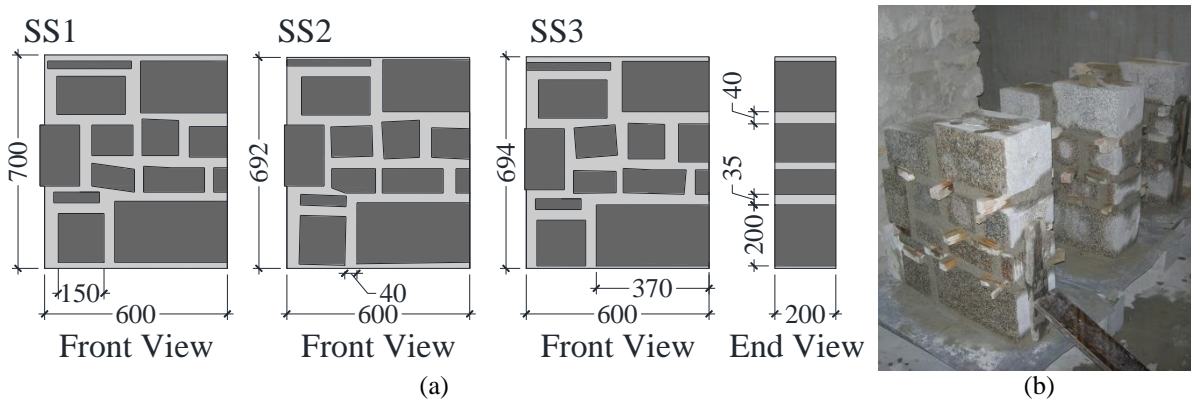
Figure 4-19 Semi-irregular masonry wallets: (a) geometries (dimensions in mm); and (b) construction

The greater irregularity of the granite stones used for the irregular wallets produced wallets with greater irregularity in joint widths and overall dimensions of each specimen. The geometries and construction of the three irregular wallets are shown in Figure 4-20.
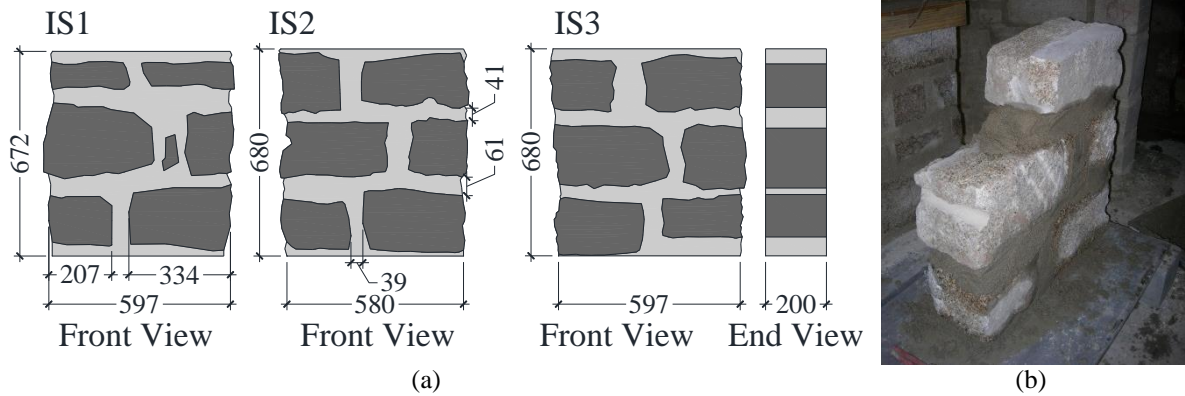
Figure 4-20 Irregular masonry wallets: (a) geometries (dimensions in mm); and (b) construction

4.6.2 Test set-up and procedure

The masonry wallets were tested in a steel reaction frame, which supported the actuator and load cell. The first step in setting up the test was to move the specimen into place under the actuator. Then a thin layer of quick curing cement paste was applied to the top of the specimen to smooth and level the surface and ensure even contact between the specimen and the steel profile that was placed on top of this layer to distribute the load. Figure 4-21 shows the process of preparing the specimens for testing.
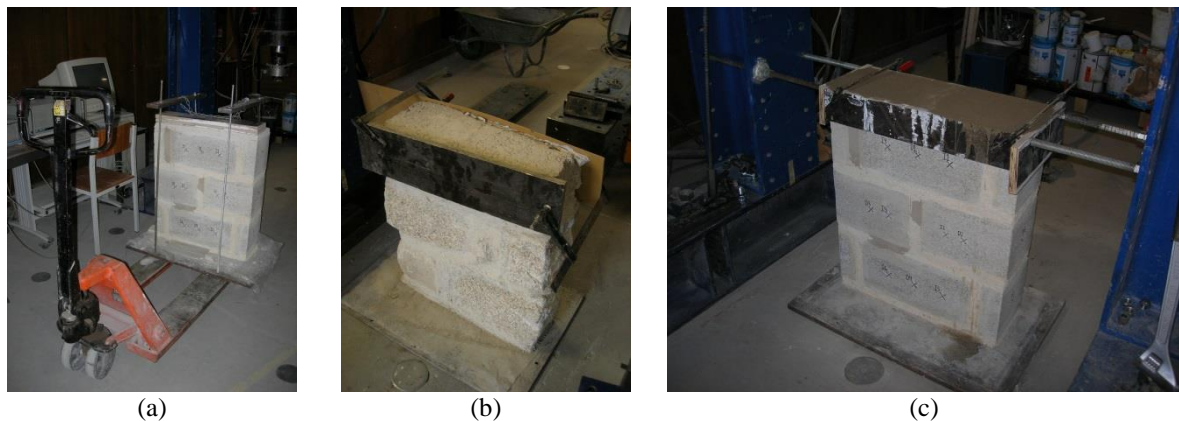
Figure 4-21 Masonry wallet preparation for testing: (a) transporting the specimen to the reaction frame; (b) positioning of formwork; and (c) application of thin mortar paste to the top of the specimen

While the fast curing cement paste was curing, the locations for the LVDTs were measured and marked on the surface of the specimen. The locations for the LVDTs were based on the European Standard [64]. Two vertical LVDTs were positioned on both the front and back of the specimen. These vertical LVDTs spanned over two mortar joints. One horizontal LVDT, spanning over one mortar joint, was used on both the front and the back of the specimen at approximately mid-height. Holes were drilled in the granite units at the marked LVDT locations and screws were used to attach the LVDT holders and stands. The locations, dimensions, and labeling of the LVDTs for the regular wallets are shown in Figure 4-22.
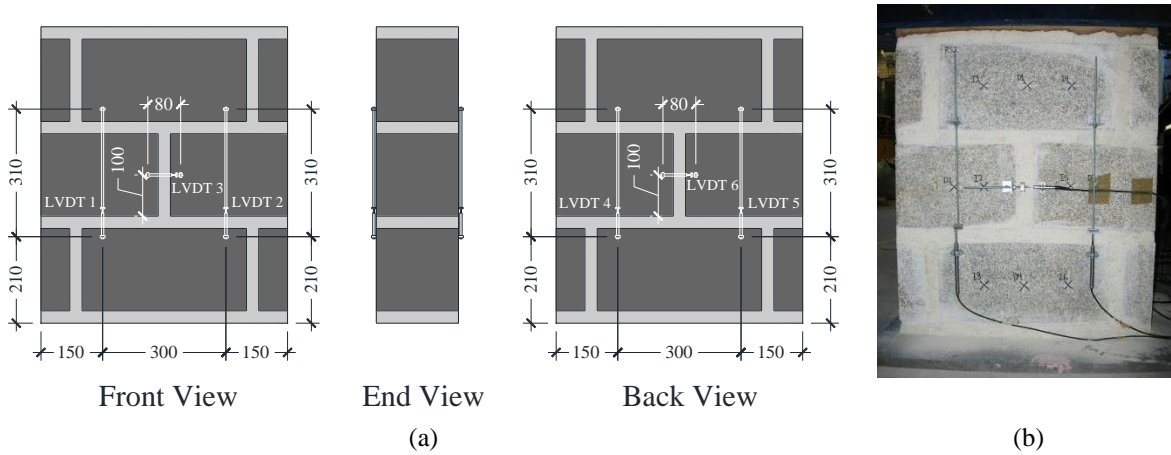
Figure 4-22 Regular masonry wallet LVDT locations: (a) dimensions in mm; and (b) photo of LVDTs attached to the RS2 wallet

A similar configuration for the LVDTs on the semi-irregular wallets was used. In this case however, the horizontal LVDT spanned over three joints and measured over a distance of 500 mm. In order to screw the holders and stands into solid granite, the span of the vertical LVDTs was also increased to 390 mm. The labeling of the LVDTs was the same. LVDTs 1, 2, 4, and 5 measured vertically and LVDTs 3 and 6 measured horizontally. The layout and dimensions of the LVDTs for the semi-irregular wallets is shown in Figure 4-23.
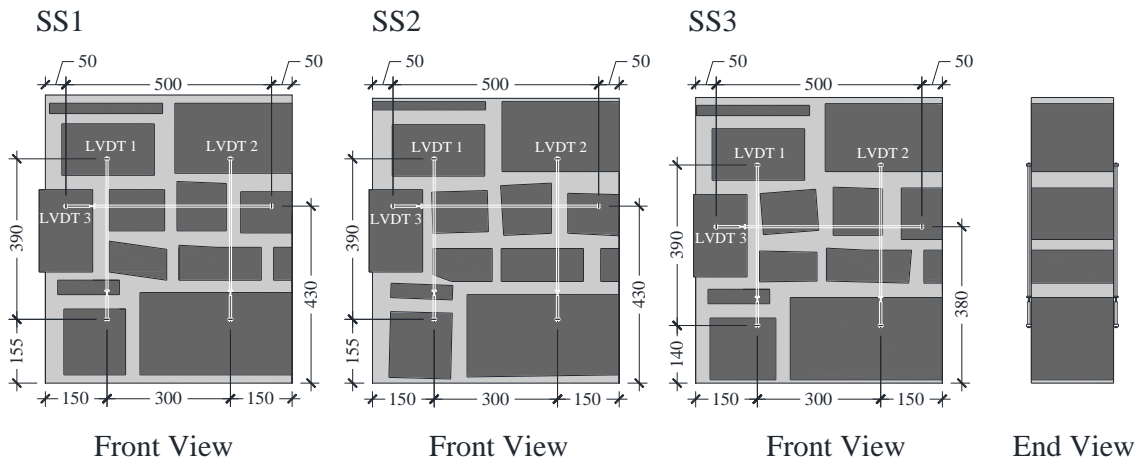
Figure 4-23 Semi-irregular masonry wallet LVDT locations

All three of the irregular wallets had the same dimensions and spacing for the LVDTs. To accommodate the irregular stones, the vertical LVDTs spanned over a distance of 480 mm and the horizontal LVDTs spanned over a distance of 400 mm. The labeling of the LVDTs was the same as for the regular and semi-irregular wallets. The dimensions and layout of the LVDTs on the three irregular wallets is shown in Figure 4-24.
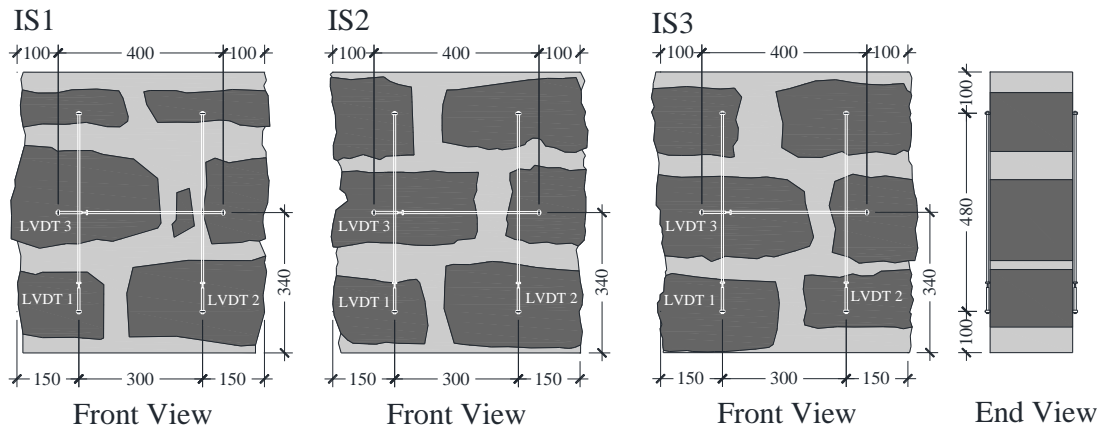
Figure 4-24 Irregular masonry wallet LVDT locations

Once the LVDTs were installed, the formwork for the thin cement paste was removed, and the steel profile was placed on top, the specimen was ready for testing. The complete test set-up is shown in Figure 4-25.
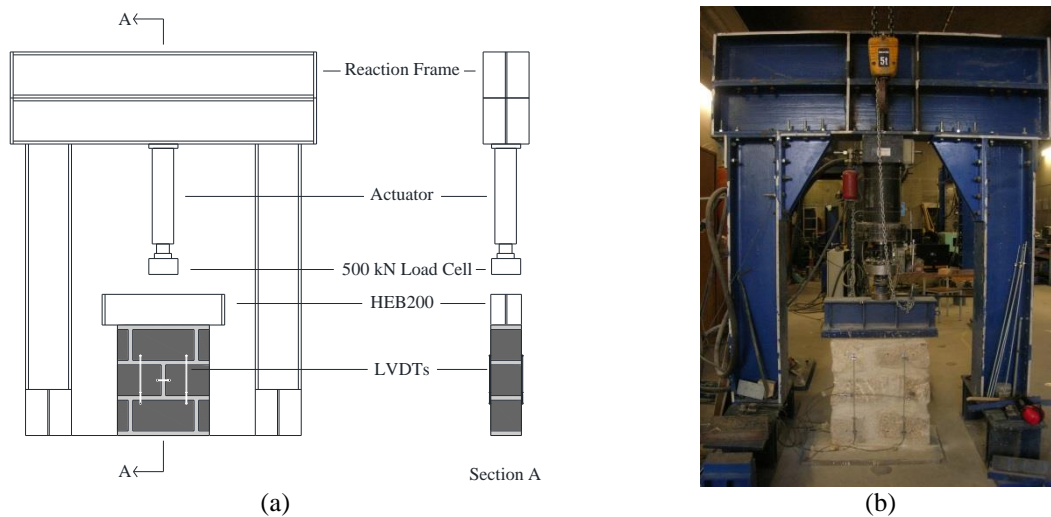
Figure 4-25 Complete test set-up for small masonry wallet tests: (a) schematic; and (b) photo

4.6.3 Young's Modulus Tests

Cyclic compression tests were performed on the small masonry wallets to determine the Young's modulus of each masonry typology. Each specimen was loaded and unloaded three times up to a maximum load of approximately half of the ultimate strength of the masonry. Thus, to determine the maximum load for the test a preliminary estimation of the ultimate strength had to be made. The compressive strength of the masonry was estimated to be 2.25 MPa using the European Standard 1996-1-1 part 3.6.1.2 [65]. The estimated ultimate strength was equivalent to a 270 kN load based on the cross-sectional area of the specimens. Half of this load, 135 kN, was reduced further to 60 kN due to the low mortar strength. Thus, the first specimen, RS3, was tested with a loading rate of 0.1 kN/s and a maximum load of 60 kN. Following the first Young's Modulus test, the results of the first compressive test on the RS3 specimen revealed that the compressive strength of the masonry was much higher than the estimated value. The rest of the regular and semi-irregular masonry wallets were tested with a loading rate of 0.3 kN/s and a maximum load of 250 kN. The irregular wallets were tested with a loading rate of 0.3 kN/s but the maximum load was reduced to 200 kN.

The results of the Young's modulus test on the RS3 specimen were not accurate due to the low level of stress in the specimen in comparison with the real compressive strength of the masonry. During the Young's modulus test of the RS2 specimen, it was discovered that there was a small eccentricity in the loading by the actuator that was resulting in bending and tipping of the specimen. Thus, the RS3 and RS2 results were discarded. The eccentricity of the actuator was corrected for the RS1 specimen testing and the remainder of the semi-irregular and irregular tests. RS1 results are presented in Figure 4-26.
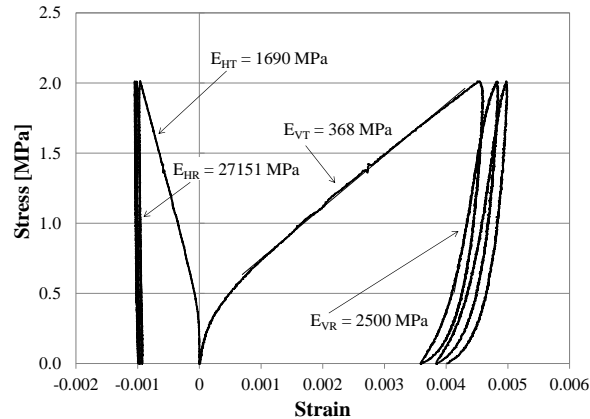
Figure 4-26 Results of the RS1 Young's modulus test

These results show the stress-strain behavior of the regular masonry wallet as recorded by the LVDTs. The positive strain curve is the average strain of the four vertical LVDTs due to their downward displacement during loading of the specimen. The negative strain curve is the average strain of the two horizontal LVDTs due to the outward expansion of the specimen as it was compressed.

Four moduli are indicated on the results graph. The initial loading tangent modulus, E_{VT}, is the slope of the linear portion of the initial loading curve from a stress level of 0.6 MPa to approximately 2.0 MPa. This stress-strain relationship occurs in the masonry the first time the masonry is subjected to that amount of stress. After the initial loading, the stress-strain relationship changes. This is why the slope of the second cycle of loading is different.

The reloading modulus, E_{VR}, is the slope of the linear portion of the reloading curve. During double tube-jack and flat-jack testing, the masonry is unloaded when the slots are cut and then reloaded during pressurization of the jacks. Thus, the tube-jack and flat-jack tests measure the reloading modulus of the masonry. However, depending on the capabilities of the jacks, these tests measure the reloading modulus at a lower stress level, as is described in the following chapter. If the stress level during tube-jack and flat-jack testing goes beyond the stress level previously seen by the masonry, the slope of the stress strain curve will change at this point to the slope of the initial loading modulus because the masonry is seeing that level of stress for the first time. This effect will be exemplified both in the compression tests on the masonry wallets in the next section and in the flat-jack testing presented in the next chapter.

The horizontal initial loading tangent modulus, E_{HT}, and horizontal reloading tangent modulus, E_{HR}, are also shown on the graph. These were used to determine the Poisson ratio of the masonry.

The results of the Young's modulus tests on specimens SS1 and SS2 are presented in Figure 4-27.

(a)　　　　　　　　　　　　　　　(b)
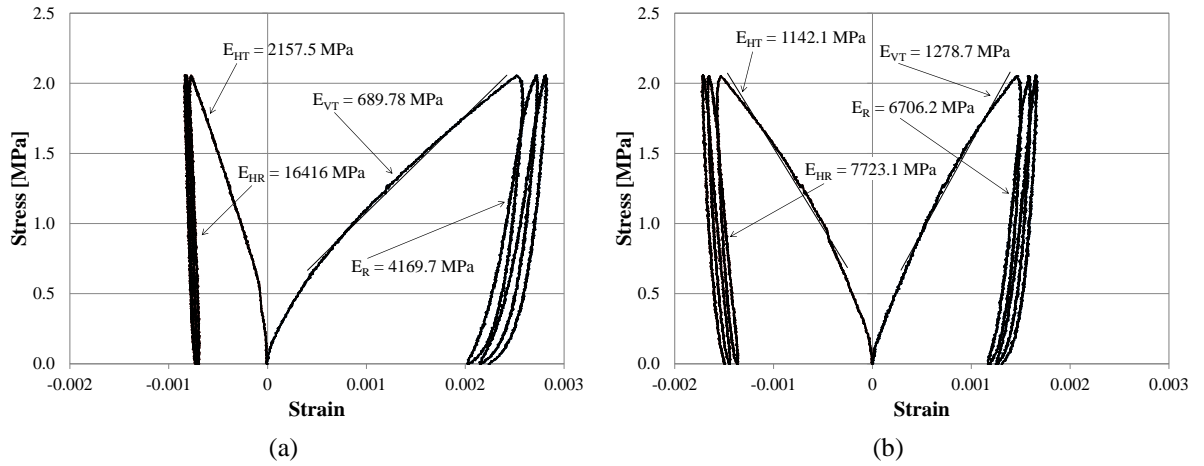
Figure 4-27 Results of the Young's modulus test on semi-irregular wallet specimens: (a) SS1; and (b) SS2

The results of the Young's modulus test on the third semi-irregular wallet are shown in Figure 4-28, along with a photo of the test.

(a)　　　　　　　　　　　　　　　(b)
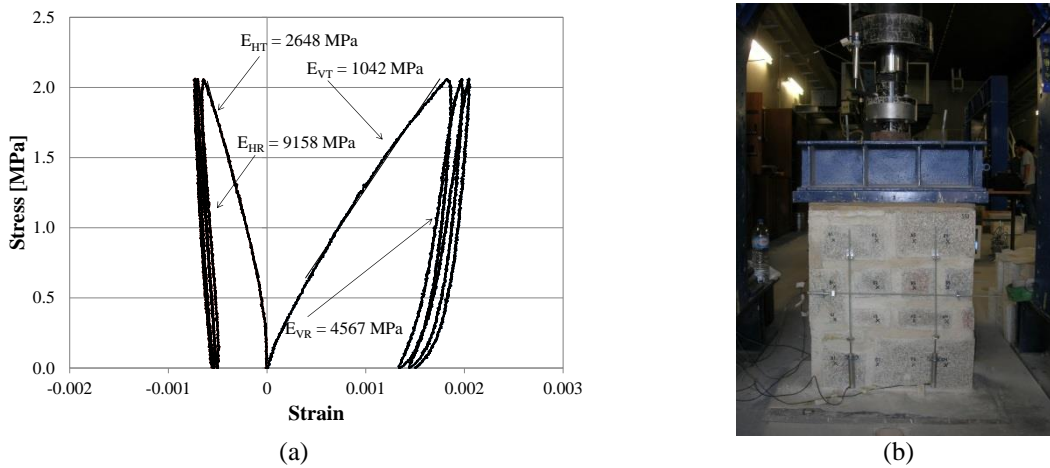
Figure 4-28 Young's modulus test on semi-irregular wallet SS3: (a) results; and (b) photo

The results of the Young's modulus tests on the irregular wallet specimens IS1 and IS2 are shown in Figure 4-29.

(a)　　　　　　　　　　　　　　　(b)
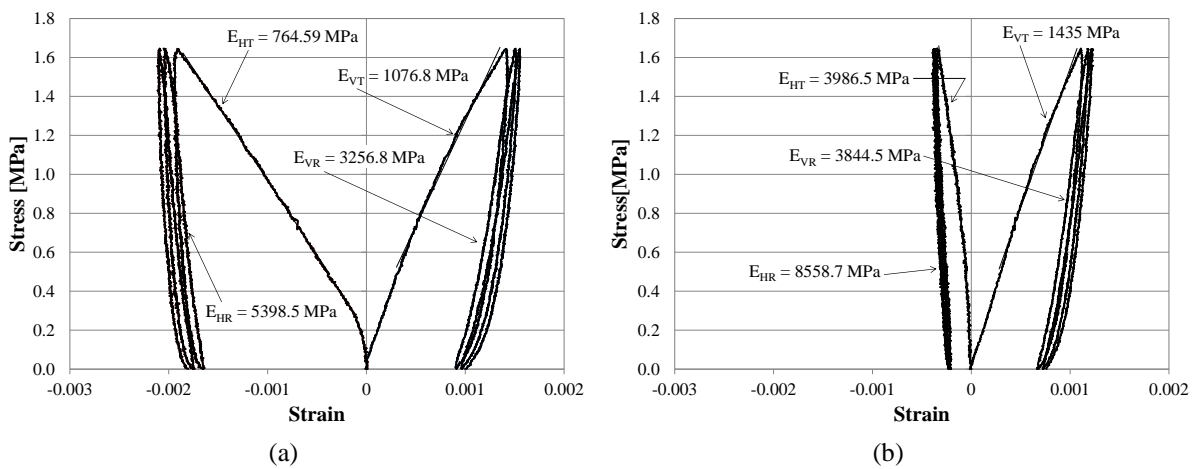
Figure 4-29 Results of the Young's modulus test on irregular wallet specimens: (a) IS1; and (b) IS2

The results of the Young's modulus test on the third irregular wallet are shown in Figure 4-30, along with a photo of the test.

| (a) | (b) |
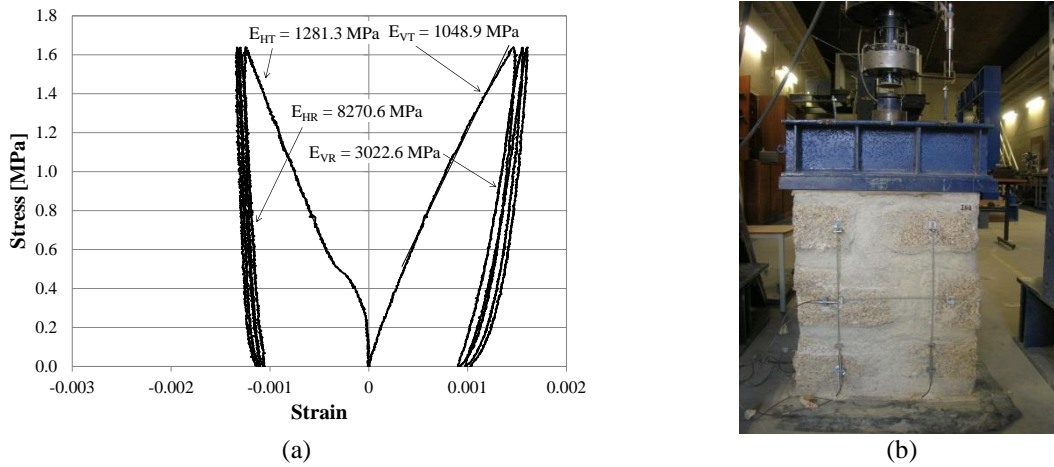
Figure 4-30 Young's modulus test on irregular wallet IS3: (a) results; and (b) photo

The average results of all of the Young's modulus tests on the small masonry wallets are presented in Table 4-1. For a complete table of results including standard deviations, and coefficients of variation see Appendix C.

Table 4-1 Average initial vertical loading modulus of elasticity and vertical reloading modulus of elasticity for the small masonry wallet Young's modulus tests

Masonry Typology	E_{VT}			E_{VR}		
	Average	St. Dev.	CV	Average	St. Dev.	CV
	[MPa]	[MPa]	[%]	[MPa]	[MPa]	[%]
Regular	368	-	-	2500	-	-
Semi-irregular	1003.6	296.4	29.5	5147.6	1364.3	26.5
Irregular	1186.9	215.3	18.1	3374.6	423.4	12.5

A graph comparing all of the Young's modulus tests performed on the masonry wallets is shown in Figure 4-31.
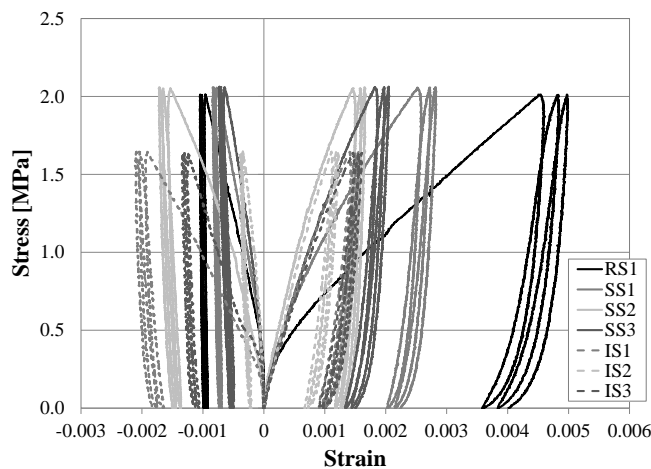
Figure 4-31 Comparison of all of the small masonry wallet Young's modulus tests

Note that in Figure 4-31 the vertical strain in the RS1 specimen is much larger than in the other specimens. This equates to a much lower modulus of elasticity, as shown in Table 4-1. The regular masonry wallets contained a mortar with a much lower strength and stiffness than both the semi-irregular and irregular masonry wallets, as presented in section 4.5.2. The results of the Young's modulus tests on the masonry wallets seem to have been greatly influenced by the properties of the mortar. A comparison of the mortar elastic modulus with the masonry initial loading elastic modulus is shown in Table 4-2.

Table 4-2. Comparison of mortar and masonry elastic modulus results

Masonry Typology	Masonry E_{VT}			Mortar E_{VT}		
	Average [MPa]	St. Dev. [MPa]	CV [%]	Average [MPa]	St. Dev. [MPa]	CV [%]
Regular	368	-	-	260	73	28
Semi-irregular	1003.6	296.4	29.5	1017.0	337.0	33.0
Irregular	1186.9	215.3	18.1			

Finally, the Poisson ratios for each of the tests were calculated based on the initial loading curves and the reloading curves. The results are presented in Table 4-3. The Poisson ratios calculated from the slopes of the initial loading curves were, on average, higher than the Poisson ratios found for the reloading curves. Overall, the Poisson ratio estimations are higher than the maximum theoretical value of 0.5 and are higher than typical values found for masonry in the literature [66].

Table 4-3 Poisson Ratio results for the masonry wallet tests

Masonry Specimen	Initial Loading Curves			Reloading Curves		
	Poisson Ratio	Average	CV	Poisson Ratio	Average	CV
RS1	0.218	0.218	-	0.092	0.092	-
SS1	0.319			0.254		
SS2	1.123	0.612	72.6%	0.869	0.541	57.2%
SS3	0.392			0.499		
IS1	1.412			0.604		
IS2	0.361	0.864	61.0%	0.449	0.472	25.6%
IS3	0.820			0.365		

4.6.4   Results of the Compression Tests

Compression tests were performed on each of the masonry wallets after all other testing on each wallet was complete. The test set-up was the same as for the Young's modulus tests except that displacement control with an external LVDT was used to load the specimen. The loading rate was 5 μm/s. All of the specimens were loaded to 500 kN, the capacity of the testing equipment. However, none of the specimens failed or yielded at this maximum load, equivalent to a stress level of 4.17 MPa. Thus, the compressive strength of all three masonry typologies was greater than 4.17 MPa. Figure 4-32 shows the results of the compression tests on the masonry wallets. The displacements of the vertical LVDTs on both sides of each specimen were used to determine the average strain in the specimen in comparison with the stress level. Since each of the specimens had been previously loaded for both the Young's modulus and sonic tests, there

is a steep reloading curve shown at the lower stress levels. Once the stress level went beyond what the specimen had seen previously, the stress-strain relationship became linear again with a lower stiffness trend.
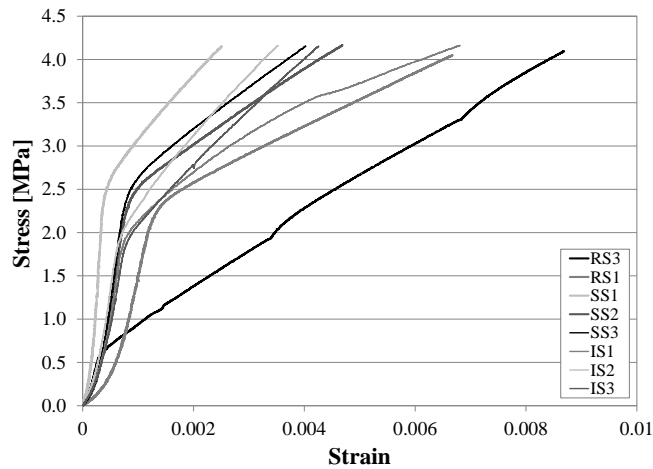
Figure 4-32 Results of the masonry wallet compression tests

While overall failure was not observed in either the collapse of the specimen or the stress-strain data collected from the test, some damage was observed during the tests. Separation between the granite units and the mortar joints as well as spalling of some mortar was evident in all of the specimens (see Figure 4-33a). In specimen SS1 one crack was observed in the smallest granite unit where it was likely experiencing flexure at the head joint between the two units above (see Figure 4-33b). In general, cracking was observed throughout the mortar joints as highlighted by the markings tracing the visible cracks in Figure 4-33c.

| (a) | (b) | (c) |
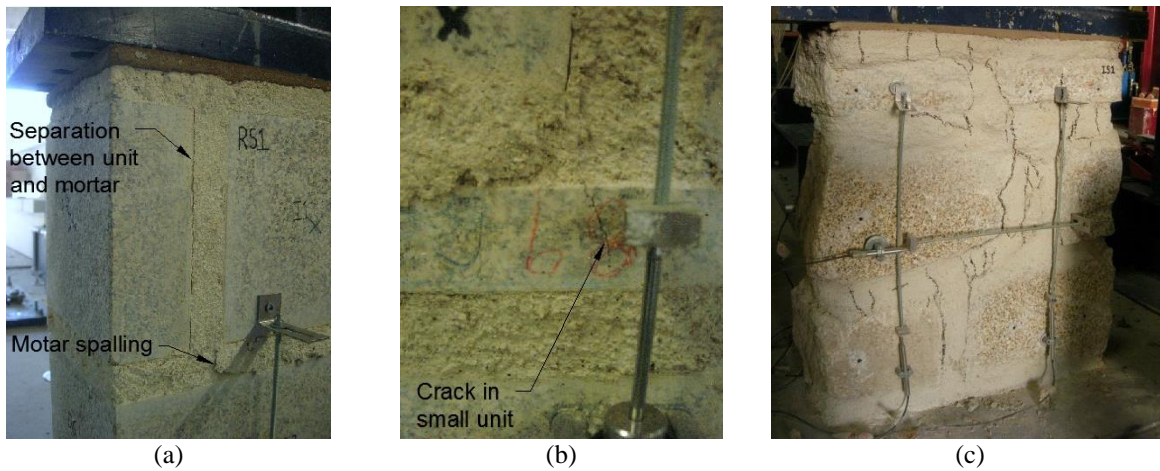
Figure 4-33 Damage observed in the masonry wallets during the compression tests: (a) separation between units and mortar, and mortar spalling; (b) crack in small unit in SS1 specimen; and (c) cracks traced in mortar joints

4.7   Conclusions

In this chapter the design and construction of three masonry walls with three different masonry typologies based on traditional masonry found in Northern Portugal, which were intended for testing the tube-jack and flat-jack tests, was presented. The mechanical characteristics of the granite units and mortar used to construct the wall were determined by performing Young's modulus and compression tests on mortar cylinders and granite cores. The results of these tests

showed the granite to have an average elastic modulus of 30 GPa and an average compressive strength of 65 MPa. The mortar used for the regular masonry wall was very weak with an elastic modulus of 260 MPa and a compressive strength of 0.327 MPa. It was decided after testing the regular wall that the mortar in the semi-irregular and irregular walls should be adjusted to be slightly stiffer. However, the result was a much stiffer mortar with an average elastic modulus of 1017 MPa and an average compressive strength of 3.08 MPa.

The properties of the units and mortar can give a basis for the mechanical properties of the masonry as a whole but it is best to test the masonry to get a better estimate. Thus, masonry wallets of each typology were constructed and tested to determine their elastic modulus and compressive strength. The results of these tests showed two stress-strain relationships, an initial loading modulus and a reloading modulus. The initial loading modulus was very similar to the elastic modulus found for the mortar specimens. Since the tube-jack and flat-jack tests will mostly be reloading the masonry after its original loading, the reloading modulus will usually be compared between the tests. Finally, the masonry wallets were tested to the capacity of the testing machine. None of the specimens failed, indicating that the compressive strength of the masonry was greater than 4.17 MPa.

5.   TUBE-JACK AND FLAT-JACK TESTING IN LABORATORY WALLS

5.1   Introduction

Tube-jack and flat-jack tests were performed on the three large masonry walls that were built in the laboratory for this purpose. The construction of the regular, semi-irregular and irregular walls and their characterization was described in Chapter 4. The purpose of the tube-jack tests in these walls was to test the tube-jack system in controlled laboratory conditions before testing the system in-situ. The goal was to perform as many tube-jack tests as possible in each wall to evaluate the consistency and the repeatability of the test and to maximize the opportunities for analysis of the particularities of the test. The purpose of performing flat-jack tests in these walls was to both assess the capability of the flat-jack method in determining the state of stress and the Young's modulus in this type of large unit masonry and to compare the flat-jack test method with the tube-jack test method in the same masonry walls under the same laboratory conditions.

This chapter presents the results of the tube-jack and flat-jack tests in the masonry walls that were carried out in the Structural Laboratory at University of Minho (LEST), in the order in which they were tested, the regular masonry wall, the semi-irregular masonry wall, and then the irregular masonry wall. Following these three subsections a final section is devoted to discussing and comparing the results from all of the walls.

5.2   Regular Masonry Wall

The first wall that was constructed and tested was the regular masonry wall. The testing was performed on this wall first because it had the simplest design and most regular construction. This would make it the easiest to understand when interpreting the results from the tests.

The wall was loaded from above to simulate the load from additional masonry and loads from levels above in a traditional masonry structure. A rubber mat was placed on top of the wall to provide uniform contact between the wall and the load above. Two hydraulic jacks were used to load the wall by applying pressure to a reaction floor above. The load was applied a day in advance of each test to allow the wall to stabilize and the pressure in the hydraulic jacks was checked and kept constant throughout each test. To distribute the load from the hydraulic jacks to the wall, a 20 cm × 20 cm × 2 m long H steel profile was placed between the rubber mat and the hydraulic jacks. To increase the height of the hydraulic jacks, they were placed on granite blocks above the steel profile. For most of the tests, the pressure in the hydraulic jacks loading the wall was 2.82 MPa, which equated to an applied pressure of 0.2 MPa on the top of the wall. Differences in loading for individual tests are discussed in the following subsections. For each test the stress state in the wall at the joint being tested was calculated based on the pressure in the hydraulic jacks loading the wall and the weight of the masonry and equipment above the joint. This loading set-up was used for all three of the masonry walls and is shown in Figure 5-1.

Several single tube-jack tests, a double tube-jack test, a single flat-jack test and a double flat-jack test were performed on the regular masonry wall. The tube-jack tests were performed first on the left side of the wall and then the flat-jack tests were performed on the right side of the wall. The test set-up, procedure and results for each test are presented in the following subsections.
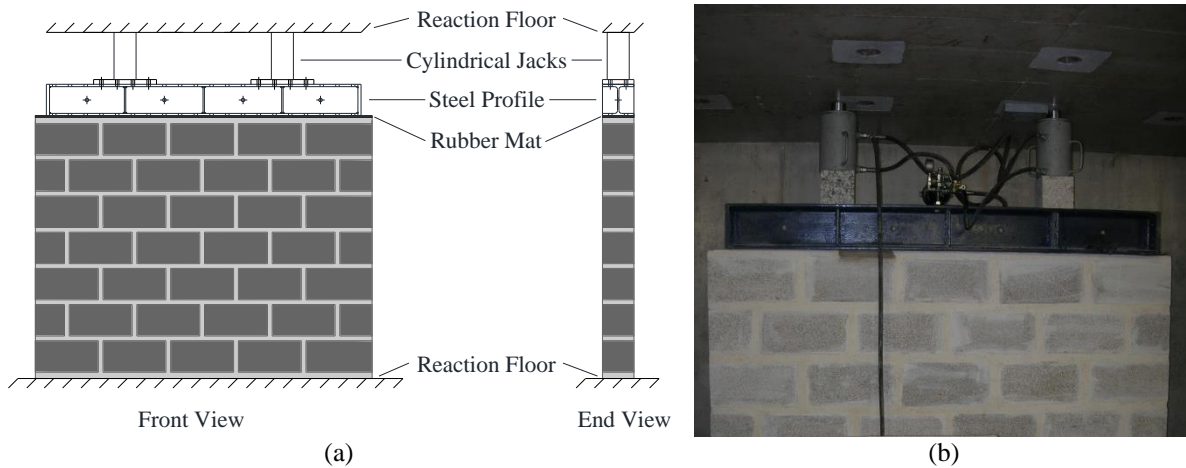
Figure 5-1 Loading of masonry walls: (a) Schematic layout; and (b) Photo of loading the regular wall

5.2.1   Single Tube-Jack Tests

Single tube-jack tests were performed in three of the horizontal mortar joints of the regular granite masonry wall. These were the first single tube-jack tests to be performed using the water pressure system as described in Chapter 3. To prevent holes from previous tests from influencing subsequent tests, the holes were filled with mortar, which was allowed to harden, before subsequent tests were performed.

The set-up for each of the single tube-jack tests was the same, except where noted in the following sections. The holes for the tube-jacks were spaced approximately 7.5 cm from center to center. The holes were labeled Hole 1 through Hole 12 from left to right.

Eight LVDTs were used to measure the relative displacement of the masonry, four on the front of the wall and four on the back. The measuring ranges of the LVDTs were ±2.5 mm for LVDTs 1-5, ±10 mm for LVDTs 6-7 and ±7.5 mm for LVDT 8. The placements of the LVDTs were between the 2nd and 3rd holes, between the 5th and the 6th holes, between the 7th and the 8th holes, and between the 10th and 11th holes, on both sides of the wall. They were labelled LVDT 1 through 4, respectively, on the front of the wall and LVDT 5 through 8, respectively, on the back of the wall, as shown in Figure 5-2.
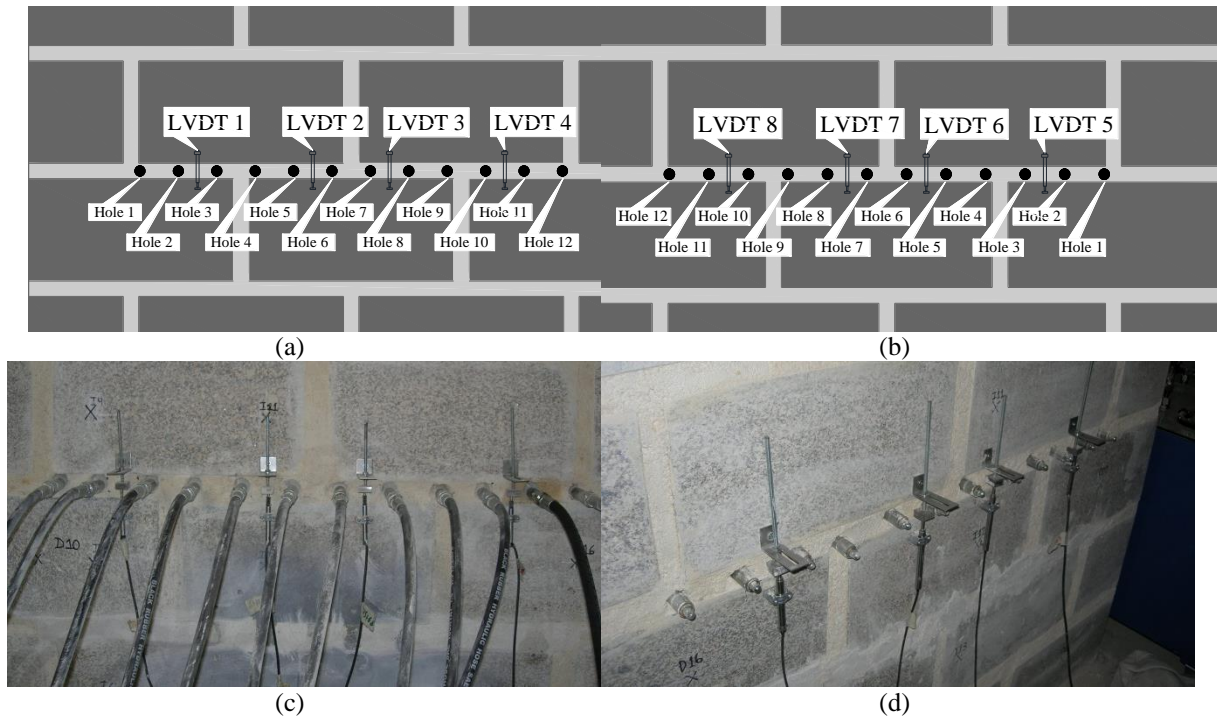
Figure 5-2 Holes and LVDT positions for the single tube-jack tests: (a) front of the wall; (b) back of the wall; (c) tube-jacks inserted in the front of the wall; and (d) tube-jack ends sticking out the back of the wall

During the test, the holes for the tube-jacks were drilled starting with the center holes and then working toward the outer holes. The LVDTs recorded the relative displacements both during the drilling process and after the drilling was complete. The tube-jacks were not inserted into the holes or pressurized until the wall had stabilized and the movement of the LVDTs had reduced to nearly zero.

Following all of the tests on the regular masonry wall, the holes drilled for the last test in the fifth horizontal joint were injected with foam. The wall was dismantled and the foam pieces extracted carefully. The diameter of each foam piece was measured every five centimeters. The process is shown in Figure 5-3 and the results are shown in Appendix D. The results were averaged and used as the average diameter of the tube-jack holes. The average diameter, 26 mm, is assumed to be the outer diameter of the deformed tube when the tube-jack is inflated to the size of the hole. This value was used in the calculation of the pressure applied to the masonry by the tube-jacks, p_m, as described in section 2.3.2 and equation (32).
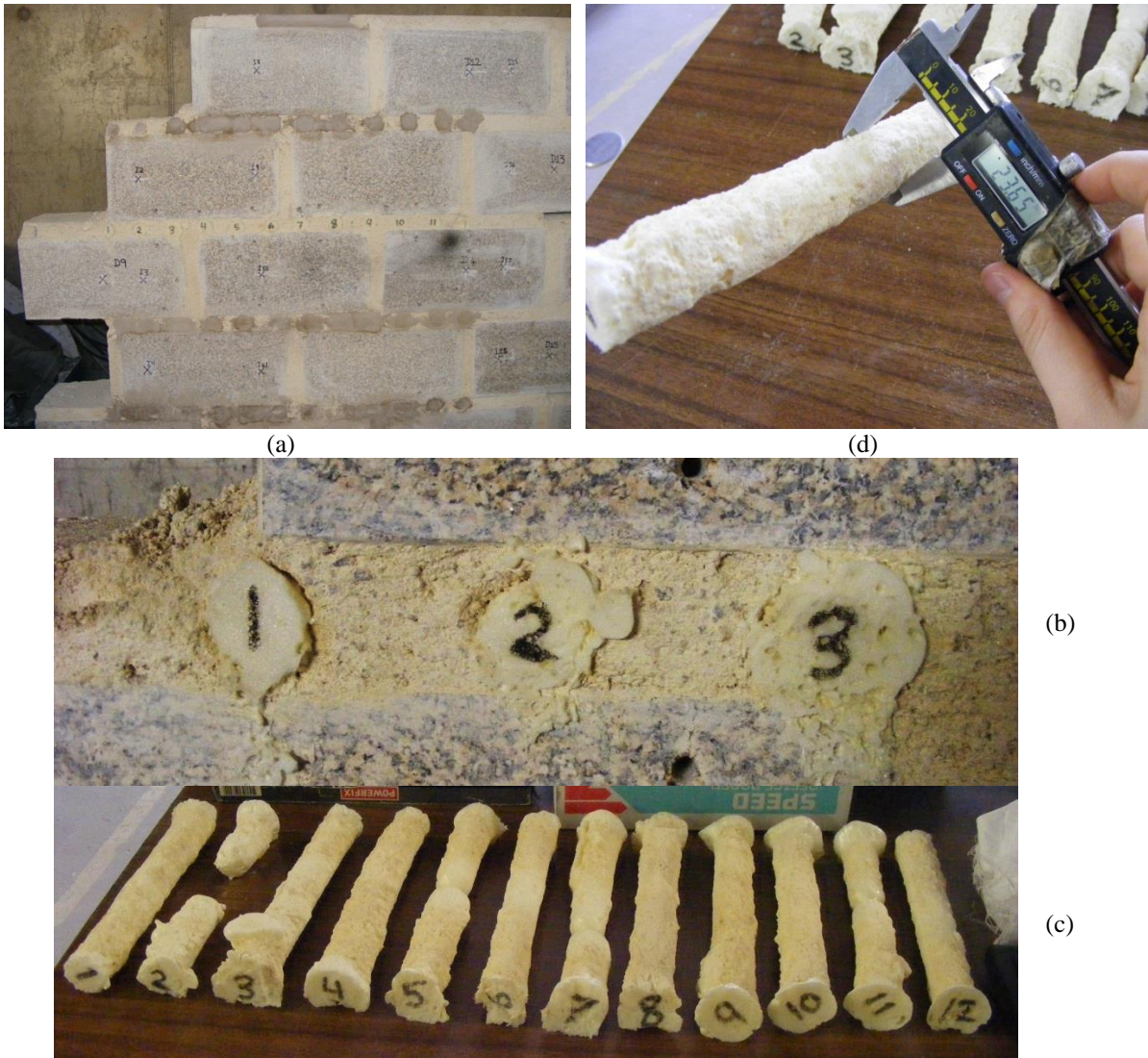
Figure 5-3 Foam used to determine the hole diameters: (a) regular wall being deconstructed to remove foam; (b) close-up of foam in the holes; (c) removed foam pieces; and (d) measuring the diameter of each piece

The area correction factor for the single tube-jack tests was calculated following the tests. Since the tube-jacks expand to fill the holes, the area correction factor can be simplified to the ratio of the average contact length of the tubing material to the wall thickness (20.0 cm). The average contact length of the tubing material was measured to be 16.5 cm. Thus, the area correction factor, k_A, for the single tube-jack tests was 0.825. The area correction factor was multiplied by the pressure applied to the masonry by the tube-jacks, p_m, to produce the applied pressure, $p_{Applied}$, which is shown in the graphs in the following sections. At the point when the average LVDT displacements are restored to zero, the applied pressure value is an estimate of the stress state in the masonry.

5.2.1.1 Single Tube-jack Test in the 3rd Horizontal Joint

The first complete tube-jack test performed on the regular granite masonry wall was conducted in the 3rd horizontal mortar joint up from the base of the wall, where the stress level was calculated to be approximately 0.23 MPa. Rubber tube-jacks were used for this test.

The drilling results of the test are presented in Figure 5-4. It can be seen in Figure 5-4a that while most of the movement of the masonry is complete shortly after the holes had been drilled, movement was observed for over one hour as the wall stabilized. Figure 5-4b shows the average relative displacement of all of the LVDTs, approximately 8.5 μm, and the average of the front and back LVDTs separately. This graph shows that the front of the wall had a much more negative relative displacement than the back of the wall. It was discovered that the steel profile on top of the wall was out of alignment and causing a slight eccentricity of the loading resulting in a higher stress level on the front of the wall than on the back. Following the test, the alignment of the steel profile was corrected by moving the steel profile slightly towards the back of the wall.

Figure 5-4 Hole drilling results for the 3rd horizontal joint: (a) individual LVDT relative displacements; and (b) average LVDT relative displacements

Once the wall had stabilized, the tube-jacks were inserted and three pressurizations performed (see Figure 5-5a). After the first pressurization, the wall was allowed to stabilize again before the second pressurization. After each pressurization it can be seen that the front LVDTs show a drop in relative displacement and the back LVDTs show an increase in relative displacement. This can be attributed to the larger stress on the front of the wall than on the back of the wall. In Figure 5-5b the relative displacements are compared to the applied pressure over time. When the applied pressure is negative the water pressure in the tube-jacks is being used to inflate the tube-jacks to the size of the holes. When the applied pressure reaches zero the water pressure inside the tube-jacks has reached a point when it has inflated the tube-jacks to the size of the holes and counteracted the containing hoop stress applied by the tubing material itself and is now starting to apply pressure to the masonry surrounding the holes. Comparing this time point with the average relative displacement of the masonry as shown by the LVDTs, it can be seen that this is the same point when the LVDTs start to move and react to the pressure being applied.
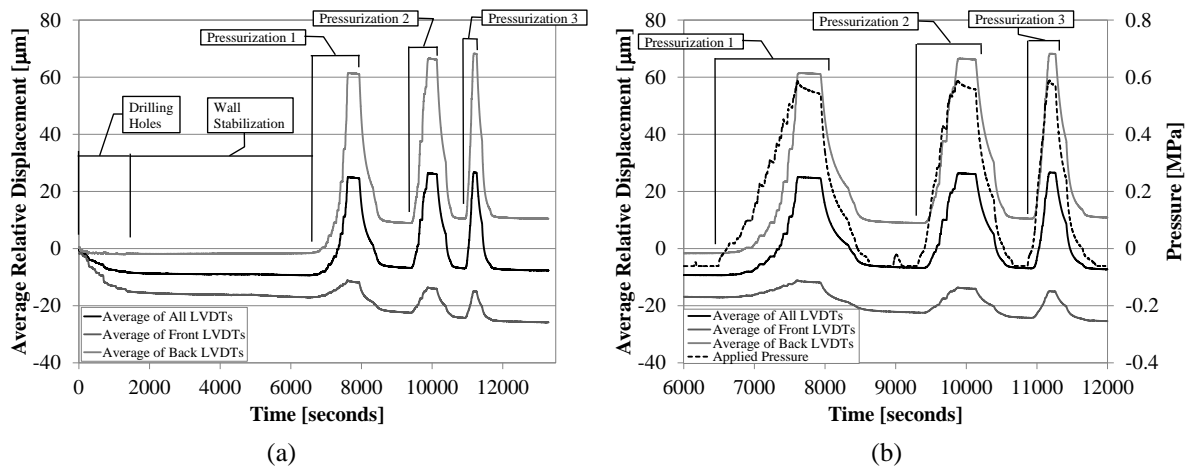
Figure 5-5 Relative displacement results: (a) over the course of the entire test; and (b) during the pressurizations as compared to the applied pressure

Figure 5-6 shows the applied pressure versus the average relative displacement results. The lower curve of each pressurization cycle is the loading portion and the upper curve is the pressure release portion of the cycle. The applied pressure value when the average relative displacement has reached zero on the loading curve estimates the state of stress in the masonry. The first pressurization has a different curvature because the masonry is adjusting to being pressurized by the tube-jacks. A similar effect occurs in flat-jack testing as noted by Binda et al. [36]. Pressurizations 2 and 3 come closest to the calculated stress level and estimate it to be 0.26 MPa, with an error of 13%.
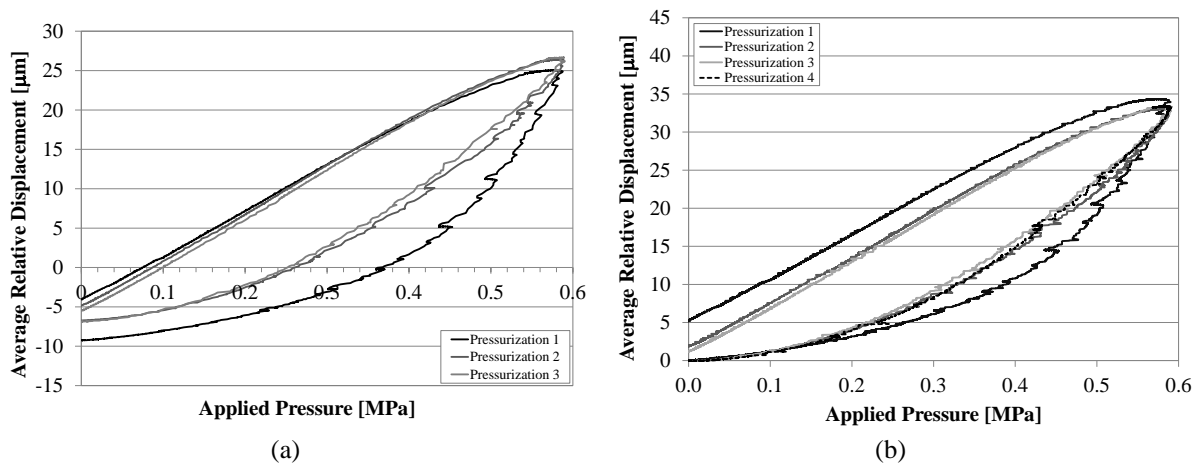
Figure 5-6 Tube-jack test applied pressure vs. relative displacement results for the 3rd horizontal mortar joint (a) during the first test; and (b) subsequent pressurization in comparison with the first test, with initial LVDT relative displacements zeroed for each pressurization

Three days after the single tube-jack test in the third horizontal joint, a pressurization test was performed in the same joint and holes and with the same set-up as the previous test. Since the holes were not drilled at the same time as the test and the wall had been allowed to settle during the previous three days, this was not considered a complete single tube-jack test. The tube-jacks were pressurized to approximately 0.8 MPa of internal water pressure. At this pressure, tube-jack #2 burst, reducing the pressure in the jacks to zero and ending the test. The results, labelled Pressurization 4, are shown in Figure 5-6b in comparison with the pressurizations from the first test. After the initial pressurization, all subsequent pressurizations followed approximately the same pressure-displacement curve.

5.2.1.2 Single Tube-jack Test in the 4th Horizontal Joint

Following the single tube-jack test in the 3rd joint, a double tube-jack test was performed in the 3rd and 6th horizontal joints of the regular wall. This double tube-jack test is described in section 5.2.3. The holes from the tests in the 3rd and 6th joints were filled with a quick curing cement mortar while zero load was applied to the top of the wall (see Figure 5-7). When this mortar had cured, a single tube-jack test was performed in the 4th horizontal mortar joint up from the base of the regular masonry wall. Rubber tube-jacks were used for this test. The stress level at the 4th horizontal joint was calculated to be approximately 0.224 MPa.

The test set-up and procedure were the same as for the single tube-jack test in the 3rd joint. The holes were drilled starting at the center and working outward and the tube-jacks weren't pressurized until the wall had stabilized. Figure 5-7 shows the test set-up at a point midway through the drilling procedure when only the center holes had been created.

Figure 5-7 Photo of the drilling process during the single tube-jack test in the 4th horizontal mortar joint

The results of the hole drilling are presented in Figure 5-8. In the graph of the individual LVDT relative displacements, Figure 5-8a, it can be seen that LVDTs in the same location but on opposite sides of the wall have similar negative relative displacements. For example, LVDTs 2 and 6 both have a relative displacement of approximately −5 μm after the drilling is complete. Similarly, LVDTs 3 and 7 have a relative displacement of approximately −6 μm. The time required for the wall to stabilize was much less than in the test performed in the 3rd joint. The graph of the average LVDT relative displacements, Figure 5-8b, shows that the movement of the front and the back of the wall is similar and that the eccentricity of the loading on the top of the wall had been corrected. The average relative displacement of the LVDTs resulting from drilling the holes was approximately −6.5 μm.
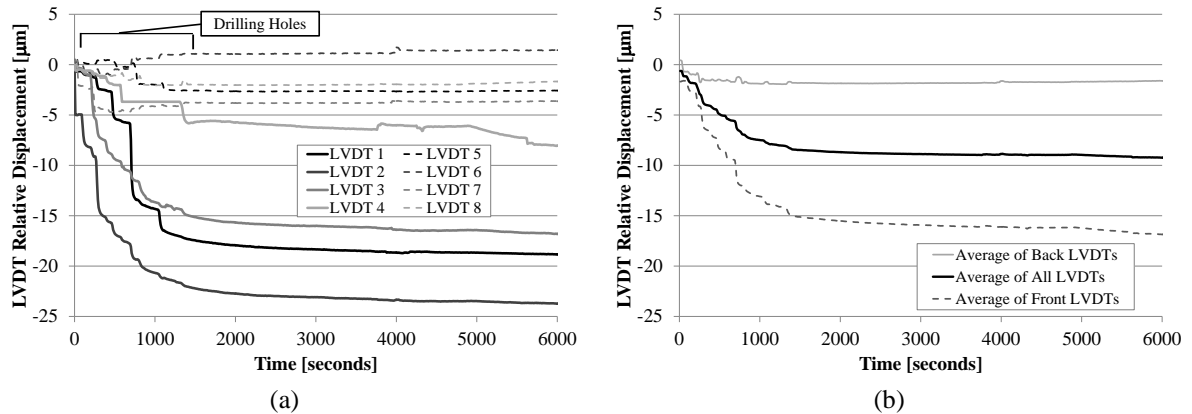
(a) (b)
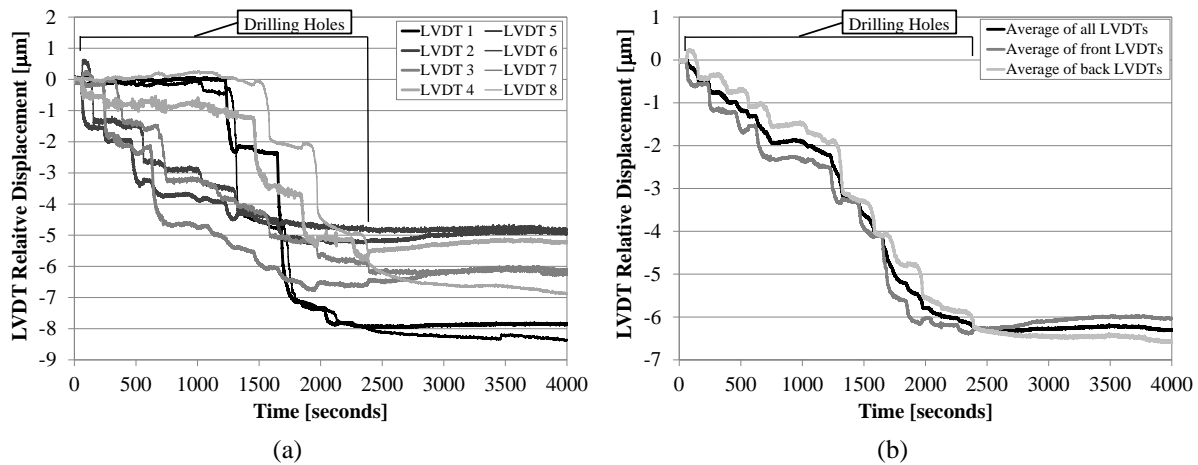
Figure 5-8 Hole drilling results for the 4th horizontal joint: (a) individual LVDT relative displacements; and (b) average LVDT relative displacements

After the movement of the LVDTs had reduced to nearly zero, the rubber tube-jacks were inserted into the holes and pressurized. Two pressurization cycles were conducted; the first one to 0.50 MPa of internal water pressure and the second to 0.60 MPa of internal water pressure. As in the single tube-jack test performed in the 3rd horizontal joint, the pressurizations performed in the 4th horizontal joint show a consistent loading curve (see Figure 5-9). The average LVDT relative displacements are restored to zero at an applied pressure of 0.34 MPa. Unfortunately, this estimated stress does not correspond to the calculated stress level at this joint, 0.224 MPa, and has an error equal to 52%. At the beginning of this test, it was assumed that filling the holes from the previous tests and performing this test in the area where the double tube-jack test had been performed would not affect the results of this test. However, due to this large error in the results, that was much greater than the error of the single tube-jack test in the 3rd horizontal joint, it is very likely that the previous tests had an impact on these test results.

(a) (b)
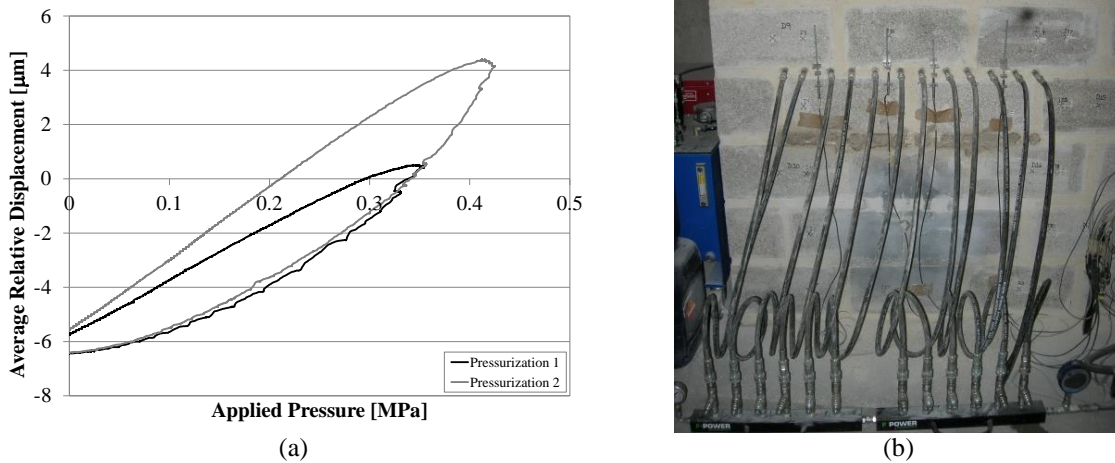
Figure 5-9 Tube-jack test results for the 4th horizontal mortar joint: (a) applied pressure versus average LVDT relative displacement results; and (b) photo of the tube-jack pressurization

Immediately following the single tube-jack test with the rubber tube-jacks in the 4th horizontal joint, a pressurization test was performed using 12 latex tube-jacks. The procedure for the test was the same as for the rubber tube-jack pressurization test. During the pressurizations, several of the tube-jacks were leaking at the back of the wall around their bolt connections, reducing the pressure in the tube-jacks whenever water was not being pumped into the system, as shown in the graph of pressurization over time in Figure 5-10a. The latex tubing allowed the tube-jacks to be pressurized to 1.0 MPa of internal water pressure, 0.2 MPa higher than the maximum

internal water pressure for the rubber tube-jacks. The second and third pressurization results are presented in Figure 5-10b. Unlike the pressurization of the rubber tube-jacks, the latex tube-jacks showed different pressurization curves for each cycle.

(a)   (b)
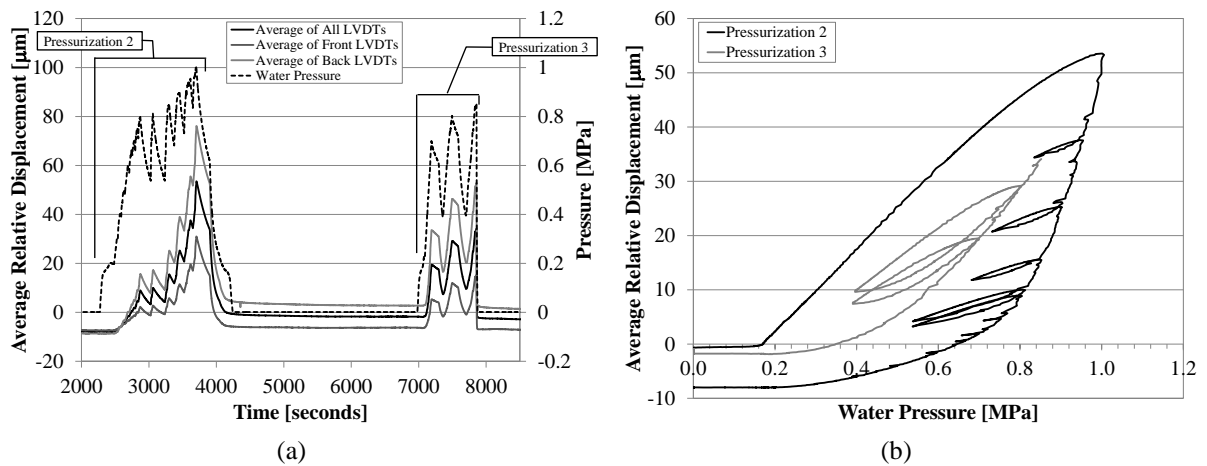
Figure 5-10 Pressurization of the latex tube-jacks: (a) water pressure compared to average relative displacements over the length of the test; and (b) results of the second and third pressurization cycles

During the third pressurization cycle with the latex tube-jacks, at a water pressure of approximately 0.85 MPa, tube-jack #9 burst (Figure 5-11a). The rupture released the pressure in the tube-jacks and the water was drained from the system. In addition to water spraying out of the tube and onto the wall, the rupture caused some of the mortar in the joint to expel from the surface of the joint in that area (Figure 5-11b).

(a)   (b)
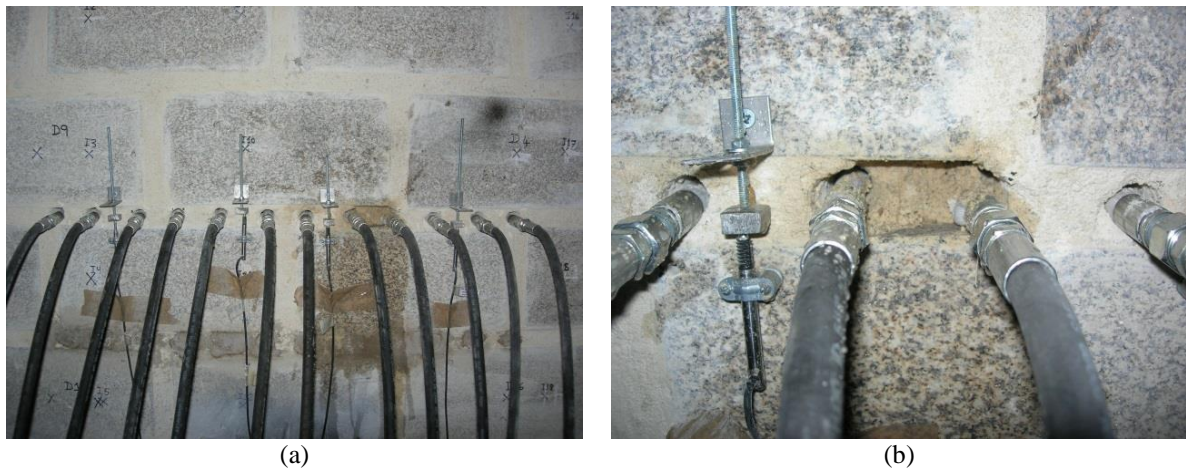
Figure 5-11 Rupture of latex tube-jack #9: (a) photo showing water on the wall following the tube-jack rupture; and (b) photo showing the mortar expelled between tube-jacks #8 and #9

5.2.1.3   Single Tube-jack Test in the 5th Horizontal Joint

The final single tube-jack test in the regular masonry wall was performed in the 5th horizontal mortar joint from the base of the wall. This test was different from the previous tests in two respects: it was performed after the flat-jack tests had been performed at the other end of the wall and the load on the wall was doubled, producing an estimated stress level of approximately 0.42 MPa at the joint. It was assumed that the flat-jack tests on the other end of the wall would have no effect on this tube-jack test and thus the flat-jack slots were not filled with mortar before this tube-jack test was begun. This hypothesis proved to be incorrect. The flat-jack slots

weakened the front face of the wall since they were only cut half way through the wall. When the holes were drilled for the tube-jack test, the relative displacements were much more negative on the front of the wall than on the back of the wall, see Figure 5-12a. The average relative displacement of the LVDTs, due to the hole drilling in the fifth horizontal joint, was approximately −54 μm, over eight times the average relative displacement of the wall when the stress in the wall was half as much. During the time allowed for the wall to adjust to the holes, the displacement decreased a further 6 μm.
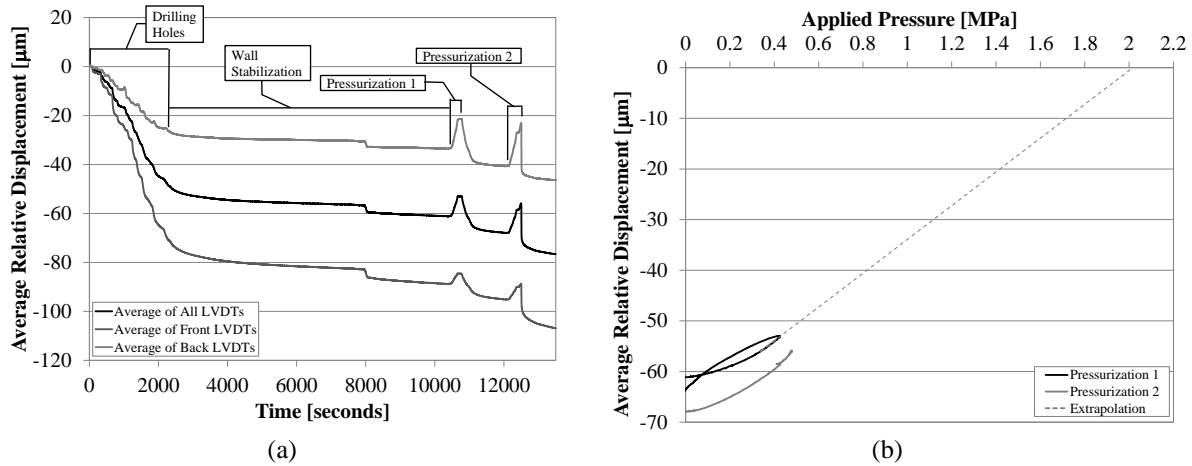
Figure 5-12 Average LVDT relative displacement results for the single tube-jack test in the 5th horizontal joint: (a) during hole drilling; and (b) versus applied pressure during the pressurizations with extrapolation to estimate the state of stress at the joint

After the movement of the LVDTs had reduced to nearly zero, the rubber tube-jacks were inserted into the holes and pressurized. The tube-jacks were pressurized to applied pressure values of approximately 0.4 MPa in the first cycle and 0.5 MPa in the second cycle. During the second pressurization cycle, tube-jack #3 burst. The results of the two pressurization cycles are shown in Figure 5-12. The results show that the average relative displacement of the LVDTs due to drilling the holes was not recovered during the first pressurization. At most only 12 μm was recovered during each pressurization. When the pressure was released in the tube-jacks after each pressurization, the relative displacement continued to decrease as the wall continued to settle. Thus, during this test, the wall was still establishing equilibrium.

Immediately following the single tube-jack test in the 5th horizontal joint with the rubber tube-jacks, several pressurizations were performed in the same holes with the latex tube-jacks. Four pressurization cycles were conducted with the maximum water pressure almost 0.9 MPa. However, even at the maximum pressure the relative displacement recovery was still only 21.5 μm and the negative relative displacement due to drilling the holes was not able to be recovered.
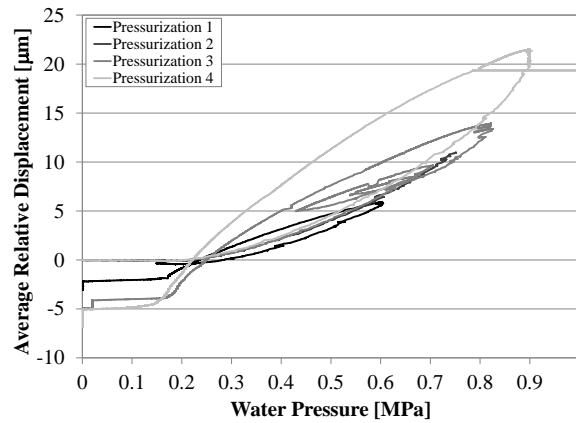
Figure 5-13 Results of the latex tube-jack pressurization test in the 5th horizontal mortar joint with all pressurization cycles adjusted to start at zero relative displacement

Since the continuous movement of the wall over the course of the test made it difficult to compare the pressurizations, the average relative displacement before each of the pressurizations was set to zero for a better comparison in Figure 5-13. This comparison shows that there are variations in the pressure versus relative displacement curves for each of the pressurizations. This is in contrast to the very similar curves for rubber tube-jack tests and pressurizations as shown in Figure 5-6b and Figure 5-9a. While the difference in the slopes of the curves could be due to the continuous negative relative displacement of the wall over the course of the tube-jack testing and pressurization in this joint, it is likely that the latex tubing material is also a factor. Inconsistency in the pressurization curves, water leakage from the tube-jacks and unpredictability of the maximum pressure are reasons the use of latex tube-jacks was discontinued after this test.

5.2.2 Single Flat-Jack Test

Following the single tube-jack test in the 4th horizontal mortar joint, a single flat-jack test was performed on the right side of the wall in the 3rd horizontal mortar joint up from the base of the wall (see Figure 5-14a). The loading on the wall was the same as it was for the single tube-jack test in the 3rd horizontal mortar joint, which produced a stress level of approximately 0.23 MPa in the joint tested. A flat-jack with dimensions of 40 cm long by 10 cm deep and jack calibration factor, K_m, of 0.77 was used for the test.
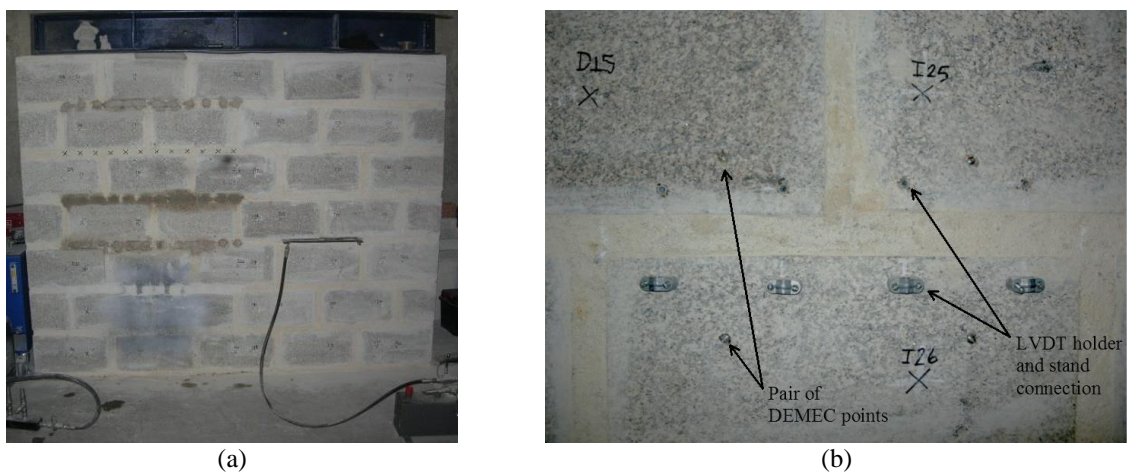
Figure 5-14 Single flat-jack test setup: (a) flat-jack test position in the regular masonry wall; and (b) attachment of LVDT holders and DEMEC points

In preparation for the single flat-jack test, holes were drilled to attach the LVDT holders and the measuring points for the demountable mechanical strain gage (DEMEC) were glued in place (Figure 5-14b). Four LVDT holders were positioned on either side of the wall, each 10 cm apart with the outer LVDTs 5 cm from the end of the slot. The LVDTs measured over a vertical distance of 8 cm. Two sets of DEMEC points were placed on each side of the wall, half way between the LVDT lines and measuring over a vertical distance of approximately 20 cm.

The vertical measurements for the DEMEC point pairs were taken before the slot was made, after the slot was made, and throughout the test, using the DEMEC shown in Figure 5-15a. The slot was made using the saw in Figure 5-15b. Since the saw was unable to make a clean and even slot, additional chiseling was necessary to complete the slot (Figure 5-15c).

(a)	(b)	(c)
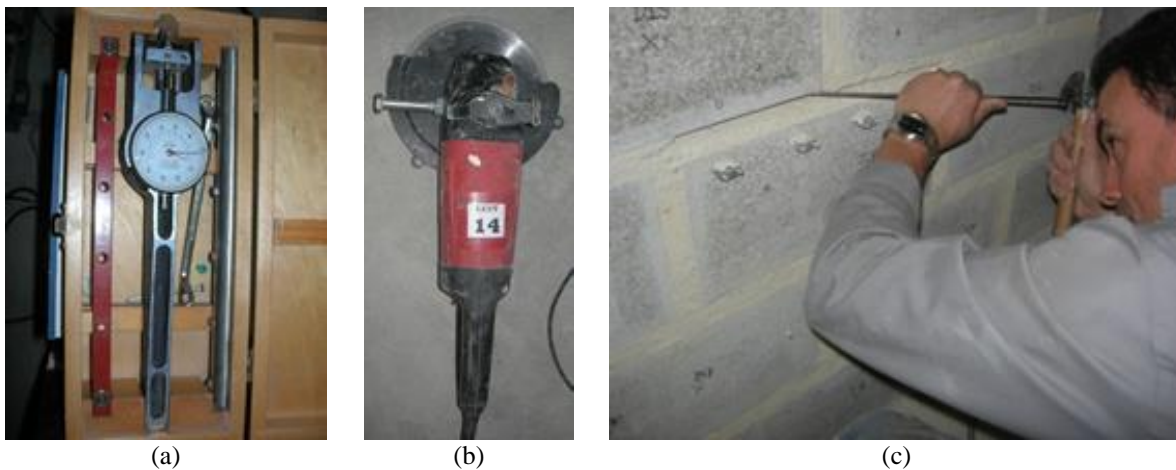
Figure 5-15 Testing equipment and slot preparation: (a) DEMEC; (b) circular handsaw; and (c) additional chiseling necessary to complete the slot

When the slot was prepared and the DEMEC measurements had been taken, the flat-jack was inserted into the slot. As allowed by ASTM C1196 [31], several shims were required above and below the flat-jack to fill in the extra space around the flat-jack and to correct for any irregularities in the slot. Once the flat-jack was in place, the LVDTs were attached (Figure 5-16a). The final setup, including the oil hand pump and the data acquisition system, is shown in Figure 5-16b.

(a)	(b)
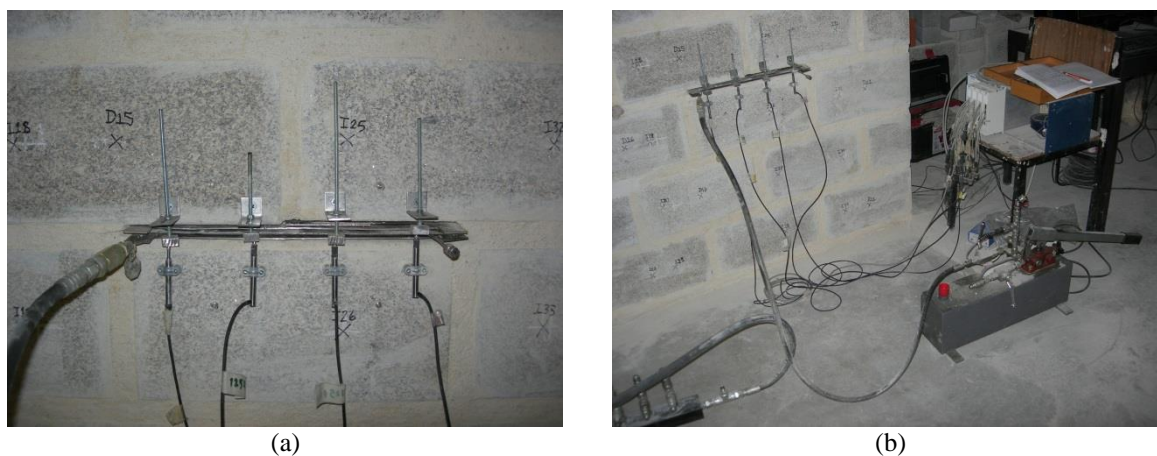
Figure 5-16 Final single flat-jack test setup: (a) flat-jack inserted and LVDTs attached; and (b) complete setup including oil hand pump and data acquisition system

The results of the DEMEC measurements are shown in Figure 5-17a. Measurements were taken at five points in time. The time points are described in Figure 5-17b. At each time point, three measurements were made for each set of points. While the DEMEC device could read measurements as small as 0.002 mm, the measurements taken were variable. The standard deviation for each set of three measurements was on average 0.033 mm. As shown in the results after the slot was opened, there was a negative relative displacement of the point sets on the back of the wall (Line 3 and 4), a very slight negative relative displacement of the point set on the front left side of the slot (Line 1) and a positive relative displacement on the front right side of the slot (Line 2). The expansion shown on the right side of the slot and greater contraction on the back of the wall could be due to movement of the individual units, since the slot is only the length of one unit. The average relative displacement of the DEMEC point sets was -0.16 mm at time point 2, indicating an overall contraction of the masonry due to the creation of the slot. The stabilization of the wall after the removal of the mortar in the slot is seen by comparing time points 2 and 3. The stabilization resulted in a further average contraction of 0.02 mm resulting in a total relative displacement average of -0.18 mm.
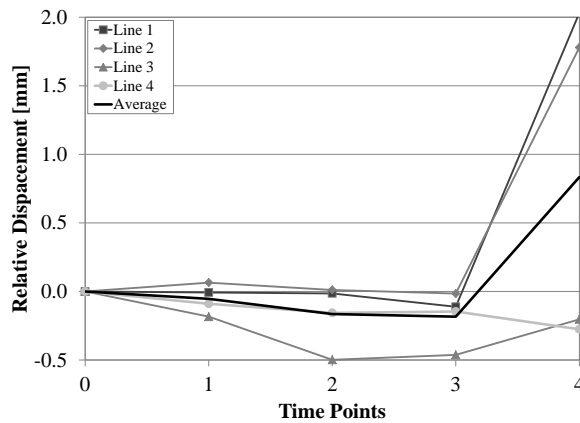
Time Point	Description
0	Before opening the slot
1	After opening the slot (vertical load = 2.66 MPa)
2	Vertical load returned to 2.82 MPa
3	30 minutes after opening the slot
4	During flat-jack pressurization to 2.8 MPa

(a)   (b)

Figure 5-17 DEMEC results: (a) relative displacement at time points during the test; and (b) time point descriptions

The calculation of the relative displacement of the wall from the DEMEC point measurements was performed following the completion of the test. Thus, this information was not available during the pressurization of the flat-jack. Also following the single flat-jack test, the flat-jack was removed and the slot was measured to determine the area of the slot and the area correction factor. The depth of the slot was measured every 5 cm along its length. The profile of the slot is shown in Figure 5-18. The area of the slot was calculated to be approximately 533 cm^2. The inflation of the flat-jack applied pressure to the masonry in an area approximately 38 cm long by 8 cm wide, 304 cm^2, 1 cm less on each edge of the jack due to the curvature of the jack edges. Thus, the area correction factor, K_a, for this single flat-jack test was 0.571.
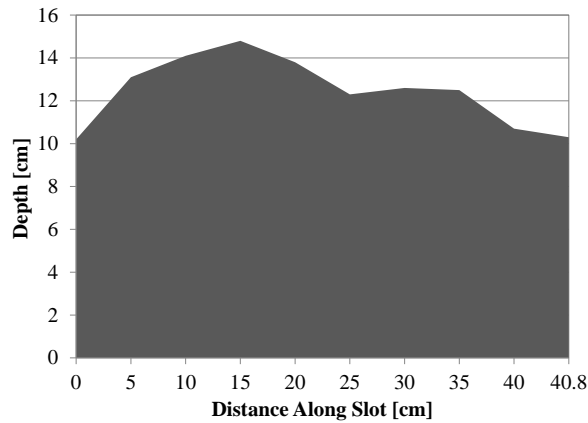
Figure 5-18 Slot profile for the single flat-jack test in the regular masonry wall

The results of the DEMEC point measurements and the correction factors were used in preparing and analyzing the pressure and LVDT results following the test. The oil pressure measured with the oil pressure gage was multiplied by the area correction factor and the jack calibration factor to determine the applied pressure. The applied pressure is shown in the graphs below. The relative displacement of the DEMEC points, -0.18 mm, was taken as the initial value of the LVDTs.

The results of the LVDTs and the applied pressure are shown in Figure 5-19. Before starting the pressurization cycles, the flat-jack was pressurized to an oil pressure of 0.8 MPa to seat the jack in the slot. Four pressurization cycles were performed with the single flat-jack. The first cycle was to an oil pressure of 2.8 MPa (applied pressure of 1.23 MPa) and each subsequent cycle was to an oil pressure of 2.0 MPa (applied pressure of approximately 0.88 MPa). Note that the small dips in the pressure shown in the graph were disruptions in the electrical power supply for the oil pressure gage and were not actual dips in the pressure.

(a)

(b)
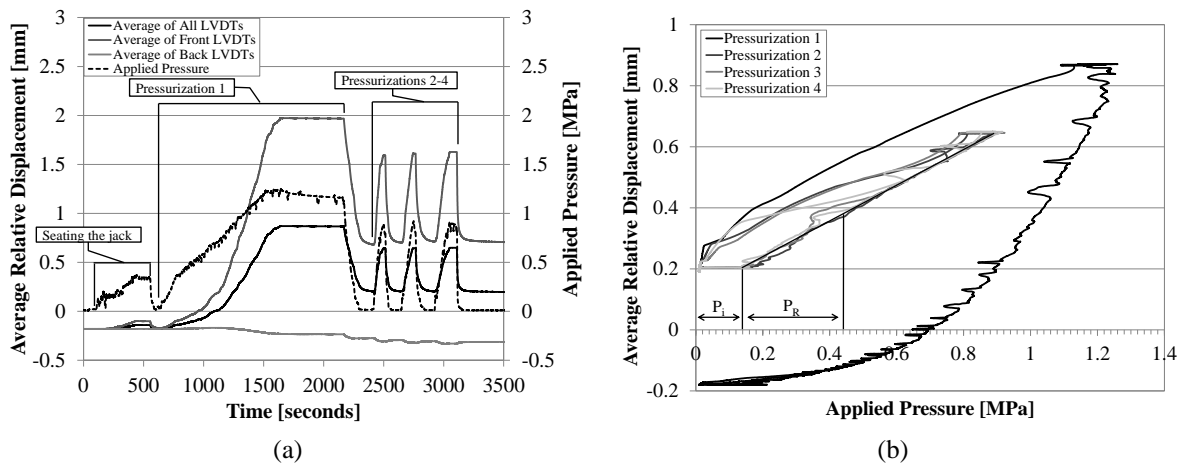
Figure 5-19 Regular masonry wall single flat-jack test results: (a) applied pressure and average LVDT relative displacements over the length of the test; and (b) average relative displacement versus applied pressure

The applied pressure versus the average relative displacement results show that the applied pressure required to return the average relative displacement to zero was approximately 0.7 MPa. The curvature in the first loading cycle was likely due to the jack and masonry adjusting to the loading. The 2nd through 4th cycles show the linear elastic behavior of the masonry. The author believes that the thickness of the joints and slot resulted in an initial inflation pressure, P_i, before the flat-jack applied pressure to the masonry in each cycle. Given

the relative displacement to be restored was -0.18 mm, the restoring pressure, P_R, and state of stress estimate was 0.3 MPa. This result is much higher than the assumed stress level in the masonry, 0.23 MPa, and has an error of 30.4%. One possible cause for the difference in values could be the variability and error in the DEMEC point measurements. The result could also be incorrect because the flat-jack is only pressurizing a very small portion of the masonry, one quarter of each of the units above the slot and half of the unit below the slot. It should also be noted that the pressure applied during the first pressurization was much too large and it caused a compaction of the masonry above the slot. This is evident in the residual relative displacement after the first pressurization.

5.2.3 Double Tube-Jack Test

A double tube-jack test was performed for the first time in the regular masonry wall. The double tube-jack test is similar to the double flat-jack test. A second row of holes is drilled in a mortar joint above the first row of holes, made for the single tube-jack test. The idea is that the two rows of holes vertically separate a masonry specimen within the wall. Tube-jacks are inserted in both rows of holes and pressurized simultaneously with an equal amount of pressure in both rows. The tube-jacks compress the specimen vertically. LVDTs placed between the two rows of tube-jacks measure the strain of the specimen. The goal of the test is to use the applied pressure and strain measurements to estimate the Young's modulus of the masonry.

The double tube-jack test was performed following the single tube-jack test and pressurization in the 3rd horizontal masonry joint. The 6th horizontal joint above the floor was chosen for the second row of tube-jacks. The locations for the holes were measured and marked directly above the holes in the third row. The locations for the LVDT holders and stands were also measured and marked. Holes were drilled in the granite units and the LVDT holders and stands attached with screws. Three vertical LVDTs were placed measuring over two mortar joints and a vertical distance of 31 cm. A horizontal LVDT was placed midway between the two lines of tube-jack holes and spanning over two mortar joints and a horizontal distance of 51 cm. This arrangement and those designed for the other double tube-jack tests performed in this work were based on the configuration shown in the recommendations and standards for the double flat-jack test [33], [3]. The complete setup is shown in Figure 5-20.

| (a) | (b) | (c) |
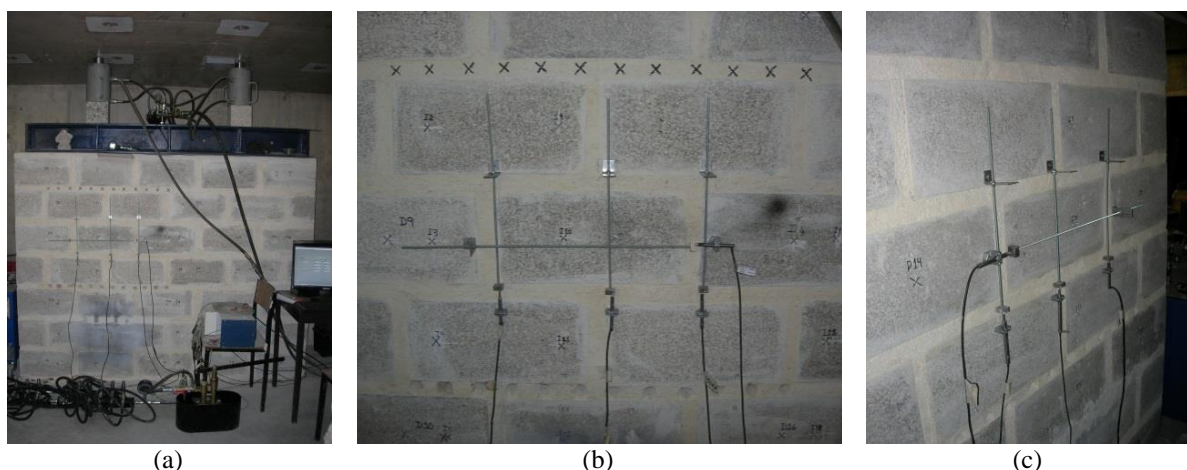
Figure 5-20 Double tube-jack test setup: (a) complete setup; (b) close-up of the front of the wall; and (c) LVDT setup on the back of the wall

The pressure applied to the top of the wall for this test was approximately 0.2 MPa. This was the same loading as for most of the single tube-jack tests and both of the single and double flat-

jack tests. The procedure for drilling the second line of holes was the same as for drilling the single tube-jack holes. Following the hole drilling, the wall was allowed to stabilize for some time before the tube-jacks were inserted into the holes.

The area correction factor for the double tube-jack test was determined using Equation (35) from section 2.3.2. The estimated lengths of the tube-jacks applying pressure to the masonry, 16.5 cm, and the estimated diameter of each of the holes, 2.6 cm, were determined following the single tube-jack test in the 5th horizontal joint, as presented in section 5.2.1. These values were used to calculate an average total surface area of the tube-jacks in a plane through the centroid of the jacks, 515 cm^2. The length of the equivalent flat-jacks was 85.5 cm, giving a cross-sectional area of the separated specimen of 1710 cm^2. Thus, the area correction factor used for determining the applied pressure to the masonry was 0.301.

Once the tube-jacks were inserted in the prepared holes (Figure 5-21a), they were pressurized to an internal water pressure of 0.2 MPa, an applied pressure of approximately 0.035 MPa, to check the performance of the tube-jacks. Two of the tube-jacks were leaking, so the water pressure was released and the leaking tube-jacks were replaced before continuing with additional pressurization cycles.

The LVDT relative displacements and the pressure applied by the tube-jacks throughout the course of the test are presented in Figure 5-21b. These results show that, as the tube-jacks were pressurized, the front vertical LVDTs showed expansion of the masonry (positive relative displacement) and the back vertical LVDTs showed a larger contraction of the masonry (negative relative displacement). The tube-jacks were compressing the masonry on the back of the wall but not on the front of the wall. If this test was done in the field and no LVDTs were placed on the back of the wall, the results of the test would only show expansion of the masonry and the test would not be usable. In this case, the averages of the front and back LVDTs for both the vertical and horizontal movements were used for the final stress versus strain calculations.

(a)	(b)
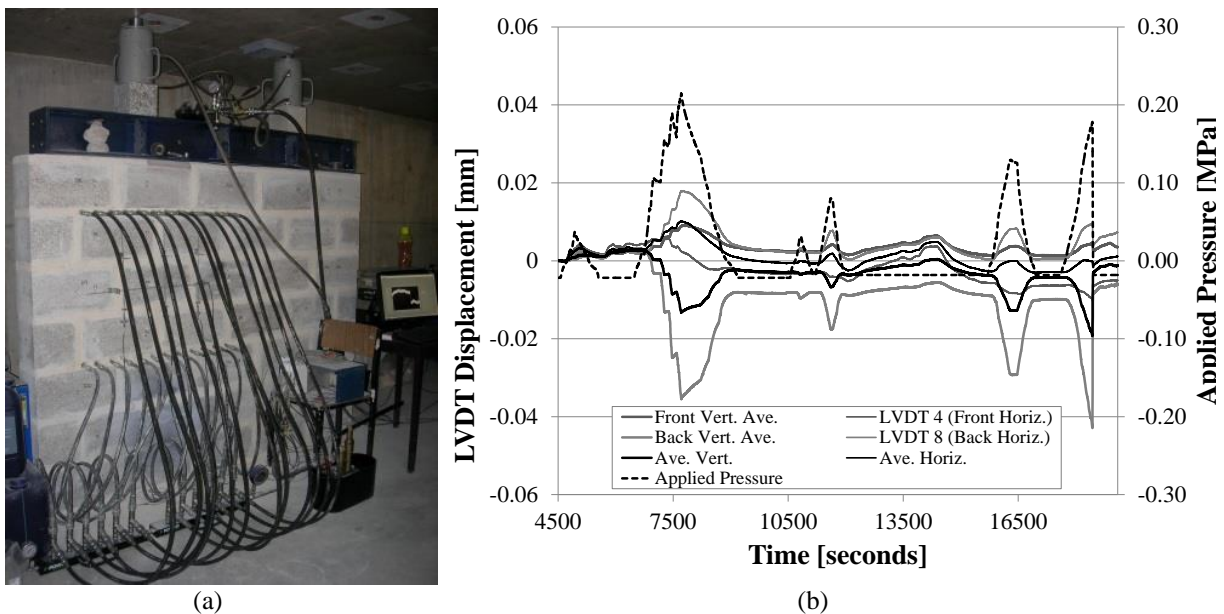
Figure 5-21 Double tube-jack testing in the regular masonry wall: (a) tube-jacks inserted in the two horizontal rows of holes; and (b) LVDT relative displacement and applied pressure throughout the test

During the second pressurization, some of the tube-jacks were leaking on the backside of the wall (Figure 5-22a) but the pressurization was continued up to an applied pressure of approximately 0.2 MPa.

After the first two pressurization cycles, four tube-jacks were removed so that there were only 10 tube-jacks in each row, the end holes in each row remaining empty. The cross-sectional area of the tube-jacks applying pressure to the masonry was reduced to 429 cm^2, resulting in a reduction of the area correction factor to 0.251. With this new set-up, four more pressurizations were conducted with successively higher applied pressure peaks. During the last pressurization, at a water pressure of approximately 0.8 MPa, tube-jack #16 burst (Figure 5-22b).

(a)   (b)
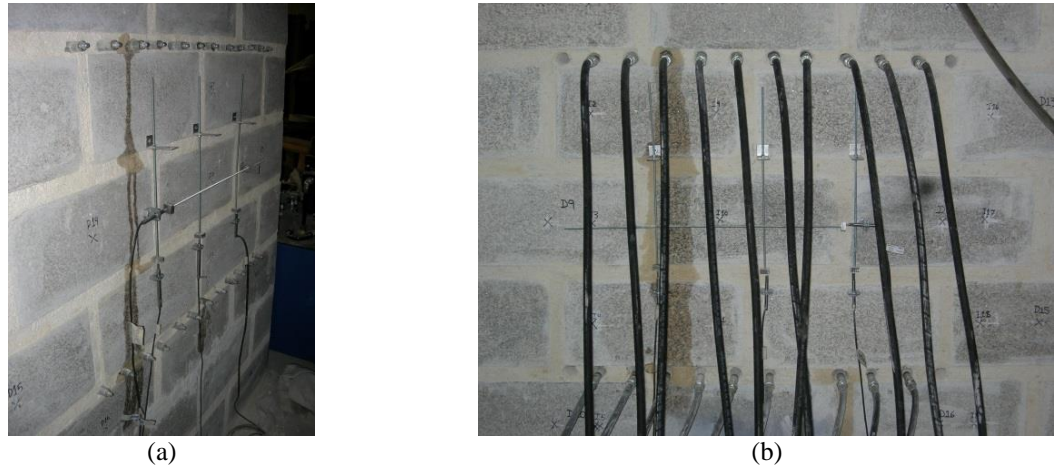
Figure 5-22 Photos during the double tube-jack test pressurizations in the regular masonry wall: (a) tube-jacks leaking on the back of the wall during the first two cycles; and (b) rupture of tube-jack #16 during the final cycle

The applied pressure versus the strain results are shown in Figure 5-23. The slopes of the later portions of the curves, indicated as E_2, are comparable to the Young's modulus results of the regular masonry wallet during the reloading phase. These results estimate an elastic modulus of approximately 2.2 GPa, whereas the wallet reloading modulus was estimated at 2.5 GPa, a 12.77% difference.
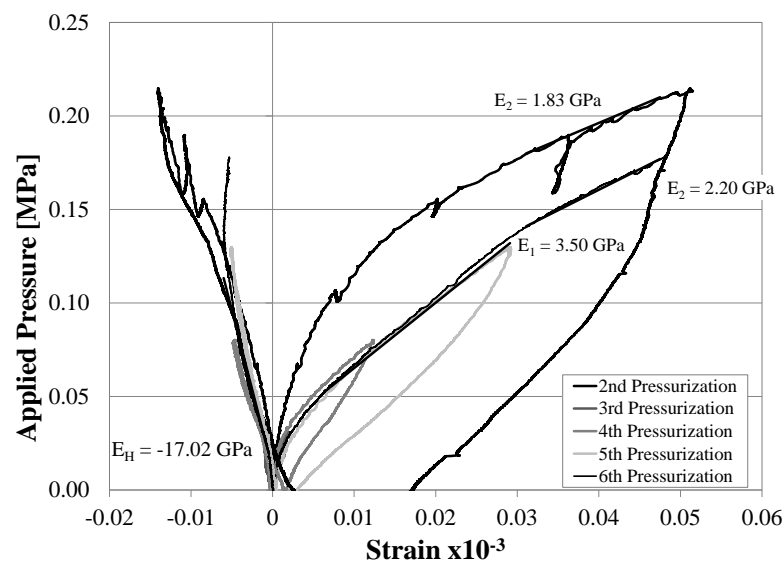
Figure 5-23 Applied pressure versus strain results for the double tube-jack test in the regular masonry wall

To estimate the Poisson ratio of the masonry using the double tube-jack test results, the vertical elastic modulus of 2.20 GPa was divided by the horizontal elastic modulus of 17.02 GPa to get a Poisson ratio of 0.129.

5.2.4   Double Flat-Jack Test

A double flat-jack test was performed following the single flat-jack test on the right side of the regular masonry wall (Figure 5-24). Both the ASTM standard and RILEM recommendation suggest that the flat-jacks should be placed between *A* and 1.5*A*, where *A* is the length of the jack [33] [3]. Thus, the location for the second flat-jack was marked on the 5th joint up from the base of the wall, directly over the single flat-jack test slot.

Four LVDTs were used on each side of the wall to record the relative displacements of the masonry during the test. Holes were drilled in the granite units to attach the LVDT stands and holders using screws. Since the mortar was so much weaker than the granite, it was expected that most of the movement in the masonry would be due to the movement of the mortar. Thus, three LVDTs were positioned to measure the vertical displacements over the center horizontal mortar joint and one LVDT was positioned to measure the horizontal displacement of the vertical mortar joint. The dimensions and locations of the LVDTs are shown in Figure 5-24b.
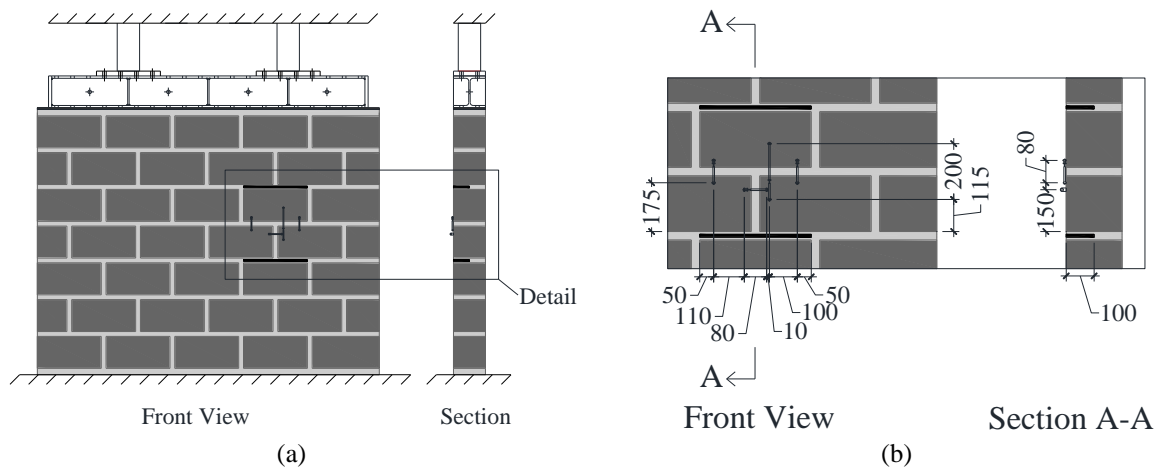
Figure 5-24 Double flat-jack test schematic layout: (a) location of flat-jack slots within the regular masonry wall; and (b) detailed view including the dimensions and locations of the LVDTs in millimeters.

The preparation of the second slot was done using the stitch drilling method, as allowed by the ASTM standard [33] (Figure 5-25). The softness of the mortar made the drilling process easy and it produced less dust than using a circular saw, as was used for the first slot.

(a)   (b)
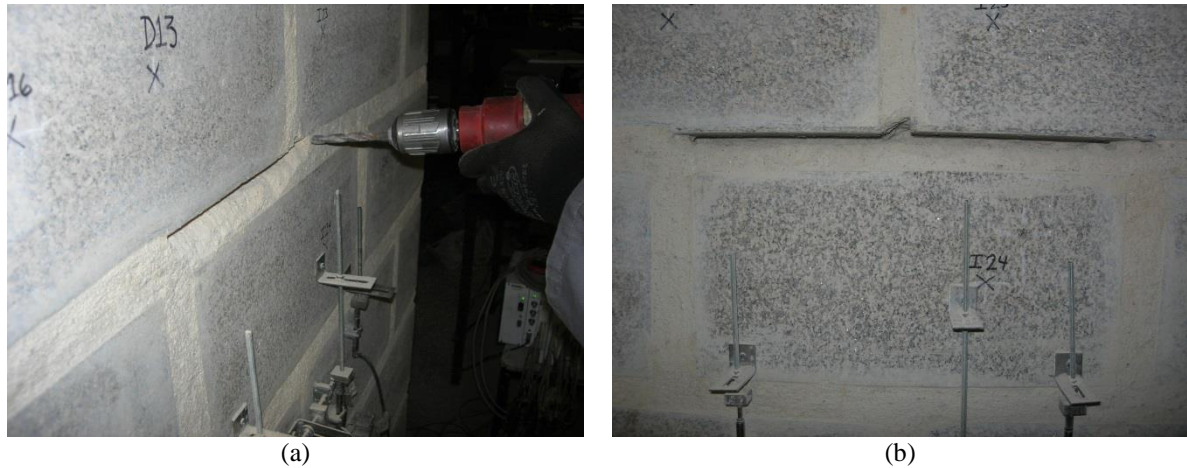
Figure 5-25 Preparing the second slot for the double flat-jack test in the regular masonry wall: (a) stitch drilling; and (b) the completed slot

After the slot was prepared and cleaned, the depth of the slot was measured to determine the slot area and the area correction factor to be used for analyzing the results. The same procedure was used for measuring the depth of the slot as was used for the single flat-jack slot. The profile of the slot is shown in Figure 5-26a. The area of the slot was calculated to be approximately 484 cm^2. The flat-jack used in the top slot had the same dimensions as the flat-jack used in the bottom slot. The areas of the top and bottom slots and jacks were combined to determine the area correction factor, K_a, for the double flat-jack test, 0.598.

The flat-jack was inserted into the top slot and full-length shims were added to fill the additional space between the flat-jack and the masonry. The flat-jack used for the top slot had a jack calibration factor of 0.8. The calibration factors from the top and bottom jacks were averaged to get the jack calibration factor, K_m, for the double flat-jack test, 0.785. The complete test set-up is shown in Figure 5-26b.

(a)   (b)
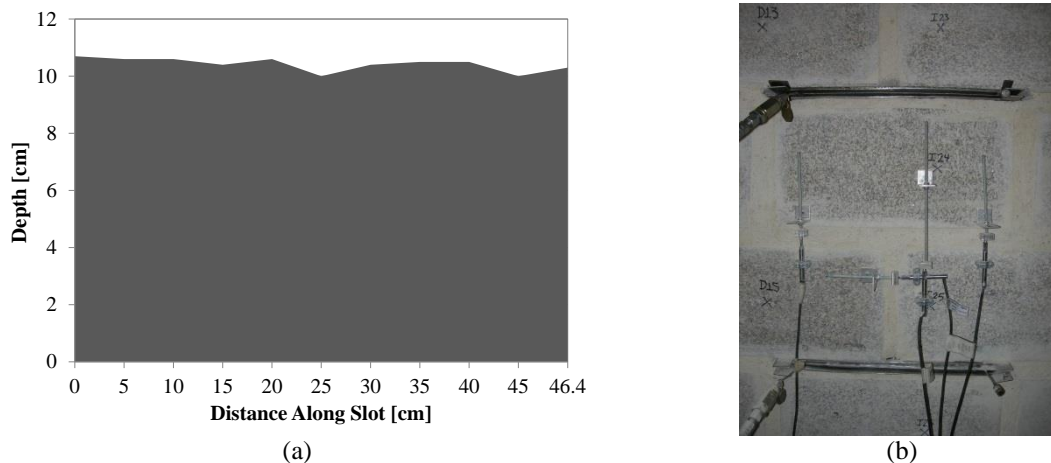
Figure 5-26 Completion of the double flat-jack test set-up: (a) depth measurements of the top slot; and (b) insertion of the top flat-jack and shims

Four pressurizations were performed during the double flat-jack test, with each subsequent pressurization obtaining a higher maximum pressure level. The LVDT relative displacements and the pressure applied by the flat-jacks throughout the course of the test are presented in Figure 5-27. The difference between the front and back of the wall is apparent in the double flat-jack test, just as it was in the double tube-jack test. However, in the double flat-jack test the flat-jacks are pressurizing only the front of the wall and not the back. This is because the flat-

jacks are only half the depth of the wall. If this test was performed in-situ and there were no LVDTs measuring the displacement on the back of the wall, the test would still produce results indicating that the flat-jacks are pressurizing the masonry. However, the results would indicate much larger strains than the wall was actually experiencing throughout its depth. For the pressure versus strain results in this test, the averages of the front and back LVDTs were used for both the vertical and horizontal strains.
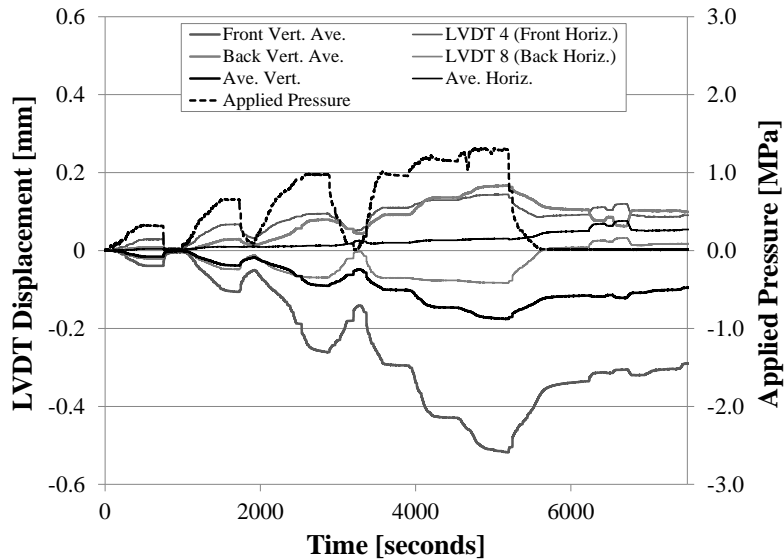
Figure 5-27 LVDT relative displacement and applied pressure throughout the double flat-jack testing in the regular masonry wall

The applied pressure versus the strain results are shown in Figure 5-28. In this graph, the results from the average of the front vertical LVDTs are shown as well. This is to show how different the results would be if this test only considered the LVDTs on the front of the wall, as is usually done during in-situ tests.

Considering the results including both the front and back LVDTs, the modulus results can be compared to those found in the Young's modulus tests of the masonry wallets. The large masonry wall has been loaded using the hydraulic jacks above the wall prior to this double flat-jack test loading, so the first part of each loading curve should be considered a reloading of the masonry. The slope of this portion of the curve is approximately 2 GPa, a 22.22% difference from the reloading modulus found in the wallet testing, 2.5 GPa. Beyond an applied pressure of approximately 0.9 MPa the slope of the loading curve changes. This suggests that the masonry has not been subject to this stress level beyond this applied pressure. This second slope can be compared to the initial loading tangent modulus of the regular masonry wallet. For the flat-jack test, it is estimated to be 0.41 GPa, a 10.8% difference from the regular masonry wallet value of 368 MPa. It can be concluded that the double flat-jack test produced results that were similar to those found in the Young's modulus testing of the masonry wallets, despite only testing a small portion of the masonry.

As in the double tube-jack test, the Poisson ratio was estimated from the results of the double flat-jack test. Using the average results from the LVDTs both on the front and back of the wall results in a Poisson ratio of 0.327, considering only the slopes of the curves where the jacks are reloading the masonry.
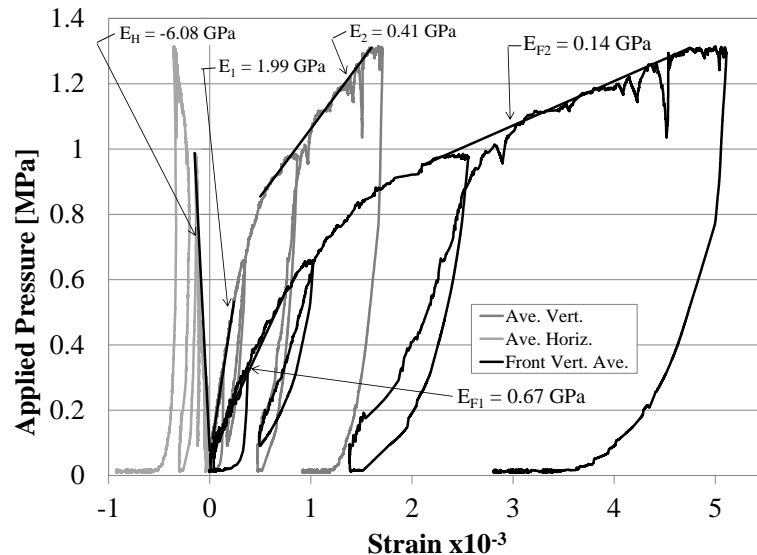
Figure 5-28 Double flat-jack test in regular wall applied pressure versus strain results

5.3 *Semi-Irregular Masonry Wall*

The second wall that was constructed and tested was the semi-irregular masonry wall. The semi-irregular wall had a slightly more complex geometry than the regular wall, as described in section 4.3. Accordingly, it was expected that the test results would be slightly more complex but closer to actual historical masonry structures in northern Portugal. The loading of the semi-irregular wall was the same as for the regular wall and was shown in Figure 5-1. The semi-irregular wall was slightly shorter than the regular wall, reducing the cross-sectional area of the wall and the pressure in the hydraulic jacks (2.64 MPa) required to apply the same pressure on top of the wall, 0.2 MPa. The approximate stress level in the wall was calculated in each joint that was tested based on this applied pressure and the weight of the equipment and the masonry above that joint. Only rubber tube-jacks were used in the tests on the semi-irregular wall. The latex tube-jacks used for some tests in the regular wall were no longer used due to several issues, including inconsistency in the loading curve and leakage from the tubes. See section 5.2.1.3 for more information.

Four minor-destructive tests were performed on the semi-irregular wall. The single tube-jack test and double tube-jack test were performed first on the left side of the wall. Following these two tests, the holes were filled with mortar. The single and double flat-jack test were performed after the tube-jack tests were complete. The flat-jack tests were performed in horizontal joints on the right side of the wall that were at the same height as the ones used for the first single and double tube-jack test. Thus, both single tests were performed at the same stress level and both double tests were performed over the same vertical distance. The arrangement for the four tests in the semi-irregular wall and the equipment used in the tube-jack tests is shown in Figure 5-29. The complete test set-up, procedure and results for each test are presented in the following subsections.

Figure 5-29 Test arrangement for the semi-irregular wall

5.3.1 Single Tube-Jack Test

A single tube-jack test was performed on the semi-irregular granite masonry wall in the 3rd horizontal mortar joint up from the base of the wall that ran the length of the wall, at an approximate height of 60 cm. The stress state at this level in the wall was calculated to be approximately 0.23 MPa, the same level of stress as for the first tube-jack test in the regular masonry wall.

As much as possible, the holes for the tube-jacks were spaced approximately 7.5 cm from center to center horizontally. However, the slightly irregular joints sometimes prevented this exact spacing. Twelve tube-jacks were used for the test, the same number as was used in most of the regular masonry wall tube-jack tests. The holes were labeled Hole 1 through Hole 12 from left to right. The positions and number of the holes for the tube-jacks and for the LVDTs are shown in Figure 5-30.

Ten LVDTs were used to measure the relative displacement of the masonry, five on both the front and back of the wall. All of the LVDTs used for the semi-irregular masonry wall tests had a range of ±2.5 mm. An equal spacing of the LVDTs was not possible for the semi-irregular wall because of the locations of the vertical mortar joints between the units. However, the LVDTs were distributed as evenly as possible along the length of the equivalent flat-jack. The placements of the LVDTs were between the 1st and 2nd holes, between the 3rd and 4th holes, between the 5th and 6th holes, between the 8th and 9th holes and between the 11th and 12th holes, on both sides of the wall. They were labelled LVDT 1 through 5, respectively, on the front of the wall and LVDT 6 through 10, respectively, on the back of the wall.

110

Figure 5-30 Holes and LVDT positions for the first single tube-jack test in the semi-irregular wall: (a) front of the wall; (b) back of the wall; (c) tube-jacks inserted in the front of the wall; and (d) tube-jack ends sticking out the back of the wall

The same drilling procedure was used for the semi-irregular wall as for the regular wall. The holes for the tube-jacks were drilled starting with the center holes and then working toward the outer holes. The LVDTs recorded the relative displacements throughout the test, including during the drilling. The tube-jacks were inserted into the holes once the wall had stabilized and the movement of the LVDTs had reduced to nearly zero.

The drilling process was much more difficult than it was for the regular masonry wall. This was due to the strength of the mortar, see section 4.5.2 for the results of the mortar compression tests. During the drilling process, after drilling a couple of holes, the drill would overheat and would need some time to cool or the operator would need to switch between two drills to continue the drilling. Due to these difficulties, the drilling took approximately two and a half hours to complete, much longer than for the regular masonry wall. In addition, when the drill pushed through to the backside of the wall several larger chunks of mortar were expelled (Figure 5-31a and b). These chunks were determined to be the fill mortar that was placed where wooden blocks were used to hold the units in place during the construction process. This fill mortar can be seen as the dark patches in Figure 5-31c. The LVDTs were able to record the displacement of the wall while the holes were being drilled. However, a couple of the LVDTs were disrupted when the mortar chunks were expelled from the back of the wall. The disrupted LVDTs had to be adjusted and the data corrected during the analysis of the results following the test.
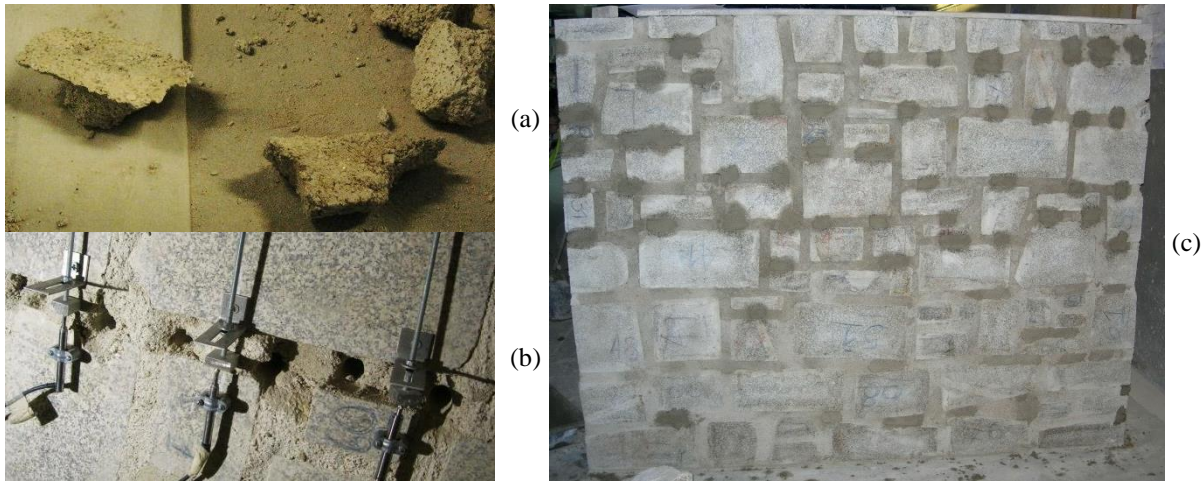
Figure 5-31 Fill mortar in the semi-irregular wall: (a) chunks expelled from the back of the wall; (b) spaces left where mortar was expelled from the joint; and (c) dark wet patches of fill mortar during construction

The average displacement of the LVDTs throughout the test is presented in Figure 5-32. This figure shows the displacement during drilling, time allowed for the wall to stabilize, and pressurization cycles. Note that the average displacement of the LVDTs on the front of the wall was greater than on the back of the wall. There could be two possible reasons for this difference: one, there could be some eccentricity in the applied load on top of the wall or, two, the pressure from the drilling could be inducing some bending in the wall.
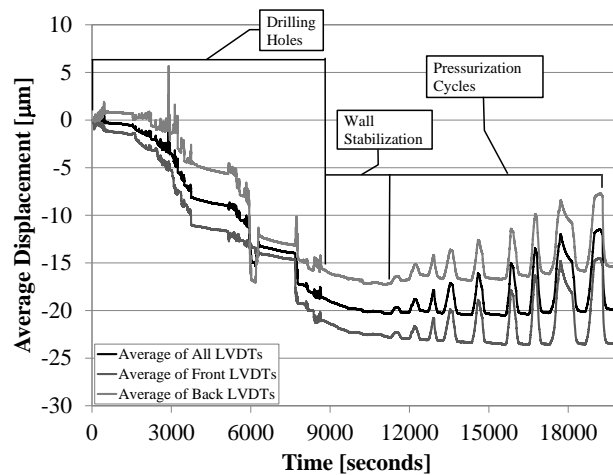
Figure 5-32 Average LVDT displacement during the single tube-jack test in the semi-irregular wall

Following the test, the area correction factor, k_a, was calculated as the ratio of the surface area of the tube-jacks, A_T, to the surface area of the holes, A_H, in the plane of the equivalent flat-jack (see Figure 2-30). The area of the expelled mortar in the plane of the equivalent flat-jack was estimated and included in the calculation of the area of the holes, A_H. The resulting area correction factor was 0.787.

The diameter of the holes was estimated to be 26 mm based on average measurements taken of the foam samples from the holes in the regular masonry wall (see section 5.2.1). The hole diameter was used in the calculations of the pressure applied to the masonry by the tube-jacks, p_m, see section 2.3.2 for the calculation. This pressure, p_m, was multiplied by k_a, to obtain the applied pressure, $P_{Applied}$, shown in the result graphs.

Ten pressurization cycles were conducted with each subsequent cycle having a greater maximum pressure up to an applied pressure of 0.65 MPa. Figure 5-33a shows the average LVDT displacement and the applied pressure during the pressurization cycles.
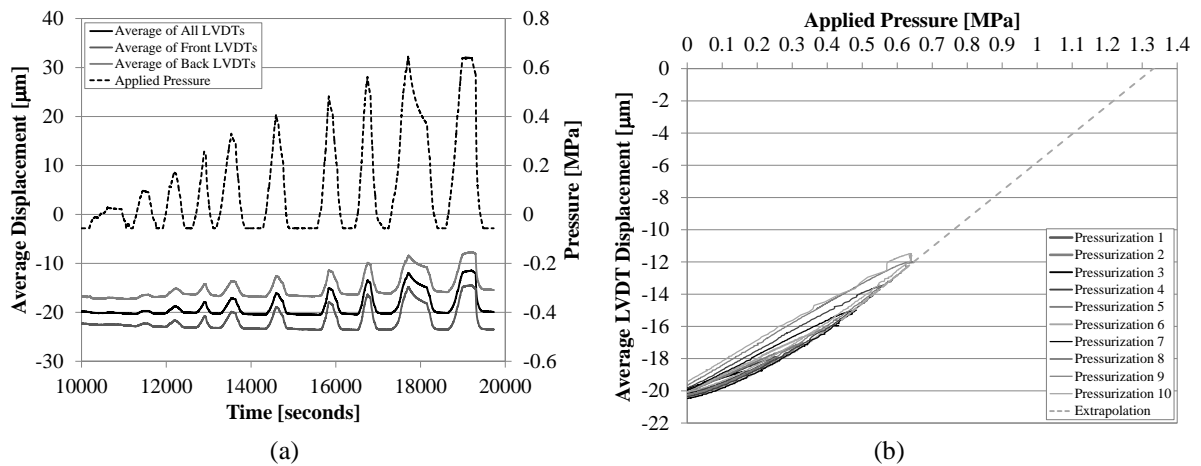
Figure 5-33 Semi-irregular wall single tube-jack test results: (a) comparison of average relative displacement and applied pressure over time; and (b) average relative displacement versus applied pressure

The average LVDT displacement versus the applied pressure is shown in Figure 5-33b. In this tube-jack test, the tube-jacks were not able to reestablish the initial position of the masonry before drilling the holes, see also Figure 5-33a. A linear extrapolation is shown in Figure 5-33b that estimates what the applied pressure would have to be to restore the masonry to its original position, over 1.3 MPa. This estimate is more than 5.5 times the approximate stress level of 0.23 MPa. Further study must be done to determine the reason for this error.

5.3.2 Single Flat-Jack Test

Following both the single and double tube-jack tests on the semi-irregular wall, a single flat-jack test was performed on the right side of the semi-irregular wall at approximately the same height as the single tube-jack test, see Figure 5-29. The purpose of this test was to compare the tube-jack test to the flat-jack test under the same conditions for both tests. The loading on the wall was the same as for the single tube-jack test, resulting in an approximate stress level of 0.23 MPa at the location of the single flat-jack test. A flat-jack with dimensions of 40 cm long by 10 cm deep and jack calibration factor, K_m, of 0.8 was used for this test.

(a)   (b)
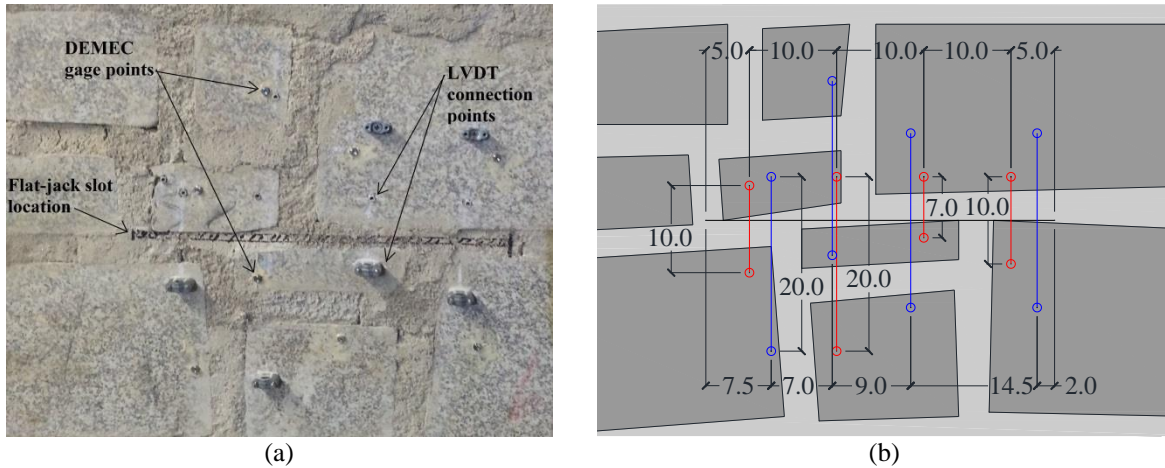
Figure 5-34 Attachment of DEMEC gage points and LVDT connection points for the single flat-jack test in the semi-irregular wall: (a) photo of points attached; and (b) dimensions of DEMEC points shown in blue and LVDT points shown in red (dimensions in [cm])

As in the single flat-jack test performed on the regular masonry wall, two measuring methods were used to determine the relative displacements of the masonry, DEMEC and LVDTs. The location of the slot was marked on the mortar joint and then the DEMEC gage points were glued in place and LVDT holders were screwed into the granite units (Figure 5-34a). Four sets of DEMEC points were used on the front face of the wall. Eight LVDTs were used for the test, four on the front of the wall and four on the back.

The dimensions and locations of the DEMEC gage points and LVDT connection points in relation to the slot are shown in Figure 5-34b. Note that the DEMEC points and LVDT connection points could not be spaced equally along the length of the flat-jack. They also could not be spaced equidistant above and below the slot due to the locations of the semi-irregular granite units and mortar joints. Some of the middle measuring sets measured over two mortar joints whereas the outer sets measured over only one joint. Each set of DEMEC points measured over a distance of approximately 20 cm.

(a)   (b)   (c)
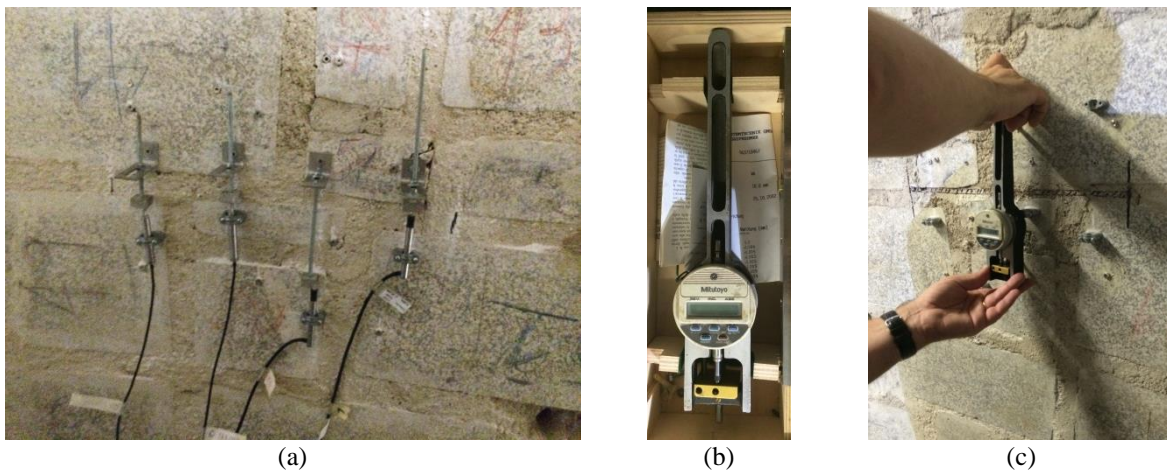
Figure 5-35 Preparation for the single flat-jack test in the semi-irregular wall: (a) LVDT attached to the back of the wall; (b) digital DEMEC; and (c) DEMEC measurements before cutting the slot

LVDTs were attached on the back of the wall as shown in Figure 5-35a so that they would be ready for the jack pressurizations once the slot was cut and the jack inserted. Once the glue had dried and the DEMEC gage points were secure, several measurements were taken with the digital DEMEC, as shown in Figure 5-35b and c, before the slot was opened. The slot was

created using a disk saw with a 10 cm radius (Figure 5-36a). Water was used to wet the saw blade and reduce the amount of dust, as shown in Figure 5-36b. Several passes with the saw were required to cut the slot to a depth and thickness so that the flat-jack could be inserted. Since the saw blade was larger than that used for the regular masonry wall tests, no additional chiseling was required to create the slot.

| (a) | (b) |
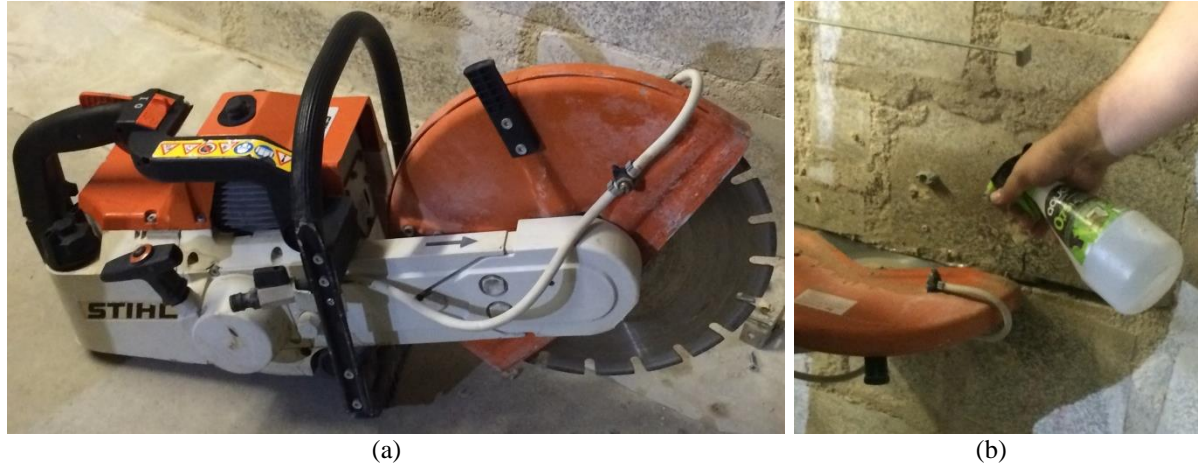
Figure 5-36 Sawing the slot for the single flat-jack test in the semi-irregular wall: (a) 10 cm radius disk saw; and (b) wetting the saw blade to reduce dust during cutting

Once the slot was large enough for the flat-jack to be inserted, DEMEC measurements were taken to determine the relative displacement of the masonry due to sawing the slot. Six measurements were taken before and after sawing the slot at each point combination. The average results are shown in Table 5-1.

Table 5-1 DEMEC results for the single flat-jack test in the semi-irregular wall

Measurement Time	Point Combination			
	1	2	3	4
Before Sawing	9.776	9.925	5.258	4.603
After Sawing	9.857	10.050	5.343	4.689
Relative Displacement [mm]	-0.081	-0.124	-0.085	-0.086

The flat-jack was inserted in the slot and the LVDTs attached and positioned over the slot. Since the LVDTs blocked access to the DEMEC points, only the LVDT measurements were used for the rest of the test. Each of the relative displacements from DEMEC point combinations 1-4 were set as the initial values for LVDTs 1-4, respectively. The complete setup for the single flat-jack test is shown in Figure 5-37a.

(a)   (b)
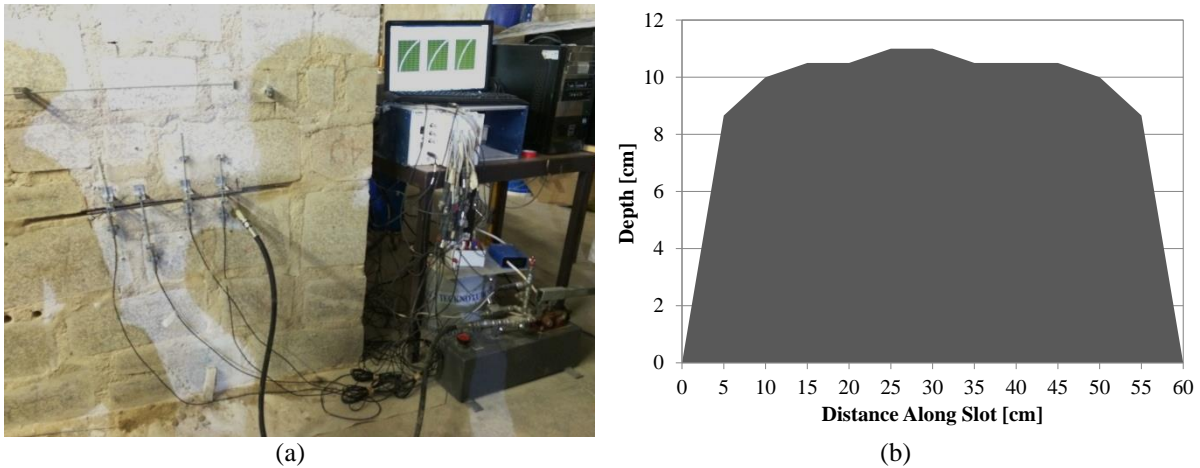
Figure 5-37 Single flat-jack test in the semi-irregular wall: (a) complete setup; and (b) measured slot area

Following the flat-jack test, the length and depth of the slot were measured in order to determine the area correction factor. The area of the slot is shown in Figure 5-37b. The flat-jack was inserted in the center of this slot. Note that the length of the slot is much longer than the length of the jack and that on either end of the slot there is some curvature due to the circular saw blade. Calculating the area of the slot to be approximately 612.6 cm^2 resulted in an area correction factor of 0.496.

Two pressurization cycles were performed with the flat-jack. The average LVDT displacements on the front and back of the wall and the applied pressure for these cycles are shown in Figure 5-38a. There are a couple of things to note about the presented results. For the flat-jack test, the applied pressure presented takes into account both the area correction factor and the jack calibration factor. In addition, as described previously, the LVDT measurements on the front of the wall have been adjusted for the initial relative displacement due to creating the slot, as measured using the DEMEC points. The front LVDTs in Figure 5-38a indicate that the slot is opening during the pressurization of the jack. The LVDTs on the back of the wall are moving in the opposite direction, indicating additional compressive stresses. Negative relative displacements were also observed on the back of the wall in the single flat-jack test on the regular masonry wall (see Figure 5-19).

(a)   (b)
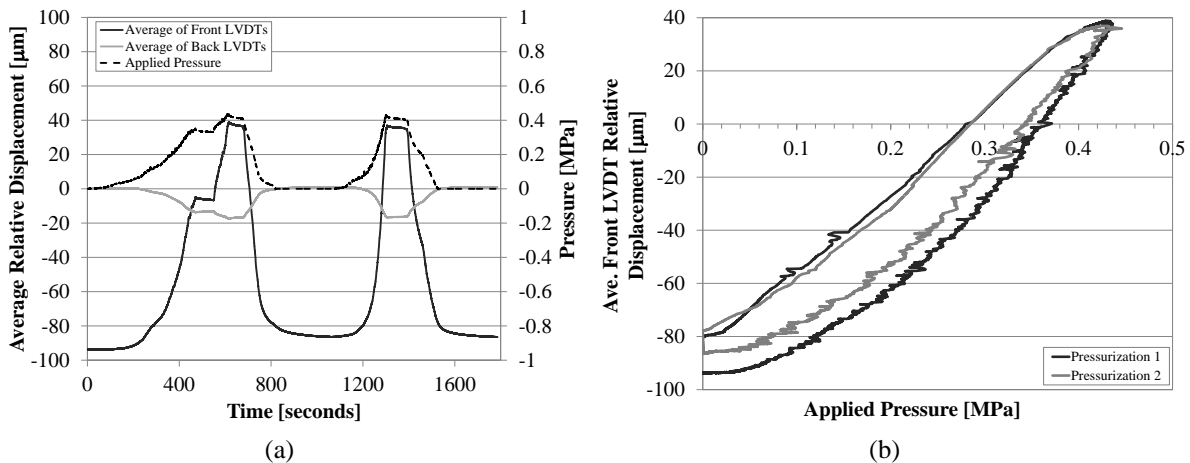
Figure 5-38 Results of the single flat-jack test in the semi-irregular wall: (a) average LVDT relative displacement and applied pressure during the pressurization cycles; and (b) average front LVDT relative displacement versus the applied pressure

The graph of pressure versus average front LVDT relative displacement (Figure 5-38b) shows that the flat-jack was able to apply enough pressure to return the masonry to its approximate position before the slot was cut. The applied pressure when the displacement was returned to zero, or the estimated local state of stress, was 0.36 MPa. While the estimated local state of stress is closer to the stress level due to the loading on the wall, 0.23 MPa, than in the tube-jack test, the flat-jack test is still over estimating the stress level in the wall by over 1.5 times.

The error in the flat-jack results could be because of the size of the flat-jack in relation to the size of the masonry units in this type of masonry. The flat-jack slot and flat-jack are only half of the depth of the masonry units in this wall. In traditional brick masonry and other small unit masonry, the slot and flat-jack would have been deep enough to test at least one full wythe of the wall. Here, the flat-jack is only deep enough to apply pressure to the front half of the units in the single wythe wall. Pressurizing only half of the wythe created an unequal distribution of stresses through the thickness of the wall, which was shown by the positive relative displacements on the front of the wall and negative relative displacements on the back of the wall during the pressurizations. If DEMEC measurements had been taken on the back of the wall, the LVDT results on the back of the wall could have been used in an overall average vertical displacement result for the test. Adding these results could have produced a more accurate estimation of the state of stress.

5.3.3 Double Tube-Jack Test

The double tube-jack test in the semi-irregular wall was performed following the single tube-jack test and before the flat-jack test. The loading on the wall was the same as for the single tube-jack test. The general location for the second line of holes was shown in Figure 5-29. Each of the holes in the second line was aligned directly over the corresponding hole in the first line. Thus, the holes had the same horizontal spacing in both lines but the vertical spacing varied based on the irregularity in the mortar joints. The two lines of holes separated a specimen within the masonry wall that was approximately 615 mm high and 825 mm long. When the tube-jacks were inserted and pressurized, the two lines of holes became equivalent flat-jacks pressurizing that masonry specimen.

LVDTs were attached to the masonry surface between the two lines of holes to measure the displacement of the masonry throughout the test. Four LVDTs were used on each side of the wall, three vertical LVDTs and one horizontal LVDT. The set-up of the LVDTs and the measuring distances on the front of the wall is shown in Figure 5-39a. The LVDTs were arranged in the same way and with the same measuring distances on the back of the wall. A photo of the LVDTs attached to the masonry during the drilling process is shown in Figure 5-39b.

(a)   (b)
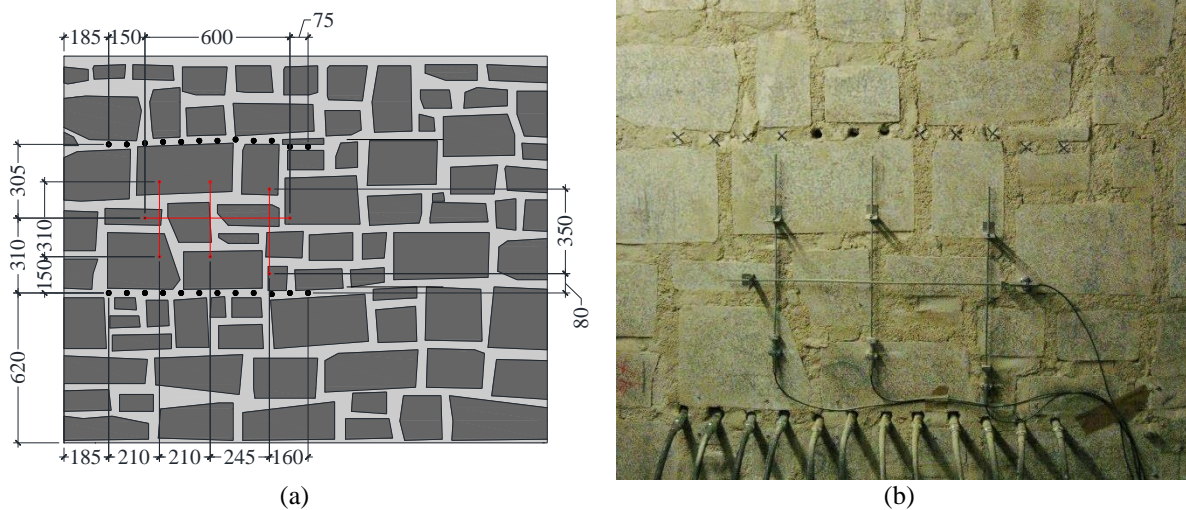
Figure 5-39 LVDT arrangement for the double tube-jack test on the semi-irregular wall: (a) locations and dimensions [mm]; and (b) photo of LVDTs attached to the wall

The hole drilling process was the same as in the single tube-jack test. As in the single tube-jack test in the semi-irregular wall, chunks of mortar were expelled from the back of the wall as the drill bit pushed through to the backside of the wall. The holes left behind after the mortar chunks had fallen out can be seen on the backside of the wall in Figure 5-40a after the drilling was complete. The final test setup with the second set of tube-jacks inserted in the holes is shown in Figure 5-40b and c.

(a)   (b)   (c)
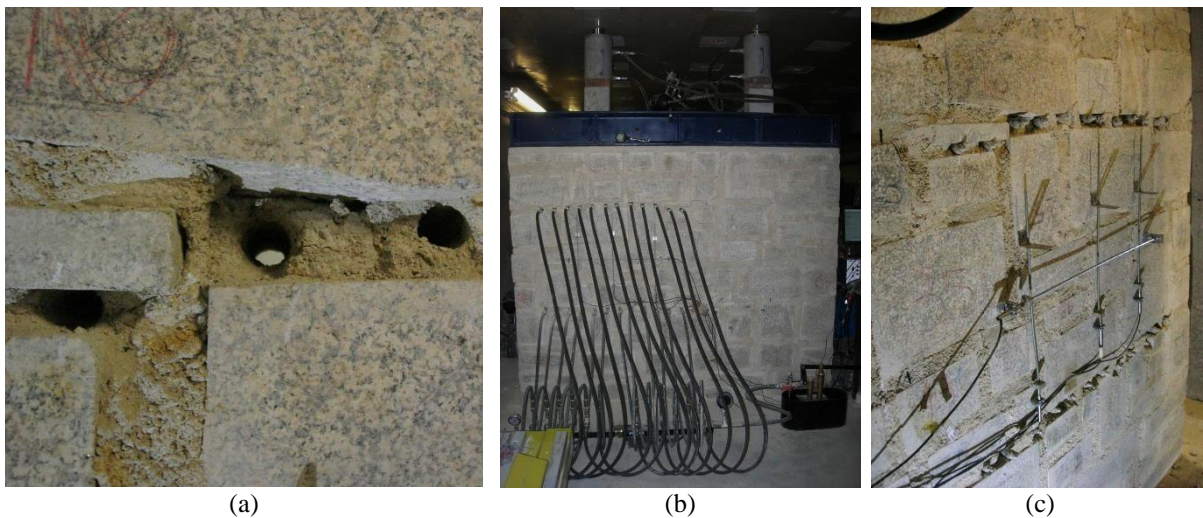
Figure 5-40 Drilling holes and inserting tube-jacks for the double tube-jack test on the semi-irregular wall: (a) holes from expelled mortar chunks on the backside of the wall; (b) complete set-up on the front of the wall; and (c) complete set-up on the back of the wall

The area correction factor for the double tube-jack test was determined using Equation (35) from section 2.3.2. The estimated length of the tube-jacks applying pressure to the masonry was 17 cm and the estimated diameter of each of the holes was 2.6 cm. These measurements gave an average total surface area of the tube-jacks in a plane through the centroid of the jacks of 530 cm^2. The length of the equivalent flat-jacks was 82.5 cm, giving a cross-sectional area of the separated specimen of 0.165 m^2. Thus, the area correction factor was 0.321. The area correction factor, k_a, was multiplied by the pressure the tube-jacks were applying to the masonry, p_m, to determine the applied pressure, shown in the result graph below.

118

Five pressurization cycles were performed during the double tube-jack test. During the fifth pressurization one of the tube-jacks burst, ending the test. Unfortunately, there was interference with the LVDTs on the front face of the wall due to another test taking place in the laboratory, so only the results from the LVDTs on the back of the wall from two of the pressurizations are presented here (see Figure 5-41).
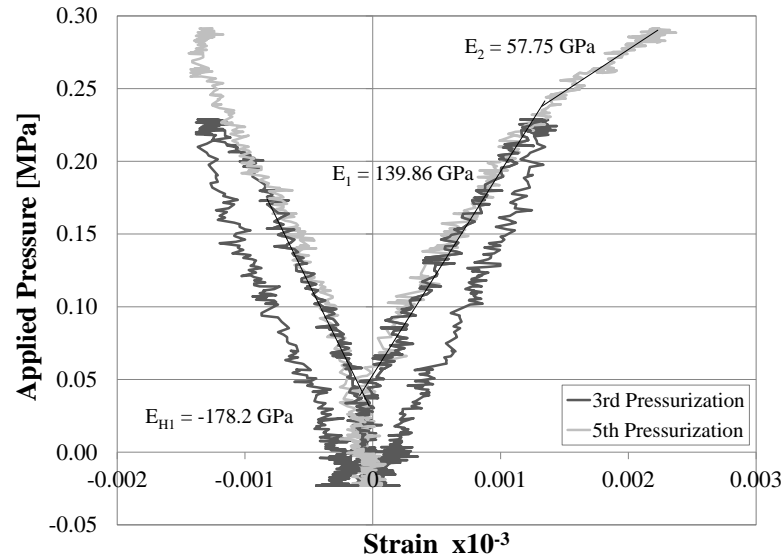
Figure 5-41 Applied pressure versus stain results on the back of the wall for the double tube-jack test on the semi-irregular wall

In Figure 5-41 it can be seen that the tube-jacks pressurize the masonry consistently in repeatable cycles. Note also that the displacements on the back of the wall were very small, resulting in very small strains and high estimates for the Young's modulus. If it had been possible to use the data from the front of the wall, the larger strains shown there could have been incorporated into an average showing a more realistic estimate of the Young's modulus. Even though the Young's modulus estimates shown are not accurate, there is one important observation to make from the graph. There is a definite change in the slope of the stress-strain curve at an applied pressure level of approximately 0.23 MPa. While this needs to be confirmed in further testing, this change in slope is likely indicating the maximum level of stress that the masonry has seen. A similar change in slope was also seen in the results of the double flat-jack test on the regular masonry wall.

The Poisson ratio of the semi-irregular masonry was estimated using the double tube-jack test results shown in Figure 5-41. The reloading vertical elastic modulus of 139.86 GPa was divided by the reloading horizontal elastic modulus of 178.2 GPa to get a Poisson ratio of 0.785. This value is much too high to be accurately representing the Poisson ratio of the material. The results from only the back of the wall do not represent the masonry as a whole.

5.3.4   Double Flat-Jack Test

The double flat-jack test was performed on the right side of the semi-irregular wall after the single flat-jack test. The loading on the wall was the same as for the single flat-jack test. The location for the second slot was directly above the first slot and at approximately the same height as the second line of holes for the double tube-jack test. Ten LVDTs were used in this test to record the relative displacements of the wall between the two flat-jack slots. Four vertical LVDTs and one horizontal LVDT were used on each side of the wall. The locations of the flat-

jack slots and LVDT connection points on the front of the wall are shown in Figure 5-42. The locations for the LVDTs on the back of the wall were the same as on the front.
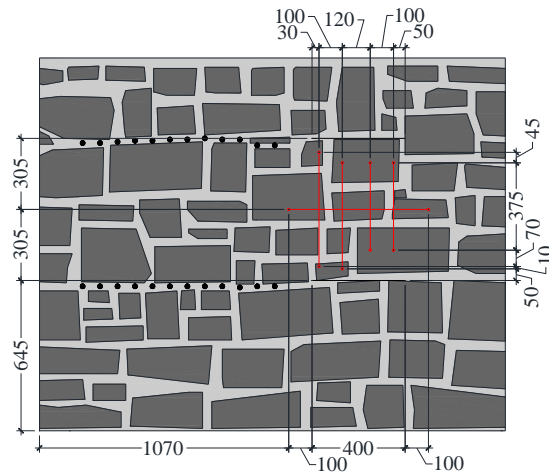
Figure 5-42 Double flat-jack test setup for the semi-irregular wall

The upper flat-jack slot was cut using the same circular saw as was used for the single flat-jack test (Figure 5-43a). Water was again used to reduce the amount of dust and a vacuum was used to suck up dust during sawing and in the slot (Figure 5-43b). Because the upper mortar joint was not long enough one of the granite blocks was cut into in order to cut the slot to the proper length and depth. If this wall had been in a historic structure, this cut would have damaged irreplaceable masonry units. If the historic masonry was visible, (without plaster) cutting through the stones likely would not have been allowed and the test would have had to be performed elsewhere or not at all.

(a)   (b)   (c)
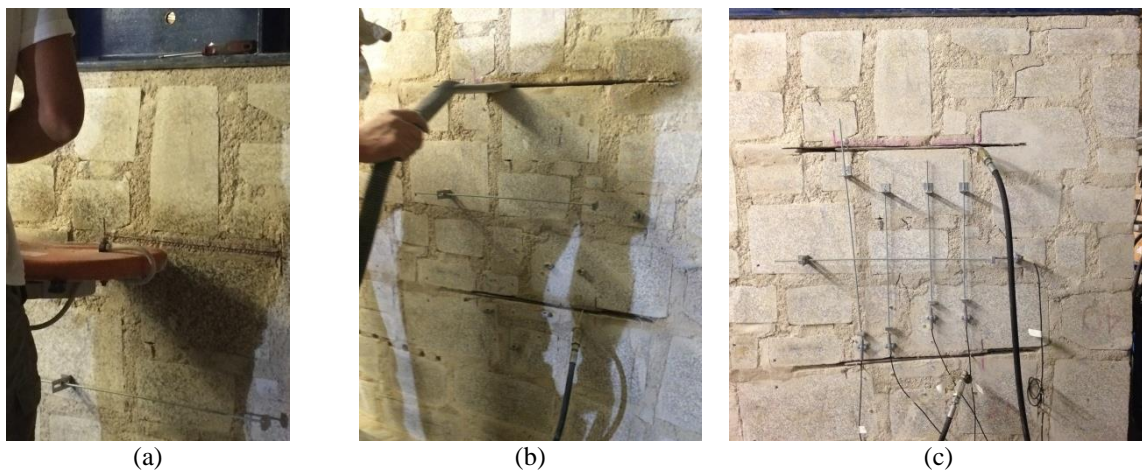
Figure 5-43 Preparation for the double flat-jack test in the semi-irregular wall: (a) cutting the upper slot; (b) vacuuming out dust; and (c) the complete setup

The area of the upper slot was assumed to be approximately the same as the area of the lower slot. The same size flat-jack was used for this slot as for the lower slot. Thus, the area correction factor was the same as in the single flat-jack test, 0.496. A flat-jack with a jack calibration factor of 0.77 was inserted into the slot. The jack calibration factors of the upper and lower flat-jacks were averaged to obtain the total jack calibration factor of 0.785. The complete test setup is shown in Figure 5-43c.

Ten pressurization cycles were performed during the double flat-jack test, with each subsequent pressurization obtaining a higher maximum pressure level. The LVDT relative displacements and the pressure applied by the flat-jacks throughout the course of the test are presented in Figure 5-44. The difference between the front and back of the wall is significant. The negative relative displacement on the front of the wall indicates the masonry is being compressed. On the back of the wall the relative displacement is positive, indicating that the masonry is moving apart. Even the horizontal LVDT on the back of the wall shows a positive relative displacement and a horizontal separation of the masonry. Because the flat-jacks are only half the depth of the wall, the applied pressure through the thickness of the wall varies greatly. In this sense, the results of this double flat-jack test are similar to the results of the double flat-jack test in the regular masonry wall. If LVDTs are only used on the front of the wall and jacks only pressurize part of the wall, the results are not representative of the masonry through the thickness of the wall. This is the case for this typology of masonry where the unit is the same depth as the thickness of the wall. However, this may not be the case in a multi-wythe wall.
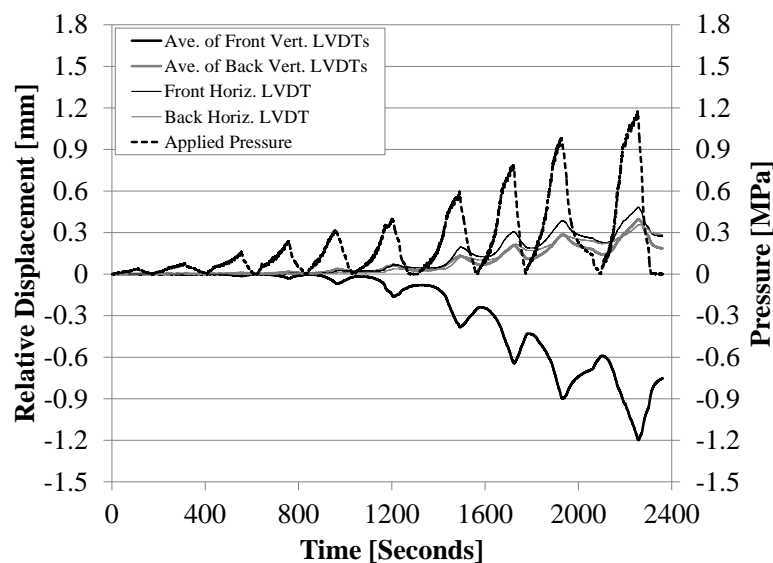
Figure 5-44 Relative displacement and applied pressure during the double flat-jack test pressurization cycles

Two sets of applied pressure versus strain results are shown in Figure 5-45, the average of all of the LVDTs (back and front of the wall) and the average of only the front LVDTs. Estimates were made for the moduli with tangent trend lines. Note the significant difference in the tangent slopes of the curves, particularly for the vertical LVDTs showing positive strains (compression). The initial slopes of the curves are greater because the masonry is being reloaded. The masonry has already been compressed to this level of applied pressure by applying load to the top of the wall. The initial slope of the average of all vertical LVDTs, 8.57 GPa, is high but still on the same order (a 50% difference) as the vertical reloading modulus found in the semi-irregular masonry wallet testing, 5.15 GPa (see Section 4.6.3).

The tangent slope of the curves changes at an applied pressure of approximately 0.3 MPa. It is theorized that the change in slope occurs at the maximum stress level that has occurred in the masonry up to that point in time. This change in slope was also seen in the double tube-jack test. It is at a higher stress level in this test because during the adjustment of the applied load on the wall, the pressure was at one point as high as 0.3 MPa. The second slope for the average of all vertical LVDTs, 0.92 GPa, is close to the value found for the initial loading of semi-irregular masonry wallets, 1.0 GPa, only an 8.3% difference. The results considering only the

movements of the front of the wall show much lower estimations for the elastic modulus and are not in the same range as the results from the masonry wallet tests.
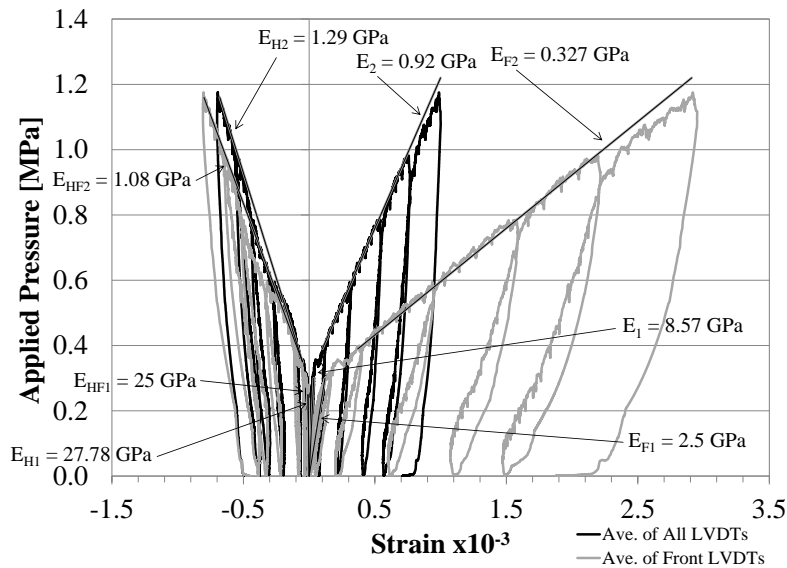
Figure 5-45 Results of the double flat-jack test in the semi-irregular wall

The Poisson ratio was estimated to be 0.31 using the reloading slopes for the vertical and horizontal LVDTs, considering all of the LVDT. This value is much more reasonable than the Poisson ratio result from the double tube-jack test on this wall. Using the reloading results from only the LVDTs on the front of the wall, the estimate for the Poisson ratio was 0.1, much lower than what would be expected for this masonry. However, using the initial loading slopes, the results are much different. The Poisson ratio estimation considering all of the LVDTs, 0.71, is much too high. The estimation for only the front LVDTs is a more reasonable value at 0.30.

5.4   *Irregular Masonry Wall*

The final wall to be constructed and tested was the irregular masonry wall. The irregular wall had irregular shaped granite units with irregular surfaces, as described in section 4.3. It was expected that the results from this wall would be the most irregular and most complex, similar to traditional historical Portuguese masonry. The loading of the irregular wall was similar to the loading for the regular and semi-irregular wall except that four hydraulic jacks were used to load the wall instead of two (see Figure 5-46) to create a better stress distribution. The pressure in the hydraulic jacks loading the wall was adjusted to 1.41 MPa. This loading was approximately equal to an applied pressure of 0.22 MPa on top of the wall, but the exact loading and stress in the wall are unknown due to the irregularity in the thickness of the wall (see Figure 5-46). The approximate stress level in the wall was estimated in each joint that was tested based on this applied pressure and the weight of the equipment and the estimated weight of the masonry above that joint.

Four minor-destructive tests were performed on the irregular wall. The single tube-jack test and double tube-jack test were performed first on the left side of the wall. Only rubber tube-jacks were used in the tests on the irregular wall. Following these two tests, the holes were filled with mortar. The single and double flat-jack test were then performed in horizontal joints on the right side of the wall. For this wall, due to the arrangement of the granite units, the flat-jack slots were not at the same heights as the lines of holes for the tube-jack tests. The arrangement for

122

the four tests in the irregular wall is shown in Figure 5-46. The complete test set-up, procedure and results for each test are presented in the following subsections.
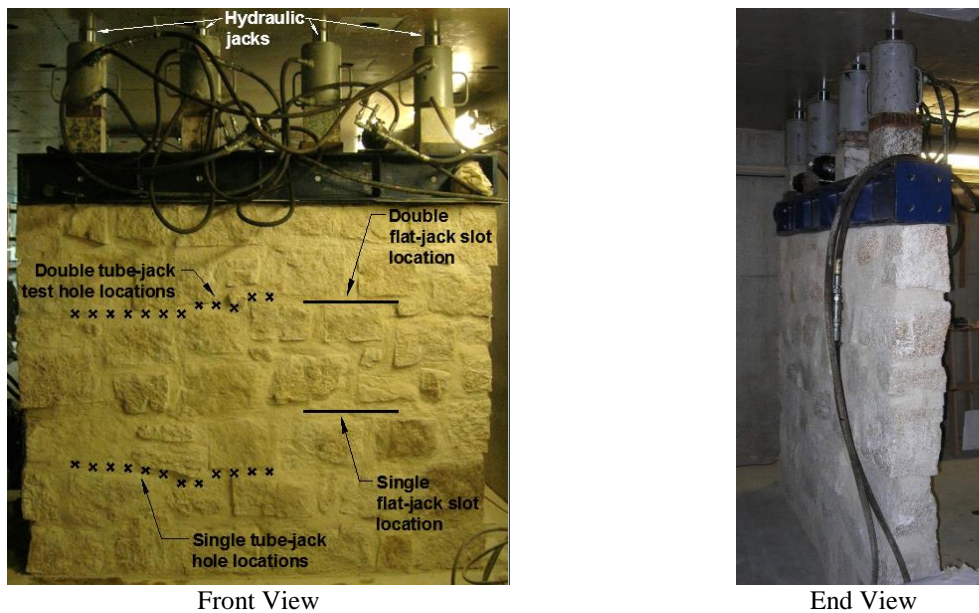
Figure 5-46 Irregular masonry wall loading and test arrangement

5.4.1 Single Tube-Jack Test

A single tube-jack test was performed on the irregular granite masonry wall in the 2nd horizontal mortar joint up from the base of the wall, at an approximate height of 47 cm. The stress state at this level in the wall was estimated to be approximately 0.247 MPa. This is a slightly higher stress level than for the single tube-jack tests performed on the regular and semi-irregular walls. Twelve tube-jacks were used for the test, the same number as was used in most of the other tube-jack tests. As much as possible, the holes for the tube-jacks were spaced approximately 7.5 cm from center to center horizontally, resulting in an overall equivalent flat-jack length of 82.5 cm. In the irregular wall test, the holes were labeled Hole 1 through Hole 12 from right to left, opposite from the labeling in the previous tests. The labeling of the holes was changed because the order of drilling the holes was changed as described below. The positions and numbers of the holes for the tube-jacks and for the LVDTs are shown in Figure 5-47.

Ten LVDTs were used to measure the relative displacement of the masonry, six on the front of the wall and four on the back of the wall. In the regular and semi-irregular masonry wall single tube-jack tests, the LVDTs measured over a distance of 8 cm. In the irregular wall test some of the measuring distances for the LVDTs had to be varied in order to accommodate the irregular joints and attachment to irregular shaped units. The LVDT measuring distances are shown in Table 5-2. All of the LVDTs used for the irregular masonry wall tube-jack tests had a range of ±2.5 mm.

Table 5-2 LVDT measuring distances for the single tube-jack test in the irregular wall

Front of the wall		Back of the wall	
LVDT #	Measuring Distance [cm]	LVDT #	Measuring Distance [cm]
LVDT 1	10	LVDT 7	12
LVDT 2	40		
LVDT 3	10	LVDT 8	11
LVDT 4	10	LVDT 9	10
LVDT 5	35		
LVDT 6	10	LVDT 10	10

As in the semi-irregular wall single tube-jack test, an equal spacing of the LVDTs was not possible for the irregular wall. However, the LVDTs were distributed as evenly as possible along the length of the equivalent flat-jack. They were labelled LVDT 1 through 6 on the front of the wall and LVDT 7 through 10 on the back of the wall.
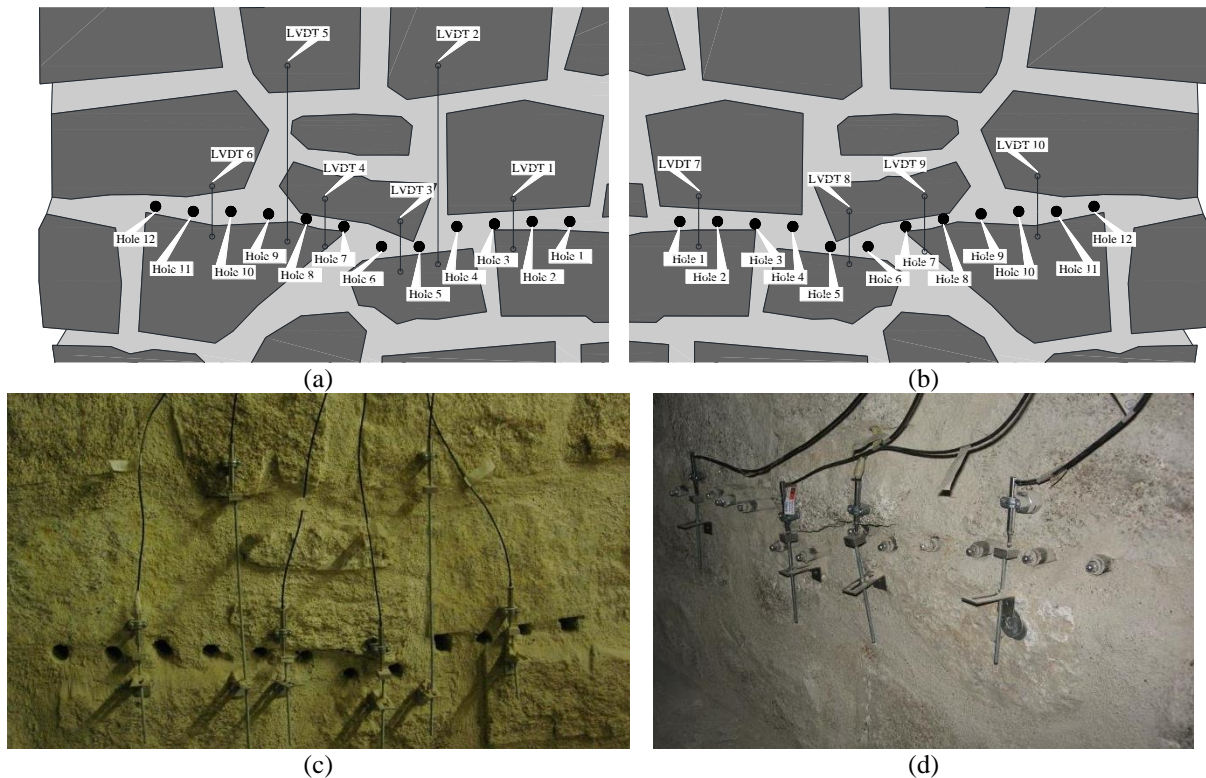
Figure 5-47 Holes and LVDT positions for the single tube-jack test in the irregular wall: (a) front of the wall; (b) back of the wall; (c) holes drilled in the front of the wall; and (d) tube-jack ends sticking out the back of the wall

The mortar used for the irregular wall was the same mixture as for the semi-irregular wall and the properties were similar, see section 4.5.2. Due to the difficulties experienced in drilling the holes for the semi-irregular wall, an alternative drilling method was tested for the irregular wall. A core drill was used to drill the holes. Water was not used to wet the drill during this process. The hope was that this technique could be used to improve the simplicity of the drilling process, produce more regular diameter holes, and be used to collect samples of the mortar in tests on a historical structure.

In the previous tube-jack tests, a 20 mm drill bit was used to drill the holes. During the drilling, the curved blade of the drill bit pushed the mortar towards the edges of the hole as it drilled, creating a larger diameter. It was expected that the displaced mortar material during coring would stay within the core drill bit. Thus, the core drill would create a hole the same diameter as the drill bit. Therefore, a slightly larger core drill bit with a 22 mm diameter was chosen so that the holes in the irregular wall would be approximately the same diameter as the holes in the regular and semi-irregular walls.

Because of the weight of the core drill and the necessity to keep it steady during the drilling process, the core drill was mounted to an adjustable steel expansion pole. The expansion pole was tightened against the reaction ceiling and floor to secure the core drill in place. The mounting sleeve allowed the core drill to be positioned vertically and secured by tightening a bolt. A different setup would be required for securing the core drill in the field. The core drill setup is shown in Figure 5-48. To reduce the distance required to move the drill between holes, it was decided to start drilling the holes on the right side and work to the left rather than starting in the center of the row of holes and working outward.

Figure 5-48 Core drill setup for the single tube-jack test in the irregular wall

Moving the core drill in between drilling each hole took more time than expected. Drilling the holes for the single tube-jack test on the irregular wall took longer than for the semi-irregular wall, over three hours. In some cases, the core drill was not long enough to reach completely through the thickness of the wall. The drilling had to be completed with a regular drill. This resulted in some holes having larger diameters toward the front of the wall and smaller diameters at the back of the wall. If this system is to be used in future tests, the setup must be modified to make it easier to move and adjust the core drill.

The core drill did not create holes with the diameter of the core drill bit. Small chunks of mortar and aggregate would break off the surface of the mortar joint as the drill started to cut the hole. Chunks of mortar or edges of the granite units would disrupt the core drill bit as it drilled through the wall causing the drill to vibrate and increase the size of the holes. However, there were no problems with large mortar chunks breaking off the front or back of the wall, as there were during drilling in the semi-irregular wall. After the drilling was complete, the diameters of the holes were estimated on the front and back of the wall using a digital micrometer. The average diameter of the holes was 25.14 mm. The individual measurements are included in Appendix E. The average diameter was used to determine the pressure the tube-jacks applied to the masonry, p_m.

The LVDTs were able to record the displacement of the wall while the holes were being drilled. Approximately 20 minutes was given for the wall to stabilize before the tube-jacks were

inserted into the holes and the pressurizations were begun. The complete test setup and the average relative LVDT displacement results are shown in Figure 5-49.

(a)   (b)
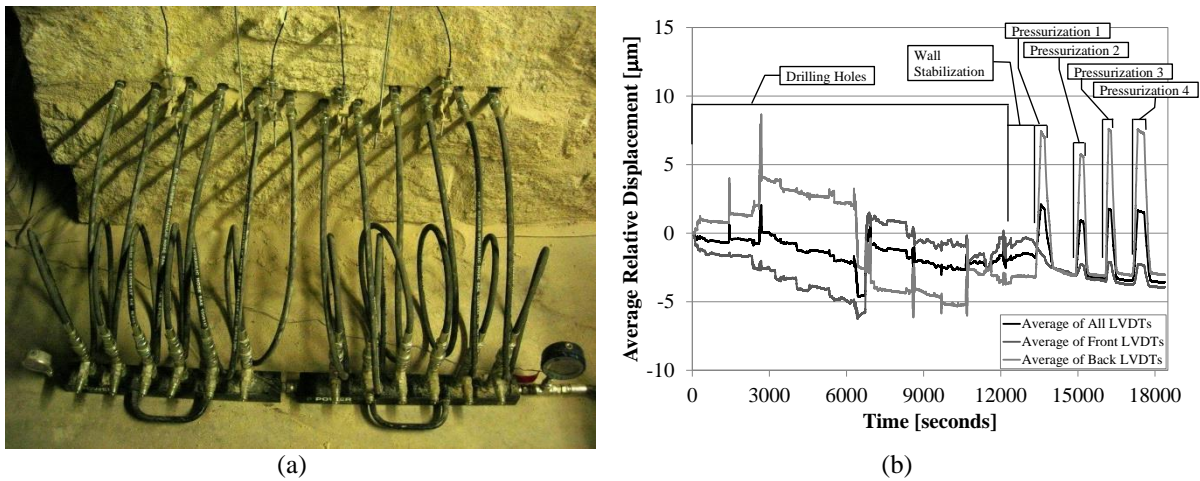
Figure 5-49 Single tube-jack test in the irregular wall: (a) complete test setup; and (b) average relative LVDT displacements

The drilling results show that there was some expansion of the masonry on the back of the wall at the beginning of the drilling. After about half way through drilling the holes, there was a significant contraction of the wall and shortly afterward an expansion of the front of the wall. The opposite movements of the front and back of the wall indicate the shifting and tilting of the granite units within the wall. As two units move together on one side of the wall, they move apart on the other side of the wall. This is why it is important to be recording the movement on both sides of the wall. The overall average relative displacement is negative indicating a contraction or coming together of the masonry as the holes are being drilled.

The relative displacement results also show some expansion on the front of the wall after the drilling is complete. It was hypothesized that this movement is due to the redistribution of stresses throughout the wall due to drilling the holes. The expansive movement of the wall meant that the LVDTs on the front of the wall were not as affected by the pressurization cycles as the LVDTs on the back of the wall. It is likely that the LVDTs on the back of the wall also showed more response to the pressurization cycles because the diameters of the holes were smaller toward the back of the wall, allowing more of the inner water pressure to be applied to the masonry rather than inflating the tube-jacks. The average relative displacements and the applied pressure are shown in Figure 5-50 during the four pressurization cycles performed.
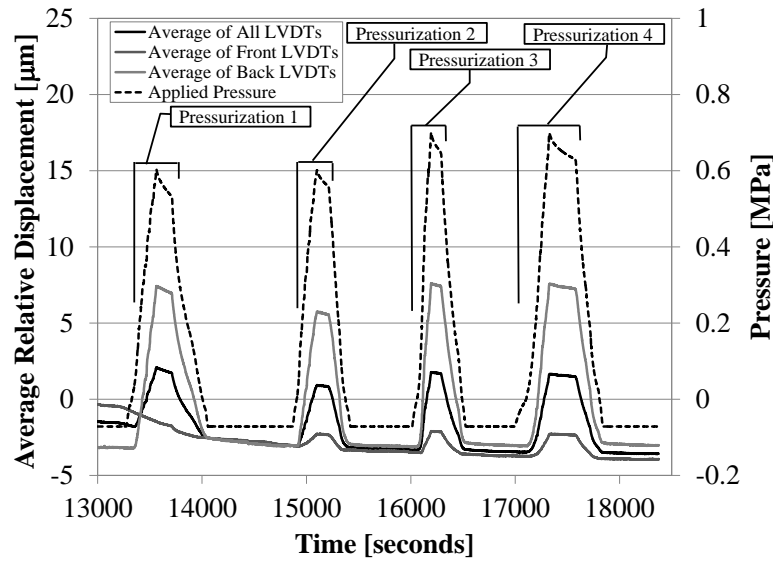
Figure 5-50 Average relative displacements and applied pressure during pressurization cycles

Following the test, the area correction factor, k_a, was calculated as the ratio of the surface area of the tube-jacks, A_T, to the surface area of the holes, A_H, in the horizontal plain through the centroid of the holes (see Figure 2-30). The individual measurements for each hole are shown in Table E-2 in Appendix E. The average length of the holes was only 17.3 cm. If this is taken as the average width of the wall, then the estimated stress level in the wall is increased to 0.281 MPa from the value estimated at the beginning of the test, 0.247 MPa. Since the length of the tube-jacks applying pressure to the masonry was in most cases as long as the hole depth, the area correction factor, k_a, for the single tube-jack test was very high for this test, 0.983. The pressure that the tube-jacks apply to the masonry, p_m, was multiplied by k_a, to obtain the applied pressure, $P_{Applied}$, shown in the result graphs, Figure 5-50 and Figure 5-51.
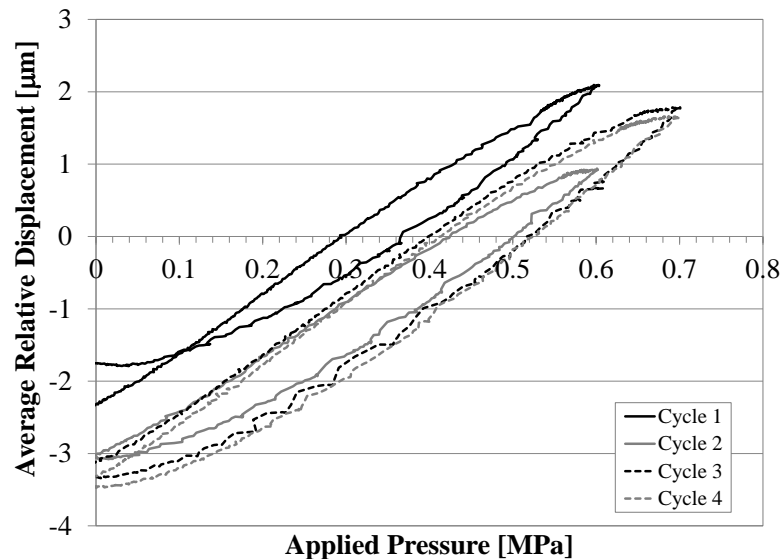
Figure 5-51 Average relative displacement vs. applied pressure for the single tube-jack test on the irregular wall

The results presented in Figure 5-51 show again how the masonry was still adjusting to the holes during the first pressurization cycle. During the second through fourth cycles the curves follow the same paths. Based on the results from this graph, the estimated state of stress in the

127

wall at this joint would be approximately 0.5 MPa. This value is much higher than the assumed state of stress of 0.281 MPa. One of the reasons for the difference could be the variation in the hole diameters from the front of the wall to the back of the wall. Another source for error could have been the readings from the LVDTs. In some cases the LVDTs were not perfectly vertical due to the irregularity of the granite surfaces they were attached to. Also, six LVDTs were mounted to the front of the wall but only four could be mounted to the back of the wall. It would have been ideal to have an equal number of LVDTs on both sides. More research should be done in the future to better understand the reasons for the error in this test.

5.4.2   Single Flat-Jack Test

Following all of the tube-jack tests on the semi-irregular wall, a single flat-jack test was performed on the right side of the semi-irregular wall, approximately one course higher than the single tube-jack test, see Figure 5-46. The loading on the wall was the same as for the single tube-jack test. If the wall is assumed to be the same depth as measured during the single tube-jack test, 17.3 cm, the approximate stress level at the location of the single flat-jack test was 0.276 MPa. A flat-jack with dimensions of 40 cm long by 10 cm deep and jack calibration factor, K_m, of 0.78 was used for this test.

As in the previous single flat-jack tests, DEMEC and LVDTs were used to measure the relative displacements of the masonry. The location of the slot was marked on the mortar joint and then the DEMEC gage points were glued in place and LVDT holders were screwed into the granite units (Figure 5-52a and c). Two sets of DEMEC points were used on both the front and back of the wall, similar to the test on the regular wall. Six LVDTs were used for the test, three on each side of the wall. The dimensions and locations of the DEMEC gage points and LVDT connection points in relation to the slot are shown in Figure 5-52b and d. As in the semi-irregular test, the LVDTs and DEMEC points could not be spaced equally along the slot or equidistant vertically from the slot. Each set of DEMEC points measured over a distance of approximately 20 cm and the measuring distances for the LVDTs are shown in Figure 5-52. The DEMEC point combinations and LVDTs were labeled from right to left on the front of the wall and left to right on the back of the wall. This is the same labeling method as used for the single tube-jack test on the irregular wall.
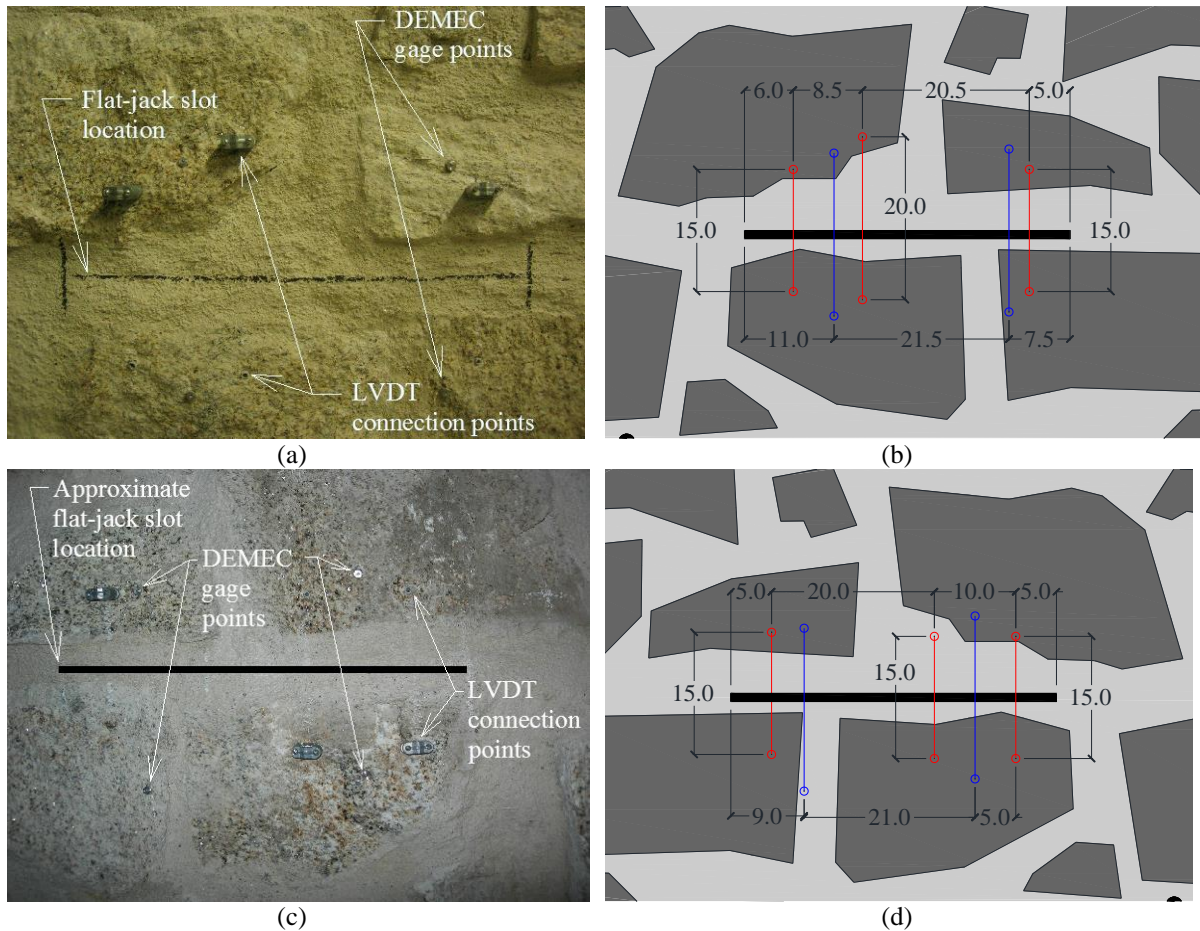
Figure 5-52 Attachment of DEMEC gage points and LVDT connection points for the single flat-jack test in the irregular wall: (a) and (b) show the front of the wall; and (c) and (d) show the back of the wall (DEMEC points in blue and LVDT points in red, dimensions in [cm])

Once the glue had dried and the DEMEC gage points were secure, several measurements were taken with the analog DEMEC used in the regular wall tests and shown in Figure 5-15a. The slot was created using the same disk saw used in the semi-irregular wall tests (Figure 5-36a). Several passes with the saw were required to cut the slot to a depth and thickness so that the flat-jack could be inserted. Water was not used during the sawing process.

After the slot was complete, DEMEC measurements were taken to determine the relative displacement of the masonry due to sawing the slot. The average results are shown in Table 5-3. The relative displacement results show that there was a closing of the masonry on the front of the wall, point combinations 1 and 2, and an opening of the masonry on the back, point combinations 3 and 4. This shows the uneven stress distribution through the wall depth.

Table 5-3 DEMEC results for the single flat-jack test in the irregular wall

Measurement Time	Point Combination			
	1	**2**	**3**	**4**
Before Sawing	7.075	4.731	5.807	10.571
After Sawing	7.094	4.905	5.766	10.568
Relative Displacement [mm]	-0.019	-0.174	0.041	0.002

Following the DEMEC readings, the flat-jack was inserted in the slot and the LVDTs attached and positioned over the slot and on the back of the wall. The LVDTs blocked access to the DEMEC points, so only the LVDT measurements were used for the rest of the test. The initial relative displacement for each LVDT was set as the relative displacement result from the DEMEC point combination closest to that LVDT. For example, the initial relative displacement of LVDTs 1 and 2 was the relative displacement due to sawing the slot from DEMEC point combination 1. LVDT 3 had an initial relative displacement the same as the relative displacement of DEMEC point combination 2. The complete setup for the single flat-jack test is shown in Figure 5-53.

(a)   (b)

Figure 5-53 Complete test setup for the single flat-jack test in the irregular wall with the flat-jack inserted in the slot and LVDTs attached: (a) front of the wall; and (b) back of the wall

The depth of the slot was measured along its length after the flat-jack test was finished. With these measurements, the area correction factor was calculated. A plot of the slot area is shown in Figure 5-54. Calculating the area of the slot to be approximately 701.5 cm^2 resulted in an area correction factor of 0.433.
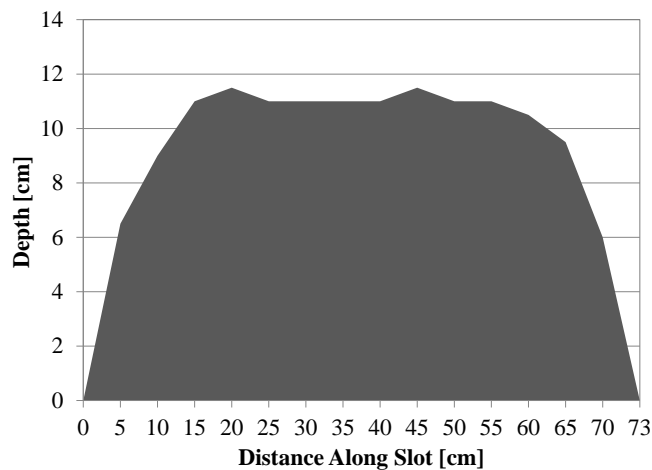
Figure 5-54 Irregular wall single flat-jack slot area

Before the pressurization cycles were conducted, the oil pressure in the flat-jack system required to return the relative displacements to zero was estimated prior to the determination of the area correction factor. It was estimated that an oil pressure of approximately 0.4 MPa would be required, given the jack correction factor of 0.78. Since the area correction factor was found to be much lower than expected, the require restoration oil pressure proved to be greatly

130

underestimated. Thus, in the result graphs below showing the pressure applied to the masonry, considering both the area correction factor and the jack correction factor, the relative displacements were not returned to zero.

During the test, three pressurization cycles were performed with the flat-jack. The average relative displacements are shown in Figure 5-55a for the LVDTs on the front of the wall, back of the wall, and for all of the LVDTs. During each of the pressurization cycles the LVDTs on both sides of the wall move toward restoring a zero relative displacement. As expected, the front of the wall is more affected by cutting the slot and by pressurizing the flat-jack in the slot than the back of the wall. The LVDTs on the front of the wall had a large negative initial relative displacement due to opening the slot and show positive relative displacements during the pressurization cycles. The LVDTs on the back of the wall had small positive initial relative displacements and show very small negative relative displacements during the pressurization cycles.

The average of all of the LVDTs is plotted versus the applied pressure in Figure 5-55b. Since the average relative displacement was not restored to zero, a linear extrapolation line was fit to the 2nd pressurization curve with a high coefficient of determination of 0.991. This line estimates that the local state of stress in the wall was approximately 0.42 MPa. As in the single tube-jack test on the irregular wall, this estimate is much higher than the state of stress calculated based on the load on the wall and density of the materials, 0.276 MPa. In the case of the flat-jack test, it is likely that the error is due to the small size of the flat-jack and only being able to pressurize half of the depth of the units and half the thickness of the wall.
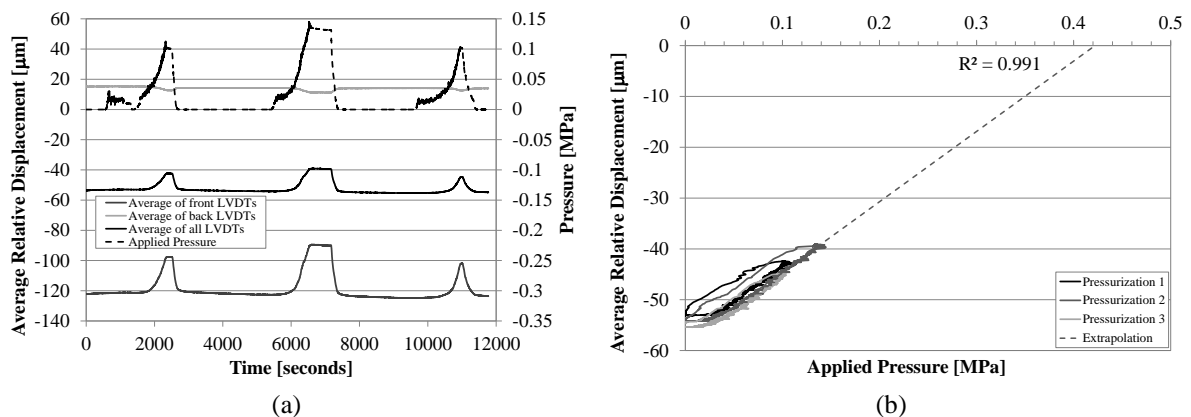
Figure 5-55 Results of the single flat-jack test in the irregular wall: (a) applied pressure and average relative displacements on the front and back of the wall throughout the test; and (b) average relative displacement versus the applied pressure

5.4.3   Double Tube-Jack Test

The double tube-jack test in the irregular wall was performed following the single tube-jack test and before the flat-jack tests. The loading on the wall was the same as for the single tube-jack test. The general location for the second line of holes was shown in Figure 5-46. The test setup was very similar to the setup for the double tube-jack test in the semi-irregular wall. The holes in the second line were aligned directly over the corresponding holes in the first line and were labeled Hole 13 through Hole 24 from right to left. The vertical spacing varied even more than in the semi-irregular test due to the irregularity of the mortar joints. The two lines of holes separated a specimen that was approximately 692.5 mm high and 825 mm long.

Four LVDTs were used on each side of the wall to measure the displacement of the masonry throughout the test, three vertical LVDTs and one horizontal LVDT. The vertical LVDTs were labeled from right to left on the front of the wall, LVDTs 1-3, and from left to right on the back of the wall, LVDTs 5-7. LVDT 4 was the horizontal LVDT on the front of the wall and LVDT 8 was the horizontal LVDT on the back of the wall. The setup for the LVDTs and the measuring distances on the wall are shown in Figure 5-56. Note that some of the LVDT stands had to be bent to avoid the irregular units on the back of the wall and line up with the LVDT holders. This could have contributed to some measurement errors in the results.

(a)

(b)

(c)

(d)

Figure 5-56 Arrangement of LVDTs for the double tube-jack test on the irregular wall: measuring distances on (a) the front of the wall and (c) back of the wall; and photos of LVDTs attached to (b) the front of the wall and (d) the back of the wall

The holes for the second line of tube-jacks were drilled using the same procedure and equipment as used in the single tube-jack test on the irregular wall. The core drill was used to drill the holes starting with the hole furthest to the right on the front of the wall and moving to the left. The drilling took approximately an hour and forty-five minutes. Once the drilling was complete, the tube-jacks were connected to the tube-jack system and placed in the holes. The complete test setup is shown in Figure 5-57.

Figure 5-57 Complete double tube-jack test setup on the irregular wall

Following the double tube-jack test, the diameters and lengths of the holes were measured and recorded. The diameters of the holes in the upper equivalent flat-jack are displayed in Table E-3 in Appendix E. Using the equations presented in section 2.3.2 and the average diameter of all of the holes in the double tube-jack test, 25.6 cm, the pressure applied by the tube-jacks on the holes, p_m, was calculated for the test.

The area correction factor was determined as described by Equation (35) in section 2.3.2. First, the cross-sectional area of the specimen between the two equivalent flat-jacks, A_S, was determined. To determine the average depth of the specimen, the depth of each of the holes was measured for the bottom line of holes, Table E-2, and the top line of holes, Table E-4. The average depth of each line of holes was multiplied by the length of the equivalent flat-jack, 82.5 cm, to determine the area of the top equivalent flat-jack, 1300 cm^2, and the bottom equivalent flat-jack, 1430 cm^2. These two areas were averaged to estimate the cross-sectional area of the separated masonry specimen, 1360 cm^2.

Second, the total surface area of the tube-jacks applying pressure to the masonry projected on a plane through their centroids was determined for the lower, A_{T1}, and upper, A_{T2}, equivalent flat-jacks. To determine the area pressurized by each tube-jack, the length of each tube-jack pressurizing the masonry was multiplied by the average horizontal diameter of each hole (see Table E-2 and Table E-4). In the case of the irregular wall, the depths of the holes were usually less than the pressurization lengths for the tube-jacks. Thus, the length of the tube-jack pressurizing the masonry was the same as the length of the hole. The areas pressurized by each tube-jack were summed to determine the total area pressurized by the lower equivalent flat-jack, $A_{T1} = 506$ cm^2, and the total area pressurized by the upper equivalent flat-jack, $A_{T2} = 496$ cm^2. These two areas were averaged to get 500 cm^2.

The average area pressurized by the tube-jacks, 500 cm^2, was divided by the cross-sectional area of the separated specimen, 1360 cm^2, to determine the area correction factor, 0.367. The area correction factor, k_a, was multiplied by the pressure the tube-jacks applied to the masonry, p_m, to determine the applied pressure, shown in the result graphs below.

Two rounds of pressurizations were performed in the double tube-jack test on the irregular wall. In the first round of pressurizations, three cycles were performed. During the second cycle, tube-jack number four broke at an internal water pressure of 0.57 MPa, ending the second cycle. This tube-jack was replaced and a third pressurization cycle was conducted. The average LVDT results and the applied pressure are shown in Figure 5-58. Comparing the relative displacements

on both sides of the wall, the front and the back of the wall show similar trends throughout the test. Both sides of the wall show negative vertical relative displacements, indicating compression of the masonry, and positive horizontal relative displacements, indicating expansion of the masonry due to Poisson effects, during the pressurization cycles. This suggests that the tube-jacks were pressurizing the masonry approximately equally throughout the thickness of the wall.

(a)   (b)
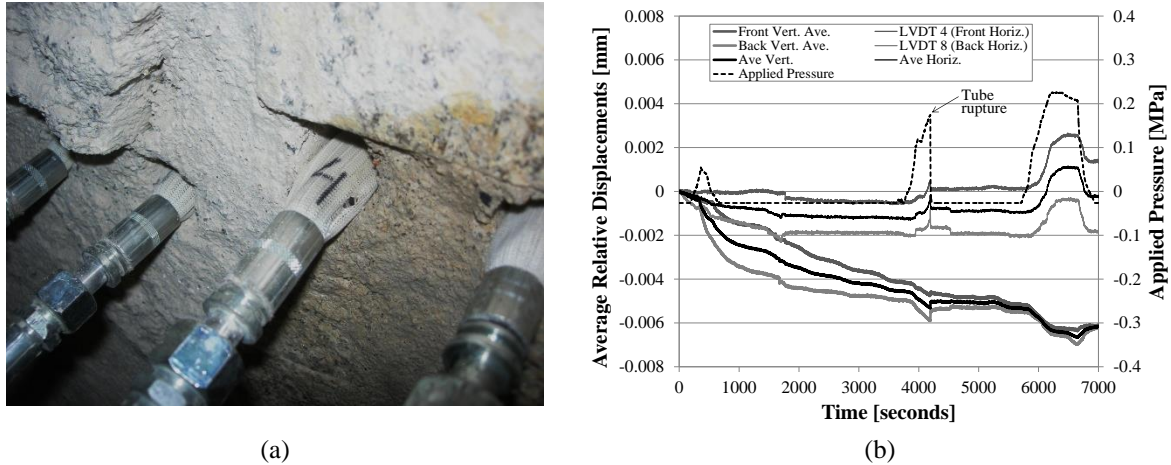
Figure 5-58 First round of pressurizations: (a) rupture of tube-jack four during second cycle; and (b) average relative displacements and applied pressure during cycles

It is also important to note the continuous downward trend of the vertical relative displacement throughout the test. This could be due to the masonry continuing to adjust from drilling the second line of holes and loading from the jacks above. To make the pressurization cycles more comparable, the strains were zeroed before each pressurization cycle for presentation in the applied pressure versus strain graph shown in Figure 5-59. The strains were very small, on the same order of magnitude as seen in the semi-irregular wall double tube-jack test. This produced high estimations of the elastic modulus of the material. An estimation of the Poisson ratio of the material based on the vertical and horizontal moduli gives a value of 0.51. As in the double tube-jack test on the semi-irregular wall, this value is above 0.5, suggesting it is not an accurate value for the material.
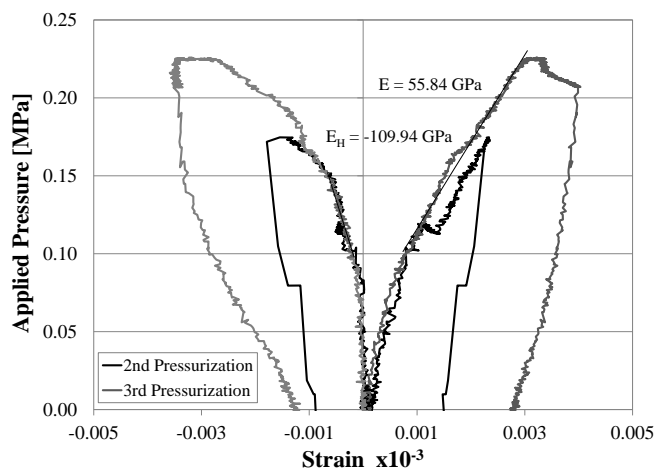
Figure 5-59 Applied pressure versus strain results for the first round of pressurizations in the double tube-jack test in the irregular masonry wall

A second pressurization round was performed one day after the first pressurization round. It was expected that the wall would have stabilized in the time between the pressurization rounds so that no movement would be observed unless it was due to the tube-jack pressurizations. To determine if power fluctuations were causing a disruption in the LVDT data, one LVDT was used as a control LVDT and was not attached to the wall. All of the other LVDTs attached to the wall were normalized using this LVDT. One pressurization cycle was performed in this second pressurization round. The average relative displacements and applied pressure throughout the test are shown in Figure 5-60a. The results show that there was still some movement of the wall as recorded by the LVDTs before and after the pressurization cycle. The strain results were again zeroed before the pressurization cycle for display in the applied pressure versus strain graph, Figure 5-60b.

(a)

(b)
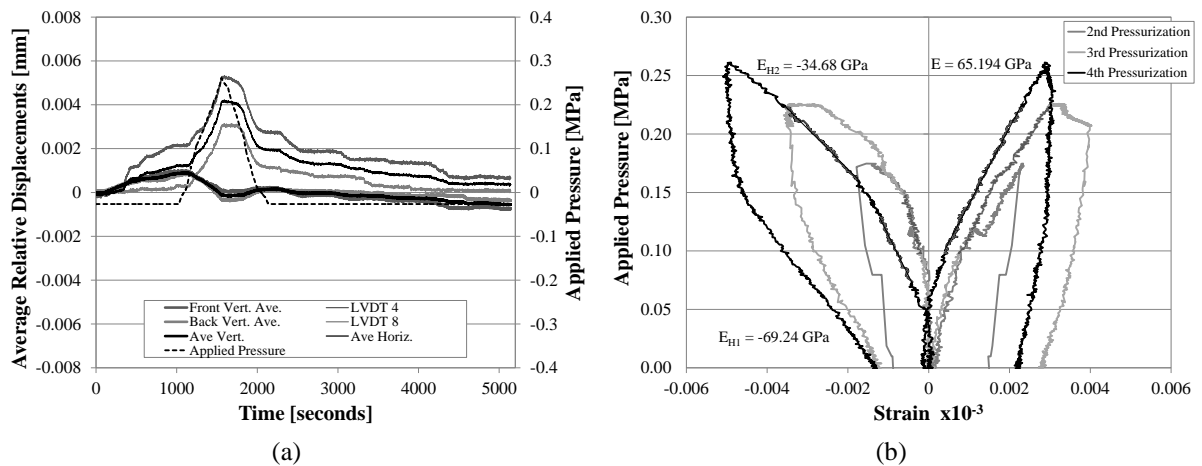
Figure 5-60 Results of the second round of pressurizations in the double tube-jack test on the irregular wall: (a) relative displacements and applied pressure throughout the test; and (b) applied pressure versus strain as compared to the first round pressurizations

The elastic modulus estimations presented in Figure 5-60 are from trend lines fit only to the fourth pressurization cycle. Comparing the two pressurization rounds, the second round has a higher vertical stiffness and a lower horizontal stiffness. This resulted in an estimation of the Poisson ratio even higher than in the first round, 1.88. These results could suggest that the pressurization cycles and loading consolidated and compressed the masonry vertically increasing the stiffness. In the horizontal direction, it is possible that the proximity to the end of the wall is allowing the masonry to expand horizontally more easily, especially after continuous loading on the top of the wall and two lines of holes through the thickness of the masonry.

5.4.4   Double Flat-Jack Test

The double flat-jack test was performed on the right side of the irregular wall after the single flat-jack test. The loading on the wall was the same as for the other tests on the irregular wall. The location for the second slot was directly above the first slot and at approximately the same height as the second line of holes for the double tube-jack test. The specimen separated by the two flat-jacks was approximately 46.5 cm in height. Eight LVDTs were used in this test to record the relative displacements of the wall between the two flat-jack slots, three vertical LVDTs and one horizontal LVDT on each side of the wall. The vertical LVDTs were labeled from right to left on the front of the wall, LVDTs 1-3, and from left to right on the back of the wall, LVDTs 5-7. LVDT 4 was the horizontal LVDT on the front of the wall and LVDT 8 was the horizontal LVDT on the back of the wall. The locations of the flat-jack slots and LVDT

connection points are shown in Figure 5-61. As in the double tube-jack test on this wall, attachment of the LVDTs on the back of the wall was difficult and some of the stands had to be bent to align them with the LVDT holders, see Figure 5-61d.
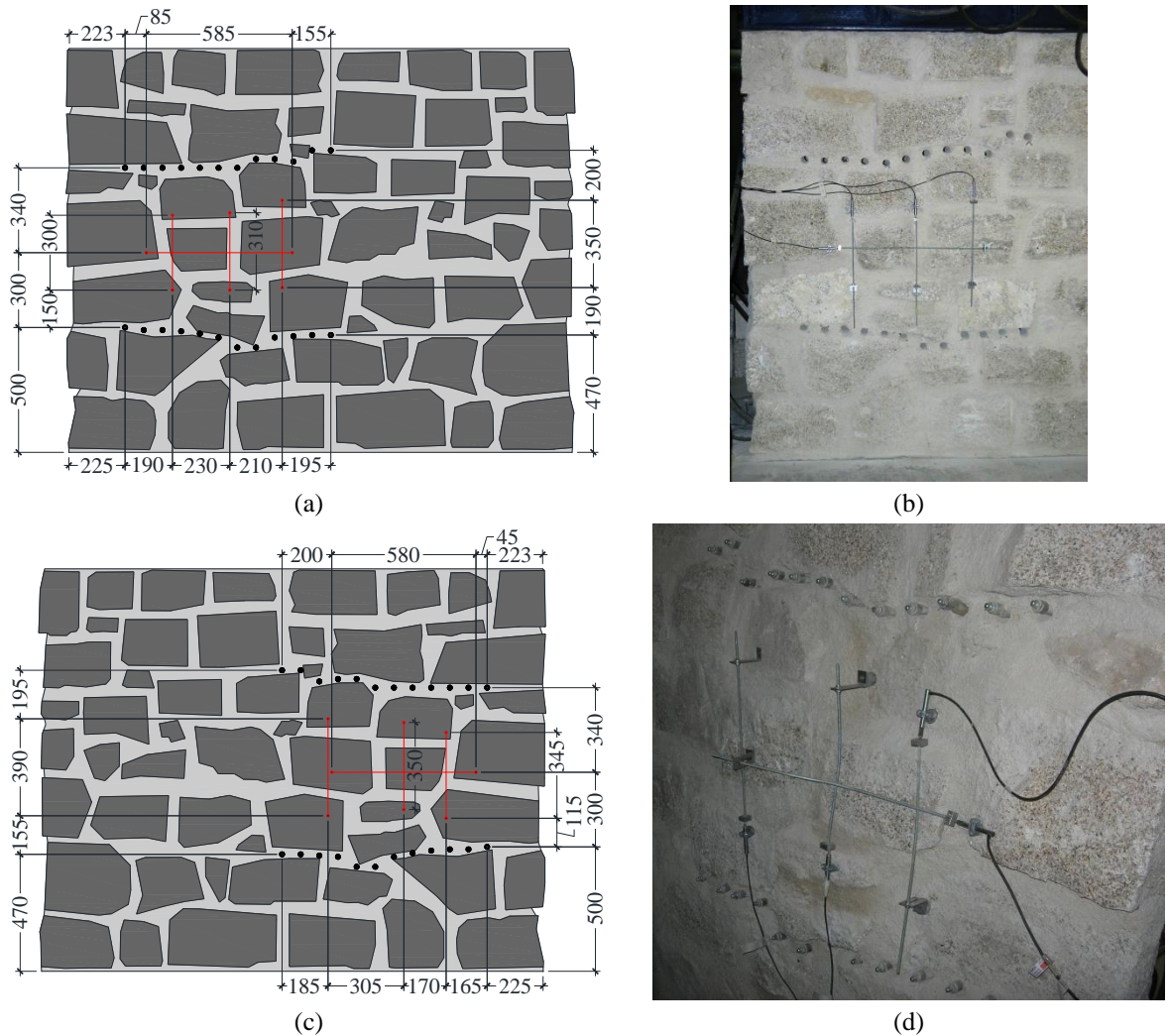

(a)

(b)

(c)

(d)
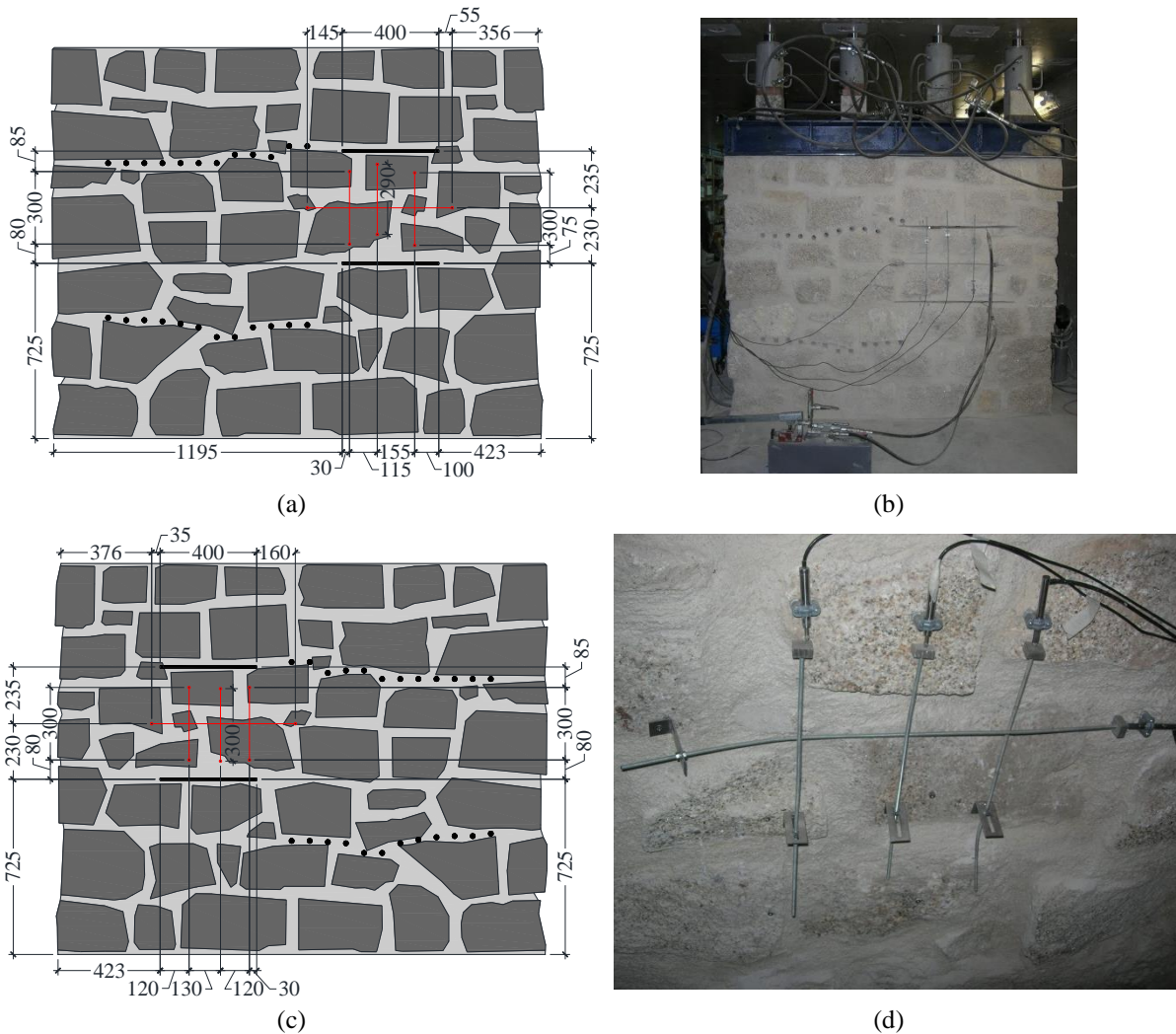
Figure 5-61 Arrangement of LVDTs for the double flat-jack test on the irregular wall: measuring distances on (a) the front of the wall and (c) back of the wall; and photos of LVDTs attached to (b) the front of the wall and (d) the back of the wall

The upper flat-jack slot was cut using the same circular saw as was used for the single flat-jack test (Figure 5-36a). A couple of the granite stones were cut into during the sawing process and several passes with the saw were required to make the slot the correct depth and width of the flat-jack. Some shims were required, both above and below the flat-jack, to fill some gaps between the flat-jack and the masonry (see Figure 5-62a).
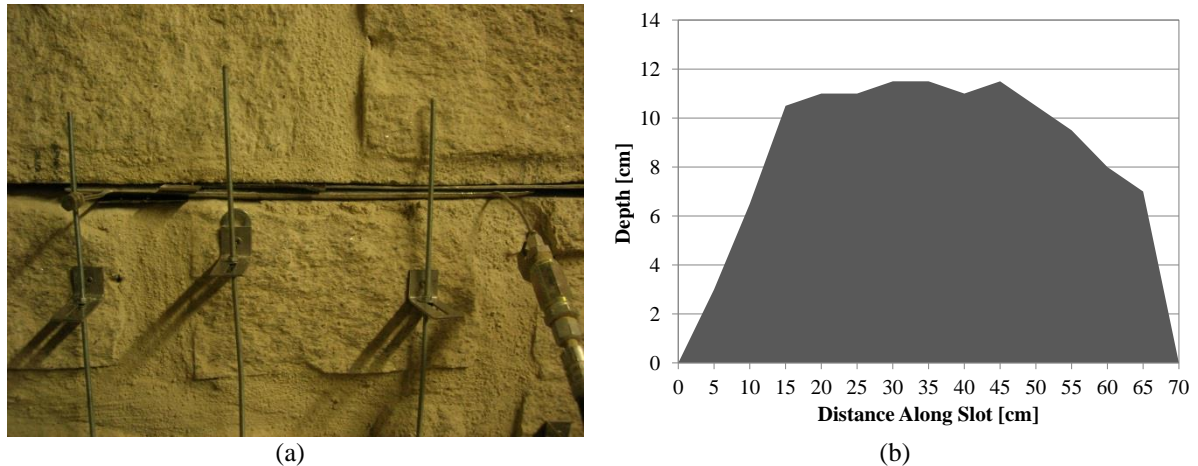
Figure 5-62 Double flat-jack test in the irregular wall upper flat-jack slot: (a) shims inserted above and below the flat-jack; and (b) slot depth along its length

After the test was complete, the depth of the slot was measured every 5 cm along its length. A plot of the upper flat-jack slot is shown in Figure 5-62b. The area of the slot was calculated to be 612.5 cm^2. The area of the upper slot was added to the area of the lower slot, 701.5 cm^2, to find the total slot area. The same size flat-jack was used for the upper slot as for the lower slot. The total flat-jack area was divided by the total slot area to obtain the area correction factor, 0.463. A flat-jack with a jack calibration factor of 0.8 was inserted into the upper slot. The jack calibration factors of the upper and lower flat-jacks were averaged to obtain the total jack calibration factor of 0.785. The area correction factor and the jack calibration factor were multiplied to get the total correction factor, 0.363, which was multiplied by the oil pressure to obtain the applied pressure.

Three pressurization cycles were performed during the double flat-jack test on the irregular wall, with each subsequent pressurization obtaining a higher maximum pressure level. The average LVDT relative displacements and the pressure applied by the flat-jacks throughout the course of the test are presented in Figure 5-63. These results are very similar to the double flat-jack test on the semi-irregular wall. As the flat-jacks pressurize the masonry, the front of the wall compresses vertically and the back of the wall expands vertically. In the horizontal direction both the front and back LVDTs show some expansion. There seems to be some error and residual displacements for the horizontal LVDT on the back of the wall. The error could be due to the bend in the LVDT stand caused by the irregularity of the masonry. These results show again that the applied pressure through the thickness of the wall varies greatly and the results on the front of the wall are not representative of the masonry through the thickness of the wall for this type of masonry.

137
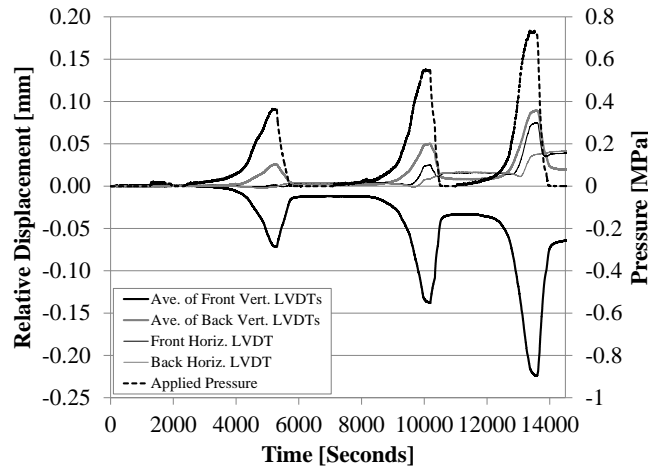
Figure 5-63 Relative displacement and applied pressure results for the double flat-jack test on the irregular wall

Two sets of applied pressure versus strain results are shown in Figure 5-64, the average of all of the vertical or horizontal LVDTs and the average of only the LVDTs on the front of the wall. Estimates for the elastic moduli were made using tangent trend lines and are shown on the graph. As in the other double tube-jack and flat-jack tests, there seems to be two tangent slopes, an initial slope corresponding to reloading the masonry and a second slope at pressure levels that the masonry has not yet seen. The tangent slope of the curves changes at an applied pressure of a little over 0.2 MPa, the approximate maximum load that has been applied to the wall. The initial slope of the average of all vertical LVDTs, 6.67 GPa, is almost double the average reloading modulus for the elastic modulus tests on the irregular masonry wallets, 3.37 GPa (see Section 4.6.3). It is likely that the confinement of the masonry in the wall is affecting the results along with the fact that the flat-jacks are only pressurizing half the thickness of the wall. Note that the estimate of the reloading modulus from just the LVDTs on the front of the wall, 1.93 GPa is much lower than the average value from the masonry wallet tests. The second slope for the average of all vertical LVDTs, 2.67 GPa, also overestimates the initial loading modulus, as compared to the average value found in the masonry wallet tests, 1.19 GPa. Here the value found from the LVDTs on the front of the wall, 0.82 GPa, is closer to the masonry wallet results.
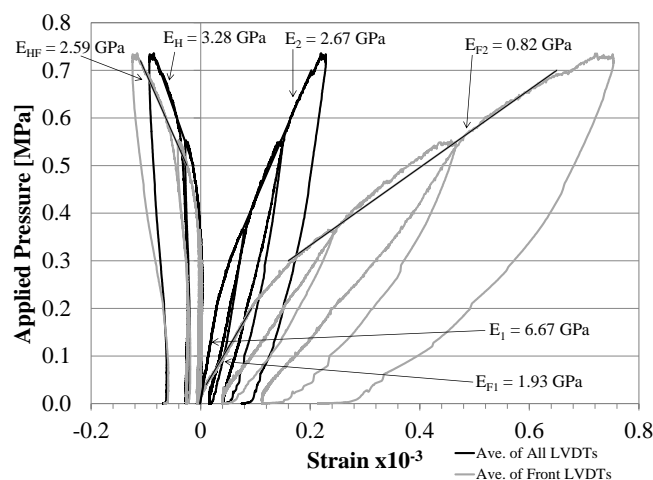
Figure 5-64 Applied pressure versus strain results for the double flat-jack test in the irregular wall

In order to estimate the Poisson ratio from these results, a slope for the horizontal LVDTs for the reloading pressure levels is required. However, as shown in Figure 5-64, almost no strain was recorded for these pressure levels. Thus, the only Poisson ratio that could be estimated was

138

for the second slope. The estimate for the Poisson ratio considering the LVDTs on the front and back of the wall was 0.81. The estimate for the Poisson ratio, only considering the LVDTs on the front of the wall, was 0.32.

5.5   Discussion

5.5.1   Further Development of the Tube-Jack Test System

The tube-jack tests in the regular masonry wall helped to make the final decision regarding the material for the tube-jacks. The latex tube-jacks were found to be inconsistent in their maximum allowable pressure and were inconsistent in loading the masonry. Thus, it was decided to continue testing with only the rubber tube-jacks.

5.5.2   Refining the Procedure for Tube-Jack and Flat-Jack Testing

One important aspect of the tube-jack and flat-jack test procedure is that the masonry can take some time to stabilize after new loads are applied and after mortar is removed from holes or slots. Even one hour after the drilling of the holes in the 3rd horizontal joint in the regular masonry wall, there was still some slight movement observed. In the single tube-jack test on the 5th horizontal mortar joint, where the load on the top of the wall was doubled and the flat-jack slots were still open, the redistribution of stresses was occurring throughout the test and affected the test results. In the single tube-jack test on the irregular wall, the first pressurization cycle was affected by the redistribution of stresses. Thus, it is important in conducting tube-jack and flat-jack tests that enough time be given for the masonry to adjust to new loading conditions before the tests are performed.

Another important finding regarding the testing procedures was the proximity of the test locations. Initially, it was thought that single tube-jack tests, performed following other tube-jack and flat-jack tests in the same area, would not be affected by the prior tests as long as either the mortar was replaced in the holes or the test was at the other end of the wall. This was not the case. The single tube-jack test performed in the 4th horizontal joint in the regular wall was affected by the previous double tube-jack test performed in the 3rd and 6th joints, which compressed the masonry in the area. The single tube-jack test in the 5th horizontal joint was likely affected by the open flat-jack slots on the other side of the wall, which weakened the front half of the wall. The effect of the flat-jack slots being open during this test is analyzed further in the numerical modeling chapter.

While the single wythe construction of the walls allowed the tube-jacks to test the entire thicknesses of the walls, the thinness of the walls caused some issues with the tests and led to some important conclusions. Due to the height to depth ratio of the walls and the depth irregularity of the irregular wall, it was difficult to ensure that the loading was centered on the walls. This resulted in eccentricities in the loading that were observed in several tests.

Unequal pressurization through the thickness of the masonry was observed in both flat-jack tests and tube-jack tests. The flat-jacks were only able to pressurize the front half of the wall. When double flat-jack test results from just the front of the regular wall were compared with average results from both sides of the wall, they were very different and the average of both sides was closer to the properties found in the masonry characterization. In some tube-jack tests, (regular wall double tube-jack test and irregular wall single tube-jack test) the tube-jacks

pressurized the back side of the wall more than the front, which was likely due to the variation in size of the holes through the thickness of the wall.

The eccentricities in loading and pressurization differences from the front of the wall to the back were observed in the different movements on the front and the back of the wall in many tests. These results led to the important conclusion that the movement of the masonry should be monitored on both sides of the wall, especially when the wall is only one wythe thick. For example, in the single flat-jack test on the semi-irregular wall, pressurization of the flat-jack resulted in positive displacements on the front of the wall and negative displacements on the back of the wall. If the relative displacement, due to opening the slot, had been measured on the back of the wall, the estimated state of stress results might have been closer to the expected value.

5.5.3   Applicability of Each Test Method to the Masonry Typology

The mortar strength and stiffness made a big difference in creating the holes for the tube-jack tests. Drilling the holes in the regular masonry wall, where the mortar was very weak, was very easy and did not take much time. In contrast, the stronger mortar in the semi-irregular and irregular walls required much more time regardless of the drilling method, regular drill or core drill. Therefore, the tube-jack test method may be more suitable for masonry will low strength and stiffness mortars.

The large unit masonry posed problems for the flat-jack tests. The unequal displacements on the front and back of the wall and from one side of the slot to the other, in single flat-jack tests on the regular and irregular wall, suggested that the units were rotating and the masonry was not just expanding and contracting. This is explained by the small size of the flat-jacks in comparison with the size of the masonry units. The flat-jack slots and flat-jacks were only half the depth of the masonry units. When the slot was created, the back half of the units above the slot were supported and the front half of the units were left unsupported. Due to the short length of the flat-jacks, the flat-jack slot was usually only the length of one or two units. Along the length of the wall, the slot only removed support from part of the units above the slot. The effects of the size of the flat-jacks in comparison with the size of the masonry will be explored more in the analysis of the flat-jack tests in the numerical models.

5.5.4   How the Masonry Behaves During Tube-Jack and Flat-jack Tests

In some of the double tube-jack and double flat-jack tests two loading slopes were observed. It is hypothesized that the first slope is the reloading of the masonry and the second slope is the loading of the masonry beyond stress levels that the masonry has seen. These slopes were found comparable in value to the corresponding slopes of the Young's modulus test on the masonry wallets, suggesting that this hypothesis might be correct. In the double flat-jack test on the regular masonry wall, both slopes were within 25% of the slopes found in the Young's modulus tests on the regular masonry wallets. In the double flat-jack test on the semi-irregular wall, the initial loading modulus was within 10% of the initial loading modulus of the semi-irregular wallet. If this finding is correct then double tube-jack and flat-jack tests could be able to indicate the maximum stress level that a masonry structure has seen in its lifetime.

In the single tube-jack test on the semi-irregular wall, the tube-jacks were unable to restore the displacements caused by opening the holes. Study of the numerical model of this test may help determine if the stress level was too high for the tube-jacks or if there was some error in tube-jack test that is yet to be identified.

The double tube-jack tests in both the semi-irregular and irregular wall showed the stiffness of the masonry to be much higher than the masonry wallet tests suggest that it is. The double flat-jack tests in both the semi-irregular and irregular walls also overestimate the Young's modulus of the masonry, though not by as much as the double tube-jack tests, when compared to the results of the Young's modulus test on the masonry wallets. One reason for this could be that the stiffness of the masonry in the wall is greater due to the confinement of the masonry around the separated flat-jack specimen. However, this might not be the only reason for the difference, since the double tube-jack tests also overestimated the stiffness of the masonry. The numerical modeling of these tests will explore this further.

5.6 Conclusion

The tube-jack and flat-jack testing in the laboratory walls helped to further develop the tube-jack test system, refine the procedure for performing these tests, provide insights into how the masonry is behaving during these tests, and define the applicability of each type of test for this typology of masonry. Questions left unanswered regarding the reasons why some of the tests were not as successful as expected, are explored further in the modeling of the tests. Following the numerical analysis, comparisons between the results of the laboratory tests, simulations, and masonry wallet tests are made and discussed.

6.   NUMERICAL ANALYSIS

A numerical analysis campaign was conducted following the laboratory testing phase of the thesis. The main goal of the numerical analysis was to better understand the experimental tests through modeling of each test, careful analysis, and comparison with the experimental results. Additional goals of the numerical analysis were to test multiple parameters of the models to determine their impacts on the test results and to use the extensive amount of data in the finite element models to examine the results from areas on the walls that could not be examined with a limited number of LVDTs in the laboratory.

In this chapter the results of finite element modeling of the three large masonry walls, the regular, semi-irregular, and irregular, are presented. In the first section, the preparation of the model is described, including the geometries, material properties, meshing, boundary conditions and loading, and phased analysis. Sections two through four each focus on one of the masonry walls. Five tests were simulated on each wall model; a Young's modulus test, a single tube-jack test, a single flat-jack test, a double tube-jack test, and a double flat-jack test. The initial simulations were created as close as possible to the laboratory test so that they could be compared with the experimental results presented in Chapter 5. In the analysis of the regular masonry wall model, additional analyses were performed for each of the tests to better understand the behavior of the masonry, through examination of the displacements, strains, and stresses throughout the wall. The final sections of this chapter provide some discussion and comparisons between the laboratory, modeling, and mechanical characterization results, followed by conclusions.

6.1   Model Preparation, Analysis and Processing

6.1.1   Geometries

Three models were created, one of each of the masonry typologies, the regular, the semi-irregular, and the irregular. The 2D geometry of each model was created in a computer aided design software (CAD) [67]. The geometry of the regular wall was based on the design geometry of the wall. For the semi-irregular and irregular walls, photos were taken of the front faces of the walls. These photos were scaled in the CAD software and the edges of the units were traced in the CAD drawing. Thus, these models approximate the arrangement of the units on the front face of the walls but do not take into account the size or location of the units through the thickness of the masonry. For the semi-irregular wall, most of the units did not change in width or height through the thickness of the wall. Thus, the numerical model should fairly accurately represent the actual wall. The irregular wall had many irregular granite units that varied in width and height through the thickness of the wall. Thus, the irregular wall model is only an approximation of the actual wall.

The geometries of each of the models are shown in Figure 6-1. See Figure 4-7, Figure 4-8, and Figure 4-9 in section 4.3 for the dimensions and characteristics of the laboratory walls, units, and mortar. All of the hole and slot locations for tube-jack and flat-jack tests were included in the geometry of each model, requiring only one model to be created for each wall. The holes were modeled with 2 cm diameters and the slots as 40 cm long by 1 cm high. Note that in the 2D modeling of the walls, the slots reach through the entire thickness of each of the walls, even though in the experimental tests the slots only reached half way through the thickness of each of the walls.
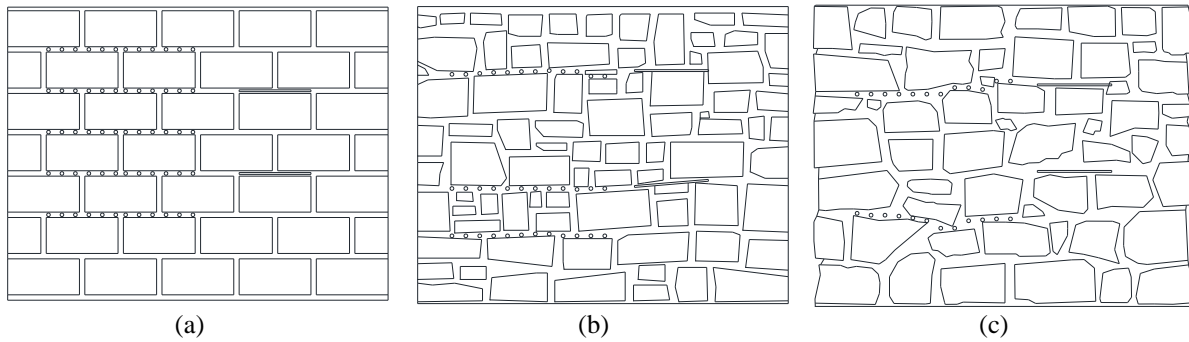
Figure 6-1 CAD geometries created for modeling purposes: (a) regular wall; (b) semi-irregular wall; and (c) irregular wall

The geometry was imported into FX+ [68], a pre- and post-processor for the finite element analysis program, DIANA [50]. The geometries only included lines and care was taken to have no lines crossing over each other, no gaps between lines, and no duplicate lines, to prevent errors in mesh generation.

6.1.2   Material and Element Properties

The material properties for the granite units and the mortar were defined in FX+ based on the mechanical characterization tests performed and presented in Chapter 4. The input values for the elastic modulus, Poisson ratio, and mass density are shown in Table 6-1. Since the Poisson ratio for the granite and mortar were not tested in the mechanical characterization, the values were all set equal to 0.2. This value is within the range found by Vasconcelos [5] for granite in a low stress state of approximately 0.2 MPa. The elastic constitutive model was used for all materials since the loads, both above the wall and from the jacks, were in the elastic ranges of the materials.

Table 6-1 Material properties for masonry wall modelling in FX+

Material	Elastic Modulus	Poisson Ratio	Mass Density
	[N/m^2]	-	[N/m^3/g]
Granite for All Walls	3.00E+10	0.2	2614
Regular Wall Mortar	2.60E+08	0.2	1735
Semi-Irregular and Irregular Wall Mortar	1.017E+09	0.2	1794

Two element property labels were created, "units" and "mortar". The granite material was assigned to the "unit" property and the mortar material was assigned to the "mortar" property. Both the "unit" property and the "mortar" property were defined as 2D plane stress elements with a thickness of 0.2 m, the thickness of the wall. Plane stress elements were chosen because no load was applied perpendicular to the plane of the wall and the intent was not to look at the bending or other out-of-plane movement of the wall. Plane stress elements were also chosen over plane strain elements because there was expected to be some strain perpendicular to the plane of the wall due to the load being applied to the top of the wall and zero stress perpendicular to the face of the wall.

6.1.3   Meshing

The entire geometry of each model wall was meshed. Elements were created not only in the units and mortar but also in all of the hole and slot locations defined in the geometry. During

144

an analysis of a tube-jack or flat-jack test in these model walls, the hole or slot elements corresponding to the test being performed would be deactivated. However, all of the other hole and slot elements in the model would remain activated. Thus, it was important for the hole and slot elements to have similar sizes and properties to the other elements in the model representing the same materials.

Prior to creating the mesh, some size controls were set for the mesh elements. Each of the edges of the holes was divided into eight equal lengths. This was to ensure that each hole had an approximately uniform mesh, equivalent to each of the other holes and with similar sized elements as for the rest of the mesh. The adaptive seeding of one of the holes and the resulting mesh is shown in Figure 6-2a. The element size for all of the elements was set to 1 cm. This would create approximately three rows of elements in each joint, also seen in Figure 6-2a on either side of the hole.

| (a) | (b) |
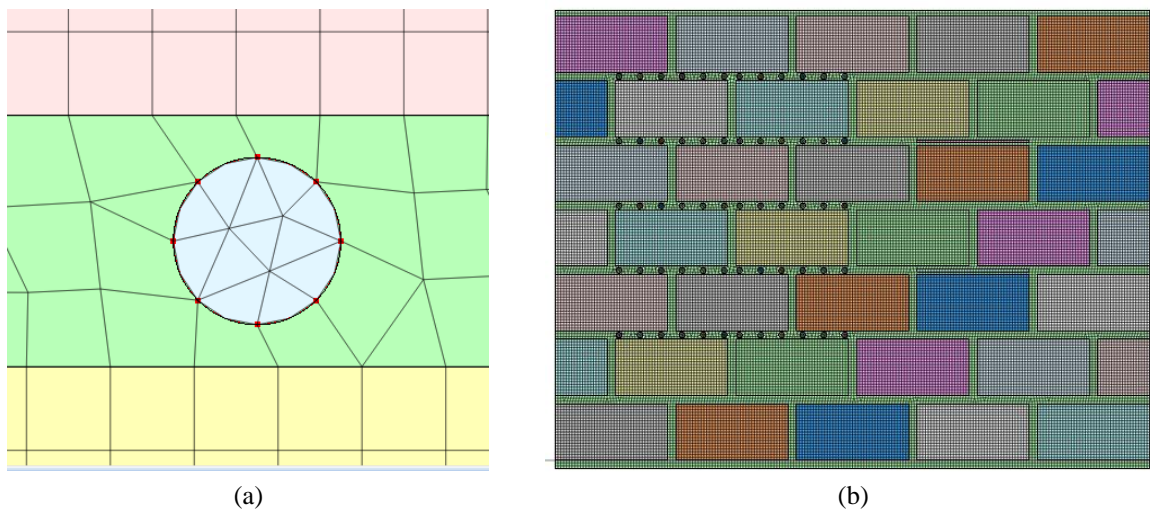
Figure 6-2 Meshing: (a) adaptive seeding of hole edges and example of a final hole mesh configuration; and (b) different colors used to distinguish mesh sets in the regular masonry wall mesh

The mesh for each model was automatically generated in FX+. During meshing, mid-side nodes were generated producing triangular elements with six nodes and quadrilateral elements with eight nodes. Different mesh sets were created for each unit, each hole, each slot, and for the mortar. The mesh sets were displayed with different colors to distinguish them from one another, see Figure 6-2b for the mesh of the regular masonry wall. The "units" property was assigned to each unit mesh set and the "mortar" property was assigned to the mortar mesh set. All of the holes were created in the mortar so they were assigned "mortar" element properties. Either the "units" or the "mortar" properties were assigned to the slot mesh sets depending on if the slots were created in the mortar or the granite units. Parts of the slots were created in the granite units, so the elements in those parts were assigned "units" element properties. An example of this is shown in Figure 6-3 where the last element in the upper slot on the semi-irregular wall is in its own mesh set and was given granite unit properties because the slot was cut into the granite unit at this location. The mesh for the irregular wall is shown in Figure 6-4. Note that the holes look like they are darker and have "units" properties but this is not the case. They appear darker because element edges are closer together in these areas.
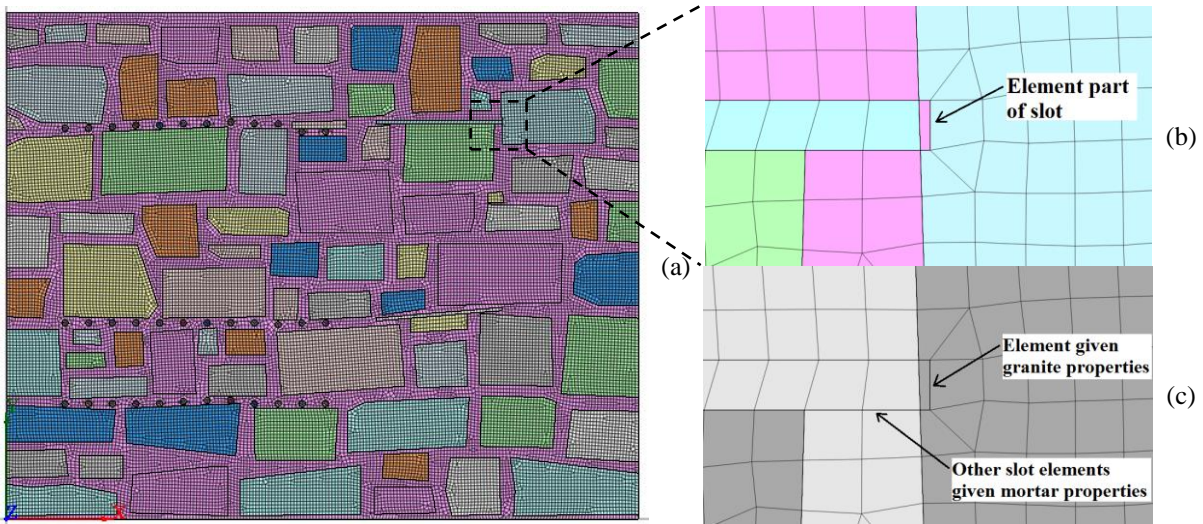
Figure 6-3 Semi-irregular wall mesh: (a) color coded mesh sets; (b) zoom of the upper flat-jack slot showing colored mesh sets; and (c) zoom of the upper flat-jack slot showing assigned element properties (dark gray for "units" and light gray for "mortar")
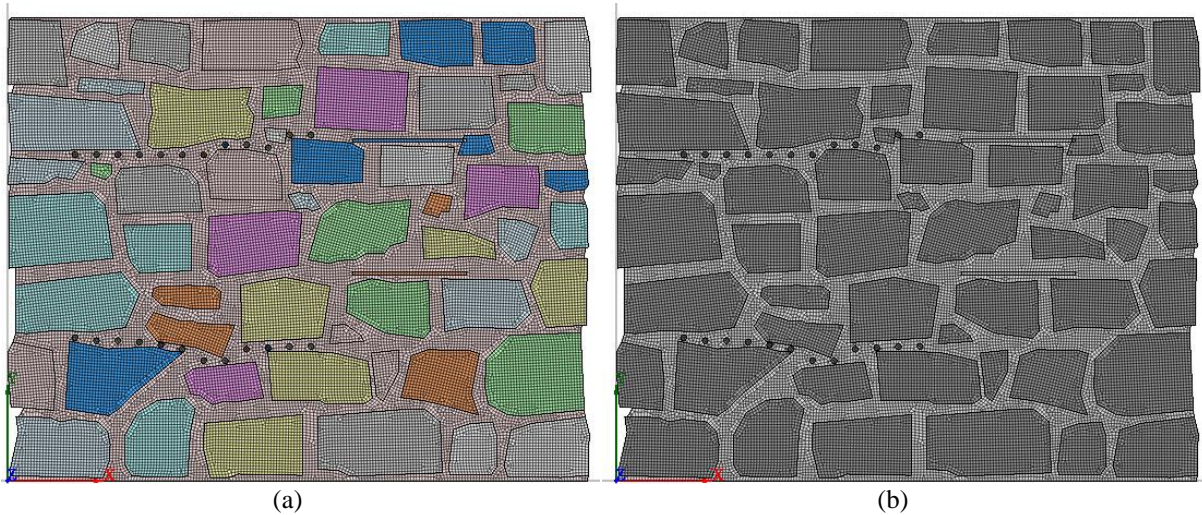
Figure 6-4 Irregular wall mesh: (a) color coded mesh sets; and (b) element properties of mesh sets (dark gray for "units" and light gray for "mortar")

6.1.4 Boundary Conditions and Loading

Initially only one boundary condition was applied to each of the walls. The translations of the nodes along the bottom of the walls were fixed in all three directions (Figure 6-5a). This condition represented the floor supporting the walls, preventing them from moving in any direction. All of the other sides of the walls were free to move. Confining the top of the wall by locking the horizontal movement of the top nodes of the wall was considered initially. However, this would have prevented all horizontal movement including movement resulting from removing the mortar in the holes and slots. Thus, the top of the wall was left free to move. If the masonry walls being modeled were part of a larger structure where masonry was to either side of these masonry specimens, the wall could have been modeled as confined horizontally.

For some tests, the self-weight of the masonry was applied as a body force to the elements. In other tests, the self-weight of the masonry was not considered in order to more clearly see the effects of only the vertical load above the wall and the pressures applied by the tube-jacks

and flat-jacks. Whether or not the self-weight was being applied is indicated in the sections discussing the results of each test.

<div align="center">(a)   (b)   (c)</div>
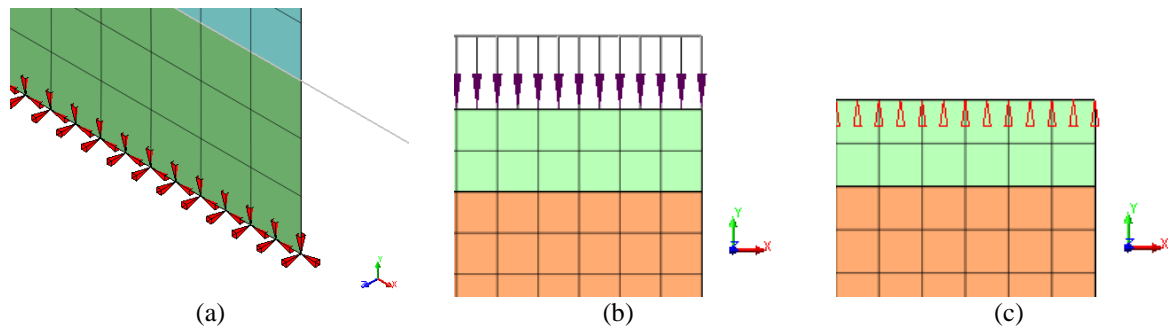
Figure 6-5 Boundary conditions and loading of the model: (a) translational fixity at each node along the bottom of each wall; (b) constant edge pressure loading along the top of the wall; and (c) constant displacement for all nodes on the top of the wall

Two ways of applying load to the top of the wall were used in the finite element modeling. The first was to apply a constant edge pressure load along the element edges at the top of the wall (Figure 6-5b). Applying the load in this way ensures that the wall is loaded with a constant load throughout the single tube-jack and flat-jack tests. In the laboratory testing, this loading method represents the case where the pressure in the hydraulic jacks loading the wall is adjusted throughout the tests to ensure that the pressure remains the same despite any vertical displacement of the wall. In an in-situ test, this loading method represents the case where there is a set amount of load being applied to the wall that will not change during the test, such as another story of masonry.

The second way of applying load to the top of the wall was to apply a constant vertical displacement at all of the nodes on the top of the wall (Figure 6-5c). The value of the constant displacement was determined by first applying the constant edge pressure load along the element edges at the top of the wall, as described above, running the analysis, and recording the vertical displacements of the nodes at the top of the wall. The vertical displacements were then applied as the constant displacement for all of the nodes at the top of the wall without the vertical load being applied. This produced approximately the same stress levels throughout the wall as the first method. In the laboratory testing, this loading method represents the case where the displacement of the steel profile on top of the wall is maintained throughout the test but the pressure in the hydraulic jacks is not maintained throughout the test. As the holes or slots for the tube-jack or flat-jack tests are created, the stress in the wall is relieved slightly. As the jacks pressurize the wall, the wall is not allowed to expand upward, and thus the load on the wall and the stresses within the wall increase. In an in-situ test, this could be the case if the masonry above the testing location is very stiff or the structure above prevents any change in vertical displacement above the testing location.

In tube-jack tests, the masonry is pressurized radially by inflating the tube-jacks. To simulate this pressurization in the models, a constant radial edge pressure was applied to the edges of the elements surrounding each of the holes in the equivalent flat-jack line that was being tested. The pressure applied was equivalent to applying pressure along the entire length of the hole through the thickness of the wall. Since the applied pressure presented in the experimental results was already adjusted for the length of the tube-jack applying pressure to the hole, the applied pressure can be compared to the pressures shown in the modeling results. The application of the edge pressure is shown in Figure 6-6a.

In flat-jack tests, the masonry is pressurized perpendicular to the surface of the flat-jack. To simulate this pressurization, a constant edge pressure was applied normally to the edges of the elements above and below the flat-jack slots, along the length of the slots (Figure 6-6b). No pressure was applied to the ends of the flat-jack slots. This pressurization is an idealization because in most experimental and in-situ flat-jack tests, the flat-jack does not pressurize the masonry uniformly along the entire length and depth of the slot. The slot is usually larger than the flat-jack, requiring an area correction factor. Since an area correction factor has been applied in the experimental flat-jack test results, the applied pressure shown in the experimental results can be compared to the modeling pressures presented.

| (a) | (b) |
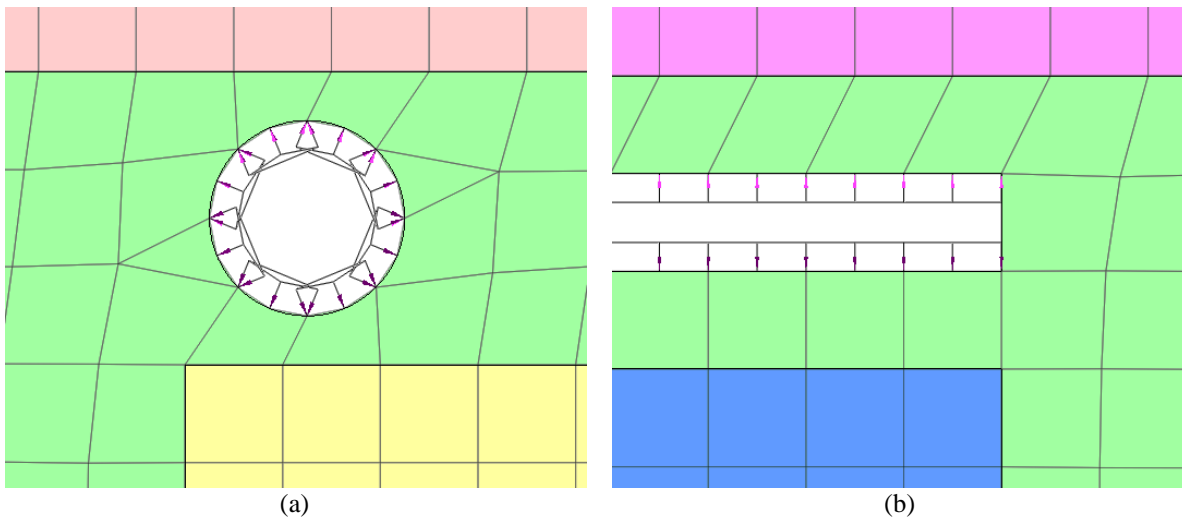
Figure 6-6 Application of jack pressures: (a) radial edge pressure on edges of elements surrounding each hole; (b) normal edge pressure on edges of elements above and below each slot

6.1.5   Phased Analysis

The analysis commands were created and edited in the Mesh Editor module of the DIANA program. Phased analyses were used for all of the tests performed. This analysis type allowed for the definition of different phases with different loads, load combinations, load factors, and element mesh sets activated or deactivated. In order to perform a phased analysis in the DIANA analysis program, a structural nonlinear analysis must be performed in each phase of the test, regardless of the structural nonlinearity of the model. In this model, only linear-elastic characteristics were included in the structural nonlinear analysis. The tests consisted of two phases. In the first phase the program analyzes the model based on the elements activated and the loads applied in that phase. When the analysis is complete for the first phase, the result becomes the initial condition for the second phase. The program then activates or deactivates elements and applies the loads for the second phase. With these inputs, the analysis is performed again. In the second phase of the analysis, the pressurization loads in the holes and slots were applied in load increments so that the pressurization could be analyzed in load increments. The elements activated and the loads applied in each phase for each test are presented in Table 6-2.

Note in Table 6-2 that for the double tube-jack and double flat-jack test, the vertical displacement method was used to load the top of the wall. This method was chosen after several analyses were run using the vertical load method. When the displacement was not set at the top of the wall, the wall was free to expand vertically due to the pressure applied by the flat-jacks or tube-jacks. This reduced the amount of pressure that was applied to the masonry between the jacks. The low amount of pressure being applied to the masonry in the model resulted in much smaller displacements than were seen in the laboratory tests. Since the movement of the top of

148

the wall was somewhat restricted during the experimental tests due to the steel profile and hydraulic jacks, it was hypothesized that reality was somewhere between the two load application methods. Thus, the vertical displacement control method was assumed to more closely represent the laboratory test situation and is presented in the thesis.

Table 6-2 Analysis phases for each of the tests run on the masonry wall models

Tests Modeled	Phase 1		Phase 2	
	Elements	Load	Elements	Load
Elastic Modulus	All elements activated	Load applied in increments to the top of the wall	-	-
Single Tube-Jack	All elements activated	Full load applied to the top of wall	Only hole elements in one equivalent flat-jack deactivated	Radial hole pressure applied in increments
Single Flat-Jack			Only slot elements in lower slot deactivated	Normal slot pressure applied in increments
Double Tube-Jack	Hole elements in two equivalent flat-jacks deactivated	Vertical displacement applied	No change from Phase 1	Radial hole pressure applied in increments to both rows of holes
Double Flat-Jack	Slot elements in both upper and lower slots deactivated	Vertical displacement applied	No change from Phase 1	Normal slot pressure applied in increments to both slots

6.1.6   Post-processing of the Results

Following the analysis by the program, the results had to be processed to create presentable and comparable graphics. The contour plots and images of the model were created in FX+. This software allowed the creation of plots of the stresses, strains, and absolute displacements. In order to make comparisons and averages of the data, the values for some or all of the elements were extracted and analyzed using spreadsheets.

In tube-jack and flat-jack testing, the absolute displacements of the masonry are not known. The only way to see the movement of the masonry is to apply LVDTs or other measuring devices to measure the relative displacement of the masonry. To compare the model results with experimental results, the relative displacement of the modeled masonry also needed to be analyzed. This was done using virtual LVDTs. To analyze a virtual LVDT, two node points were selected to represent the connection points of the virtual LVDT. The relative displacement of each set of nodes, or virtual LVDT, was determined by subtracting the absolute displacement of the lower node from the absolute displacement of the upper node. To determine the strain of a virtual LVDT, the relative displacement was divided by the distance between the two node points.

6.2   Regular Masonry Wall Model

6.2.1   Young's Modulus Test

The Young's modulus test was the first test to be performed on the regular masonry wall model. Since the model was perfectly linear-elastic, only one loading was performed up to an applied

149

pressure of 0.22 MPa. The self-weight of the masonry was included in the loading of the wall. Following the standards for masonry wallet testing [64], two virtual LVDTs were analyzed. The distances between the node points on the regular masonry wall are 54 cm apart vertically and 1.06 m apart horizontally and are shown in Figure 6-7.

Before continuing with the analysis of the Young's modulus test, the vertical stresses in the masonry wall, due to the self-weight of the masonry, should be discussed. In Figure 6-7, a contour plot of the vertical stresses is shown with some of the nodal values displayed in flags. In general, the compressive stress increases from the top of the wall to the bottom. However, at each of the vertical mortar joints the vertical stress is very low. This is due to the difference in stiffness of the mortar and granite materials. The granite is much stiffer than the mortar so it does not deform as much as the mortar under the same load. Therefore, the granite takes most of the load from the masonry above and the vertical mortar joints take almost none. Since the stress is so low in the vertical mortar joints, the load above those joints is transferred to the granite units on either side of each joint, producing a high compressive stress concentration. These effects were seen in all of the masonry modeling but they are most clear in the regular masonry wall, due to its perfectly vertical head joints.
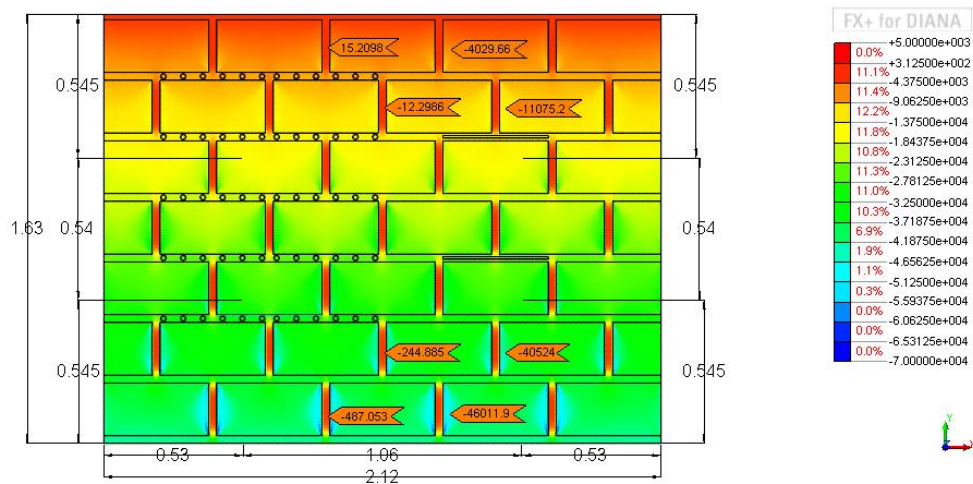
Figure 6-7 Contour plot of the vertical stresses [Pa] in the wall due to the masonry self-weight only and the locations of the virtual LVDTs (dimensions in meters)

The displacements and strains resulting from the self-weight of the masonry were not considered in the Young's modulus test. The initial condition, or zero point of the test, is when the self-weight has already been applied, which is the same case as in the experimental and in-situ tests. Contour plots of the vertical displacement and strain at an applied pressure of 0.2 MPa on the top of the wall are shown in Figure 6-8. At the bottom of the wall, the displacement is zero since the floor boundary prevents the wall from moving. The displacement increases at each successive course moving up from the base of the wall. The strain is much higher in the horizontal mortar joints than in the granite due to the difference in stiffness of the two materials. At the same level of stress, the mortar deforms much more than the granite.

(a)	(b)
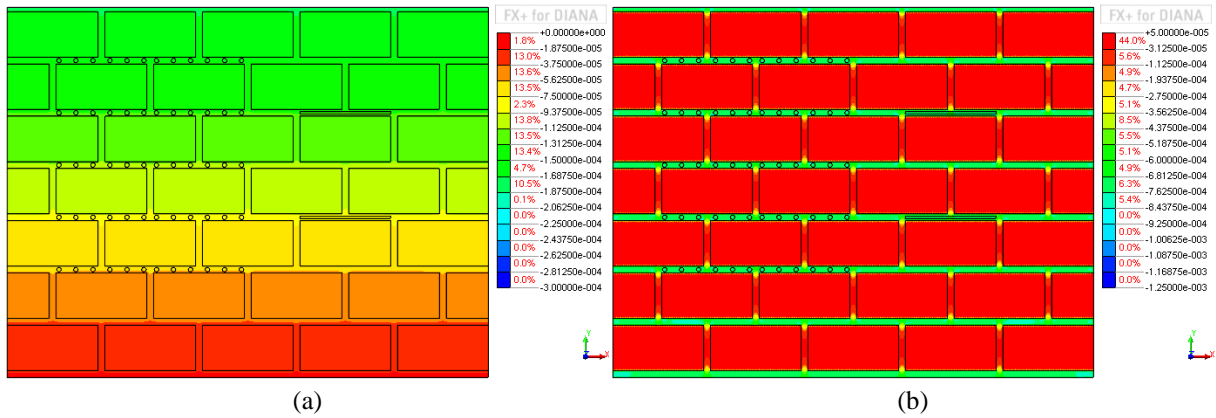
Figure 6-8 Regular wall loading of 0.2 MPa on top of the wall: (a) vertical displacement contour plot [m]; and (b) vertical strain contour plot

The stress versus strain results of the two virtual LVDTs during Young's modulus test are shown in Figure 6-9. The difference between the two virtual LVDTs is almost indistinguishable since they measure over the same distances and joints, are at the same height on the wall, and are spaced equal distances from the edge of the wall horizontally. The slope of the trend line fit to the data results in a Young's modulus estimation of approximately 2.2 GPa. This value is not far from the reloading elastic modulus found in the Young's modulus testing of the regular masonry wallets, which was estimated to be equal to 2.5 GPa, a difference of approximately 13% (see section 4.6.3for the masonry wallet results). However, if it is compared to the initial loading modulus of the masonry wallets, 0.368 MPa, there is a difference of approximately 143%.
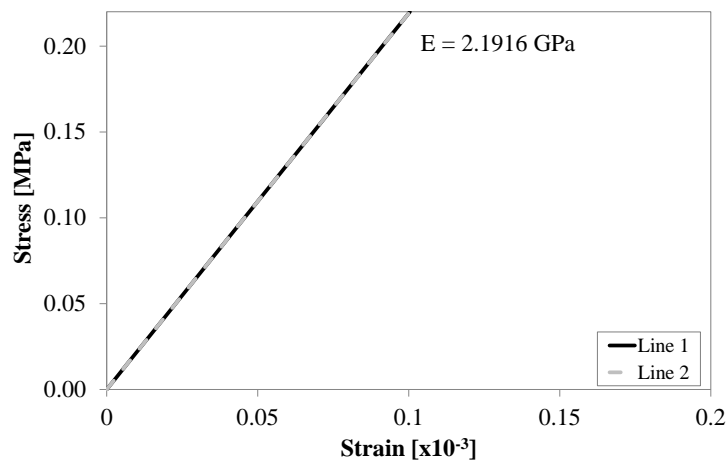
Figure 6-9 Virtual LVDT stress versus strain results for the Young's modulus test on the regular wall model

There are several possible reasons for the difference between the experimental and numerical results for the elastic modulus of the regular masonry. First, the model was of the entire wall and not of just the small masonry wallet. Thus, the size of the specimen being tested could have influenced the results. The units and mortar joints in the model are all perfectly regular and homogeneous, whereas in the wallet specimens there were small imperfections in the materials, the thicknesses of the joints, and the dimensions of the units. The model also perfectly loaded the wall, whereas in experimental testing slight eccentricities in the loading and slightly unequal load distributions are unavoidable.

As mentioned in the introduction to this chapter, numerical modeling allows for the analysis of much more data (and different scenarios) than experimental testing. One aspect of the Young's modulus test that was investigated was the placement of the connection points for the virtual LVDTs. What happens if a set of points measures over a larger or smaller percentage of mortar vertically? As shown in the contour plots of the displacement and strain of the wall, the horizontal mortar joints show much larger vertical stains than the granite courses due to the lower stiffness of the mortar in comparison with the granite. Therefore, it could be expected that, if the percentage of mortar is higher between a set of two vertical measuring points, the strain will also be higher and the resulting elastic modulus will be lower.

In the initial analysis presented above, the virtual LVDTs measured over a distance of 54 cm and two mortar joints. Thus, 11.11% of the material between the measuring points was mortar. This resulted in an elastic modulus of 2.1916 GPa. Another two sets of measuring points were selected as shown in Figure 6-10. These points measured over a distance of 30 cm and the same two mortar joints as the previous sets. This arrangement resulted in 20% of the material between the measuring points being mortar and an elastic modulus estimation of 1.2595 GPa, 57.5% of the modulus found with the first set of virtual LVDTs. This illustrates the difference in elastic modulus results due to the difference in percentage of mortar between the measuring points.
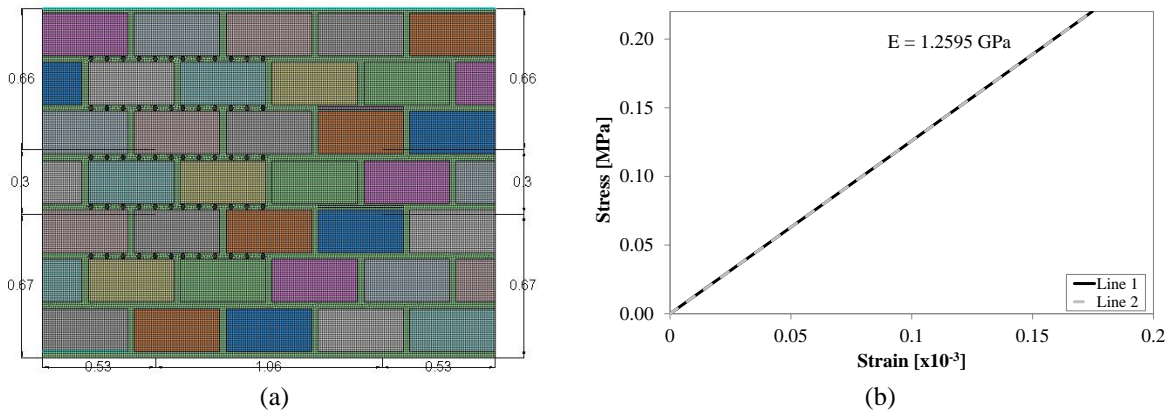
Figure 6-10 Results from a second set of virtual LVDTs: (a) location of the connection points (dimensions in meters); and (b) stress versus strain results

Several more measuring point sets, with different percentages of mortar between the measuring points, were analyzed and the elastic modulus results versus the mortar percentage between the measuring points are presented in Figure 6-11. As the percentage of mortar between the measuring points decreases below 10% the elastic modulus estimation increases rapidly; the LVDTs are measuring more of the granite properties than the mortar properties. On the other end of the spectrum, as the percentage of mortar between the measuring points increases, the LVDTs are measuring mostly the strain of the mortar and the elastic modulus estimation gets closer to the value for the mortar elastic modulus, 0.26 GPa. A power trend line seems to fit the data points the best given the apparent curvature. The power curve equation is shown on the graph.
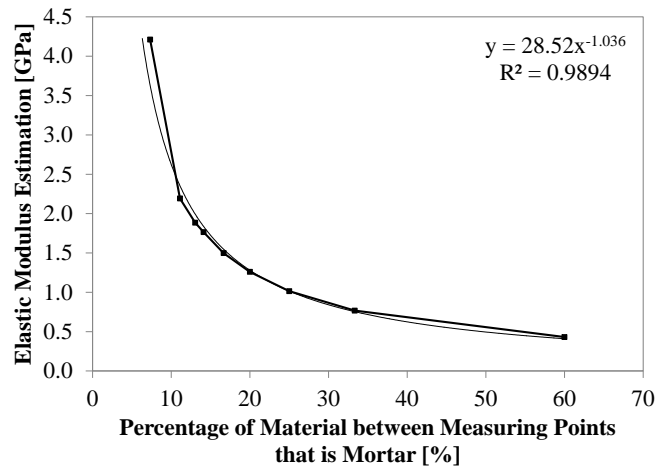
Figure 6-11 Numerical model estimation of elastic modulus of the regular masonry wall for different sets of virtual LVDTs measuring over different percentages of mortar

Since this masonry typology is regular, the vertical percentage of mortar can be calculated for the masonry as a whole. Each course of masonry is the same height, 23 cm, and consists of 3 cm of mortar and 20 cm of granite. The percentage of mortar is 13.04%. If measuring points are set so that the percentage of mortar between them is 13.04%, the same as the masonry as a whole, the elastic modulus estimation is 1.8844 GPa. The relationship between the percentage of mortar between the LVDT measuring points will be discussed briefly in modeling of the Young's modulus tests on the semi-irregular and irregular walls. However, more research should be done, including a parametric study considering the material properties, to better understand this relationship. This finding has the potential to be very important for selecting appropriate locations for measuring points for Young's modulus tests on masonry wallets and prisms, and double tube-jack and flat-jack tests in masonry walls.

6.2.2 Single Tube-Jack Tests

In this section, the results of modeling single tube-jack tests in the 3rd, 4th, and 5th horizontal joints are presented and compared to the results found in the laboratory tests (see Chapter 5). Following these comparisons, the test in the 3rd horizontal joint will be analyzed more deeply by looking at the vertical displacements, strains, and stresses and the horizontal strains and stresses.

6.2.2.1 Simulation of Experimental Tests

Single Tube-jack Test in the 3rd Horizontal Mortar Joint

Several single tube-jack tests were modeled in the regular masonry wall model. The first test to be performed was the single tube-jack test on the 3rd horizontal mortar joint up from the base of the wall, in the same location as the first experimental tube-jack test performed with the water pressure system. In this test, a pressure load was applied to the top of the wall in the first phase along with the self-weight of the masonry. In the second phase of the test, the elements in the holes in the 3rd joint up from the base of the wall were deactivated and then the radial pressure was applied in increments to the element edges surrounding the holes.

The first aspect of the modeled test to be analyzed was the displacements of the masonry within the wall. All displacements were measured taking the first phase as the reference. Thus, displacements were only affected by the deactivation of the hole elements and the radial

pressure applied around the edges of the holes. Eight vertical sets of nodes were selected to measure the relative displacement over the line of holes. The nodes were two centimeters above and below the edge of the mortar joint, resulting in a measurement distance of 7 cm. Each set, or virtual LVDT, was horizontally centered between the holes on either side. The node locations and virtual LVDT labels are shown in Figure 6-12. These node locations were chosen to be as close as possible to the actual connection points for the LVDTs in the experimental test. Virtual LVDTs 2, 4, 5, and 7 correspond to LVDTs 1 through 4, respectively, in the experimental test.
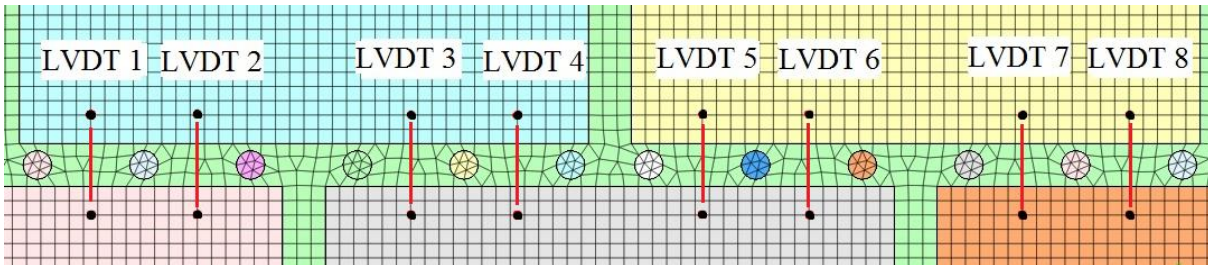
Figure 6-12 Locations for the vertical node sets, or virtual LVDTs, for modeling the single tube-jack test in the regular masonry wall

The relative displacement results for the virtual LVDTs at several radially applied pressure increments are shown in Figure 6-13. The values for zero applied pressure are the relative displacements due to drilling the holes. The average relative displacement at zero applied pressure for virtual LVDTs 2, 4, 5, and 7, is −7.03 μm. This value is very close to the average relative displacement due to drilling the holes in the single tube-jack test on the regular wall in the 3rd horizontal joint, −8.5 μm (see section 5.2.1.1).
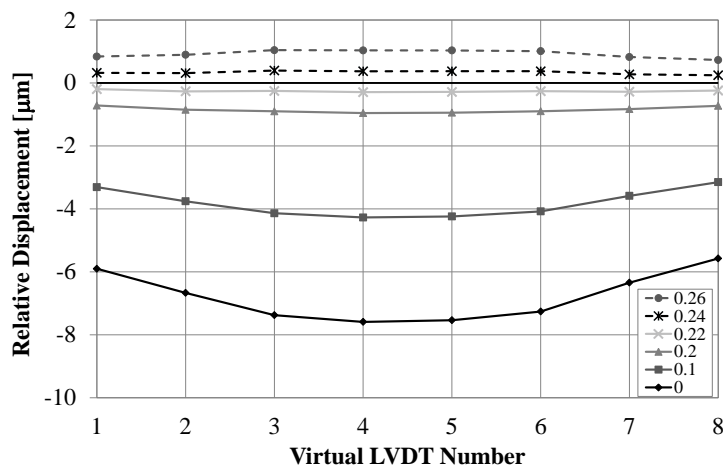
Figure 6-13 Relative vertical displacements for each virtual LVDT at several increments of radial pressure applied to the edges of the holes (pressure values in MPa)

Several observations can be made regarding the relative displacement results for each of the virtual LVDTs. The masonry closes or contracts more at the center of the equivalent flat-jack after drilling the holes than at the ends of the equivalent flat-jack, as shown by the more negative relative displacements of the middle virtual LVDTs. The same behavior along the slot has been described in flat-jack testing by Cucchi et al. [38] (see Figure 2-25a). As pressure is applied to the holes radially, the relative displacement values increase, indicating that the masonry is expanding vertically. The relative displacement of all of the virtual LVDTs reaches zero at a pressure level between 0.22 MPa and 0.24 MPa. To determine the exact restoring pressure, the relative displacement was plotted against the applied radial pressure in Figure 6-14.

154

Figure 6-14 Relative vertical displacements of the virtual LVDTs versus applied radial pressure: (a) over all applied pressure values; and (b) zoomed in at the restoring pressure value

Figure 6-14a shows that the relative displacements for the virtual LVDTs are restored to zero at an approximate applied pressure of 0.23 MPa. Zooming in to see the restoring values of each measuring line in Figure 6-14b reveals that the lines do not all cross at the same pressure level. Averaging the crossing values results in an estimation of 0.2287 MPa for the state of stress in the simulated wall at the 3rd horizontal mortar joint, with a coefficient of variation of 0.40%. The stresses in all of the elements in the joint prior to creating the holes were averaged to determine the stress level at the 3rd joint in the model, 0.2252 MPa. This results in an error of 1.56% for the virtual LVDTs. The experimental test estimated the stress level at 0.26 MPa, a 15% error in comparison to the average stress in the 3rd joint of the model.

Single Tube-jack Test in the 4th Horizontal Mortar Joint

The procedure for modeling the single tube-jack test in the 4th horizontal mortar joint was the same as for the single tube-jack test in the 3rd horizontal joint. The only difference was that in the second phase of the test, the elements in the holes in the 4th joint were deactivated and the elements in the holes in the 3rd joint remained activated. The vertical load on the wall was a pressure of 0.2 MPa and the self-weight of the masonry was included in the analysis.

The locations of the virtual LVDTs were the same as shown in Figure 6-12, except that they were centered over the 4th joint. The relative displacements of the virtual LVDTs versus the applied radial pressure to the edges of the holes are shown in Figure 6-15. Averaging the relative displacements from virtual LVDTs 2, 4, 5, and 7, results in a relative displacement of −6.88 μm due to opening the holes. This value is very close to the average results of the LVDTs in the same locations in the experimental test, -6.5 μm (see section 5.2.1.2).
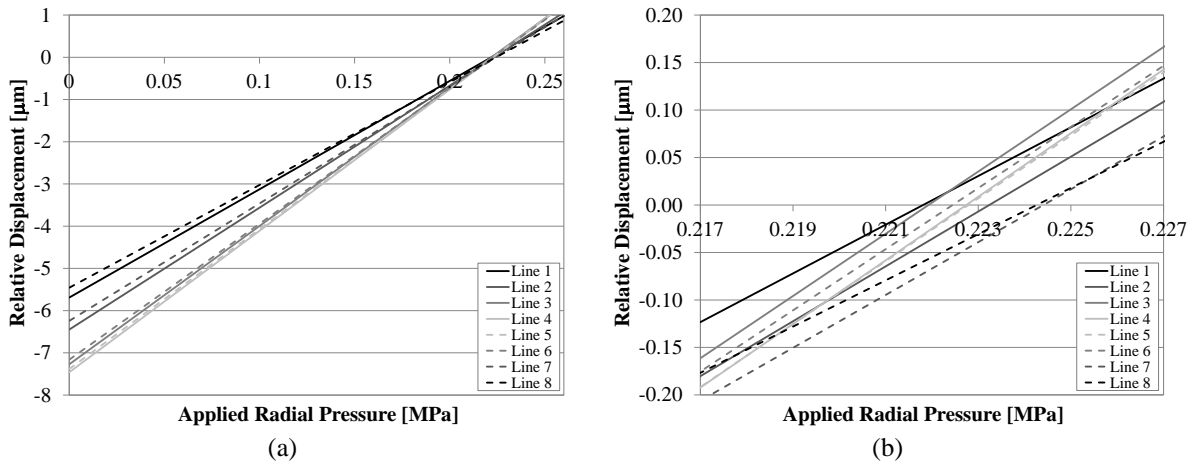
Figure 6-15 Modeling results for the single tube-jack test in the 4th horizontal joint: relative vertical displacements of the virtual LVDTs versus applied radial pressure (a) over all applied pressure values; and (b) zoomed in at the restoring pressure value

The results shown in Figure 6-15a are very similar to those shown in Figure 6-14a. However, the restoring pressure is slightly lower than in the previous test due to one less course of masonry above the joint being tested. All of the lines pass between 0.221 MPa and 0.225 MPa at zero relative displacement in Figure 6-15b. The estimate for the state of stress at the 4th horizontal joint based on the average results of the virtual LVDTs is 0.223 MPa, with a coefficient of variation of 0.44%. The stresses in all of the elements in the joint prior to creating the holes were averaged to determine the stress level at the 4th joint in the model, 0.2202 MPa. This results in a 1.24% error for the virtual LVDTs, similar to the 1.56% error found in the test on the 3rd joint.

While the virtual test was performed in a perfect model wall undisturbed by previous tests, the laboratory test in the 4th joint was performed after the double tube-jack test in the same area. The laboratory test estimated the stress level at 0.34 MPa. This is a 43% difference from the average stress in the 4th joint of the model. Assuming there were no other errors in the experimental test, these results suggest that the double tube-jack test affected the state of stress at the 4th joint in the laboratory wall.

Single Tube-jack Test in the 5th Horizontal Mortar Joint

For the single tube-jack test in the 5th horizontal mortar joint, the load on the model wall was doubled to a pressure of 0.4 MPa, as it was in the experimental test. The procedure for modeling the test was the same as the other modeled single tube-jack tests except that the elements in the holes in the 5th horizontal mortar joint were deactivated in the second phase of the test. Since the load applied to the top of the wall was double the previous load, the applied pressures on the edges of the holes were also doubled. The virtual LVDTs had the same spacing and measured over the same distances as in the previous tests. The only difference was that they were centered over the 5th joint.

In the experimental test, the flat-jack tests had been performed prior to this tube-jack test and the slots were left without mortar. The flat-jack slots affected the front face of the wall, increasing the relative displacements on the front. Two analyses were run for the model test, one disregarding the flat-jack slots and one with the slot elements deactivated. Note that in the model, the flat-jack slots are the entire width of the wall and not just half of the thickness.

The first analysis run for the single tube-jack test on the 5th joint was without the flat-jack slots. The virtual LVDT results, shown in Figure 6-16, were very similar to the results of the other modeled single tube-jack tests. Since the load on the wall was doubled, the initial relative displacement due to opening the holes was also doubled. The average of virtual LVDTs 2, 4, 5, and 7, was −13.5 μm. The average relative displacement found in the laboratory test was much greater at −54 μm (see section 5.2.1.3).

The estimation for the state of stress, based on all of the virtual LVDTs in the model, was 0.424 MPa, with a coefficient of variation of 0.36%. Comparing this to the average stress in the joint before deactivating the hole elements, 0.4175 MPa, results in a 1.49% error. This error is almost the same as for the model results of the single tube-jack tests on the 3rd and 4th joints. Thus, the error in using the virtual LVDTs to estimate the state of stress in the model is not affected by the applied loads.

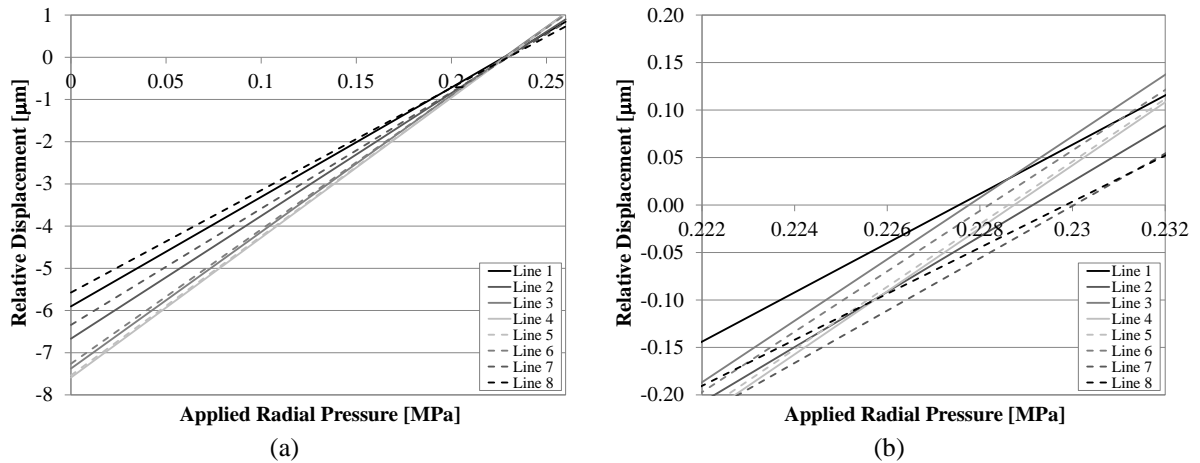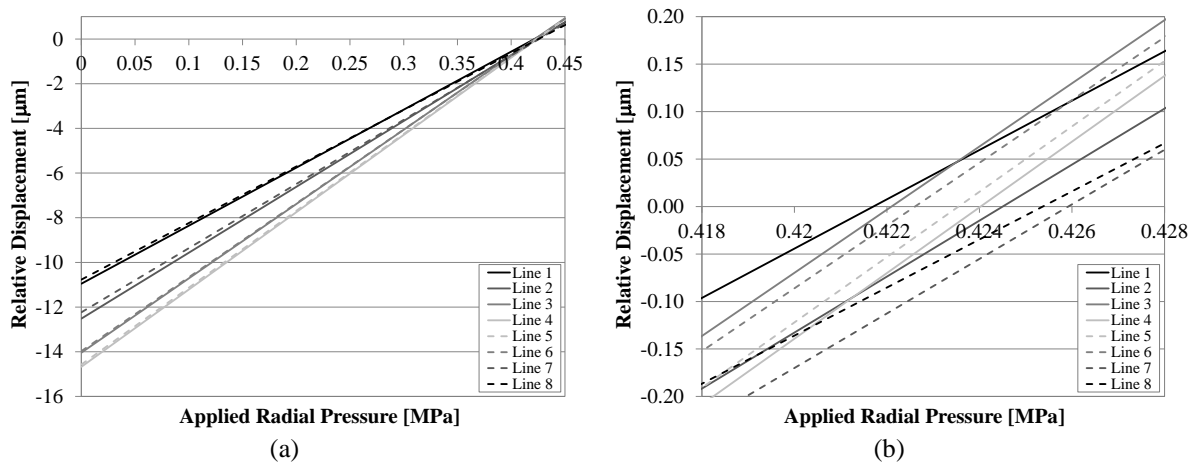Figure 6-16 Modeling results for the single tube-jack test in the 5th horizontal joint: relative vertical displacements of the virtual LVDTs versus applied radial pressure (a) over all applied pressure values; and (b) zoomed in at restoring pressure value

The second analysis run modeling the single tube-jack test in the 5th horizontal joint considered the impact of the two flat-jack slots by deactivating the elements in the slots for both the first and second phases. This influenced the relative displacements on the right side of the equivalent flat-jack as shown in Figure 6-17a. The virtual LVDTs measured larger relative displacements on the right side of the equivalent flat-jack, the side closer to the flat-jack slots. However, the average relative displacement of lines 2, 4, 5, and 7 due to creating the holes, -14.1 μm, was not much larger than in the first run of the model. Thus, the much larger relative displacement seen in the laboratory test was likely due to the slots being made only partway through the wall, causing eccentric loading and bending of the wall.

157
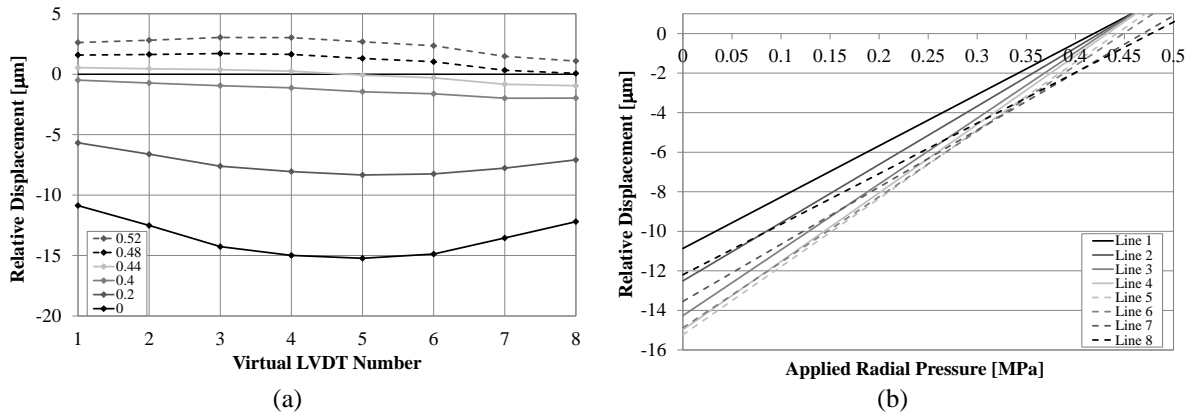
Figure 6-17 Modeling results for the single tube-jack test in the 5th horizontal joint considering the existing flat-jack slots: (a) relative displacements for the virtual LVDTs; and (b) relative vertical displacements of the virtual LVDTs versus applied radial pressure

The average restoring pressure for the virtual LVDTs in this analysis was 0.443 MPa, with a coefficient of variation of 4.76%. This variation in restoring pressure is much higher than for the analysis that did not consider the flat-jack slots. The high dispersion of the virtual LVDT restoring pressures is due to the variation of relative displacements along the length of the slot shown in Figure 6-17a and can be seen visually in Figure 6-17b. Regardless of the variation in restoring pressures, the average estimated state of stress only has an error of 0.68% considering the stress level in the model at the 5th joint at the location of the single tube-jack test, 0.4397 MPa.

The laboratory test results and the results of modeling of the single tube-jack test in the 5th horizontal joint show that the single tube-jack test results were affected by the flat-jack slots in the wall to the right. Thus, future tube-jack and flat-jack test should take this into consideration and ensure that the tests are far enough away from each other horizontally or that any holes or slots are repaired with mortar prior to subsequent testing in the vicinity.

6.2.2.2   Analysis of Displacement, Strain, and Stress

The application of the self-weight of the masonry complicates the analysis of the model since the stress level decreases moving up the wall. To see the effects of drilling and pressurizing the holes on the displacements, strains, and stresses more clearly, the model of the single tube-jack test in the 3rd horizontal mortar joint was run without the self-weight of the masonry. The results of the relative displacements versus the applied pressure are shown in Figure 6-18. Again, the virtual LVDT results overestimate the stress level in the wall at an average value of 0.2060 MPa (COV 0.39%), a 2.98% error in comparison with the stress level induced in the wall by the pressure on top of the wall, 0.2 MPa.
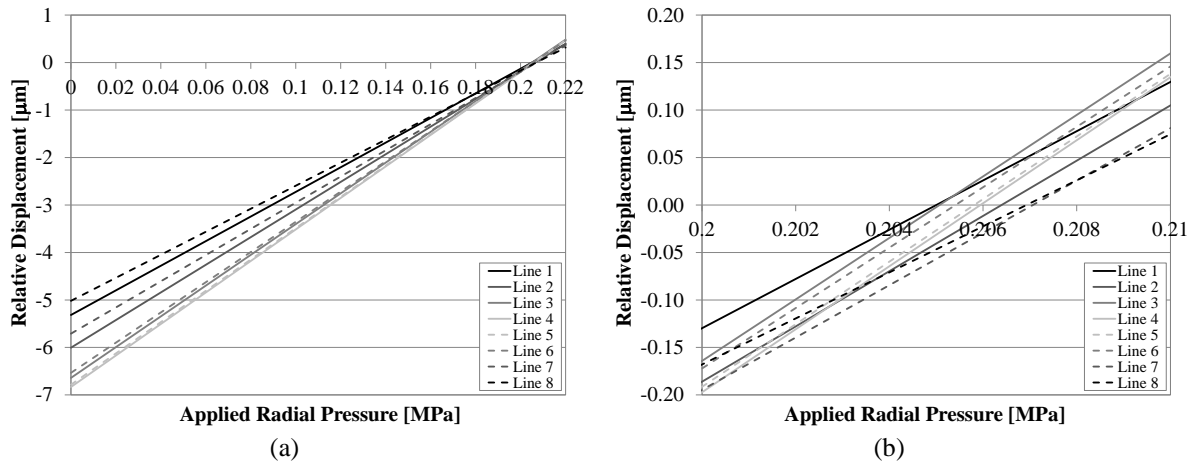
Figure 6-18 Relative vertical displacement versus applied pressure results without considering the self-weight of the masonry: (a) over all applied pressure values; and (b) zoomed in at restoring pressure value

Contour plots of the displacement of the wall can show more clearly how the wall is reacting to the removal of material from the holes and pressurization in the holes. After the holes are drilled (hole elements are deactivated), the masonry moves together. The masonry above the line of holes moves downward and the masonry below the line of holes moves upward slightly, see the first contour plot in Figure 6-19 at zero applied pressure. The vertical displacement is not equal along the length of the wall. Because the wall is unconfined on the left side of the equivalent flat-jack, the masonry is allowed to displace more toward the edge of the wall than at the center of the wall. As pressure is applied radially on the inside of the holes, the masonry above the holes moves upward and the masonry below the holes moves downward and the displacements are reduced (see 0.10 MPa contour plot). Appling a pressure of 0.20 MPa on the inside of the holes reduces the displacements to zero almost everywhere in the wall. Continuing to pressurize the holes beyond the restoring pressure starts to lift the masonry above the line of holes, producing positive displacements (see 0.24 MPa contour plot).

Observing how much the edges of the wall impact the displacement during the single tube-jack test, future testing should be performed on longer walls and further away from the ends of the walls. If tests must be performed near the ends of a wall, greater displacements should be expected at the end of the equivalent flat-jack closest to the edge of the wall.
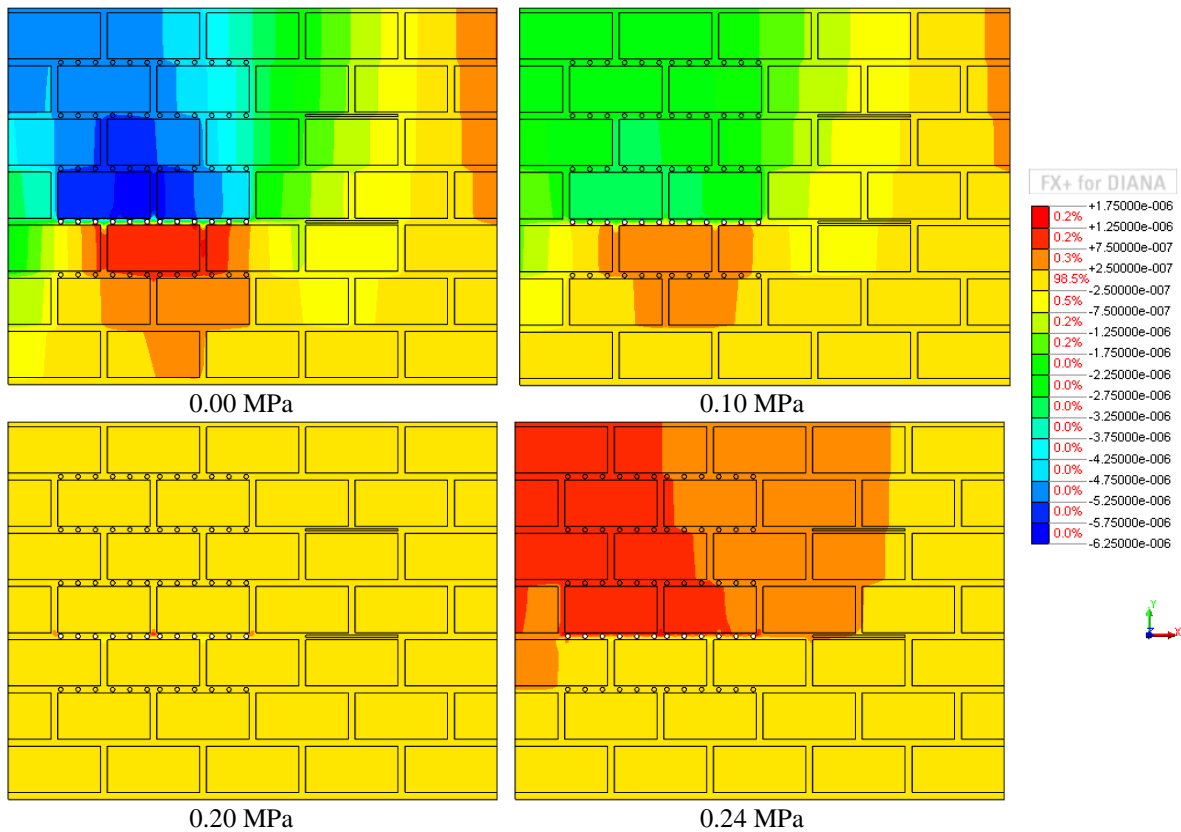
Figure 6-19 Contour plots of the absolute vertical displacement of the wall [m] at various applied pressure values

What is happening around the holes can be observed by zooming in on the vertical displacement contour plots at the center of the line of holes. In the contour plots shown in Figure 6-20, the undeformed mesh is shown over the deformed outlines of the granite units. After the mortar is removed from the holes, the circular holes become oval as the masonry contracts vertically over the line of the holes. The granite units seem to move as rigid blocks having displacement values all within the same color band, whereas the displacement varies from positive to negative from the bottom to the top of the mortar joint.

As pressure is applied radially to the holes, the holes get larger both vertically and horizontally. When the restoring pressure is reached, the displacements are zero almost everywhere. The last locations to reach zero displacement are directly above and below the holes. Note that at this pressure the holes have restored their original diameter vertically but are now wider than they originally were, retaining the oval shape. Continuing to pressurize the holes, the masonry above the joint begins to move upward and the variation of the displacement is again seen mostly in the mortar joint.

The mortar in the vertical mortar joint shows less vertical displacement as a result of drilling the holes. This is because there was less stress in the vertical mortar joints to be relieved, as shown in Figure 6-7. Since less displacement has occurred due to the removal of mortar material, there is less displacement to be recovered during the pressurization. Therefore, the displacements at the vertical mortar joints are recovered at a lower pressure level than the stress state in the wall. At 0.20 MPa, the mortar in the vertical mortar joint is already showing positive displacements. The variation in stress at the vertical joints and the difference in restoring pressure are two reasons why LVDT connection points should not be located in vertical mortar joints.
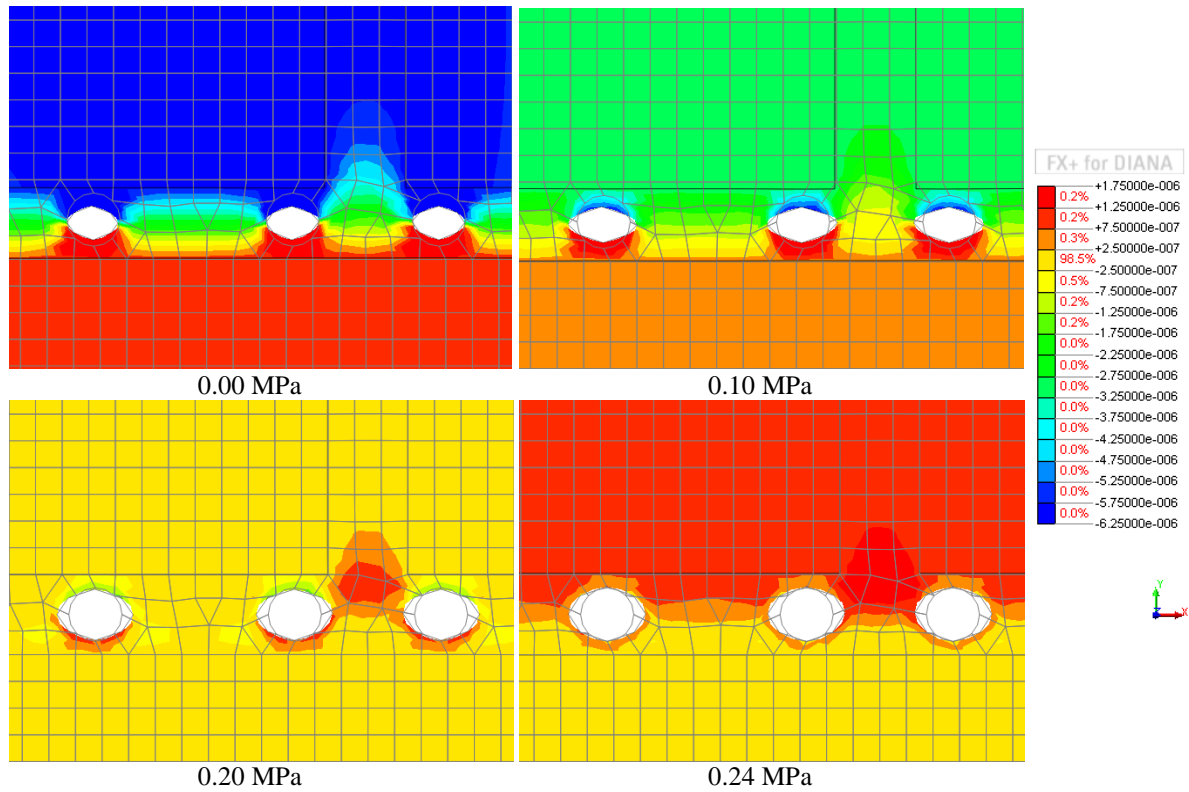
Figure 6-20 Contour plots of the absolute vertical displacement of the masonry [m] around the holes at various applied pressure values

With the finite element model, it is possible to observe the displacement of the masonry above and below the mortar joint throughout the entire length of the equivalent flat-jack, not just at a few virtual LVDTs. The absolute vertical displacements of all of the nodes 2 cm above and below the mortar joint are shown in Figure 6-21. As shown in the contour plots, the masonry above the joint moves downward when the mortar in the holes is removed. The masonry below the joint moves upward by a smaller amount. The movement of the masonry is greater at the center of the equivalent jack than at the ends. It can also be seen how the proximity of the equivalent flat-jack to the edge of the wall affects the results. Displacements that are more negative are seen on the left side of the equivalent flat-jack. Below the joint, the displacements are negative on the left side, as additional load from the tilting of the wall above does not allow the masonry to move upward. As discussed in regards to the contour plots, at each of the vertical mortar joints, the displacement is less than for the granite due to the lower stress in the vertical joints prior to removing the mortar in the holes.
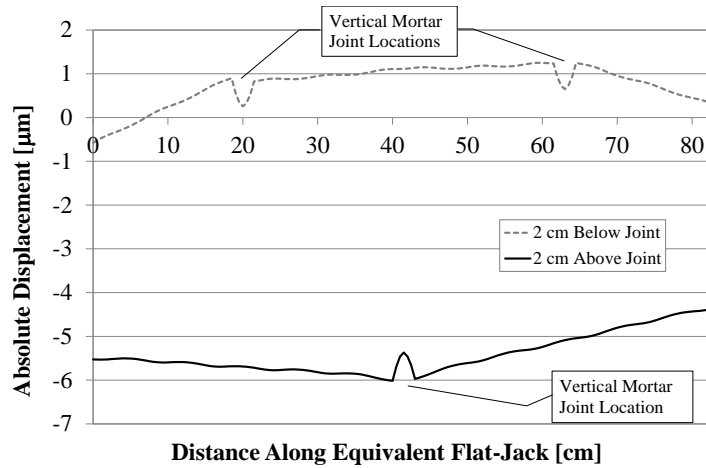
Figure 6-21 Absolute vertical displacements (due to opening the holes) 2 cm above and 2 cm below the joint

The absolute vertical displacements below the joint were subtracted from the absolute vertical displacements above the joint to obtain the relative displacements at various applied pressure levels. The results are shown in Figure 6-22. The results show the same general shape as presented in Figure 6-13. However, more details can be seen including the locations of the mortar joints where the displacements are less than for the granite units and slight waves in the line segments where the granite units are both above and below the joint. Each of these dips in the relative displacement is where a hole is located. The results in Figure 6-22 also indicate that the applied radial pressure that will restore the average displacements is slightly larger than the original stress state in the wall, 0.2 MPa. Due to the dips in the relative displacement along the length of the equivalent flat-jack, not all points will be restored at the same pressure. Thus, in an in-situ test, it cannot be expected that all LVDTs will be restored to zero relative displacement at the same pressure level.
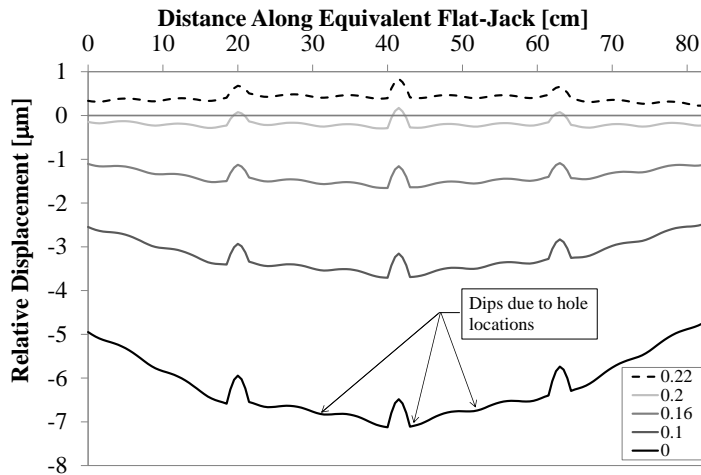
Figure 6-22 Relative vertical displacement of the masonry along the length of the equivalent flat-jack at various applied radial pressure values (Pressure in MPa)

The vertical strains were also analyzed and contour plots are provided in Appendix F. The vertical strains were limited to the horizontal joint where the holes were created for the equivalent flat-jack. The creation of the holes result in a redistribution of stresses causing positive strains above and below each hole and negative strains to the left and right of each hole. Applying a restoring pressure of 0.2 MPa to the holes returns the strain nearly to zero.

Pressurizing beyond that value results in positive strains as the joint is separated by the tube-jacks.

The horizontal strains were also contained almost entirely to the mortar joints. Contour plots of the horizontal strains can be found in Appendix F.2. When the holes are created, positive horizontal strains result as the mortar expands into the holes. When pressure is applied to the holes, the horizontal strains return to zero in most areas. The pressure required to restore the horizontal strains to zero is 0.04 MPa, only 20% of the vertical restoring pressure. Thus, as pressurization continues up to 0.2 MPa, negative horizontal strains result in between the holes.

Contour plots of the vertical stresses in the masonry at different points during the test are shown in Figure 6-23. Before the holes are created, the stresses in the masonry are similar to those presented in Figure 6-7 but without the variation from top to bottom due to the self-weight of the masonry. When the holes are created, the stress is relieved above and below each hole. This results in the positive strains and negative displacements discussed in the sections above. The release of stress at each of the holes results in a redistribution of stresses and concentrations of vertical compressive stresses on either side of each hole.
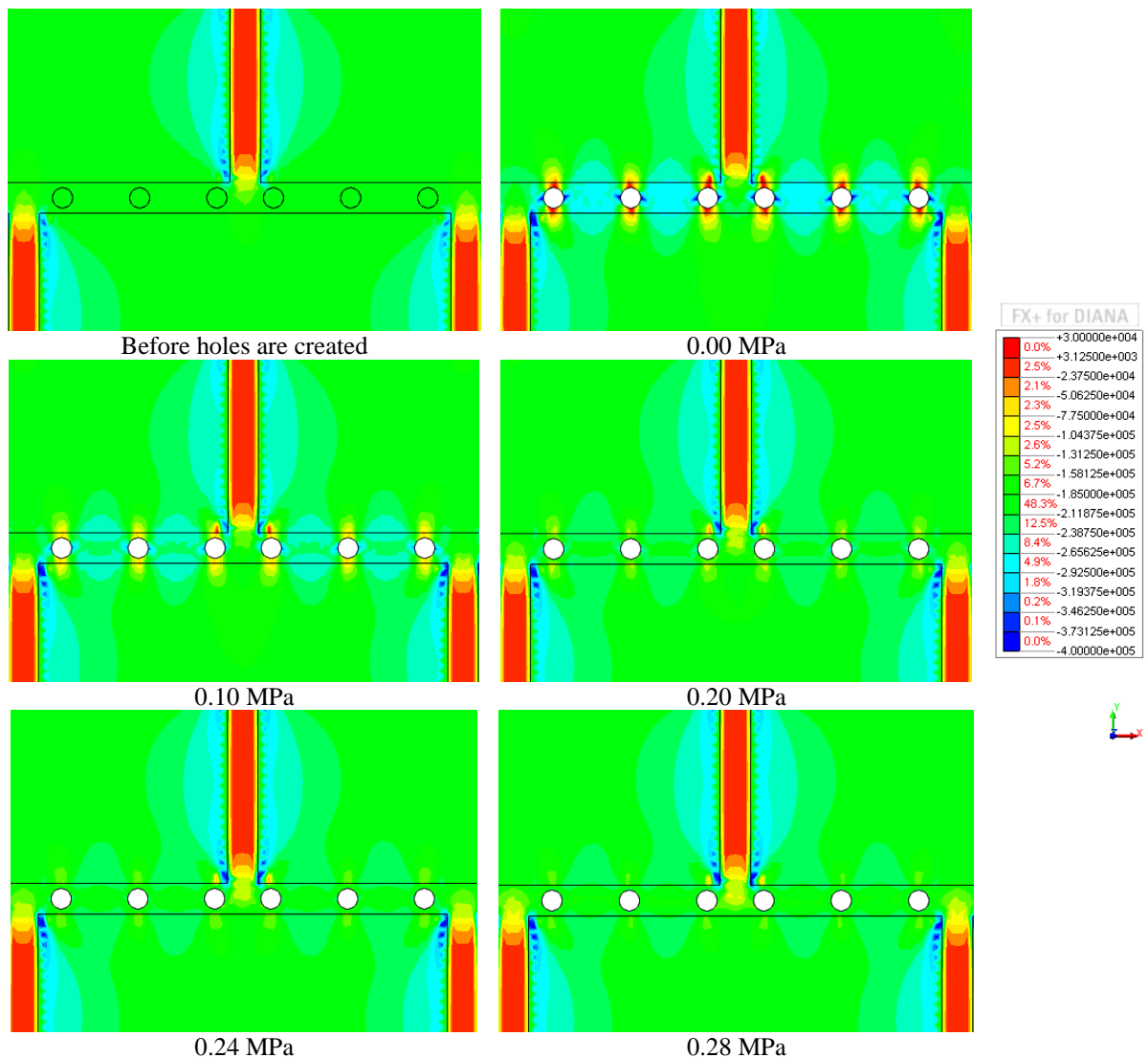
Figure 6-23 Contour plots of the masonry vertical stress [Pa] at various applied pressure values

Radial pressurization of the edges of the holes reduces the vertical compressive stresses to either side of each hole and increases the compressive stress above and below each hole. At the restoring pressure, 0.20 MPa, most of the mortar joint is again at a stress level of 0.2 MPa, however not all of the stresses have returned to their original values. Even increasing the applied pressure to 0.28 MPa does not entirely restore the stress distribution that existed before the holes were created. Given the linear-elastic properties of the model, it was originally expected that the stresses would be restored since the displacements were restored.

(a)   (b)
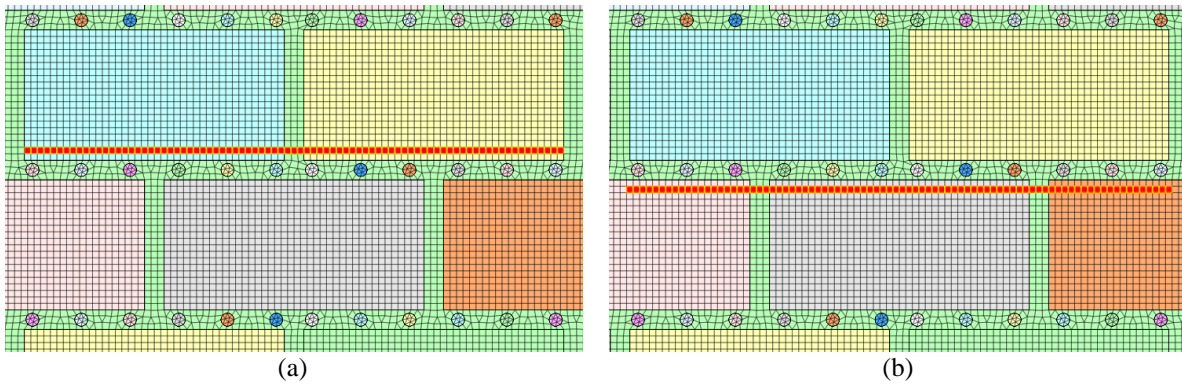
Figure 6-24 Elements selected to analyse vertical stresses: (a) 2 cm above the joint; and (b) 2 cm below the joint

The vertical stresses in the elements 2 cm above and below the joint (Figure 6-24) were examined more closely. The vertical stresses in these elements were plotted at various applied pressures during the simulated tube-jack test, as shown in Figure 6-25. Note that negative values signify compressive stresses. Initially, before the holes are drilled, the compressive stress is relatively level at 0.20 MPa, except where there are vertical joints. When the holes are created, the redistribution of stresses is observed, a reduction in compressive stress at each hole and an increase in compressive stress between the holes. In Figure 6-25, the vertical lines indicate the approximate centerline of each hole.
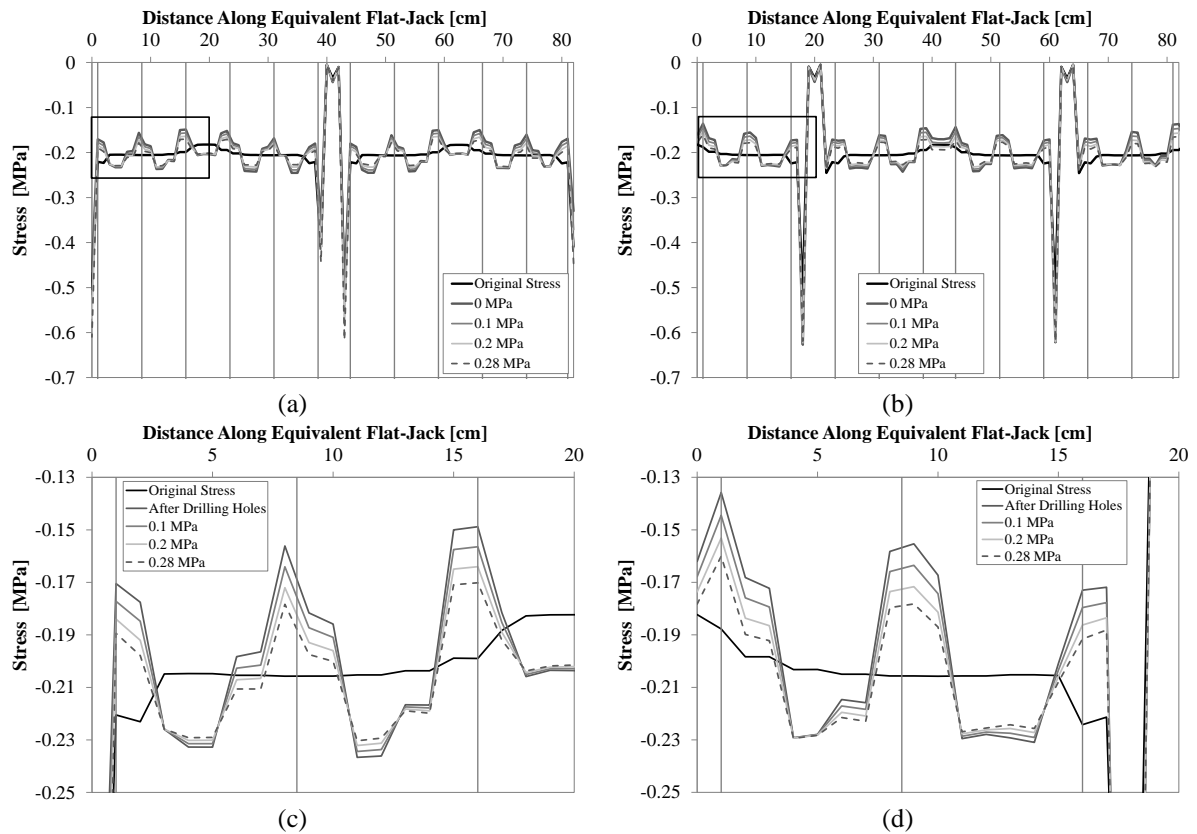
Figure 6-25 Stress in the masonry at various applied pressure levels: along the entire length of the equivalent jack (a) 2 cm above the joint; and (b) 2 cm below the joint; and zoomed in at the beginning of the equivalent flat-jack (c) 2 cm above the joint; and 2 cm below the joint (Vertical lines indicate the centerline of each hole)

As pressure is applied radially to the edges of the holes and increased in increments, the zoomed in plots of the stresses above and below the joint (Figure 6-25c and d) show that the stress starts to return to its original levels. However, similarly to the contour plots of the vertical stresses, at the pressure required to restore the displacements, slightly over 0.2 MPa, the stress level is not completely restored.

It was also observed in Figure 6-25c and d that some areas along the joint saw more stress restored than other areas. To quantify this difference along the equivalent flat-jack, the change in compressive stress, 2 cm above the joint, due to the change in applied pressure was graphed as a percentage in Figure 6-26a. In this graph, a positive percentage represents an increase in compressive stress due to the application of a compressive pressure on the edges of the holes. In the same graph, the change in stress due to opening the holes was graphed. Again, a positive change in stress represents an increase in compressive stress.
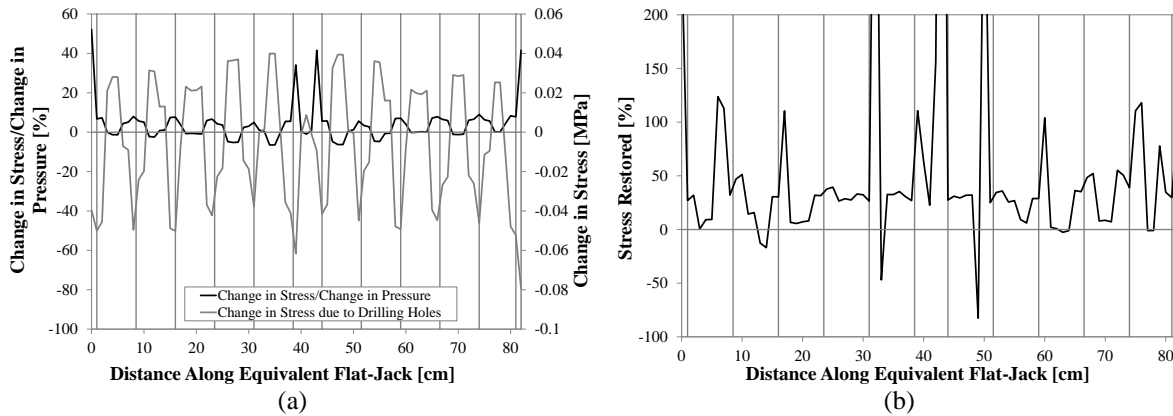
Figure 6-26 Results 2 cm above the equivalent flat-jack for (a) the change in stress due to the change in applied radial pressure on the edges of the holes and the change in stress due to creating the holes; and (b) the percentage of the stress restored to its original value (before the holes were created) at a pressure of 0.2 MPa

In order to restore the original stress level by applying the restoring pressure to the holes, the two lines in Figure 6-26a would need to be mirrored. In locations where drilling the holes caused an increase in pressure, the applied pressure to the edges of the holes would need to cause a decrease in pressure, and vice versa. This is not always the case. Toward the edges of the equivalent flat-jack, pressure application to the holes results in almost no decrease in stress in between the holes. Another reason that the stress state is not restored is that the percentage of stress restored in comparison to the pressure applied is very low. The change in compressive stress due to opening the holes was around 15%-20% at each hole and in between each hole. Thus, a 20% change in compressive stress due to the applied pressure would be required in these locations to restore the stress level. However, for most of the length of the equivalent flat-jack, the change in stress due to the change in applied pressure is below an absolute value of 10%.

The percentage of the stress recovered at the restoring pressure of 0.20 MPa is shown in Figure 6-26Figure 6-26b. A value of 100% would indicate that the stress value seen before the holes were created was recovered at the restoring pressure. There were only a few points along the length of the equivalent flat-jack that were close to this value.

Regarding the horizontal stresses, the initial vertical loading on the wall causes horizontal compressive stresses in the joints. When the holes are created, the redistribution of stresses and the increase in vertical stress between the holes also results in an increase in horizontal stress due to the confinement of the granite units above and below each joint. As the holes are pressurized, the horizontal stresses increase further. Additional discussion and contour plots of the horizontal stresses are provided in Appendix F.3.

6.2.3 Single Flat-Jack Test

6.2.3.1 Simulation of the Experimental Test

The single flat-jack test performed on the regular masonry wall in the laboratory was simulated. The pressure load on the top of the wall was 0.2 MPa for this test and was applied, along with the self-weight of the masonry, in the first phase of the analysis. In the second phase the elements located in the lower flat-jack slot were deactivated, simulating the sawing of the slot. Pressure was then applied in load steps to the elements on the top and bottom edges of the slot as described in section 6.1.4. The locations of the nodes used to simulate the DEMEC points

and LVDT connection points are shown in Figure 6-27. The virtual DEMEC nodes were spaced 19 cm apart and the virtual LVDT nodes were spaced 7 cm apart.
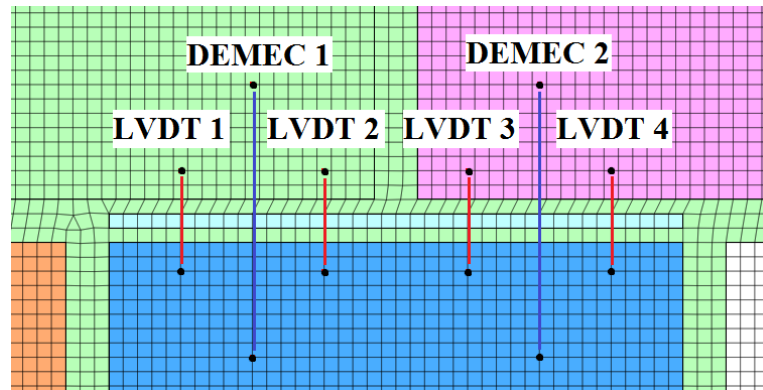
Figure 6-27 Locations for the vertical node sets in modeling the single flat-jack test

The relative displacements of the virtual LVDTs are shown in Figure 6-28. The average virtual LVDT relative displacement due to opening the slot (deactivating the slot elements) is almost ten times greater than in the single tube-jack tests simulation; −69.79 μm for the flat-jack slot versus −7.03 μm for the tube-jack holes in the 3rd joint. Despite the scale of the relative displacements, the distribution of relative displacement over the length of the flat-jack is similar to that found in the single tube-jack test, shown in Figure 6-13. More negative relative displacements are seen at the middle of the slot than at the edges of the slot, indicating the slot closes more in the middle.
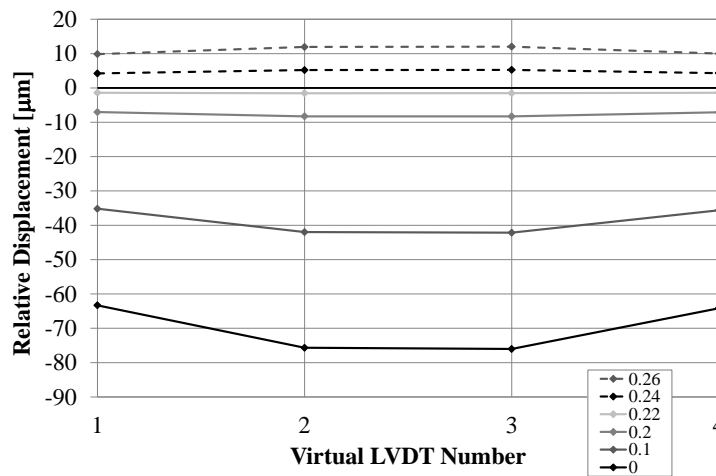
Figure 6-28 Relative vertical displacements for each virtual LVDT at several increments of radial pressure applied to the edges of the holes (pressure values in MPa)

Figure 6-28 shows that as the pressure is applied to the upper and lower edges of the flat-jack slot, the relative displacements decrease. Between 0.22 MPa and 0.24 MPa the relative displacements are restored to zero. The exact restoring pressure for each virtual LVDT can be seen in the graph of the relative displacement versus the applied pressure in Figure 6-29a. LVDTs 1 and 4 follow the same loading curve and LVDTs 2 and 3 follow another loading curve. The average restoring pressure for the four LVDTs estimates the state of stress to be 0.2247 MPa. This is an error of only 0.22% comparing with the average stress in the joint prior to opening the slot, 0.2252 MPa.
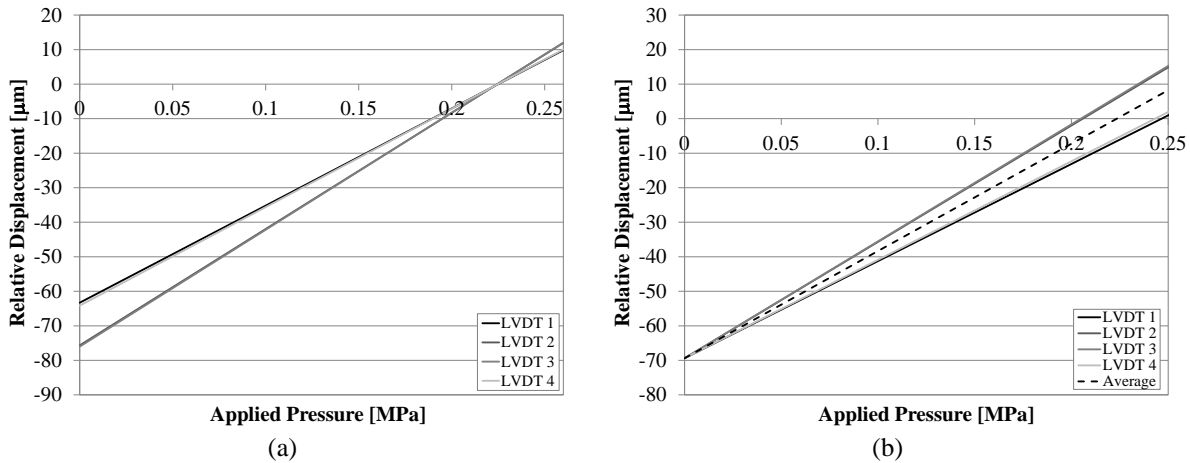
Figure 6-29 Relative vertical displacements of the virtual LVDTs versus applied radial pressure: (a) with LVDT initial relative displacements; and (b) with average DEMEC relative displacement at the initial displacement

Relying on the virtual LVDTs to determine the relative displacement due to opening the slot is not realistic in the physical test since the LVDTs cannot be in place during the sawing of the slot. Thus, to simulate the procedure used in the laboratory test, the average relative displacement value found using the virtual DEMEC measurements as a result of deactivating the slot elements, −69.40 μm, was used as the initial relative displacement value for the virtual LVDTs. This is shown in Figure 6-29b. The average relative displacement due to cutting the slot in the laboratory test was −180 μm, much larger than in the model. However, the relative displacement varied greatly between the four sets of DEMEC points and the slot was only through half the thickness of the wall. Since the slopes of the pressurization curves for each of the LVDTs are the same in Figure 6-29b as in Figure 6-29a, the lines diverge instead of converging on the restoring pressure value. However, plotting the average of the LVDT relative displacements results in a good estimation of the state of stress of the masonry, 0.2252 MPa; a 0.02% error from the average stress value before opening the slot. The laboratory test resulted in an estimated state of stress of 0.3 MPa, a 33% error in comparison to the average stress in the 3rd joint in the model wall. The difficulties found in performing the test in the laboratory, which were discussed in the previous chapter, likely led to this error.

6.2.3.2   Analysis of Displacement, Strain, and Stress

As previously done with single tube-jack, the model was run without the self-weight of the masonry being applied. The relative displacement of the virtual LVDTs resulting from simulating the slot opening was −62.8 μm, 7 μm less than when the self-weight was applied. The relative vertical displacements of the virtual LVDTs versus the applied pressure results are shown in Figure 6-30. The average virtual LVDT results overestimate the stress level in the wall. The average restoring pressure is 0.2022 MPa, a 1.12% error in comparison with the pressure applied to the top of the wall, 0.2 MPa.
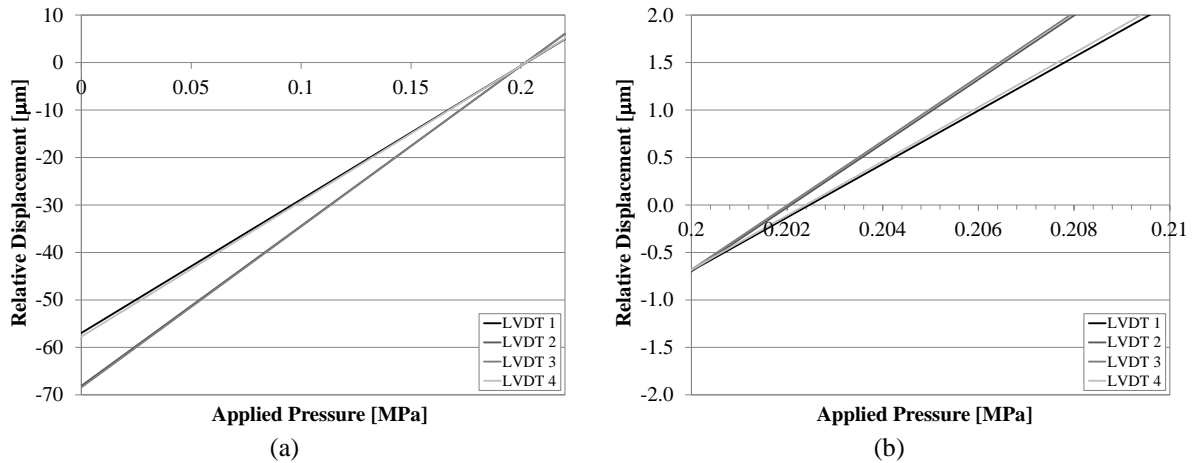
Figure 6-30 Relative vertical displacements of the virtual LVDTs versus applied pressure: (a) over all pressure values; and (b) close to the restoring pressure

Contour plots of the vertical displacement over the entire regular masonry wall are shown in Figure 6-31. Note that the scale of the contour plots in Figure 6-31 is different from the scale of the contour plots in the analysis of the single tube-jack tests in Figure 6-19. The vertical displacement above and below the flat-jack is larger than it was above and below the line of tube-jacks. However, the same distribution of displacements seems to be happening in both tests. Following cutting of the slot, negative displacements are seen above the slot and positive displacements are seen below the slot. The magnitudes of the displacements are largest closer to the slot and diminish farther away from the slot. The end of the flat-jack slot is half a unit farther away from the edge of the wall than the end of the equivalent flat-jack in the tube-jack test, reducing the edge effect on the vertical displacements, although some edge effects can still be seen. The magnitudes of the displacements above and to the right of the flat-jack slot are greater than they are the same distance away to the left of the slot.

As pressure is applied to the edges elements above and below the slot, the magnitudes of the displacements reduce until they are nearly zero everywhere in the wall at an applied pressure of 0.2 MPa, the same as the pressure applied on top of the wall. Continuing to apply pressure to the edges of the slot beyond 0.2 MPa results in positive vertical displacements above the slot and negative displacements below the slot.
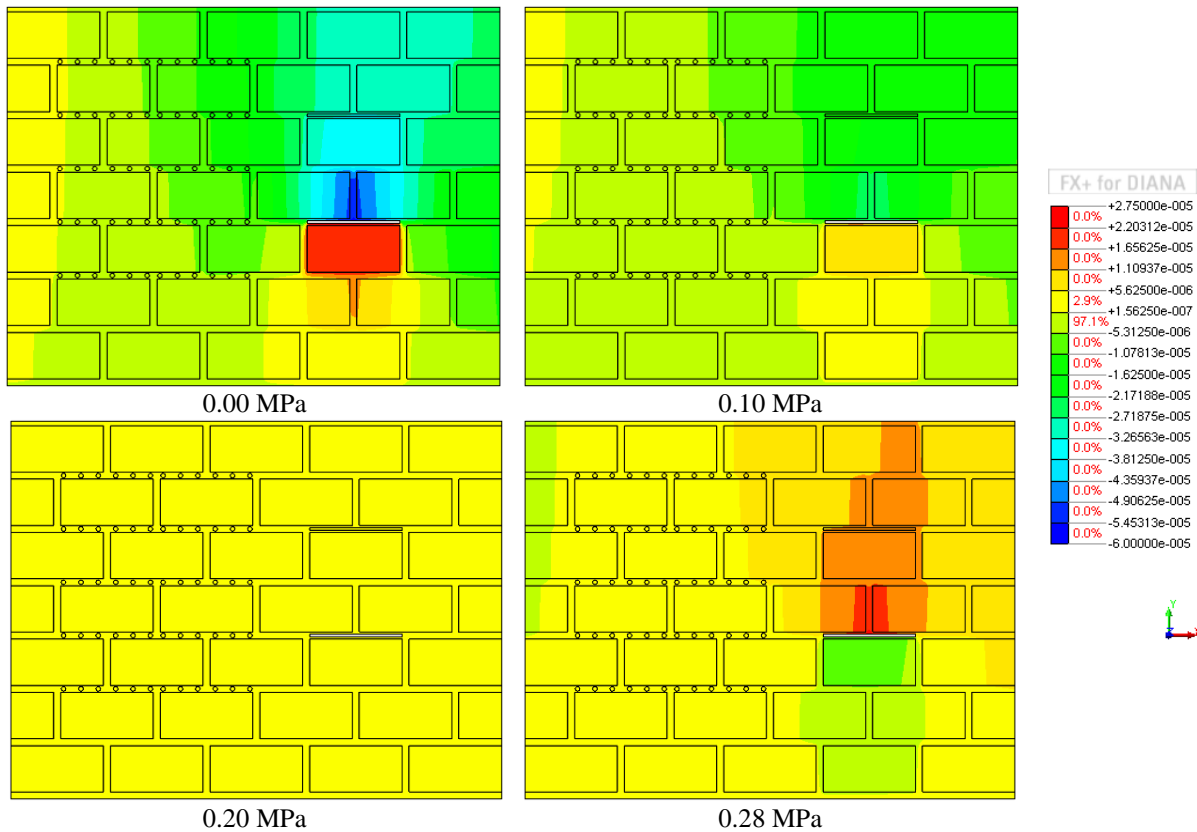
Figure 6-31 Contour plots of the masonry absolute vertical displacement [m] at various applied pressure values

The movement of the masonry surrounding the slot can be examined using the contour plots of the vertical displacement zoomed in around the slot, as shown in Figure 6-32. The deformation of the slot is also shown with a magnification factor of 100 in these contour plots. Following the opening of the slot, the slot closes and a slight horizontal expansion of the slot occurs to the right, the side closest to the free edge of the wall. As pressure is applied by the flat-jack to the top and bottom edges of the slot, the slot is ideally pushed back open to its original size. At 0.2 MPa of applied pressure, the vertical displacements are nearly zero everywhere and the slot is indistinguishable from its original size and shape. Continued pressurization opens the slot and vertical movement is most notable above the slot in the center where there is the least resistance due to the vertical joint. Since the flat-jack only applies pressure vertically and not horizontally, very little movement is seen horizontally due to the pressurization. The opposite was the case in the tube-jack test, where the height of the holes was restored at 0.2 MPa of applied pressure but the width of the holes was restored at 0.04 MPa and additional pressure continued to increase the width of the holes.
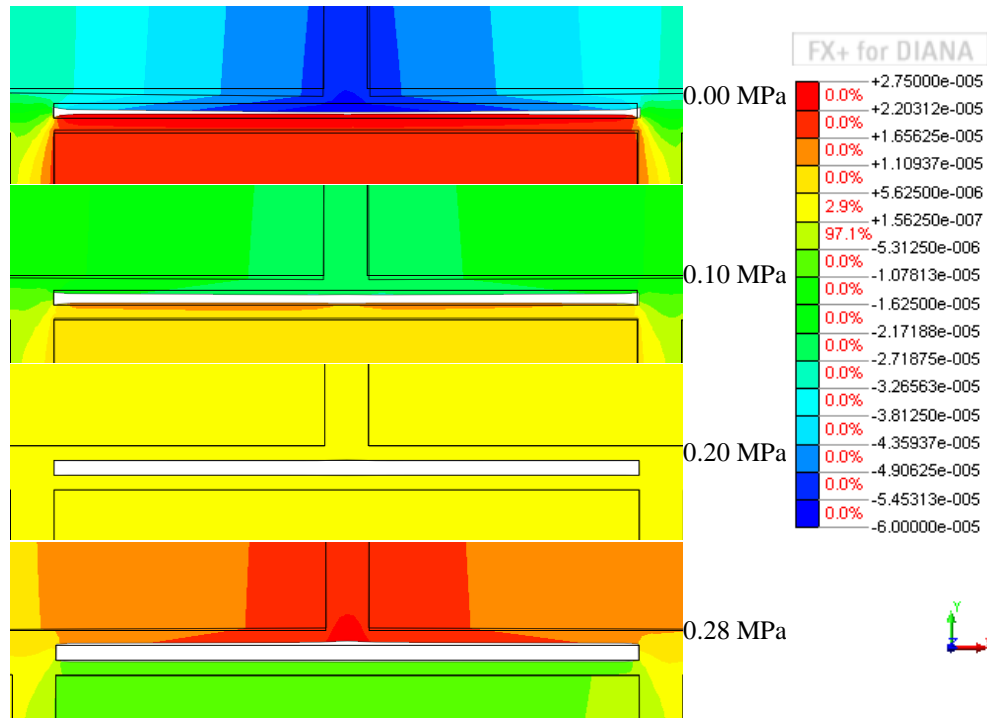
Figure 6-32 Absolute vertical displacement [m] contour plots at various applied pressure values close to the slot

The vertical displacement was also analyzed at each node 2 cm above and below the mortar joint along the entire length of the slot. The graphs of the displacements due to opening the slot are shown in Figure 6-33.
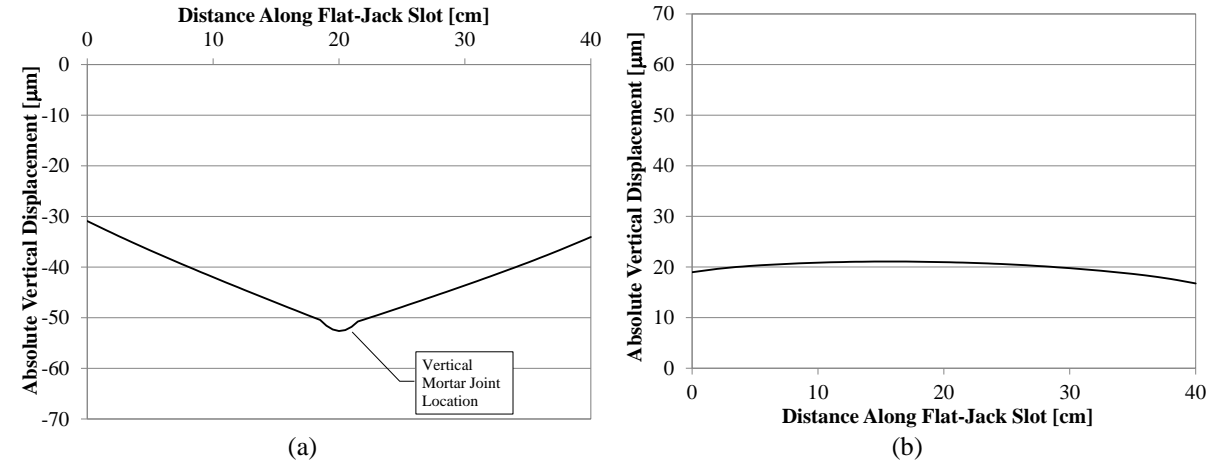
Figure 6-33 Absolute vertical displacements (due to opening the slot) of the masonry: (a) 2 cm above the joint; and (b) 2 cm below the joint

The scale of the displacements along the slot are approximately ten times greater than in the single tube-jack test (see Figure 6-21). However, some aspects of the vertical displacement graphs are similar in both tests. The vertical mortar joint influences the displacements above the slot and a small increase in downward displacement is seen at its location. The vertical joint also allows the two units above the bed joint to tip inward toward the center of the slot when the mortar in the slot is removed. The slopes of the tilted units are seen in Figure 6-33a as the slopes of the vertical displacement on either side of the vertical joint. The unit under the slot seems to move upward almost uniformly as shown by the vertical displacements in Figure 6-33b. Only a slight increase in deformation is seen toward the center of the slot.

171

Similarly to the tube-jack test, the displacements are less on the side of the slot closer to the edge of the wall both above and below the slot.

Horizontal strains result in the vertical joint directly above the flat-jack slot due to the tilting of the masonry units in toward the slot when the slot is cut, as seen in the plots of the deformation. A contour plot of the horizontal strains is shown in Appendix F.5.

The absolute vertical displacements 2 cm below the mortar joint were subtracted from the absolute displacements 2 cm above the mortar joint to determine the relative displacement of the masonry over the same distance as the virtual LVDTs. The results at various applied pressure levels are shown in Figure 6-34. The relative displacements at the vertical mortar joint at the center of the slot are restored to zero at a lower applied pressure level than the displacements along the length of the granite units. This was also the case in the single tube-jack test. With increasing complexity of the masonry typology and a larger number of vertical mortar joints along the length of the flat-jack slot it could be expected that restoration of the relative displacements to zero will vary along the length of the slot. As higher pressures are applied by the flat-jack to the slot, the variations in displacement due to increased mortar thicknesses in some locations could lead to deformations of the flat-jack in those areas and non-uniform distributions of the applied pressure.
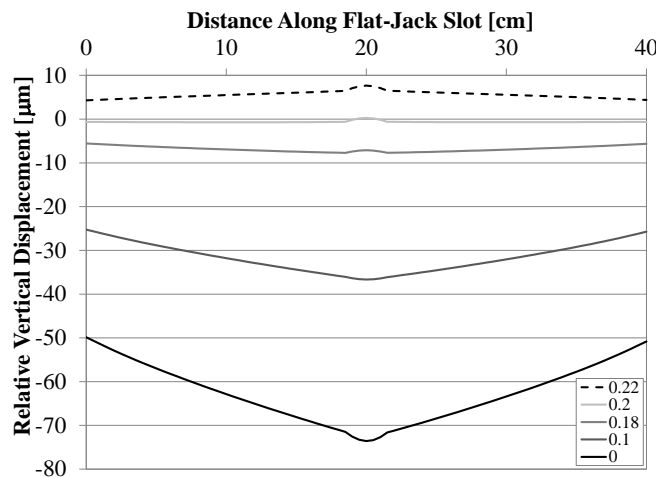
Figure 6-34 Relative vertical displacement of the masonry along the length of the flat-jack slot at various applied pressure values (Pressure in MPa)

The vertical stresses throughout the masonry wall for different applied pressure values are shown in the contours in Figure 6-35. The pattern of stresses before the slot is opened is the same as presented in the single tube-jack test and the variations were discussed in that section.
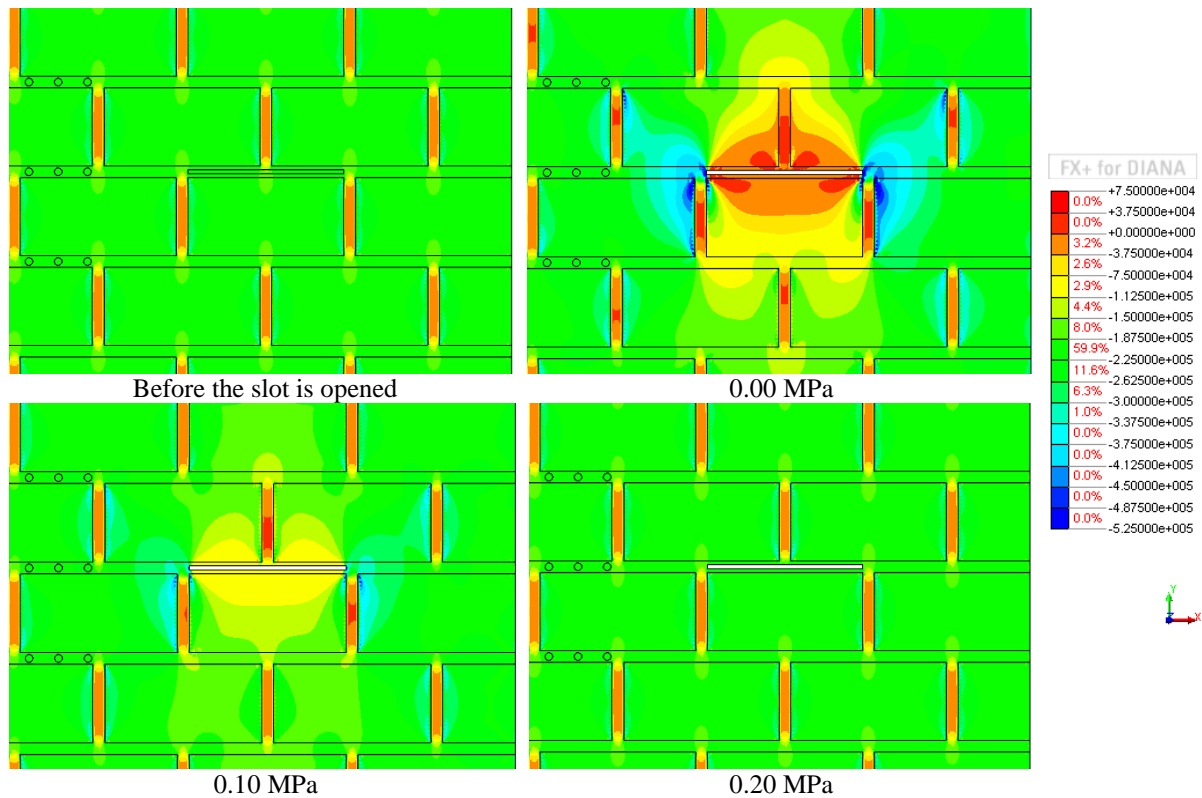
Figure 6-35 Contour plots of the masonry vertical stress [Pa] at various applied pressure values

When the slot is opened, the distribution of stresses is similar to that seen in the single tube-jack test but on a much larger scale. At each of the tube-jack holes, the stress was relieved above and below the hole and the compressive stress increased to either side (see Figure 6-23). In the flat-jack test, the stress is relieved above and below the slot. In the center above the slot, tensile stresses occur as the masonry is suspended above the opening. As the load from the masonry and applied pressure above the joint is redistributed due to the slot opening, the stresses increase significantly to either side of the slot. In some areas, the compressive stress is more than double the applied pressure on top of the wall. The maximum compressive stresses occur at the ends of the flat-jack where they are approximately 0.86 MPa. In the single tube-jack test, the maximum vertical compressive stresses were approximately 0.45 MPa and only occurred in small areas to the right and left of each hole (see Figure 6-23). In the flat-jack test, the stress redistribution affects a large portion of the wall including several units above, below, and to the sides of the flat-jack slot. On the other hand, in the single tube-jack test, the stress redistribution was localized at each hole and was mostly contained within the mortar joint being tested.

Another difference between the single flat-jack test and the single tube-jack test is that, when the pressure is applied to the flat-jack slot, the vertical stresses return to the distribution that occurred before the slot was created, see the final contour plot in Figure 6-35. In the tube-jack test at and above the restoring pressure, there continued to be larger compressive stresses to either side of each hole and lower compressive stresses above and below each hole.

The stress redistribution observed in the analysis of the vertical stresses produces vertical strains in the mortar joints around the flat-jack. When the slot is created, positive strains are seen above and below the slot as the mortar expands into the slot. On either side of the flat-jack, the redistribution of stresses causes high compressive stresses and negative vertical strains. Pressurization of the flat-jack to 0.2 MPa reduces the strains to zero almost everywhere. As in the tube-jack test, additional pressurization causes positive strains on either side of the jack as

the joint is pushed apart. Additional discussion and contour plots of the vertical strains are presented in Appendix F.4.

As in the analysis of the vertical stresses for the single tube-jack test, elements were selected 2 cm above and below the mortar joint to study the vertical stresses in the masonry due to the flat-jack test (see Figure 6-36). In order to compare the results, the same number of elements was selected above and below the flat-jack slot as was selected in the single tube-jack test, even though the flat-jack slot was half as long.

(a)   (b)
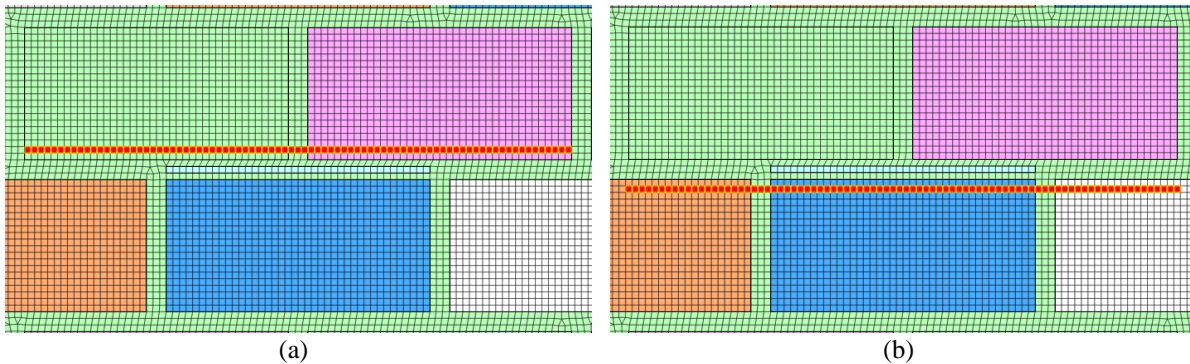
Figure 6-36 Elements selected to analyze vertical stresses: (a) 2 cm above the mortar joint; and (b) 2 cm below the mortar joint

The results of the vertical stresses above and below the tested joint are shown in Figure 6-37. Vertical lines indicate the start and end of the flat-jack slot. Before the slot is created, the original stress line indicates that the stress level is approximately 0.2 MPa along most of the joint except where there are vertical joints. When the slot is created but no pressure has been applied yet, the stress level reduces to around zero along the length of the slot. To either side of the slot, the compressive stress doubles to 0.4 MPa. As pressure is applied by the flat-jack to the masonry around the slot, the stresses return to their original state.

(a)   (b)
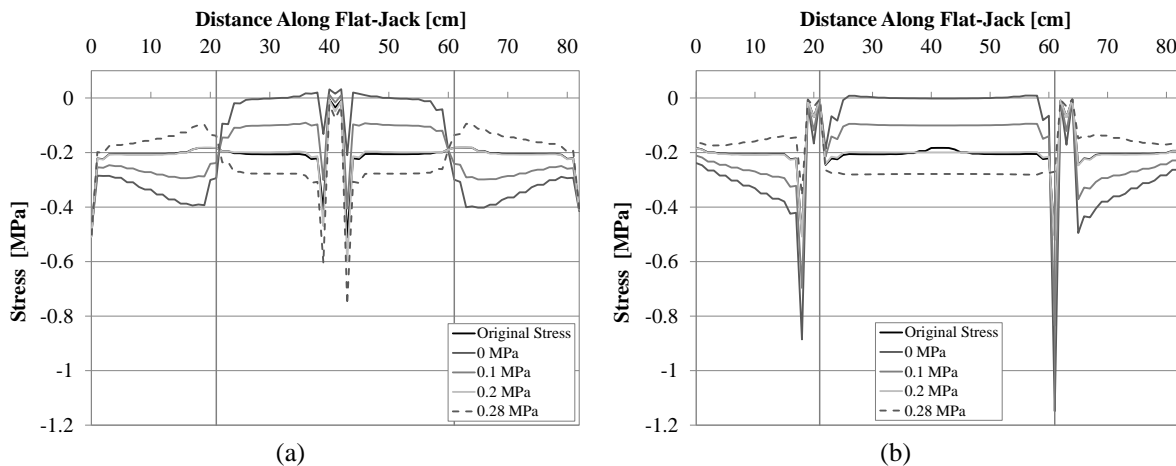
Figure 6-37 Vertical stress in the masonry along the length of the flat-jack at various applied pressure levels at: (a) 2 cm above the joint; and (b) 2 cm below the joint

In Figure 6-38 the vertical stresses are compared between the single tube-jack test and the single flat-jack test for the lines of elements above and below the joints tested. These graphs were created by combining the graphs in Figure 6-25 with the graphs in Figure 6-37. For clarity, only the stress levels right after opening the holes or slot (zero applied pressure) and the restoring pressure (0.2 MPa) are shown, along with the original stress distribution. These graphs show clearly how the variation in the vertical stress distribution is much greater due to opening the

174

flat-jack slot than in opening the tube-jack holes. The compressive stress at each hole is slightly decreased, whereas at the flat-jack slot the compressive stress goes nearly to zero. On either side of each hole, the compressive stress increases slightly, whereas on either side of the flat-jack slot, the compressive stress nearly doubles. In the flat-jack test, the vertical stresses are restored to their original distribution at the restoring pressure. In contrast, in the tube-jack test, only a small percentage of the original stress values are restored during the tube-jack pressurization to the restoring pressure.
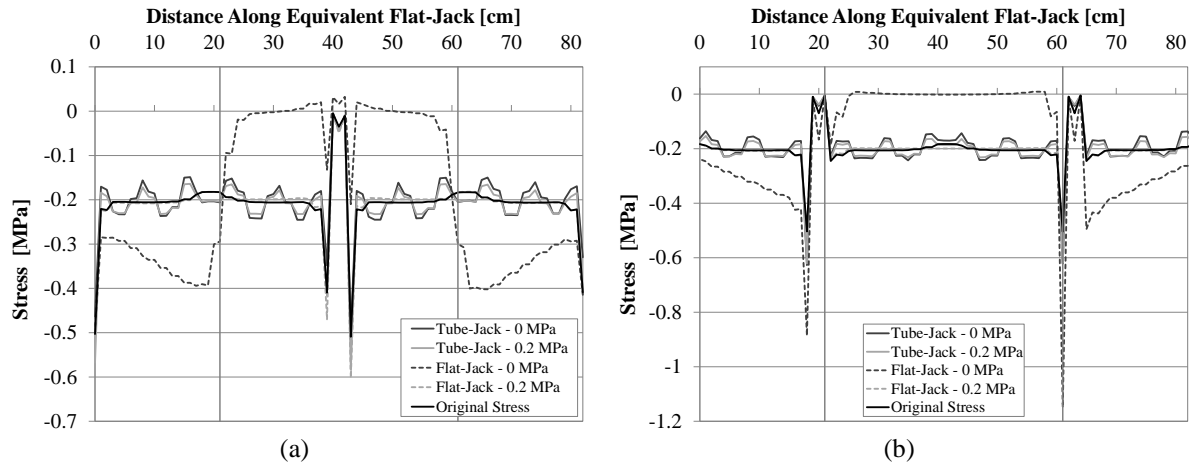
Figure 6-38 Vertical stress comparison between the single tube-jack test and the single flat-jack test at various applied pressure levels at: (a) 2 cm above the tested joint; and (b) 2 cm below the tested joint

The reason why the stresses are restored to their original values by pressurizing the edges of the slot is shown in Figure 6-39. This graph shows the stress change due to opening the slot and the change in stress due to the change in applied pressure to the slot, along the length of the mortar joint. The two curves are almost exact reflections of each other. Thus, pressure applied to the edges of the slot causes a change in stress that is proportional to the change in stress that occurred when the slot was opened. For example, in an area where a large stress reduction resulted from opening the slot, a large stress increase results from applying pressure to the edges of the slot, restoring the stress level to its original value. This was not the case in the single tube-jack test, which resulted in the stresses not being restored at the restoring pressure (see Figure 6-26).
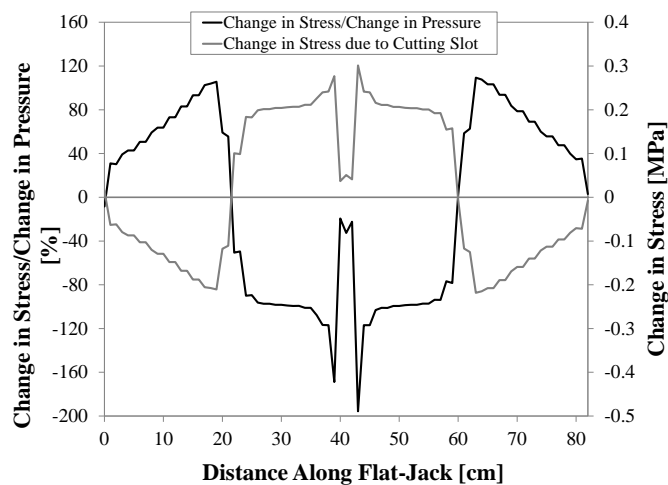
Figure 6-39 Change in vertical stress due to the change in applied pressure on the edges of the slot and the change in vertical stress due to creating the slot

Horizontal stresses also occur due to the opening of the flat-jack slot. Contour plots of the horizontal stresses are shown in Appendix F.5.These stresses are much larger than those found in the single tube-jack test and they affect not only the mortar but also the units above and below the slot. Tensile stresses occur in the units above and below the slot and compressive stresses occur to either side of the slot. In contrast with the single tube-jack test, the horizontal stresses return to their original values before the slots were created at a restoring pressure equal to the load on the wall.

6.2.4 Double Tube-Jack Test

6.2.4.1 Simulation of the Experimental Test

The double tube-jack test was performed by deactivating the elements within the holes in the 3rd horizontal joint and the 6th horizontal joint, and radially pressurizing the edges of the elements surrounding the holes. In this test, the displacement loading method was used. The beginning of the recorded portion of the double tube-jack test is after the holes have been drilled, the stresses have redistributed in the masonry, and the tube-jacks have been inserted into the holes. Thus, this situation was simulated in the model to determine the displacement to use at the top of the wall. The model, with the hole elements in the 3rd and 6th joints deactivated, was loaded with a vertical pressure of 0.2 MPa on the top of the wall and the self-weight of the masonry. The vertical displacement along the top of the wall was recorded and is presented in Figure 6-40a. The sharp dips in the displacement are due to the vertical mortar joints. The holes in the mortar joints on the left side of the wall did affect the displacement on the top of the wall; however, the variation due to the holes and the vertical joints was at most 0.02 mm. Since the steel profile on top of the wall in the experimental test would only allow a linear deformation, a linear displacement line is shown connecting the points of least displacement. This linear displacement was used as the prescribed displacement in modeling the double tube-jack test. Refer to Table 6-2 for the phases of the test.
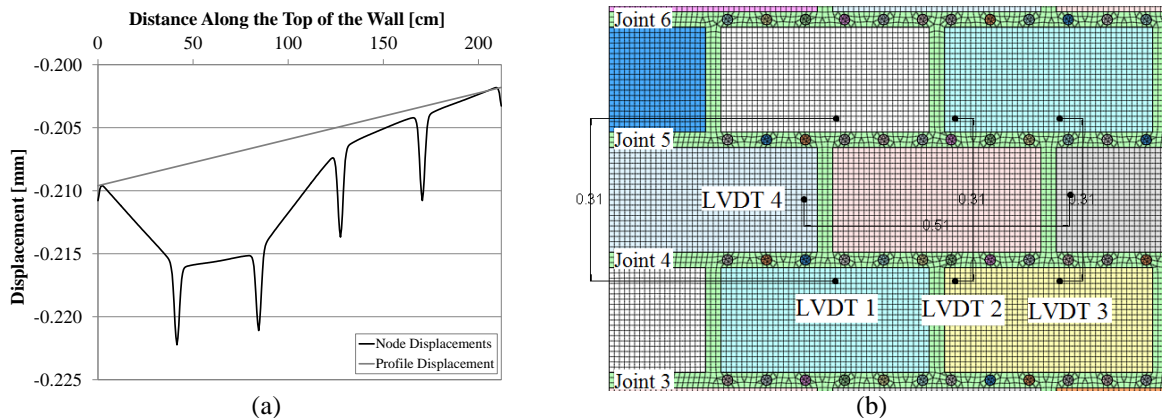
Figure 6-40 Double tube-jack test modeling set-up: (a) displacements at the top of the wall due to the vertical pressure and self-weight and estimated linear profile displacement; and (b) locations of the virtual LVDT connection points (Dimensions in [m])

The first aspect of the modeled test to be analyzed was the displacements of the masonry within the wall. All displacements were measured taking the first phase as the reference. Thus, displacements were only affected by the radial pressure applied around the edges of the holes. Three vertical sets of nodes and one horizontal set of nodes were selected to measure the relative displacement of the masonry separated by the two equivalent flat-jacks. The point locations and the virtual LVDT line labels are shown in Figure 6-40b.

The relative displacements for the vertical and horizontal virtual LVDTs during the pressurization of the edges of the holes are shown in Figure 6-41a. As expected, the pressure applied to the edges of the holes in the two equivalent flat-jacks causes a negative relative displacement vertically, a contraction of the masonry between the equivalent flat-jacks, and a positive relative displacement horizontally, an expansion of the masonry due to the Poisson effect.

A comparison can be made between the relative displacements of the model and the relative displacements in the experimental test (see Figure 5-23). During the final pressurization cycle of the experimental test, the average vertical relative displacement was approximately −20 μm at the maximum applied pressure of approximately 0.18 MPa. In the model at an applied pressure of 0.18 MPa, the relative vertical displacement is approximately −3.3 μm, about 6 times smaller.
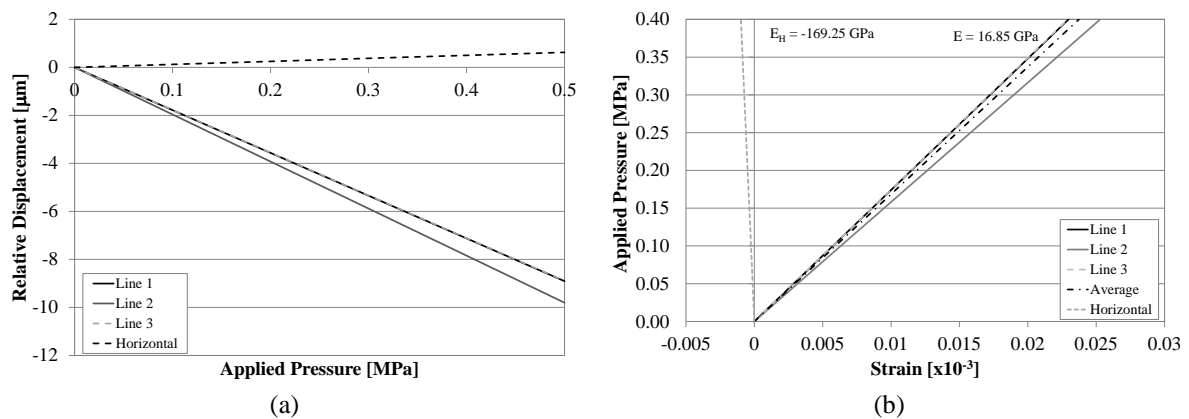
Figure 6-41 Double tube-jack test modeling results: (a) relative vertical and horizontal displacements of the virtual LVDTs; and (b) applied pressure versus strain for the virtual LVDTs

In Figure 6-41b, the applied pressure versus the strain for the virtual LVDTs is shown. The three vertical LVDTs were averaged and a trend line fit to the average to estimate the elastic modulus for the modeled test. The result was an elastic modulus of 16.85 GPa. In the experimental double tube-jack test on the regular wall the elastic modulus was estimated at 2.2 GPa, much closer to the Young's modulus found in the masonry wallet tests, 2.5 GPa.

These results can also be compared to the modeled Young's modulus test, see section 6.2.1. The elastic modulus found in that test using the virtual LVDTs was 2.19 GPa. However, the change in Young's modulus value due to the amount of mortar between the measuring points showed that the percentage of mortar between the measuring points makes a difference. Considering that the virtual vertical LVDTs measured over a distance of 31 cm including two joints, 19.35% of the material between the nodes being mortar, the expected elastic modulus based on the curve in Figure 6-11 would be approximately 1.3 GPa. This expected value is even farther away from the result than any of the previous comparisons.

Since the estimated elastic modulus from the modeled double tube-jack test is higher than the expected value based on the modeled elastic modulus test, the strains in the modeled double tube-jack test are not as large as they are expected to be. Therefore, the applied pressure in the holes must not be creating the same change in stress in the masonry between the equivalent flat-jacks that would cause the expected strains. To determine if this is the case, the stress was recorded for all of the elements between the two equivalent flat-jacks. For a change in applied pressure of 0.1 MPa, the average change in stress in the elements between the two equivalent

flat-jacks was only 0.0078 MPa. Thus, the change in stress in the masonry is only 7.8% of the pressure applied by the tube-jacks in this modeled double tube-jack test. In the analysis of the single tube-jack test it was also shown that the change in stress due to the change in applied pressure was not equal to 100% and the variation was shown at 2 cm above the mortar joint in Figure 6-26a.

The average change in stress between the equivalent flat-jacks due to the applied pressure versus the strain of the virtual LVDTs is shown in Figure 6-42. These results give an elastic modulus of 1.33 GPa. This is almost exactly the same as the expected result based on the curve developed from the simulated Young's modulus of the regular wall (Figure 6-11).
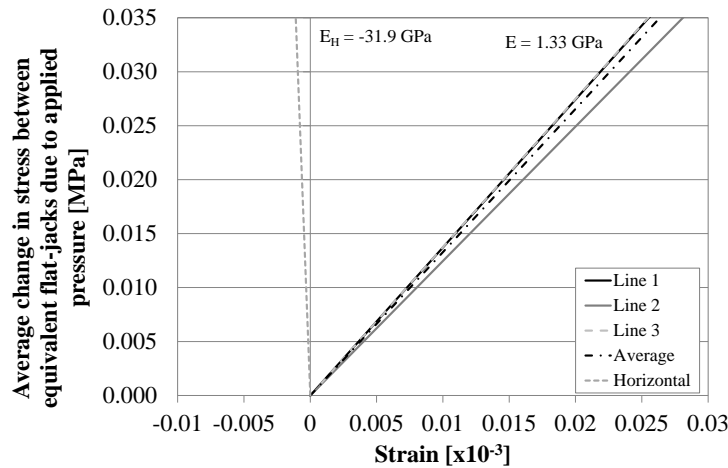
Figure 6-42 Average change in stress between equivalent flat-jacks due to applied pressure versus the strain of the virtual LVDTs in the modeled double tube-jack test

Finally, the Poisson ratio was calculated based on the results presented in Figure 6-41. The result is 0.100. This value is very close to the Poisson ratio found in the Young's modulus test on the regular masonry wallet using the reloading curve. In that test the value was 0.092, an 8.3% difference.

6.2.4.2 Analysis of Displacement, Strain, and Stress

Contours of the vertical displacements are shown in Figure 6-43. Note that the contour plots start at an applied pressure of 0.1 MPa because the reference condition was at zero applied pressure, after the load had been applied and the holes were created. The maximum vertical displacement at an applied pressure of 0.4 MPa was no more than -15 μm.
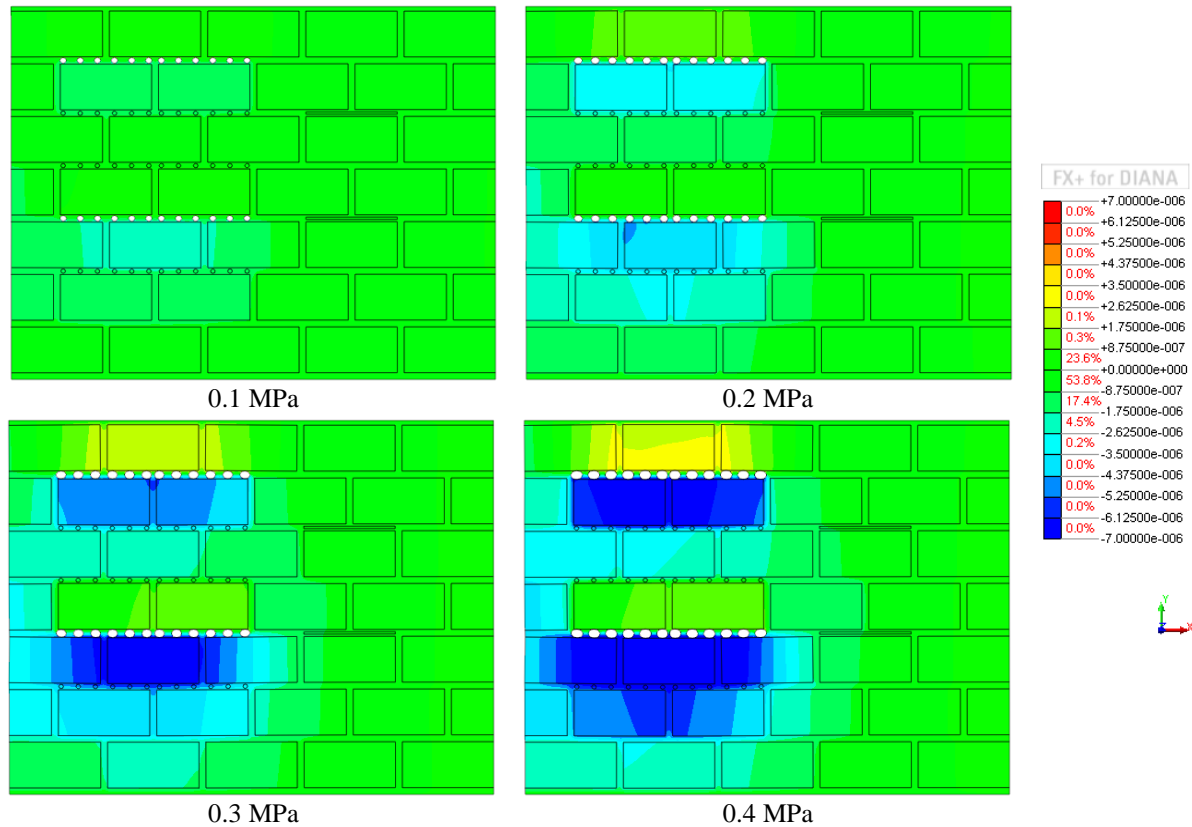
Figure 6-43 Contour plots of the masonry vertical displacements [m] during the double tube-jack test simulation (1000 times amplification factor for deformation)

As pressure is applied to the edges of the holes in each of the equivalent flat-jacks, vertical displacements occur above and below each line of holes. In general, larger displacements occur toward the center of each line of holes. However, due to the slightly larger displacement applied to the left side of the top of the wall and the proximity of the test to the left edge of the wall, larger negative displacements are seen toward the edge of the wall.

In general, positive displacements occur above each line of holes and negative displacements occur below each line of holes. However, the positive displacements above the equivalent flat-jacks are smaller than the negative displacements below. This can be explained by the number of courses of masonry above and below each equivalent flat-jack and the distance to each boundary. For example, below the bottom line of holes there are three courses of masonry, which allow larger displacements in comparison with the one course of masonry above the top line of holes. In these masonry walls, the 0.2 MPa load on the top of the walls was to represent load from additional masonry above the wall so that a taller wall would not need to be constructed. However, these vertical displacement results show that having the equivalent flat-jacks close to the top and bottom of the wall affects the results of the tests.

The vertical stresses in the regular masonry wall during the double tube-jack test are shown in the contours in Figure 6-44. The stress variation due to applying pressure in the holes is small in comparison with the stress variation due to the difference in stiffness between the granite and vertical mortar joints. Thus, the range of stresses represented in the contours has been narrowed to see the differences in stress between the different levels of applied pressure. Values beyond the range shown in the legend are shown as the maximum or minimum colors in the legend. The maximum observed vertical compressive stress in the model for all of these applied pressure levels was not over 0.555 MPa.
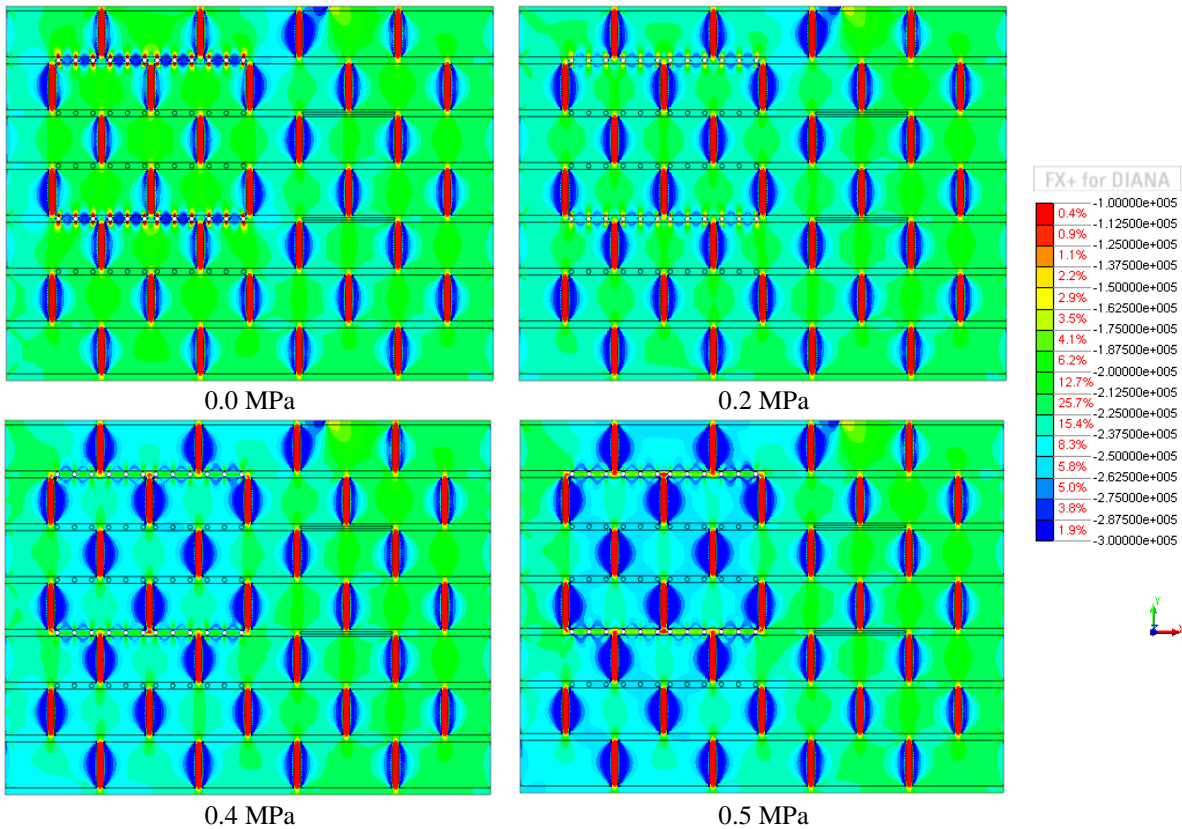
Figure 6-44 Contour plots of the masonry vertical stresses [Pa] during the double tube-jack test simulation

At zero applied pressure, the vertical displacement loading and the absence of elements in the holes creates an area between the two lines of holes where the compressive stress is slightly less than to the right or left of this area. However, only directly above and below each of the holes is the stress completely released due to the holes. The distribution of stresses near the holes is the same as in the single tube-jack test (see Figure 6-23).

At an applied pressure of 0.2 MPa, the same pressure as applied to the top of the wall to determine the prescribed displacement, the stress distribution seems to have returned in general to the distribution occurring before any holes are created. This is the case except for the areas just above and below each line of holes, where the stress distribution is similar to the one seen in the single tube-jack test at an applied pressure level of 0.2 MPa (see Figure 6-23).

Continuing to apply pressure to the edges of the holes to 0.4 MPa and 0.5 MPa increases the areas of higher compressive stress between the two equivalent flat-jacks. However, this is not the only area where compressive stresses are increasing. Compressive stress also increases above the top equivalent flat-jack and below the bottom equivalent flat-jack. Overall, the entire left half of the wall shows higher compressive stresses.

The distribution of the vertical strains, horizontal strains, and horizontal stresses close to the equivalent flat-jack joints are very similar to the distribution seen in the single tube-jack test. Contour plots of the vertical strains during the pressurization of the tube-jacks are presented in Appendix F.6. Above the top equivalent jack and below the bottom equivalent jack during their pressurization, horizontal strains vary from negative to positive in the vertical joints moving away from the equivalent jacks, as shown in Appendix F.7. This distribution indicates that the masonry units are tilting and deflecting away from the equivalent flat-jacks due to the pressure. Finally, the change in horizontal stress distribution between the equivalent flat-jacks during the

pressurization, is almost indistinguishable, as shown in Appendix F.7. Most of the horizontal stress change is localized around the two equivalent flat-jacks.

6.2.5   Double Flat-Jack Test

6.2.5.1   Simulation of the Experimental Test

The double flat-jack test was modeled by deactivating the elements within the two flat-jack slots and then vertically pressurizing the edges of the elements on the top and bottom of both of the slots. The procedure to determine the prescribed displacement on the top of the wall was similar to the one used in modeling the double tube-jack test. The model, with the slot elements deactivated, was loaded with a vertical pressure of 0.2 MPa on the top of the wall and the self-weight of the masonry. The vertical displacement along the top of the wall was recorded and is presented in Figure 6-45a. A linear displacement line is shown connecting the points of least displacement in the figure, indicating the estimated displacement of the steel profile above the wall. This linear displacement line was used as the prescribed displacement on the top of the wall. Refer again to Table 6-2 for the phases of the test.

Comparing the variation of the displacement of the top of the wall due to the double tube-jack holes (see Figure 6-40a) and the double flat-jack slots, the latter creates a much larger variation in displacement. Due to the double flat-jack slots, the estimated displacement of the profile varies by about 0.04 mm as compared to about 0.02 mm for the double tube-jack holes. Thus, creating the flat-jack slots for the double flat-jack test has a greater impact on the masonry above the test area than creating tube-jack holes for a double tube-jack test.
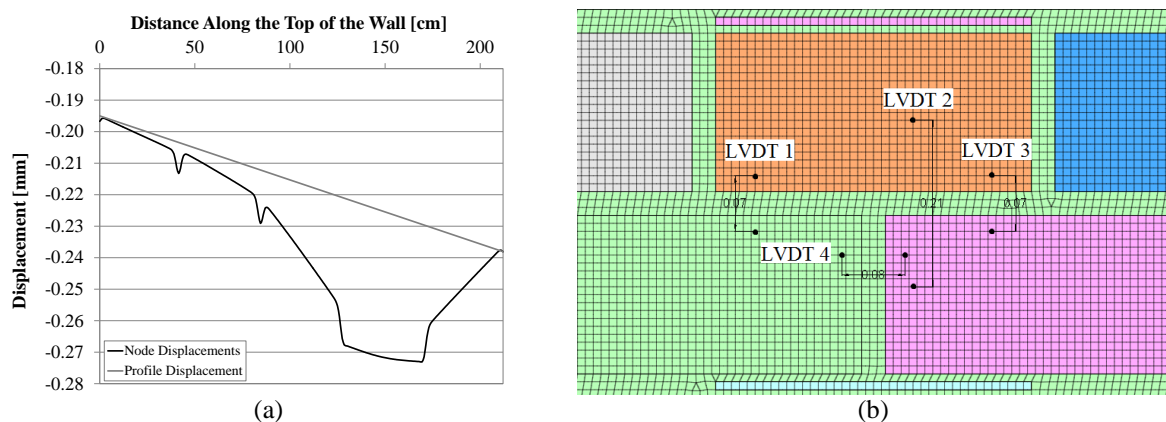
Figure 6-45 Double flat-jack test modeling set-up: (a) displacements at the top of the wall due to the vertical pressure and self-weight and estimated linear profile displacement; and (b) locations of the virtual LVDT connection points (Dimensions in [m])

Three vertical sets of nodes and one horizontal set of nodes were selected to measure the relative displacement of the masonry separated by the two flat-jacks. The point locations and the virtual LVDT line labels are shown in Figure 6-45b.

The relative displacements for the vertical and horizontal virtual LVDTs during the pressurization are shown in Figure 6-46a. Note that LVDTs 1 and 3 have nearly the same relative displacements. The relative displacements are much larger for the double flat-jack test than for the double tube-jack test. At an applied pressure of 0.5 MPa, the average vertical displacement for the modeled double flat-jack test was approximately −41 μm, approximately 4.5 times greater than the average vertical displacement in the modeled double tube-jack test at the same applied pressure, approximately −9 μm.

A comparison can also be made between the relative displacements of the model and the relative displacements in the experimental test (see Figure 5-28). During the final pressurization cycle of the experimental test, the average vertical relative displacement was approximately −175 μm at the maximum applied pressure of approximately 1.29 MPa. Extrapolating the model results to an applied pressure of 1.29 MPa produces an average vertical displacement of approximately −106 μm, about 0.6 times smaller than the experimental results.
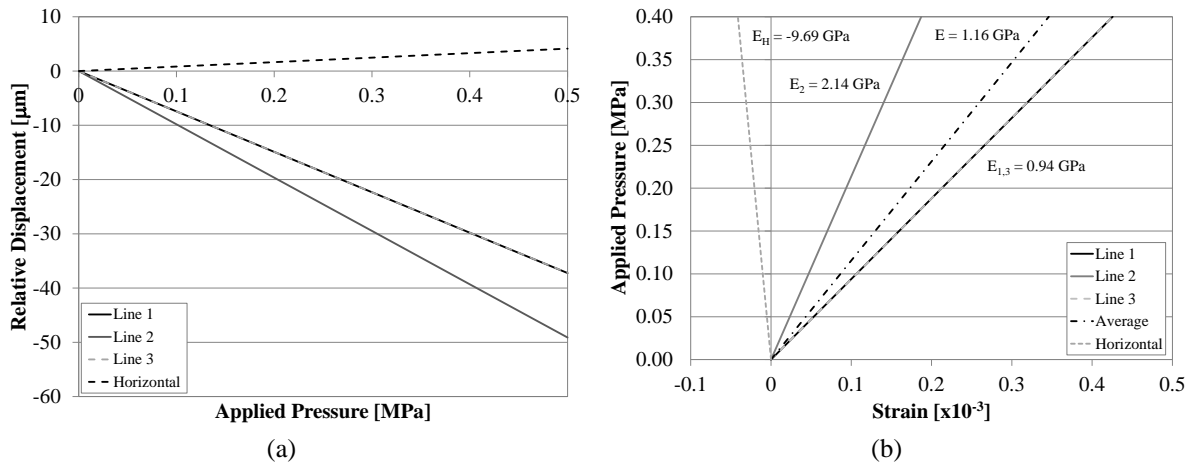
Figure 6-46 Double flat-jack test modeling results: (a) relative vertical and horizontal displacements of the virtual LVDTs; and (b) applied pressure versus strain for the virtual LVDTs

In Figure 6-46b, the applied pressure versus the strain for the virtual LVDTs is shown. The three vertical LVDTs were averaged and a trend line fit to the average to estimate the elastic modulus for the modeled test. The result was an elastic modulus of 1.16 GPa. In the experimental double flat-jack test on the regular wall, the elastic modulus was estimated at 2.0 GPa. The Young's modulus found in the masonry wallet tests for the reloading curve was 2.5 GPa. The average virtual LVDT results underestimate the stiffness of the actual masonry by 60% compared to the experimental test results and by 46% compared to masonry wallet reloading results. However, the double flat-jack test overestimates the elastic modulus by 215% in comparison with the initial loading curve result from the masonry wallet test, 0.368 GPa.

The results from virtual LVDT lines 1 and 3 and from LVDT line 2 can be compared to the results of the modeled Young's modulus test (see section 6.2.1). Virtual LVDT lines 1 and 3 measure over a distance of 7 cm including one joint. Thus, 42.8% of the material between the sets of nodes is mortar. Based on this percentage of mortar, the expected estimation Young's modulus of the masonry based on the curve in Figure 6-11 would be approximately 0.6 GPa. The elastic modulus shown in Figure 6-46b for lines 1 and 3, $E_{1,3}$, is 0.94 GPa, 57% larger than the expected value. For LVDT line 2, 14.3% of the material between the nodes is mortar resulting in an expected Young's modulus of 1.8 GPa for this LVDT based on the curve in Figure 6-11. Instead, the elastic modulus shown in Figure 6-46b for line 2, E_2, is 2.14 GPa, about 19% larger than the expected value. Therefore, the virtual LVDTs in the modeled flat-jack test are over estimating the elastic modulus of the modeled masonry based on the Young's modulus test of the modeled masonry. The reason is the same as in the analysis of the double tube-jack test. The pressure applied by the flat-jacks does not produce the same change in stress in the masonry between the flat-jacks.

The stress was recorded for all of the elements between the two flat-jacks, from the bottom edge of the mortar joint containing the top flat-jack to the top edge of the mortar joint containing the bottom flat-jack. For a change in applied pressure of 0.1 MPa, the average change in stress in

the elements between the two equivalent flat-jacks was only 0.0814 MPa. Thus, the change in stress in the masonry is 81.4% of the pressure applied by the flat-jacks in this modeled double flat-jack test.

The average change in stress between the flat-jacks, due to the applied pressure, versus the strain of the virtual LVDTs is shown in Figure 6-47. These results show an elastic modulus of 1.79 GPa from virtual LVDT 2 and an elastic modulus of 0.79 GPa from virtual LVDTs 1 and 3. The result from LVDT 2 is almost exactly what was expected based on the curve developed for the Young's modulus results of the modeled wall, 1.8 GPa. The result from LVDTs 1 and 3 is closer to the expected result of 0.6 GPa but still is not the same. The difference can be explained by the locations of the virtual LVDT lines. Lines 1 and 3 are at the edges of the separated specimen where the stress change is likely less than at the center of the separated specimen.
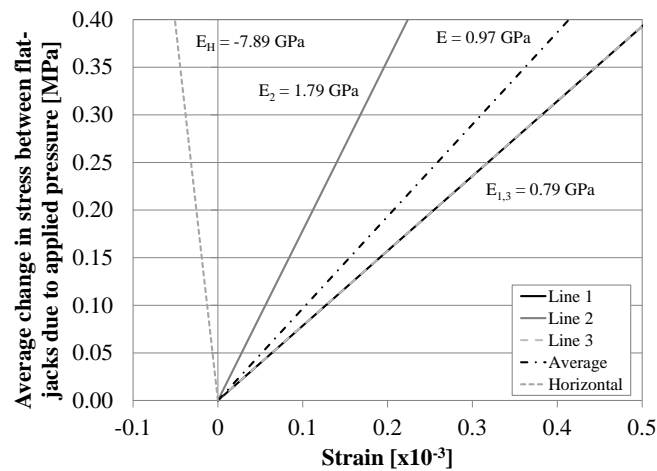
Figure 6-47 Average change in stress between flat-jacks due to applied pressure versus the strain of the virtual LVDTs in the modeled double flat-jack test

The Poisson ratio was calculated to be 0.120 based on the average results of the LVDTs shown in Figure 6-46. This is a 26.4% difference in comparison with the Poisson ratio calculated from the reloading curves of the masonry wallet test, 0.092.

6.2.5.2 Analysis of Displacement, Strain, and Stress

Contours of the vertical displacements are shown in Figure 6-48. Comparing the double tube-jack with the double flat-jack, it is obvious by the scale of the contours and the deformations that the vertical movement caused by the flat-jacks is greater than the vertical movement caused by the line of tube-jacks. For example, the maximum vertical displacement at an applied pressure of 0.4 MPa was -76 μm for the double flat-jack test, over 5 times greater than in the double tube-jack test at the same applied pressure. Several differences in the distributions of the displacements can be noted when comparing the double flat-jack test to the double tube-jack test. Since the length of the double flat-jack test is half the length of the double tube-jack test, less of the masonry is affected by the double flat-jack test. The area affected by the test may not be representative of the masonry as a whole. Most of the displacements are focused directly above and below each flat-jack, only affecting one or two units above and below. The edge of the wall also has less of an impact on the displacement since the test is a full unit away from the edge. More tilting of the units is seen in the deformations of the double flat-jack test because load is applied to only half of the lengths of the units above each flat-jack. Also, relative

to the negative displacements within the wall during the flat-jack test, larger positive displacements are seen above the top flat-jack. These displacements are possible because there are two courses of masonry above the top jack as opposed to only one in the case of the double tube-jack test.
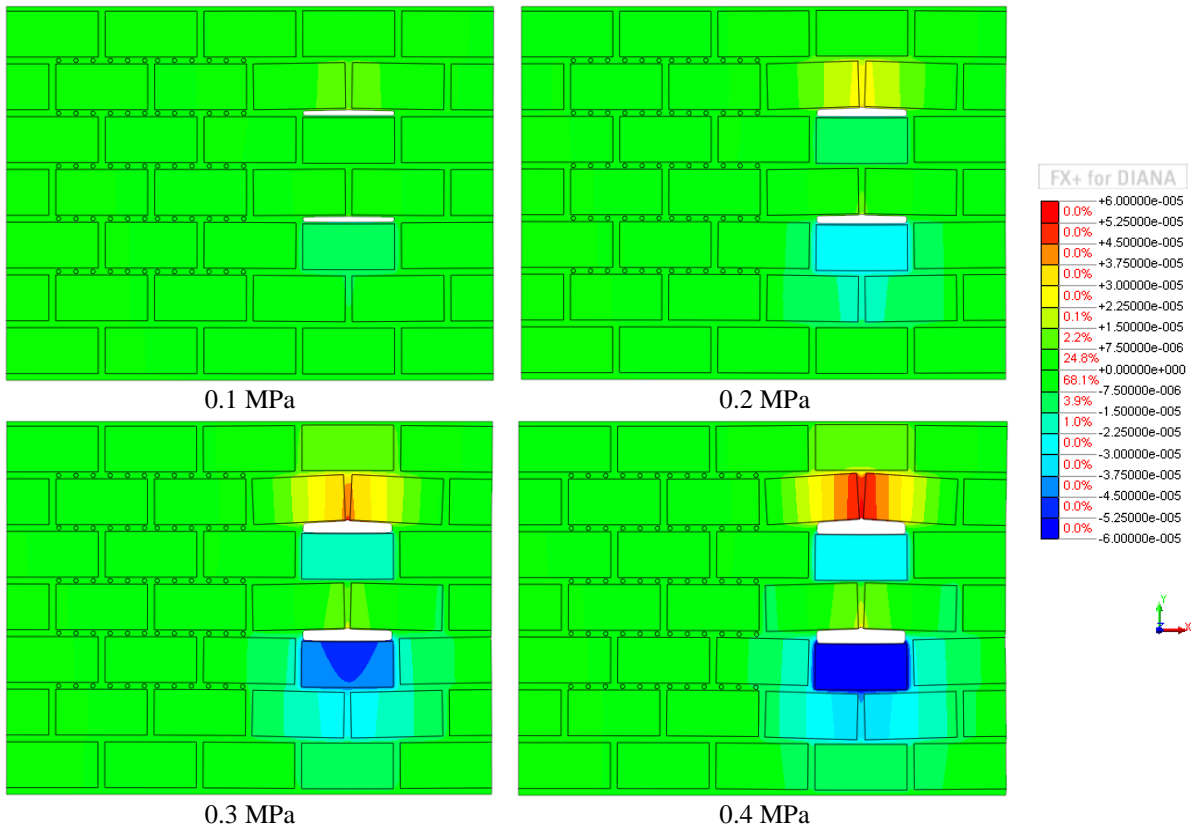
Figure 6-48 Contour plots of the masonry vertical displacements [m] during the double flat-jack test simulation (500 times the actual deformation)

The vertical stresses in the regular masonry wall during the double flat-jack test are shown in the contours in Figure 6-49. The variation in stresses due to the flat-jack slots and applied pressure is much greater than the variation in stresses due to the difference in stiffness between the granite and vertical mortar joints. The larger variation in stresses allows the effects of the flat-jack slots and applied pressure to be seen more clearly in the contour plots than in the case of the double tube-jack test.

At zero applied pressure, the slots create areas above and below each slot where the stress is relieved. However, the stress is not reduced to zero everywhere between the two flat-jack slots. The redistribution of stresses creates higher compressive stresses on either side of each slot and on the sides of the specimen separated by the flat-jacks.

When the applied pressure is 0.2 MPa, equivalent to the pressure applied to the top of the wall to create the prescribed displacement, the stress distribution returns, for the most part, to the distribution seen before any slots were created. The same result was seen at this pressure level for the double tube-jack test.

Continuing to apply pressure to the edges of the slots to 0.4 MPa and 0.5 MPa, results in areas of compressive stress both above and below each flat-jack. The compressive stress in the

masonry between the flat-jacks is not uniform and varies due to the vertical mortar joint. This variation in compressive stress is especially evident in the contour plot at 0.4 MPa.
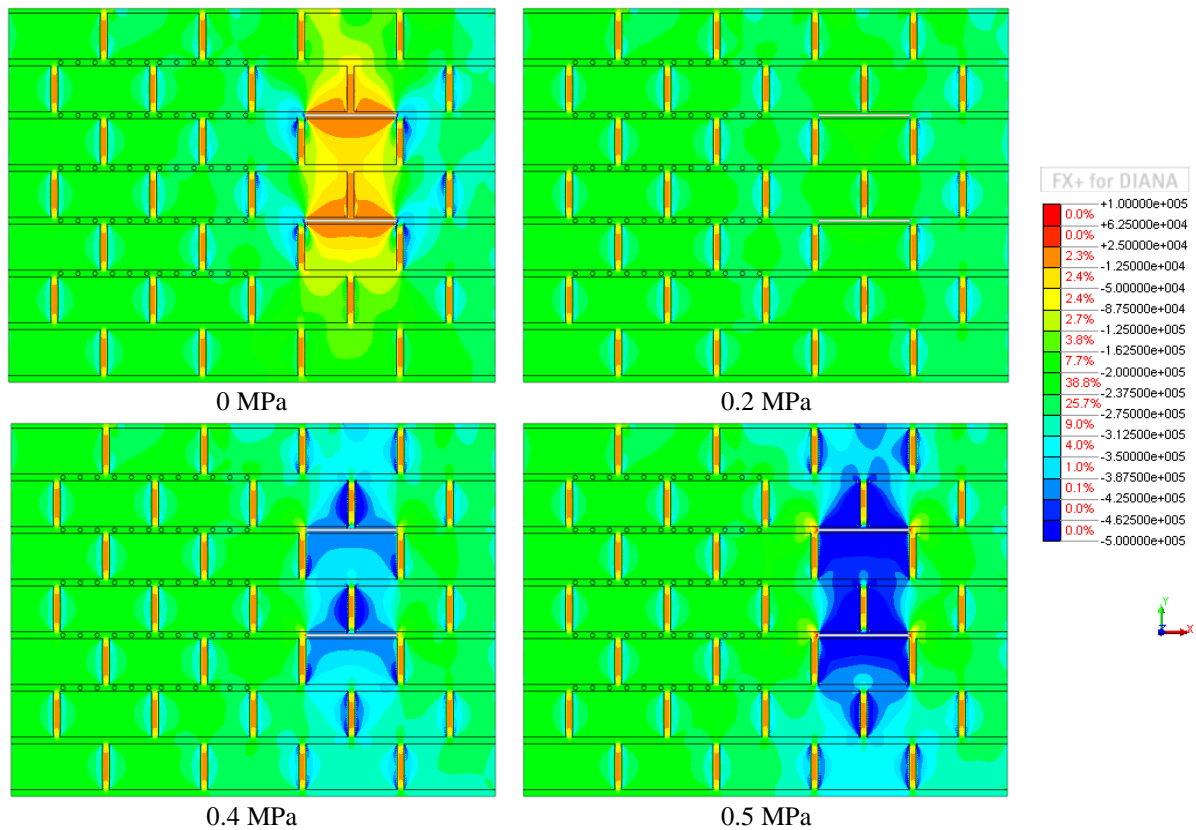
Figure 6-49 Contour plots of the masonry vertical stresses [Pa] during the double flat-jack test simulation

An analysis of the vertical strains, horizontal strains, and horizontal stresses is presented in Appendices F.8 and F.9. The results of these analyses show that the distributions of strains and stresses to be similar to those found in the single flat-jack test. Most of the vertical and horizontal strains occur within the mortar joints, above, below, and between the two jacks. Negative vertical strains result in the joints above and below the flat-jack due to the pressurizations. Positive vertical strains are seen to each side of each of the flat-jacks as they push the mortar joints apart. The tilting of the masonry units due to the pressurization are shown by the variation of horizontal strains in the vertical joints and the horizontal stresses indicating flexure in the units.

6.3   Semi-irregular Masonry Wall model

6.3.1   Young's Modulus Test

Two Young's modulus tests were conducted on the semi-irregular masonry wall model. The first was carried out with the material properties shown in Table 6-1 in section 6.1.2 for the semi-irregular wall mortar. This model was used to compare with the Young's modulus test results from the semi-irregular masonry wallet tests. The second Young's modulus simulation was conducted with the mortar properties from the regular masonry wall mortar in order to see the effects of masonry typology and mortar material properties separately.

In the first test, the load was applied to the top of the wall up to a pressure of 0.2 MPa. The self-weight of the masonry was included. However, the reference condition, or zero point, of the

185

test is when the self-weight of the masonry has already been applied. Thus, the displacements and strains resulting from the self-weight of the masonry were not considered in the Young's modulus test.

Two vertical virtual LVDTs were used to analyze the displacement of the wall during the test, with the nodes chosen as close as possible to the positions suggested by the standards for masonry wallets [64]. The distances between the nodes on the semi-irregular masonry wall are shown in Figure 6-50.

Also shown in Figure 6-50 is a contour plot of the vertical stresses due to the self-weight of the masonry only. A comparable plot was shown for the vertical stresses in the regular masonry wall due to only the self-weight of the masonry. In general, the two contour plots are similar. The compressive stress increases from the top of the wall to the bottom and stresses are low at the vertical mortar joints due to the difference in stiffness between the granite and mortar materials. However, in the semi-irregular wall, the geometry has increased in complexity, increasing the variability of the vertical stress distribution throughout the wall.
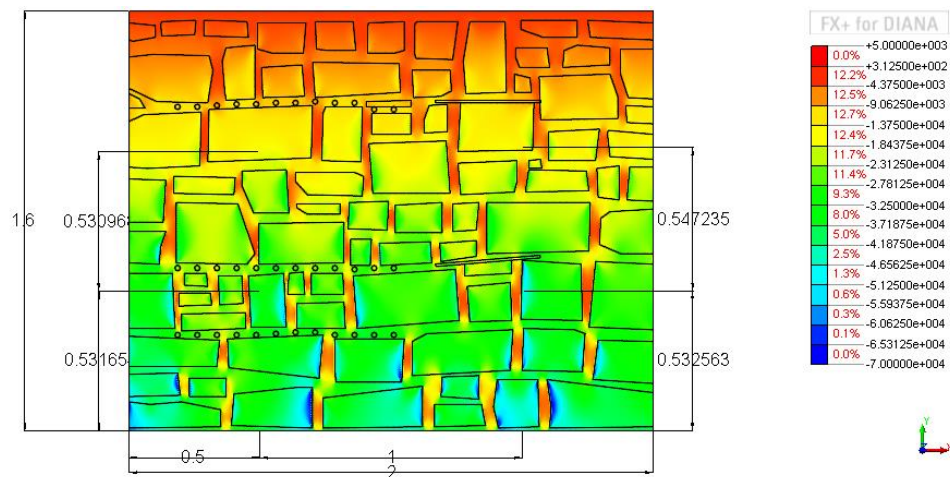
Figure 6-50 Contour plot of the vertical stresses [Pa] in the semi-irregular wall due to the masonry self-weight only and the locations of the virtual LVDTs [m]

The stress versus strain results of the two virtual LVDTs during the Young's modulus test are shown in Figure 6-51. As in the regular masonry wall Young's modulus test simulation, the difference between the two virtual LVDTs is almost indistinguishable. For the semi-irregular wall, the Young's modulus estimation is 3.4314 GPa. This value underestimates the elastic modulus of the masonry when compared to the average reloading elastic modulus for the masonry wallet tests, 5.15 GPa (see section 4.6.3). One explanation for the difference in results between the laboratory tests on the masonry wallets and the simulation of the Young's modulus test on the semi-irregular wall, is the variability in the mortar stiffness and the masonry wallet stiffness. Coefficients of variation for the Young's modulus tests on the mortar and on the masonry wallets were both near 30% (see sections 4.5.2 and 4.6.3). Another explanation for the difference could be the different proportions of mortar and stone that the LVDTs measure over in each test. This effect will be examined further below.
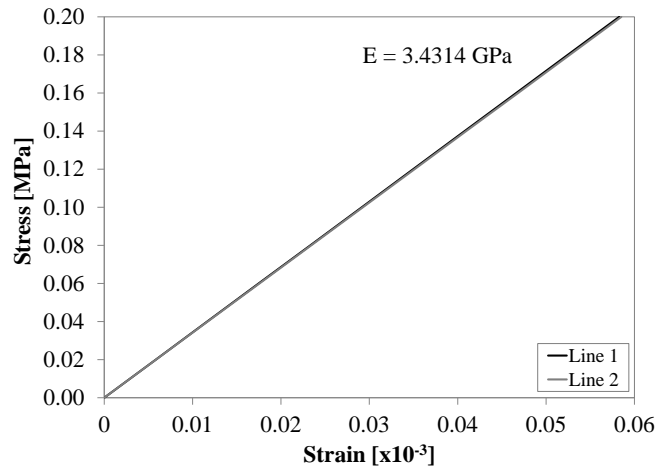
Figure 6-51 Virtual LVDT stress versus strain results for the semi-irregular wall Young's modulus test

Since the material properties for the mortar are different between the regular and the semi-irregular masonry walls, it would be difficult to compare the simulated test results for these two walls. To see the effect of changing the geometry of the wall and the material properties individually, a second Young's modulus test was performed on the semi-irregular wall model using the regular wall mortar material properties. For simplicity, the regular wall mortar is referenced as RM mortar and the semi-irregular wall mortar is referenced as SM mortar. See Table 6-1 for the mortar properties.

Contour plots of the vertical displacement and strain due to an applied pressure of 0.2 MPa on the top of the semi-irregular wall are shown in Figure 6-52 and Figure 6-53. The SM mortar is much stiffer than the RM mortar. Correspondingly, the displacement contours shown in Figure 6-52a are smaller than those in Figure 6-52b and the strain contours shown in Figure 6-53a are smaller than those in Figure 6-53b. The average vertical displacement at the top of the wall when the SM mortar properties are used is approximately −0.085 mm, approximately 28% of the displacement at the top of the wall when the RM mortar properties are used, −0.303 mm. Therefore, using a stiffer mortar results in less deformation if the wall geometry remains unchanged.

When comparing the regular wall with the semi-irregular wall both using the RM mortar properties, the following was obtained. In the semi-irregular wall, the displacements are not uniform across the length of the wall because of the varying stiffness of the wall due to the arrangement and size of the granite units. Comparing the vertical displacements at the top of the walls, the average vertical displacement of the regular masonry was −0.185 mm, about 61% of the average vertical displacement on the top of the semi-irregular wall. In the regular masonry wall, the vertical strains were relatively uniform in the horizontal joints. In contrast, the increased irregularity of the units causes variations in the vertical strains in the mortar joints with concentrations of high compressive strains in certain locations. Thus, the geometry and typology of the masonry does affect the vertical displacement and strain of the wall.

(a)   (b)
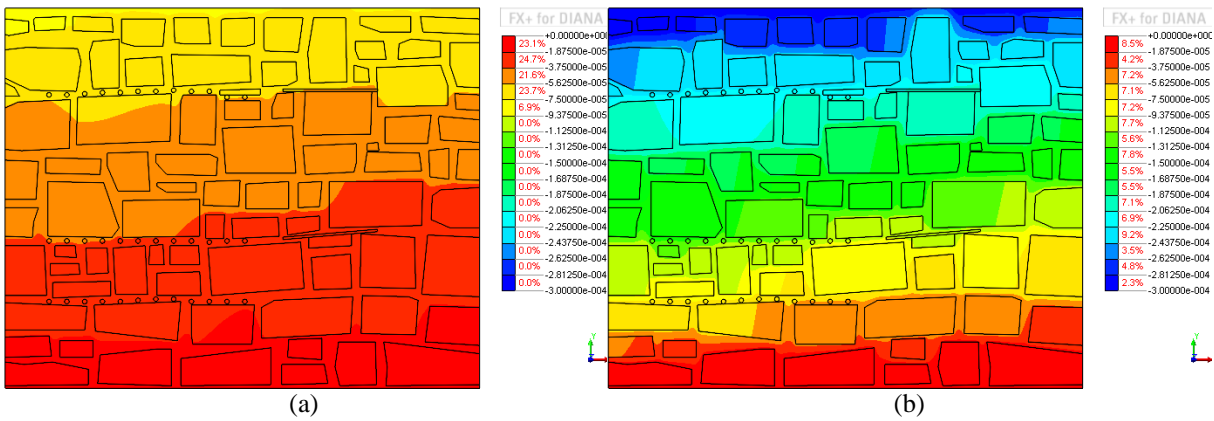
Figure 6-52 Semi-irregular wall loaded to 0.2 MPa on top of the wall: vertical displacement [m] contour plots when; (a) the SM mortar properties are used; and (b) the RM mortar properties are used

(a)   (b)
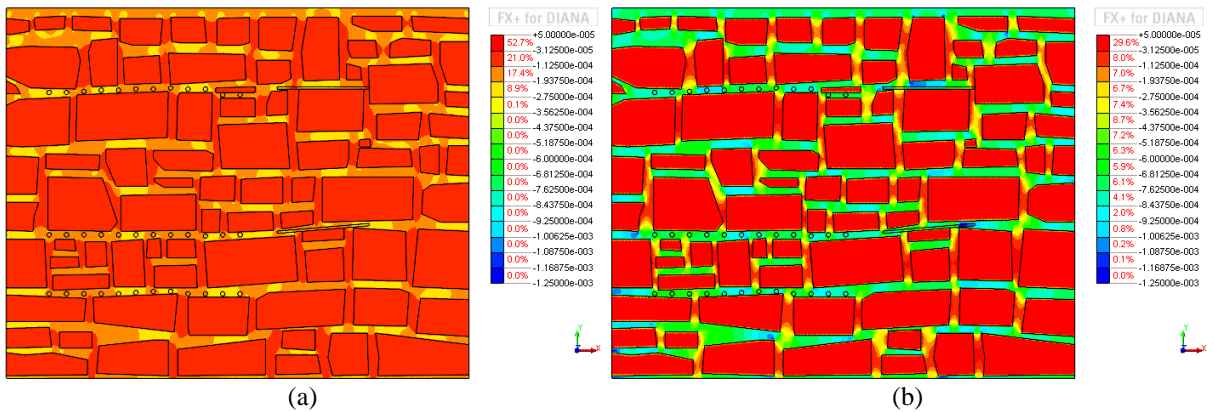
Figure 6-53 Semi-irregular wall loaded to 0.2 MPa on top of the wall: vertical strain contour plots when; (a) the SM mortar properties are used; and (b) the RM mortar properties are used

The stress versus strain results for virtual LVDT line 1 (Line 2 would have the same results as in Figure 6-51) for the Young's modulus test simulations are shown in Figure 6-54 for the three models: the regular wall, the semi-irregular wall with RM mortar, and the semi-irregular wall with SM mortar. Moving from the regular wall to the semi-irregular wall with the RM mortar properties, the stiffness of the wall was reduced due to the increase in mortar joints and the change in typology of the wall. When the mortar properties are changed in the semi-irregular wall from the RM mortar to the SM wall mortar, the increase in stiffness in the mortar properties contributes to the increase in stiffness of the masonry overall.
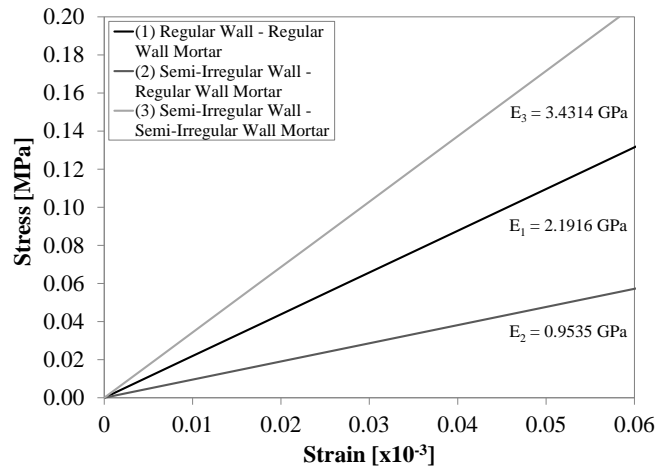
Figure 6-54 Modeled Young's modulus test stress versus strain results for virtual LVDT line 1 for the regular masonry wall, semi-irregular masonry wall with RM mortar, and semi-irregular wall with SM mortar

To determine how the location of the node points contributed to the estimation of the Young's modulus in the simulations, several more virtual LVDTs were analyzed for each test. They were compared based on the percentage of mortar between each set of node points. The percentage of mortar between the nodes defining the first two virtual LVDTs was estimated to be approximately 22.6%. The elastic modulus estimations from this set of virtual LVDTs and several others are presented in Figure 6-55. The power curve trend lines fit to the data and their equations are shown on the graph. The scatter in the data points is larger for the semi-irregular wall models than for the regular wall model because the node points were not on a regular grid in the semi-irregular wall model, as they were in the regular wall model. Thus, the amount of mortar between the nodes for each node set was estimated to the nearest centimeter for the semi-irregular wall.
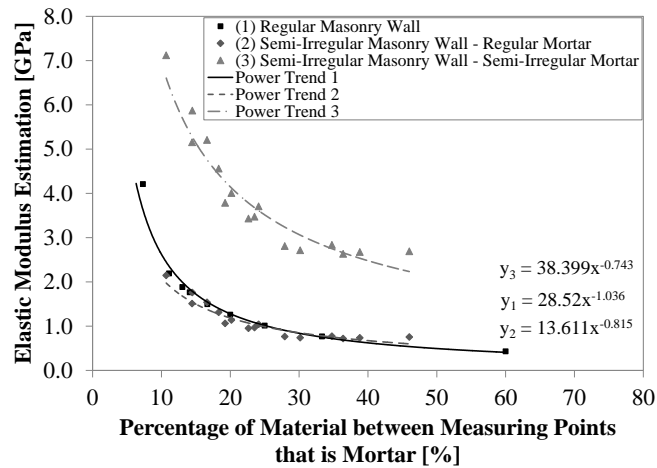
Figure 6-55 Numerical model estimation of elastic modulus for various percentages of mortar between the virtual LVDT nodes for: the regular masonry wall, semi-irregular masonry wall using regular wall mortar properties, and semi-irregular masonry wall using the semi-irregular wall mortar properties

Comparing the results of the semi-irregular model using the regular wall mortar with the model using the semi-irregular wall mortar in Figure 6-55, it seems that changing the stiffness of the mortar changed both the range of stiffness values and the curvature of the trend line. The points shown for both the regular wall and the semi-irregular wall using the regular wall mortar are very close together. Further research including a detailed analysis of how the typology of the

189

masonry and the material properties affect these curves is required to understand them more fully. Although these analyses are out of the scope of this work, it is evident from these findings that the proportion and mechanical characteristics of the mortar play a fundamental role in the stiffness of masonry walls.

6.3.2   Single Tube-Jack Test

The single tube-jack test that was performed in the semi-irregular masonry wall in the laboratory was simulated using the semi-irregular masonry wall model. In this simulation a 0.2 MPa load was applied to the top of the wall along with the self-weight of the masonry. The semi-irregular wall mortar properties were used in this model and in the following tube-jack and flat-jack simulations.

The five virtual LVDTs used in modeling the test were placed as close as possible to the actual locations of the LVDTs on the wall. The locations and distances between the node points are listed in Table G-1. The placement of the virtual LVDT node points in relation to the mortar joints and granite units is shown in Figure 6-56.
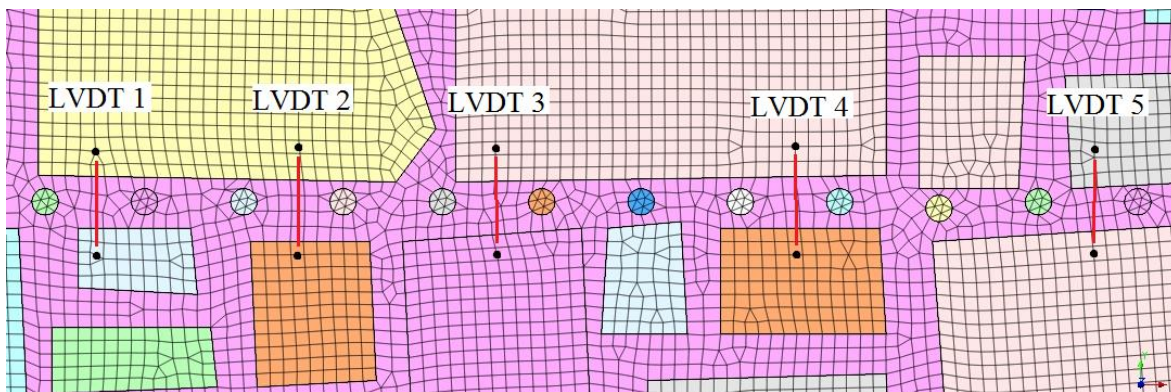
Figure 6-56 Locations for the vertical node sets in modeling the single tube-jack test in the semi-irregular wall

The relative displacements of the virtual LVDTs are shown in Figure 6-57 for various levels of radially applied pressure to the edges of the holes. The relative displacements shown for zero applied pressure are due to the drilling of the holes, i.e., due to the deactivation of the elements within the holes. The average relative displacement due to drilling the holes is −1.76 μm. This relative displacement is much less than the average relative vertical displacement due to drilling the holes in the laboratory test, where it was approximately −20 μm.

(a)

(b)
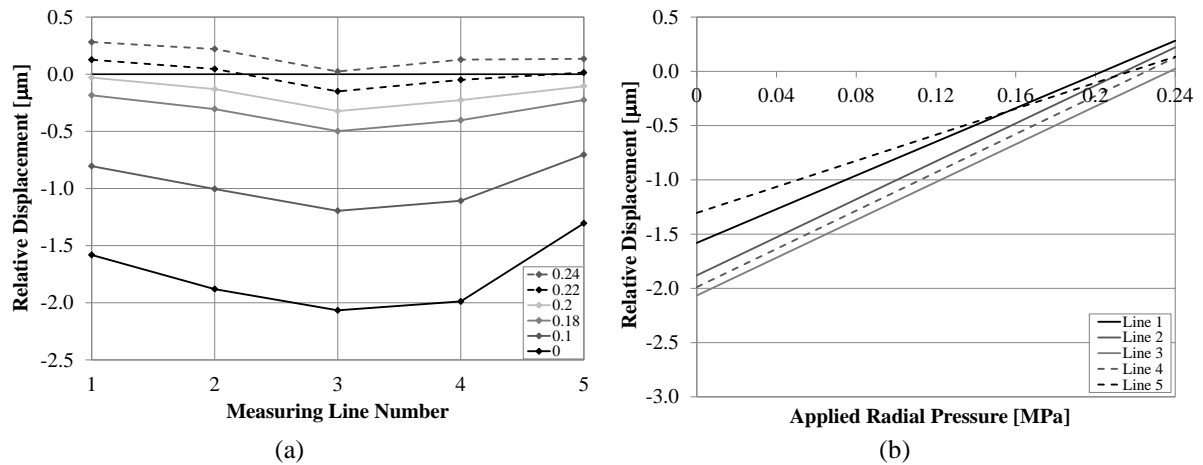
Figure 6-57 Results of the simulation of the single tube-jack test in the semi-irregular wall: (a) relative vertical displacements of the virtual LVDTs at various applied pressure levels; and (b) relative vertical displacements versus the applied radial pressure

Figure 6-57a shows that the line of holes in the semi-irregular wall works as an equivalent flat-jack, with more negative vertical relative displacements toward the center of the equivalent flat-jack than at the ends. The more negative relative vertical displacement due to drilling the holes at the left side of the equivalent flat-jack than at the right side shows that the edge of the wall affected the results in this test, just as it did in the regular wall tests.

Applying pressure to the edges of the holes reduced the relative displacements, restoring them to zero at an applied pressure between 0.2 and 0.24, as shown in Figure 6-57b. The increased irregularity of the masonry has resulted in an increased variability in the restoring pressure. The average restoring pressure for this simulation was 0.2197 MPa, with a coefficient of variation of 5.65%.

To determine how well the virtual LVDTs estimate the state of stress in the semi-irregular wall model, the vertical stress in the elements at the height of the equivalent flat-jack was recorded and averaged after applying the loads to the wall but before deactivating the elements within the holes. The stress level at the height of the test was on average 0.2243 MPa. Thus, the virtual LVDTs estimated the stress level in the wall with an error of only 2.08%. This error is only slightly larger than the errors seen in estimating the stress level using the virtual LVDTs in the regular masonry wall single tube-jack tests. Thus, the virtual LVDTs produce results with good accuracy, even though they can only provide discrete measurements along the length of the equivalent flat-jack.

The results of the single tube-jack test in the idealized semi-irregular wall model show that the test is not only possible but also very accurate. However, in the laboratory test, the tube-jacks were not able to restore the vertical displacements caused by drilling the holes, even at an applied pressure of 0.6 MPa, much higher than the estimated stress level. Additional study is required to determine what other aspects of the test are causing the disparity between the idealized results and the actual laboratory results.

6.3.3   Single Flat-Jack Test

In the setup for the single flat-jack test in the semi-irregular wall model, the loading was kept the same as for the single tube-jack test in the semi-irregular wall. The distances between the node points for the virtual LVDTs and their locations in relation to the bottom left corner of the

wall are shown in Table G-2. In Figure 6-58 the node point sets are labeled and shown in relation to the flat-jack slot on the semi-irregular wall mesh.
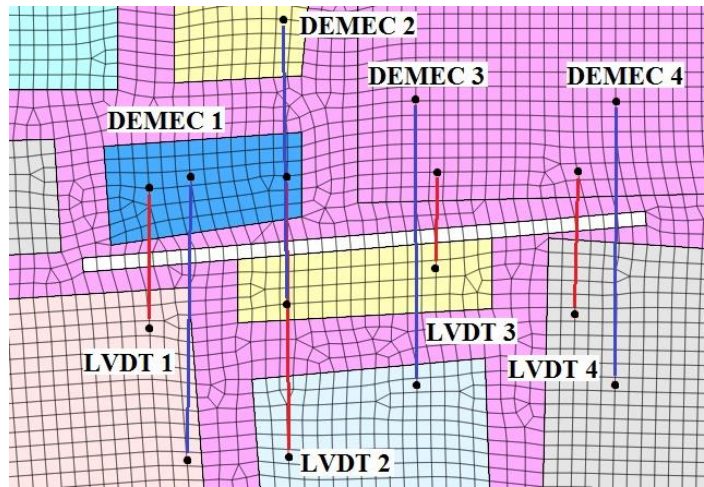
Figure 6-58 Locations for the vertical node sets in modeling the single flat-jack test in the semi-irregular wall

The relative displacements of the virtual LVDTs are shown in Figure 6-59 for various applied pressure values. The average virtual LVDT relative displacement due to opening the slot (deactivating the slot elements) was −30.7 μm, over 17 times greater than for the modeled single tube-jack test in the semi-irregular wall. In the regular wall simulations, the relative displacement due to opening the slot in the single flat-jack test was about ten times greater than the relative displacement due to opening the holes in the single tube-jack test. Thus, the increase in stiffness of the mortar has impacted the displacements due to drilling the holes more than the displacements due to sawing the slot.
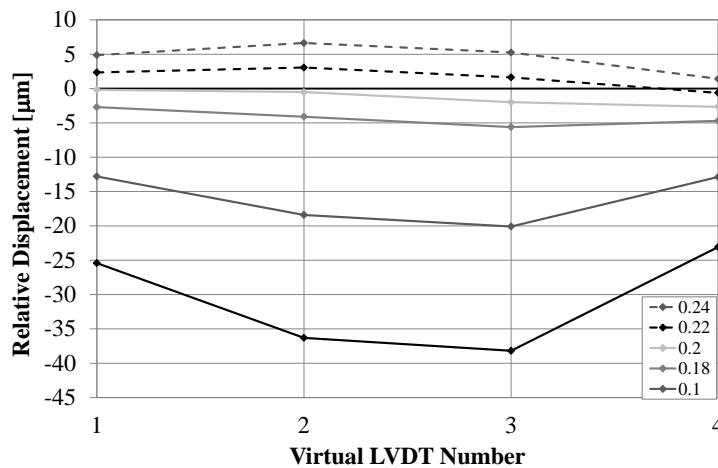
Figure 6-59 Relative vertical displacements for each measuring line at several increments of pressure applied in a normal direction to the upper and lower edges of the slot (pressure values in MPa)

The relative displacement versus the applied pressure graph in Figure 6-60a shows that the relative displacements were restored to zero between 0.2 MPa and 0.22 MPa. The average restoring pressure for the four virtual LVDTs estimates the state of stress to be 0.2104 MPa with a coefficient of variation of 5.39%. In the simulated single flat-jack test on the regular wall the coefficient of variation was only 0.11%. There are a couple of possible reasons for the increased variability; the increase in irregularity of the masonry, both in terms of geometry and mortar characteristics and the angle of the flat-jack slot and angle of the applied pressure.

192

Comparing the estimate of the state of stress to the average stress in the flat-jack slot elements prior to deactivating them, 0.2190 MPa, results in an error of 3.93% for the estimate given by the virtual LVDTs. In the simulated flat-jack test in the regular masonry wall, the error in the estimate given by the virtual LVDTs was only 0.22%.
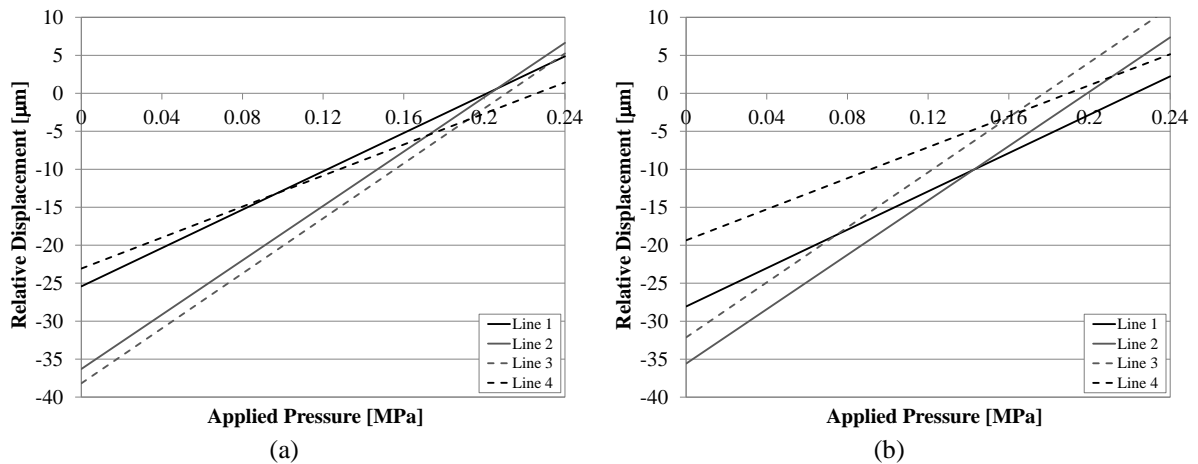
Figure 6-60 Relative vertical displacements of the virtual LVDTs versus applied pressure: (a) with LVDT initial relative displacements; and (b) with average DEMEC relative displacement as the initial displacement

The results of only the virtual LVDTs cannot be compared to the results of the laboratory test because the LVDTs in the laboratory test could not be in place during the sawing of the slot. Thus, to replicate the procedure used in the laboratory test, the relative displacements of the four DEMEC point sets due to deactivating the elements in the slot were used as the initial relative displacements of the four LVDTs, respectively. The revised results of the virtual LVDTs are shown in Figure 6-60b. The average relative displacement of the DEMEC point sets due to opening the slot was −29 μm. The average relative displacement due to cutting the slot in the laboratory test was −94 μm (see Table 5-1), over three times greater than in the model.

Using the DEMEC point relative displacements as the initial virtual LVDT relative displacements results in an even larger variation in restoring pressures. The average restoring pressure determined from Figure 6-60b is 0.1970 MPa with a coefficient of variation of 9.62%. This estimation of the state of stress in the semi-irregular wall model has an error of 10.04%. The laboratory test resulted in an estimated state of stress of 0.36 MPa, a 64% error in comparison to the average stress in the slot in the model wall before opening the slot.

6.3.4 Double Tube-Jack Test

In the simulation of the double tube-jack test in the semi-irregular masonry wall model, a prescribed displacement was applied to the top of the wall. To determine the prescribed load, the semi-irregular wall model, with the elements in the two lines of holes deactivated, was analyzed with both the pressure applied to the top of the wall and the self-weight of the masonry. The absolute vertical displacements of the nodes at the top of the wall were graphed and are shown in Figure 6-61a. The vertical displacements on top of the semi-irregular wall are more irregular than the ones on the top of the regular wall, shown in Figure 6-40. While the deactivation of the hole elements has caused greater vertical displacements on the left side of the wall, there is no distinct area along the top of the wall with greater vertical displacements, as there was on the top of the regular masonry wall. A linear trend line was fit to the data to represent the displacement of the steel profile on top of the wall. This trend line was used as the prescribed displacement at the top of the wall for the double tube-jack test simulation.
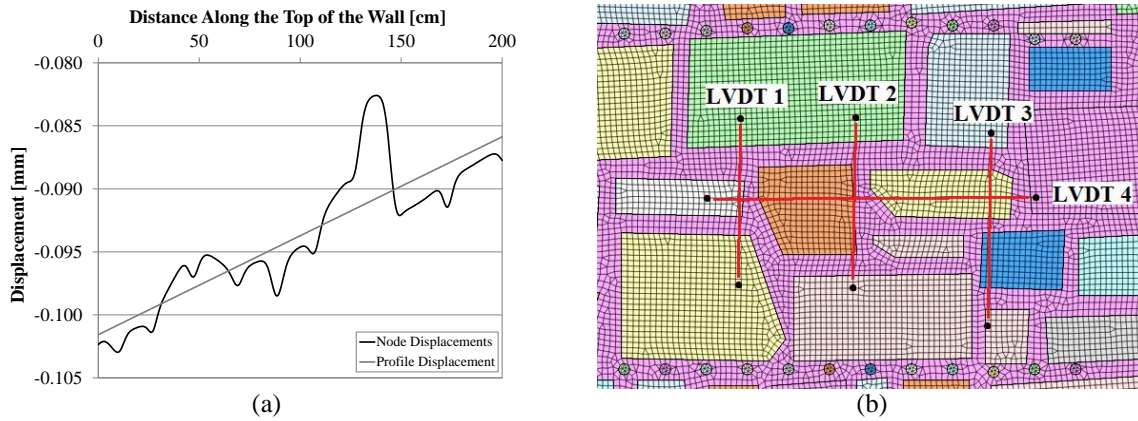
Figure 6-61 Double tube-jack test modeling set-up: (a) displacements at the top of the wall due to the vertical pressure and self-weight and estimated linear profile displacement; and (b) locations of the virtual LVDT nodes

The nodes used for the virtual LVDTs in the double tube-jack test simulation are shown in Figure 6-61b. The distances between the nodes and to the bottom left corner of the semi-irregular masonry wall model are displayed in Table G-3 and Table G-4.

The relative displacements for the vertical and horizontal virtual LVDTs during the pressurization of the edges of both lines of tube-jack holes are shown in Figure 6-62a. A comparison can be made between the relative displacements of the model and the relative displacements on the back of the laboratory test wall (see section 5.3.3). During the fifth pressurization cycle of the experimental test, the average vertical relative displacement on the back of the wall was approximately −1 μm at the maximum applied pressure of approximately 0.3 MPa. In the model at an applied pressure of 0.3 MPa, the average vertical displacement is approximately −1.38 μm. Thus, the model fairly accurately represents the movements of the back of the wall in the laboratory test.
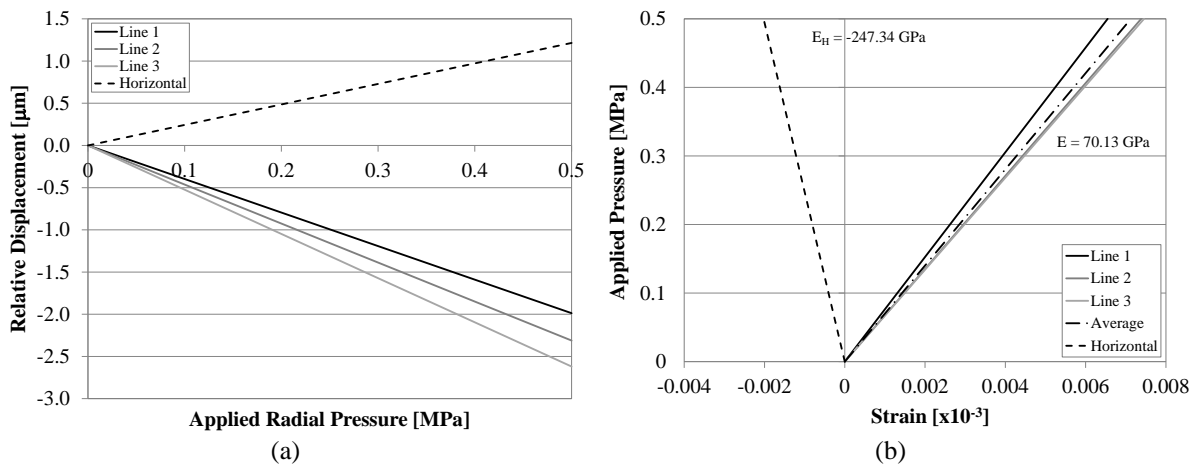
Figure 6-62 Double tube-jack test modeling results: (a) relative vertical and horizontal displacements of the virtual LVDTs; and (b) applied pressure versus strain for the virtual LVDTs

Figure 6-62b shows the applied pressure versus the strain for the virtual LVDTs. The three vertical LVDTs were averaged and a trend line fit to the average to estimate the elastic modulus for the modeled test. The result was an elastic modulus of 70.13 GPa. In the experimental double tube-jack test the elastic modulus was estimated at 139.86 GPa using the LVDTs only on the back of the wall. Neither the model nor the double tube-jack laboratory test comes close to the values found in the Young's modulus tests on the semi-irregular masonry wallets. The average reloading elastic modulus for the wallet tests was 5.15 GPa (see Table 4-1)

These results can also be compared to the modeled Young's modulus test results presented in section 6.3.1. The virtual vertical LVDTs measured over an average distance of 32.3 cm, of which, 9 cm on average was mortar. Thus, 29% of the material between the nodes was mortar. Based on the curve in Figure 6-55 for the semi-irregular wall with the SM mortar, the expected elastic modulus result from the virtual LVDTs would be approximately 3.15 GPa, if the pressurization of the tube-jacks resulted in a change in stress between the equivalent flat-jacks equal to the applied pressure. Since the estimated elastic modulus shown in Figure 6-62b is much larger than the expected value based on modeling the Young's modulus test, the change in stress level between the two equivalent flat-jacks must be much less than the pressure being applied by the tube-jacks. The same result was seen in the double tube-jack test in the regular masonry wall.

The stresses of all of the elements between the two equivalent flat-jacks were recorded for two applied pressure levels. For a change in applied pressure of 0.1 MPa, the average change in stress was only 0.0043 MPa. Thus, the change in stress in the masonry is only 4.3% of the pressure applied by the tube-jacks. In the double tube-jack test in the regular masonry wall, the change in stress was approximately 7.8% of the pressure applied by the tube-jacks. This means that the tube-jacks were less effective in changing the stress level between the two equivalent flat-jacks in the semi-irregular wall than they were in the regular wall. One reason for this could be the positioning of the tube-jacks in relation to the vertical mortar joints. Since there were more vertical joints in the semi-irregular wall and the distance between tube-jacks was maintained, some of the tube-jacks were positioned over or under vertical joints. This is one aspect of the test that requires further study in order to make any conclusions.

The average change in stress between the equivalent flat-jacks, due to the applied pressure, versus the strain of the virtual LVDTs is plotted in Figure 6-63. These results give an elastic modulus of 3.01 GPa. This result is close to the estimation given by the curve produced in the Young's modulus test of semi-irregular wall model in Figure 6-55.
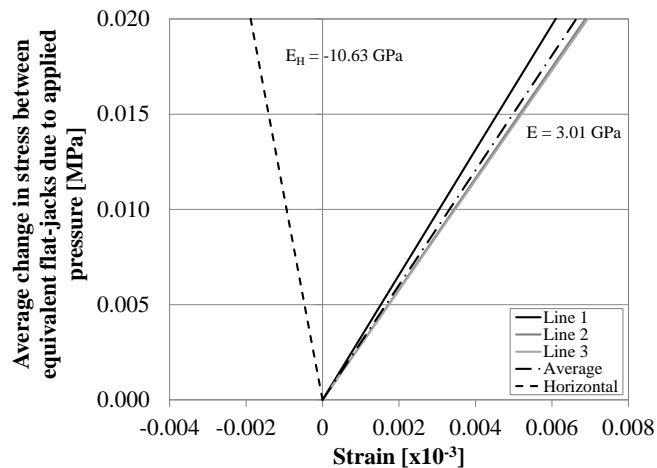
Figure 6-63 Average change in stress between equivalent flat-jacks due to applied pressure versus the strain of the virtual LVDTs in the modeled double tube-jack test

The Poisson ratio was calculated using the average results of the virtual LVDTs presented in Figure 6-62b. The result was a Poisson ratio of 0.284, a 62.3% difference from the Poisson ratio results from the masonry wallet tests, 0.541, see Table 4-3. However, the wallet tests results had a very high variation, 57.2%.

6.3.5   Double Flat-Jack Test

The double flat-jack test was also modeled by applying a prescribed displacement to the nodes at the top of the semi-irregular wall. The vertical displacement along the top of the wall, for the model with the slot elements deactivated and the self-weight and pressure loads applied, is presented in Figure 6-64a. The line for the estimated position of the bottom of the steel profile was placed at the height of the two ends of the wall and disregarded the dip due to the creation of the slots. The estimated profile displacement was used as the prescribed displacement in modeling the double flat-jack test. Since the profile displacement is level, the proximity to the edge of the wall seems to have affected this test less than in the regular masonry wall test.
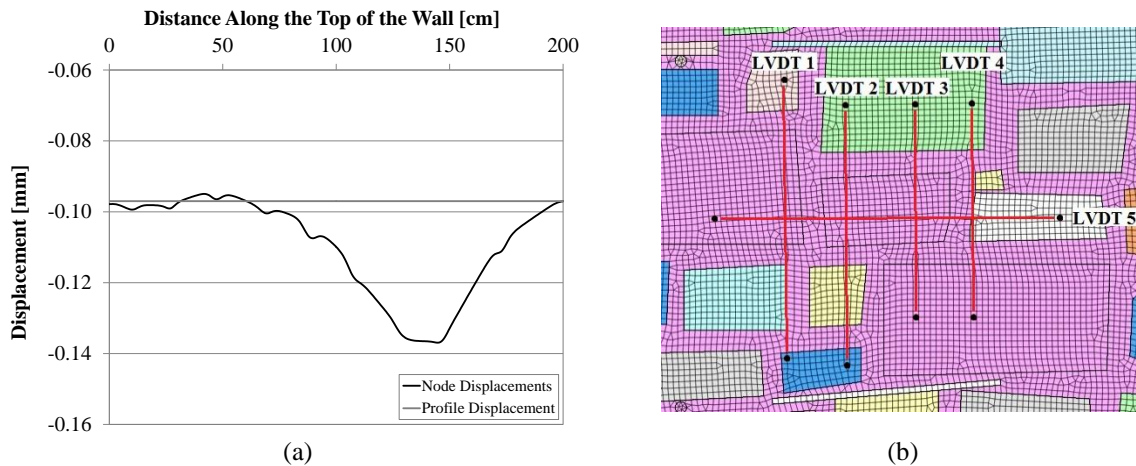
Figure 6-64 Double flat-jack test modeling set-up: (a) displacements at the top of the wall due to the vertical pressure and self-weight and estimated linear profile displacement; and (b) locations of the virtual LVDT nodes

The locations of the virtual LVDT nodes and their labels are shown in Figure 6-64b. The distances between the points in each set and from the bottom left corner of the semi-irregular model wall are shown in Table G-5 and Table G-6.

The relative displacements of the vertical and horizontal virtual LVDTs during the pressurization are shown in Figure 6-65a. Again, a comparison is made between the relative displacements of the model and the relative displacements in the experimental test (see section 5.3.4). During the final pressurization cycle of the experimental test, the average vertical relative displacement reached a maximum value of −1.2 mm at the maximum applied pressure of nearly 1.2 MPa. If the model results are extrapolated to an applied pressure of 1.2 MPa, the average vertical displacement is approximately −0.088 mm, over 13 times smaller than the experimental results.

196
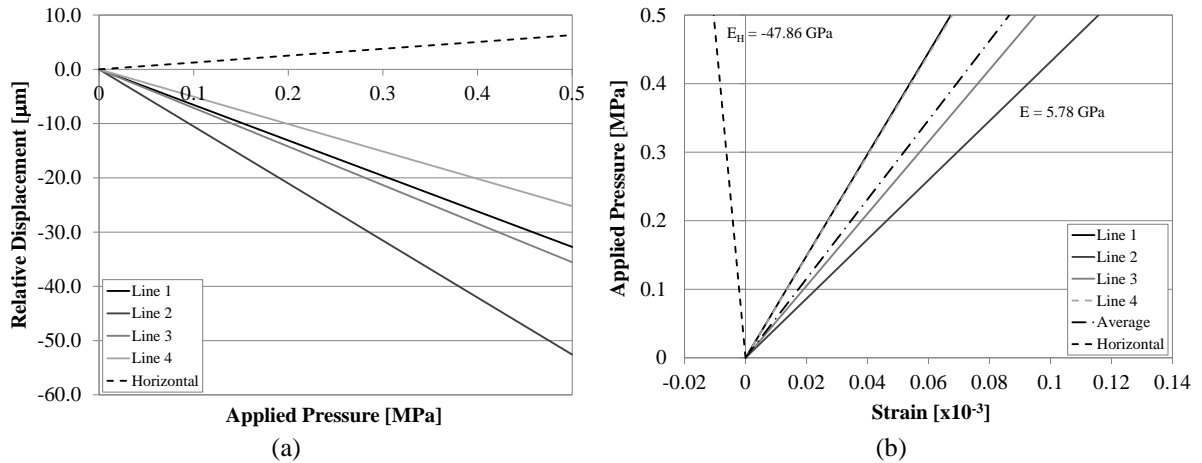
Figure 6-65 Double flat-jack test modeling results: (a) relative vertical and horizontal displacements of the virtual LVDTs; and (b) applied pressure versus strain for the virtual LVDTs

In Figure 6-65b, the applied pressure versus the strain for the virtual LVDTs is shown. The estimate shown for the elastic modulus is the slope of the trend line fit to the average of the vertical virtual LVDTs. The result was an elastic modulus of 5.78 GPa. In the experimental double flat-jack test on the semi-irregular wall, the elastic modulus was estimated at 8.57 GPa for the reloading modulus considering the LVDT results on both sides of the wall. The Young's modulus found in the semi-irregular masonry wallet tests was 5.15 GPa. The model results come closer to the value found in the wallet tests than to the result of the double flat-jack test in the laboratory.

The results of the modeled double flat-jack test in the semi-irregular wall can also be compared to the expected results based on modeling the Young's modulus test in the semi-irregular wall. The vertical virtual LVDTs measured over an average distance of 0.42 m with an average of 9.5 cm of mortar between the nodes of each virtual LVDT. Thus, on average, 22.5% of the material between each node set was mortar. Based on this mortar ratio and the Young's modulus test curve for the semi-irregular wall with the semi-irregular mortar (Figure 6-55), the expected elastic modulus result would be 3.79 GPa. Therefore, even though the modeled double flat-jack test results are close to the results of the wallet tests, the results are not the expected results for the modeled masonry. The pressure applied by the flat-jacks is not producing the same change in stress in the masonry between the flat-jacks, resulting in an overestimate of the elastic modulus.

The stress was recorded for all of the elements between the two flat-jacks. For a change in applied pressure of 0.1 MPa, the average change in stress in the elements between the two flat-jacks was 0.0762 MPa. Thus, the change in stress in the masonry is 76.2% of the pressure applied by the flat-jacks in the modeled double flat-jack test in the semi-irregular wall.

The average change in stress between the equivalent flat-jacks, due to the applied pressure, versus the strain of the virtual LVDTs is plotted in Figure 6-66. These results give an elastic modulus of 4.4 GPa. This result comes closer to the estimation given by the curve produced in the Young's modulus test of semi-irregular wall model (see Figure 6-55). However, this value is not as close as it was in the simulated double flat-jack test on the regular masonry wall. The increased irregularity is likely causing the difference.
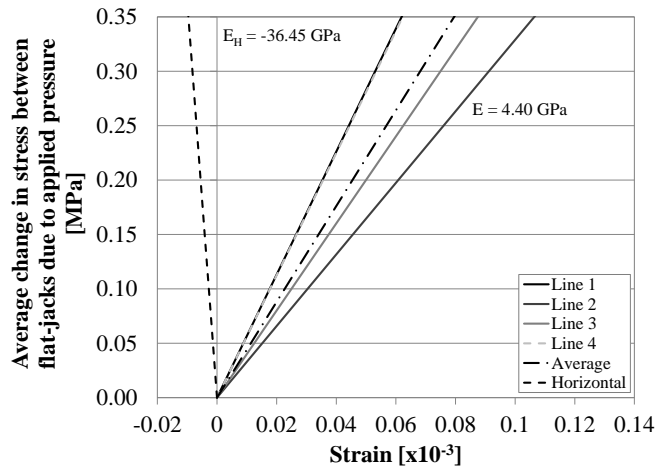
Figure 6-66 Average change in stress between flat-jacks due to applied pressure versus the strain of the virtual LVDTs in the modeled double flat-jack test

The Poisson ratio estimation for the semi-irregular masonry, based on the double flat-jack test results in Figure 6-65, is 0.121. There is a 127% difference between this estimation and the calculated Poisson ratio from the Young's modulus test reloading curves for the semi-irregular masonry wallets, 0.541, see Table 4-3. Comparing the estimations from the double tube-jack test, 0.284, and the double flat-jack test, the double tube-jack test was closer to the wallet test results.

6.4   Irregular Masonry Wall Model

6.4.1   Young's Modulus Test

One Young's modulus test simulation was performed on the irregular wall model. The set-up for the test was the same as for the regular masonry wall and semi-irregular masonry wall. The irregular masonry wall mortar properties were used for this test and the rest of the modeled tests in the irregular wall, see Table 6-1 in section 6.1.2. The self-weight of the masonry and the 0.2 MPa load on the top of the wall were applied. However, as in the previous tests, the displacements and strains resulting from the self-weight of the masonry were not considered in the Young's modulus test. Two vertical virtual LVDTs were used to analyze the displacement of the wall during the test. The distances between the node points on the irregular masonry wall are shown in Figure 6-67.

Figure 6-67 also shows a contour plot of the vertical stresses due to the self-weight of the masonry only. A comparable plot was shown in Figure 6-7 and Figure 6-50 for the vertical stresses in the regular and semi-irregular masonry walls due to only the self-weight of the masonry. In general, all three plots are similar: the compressive stress increases from the top of the wall to the bottom and stresses are lower in vertical mortar joints due to the difference in stiffness between the granite and mortar materials. In the irregular wall, the irregularity in the size and shapes of the granite units has contributed to the variation in the stresses throughout the wall. In some areas, sharp points in the units seem to be causing high stress concentrations. This is especially noticeable toward the bottom of the wall.
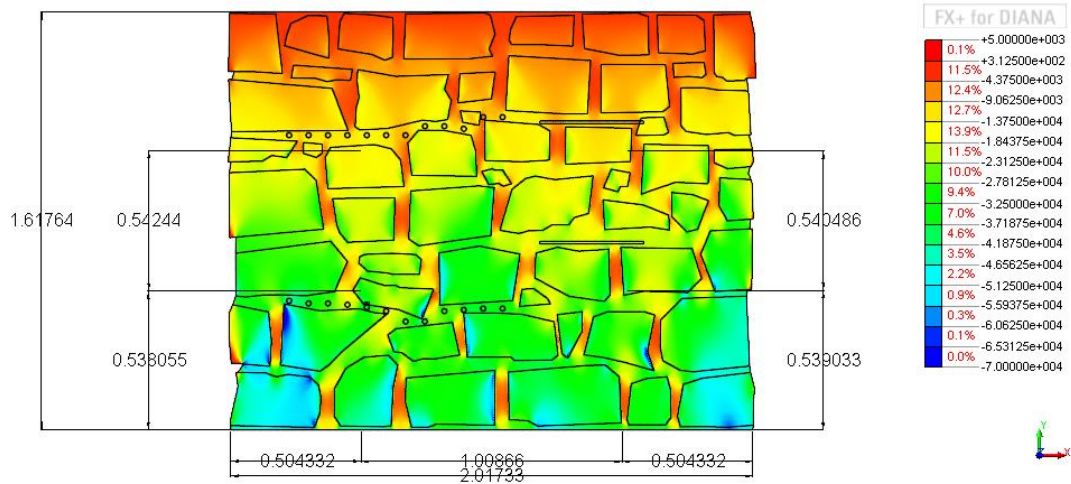
Figure 6-67 Contour plot of the vertical stresses [Pa] in the irregular wall due to the masonry self-weight only and the locations of the virtual LVDTs [m]

The stress versus strain results of the two virtual LVDTs are shown in Figure 6-68. In contrast with the results from the regular and semi-irregular walls, the results of the two virtual LVDTs in the irregular wall do not have the same slope. For the irregular wall, the Young's modulus estimation is 3.65 GPa based on the average of the two virtual LVDTs. This value is within the first standard deviation of the average reloading elastic modulus for the masonry wallet tests, 3.375 GPa (see section 4.6.3). Thus, this model seems to represent the masonry in the laboratory more closely than the semi-irregular wall model did.
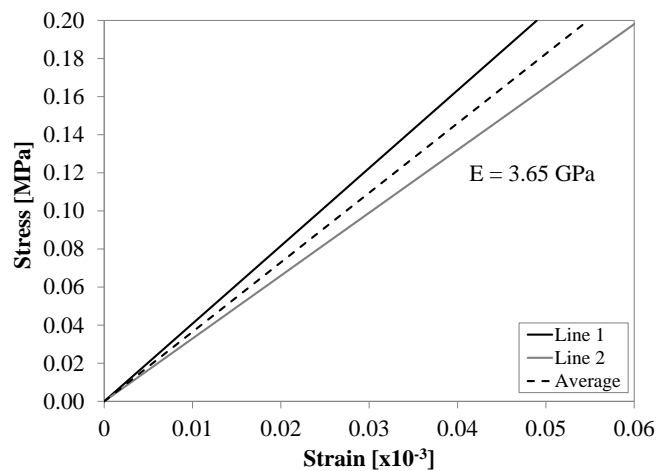
Figure 6-68 Virtual LVDT stress versus strain results for the Young's modulus test on the regular wall model

The semi-irregular and irregular wall models both used the same granite and mortar properties. Thus, the vertical displacement and strain for the two walls can be compared with only one variable changing between the two models, the geometry. The contour plots for the vertical displacement are shown in Figure 6-69 and the contour plots for the vertical strain are shown in Figure 6-70. Note that the scales are different from those presented in Figure 6-52 and Figure 6-53. In general the semi-irregular wall contours are very similar to the irregular wall contours. Both, the displacement and the strain, are in the same ranges for the walls. The irregular wall shows slightly more irregularity in the displacement contour bands than the semi-irregular wall. Also, there are some larger concentrations of negative vertical strain in the

irregular wall. These concentrations are close to the stress concentration areas identified in the stress contour plot in Figure 6-67.

(a)   (b)
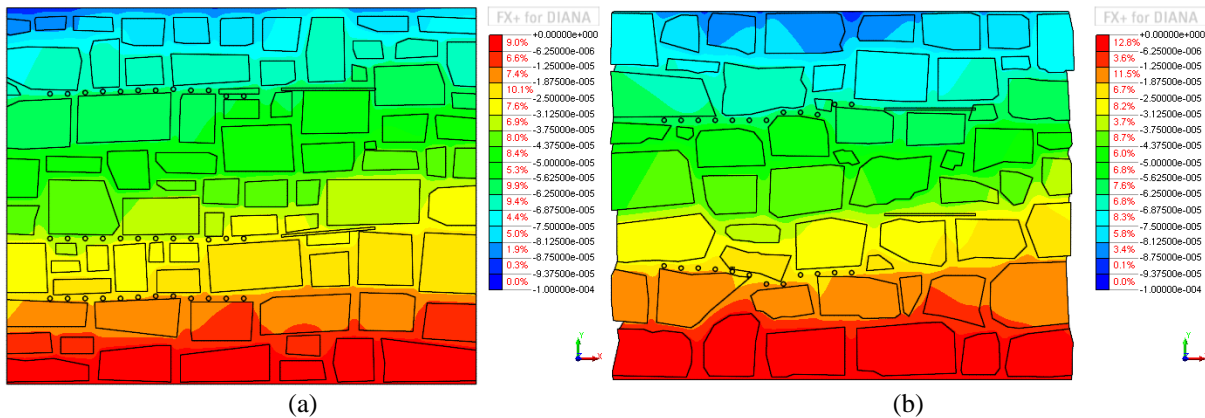
Figure 6-69 Vertical displacement [m] contour plots of the FE wall models loaded to 0.2 MPa on top of the wall: (a) semi-irregular wall; and (b) irregular wall

(a)   (b)
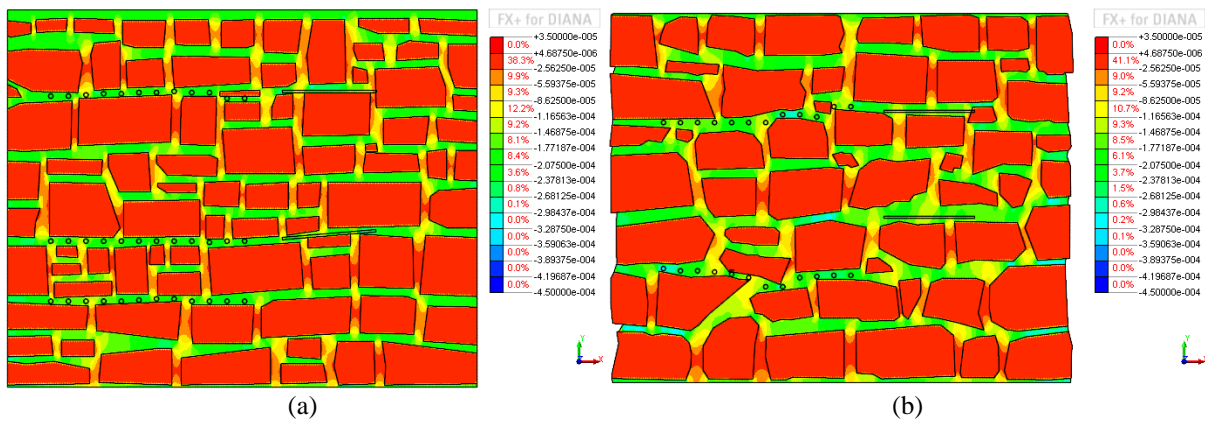
Figure 6-70 Vertical strain contour plots of the FE wall models loaded to 0.2 MPa on top of the wall: (a) semi-irregular wall; and (b) irregular wall

The influence of the amount of mortar between the measuring points of the virtual LVDTs was again studied for the irregular masonry wall. Twenty-five additional virtual LVDTs placed in various locations on the wall were analyzed. The elastic modulus estimations from all of the virtual LVDTs analyzed on the irregular wall are presented in Figure 6-71. The semi-irregular wall with the semi-irregular wall mortar elastic modulus estimations and curve are also presented in this graph. The scatter in the data points is slightly larger for the irregular wall model than for the semi-irregular wall model. However, the data points follow similar curves for both walls. It can be concluded that the geometry of the wall has less of an impact than the granite and mortar properties on the elastic modulus estimation curve. However, further research should be done to confirm these findings. To place the results of the simulated Young's modulus test on this graph, the percentage of mortar between the nodes defining the first two virtual LVDTs was estimated to be approximately 25.9%. This is the highest percentage for the three walls. Thus, for the design of these walls, the increase in irregularity corresponds with an increase in percentage of mortar and its contribution to the properties of the masonry overall.
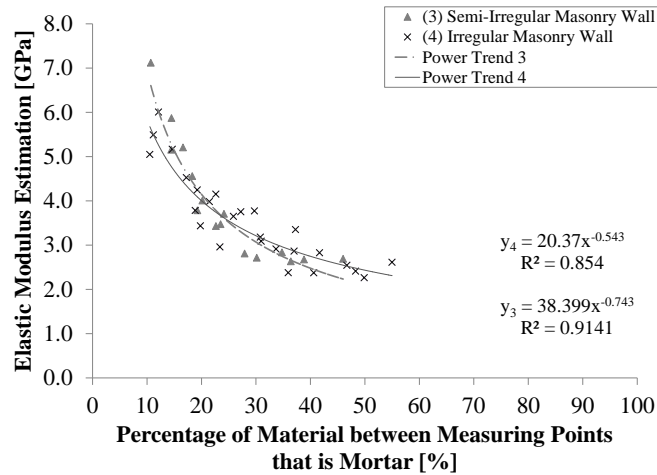
Figure 6-71 Numerical model estimation of elastic modulus for various percentages of mortar between the virtual LVDT nodes for: the regular masonry wall, semi-irregular masonry wall using regular wall mortar properties, and semi-irregular masonry wall using the semi-irregular wall mortar properties

6.4.2   Single Tube-Jack Test

A single tube-jack test was modeled to simulate the single tube-jack test performed in the same laboratory wall type. In this simulation, a 0.2 MPa load was applied to the top of the wall along with the self-weight of the masonry.

Six virtual LVDTs corresponding to the six LVDTs on the front face of the irregular wall in the laboratory were used to record the movement of the masonry above and below the equivalent flat-jack. The locations and distances between the node points are listed in Table H-1 and shown in Figure 6-72.
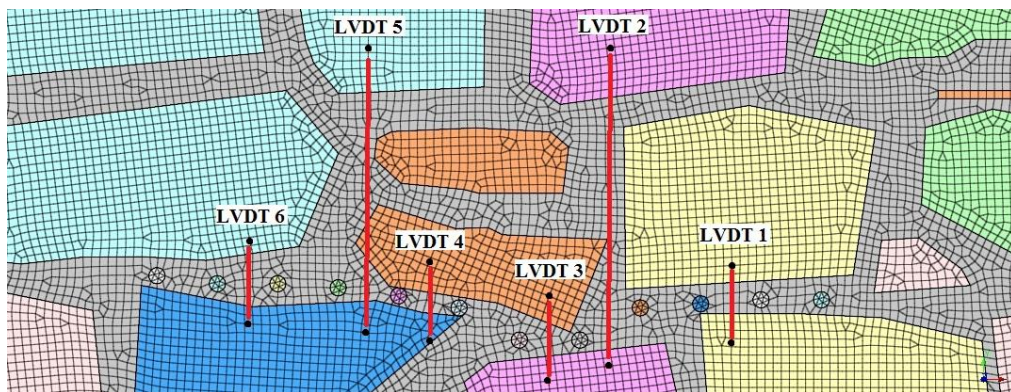
Figure 6-72 Locations for the vertical node sets in modeling the single tube-jack test in the semi-irregular wall

The relative displacements of the virtual LVDTs are shown in Figure 6-73 for various levels of radially applied pressure to the edges of the holes. The average relative displacement due to drilling the holes (zero applied pressure) is −2.11 μm, just slightly more than in the semi-irregular wall model where it was −1.76 μm. The average relative displacement due to deactivating the elements in the irregular wall model is very close to the average relative vertical displacement due to drilling the holes in the irregular wall laboratory test, where it was approximately −1.8 μm.

(a)   (b)
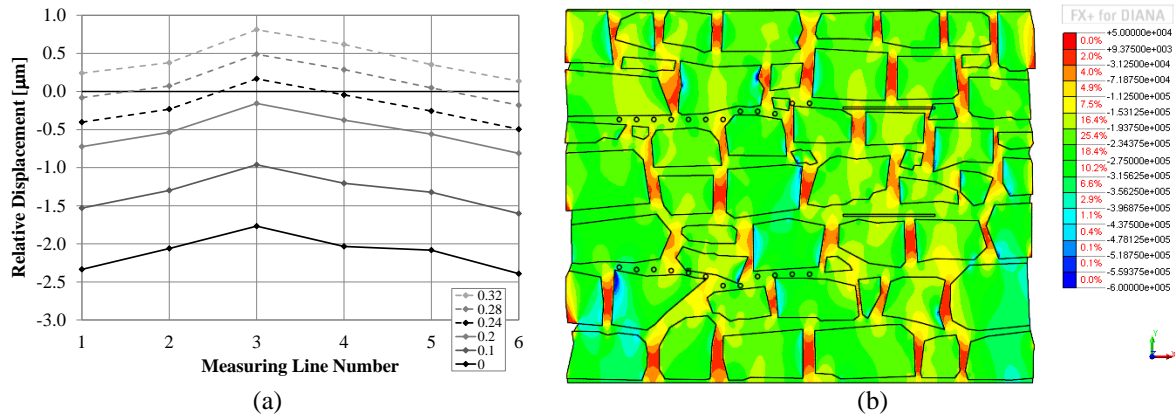
Figure 6-73 Simulation results of the single tube-jack test in the irregular wall: (a) relative vertical displacements of the virtual LVDTs at various applied pressure levels; and (b) contour plot of the vertical stresses [Pa] before deactivating the hole elements

Unlike the previously modeled single tube-jack tests in the regular and semi-irregular walls, the relative displacements due to deactivating the hole elements in the irregular wall are more negative at the ends of the equivalent flat-jack than at the center of the equivalent flat-jack. Prior to removing the mortar in the holes, the irregularity of the stress distribution resulted in lower stresses toward the center than at the edges of the line of holes, as shown in Figure 6-73b. Since the stresses are lower at the center of the line of holes, when the holes are created, there is less stress to redistribute. This results in less contraction of the masonry at the center of the line of holes.

Another difference between the previous walls and the irregular wall single tube-jack tests is the distance over which the LVDTs measured. For the irregular wall test, LVDTs 2 and 5 measured over a distances of approximately 40 cm and 35 cm respectively. Even though the distance was greater for these two LVDTs than for the other four LVDTs, their results fall within the range of the other LVDTs, as shown in Figure 6-73a. Thus, the distance over which the LVDT measures does not seem to affect the results for the single tube-jack test. This aspect of the test should be studied further to confirm this conclusion.
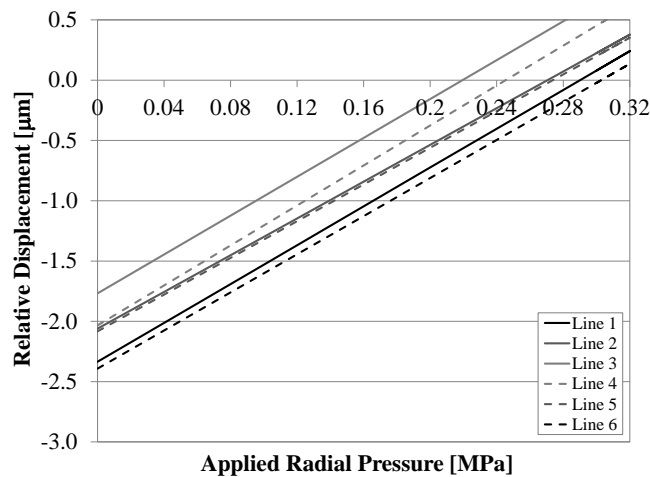
Figure 6-74 Relative displacement versus applied radial pressure results for the single tube-jack test simulation in the irregular masonry wall

The variation in the relative displacements due to deactivating the hole elements along the length of the equivalent flat-jack results in a range of pressures at which the relative

displacements are restored to zero, as shown in Figure 6-74. The average restoring pressure for this simulation was 0.267 MPa, with a coefficient of variation of 11.4%.
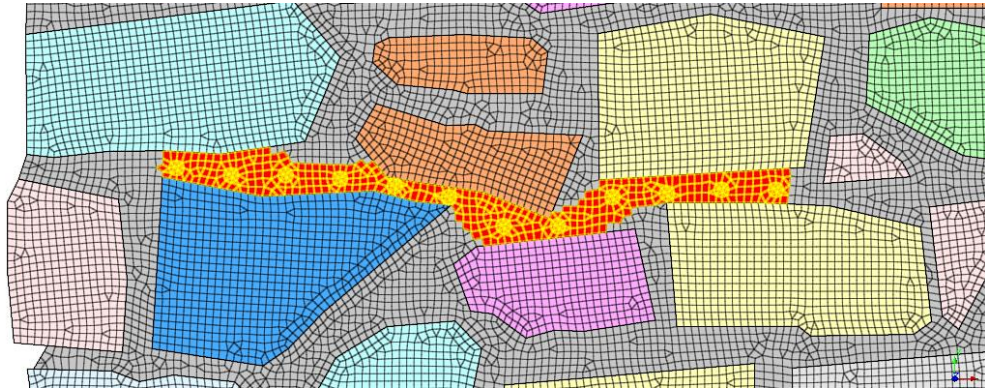
Figure 6-75 Elements selected to determine the average stress level at the location of the single tube-jack test

To determine the expected stress level at the tested joint, the initial stresses at each of the elements in the joint being tested were analyzed. See Figure 6-75 for the elements selected. The average stress level in the joint tested was 0.2336 MPa. Thus, the virtual LVDTs estimated the stress level in the model wall with an error of 14.3%. This error is much larger than the errors seen in estimating the stress level using the virtual LVDTs in the regular and semi-irregular masonry wall single tube-jack tests, which were around 2%. Thus, the irregularity of the masonry has greatly increased the error in the virtual LVDTs.

In the laboratory test of the single tube-jack test in the irregular wall, the estimated state of stress from the test was 0.5 MPa. This is a 114% error in comparison with the state of stress in the model wall joint of 0.2336 MPa. The estimated state of stress in the model wall was not nearly so far off from the stress level in the joint, with an error of 14.3%. Thus, additional factors contributing to the error in the results that were present in the laboratory test, besides the irregular typology, were not considered in the model. The laboratory wall had large variability in the depth due to the irregularity of the units and mortar that filled the joints. Also, the diameter of the holes varied from one hole to the next and also from the front of the wall to the back of the wall. The irregular wall model had a uniform depth of 0.2 m and uniform holes. With this large variability, it would be best to model this wall and test in a three-dimensional model that can capture these complexities.

6.4.3 Single Flat-Jack Test

The single flat-jack test performed in the irregular wall in the laboratory was simulated in the irregular wall model. The loading in this simulation was the same as for the single tube-jack test in the irregular wall. The locations of the virtual DEMEC points and virtual LVDTs are given in Table H-2 and shown in Figure 6-76.
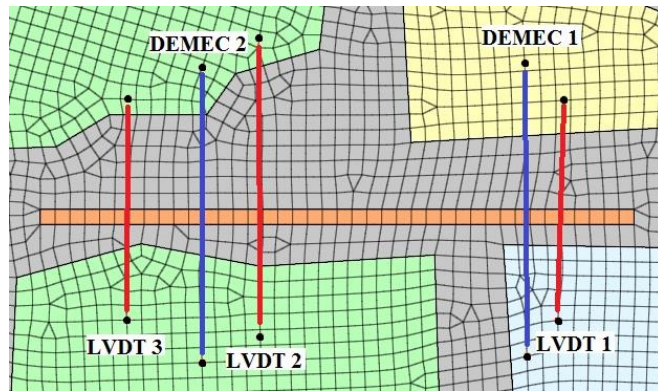
Figure 6-76 Locations for the vertical node sets in modeling the single flat-jack test in the irregular wall

The relative displacements of the virtual LVDTs are shown in Figure 6-77 for various applied pressure values. The average virtual LVDT relative displacement due to opening the slot was −30.5 µm, almost the same as in the simulation of the single flat-jack test in the semi-irregular wall. Thus, the increased irregularity did not significantly affect the relative displacements due to creating the openings in either the single tube-jack or single flat-jack tests.
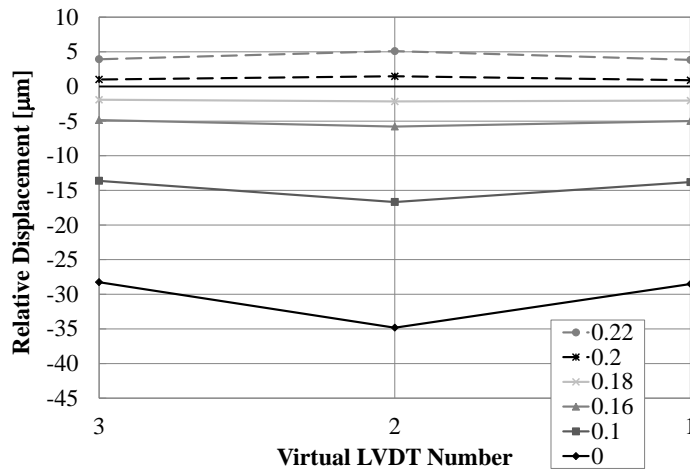
Figure 6-77 Relative vertical displacements for each measuring line at several increments of pressure applied in a normal direction to the upper and lower edges of the slot (pressure values in MPa)

The relative displacement versus the applied pressure graph in Figure 6-78a shows that the relative displacements were restored to zero between 0.18 MPa and 0.20 MPa. The average restoring pressure for the three LVDTs estimates the state of stress to be 0.1930 MPa with a coefficient of variation of 0.54%. This coefficient of variation is very low and close to the variation for the regular wall single flat-jack test, which was 0.11%. Thus, the irregularity of the masonry is not causing a significant increase in variability of the restoring pressure results. The larger variation in restoring pressures seen in the semi-irregular wall single flat-jack test, 5.39%, was most likely due to the angle of the flat-jack slot in that test.

Comparing the state of stress estimate of 0.1930 MPa to the average stress prior to deactivating the slot elements in the joint where the flat-jack slot is located, 0.1936 MPa, results in an error of 0.31% for the estimate given by the virtual LVDTs. This error is very low and is in the same range as the regular masonry wall single flat-jack test simulation. Again, the larger error of 3.93% in the virtual LVDT results in the semi-irregular wall test was most likely due to the angle of the flat-jack slot.
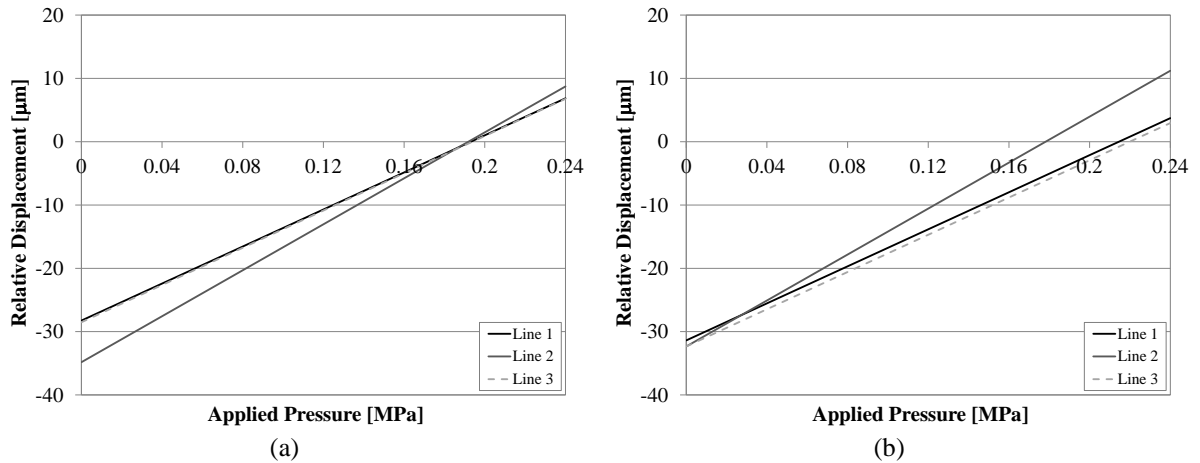
Figure 6-78 Relative vertical displacements of the virtual LVDTs versus applied pressure: (a) with LVDT initial relative displacements; and (b) with average DEMEC relative displacement as the initial displacement

To replicate the procedure used in the laboratory test, the relative displacements of the two DEMEC point sets, due to deactivating the elements in the slot, were used as the initial relative displacements of the three LVDTs. The relative displacement for DEMEC 1 was used as the initial relative displacement for LVDT 1 and the relative displacement for DEMEC 2 was used as the initial relative displacement for LVDTs 2 and 3. The revised results of the virtual LVDTs are shown in Figure 6-78b. The average relative displacement of the DEMEC point sets due to opening the slot was −32 μm. The average relative displacement due to cutting the slot in the laboratory test was −38 μm based on the DEMEC measurements on both the front and back of the wall (see section 5.4.2).

Using this procedure, rather than using only the virtual LVDT results, produces more variation in the state of stress estimation. The average restoring pressure determined from Figure 6-78b was 0.2042 MPa with a coefficient of variation of 11.13%. This estimation of the state of stress in the irregular wall model has an error of 5.46% in comparison with the average stress before the slot was opened at the level of the slot. Extrapolation of the laboratory test results produced an estimated state of stress of 0.44 MPa, a 127% error in comparison to the average stress before opening the slot at the location of the slot in the model wall.

6.4.4   Double Tube-Jack Test

In the simulation of the double tube-jack test in the irregular masonry wall model, a prescribed displacement was applied to the top of the wall. The prescribed vertical displacement was determined in the same way as for the other two walls. The absolute vertical displacements of the nodes at the top of the wall were graphed and are shown in Figure 6-79a. The displacements on the top of the wall show that drilling the holes in the irregular wall did not cause the wall to tilt as the drilling did in the other walls. The drilling did result in greater displacements above the area of the equivalent flat-jacks, which could be expected. For this test, the average vertical displacement was used as the prescribed displacement to represent the displacement of the steel profile on top of the wall.

205
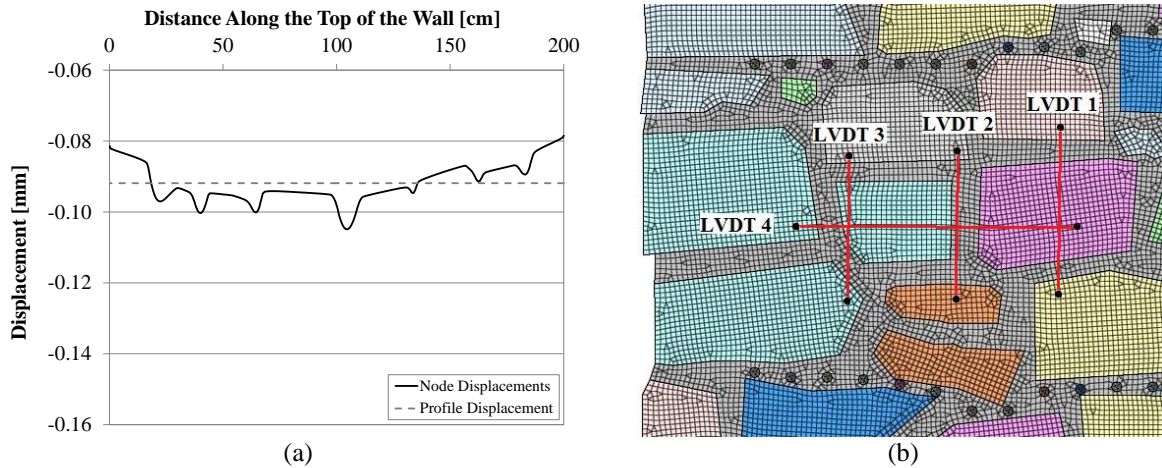
Figure 6-79 Double tube-jack test modeling set-up: (a) displacements at the top of the wall due to the vertical pressure and self-weight and estimated linear profile displacement; and (b) locations of the virtual LVDT nodes

The nodes used for the virtual LVDTs in the double tube-jack test simulation are shown in Figure 6-79b. The distances between the nodes and to the bottom left corner of the irregular masonry wall model are displayed in Table H-3 and

Virtual LVDT	Vertical Distance Between Nodes	Distance from Bottom of Wall to Bottom Node	Horizontal Distance from Bottom Left Corner of Wall to Bottom Node
	[m]	[m]	[m]
1	0.347	0.662	0.854
2	0.309	0.652	0.644
3	0.302	0.649	0.414

Table H-4.

A comparison can be made between the relative displacements of the model and the laboratory test wall. During the third pressurization cycle of the experimental test, the change in average vertical relative displacement between the start of the pressurization and the maximum applied pressure of 0.22 MPa was approximately -1 μm (see 5.4.3). In the model at an applied pressure of 0.22 MPa, the average vertical displacement shown in Figure 6-80a is approximately -1.01 μm. Thus, the model accurately represents the magnitude of vertical relative displacement of the wall in the laboratory test during pressurization.
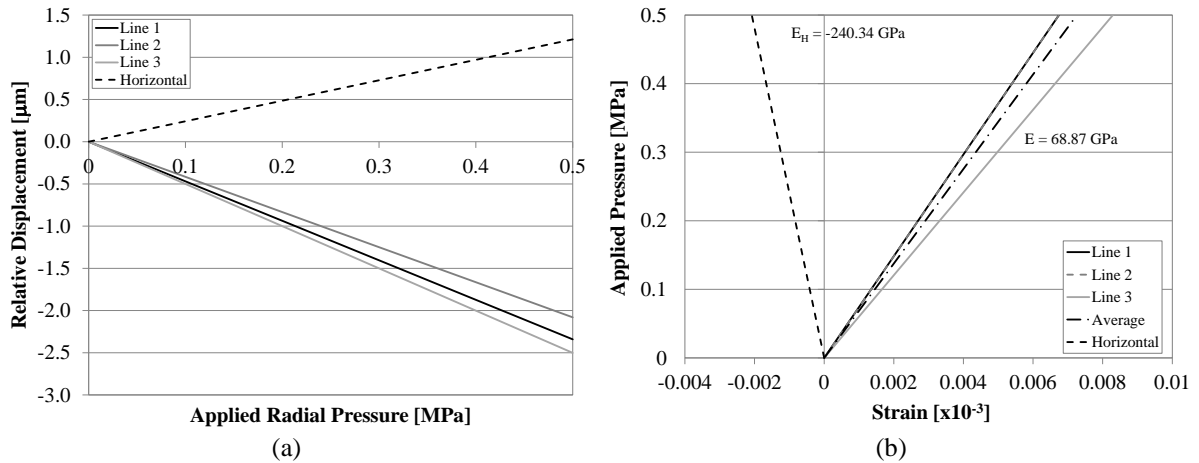
Figure 6-80 Double tube-jack test modeling results: (a) relative vertical and horizontal displacements of the virtual LVDTs; and (b) applied pressure versus strain for the virtual LVDTs

Figure 6-80b shows the applied pressure versus the strain for the virtual LVDTs. The elastic modulus for the average of the three virtual LVDTs was 68.87 GPa. In the experimental double tube-jack test, the elastic modulus was estimated at 55.84 GPa. The model results are much closer to the laboratory results in this test than they were in the semi-irregular wall test, where the laboratory results were nearly double the model results. Two conclusions can be made from these results: the semi-irregular and irregular finite element models are accurately representing the masonry and the movement of the masonry during the double tube-jack tests and the double tube-jack test on the semi-irregular wall in the laboratory did not produce accurate results.

Neither the model nor the double tube-jack laboratory test comes close to the values found in the Young's modulus tests on the irregular masonry wallets. The average reloading elastic modulus for the wallet tests was 3.37 GPa (see section 4.6.3)

These results can also be compared to the modeled Young's modulus test results presented in section 6.4.1. The virtual vertical LVDTs measured over an average distance of 31.9 cm, of which, 10 cm on average was mortar. Thus, 31% of the material between the nodes was mortar. Based on the curve in Figure 6-71 for the irregular masonry wall, the expected elastic modulus result from the virtual LVDTs would be approximately 3.16 GPa. However, the estimated elastic modulus shown in Figure 6-80b is much larger than the expected value based on modeling the Young's modulus test, implying the change in stress level between the two equivalent flat-jacks must be much less than the pressure being applied by the tube-jacks. The same result was seen in the two previously modeled double tube-jack tests.

For a change in applied pressure of 0.1 MPa during the double tube-jack test in the irregular wall, the average change in stress in the elements between the two equivalent flat-jacks was only 0.0042 MPa. Thus, the change in stress in the masonry is only 4.2% of the pressure applied by the tube-jacks. These are almost the same values as in the semi-irregular wall test. The increase in irregularity did not affect the effectiveness of the tube-jacks in changing the stress level between the equivalent jacks.

The average change in stress between the equivalent flat-jacks, due to the applied pressure, versus the strain of the virtual LVDTs is plotted in Figure 6-81. These results give an elastic modulus of 2.87 GPa. This result is closer than the applied pressure versus strain result to the expected result given by the curve produced in the Young's modulus test of irregular wall model. However, the average change in stress estimations for the elastic modulus for the semi-

irregular and the irregular wall tests both under estimated the expected results from the Young's modulus test curves.

Figure 6-81 Average change in stress between equivalent flat-jacks due to applied pressure versus the strain of the virtual LVDTs in the modeled double tube-jack test

The Poisson ratio was calculated to be 0.287 for the irregular masonry, based on the average double tube-jack test results from Figure 6-80b. Comparing this result to the value calculated from the reloading curves of the Young's modulus tests on the irregular masonry wallet, 0.472, there is a 24.4% difference between the two.

6.4.5   Double Flat-Jack Test

The double flat-jack test was also modeled by applying a prescribed displacement to the nodes at the top of the irregular wall. The vertical displacement along the top of the wall, for the model with the slot elements deactivated and the self-weight and pressure loads applied, is presented in Figure 6-82a. In this test, the proximity of the flat-jack slots to the edge of the wall has caused a greater vertical displacement on the right side of the wall. The line for the estimated position of the bottom of the steel profile was created by connecting the two points of least displacement at both ends of the wall. The estimated profile displacement was used as the prescribed displacement in modeling the double flat-jack test.

(a)   (b)
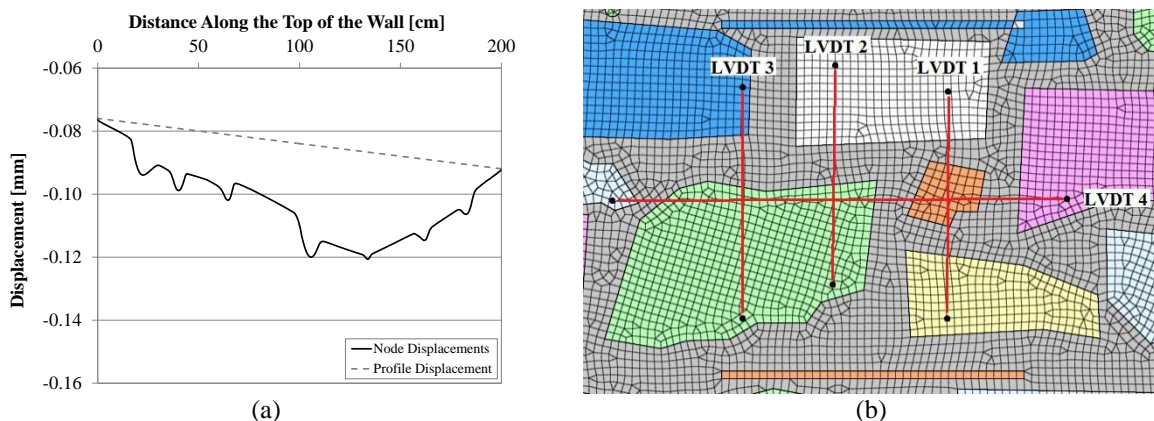
Figure 6-82 Double flat-jack test modeling set-up: (a) displacements at the top of the wall due to the vertical pressure and self-weight and estimated linear profile displacement; and (b) locations of the virtual LVDT nodes

The locations of the virtual LVDT nodes and their labels are shown in Figure 6-82b. The distances between the points in each set and from the bottom left corner of the irregular model wall are shown in Table H-5 and Table H-6.

The relative displacements of the vertical and horizontal virtual LVDTs during the pressurization are shown in Figure 6-83a. The variation in the displacements for the three vertical virtual LVDTs is large in comparison with the results of the double tube-jack test. One explanation for this is the number of joints and the amount of mortar each LVDT is measuring over. LVDT 1 measures over two mortar joints and LVDTs 2 and 3 only measure over one mortar joint. In the double tube-jack test, all of the LVDTs measured over two mortar joints. The more mortar between the node points, the greater the relative displacements since the mortar is less stiff. This is exemplified by LVDT 1, which has the greatest displacement.

Another reason for the variation in the displacement results is the location of the LVDTs along the width of the separated specimen. At the edges of the specimen the flat-jacks will have less of an effect than at the center of the specimen. See the contour plots of the displacements and stresses during the pressurization of the flat-jacks in the regular masonry wall in Figure 6-48 and Figure 6-49. LVDTs 2 and 3 measure over approximately the same amount of mortar but LVDT 3 is near the edge of the separated specimen, resulting in a low amount of displacement. In the double tube-jack test, the length of the separated specimen is much longer, there is more space to place the LVDTs and they can be placed closer toward the center of the specimen where they will be influenced by the pressurization.

The average vertical displacement results can be compared to the results obtained in the experimental test (see section 5.4.4). For this comparison, the relative displacement results from all of the vertical LVDTs in the laboratory test were averaged for the first pressurization cycle, producing a relative displacement of -0.022 mm at the applied pressure of 0.36 MPa. If the model results are interpolated at an applied pressure of 0.36 MPa, the average vertical displacement is approximately -0.019 mm. Since these values are very close, it can be concluded that the modeling of the double flat-jack test in this irregular wall model is a good representation of the laboratory test.
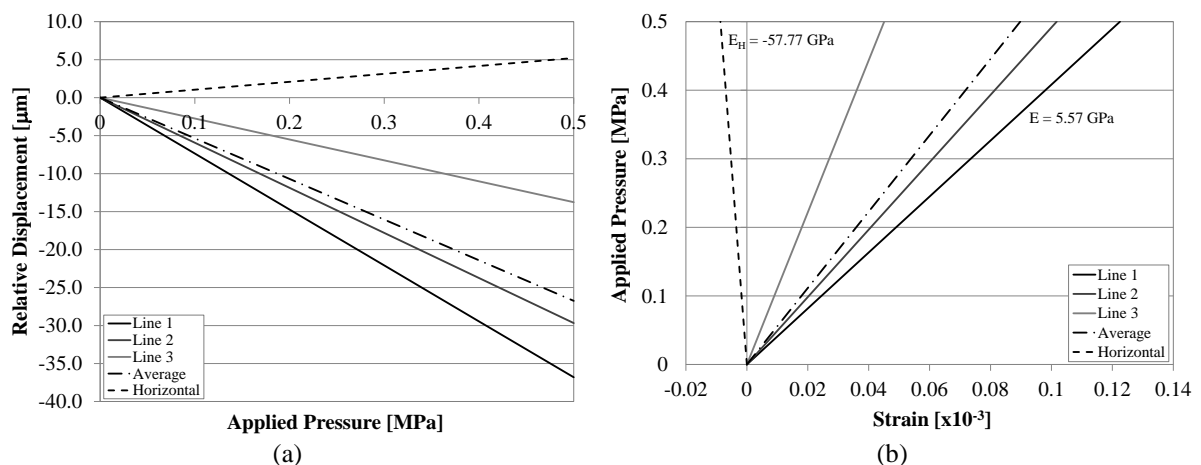
Figure 6-83 Double flat-jack test modeling results: (a) relative vertical and horizontal displacements of the virtual LVDTs; and (b) applied pressure versus strain for the virtual LVDTs

In Figure 6-83b, the applied pressure versus the strain for the virtual LVDTs is shown. The elastic modulus was estimated to be 5.57 GPa based on the average of the vertical virtual LVDTs. In the experimental double flat-jack test on the irregular wall, the elastic modulus was

estimated at 6.67 GPa for the reloading modulus considering the LVDT results on both sides of the wall. The Young's modulus found in the irregular masonry wallet tests was 3.37 GPa. The modeling and laboratory flat-jack test results are relatively close to each other, however they are both about double the experimental Young's modulus test results.

The results of the modeled double flat-jack test in the irregular wall can also be compared to the expected results based on modeling the Young's modulus test in the irregular wall. The vertical virtual LVDTs measured over an average distance of 0.3 m with an average of 6.3 cm of mortar between the nodes of each virtual LVDT. Thus, on average, 21.2% of the material between each node set was mortar. Based on this mortar ratio and the Young's modulus test curve for the irregular wall shown in Figure 6-71, the expected elastic modulus result would be 3.88 GPa. As in the modeling of the double flat-jack test in the semi-irregular wall, the pressure applied by the flat-jacks is not producing the same change in stress in the masonry between the flat-jacks, resulting in an overestimate of the elastic modulus.

The stress was recorded for all of the elements between the two flat-jacks. For a change in applied pressure of 0.1 MPa, the average change in stress in the elements between the two flat-jacks was 0.0789 MPa. Thus, the change in stress in the masonry is 78.9% of the pressure applied by the flat-jacks in the modeled double flat-jack test in the irregular wall. This value was 78.5% for the semi-irregular wall and 81.4% for the regular wall. The distance between the flat-jacks was 45 cm for the regular wall, 61 cm for the semi-irregular wall and 46.5 cm for the irregular wall. Since the change in stress is around 80% of the applied pressure for all three walls despite the differences in distance between the flat-jacks, it can be concluded that the distance between the jacks does not significantly affect the effectiveness of the flat-jacks in compressing the masonry. The slight difference in percentage for the regular masonry wall could be due either to being more regular in typology or having different mortar properties.

The average change in stress between the equivalent flat-jacks, due to the applied pressure, versus the strain of the virtual LVDTs is plotted in Figure 6-84. These results give the elastic modulus as 4.4 GPa. This is the same result as in the semi-irregular wall test. Again, it is close to the estimation given by the curve produced in the Young's modulus test of irregular wall model, however this value is not as close as it was in the double flat-jack test on the regular masonry wall. The irregular typology is likely causing the difference.

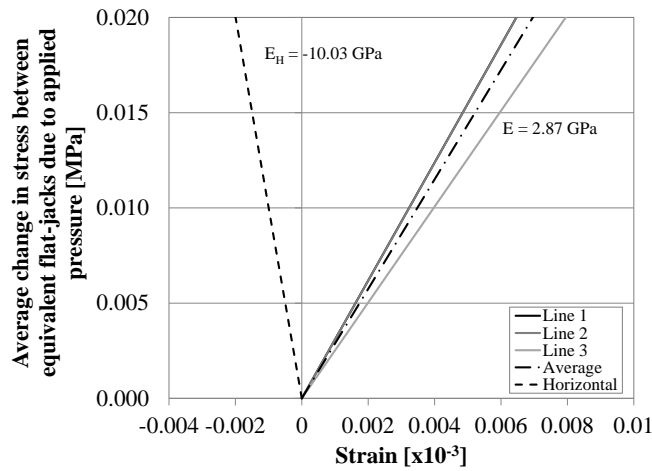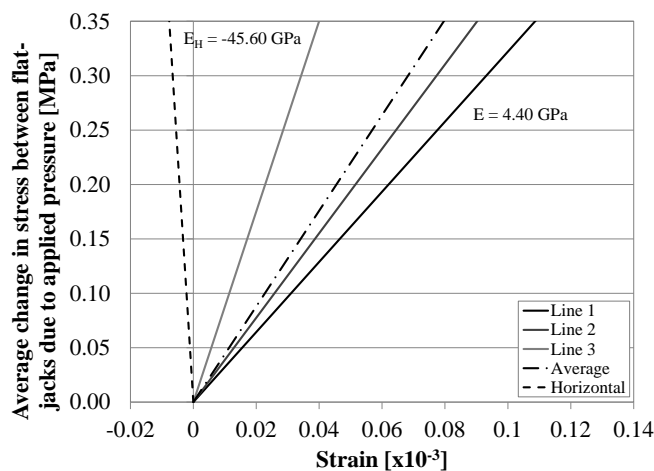

Figure 6-84 Average change in stress between flat-jacks due to applied pressure versus the strain of the virtual LVDTs in the modeled double flat-jack test

Finally, the Poisson ratio was calculated to be 0.096 based on the average results in Figure 6-83. This estimation for the Poisson ratio is 132% different from the calculated value based on the reloading curves in the Young's modulus tests on the irregular masonry wallets, where it was 0.472. Even considering the 25.6% variation in the masonry wallet results, the values are still very different. The following discussion section will address these differences and offer some hypothesis as to why they are so different.

6.5   Discussion

6.5.1   Young's Modulus Tests

The original reason for simulating Young's modulus tests on the large masonry walls was to determine if the masonry models had similar masonry properties to the masonry constructed in the laboratory. The properties for the individual granite and mortar materials in the model were based on the mechanical characterization tests performed on the same materials as those in the laboratory walls. However, since each of the materials were simulated in the wall models, the input of properties of the masonry as a whole was not possible. Thus, it was important to compare the resultant simulated masonry to characterization tests for the actual masonry. The comparison of the model Young's modulus tests with the masonry wallet Young's modulus tests performed in the laboratory, are presented in Table 6-3.

Table 6-3 Young's modulus test results for the modeled walls and the masonry wallets in the laboratory

Wall Typology	Model	Wallet	Difference
	GPa	GPa	%
Regular Wall	2.19	2.50	13.1%
Semi-irregular Wall	3.43	5.15	40.1%
Irregular Wall	3.65	3.38	7.8%

The regular wall and irregular wall have similar elastic modulus values to the masonry wallet results. This suggests that these two models fairly accurately represented the stiffness of the actual masonry in the laboratory. This means that these two models could be expected to perform similarly to the actual masonry walls during the tube-jack and flat-jack test simulations. However, this doesn't mean that the results from all of the tube-jack and flat-jack tests would be the same as the results in the laboratory. Other complications arising from the test set-ups, locations of the measuring devices, difficulties in creating the holes and slots, and other imperfections could have caused differences between the modeling and the actual tests. Differences between the models and the actual tests are discussed in other discussion sections.

The stiffness of the semi-irregular wall model is over 40% different from the results of the masonry wallet Young's modulus test. This would suggest that the model does not represent the actual masonry accurately. However, the variability in both the masonry wallet Young's modulus tests and the mortar compression tests (see section 4.5.2) suggest that the properties of the semi-irregular wall were variable. Thus, the model properties were not changed. Other reasons for the difference in the model and laboratory results were that the specimen sizes were different and the distance over which the LVDTs and virtual LVDTs measured were different for the two tests.

The placement of the LVDTs was examined further with the models. It was found that the percentage of mortar that is between the connection points of an LVDT makes a difference in

211

the resulting Young's modulus value for that LVDT. Numerous virtual LVDTs measuring over different percentages of mortar were tested and power curves were fit to the data for each of the wall models. It was discovered that changing the mortar properties affected the fitted curve. The irregularity in the masonry resulted in a larger variability in the data points but it was unclear if the typology itself affected the curves. These findings must be studied further in order to confirm them. However, it is clear that in order to have the best comparison between two Young's modulus tests, it is important that the measuring devices be measuring over the same percentage of mortar.

6.5.2   Single Tube-Jack Tests

Each of the single tube-jack tests performed in the laboratory walls was simulated in the numerical models for comparison. The first aspect of the test that can be compared is the relative displacement due to the opening of the holes. Table 6-4 shows the values for the model and laboratory tests.

Table 6-4 Relative average displacement due to deactivating the hole elements or drilling holes

Wall Typology	Joint	Applied Load	Model Relative Displacement	Laboratory Relative Displacement	Difference
		MPa	μm	μm	%
Regular Wall	3rd Joint	0.2	-7.03	-8.5	-18.9%
	4th Joint	0.2	-6.88	-6.5	-5.7%
	5th Joint	0.4	-13.50	-54	-120.0%
Semi-irregular Wall		0.2	-1.76	-20	-167.6%
Irregular Wall		0.2	-2.11	-1.8	-15.9%

Most of the relative displacements are on the same order as the laboratory tests except for the test in the 5th joint in the regular wall and the test in the semi-irregular wall. The same conclusion can be made from these results as was made about the comparison between the Young's modulus tests: the regular wall and irregular wall models are accurately representing the behavior of the actual masonry walls. The variability in the semi-irregular laboratory wall has resulted in a relative displacement that is much different from both the other laboratory walls and different from the modeled semi-irregular wall. The difference in the results for the 5th horizontal joint were likely due to the issues experienced during that test in the laboratory. The flat-jack slots on the other side of the wall were not filled in at the time of the test, the double tube-jack test had been performed previously in that area, and the wall was loaded to double the previous loading.

Analysis of the relative displacements along the length of the equivalent flat-jack showed that not all of the relative displacements would be restored at the same applied pressure level (see section 7.2.2.2). The same was true when the restoring pressures for virtual LVDTs were analyzed for each test. The average restoring pressures and their coefficients of variation are shown in Table 6-5. The variation in the restoring pressures seem to increase as the irregularity of the masonry increases. However, the irregularity of the equivalent flat-jack was also increasing with the irregularity of the masonry. Thus, it is difficult to say which of these two aspects was the contributing factor to the variation. One aspect of LVDT placement that did not seem to impact the restoring pressure recorded for the LVDTs was the distance over which the

LVDTs were recording. Since this was only observed in the single tube-jack test on the irregular wall, this aspect should be further studied.

Table 6-5 Variation of restoring pressures for virtual LVDTs

Wall Typology	Joint	Ave. Restoring Pressure	COV
		MPa	%
Regular Wall	3rd Joint	0.229	0.40%
	4th Joint	0.223	0.44%
	5th Joint - No Slots	0.424	0.36%
	5th Joint - Slots Open	0.443	4.76%
Semi-irregular Wall		0.220	5.65%
Irregular Wall		0.267	11.40%

The estimated states of stress in the walls by the simulations and the laboratory tests are compared in Table 6-6. The simulated tube-jack tests estimate the state of stress in the model wall with very small amounts of error for all but the irregular wall test. This shows that the ideal tube-jack test is possible and accurate. The error in the irregular wall simulation was much higher than for the other tests. This could be due to the irregular typology of the masonry or it could be due to the irregular spacing of the tube-jacks vertically. More research is needed to determine the cause of this error. It does suggest that there could be some error in the laboratory tube-jack test that was not due to test difficulties but was a result of the test itself.

Table 6-6 Estimated state of stress results for the single tube-jack tests

Wall Typology	Joint	Stress in model joint	Estimated State of Stress		Error based on stress in model joint	
			Model Wall	Laboratory Wall	Model Wall	Laboratory Wall
		MPa	MPa	MPa	%	%
Regular Wall	3rd Joint	0.2252	0.229	0.26	2%	15%
	4th Joint	0.2202	0.223	0.34	1%	54%
	5th Joint	0.4397	0.443	2.00	1%	355%
Semi-irregular Wall		0.2243	0.220	1.33	2%	493%
Irregular Wall		0.2336	0.267	0.50	14%	114%

Other than the regular wall test in the third joint, the single tube-jack test laboratory results were not comparable with the model stress level. The regular wall model seemed to accurately represent the actual wall in regards to stiffness and represented the wall well in stress levels given the 15% error from the 3rd joint test. Thus, the errors from the 4th and 5th joint tests were due to the other experimental test issues discussed previously. The semi-irregular wall model did not represent the stiffness of the semi-irregular masonry well and from these results, it looks like the stress level was also not represented well. The irregular wall model represented the stiffness of the irregular masonry well, but the variation in the depth of the irregular wall, that could not be modeled in the two-dimensional model, resulted in differences in the stress state between the model and the laboratory walls.

Using the model to analyze the distribution of displacements, strains and stresses provided important information about how the tube-jack test was working to pressurize the masonry. Observing the displacements along the equivalent flat-jack showed that the line of tube-jacks works as one equivalent flat-jack. A similar distribution of relative displacements is seen along the equivalent flat-jack as along the regular flat-jack due to opening the holes. When the holes are pressurized, the distribution of stresses along the length of the equivalent flat-jack is more complex that for the single flat-jack. The change in stress above the equivalent flat-jack is not equal to the change in pressure applied by the tube-jacks and varies along the length of the equivalent flat-jack.

6.5.3   Single Flat-Jack Tests

Some of the same comparisons that were made for the single tube-jack test can be made for the single flat-jack test. First the relative displacements recorded using the DEMEC points are compared in Table 6-7. Comparing the results, the model does not reflect the actual relative displacement of the masonry. This is most likely because the slots in the model walls was the same depth of the masonry, whereas the slots in the laboratory walls were only halfway through the thickness of the wall. A three-dimensional model would be required to model the relative displacement differences from the back of the wall to the front of the wall that were seen in the laboratory testing.

Table 6-7 Relative displacement of the DEMEC points due to deactivating slot elements or sawing slots

Wall Typology	Model Wall	Laboratory Wall	Difference
	μm	μm	%
Regular Wall	-69.8	-180	-88.2%
Semi-irregular Wall	-30.7	-94	-101.5%
Irregular Wall	-30.5	-38	-21.9%

The estimated state of stress found by the model tests and laboratory tests are compared in Table 6-8. The 0% error in the regular model wall results show that the single flat-jack test works perfectly in an ideal regular masonry wall. The model results for the irregular wall are also low, showing that in an irregular masonry with a uniform thickness, the test can be performed with accurate results. The higher error in the semi-irregular model test and laboratory test is likely due to the angle of the slot in this test. Therefore, it is important to ensure that the slot is created in the direction perpendicular to the direction of the compressive stress in the masonry. The difference between the model and laboratory results for the irregular wall are likely due to the variation in thickness of the laboratory wall, which was not simulated in the model.

Table 6-8 Estimated state of stress based on initial DEMEC displacements

Wall Typology	Stress in model joint	Estimated State of Stress		Error based on stress in model joint	
		Model Wall	Laboratory Wall	Model Wall	Laboratory Wall
	MPa	MPa	MPa	%	%
Regular Wall	0.2252	0.2252	0.30	0%	33%
Semi-irregular Wall	0.2190	0.1970	0.36	10%	64%
Irregular Wall	0.1936	0.2042	0.44	5%	127%

6.5.4 Single Tube-Jack and Flat-Jack Tests

One of the main reasons for including flat-jack tests in this thesis work was to compare this traditional and accepted method with the enhanced tube-jack method on the same masonry. To start, a comparison is made between the relative displacements caused by opening the holes or slots in the modeled and laboratory tests, Table 6-9. In general, for both the modeled and laboratory tests, creating the tube-jack holes resulted in far less relative displacement than creating the slot. This was expected based on the preliminary tests performed during the development phase of the thesis work.

Table 6-9 Relative displacements due to opening the holes or slot in the single tube-jack and flat-jack tests

Wall Typology	Virtual LVDTs			Laboratory LVDTs		
	Tube-Jack	Flat-Jack	Flat-Jack to Tube-Jack Ratio	Tube-Jack	Flat-Jack	Flat-Jack to Tube-Jack Ratio
	µm	µm		µm	µm	
Regular	-7.03	-69.8	9.9	-8.5	-180	21.2
Semi-irregular	-1.76	-30.7	17.4	-20.0	-94	4.7
Irregular	-2.11	-30.5	14.5	-1.8	-38	21.1

Increasing the stiffness of the mortar greatly reduced the relative displacements due to opening the holes or slots for the single tube-jack and flat-jack tests. The increase in stiffness affected the relative displacement due to opening the holes in the tube-jack test more than opening the slot in the flat-jack test, as seen by the increase in ratio between the two relative displacements. Thus, the tube-jack test is better suited for low stiffness materials where drilling the holes will result in more relative displacement of the masonry over the equivalent flat-jack.

The absolute vertical displacements due to opening the holes or slot were also examined in the regular wall model. The absolute vertical displacements were influenced by the edges of the wall in both the tube-jack and flat-jack tests. Opening the holes or slot resulted in not only a vertical displacement downward of the masonry above the test location but also some rotation or leaning of the wall. Therefore, the tests were performed too close to the edges of the wall. Analysis of the single tube-jack test in the 5th horizontal joint when the flat-jack slots were left open, also showed that the tube-jack and flat-jack tests were performed too close to each other, as well. Therefore, future tests should be performed farther from the edges and farther from each other so that the masonry at the elevation of the test is confined equally on both sides.

A comparison between the tube-jack and flat-jack modeled test results is shown in Table 6-10. The results of modeling both the single tube-jack and flat-jack were very close to the expected values (the average stress in the model joint) with low errors. This shows that both tests can accurately determine the state of stress in these types of masonry walls in the idealized model situation. In general, the tube-jack tests had higher errors than the flat-jack tests comparing between tests in the same walls. As the irregularity in the masonry typology increased, the error in the average estimated state of stress and the variation in the restoring pressure for the virtual LVDTs increased for the tube-jack tests. However, it is difficult to determine exactly how much the irregularity contributed since the mechanical properties of the mortar varied between the regular wall and the semi-irregular and irregular walls and the linearity of the lines of tube-jack holes also varied.

Table 6-10 Comparison of Single Tube-Jack and Single Flat-Jack model results based on virtual LVDT displacements

Wall Typology	Stress in model joint		Estimated State of Stress		Error based on stress in model joint		Variation in Restoring Pressure	
	Tube-Jack	Flat-Jack	Tube-Jack	Flat-Jack	Tube-Jack	Flat-Jack	Tube-Jack	Flat-Jack
	MPa	MPa	MPa	MPa	%	%	%	%
Regular	0.2252	0.2252	0.2287	0.2247	1.55%	0.22%	0.40%	0.11%
Semi-irregular	0.2243	0.2190	0.2197	0.2104	2.05%	3.93%	5.65%	5.39%
Irregular	0.2336	0.1936	0.2670	0.1930	14.30%	0.31%	11.40%	0.54%

6.5.5 Double Tube-Jack Tests

In the double tube-jack tests in the laboratory, large estimations for the stiffness of the masonry were in contrast with the results of the wallet tests for the semi-irregular and irregular wall. The modeling of the double tube-jack tests was important to determine what was happening in these tests and why the results were so different. It was found in the simulation of the Young's modulus test that the amount of mortar that each LVDT measures over makes a difference in its estimation for the elastic modulus. Thus, it was also important to compare the expected results based on the curves developed from those simulated Young's modulus tests. All of these comparisons are shown in Table 6-11.

Table 6-11 Comparison of the double tube-jack test results with the expected model results and Young's modulus test results on the masonry wallets

Wall Typology	Expected result based on curve developed in modeling the Young's modulus test	Double Tube-Jack Test		Young's Modulus Test
		Model Wall	Laboratory Wall	Wallet
	GPa	GPa	GPa	GPa
Regular Wall	1.3	16.85	2.2	2.5
Semi-Irregular Wall	3.15	70.13	139.86	5.15
Irregular Wall	3.16	68.87	55.84	3.37

The results in Table 6-11 show that neither the laboratory tests nor the model simulations of the double tube-jack tests accurately determined the elastic modulus of the masonry in comparison to the expected value from the simulated Young's modulus test. Given the trend of the other results, it seems that the laboratory test result for the regular wall is lower than it should be. It would be interesting to perform this test again on another laboratory wall of the same typology to see if the result would be different.

The difference between the expected result based on the Young's modulus simulation and the Young's modulus test on the wallets is partly due to the different percentages of mortar between the connection points of the LVDTs. Thus, it is hard to make a good comparison for either the laboratory or model results with the results of the masonry wallet tests.

In the single tube-jack test it was found that the change in stress above the joint varied along the equivalent flat-jack and was far less than the pressure applied by the tube-jacks. Thus, the change in stress was examined to see if it was the reason for the differences between the

expected results elastic modulus and the double tube-jack test results. The change in stress due to a change in pressure was found to be very low, less than 10%. When the change in stress was used, instead of the pressure applied by the tube-jacks, to determine the elastic modulus, the results were much closer to the expected values as shown in Table 6-12. More research will need to be done to see what variables affect the change in stress percentage of the change in applied pressure.

Table 6-12 Comparison of elastic modulus results for the modelled double tube-jack tests based on the pressure applied to the edges of the holes or based on the change in stress between the equivalent flat-jacks

Wall Typology	Expected result based on curves developed in modeling the Young's modulus test	Pressure vs. Strain	Stress vs. Strain	Change in stress percentage of change in applied pressure
	GPa	GPa	GPa	%
Regular Wall	1.3	16.85	1.33	7.80%
Semi-Irregular Wall	3.15	70.13	3.01	4.30%
Irregular Wall	3.16	68.87	2.87	4.20%

6.5.6   Double Flat-Jack Test

In the laboratory double flat-jack tests, the results overestimated the stiffness of the masonry when the results were compared with the masonry wallet tests. Thus, the numerical modeling was important to determine why this was the case and if the masonry typology was to blame for the errors in the results. A comparison of the results from the simulated and laboratory tests is presented in Table 6-13. The model results also overestimate the stiffness of the masonry in comparison with the expected value from the curves developed in the simulation of the Young's modulus test. However, the differences were not nearly as large as in the double tube-jack test results.

Table 6-13 Comparison of the uble flat-jack test results with the expected model results and Young's modulus test results on the masonry wallets

Wall Typology	Expected result based on curves developed in modeling the Young's modulus test	Double Flat-Jack Test		Young's Modulus Test
		Model Wall	Laboratory Wall	Wallet
	GPa	GPa	GPa	GPa
Regular Wall	0.76	1.16	2	2.5
Semi-Irregular Wall	3.79	5.78	8.57	5.15
Irregular Wall	3.88	5.57	6.67	3.37

It was theorized that the overestimation in the flat-jack test was also due to the change in stress between the flat-jacks not being the same as the applied pressure. This was confirmed by observing the contour plots of the stress distribution in the masonry and in averaging the change in stress of all of the elements between the two flat-jacks. The change in stress was around 80% of the change in applied pressure as shown in Table 6-14. When the change in stress was plotted against the strain, the elastic modulus result was much closer to the expected result.

Table 6-14 Comparison of elastic modulus results for the modelled double flat-jack tests based on the pressure applied to the edges of the slot or based on the change in stress between the flat-jacks

Wall Typology	Expected result based on curves developed in modeling the Young's modulus test	Pressure vs. Strain	Stress vs. Strain	Change in stress percentage of change in applied pressure
	GPa	GPa	GPa	%
Regular Wall	0.76	1.16	0.97	81.40%
Semi-Irregular Wall	3.79	5.78	4.4	76.20%
Irregular Wall	3.88	5.57	4.4	78.90%

The difference between the change in stress in the masonry and change in applied pressure is likely due to the connection of the masonry between the flat-jacks with the surrounding masonry. If this is the case, it could explain why the flat-jack tests overestimated the elastic modulus of the masonry walls in the laboratory. The masonry between the flat-jacks was connected to the surrounding masonry not only on either side, but also at the back side of the wall. This result suggests that the separation of the masonry during the double tube-jack and flat-jack tests makes a large difference in the results and that the tube-jacks, which can pass through the thickness of the masonry, may be a better choice for this type of large stone masonry. However, these conclusions must be researched further to confirm them.

6.6   Conclusions

The numerical modeling simulation of the tube-jack and flat-jack tests performed in the three masonry walls in the laboratory served a very important role in helping to determine if the laboratory results were accurate, understand how the tests were working, and how the masonry behaves as a result of the pressurizations. Important conclusions that can be drawn from the numerical modeling and the comparison with the experimental tests are listed below.

-   The percentage of mortar between the connection points of an LVDT makes a difference in the elastic modulus obtained from that LVDT. Therefore, in order to compare stiffness results between two tests, the percentage of mortar over which the LVDTs measure, must be the same.

-   The relative displacement due to opening the tube-jack holes is much smaller than the relative displacements resulting from opening the flat-jack slot.

-   The line of tube-jacks works as an equivalent flat-jack.

-   Pressurization of the tube-jacks in the holes results in a change in stress above the joint that is less than 10% of the applied pressure.

-   The relative displacements are not all restored at the same pressure level and vary along the length of the equivalent jack or flat-jack.

-   The variation in the restoring pressures of the LVDTs seems to increase with increasing irregularity of the masonry.

- An angle in the flat-jack led to increased error and variation in the results. The flat-jack or equivalent flat-jack should be perpendicular to the direction of the compressive stress to avoid these errors.

- Both the idealized tube-jack and flat-jack tests accurately estimated the state of stress in the model walls. This suggests that the actual tests can be accurate if no errors in the tests occur.

- Both the laboratory and the modeled double tube-jack and flat-jack tests overestimated the elastic modulus of the masonry.

- The change in stress of the masonry between the equivalent flat-jacks and between the flat-jacks is less than the change in applied pressure to the masonry. The change in stress is less than 10% of the change in pressure for the tube-jack tests and is approximately 80% of the change in pressure for the flat-jack tests.

- The change in stress as a result of the change in pressure is likely due to the connection of the masonry between the jacks to the surrounding masonry. Since the change in stress can't be measured and it is difficult to determine the connectivity of the masonry during the in-situ tests, this aspect of the test could lead to inaccuracies in the double tube-jack and flat-jack test results.

7.   IN-SITU TESTING – THE SAN FRANCISCO CONVENT

The goal of developing the tube-jack test system was to create an alternative to the flat-jack test for use in-situ on irregular or large unit historic masonry structures to determine local states of stress and mechanical characteristics of the masonry. Thus, this thesis would not be complete without testing the tube-jack system in-situ on a historical structure. The site chosen for the testing was the San Francisco Convent located in Braga, Portugal. Just as in the laboratory tests and numerical modeling, a series of four tests was performed on a masonry wall in the convent complex; a single tube-jack test, a single flat-jack test, a double tube-jack test, and a double flat-jack test. In this chapter, background information is provided about the San Francisco Convent and the location for the tests, the four tests are described along with their results, and finally, conclusions are made regarding the success of the tube-jack tests.

7.1   Background Information

The San Francisco Convent is located in the parish of Real in the city of Braga in Portugal. The convent is part of a complex of buildings and monuments including the Church of San Francisco, the Chapel of San Frutuoso, the Fountain of Santo António, and the San Francisco Convent. The complex is shown in Figure 7-1 with the convent highlighted. The convent was in a state of disrepair and ruin at the time of the tests. Most of the roof had collapsed and some of the floors and walls as well. There was a significant amount of vegetation growing on, in and around the structure. The complex will soon have a new use as the archeological research group center of the University of Minho. The inspection and diagnosis works were carried out to assess the state of conservation prior to the adaptive reuse of the structure.

| (a) | (b) |

Figure 7-1 San Francisco Convent in relation to other buildings within the complex: (a) from the South;

and (b) from the West [69]

Archaeological works, excavations and surveys were carried out at the convent by the Studies Center of the University of Minho School of Architecture and a report was written by Fontes in 2012 [70]. This document outlines the likely phases of construction of the complex, including the convent. Currently, the convent consists of three wings surrounding a cloister and an additional wing extending to the east of the northern most wing. In the sequence of construction identified by Fontes, the north wing was built first in the eleventh and twelfth centuries. The east and south wings were constructed in the sixteenth century and finally an additional wing was added on to the north wing in the eighteenth century [70].

A study by the Department of Civil Engineering (DEC) at the University of Minho was performed in 2015 to determine the condition of the convent, characterize the structure, identify

deterioration and determine if the structure could be rehabilitated and adapted to be a new facility for the archeology unit of the university [69]. This study identified four typologies of masonry corresponding to the different wings of the structure. The locations for these masonry types are shown on the main floor plan in Figure 7-2.
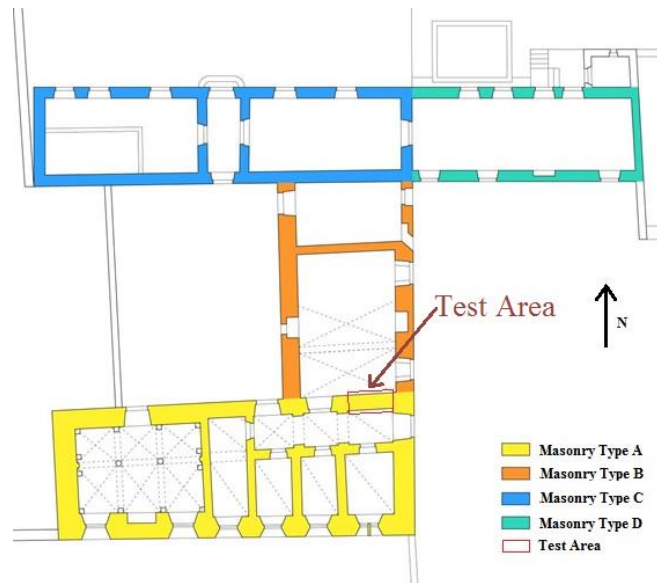
Figure 7-2 Main floor plan of the San Francisco Convent showing the four masonry types identified (image adapted from [69])

The tube-jack and flat-jack tests were performed in the wall dividing the southern wing from the eastern wing, as shown in Figure 7-2. This wall was part of the southern wing and was composed of Type A masonry. This type of masonry was characterized in the DEC study [69] by having a large variability in the size of the granite stone units, mostly rectangular larger stones with smaller stones used to fill gaps between the larger stones. The joints of the masonry were irregular and the mortar very weak. The masonry appeared to have two leaves or wythes with a weak link between them.

The tube-jack and flat-jack tests were performed from the southernmost room of the eastern wing of the convent. This room has become known as, "the fig tree room," because of the large fig tree that has taken root on the vault over half of the room. The wall to be tested and the branches of the fig tree coming through the collapsed ceiling at the other end of the room are shown in Figure 7-3.

Figure 7-3 "The fig tree room": (a) branches from the fig tree coming through the collapsed ceiling on the north side of the room; and (b) the south wall of the room where the tests were performed

The loading on the wall was assumed to be only the self-weight of the masonry and the self-weight of the walls on the second and third story direct above this wall. The second story wall, shown in Figure 7-4a, was assumed to be a continuation of the first level wall and thus the same typology as the first level wall (Figure 7-2b). The third level wall was a half-timber frame wall with brick masonry infill as shown in Figure 7-4b. A simple finite element model was created to estimate the stresses in the wall at the level of the tube-jack and flat-jack tests. The model assumed the stone masonry had a density in the range of $1800 - 2200$ kg/m^3 and an elastic modulus in the range of $1.7 - 2.1$ GPa [69]. The half-timber wall was assumed to have a density of 1500 kg/m^3 and an elastic modulus of 0.67 GPa [71]. Contour plots of the stress in the masonry are shown in Appendix I. The estimated level of stress at the level of the tube-jack and flat-jack tests ranged from 0.14 MPa to 0.17 MPa. This stress level was slightly lower than the loading on the walls in the laboratory testing. The stress estimation did not take into consideration the possible loading from the tree on ceiling above the fig tree room or the variation in loading due to the vaulting of the ceilings.

Figure 7-4 Loading on the tested masonry wall: (a) second level granite masonry wall; and (b) third level timber and brick infill masonry wall

One reason for choosing this location for the tube-jack and flat-jack tests is that other non-destructive tests were performed in this location for the study carried out by the Department of

Civil Engineering at the University of Minho [69], namely sonic direct/indirect tests, impact-echo tests and georadar measurements. Some of the main results are briefly presented here.

Regarding the sonic tests, several types of sonic velocity tests were performed. An initial direct sonic velocity test was conducted in a couple of granite stones resulting in an average p-wave velocity for the granite of 3425.7 m/s, a value deemed reasonable in the study for this type of masonry [69]. Following the direct tests through the stones, direct sonic tests were performed through the wall to qualitatively study the morphology of the wall and detect the presence of voids. A 3×3 grid of points was created with 0.5 m between points vertically and 0.75 m between points horizontally. The grid is shown in Figure 7-5. The thickness of the wall was estimated to be 0.94 m.

| (a) | (b) |
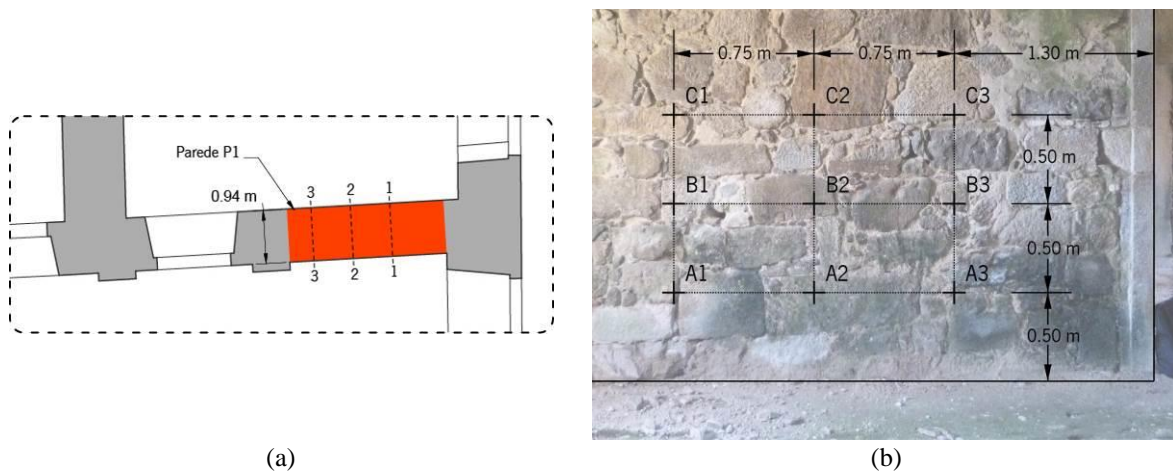
Figure 7-5 Set-up for the direct sonic tests through the wall in the San Francisco Convent wall: (a) plan of the tested wall; and (b) distances between the grid points on the wall

The average velocity of the waves passing through the wall was 1500 m/s, not considering values greater than 2500 m/s. The contour plot of the wave velocities is shown in Figure 7-6. There is a considerable amount of variability in the wave velocities indicating irregularity in the masonry on the surface and throughout the wall section. Since none of the velocities was below 1000 m/s, it was concluded in the study that large voids were not expected within the wall section.
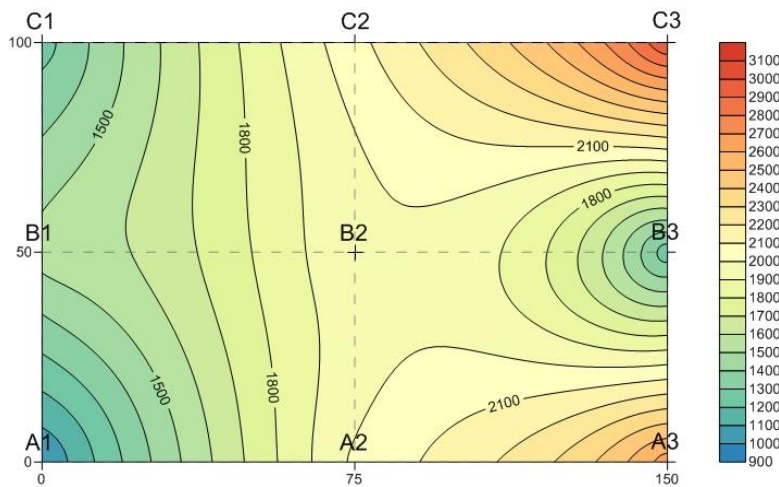
Figure 7-6 Contour plot of the direct sonic velocities through the San Francisco Convent wall [m/s]

The University of Minho study [69] also conducted indirect sonic tests on both faces of the wall between the upper and lower points of the grid. Through these tests, the average velocities of the p-waves (1051.7 m/s) and r-waves (572.6 m/s) were used by the researchers to estimate the Poisson ratio of the masonry, 0.23, and the modulus of elasticity range, 1.7-2.1 GPa, assuming a masonry density range of 1800 to 2200 kg/m^3. These values were also deemed reasonable by the researchers for this type of historic granite masonry. These results provide values for the Poisson ratio and modulus of elasticity with which to compare to the results from the double tube-jack and double flat-jack tests.

Finally, impact-echo tests were performed on nine stones on each side of the wall to determine the thickness of each stone. There was large variability in the thicknesses of the stones, with a range from 37 cm up to 88 cm. However, most of the stones were between 0.5 m and 0.7 m in thickness. The depth of the stones indicates that there are stones crossing the thickness of the wall, providing a stronger tie between the two wythes of the wall than previously predicted. The thicknesses of both the wall and the individual stones indicate that the single and double tube-jack and flat-jack tests will only be testing a portion of the wall and a portion of the thickness of the stone units. This could have an impact on the results of the test, especially since the thicknesses of the units vary so much. Future development of the tube-jacks could result in the use of variable length tube-jacks that could create an equivalent flat-jack to match the thicknesses of the units and walls that they are testing.

The layout for the single and double tube-jack and flat-jack tests on the selected wall in the fig tree room is shown in Figure 7-7. A vertical crack with 1 cm maximum width was also visible at left side of the testing area (see Figure 7-7), possibly linked to the presence of roots from the fig tree and/or a possible foundation settlement. This limited the test area to between the doorway and the crack. The tests locations were planned so that they would be less likely to be affected by these edges. The single tube-jack test was performed first using the bottom line of holes shown in the figure. This was followed by the double tube-jack test. On the second day of testing, the single flat-jack test was performed using the bottom slot location shown on the figure and then a second slot was sawed above the first, as shown in the figure, for the double flat-jack test. The details of each test setup, results and discussion are presented in the following sections.
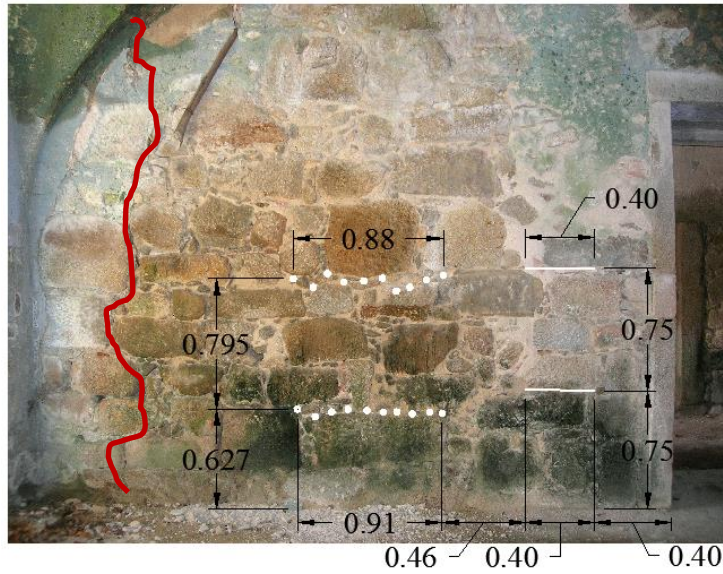
Figure 7-7 Layout of the single and double tube-jack and flat-jack tests at the San Francisco Convent with the crack location (Dimensions in meters)

7.2   Single Tube-Jack Test

The first test to be performed at the San Francisco Convent for this thesis work was the single tube-jack test. The test was performed near the center of the wall and approximately 60 cm up from the base of the wall. Ten rubber tube-jacks were used for this test. The locations for the holes were marked on the wall in preparation for drilling the holes. The holes were spaced approximately 7.5 cm from center to center to match the spacing used in the laboratory tests and modeling. In some cases, this spacing was not possible due to the irregularity of the masonry and the locations of the granite stones. The holes were labeled H_1 through H_{10} from left to right. The dimensions to each of the holes is provided in Table I-1 in Appendix I.

The movement of the masonry was measured throughout the test using six LVDTs, each with a measuring range of ±2.5 mm. The LVDTs were positioned between holes H_1 and H_2, H_2 and H_3, H_3 and H_4, H_4 and H_5, H_7 and H_8, and H_8 and H_9. The LVDTs were labeled LVDT 1 through LVDT 6 from left to right. The distances over which each LVDT measured the relative displacement of the masonry are shown in the table below.

Table 7-1 Measuring distances for the LVDTs used in the single tube-jack test at the San Francisco Convent

LVDT Number	Measuring Distance [cm]
LVDT 1	8.5
LVDT 2	19.5
LVDT 3	11.0
LVDT 4	10.5
LVDT 5	20.0
LVDT 6	12.0

The holes were drilled starting at the center of the line of holes and working outward. The mortar was very soft, allowing the holes to be drilled easily. Following the drilling, the wall

226

was allowed to stabilize for some time before the tube-jacks were inserted into the holes. Photos of the drilling and of the final test setup with the tube-jacks inserted into the holes, are shown in Figure 7-8.

(a)   (b)
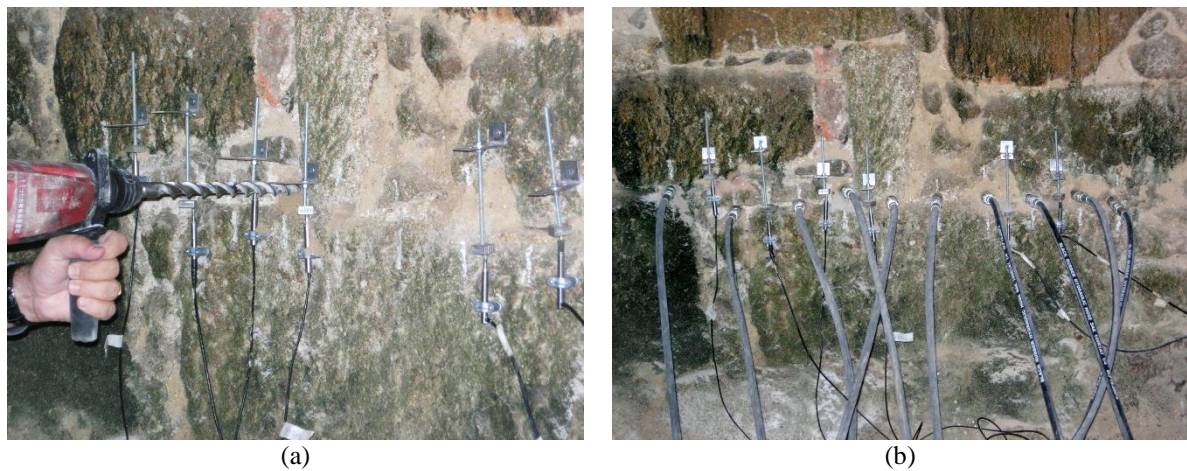
Figure 7-8 Photos of the single tube-jack test at the San Francisco Convent: (a) drilling the holes; and (b) complete setup with LVDTs attached, holes drilled, and tube-jacks inserted

The average displacement of the LVDTs throughout the test is shown in Figure 7-9. In the laboratory tests, LVDTs were placed on both the front and the back of the wall so that the relative displacements on both sides of the wall could be examined. Comparison between the front of the wall and the back of the wall often showed that the wall was not moving equally on both sides and that there were eccentricities in the loading on the wall and pressurization by the jacks. Because LVDTs were only placed on the front of the wall in this test, the movement on both sides of the wall was not observed and there is no way of knowing if the loading was equal throughout the thickness of the wall. However, due to the multiple wythes of masonry in this wall and only testing partway through the wall, LVDTs on the back of the wall might not have been affected by the test. In addition, it would have been very difficult to determine the most appropriate locations for the LVDTs on the back of the wall because the joints did not pass linearly through the thickness of the wall.
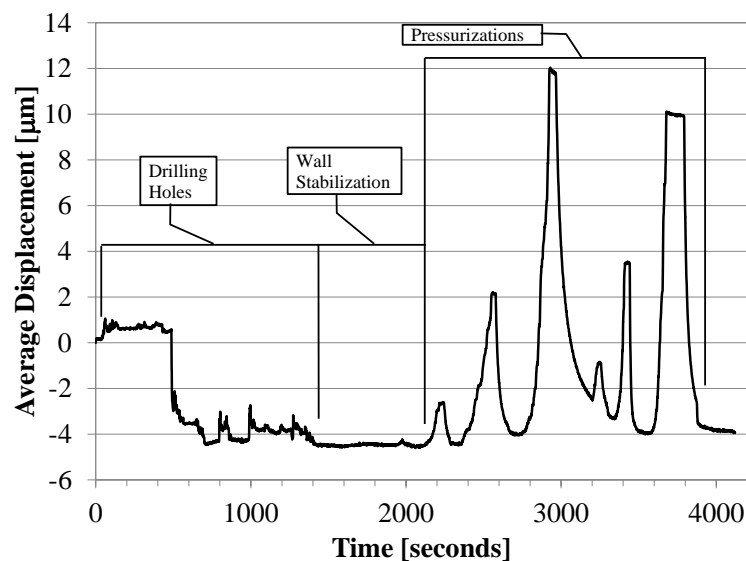
Figure 7-9 Average LVDT relative displacements during the single tube-jack test at the San Francisco Convent

The average relative displacement due to drilling the holes was approximately −4.5 μm. This is a reasonable value if it is compared to the relative displacement due to drilling the holes in the laboratory walls. This value falls between the values found when testing in the 3rd joint of the regular masonry wall, where it was −8.5 μm, and the irregular masonry wall, where it was −1.8 μm.

In order to determine the pressure that the tube-jacks applied to the masonry during the single tube-jack test, the correction factors needed to be determined. For this purpose, measurements of the holes were taken following the testing. The diameter, as measured on the surface of the wall, and the depth of each hole is provided in Table 2-1in Appendix I. Note that an additional hole, H$_{2B}$, was drilled near H$_2$ but could not be completed due to a stone blocking the drill within the wall. The depths of each of the holes in comparison with the depth of the inflated tube-jacks are shown in Figure 7-10.

Using the average hole length of 25.17 cm and the average length of the inflated portion of the tube-jacks, 17 cm, the area correction factor was determined to be 0.675. The average diameter of the holes, 22.9 mm, minus the thickness of the fabric sock, approximately 0.3 mm, was used as the outer diameter of the tube-jack in the equation to determine the pressure applied by the tube-jack on the masonry. The pressure applied by the tube-jacks on the masonry during the pressurization cycles, along with the average displacement of the LVDTs is shown in Figure 7-11.
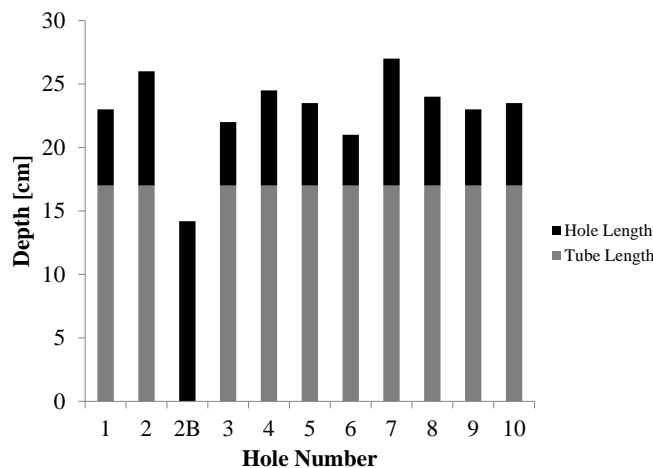
Figure 7-10 Single tube-jack test hole and inflated tube lengths

Two rounds of pressurization cycles were performed, one right after the other, with the maximum pressure applied to the masonry being slightly less than 0.4 MPa. There were some technical issues with recording the pressure and some erroneous dips in the pressure are seen right before and after each pressurization cycle. These dips were within the pressure range where the tube-jacks were still inflating to the size of the holes. Thus, they did not affect the pressure being applied to the masonry.
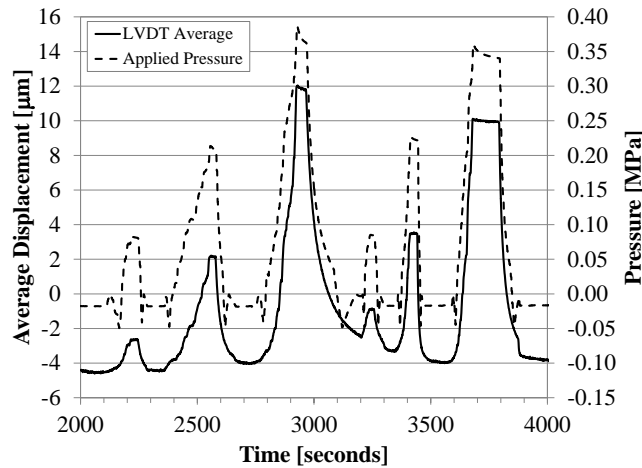
Figure 7-11 Pressure applied to the masonry and average LVDT results for the single tube-jack test

The graphs below show the average relative displacements of the LVDTs versus the pressure applied to the masonry for each of the pressurization cycles. These graphs show that the relative displacement reached approximately zero at a masonry pressure between 0.13 MPa and 0.15 MPa, depending on the pressurization cycle. Thus, the tube-jack test estimates the stress level in the wall to be between 0.13 and 0.15 MPa.
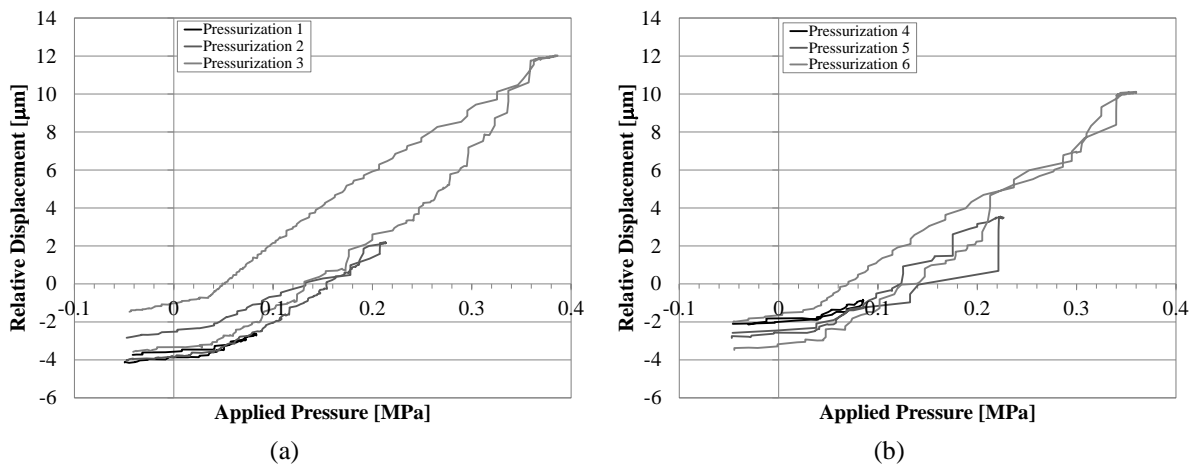
Figure 7-12 Average relative displacement versus applied pressure results for the single tube-jack test: (a) first round of pressurizations; and (b) second round of pressurizations

An additional set of pressurization cycles was conducted after one hour had passed. The relative displacements of LVDTs 1-5 over the course of the pressurization cycles are shown in Figure 7-13a. LVDT 6 did not show much movement during these cycles and is not presented or included in the averages. This graph also shows the pressure applied to the masonry for comparison. The variation in relative displacements of the LVDTs is large and shows the irregularity of the masonry.

229

(a)   (b)
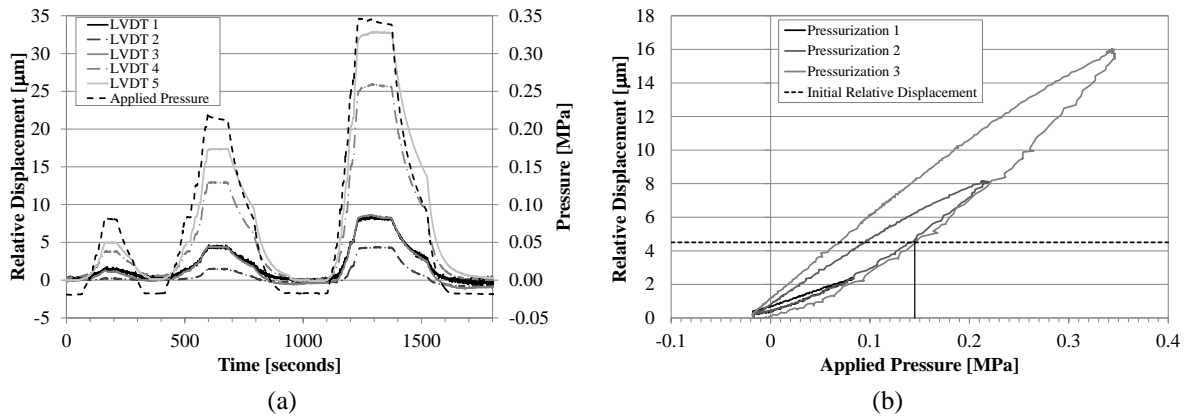
Figure 7-13 Results of the single tube-jack pressurization following the single tube-jack test: (a) relative displacements of LVDTs 1-5 during cycles; and (b) average relative displacements versus applied pressure

Figure 7-13b shows the average relative displacements of the LVDTs for the three pressurization cycles. If the initial relative displacement due to drilling the holes, approximately 4.5 µm, is subtracted from the values shown in Figure 7-13b, the restoring pressure is approximately 0.145 MPa. Thus, the same results for the estimated state of stress in each of the rounds of pressurization cycles and the final set loading curves following the same loading curve, show the consistency and repeatability of the single tube-jack test performed in a historical masonry structure. Both of the pressurizations estimate the state of stress within the expected range of 0.14 MPa – 0.17 MPa.

7.3   Single Flat-Jack Test

The single flat-jack test was performed following both the single tube-jack and double tube-jack tests at the San Francisco Convent. The slot for the single flat-jack test was created to the right of the tube-jack test and approximately 75 cm up from the base of the wall, as shown in Figure 7-7. The rectangular flat-jacks used for these tests were the same as were used in the laboratory testing. They had dimensions of 40 cm long by 10 cm deep. The jack calibration factor for the jack used in the bottom slot for the single flat-jack test was 0.77.

In the laboratory single flat-jack tests, LVDTs were used to measure the movement of the masonry after the slot was created and the flat-jack was inserted. However, the attachment of the LVDTs took extra time to set up and in some cases prevented the use of DEMEC measurements due to limited space for the measurement devices. For these reasons it was decided that only DEMEC measurements would be used in the single flat-jack test on site. Thus, three sets of DEMEC measuring points were glued to the surface of the granite units and used to measure the relative displacement of the masonry throughout the test. The point sets were located approximately at quarter points along the length of the flat-jack and were separated vertically by approximately 20 cm. Each point combination was given a label, L1 to L3, from left to right. The DEMEC points are shown in the final setup of the test with the flat-jack inserted into the slot, Figure 7-14a.

230
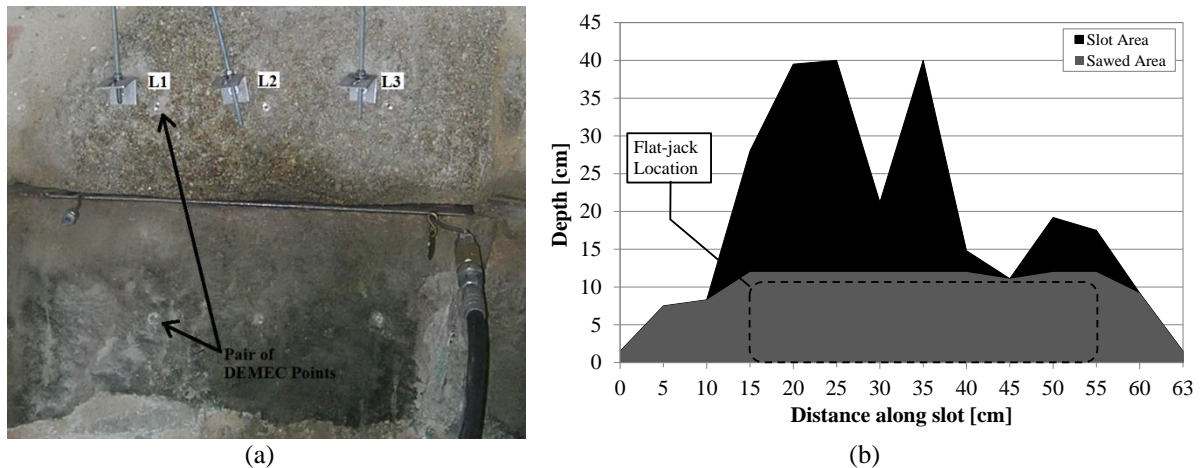
Figure 7-14 Single flat-jack test setup at the San Francisco Convent: (a) DEMEC point set locations; and (b) depth of the flat-jack slot along its length

The flat-jack slot was created using a disk saw with a radius of 12 cm, slightly deeper than the flat-jack. Following the test, the depth of the slot was measured every 5 cm along the length of the slot. The plot in Figure 7-14b shows both the total area of the slot and the area that was created due to sawing. The area of the slot created only by the saw, 0.066 m^2, was used in the calculation of the area correction factor, 0.462.

In some places along the slot there were large voids behind the slot created by the saw. Because the results of the sonic testing on this wall did not show these voids, these voids were not expected. However, the flat-jack test was performed to the right of the grid of sonic test points and the variability in the sonic results did point to large variability in the masonry.

Measurements of the movement of the masonry using the three DEMEC point sets were recorded over the course of the test at various time points. Three to five measurements were taken for each point set and then averaged for each of the time points. The standard deviation was on average 0.034 mm (CoV = 71.5%) for the measurements taken at each point set. The average relative displacement measurements along with the approximate oil pressure measured in the flat-jack system and the applied pressure, taking into account the jack calibration factor and area correction factor, are provided in Table I-2 in Appendix I. The relative displacements and applied pressure are shown in Figure 7-15. At time −1260 seconds, the DEMEC measurements were taken for the first time. Between time −1260 seconds and −240 seconds the slot was created using the saw. At time zero, the electronic data acquisition was started and the pressurization of the flat-jack begun.
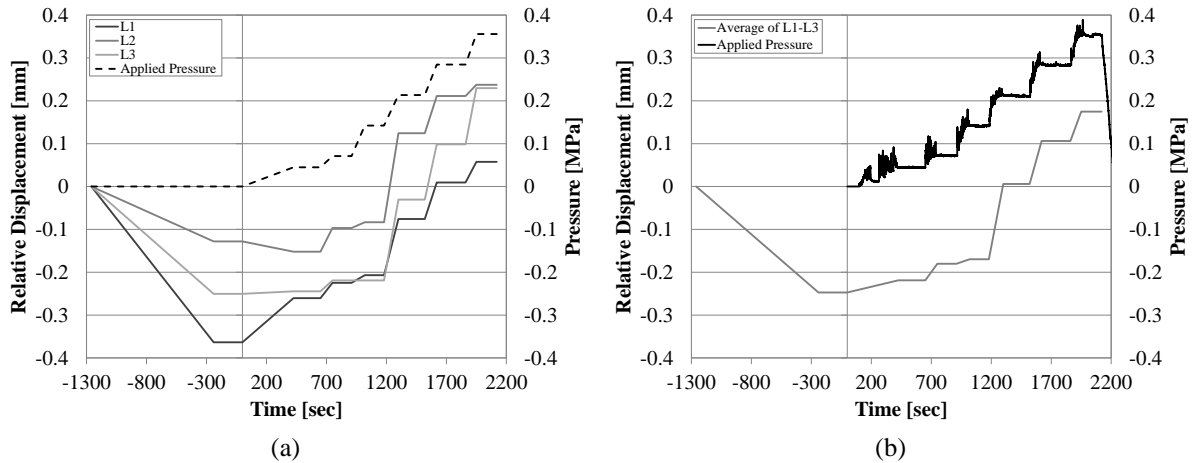
Figure 7-15 Single flat-jack test results: (a) Relative displacements for the DEMEC point sets in comparison with the approximate applied pressure throughout the test; and (b) the average relative displacements of the DEMEC point sets in comparison with the applied pressure data

In Figure 7-15a, all three of the DEMEC point sets showed negative relative displacements due to the slot being created. The average relative displacement due to sawing the slot is shown in Figure 7-15b as −0.247 mm. This average is slightly larger than the relative displacement due to sawing the slot in the regular masonry wall in the laboratory, where it was 0.18 mm.

As shown by the variability in the relative displacements for the three point sets in Figure 7-15a, the slot did not close equally along its length. The graph in Figure 7-16a shows the relative displacements of the three point sets at different applied pressure levels. The relative displacements shown for zero pressure are those resulting from sawing the slot. Unlike typical flat-jack test results, the center of the slot does not close as much as the edges of the slot due to the sawing. During the pressurization, the slot opens approximately the same amount at each of the point sets. This means that the restoring pressure varies between the three point sets.

The average relative displacement versus the applied pressure graph is shown in Figure 7-16b. At a pressure of approximately 0.21 MPa the average relative displacements are restored to zero. Thus, the single flat-jack test estimates the stress level in the masonry wall at this location to be 0.21 MPa. This estimation is very close to the assumed values of 0.14MPa – 0.17 MPa and is higher than the result from the single tube-jack test, 0.15 MPa. It is possible that both the single tube-jack and single flat-jack test results are correct. Due to the large voids in the wall behind the flat-jack test and the proximity to the door opening, it is possible that the stress level at the location of the flat-jack test is higher than at the tube-jack test location at the center of the wall where the load is distributed throughout the thickness of the wall.
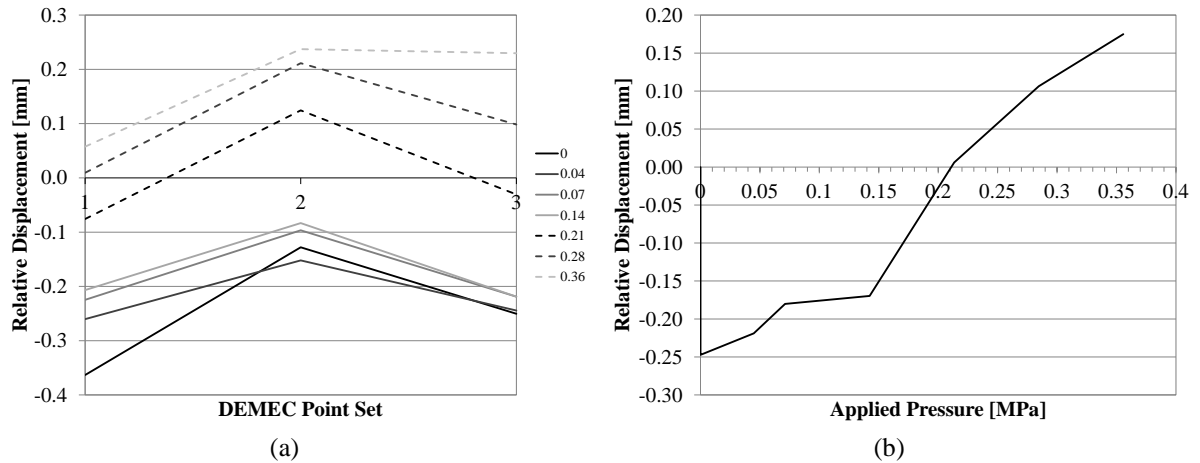
Figure 7-16 Single flat-jack test results: (a) relative displacements of the point sets as various applied pressures; and (b) average relative displacement versus applied pressure

7.4   *Double Tube-Jack Test*

The double tube-jack test was performed following the single tube-jack test at the San Francisco Convent. Locations for the second row of holes were marked on the wall above the first row of holes, approximately 80 cm above the first row, as shown in Figure 7-7. The holes were labeled H_{11}-H_{20} from left to right.

The movement of the masonry was measured throughout the test using four LVDTs, three vertical LVDTs labeled 1-3 from left to right and one horizontal LVDT labeled LVDT 4. The LVDTs used were the same LVDTs as used in the single tube-jack test and therefore had the same measurement range. The distances over which each LVDT measured the relative displacement of the masonry are shown in Table 7-2. These distances were also used to calculate the strains. The LVDTs and stands were attached to the masonry by drilling holes in the granite units and then attaching the LVDT holders and stands with screws. This was the same method of attachment as in the laboratory testing.

Table 7-2 Measuring distances for the LVDTs used in the double tube-jack test at the San Francisco Convent

LVDT Number	Measuring Distance [cm]
LVDT 1	41.5
LVDT 2	41.5
LVDT 3	41.5
LVDT 4	64

The procedure for drilling the top line of holes was the same as for the bottom line of holes. Drilling started at the center and then progressed outward, alternating sides. The drilling of the top line of holes and the LVDTs attached to the masonry between the lines of holes are shown in Figure 7-17a. The tube-jacks were inserted into the holes after some time was allowed for the wall to adjust to the holes. The final setup for the test is shown in Figure 7-17b.

(a)   (b)
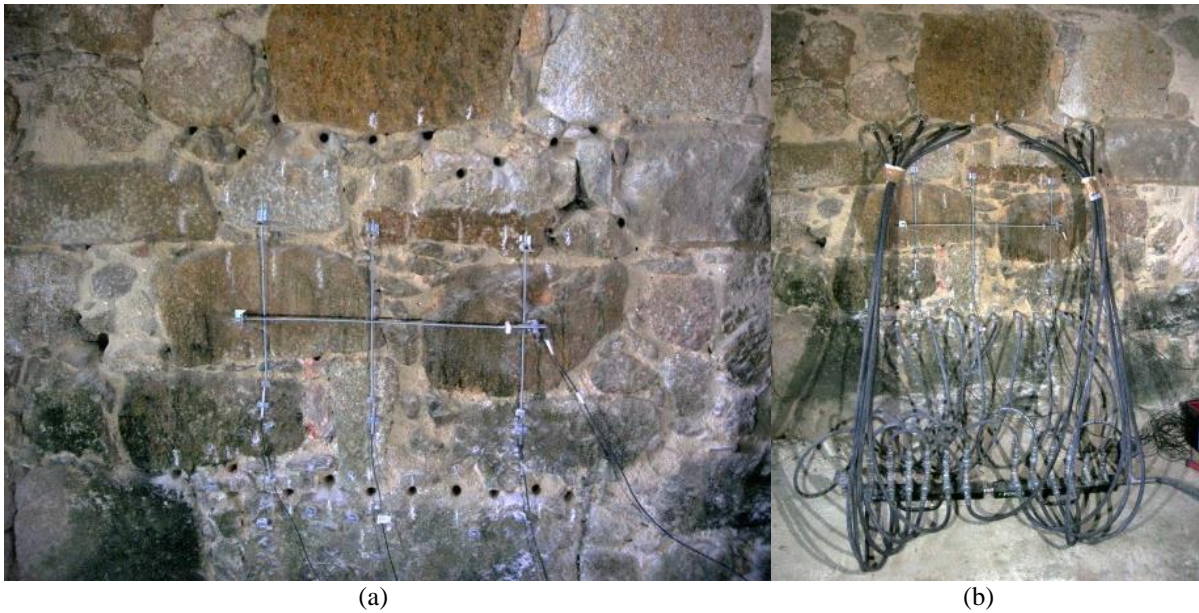
Figure 7-17 Double tube-jack test preparation at the San Francisco Convent: (a) LVDTs attached to the masonry between the two lines of holes; and (b) tube-jacks inserted in all of the holes

Following the test, the upper line of holes was measured. The dimensions of the holes in the top row are provided in Table I-3 in Appendix I. A graph showing the depths of the holes in comparison to the lengths of the inflated portion of the tube-jacks is shown in Figure 7-18. The average depth of all of the holes, including both lines of holes, was 22.75 cm. This was considered the depth of the separated specimen. The length of the separated specimen was calculated as the average of the lengths of the two lines of holes, 91.5 cm. Thus, the cross-sectional area of the separated specimen was 2081.63 cm^2.

The average diameter of all of the holes was 2.464 cm (CoV = 5.9%). Considering that ten tube-jacks were used to pressurize the masonry, the total length of the masonry pressurized by the tube-jacks was 24.64 cm. The average depth of the inflated tube-jacks was 17 cm. Thus, the cross-sectional area pressurized by the tube-jacks was approximately 419 cm^2. Dividing the cross-sectional area of the separated specimen by the cross-sectional area pressurized by the tube-jacks results in an area correction factor of 0.201. This area correction factor and equation (35) in Section 2.3.2 were used to determine the applied pressure on the masonry during the pressurization cycles.
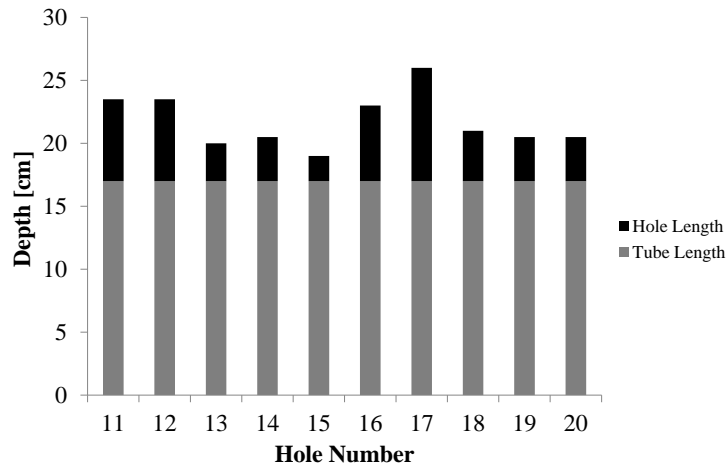
Figure 7-18 Hole and inflated tube lengths for the upper line of holes used in the double tube-jack test

Three pressurization cycles were performed during the double tube-jack test, with each cycle reaching a higher maximum pressure. The LVDT relative displacements and the pressure applied by the tube-jacks during the three pressurization cycles are presented in Figure 7-19a. Comparing the relative displacements in this test with those observed in the double tube-jack test in the regular masonry wall in the laboratory, the relative displacements are in the same range in both tests for the given applied pressures.
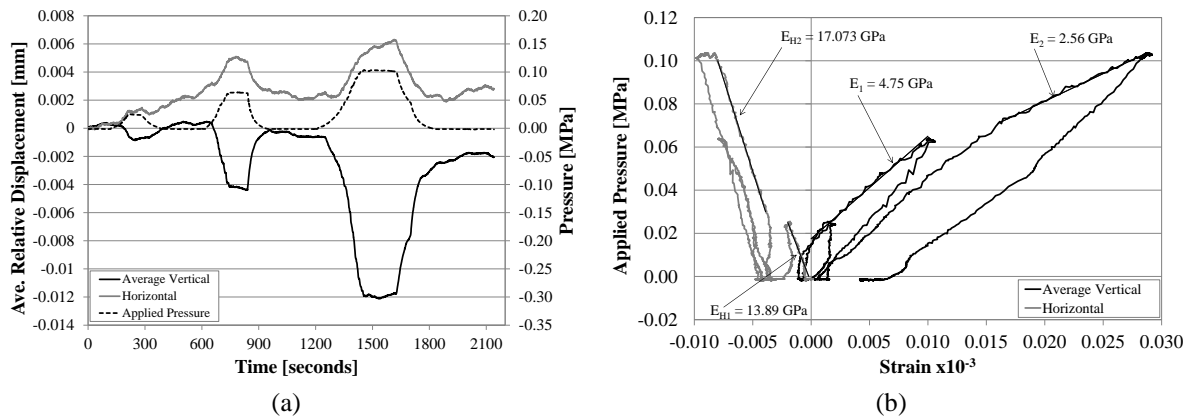
Figure 7-19 Double tube-jack test results: (a) LVDT relative displacements and applied pressure during the pressurization cycles; and (b) applied pressure versus strain

The applied pressure versus the strain results are presented in Figure 7-19b. Two trend lines were fit to the data for both the average vertical and horizontal LVDT results. The later trend line for the vertical LVDT results produces an estimate for the elastic modulus of the masonry of 2.56 GPa. This is a reasonable value for the elastic modulus of masonry of this type. Modulus of elasticity values for granite masonry with hand cut faces and sawn faces were found to be 1.2 GPa and 4.6 GPa, respectively, by Vasconcelos [5]. This elastic modulus estimation is also very similar to the elastic modulus results found for the regular masonry in the laboratory, which also had a very low strength mortar.

While the values found using the double tube-jack test results are within the probable range for this type of masonry, one factor was not yet considered, the change in stress in the masonry as a percentage of the change in applied pressure. In the numerical modeling this percentage was around 8% for the regular masonry wall, the wall with a similarly low strength mortar. Reducing the estimated modulus of elasticity to 8% for the range of values 2.56 GPa – 4.75 GPa results

235

in an estimation of 0.20 GPa – 0.38 GPa. These are very low values and are more similar to a rubble masonry [66].

A second double tube-jack test was performed approximately 45 minutes after the first test. The second test was performed with the same test setup and correction factors. The average relative displacements of the four LVDTs over the course of the test are shown in Figure 7-20a along with the applied pressure. During the 4th pressurization cycle of this test the pressure was increased to a value higher than the pressure gage could register. This resulted in the constant value shown at the highest pressure during this cycle.
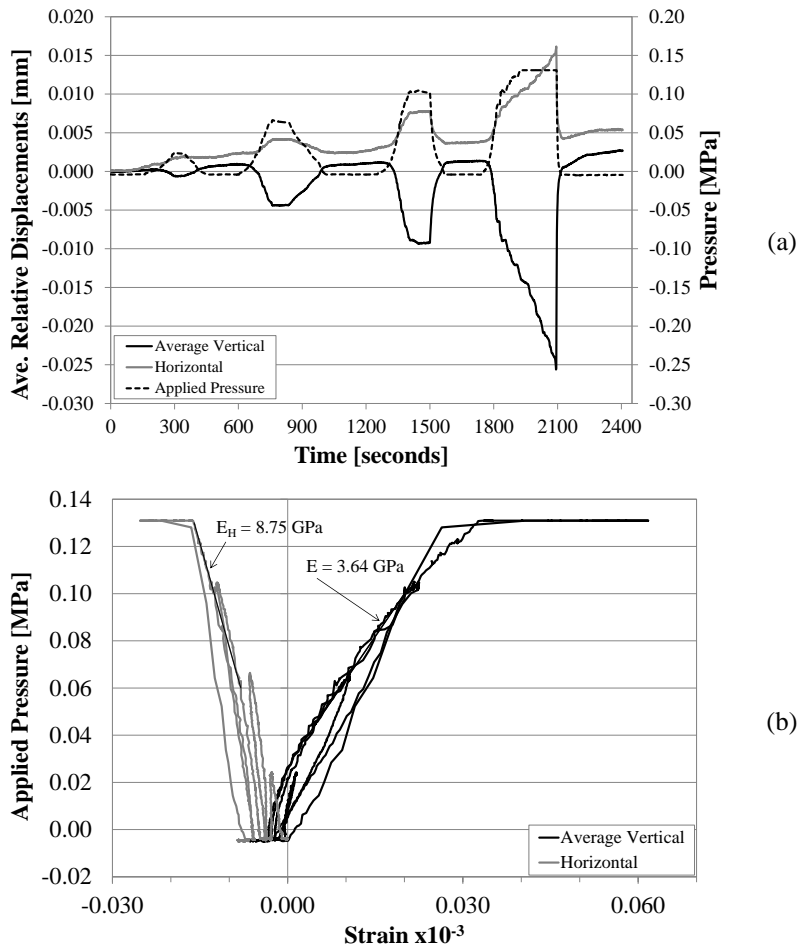
Figure 7-20 Results of the second double tube-jack test at the San Francisco Convent: (a) LVDT relative displacements and applied pressure during the pressurization cycles; and (b) applied pressure versus strain

The applied pressure versus the strain is shown in Figure 7-20b. Trend lines were fit to the results to estimate the elastic modulus of the material. The result of 3.64 GPa was between the two trend line values found in the first double tube-jack test. Reducing this value also to 8% results in an estimation of 0.29 GPa.

Finally, the Poisson ratio was calculated based on the results of both tests. The range of calculated values for the first test was 0.15 – 0.28. For the second test, the Poisson ratio was calculated to be 0.42. The results of the first test compare well with the Poisson ratio found using the sonic tests, 0.23 [69].

7.5   Double Flat-Jack Test

The double flat-jack test was the last test to be performed as part of this thesis work on the San Francisco Convent. It was performed following the single flat-jack test and the slot created for the single flat-jack test was used as the bottom slot for the double flat-jack test. The location for the test was shown in Figure 7-7. The upper slot was located approximately 75 cm above the first slot. This is a little bit farther apart than the standard recommends, however, this location allowed two horizontal mortar joints to be within the separated specimen and the distance between the jacks to be similar to the distance between the equivalent flat-jacks in the double tube-jack test.

One horizontal LVDT and three vertical LVDTs were used to measure the relative displacements of the masonry between the two flat-jacks throughout several pressurization cycles. The vertical LVDTs were labeled LVDT 1 through LVDT 3 from left to right. The horizontal LVDT was labeled LVDT 4. The distances over which each LVDT measured the relative displacement of the masonry are shown in Table 7-3. These distances were used to calculate the strains. Attachment of the LVDT holders and stands was the same as in previous tests.

Table 7-3 Measuring distances for the LVDTs used in the double flat-jack test at the San Francisco Convent

LVDT Name	LVDT Number	Measuring Distance [cm]
lvdt_173782	LVDT 1	42.2
lvdt_173778	LVDT 2	41.8
LVDT_61531	LVDT 3	41.7
LVDT_125473	LVDT 4	48.5

The same circular saw was used to create the upper slot as was used for the lower slot. Water was used to reduce the amount of dust during the sawing but, as Figure 7-21a shows, there was still quite a bit of dust in the air. Following the creation of the slot, the upper flat-jack was inserted into the slot as shown in Figure 7-21b and the LVDTs were positioned in the holders. The final test setup is shown in Figure 7-21c.

(a)   (b)   (c)
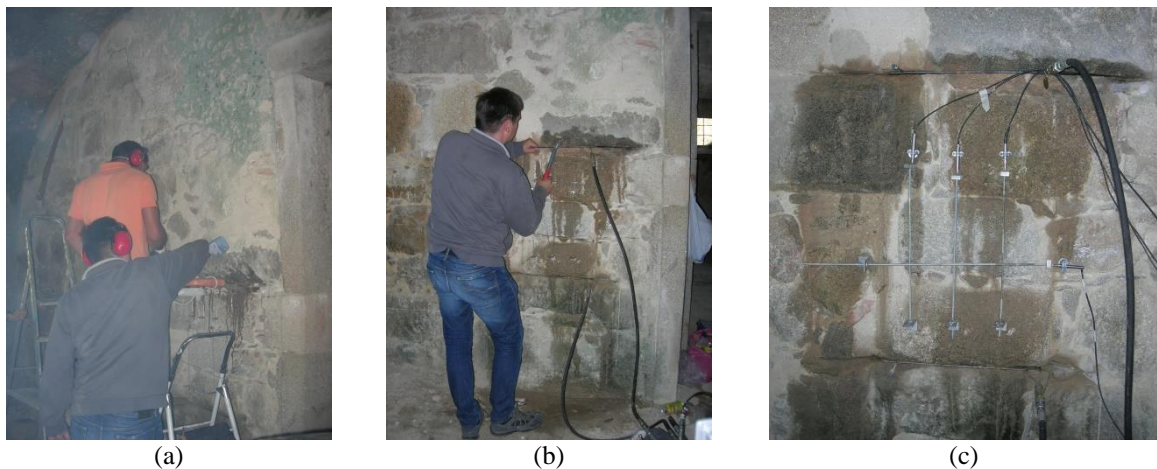
Figure 7-21 Double flat-jack test preparation at the San Francisco Convent: (a) sawing the upper slot; (b) inserting the upper flat-jack; and (c) final setup with LVDTs attached and positioned

Following the test, the depth of the upper slot was measured every 5 cm along the length of the slot. The plot in Figure 7-22 shows both the total area of the slot and the area that was created due to sawing. The area of the slot created only by the saw was estimated to be 0.083 m². Dimensions of the upper flat-jack were the same as the lower flat-jack. The total surface area of the two flat-jacks, 0.0608 m², was divided by the total sawed area of the two slots, 0.149 m², to determine the area correction factor, 0.408. The jack calibration factor for the upper jack was 0.8. This factor was averaged with the calibration factor of the lower jack, 0.77, to determine the double flat-jack calibration factor, 0.785.
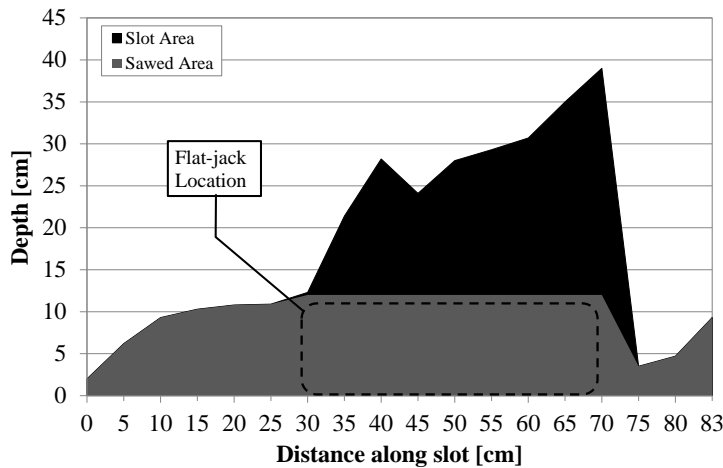
Figure 7-22 Total slot area and slot area created by the saw for the upper slot in the double flat-jack test

Several pressurization cycles were performed during the double flat-jack test, with each cycle reaching a higher maximum pressure. The LVDT relative displacements and the pressure applied by the flat-jacks during the pressurization cycles are presented in Figure 7-23. The relative displacements in this test can be compared with those observed in the double flat-jack test in the regular masonry wall in the laboratory (presented in section 6.2.4) since both walls have a very soft mortar. The relative displacements are much greater in the San Francisco Convent test than in the regular masonry wall test at the same applied pressure levels. Greater displacements do not automatically translate into lower stiffness values, however, due to the differences in measuring distances for each test.
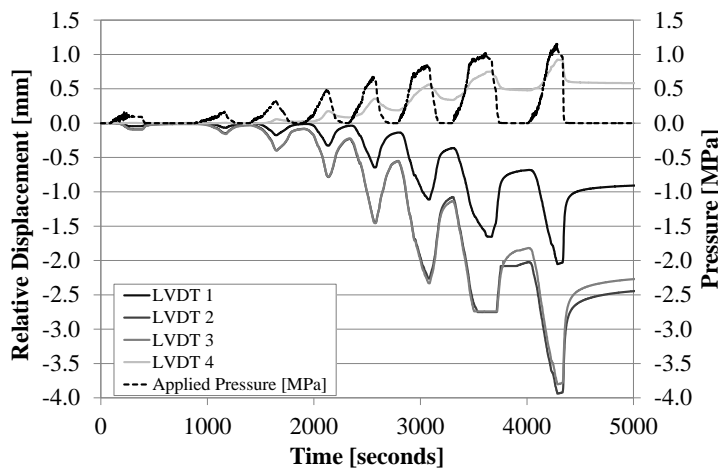
Figure 7-23 LVDT relative displacements and applied pressure during the pressurization cycles of the double flat-jack test at the San Francisco Convent

The applied pressure versus the strain results are shown in Figure 7-24. Since the results for the double tube-jack test were so close to the result of the laboratory test on the regular masonry wall, these double flat-jack test results were compared to the results of the double flat-jack test on the regular masonry wall in the laboratory as well (see section 6.2.4). The reloading elastic modulus calculated for the vertical LVDTs in this test, 0.413 GPa, is in the same range as the reloading modulus for the front vertical LVDTs in the laboratory test, 0.67 GPa. Even closer are the results for the second curve, where the elastic modulus is 0.103 GPa for the San Francisco Convent test and 0.14 GPa for the regular masonry wall laboratory test considering only the front LVDTs.

In the numerical analysis of the double flat-jack tests in the laboratory walls, the change in stress between the flat-jacks was found to be approximately 80% of the applied pressure. If 80% is taken of the reloading elastic modulus found in these in-situ tests, the result is an elastic modulus of 0.33 GPa. These results test are in the middle of the range found in the double tube-jack test when the change in stress is considered to be 8% of the change in pressure, a range of 0.20 GPa – 0.38 GPa. However, all of these results are very low for this type of masonry [5] and are more similar to a rubble masonry with lime mortar [66].
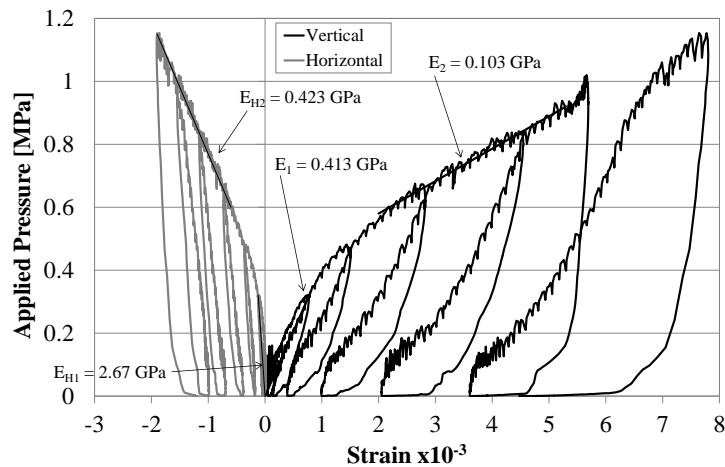
Figure 7-24 Applied pressure versus strain results for the double flat-jack test at the San Francisco Convent

The comparisons between the results of the double flat-jack tests at the San Francisco Convent and the regular masonry wall in the laboratory are only between the LVDTs on the front face of the wall. The average reloading modulus results for the LVDTs on both sides of the wall in the laboratory double flat-jack test were much higher, 2.0 GPa. If the trend is the same in the in-situ testing then the actual elastic modulus of the masonry could be higher than shown by the double flat-jack test results.

The Poisson ratio estimation for the masonry, based on the double flat-jack test results is in the range of 0.15 – 0.24, which is also similar to the result found using the sonic tests.

7.6   Conclusions

In-situ tube-jack and flat-jack tests were performed at the San Francisco Convent in Braga, Portugal. The single tube-jack and flat-jack tests estimated the state of stress to be approximately 0.15 MPa and 0.21 MPa respectively in the southern wall of the Fig Tree Room. The expected state of stress based on loading from the granite masonry in the wall and brick masonry wall above was determined in a simple model and was in the range of 0.14 MPa –

0.17 MPa. Both, the tube-jack and flat-jack test results, were close to the expected value and it is possible that they are both correct given the large variability in the masonry and the locations of each of the tests.

Double tube-jack and flat-jack tests were used to estimate the elastic modulus of the masonry. The estimate for the reloading elastic modulus was in the range of 0.20 GPa – 0.38 GPa, considering the change in stress to be 8% of the change in pressure, in the second double tube-jack test and 0.33 GPa, considering the change in stress to be 80% of the change in pressure, in the double flat-jack test. These values are very low for a granite masonry and are closer to values found for a rubble masonry with lime mortar.

The Poisson ratio was estimated from the double tube-jack test to be in the range of 0.15 – 0.28 and from the double flat-jack test to be in the range of 0.15 – 0.24. Both of these results are in the range typically found for this type of masonry [5] and were comparable to the value found with the sonic test results, 0.23.

Overall, the single and double tube-jack tests performed at the San Francisco Convent were successful and produced consistent results. Considering the change in stress as a percentage of the change in pressure applied by the tube-jacks and flat-jacks in the double jack tests proved to be an important part of analyzing the test data and resulted in comparable results between the two methods.

8.   CONCLUSIONS AND FUTURE WORK

This thesis work developed the tube-jack test system from a theoretical idea to a functioning enhanced non-destructive test that was successfully used in-situ on a historical masonry structure to estimate the state of stress and the mechanical characteristics of the masonry. The work began with a thorough literature review of traditional non-destructive and minor-destructive test methods for diagnosis of historical masonry structures. The phases of the tube-jack test development, and main chapters of this thesis, included an initial tube-jack system development, design and characterization of masonry walls for testing the system in the laboratory, tube-jack and flat-jack testing in these walls to compare the method to the traditionally used flat-jack method, numerical analysis to understand how each of the tests were affecting the masonry, and a final set of in-situ tests on a historic masonry structure. The conclusions of each of these phases of development are presented in this concluding chapter along with recommendations for future research.

8.1   *Tube-Jack System Development*

The tube-jack system development began with the testing of three tube-jack prototypes made of PVC, rubber, and latex. Testing in a small two-block specimen led to the conclusions that the PVC prototype was not deformable enough, the rubber and latex prototypes required some form of confinement, and that the test specimen was too small to adequately test the tube-jack system. These initial tests also revealed that the relative displacements resulting from drilling the holes would be very small and sensitive LVDTs or other measuring devices would be required in these tests to accurately measure the relative displacements.

To confine the rubber and latex tube-jacks, tubular knitted fibrous structures, or tube socks, were added to the tube-jack design. Several rounds of inflation tests with these tube socks helped to determine the best size and fabric construction for the tube-jacks. The inflation tests also showed that there were three phases of inflation including; filling the tube-jack with fluid, inflation of the tubing material only, and expansion of the tubing and sock together. It was later found in the laboratory testing phase that the tube-jacks were mainly inflating to the second phase where only the tubing material was engaged. Thus, the rubber tubing was also characterized in tension.

Finally, full tube-jack system tests were performed in some larger masonry walls to check how the completed system would work. These tests revealed that the air pressure system was not adequate and the system was switched to a water pressure system that reduced leaks and could maintain high pressures throughout the tests.

8.2   *Mechanical Characterization of the Masonry*

Testing the tube-jack prototypes in small masonry specimens in the tube-jack system development showed that larger masonry walls would be required to test the complete system. In this phase of the thesis work, three masonry walls were designed based on other researchers' studies of traditional Portuguese masonry typologies. The geometries of these three walls were characterized as having regular, semi-irregular and irregular typologies. The masonry consisted of granite stones and a cement-lime mortar.

To determine properties of the masonry actually constructed, mechanical characterization of each of the constituent materials and small masonry wallet specimens was carried out. Through Young's modulus and compressive tests of granite cores taken from the same granite as used for the walls, the elastic modulus of the granite, 30 GPa, and compressive strength, 65 MPa, were determined. These values were in the ranges found by other researchers [5]. Two different mortars were used for the walls. Compressive tests on mortar cylinders, cast at the time of construction of the walls, showed the mortar in the regular masonry wall to be very weak, having an elastic modulus of 260 MPa and a compressive strength of 0.327 MPa. This mortar was most like mortars found in historic structures, which tend to be low in strength and stiffness [66]. The semi-irregular and irregular masonry walls had a mortar with an elastic modulus of 1017 MPa and a compressive strength of 3.08 MPa.

Young's modulus and compression tests were also performed on small masonry wallets representing the three different masonry typologies. The Young's modulus results for the reloading curves were very similar to the results of the mortar characterization tests, showing that the mortar characteristics were the main contributor to the stiffness of the masonry. These reloading results were used to compare with the results of the double tube-jack and flat-jack tests in the masonry walls since those tests would be mainly reloading the masonry. The compression tests showed that the masonry has a compressive strength beyond 4.17 MPa.

8.3   Tube-jack and Flat-jack Testing in Laboratory Walls

The tube-jack test system developed in the first phase of the thesis was tested for the first time in the masonry walls designed and characterized in the second phase of the thesis. Flat-jack tests were also performed next to the tube-jack tests in these walls to compare the two test methods and determine which was best suited to estimate the state of stress and mechanical characteristics of this typology of large unit masonry. The tube-jack and flat-jack testing in the laboratory walls helped to further develop the tube-jack test system, refine the procedure for performing these tests, provide insights into how the masonry is behaving during these tests, and define the applicability of each type of test for this typology of masonry.

At the end of the tube-jack system development phase, two tube-jack prototypes were still being considered for the system. The testing in the regular masonry wall showed that the rubber tube-jack was more consistent in pressurizing the masonry and it was selected for the final system.

Other important improvements and recommendation for performing both tube-jack and flat-jack tests were discovered through these laboratory tests. The monitoring of the relative displacement of the wall, during the hole drilling and afterward, showed that the redistribution and stabilization of the wall takes some time. If the tube-jack or flat-jack test was started too early, the stabilization of the masonry was still occurring and the error of the test was increased. One result of performing multiple tests in the same wall was that the tests affected each other and there was not enough space to keep the tests away from the edges of the wall, which also affected the tests. Placement of tests, when they are performed in the field, should be far enough apart not to affect each other and far away from openings or edges to prevent edge effects. Another finding was that the pressure applied by both the tube-jacks and flat-jacks varied through the thickness of the wall. Thus, it is important in single wythe masonry that displacements be recorded on both sides of the wall to obtain the overall movement of the masonry.

Difficulties found during the tube-jack and flat-jack testing in the laboratory walls helped to define which of the two test methods was better suited for each masonry typology. Lower strength and stiffness mortar characteristics made for more effective and efficient tube-jack tests. In the regular wall, where the mortar strength and stiffness were low, the relative displacements due to drilling the holes were greater than in the semi-irregular and irregular walls, making their measurement easier. The strength of the mortar in the semi-irregular and irregular walls also made it difficult to drill the holes, resulting in extremely lengthy tests. For the flat-jack tests, the size of the units was an issue, since the size of the flat-jacks could not be expanded. The flat-jack slots caused rotation of the units and the flat-jacks were only able to pressurize half of the thickness of the walls.

Finally, the tube-jack and flat-jack tests in the laboratory gave a first look into how the masonry behaves during these tests. Results of the double tube-jack and double flat-jack tests showed two slopes for the pressurization curves. It was hypothesized that the first slope was the reloading of the masonry and the second slope was loading the masonry beyond a state of stress that it had previously been exposed to. If this hypothesis is correct, then double tube-jack and flat-jack tests could be able to estimate the maximum stress level that the masonry has been exposed to in its lifetime. One final conclusion was that the results from the double tube-jack and flat-jack tests overestimated the elastic modulus of the masonry in comparison with the results of the Young's modulus tests on the masonry wallets. This finding was further explored in the numerical analysis.

8.4   Numerical Analysis

The numerical analysis of the tube-jack and flat-jack tests performed in the three masonry walls in the laboratory served a very important role in helping to determine if the laboratory results were accurate and understand how the tests were pressurizing the surrounding masonry.

Modeling of a Young's modulus test on the masonry wall, not only showed if the models were reflecting the properties of the actual masonry, but also provided key insights into how the placement of LVDTs makes a difference in masonry testing. It was found that the percentage of mortar between the connection points of an LVDT makes a difference in the Young's modulus value recorded by that LVDT. Therefore, in order to compare elastic moduli between two Young's modulus tests, the percentage of mortar that the LVDTs measure over must be the same. Curves were fit to the Young's modulus results for numerous virtual LVDTs measuring over various percentages of mortar, for each typology of wall. It was clear that the stiffness of the mortar affected these curves but it was unclear as to whether the typology of the wall affected these curves.

The modeling of the single tube-jack test showed that the line of tube-jacks works in a similar way to a flat-jack and can be considered an equivalent flat-jack as originally hypothesized. Pressurization of the tube-jacks results in a change in stress in the masonry, above the equivalent flat-jack, of less than 10% of the pressure applied. Regardless, the idealized single tube-jack and flat-jack tests were able to restore the relative displacements, caused by opening the holes or slot, to zero, and estimate the state of stress accurately. Modeling of these tests also revealed that an angle in the flat-jack and nonlinearity of the line of tube-jacks likely lead to errors and variation in the results.

The double tube-jack and flat-jack tests overestimated the stiffness of the masonry in comparison with the Young's modulus tests on the masonry wallets. This confirmed the same

conclusion found in the laboratory tests. The numerical analysis provided a reason for this overestimation. The change in stress between the equivalent flat-jacks or between the flat-jacks was less than the pressure applied. In the double tube-jack tests, the change in stress was less than 10% of the pressure applied by the tube-jacks. In the double flat-jack test, the change in stress was about 80% of the pressure applied by the flat-jacks. It is hypothesized that the connection of the masonry between the jacks to the surrounding masonry influences this percentage.

8.5   *In-situ Testing*

The culmination of the thesis was the successful in-situ testing of the single and double tube-jack and flat-jack tests on a historic masonry structure. The San Francisco Convent was selected for this testing because of its similar masonry typology to that of the masonry walls studied in the laboratory and because a previous diagnostic research and testing campaign had already been carried out. Previous research included sonic testing in the same location as the tube-jack and flat-jack were to be performed. The sonic test results provided estimations of the Young's modulus and Poisson ratio that could be compared with the results of the double tube-jack and flat-jack tests.

The single tube-jack and flat-jack tests estimated the state of stress in the masonry to be 0.15 MPa and 0.21 MPa, respectively. The tube-jack result was within the state of stress range estimated using a simple finite element model of the wall, 0.14 – 0.17 MPa, and the flat-jack result was slightly over the range. Both results could be correct due to the variability in the masonry and unknown loads acting on the wall, namely the fig tree on the ceiling.

The double tube-jack and double flat-jack test results were comparable when consideration was given to the likely change in stress due to the change in applied pressure in both tests. For the double tube-jack test, the estimate for the reloading elastic modulus was in the range of 0.20 GPa – 0.38 GPa, considering the change in stress to be 8% of the change in pressure. For the double flat-jack test, the elastic modulus was estimated at 0.33 GPa, considering the change in stress to be 80% of the change in pressure. While both of these estimations are low for a granite masonry, the low strength of the mortar and the consistency between the two results suggest that the estimation is correct.

Finally, the Poisson ratio was determined using the double tube-jack and double flat-jack test results. The expected value based on the sonic test results, 0.23, was within the Poisson ratio estimated ranges for both the double tube-jack and double flat-jack tests.

In conclusion, the developed tube-jack test system was applied to a historical masonry structure and was able to estimate the state of stress in the masonry, the elastic modulus of the masonry, and the Poisson ratio of the masonry with the same amount of accuracy as the traditional flat-jack test method, while preventing any damage to the historic masonry units. The tube-jack test method is a promising enhanced non-destructive test method that, through further research and development, will likely be able to provide an alternative to flat-jack testing for irregular and large unit masonry diagnosis.

8.6   Future Research

A significant amount of work was put into this thesis; however, as knowledge was obtained new questions arose. Here is a summary of some interesting aspects of the tube-jack and flat-jack tests that have yet to be studied and the developments that have yet to be made.

Testing of the tube-jacks in the laboratory showed that their design has not yet been perfected. The design could still be improved to be more resistant to rupture and more durable. Only one length of tube-jack was tested. Masonry walls come in many sizes and it would be beneficial to determine if the tube-jacks can be effective with different lengths and sizes. The tube-jack tests were easier to perform when the mortar was weaker. Since only one of the laboratory walls had this type of mortar, it would be best to perform more laboratory tests on masonry walls with this type of mortar. If possible, the size of the walls should be made larger to avoid edge effects and to allow more space between tests in the same wall. Laboratory tests could also be performed on multi-wythe masonry walls.

Numerical modeling of some of the tube-jack and flat-jack tests suggested that an angle in the flat-jack and nonlinearity of the line of tube-jacks could result in errors and larger variations in the results. These aspects of the tests should be further investigated. Additional numerical modeling could be done in three-dimensional models of single and multi-wythe walls. These models would shed light on the distribution of stresses in the masonry and pressures applied by the tube-jacks and flat-jack through the thickness of the wall. Along with the distribution of stresses, the difference in displacements from one side of the wall to the other could be studied, especially for slender or single wythe walls.

Numerical modelling results also found that the percentage of mortar between the connection points of an LVDT makes a difference in the Young's modulus result for that LVDT. This should be researched further and a parametric study should be done to determine which variables affect the Young's modulus versus mortar percentage curves.

Finally, a parametric study could also be done to determine what variables affect the change in stress in the masonry as a result of the applied pressure in both the double tube-jack and double flat-jack tests. The result of this future study could change how traditional double flat-jack test results and double tube-jack test results are analyzed.

REFERENCES

[1] P. P. Rossi, "Non-destructive Evaluation of the Mechanical Characteristics of Masonry Structures," in *Nondestructive Evaluation of Civil Structures and Materials*, Boulder, Colorado, 1990.

[2] *RILEM Recommendation MDT.D.4: In-situ stress tests based on the flat-jack, 2004.*.

[3] *RILEM Recommendation MDT.D.5: In-situ stress-strain behavior tests based on the flat-jack, 2004.*.

[4] L. Binda and C. Tiraboschi, "Flat-jack test: A slightly destructive technique for the diagnosis of brick and stone masonry structures," Dept. Of Structural Engineering, Politecnico of Milano, Milan, 1999.

[5] G. Vasconcelos, "Experimental investigations on the mechanics of stone masonry: Characterization of granites and behavior of ancient masonry shear walls, PhD Thesis," Universidade do Minho, 2005.

[6] Z. Sharafi, "Enhanced Flat-Jack Tests for Irregular Walls," Guimaraes, 2009.

[7] S. Hum-Hartley, "Nondestructive Testing for Heritage Structures," *Bulletin of the Association for Preservation Technology,* vol. 10, no. 3, pp. 4-20, 1978.

[8] J. Scrivener, "Old Masonry Buildings: Earthquake Performance and Meterial Testing," National Research Council Canada, 1992.

[9] M. P. Schuller, R. H. Atkinson and J. L. Noland, "Structural Evaluation of Historic Masonry Buildings," *APT Bulletin,* vol. 26, no. 2/3, pp. 51-61, 1995.

[10] L. Binda and G. Cardani, "Methodology for on site evaluation of physical and mechanical properties of historic masonry," in *Structural Engineers World Congress*, Como - Villa Erba, 2011.

[11] G. R. Kingsley, "Evaluation and Retrofit of Unreiforced Masonry Buildings," in *Third National Concrete and Masonry Engineering Conference*, San Francisco, CA, June, 1995.

[12] International Conference of Building Officials, "Uniform Building Code," Whittier, CA, 1994.

[13] F. Chagneau and M. Levasseur, "Controle des materiaux de construction par dynamostratigraphie," *Mater. Struct.,* no. 22, 1989.

[14] N. Gucci and A. Moretti, "Un dispositivo per misurare in situ la resistenza delle malte," *Boll. Ingegneri Toscana,* no. 9, 1989.

[15] N. Gucci and R. Barsotti, "A non-destructive technique for the determination of mortar load capacity in situ," *Materials and Structures,* no. 28, pp. 276-283, 1995.

[16] R. Netting, "The Electromagnetic Spectrum," NASA, [Online]. Available: http://science.hq.nasa.gov/kids/imagers/ems/index.html. [Accessed 20 06 2012].

[17] "Module 3: Waves and the Electromagnetic Spectrum," Study Blue, 16 01 2014. [Online]. Available: https://www.studyblue.com/notes/note/n/module-3-waves-and-the-electromagnetic-spectrum/. [Accessed 15 08 2015].

[18] "Tontechnik-Rechner - sengpielaudio," [Online]. Available: http://www.sengpielaudio.com/calculator-wavelength.htm. [Accessed 15 08 2015].

[19] L. Binda, Role of a Rilem Committee: Calibration of Proposed Test Methods, Padua: RILEM, 1995.

[20] L. Miranda, "Ensaios acústicos e de macacos planos em alvenarias resistentes," Faculdade de Engenharia, Universidade do Porto, Porto, Portugal, 2011.

[21] F. J. Richart, J. Hall and R. Woods, "Vibrations of soils and foundations," Prentice-Hall, Inc., Englewood Cliffsm, 1970.

[22] L. Binda, A. Saisi and C. Tiraboschi, "Application of sonic tests to the diagnosis of damaged and repaired structures," *NDT&E International,* vol. 34, pp. 123-138, 2001.

[23] F. da Porto, M. R. Valluzzi and C. Modena, "Investigations of the knowledge of multi-leaf stone masonry walls," in *Proceedings of the First International Congress on Construction History*, Madrid, Spain, 2003.

[24] L. Binda, A. Saisi, C. Tiraboschi, S. Valle, C. Colla and M. Forde, "Application of sonic and radar tests on the piers and walls of the Cathedral of Noto," *Construction and Building Materials,* vol. 17, pp. 613-627, 2003.

[25] C. Colla, P. Das, D. McCann and M. Forde, "Sonic, electromagnetic and impulse radar investigation of stone masonry bridges," *NDT&E International,* vol. 30, no. 4, pp. 249-254, 1997.

[26] A. Anzani, L. Binda, A. Carpinteri, S. Invernizzi and G. Lacidogna, "A multilevel approach for the damage assessment of Historic masonry towers," *Journal of Cultural Heritage,* vol. 11, pp. 459-470, 2010.

[27] N. Carino, "The Impact-Echo Method: An Overview," Building and Fire Research Laboratory; National Institute of Standards and Technology, Gaithersburg, MD, USA, 2001.

[28] F. da Porto, M. R. Valluzzi and C. Modena, "Use of Sonic Tomography for the Diagnosis and the Control of Intervention in Historic Masonry Buildings," in *International Symposium (NDT-CE 2003): Non-Destructive Testing in Civil Engineering 2003*, 2003.

[29] L. Binda, A. Saisi and C. Tiraboschi, "Investigation procedures for the diagnosis of historic masonries," *Construction and Building Materials ,* no. 14, pp. 199-233, 2000.

[30] F. Casarin, M. Valluzzi, F. da Porto and C. Modena, "Structural Monitoring for the Evaluation of the Dynamic Response of Historical Monuments," in *on Site Assessment of Concrete, Masonry and Timber: International Rilem Conference*, Como Lake, Italy, 2008.

[31] *Standard Test Method for In Situ Compressive Stress within Solid Unit Masonry, Estimated Using Flat-jack Measurements, ASTM Standard C 1196-04, 2004.*.

[32] I. Vrkljan and B. Kavur, "Experience gained in rock mass deformability testing by large flat jacks," *Rock Mechanics - a Challenge for Society,* pp. 191-198, 2001.

[33] *Standard Test Method for In Situ Measurement of Masonry Deformability Properties, Using the Flat-jack Method, ASTM Standard C 1197-04, 2004..*

[34] P. Gregorczyk and P. B. Lourenço, "A Review on Flat-Jack Testing," *Engenharia Civil - UM,* no. 9, pp. 39-50, 2000.

[35] G. R. Kingsley and J. L. Noland, "A note on obtaining in-situ load-deformation properties of unreinforced brick masonry in the United States using flat jacks," in *Proc. Second Joint USA-Italy Workshop on Evaluation and Retrofit of Masonry Structures*, Los Angeles, 1987.

[36] L. Binda, L. Cantini, G. Cardani, A. Saisi and C. Tiraboschi, "Use of Flat-Jack and Sonic Tests for the Qualification of Historic Masonry," in *North American Masonry Conference*, St. Louis, Missouri, USA, 2007.

[37] L. Binda, C. Modena, G. Baronio and S. Abbaneo, "Repair and investigation techniques for stone masonry walls," *Construction and Building Materials,* vol. 11, no. 3, pp. 133-142, 1997.

[38] M. Cucchi, C. Tiraboschi, M. Antico and L. Binda, "Optical System for Real-Time Measurement of the Absolute Displacements Applied to Flat Jack Test," in *Structural Analysis of Historical Constructions*, Wroclaw, Poland, 2012.

[39] "A Method of Measuring the Stress in the Concrete". Japan Patent JP58097636A-1, 1983.

[40] A. Dean and R. Beatty, "Rock stress measurements using cylindrical jacks and flat jacks at North Broken Hill Limited," Broken Hill Mines Monograph No 3:1-8, Melbourne: Australian Inst. Min Metal, 1968.

[41] A. Galybin, A. Dyskin and R. Jewell, "A measuring scheme for determining in situ stresses and moduli at large scale," *Int. J. Rock Mech. Min. Sci. ,* vol. 34, no. 1, pp. 157-162, 1997.

[42] C. M. Piccirilli, "Cylindrical Jack". Italy Patent ITRM960219A1, 1996.

[43] C. M. N. V. d. Almeida, "Análise do Comportamento da Igreja do Mosteiro da Serra do Pilar sob a Acção dos Sismos: PhD Thesis," FEUP, Porto, 2000.

[44] L. F. Ramos, E. Manning, F. Fernandes, R. Fangueiro, M. Azenha, J. Cruz and C. Sousa, "Tube jack testing for irregular masonry walls: prototype development and testing," *NDT&E,* 2012.

[45] E. J. Hearn, "Ch. 10: Thick cylinders," in *Mechanics of Materials 1: An Introduction to the Mechanics of Elastic and Plastic Deformation of Solids and Structural Materials - 3rd ed.*, Woburn, MA, USA, Butterworth-Heinemann, 1997, pp. 215-253.

[46] L. F. Ramos and Z. Sharafi, "Tube-jack Testing for Irregular Masonry Walls: First Studies," *Advanced Materials Research,* Vols. 133-134, pp. 229-234, 2010.

[47] S. Moreira, L. Ramos, D. Oliveira, R. Fernandes, J. Guerreiro and P. Lourenço, "Experimental seismic behavior of wall-to-half-timbered wall connections," in *8th*

International Conference on Structural Analysis of Historical Constructions, Wroclaw, Poland, 2012.

[48] C. Sousa, "Concrete behavior under restrained shrinkage: Proposal of a new test setup," MSc Thesis. University of Minho, 2011.

[49] E. Manning, L. Ramos, F. Fernandes, C. Sousa and M. Azenha, "Tube-Jack Testing for Irregular Masonry: Preliminary Testing," in *8th International Conference on Structural Analysis of Historical Constructions*, Wroclaw, Poland, 2012.

[50] "DIANA Finite Element Analysis Program; User's Manual," 2010.

[51] D. Spencer, Knitting technology a comprehensive handbook and practical guide, Third Edition ed., Cambridge, England: Woodhead Publishing Limited, 2001.

[52] *Standard Test Methods for Vulcanized Rubber and Thermoplastic Elastomers- Tension, ASTM Standard D412,* 1998.

[53] R. J. Schaefer, "Mechanical properties of rubber," in *Harris' Shock and Vibration Handbook, Sixth edition, A. Piersol, T. Paez (Eds)*, McGraw-Hill Companies Inc, 2010, pp. 33-1.

[54] D. Chesler, "Methodology for in situ Testing of Masonry Typologies, Master's Thesis," University of Minho, 2014.

[55] P. B. Lourenço, F. Pagaimo and E. Júlio, "Caracterização das paredes de alvenaria da vila de Tentúgal," *Revista Portuguesa de Engenharia de Estruturas (RPEE),* no. N.º 51, pp. 1-7, 2005.

[56] K. E. M. D. V. MOTA, "CARACTERIZAÇÃO E TIPIFICAÇÃO IN SITU DE PAREDES DE ALVENARIA DE PEDRA, Masters Thesis," Universidade do Porto, 2009.

[57] C. Almeida, C. Q. Costa, J. Guedes, A. Arêde and A. Costa, "Mechanical Behaviour Analyzes of One Leaf Stone Masonry Walls," in *VI Congreso Internacional Sobre Patologia Y Recuperacion De Estructuras*, Cordoba, Argentina, 2010.

[58] Proceq, "Ultrasonic Pulse Velocity - Pundit Lab," [Online]. Available: www.proceq.com. [Accessed 22 December 2015].

[59] *Standard Test Method for Compressive Strength of Cylindrical Concrete Specimens, ASTM standard C39,* 2005.

[60] *Standard Test Method for Static Modulus of Elasticity and Poisson's Ratio of Concrete in Compression, ASTM standard C469,* 2002.

[61] P. Lourenço, "Computational strategies for masonry structures," Delft, the Netherlands, 1996.

[62] W. Mann and M. Betzler, "Investigations on the effect of different forms of test samples to test the compressive strength of masonry," in *10th Int. Brick and Block Masonry Conf.*, Calgary, Alberta, Canada, 1994.

[63] D. Oliveira, "Experimental and numerical analysis of blocky masonry structures under cyclic loading," Guimaraes, Portugal, 2003.

[64] EN 1052-1, "Methods of test for masonry - Part 1: Determination of compressive strength.," 1999.

[65] EN 1996 1-2, "Eurocode 6 - Design of masonry structures - Part 1-2: General," CEN, Brussels, 2005.

[66] N. Augenti, F. Parisi and E. Acconcia, "MADA: online experimental database for mechanical modelling of existing masonry assemblages," in *Proc. 15th World Conference on Earthquake Engineering*, Lisbon, Portugal (CD-ROM), 2012.

[67] Autodesk, Inc., "AutoCAD 2012," Version: F.107.0.0, (c) 2011.

[68] MIDAS Information Technology Co., Ltd., "FX+ for Diana," Version: 3.3.0, (c) 1989.

[69] P. B. Lourenço, G. Vasconcelos, J. Ortega, L. Ramos and F. Fernandes, "Relatório de Inspeção e Diagnóstico no Convento de S. Francisco, Braga," Department of Civil Engineering, University of Minho, 2015.

[70] L. Fontes, C. Braga and F. Andrade, "Salvamento de Bracara Augusta Convento de São Francisco, Real (Braga). Projecto de Adaptação a Pousada da Juventude.," Relatório Final. Trabalhos Arqueológicos da U.A.U.M., 2012.

[71] E. Poletti, "Characterization of seismic behavior of traditional timber frame walls - Tesis de Doutoramento," Universidade do Minho - Escola de Engenheria, Guimaraes, Portugal, 2013.

[72] N. J. Carino, Handbook on Nondestructive Testion of Concrete. 2nd Edition, Barr Harbor Drive: ASTM - International - CRC Press LLC, 2004.

[73] M. Schuller, M. Berra, R. Atkinson and L. Binda, "Acoustic Tomography for Evaluation of Unreinforced Masonry," *Construction and Building Materials,* vol. 11, no. 3, pp. 199-204, 1997.

[74] R. Aguilar, L. F. Ramos and L. Marques, "Report No. 1: Improved Techniques for the Diagnosis and Monitoring of Historical Masonry: Numerical Modelling of Flat-Jack and Tube-Jack Tests," 2011.

[75] G. Riva, C. Bettio and C. Modena, "The use of sonic wave technique for estimating the efficiency of masonry consolidation by injection," in *Proc. 11th International Brick/Block Masonry Conference*, Shanghai, China, October , 1997.

[76] "Reasons for Patenting Your Inventions," [Online]. Available: http://www.wipo.int. [Accessed 29 May 2012].

[77] S. Moreira, L. F. Ramos and D. V. Oliveira, "Experimental characterization of irregular stone masonry," *Construction and Building Materials,* 2013.

[78] EN 772-1, "Methods of test for masonry units - Part 1: Determination of compression strength," 2000.

[79] "Wave2000® Software for Computational Ultrasonics," CyberLogic, inc., [Online]. Available: http://www.cyberlogic.org/wave2000.html. [Accessed 20 July 2012].

[80] L. F. Ramos and Z. Sharafi, "Tube-jack Testing for Irregular Masonry Walls: First Studies," *Advanced Materials Research,* Vols. 133-134, pp. 229-234, 2010.

[81] L. Binda, A. Saisi and L. Zanzi, "Sonic tomography and flat-jack tests as complementary investigation procedures for the stone pillars of the temple of S. Nicolò l'Arena (Italy)," *NDT&E International,* vol. 36, pp. 215-227, 2003.

[82] M. R. Valluzzi, F. Da Porto, F. Casarin, N. Monteforte and C. Modena, "A contribution to the characterization of masonry typologies by using sonic waves investigations," in *Non-Destructive Testing in Civil Engineering*, Nantes, France, 2009.

[83] A. Anzani, L. Binda, M. Lualdi, C. Tedeschi and L. Zanzi, "Use of Sonic and GPR Tests to Control the Effectiveness of Grout Injections of Stone Masonry," in *European Conference on Non Destructive Testing*, Berlin, Germany, 2006.

[84] L. F. Ramos, T. Miranda, M. Mishra, F. M. Fernandes and E. Manning, "A Bayesian approach for NDT data fusion: The Saint Torcato church case study," *Engineering Structures,* vol. 84, pp. 120-129, 2015.

[85] J. Fuente, R. Fernandez and V. Albert, "Brick masonry elastic modulus determination using the numerical simulation and experiments of sonic wave propagation," in *Simulation in NDT - Online Workshop in www.ndt.net in September 2010*, 2010.

[86] "The Nature of a Wave," The Physics Classroom, [Online]. Available: http://www.physicsclassroom.com/class/waves/u10l1c.cfm. [Accessed 20 06 2012].

[87] "World Heritage List," United Nations Educational, Scientific and Cultural Organization (UNESCO), [Online]. Available: http://whc.unesco.org/en/list. [Accessed 29 June 2012].

[88] A. Provins, D. Pearce, E. Ozdemiroglu, S. Mourato and S. Morse-Jones, "Valuation of the historic environment: The scope for using economic valuation evidence in the appraisal of heritage-related projects," *Progress in Planning,* vol. 69, pp. 131-175, 2008.

[89] J. Leite, P. Lourenço and J. Ingham, "Statistical Assessment of Damage in Chruches Affected by the Christchurch Earthquakes, New Zealand (2010-2011)," in *Historical and Masonry Structures Group Meeting Presentation*, University of Minho, Azurem Campus, January 16, 2012.

[90] P. Rossi, "Analysis of mechanical characteristics of brick masonry tested by means of in-situ tests," in *6th IBMaC*, Rome, Italy, 1982.

[91] Z. Sharafi, "Enhanced Flat-Jack Tests for Irregular Walls, Master's Thesis," Guimaraes, 2009.

[92] L. F. Ramos and Z. Sharafi, "Tube-jack Testing for Irregular Masonry Walls: First Studies," Vols. 133-134, pp. 229-234, 2010.

[93] N. J. Carino, Handbook on Nondestructive Testing of Concrete. 2nd Edition, Barr Harbor Drive: ASTM - International - CRC Press LLC, 2004.

[94] PCB Group, Inc., "Impact Hammers," [Online]. Available: http://www.pcb.com/testmeasurement/impacthammers. [Accessed 21 January 2016].

[95] E. Manning, L. F. Ramos and F. Fernandes, "Direct Sonic and Ultrasonic Wave Velocity in Masonry under Compressive Stress," in *9th International Masonry Conference*, Guimaraes, Portugal, 2014.

[96] L. F. Ramos, E. Manning, F. Fernandes, R. Fangueiro, M. Azenha, J. Cruz and C. Sousa, "Tube jack testing for irregular masonry walls: prototype development and testing," *NDT&E,* vol. 58, no. September, pp. 24-35, 2013.

[97] L. Binda and C. Tiraboschi, "Flat-Jack Test as a Slightly Destructive Technique for the Diagnosis of Brick and Stone Masonry Structures," *Int. J. for Restoration of Buildings and Monuments,* pp. 449-472, 1999.

Appendices

A.   Granite Cylinder Data

Table A-1.Granite Cylinder Measurements

#	Height [cm]				Diameter [mm]				Weight [g]	Volume [m³]	Density [kg/m³]
	1	2	3	Ave.	1	2	3	Ave.			
RG1	14.9	14.9	14.9	14.90	73.67	73.75	73.73	73.72	1667.0	0.000636	2621
RG2	14.8	14.8	14.8	14.80	73.66	73.70	73.70	73.69	1660.2	0.000631	2630
RG3	14.9	14.9	14.9	14.90	73.64	73.59	73.65	73.63	1660.1	0.000634	2617
RG4	14.9	14.9	14.9	14.90	66.75	72.06	73.63	70.81	1590.5	0.000587	2710
RG5	14.9	14.8	14.8	14.83	73.68	73.52	73.50	73.57	1669.7	0.000631	2648
RG6	14.9	14.9	14.8	14.87	73.53	73.60	73.51	73.55	1669.5	0.000632	2643
RG7	14.8	14.7	14.8	14.77	73.53	73.63	73.69	73.62	1650.0	0.000629	2625
RG8	15.3	15.4	15.2	15.30	73.2	73.29	73.27	73.25	1679.7	0.000645	2605
RG9	13.5	13.6	13.5	13.53	72.87	72.96	72.84	72.89	1469.6	0.000565	2602
RG10	15.3	15.3	15.4	15.33	73.29	73.06	73.31	73.22	1682.2	0.000646	2606
RG11	15.1	14.9	15.0	15.00	73.11	73.26	73.13	73.17	1646.8	0.000631	2611
RG12	15.2	15.3	15.1	15.20	73.66	73.01	73.27	73.31	1646.8	0.000642	2566
RG13	15.0	15.0	15.1	15.03	73.68	73.42	73.17	73.42	1634.4	0.000637	2568
RG14	15.4	15.4	15.3	15.37	73.56	73.33	73.37	73.42	1672.0	0.000651	2570
RG15	14.2	14.2	14.4	14.27	73.42	73.47	73.41	73.43	1565.6	0.000604	2591

Table A-2. Granite Cylinder Test Results

#	Ultrasonic Velocity [m/s]	Loading Rate [kN/s]	Maximum Load [kN]	Young's Modulus [GPa]	Compressive Strength [MPa]
RG1	2891	5	152.9	29.4	48.36
RG2	2902	3	102.6	31.9	63.01
RG3	2773	4	132.1	25.9	60.10
RG4	2468	-	-	-	65.94
RG5	2597	4	131.4	31.0	87.96
RG6	2616	4	131.9	34.1	64.57
RG7	2528	4	132.1	26.7	85.38
RG8	-	4	121.5	31.1	48.81
RG9	-	4	121.6	38.9	79.83
RG10	-	4	122.2	32.2	63.17
RG11	-	4	121.4	36.5	-
RG12	-	4	121.8	25.2	61.43
RG13	-	4	121.5	24.1	55.63
RG14	-	4	122.2	22.8	59.00
RG15	-	4	121.3	31.0	67.39
Average	2682	-	-	30.05	65.04
St. Dev	174.10	-	-	4.71	12.01
COV	6.49	-	-	15.68	18.47

B.   Mortar Cylinder Data

Table B-1. Measurements of mortar cylinders cast during regular masonry wall construction

#	Height [cm]				Diameter [mm]				Weight [g]	Volume [m³]	Density [kg/m³]
	1	2	3	Ave.	1	2	3	Ave.			
R1	14.8	15.0	14.9	14.9	69.13	71.35	69.62	70.03	1035	0.000574	1803
R2	14.9	14.9	14.9	14.9	69.86	71.68	70.29	70.61	1025	0.000583	1757
R3	15.0	14.8	15.0	14.9	70.78	69.64	71.92	70.78	1026	0.000588	1746
R4	14.9	14.9	14.8	14.9	70.30	71.43	70.48	70.74	1021	0.000584	1748
R5	15.0	15.2	14.7	15.0	70.55	71.90	71.03	71.16	1054	0.000595	1771
R6	14.9	15.0	14.8	14.9	71.22	66.62	57.28	65.04	896	0.000495	1810
R7	14.9	14.9	14.9	14.9	71.82	70.96	70.81	71.20	1024	0.000593	1726
R8	15.1	14.9	14.9	15.0	69.85	71.50	72.21	71.19	1048	0.000596	1759
R9	14.9	14.7	14.9	14.8	70.30	69.91	70.74	70.32	990	0.000576	1719
R10	14.8	14.8	14.8	14.8	70.89	69.65	71.61	70.72	972	0.000581	1672
R11	14.7	14.8	14.7	14.7	70.15	70.45	69.84	70.15	983	0.000569	1726
R13	14.8	14.8	14.9	14.8	71.04	70.89	69.59	70.51	1007	0.000579	1739
R14	14.8	14.9	14.9	14.9	70.60	70.50	71.24	70.78	1021	0.000585	1745
R15	14.9	14.7	14.9	14.8	70.32	71.15	69.60	70.36	1021	0.000577	1770
R16	14.9	15.0	14.9	14.9	69.54	71.38	71.72	70.88	995	0.000589	1689
R17	15.0	14.8	14.7	14.8	70.65	71.27	69.57	70.50	958	0.000579	1655
R18	15.1	14.7	15.1	15.0	67.85	71.38	72.13	70.45	996	0.000583	1707
R19	14.8	14.8	14.6	14.7	68.46	70.93	65.73	68.37	922	0.000541	1704
R20	15.0	15.1	14.9	15.0	70.43	69.18	70.60	70.07	999	0.000578	1727

Table B-2. Measurements of mortar cylinders cast during semi-irregular and irregular wall construction

#	Height [cm]				Diameter [mm]				Weight [g]	Volume [m³]	Density [kg/m³]
	1	2	3	Ave.	1	2	3	Ave.			
S1	15.6	15.5	15.6	15.6	73.25	72.48	70.50	72.08	1133	0.000635	1784
S2	15.6	15.5	15.5	15.5	73.25	72.29	69.75	71.76	1148	0.000628	1827
S3	15.6	15.7	15.7	15.7	73.93	72.21	69.74	71.96	1162	0.000637	1824
S4	15.7	15.6	15.6	15.6	75.05	73.82	65.65	71.51	1143	0.000628	1821
S5	15.4	15.5	15.5	15.5	71.83	72.87	73.60	72.77	975	0.000643	1516
S6	15.6	15.6	15.7	15.6	73.74	71.77	70.74	72.08	1148	0.000638	1799
S7	15.7	15.7	15.6	15.7	73.48	71.95	70.09	71.84	1148	0.000635	1808
S8	15.8	15.9	15.9	15.9	76.47	70.95	71.06	72.83	1166	0.000661	1764
S9	15.9	15.8	15.9	15.9	71.24	71.40	71.19	71.28	1178	0.000633	1861
S10	15.9	15.9	15.8	15.9	72.90	71.90	70.92	71.91	1165	0.000644	1808
S11	15.7	15.6	15.5	15.6	72.76	71.74	71.25	71.92	1139	0.000634	1797
S12	15.5	15.7	15.6	15.6	70.25	71.63	72.93	71.60	1136	0.000628	1808
S13	16.0	15.9	15.9	15.9	73.64	71.07	70.54	71.75	1175	0.000644	1824
S14	15.5	15.6	15.5	15.5	72.74	74.11	72.14	73.00	1141	0.000650	1755
S15	15.5	15.5	15.5	15.5	73.68	71.10	71.12	71.97	1128	0.000630	1789
S16	15.8	15.8	15.8	15.8	72.79	73.23	72.11	72.71	1164	0.000656	1774
S17	15.9	15.8	15.8	15.8	73.35	72.49	72.37	72.74	1165	0.000658	1771
S18	15.8	15.7	15.8	15.8	70.71	70.77	72.30	71.26	1159	0.000629	1843
S19	15.7	15.8	15.8	15.8	71.06	71.70	73.23	72.00	1145	0.000642	1784
S20	16.2	16.1	16.2	16.2	73.36	73.68	72.39	73.14	1190	0.000679	1752
S21	16.0	16.0	16.0	16.0	73.40	71.77	70.40	71.86	1184	0.000649	1825
S22	15.9	15.9	15.8	15.9	73.53	70.31	70.04	71.29	1188	0.000633	1876
S23	16.2	16.1	16.2	16.2	73.86	71.16	71.26	72.09	1221	0.000660	1850

Table B-3. Mortar cylinder compression test results for regular masonry wall mortar

#	Ultimate Strength [MPa]	Young's Modulus [MPa]
R1	0.345	163
R2	0.336	255
R3	0.338	157
R4	0.343	252
R5	0.335	262
R6	0.289	161
R7	0.308	191
R8	0.331	237
R9	0.315	279
R10	0.328	436
R11	0.364	299
R13	0.348	187
R14	0.371	304
R15	0.388	295
R16	0.289	227
R17	0.300	331
R18	0.294	279
R19	0.247	257
R20	0.350	368
Average	0.327	260
St. Dev	0.034	73
COV	10.32	28

Table B-4. Mortar cylinder compression test results for semi-irregular and irregular masonry wall mortar

#	Ultimate Strength [MPa]	Young's Modulus [MPa]
S1	3.72	1158
S2	4.23	1144
S3	3.42	580
S4	2.74	727
S6	2.43	580
S7	2.29	655
S8	3.04	869
S9	3.74	1597
S10	3.21	1436
S11	3.06	1146
S12	3.18	970
S13	3.02	1625
S15	2.82	718
S16	2.84	830
S17	3.29	873
S18	2.69	694
S19	2.33	678
S20	2.49	1171
S21	3.54	1500
S22	3.34	1318
S23	3.29	1087
Average	3.08	1017
St. Dev	0.50	337
COV	16.30	33

C.   Masonry Wallet Test Results

Table C-1. Young's modulus test results for regular masonry wallet RS1

#	E_{VT} [MPa]	E_{VR} [MPa]	E_{HT} [MPa]	E_{HR} [MPa]
RS1	368	2500	1690	27151

Table C-2. Young's modulus test results for the semi-irregular masonry wallets

#	E_{VT} [MPa]	E_{VR} [MPa]	E_{HT} [MPa]	E_{HR} [MPa]
SS1	689.8	4169.7	2157.5	16416
SS2	1278.7	6706.2	1142.1	7723.1
SS3	1042.4	4566.8	2648.2	9157.6
Average	1003.6	5147.6	1982.6	11098.9
St. Dev	296.4	1364.3	768.1	4660.3
CV [%]	29.5	26.5	38.7	42.0

Table C-3. Young's modulus test results for the irregular masonry wallets

#	E$_{VT}$ [MPa]	E$_{VR}$ [MPa]	E$_{HT}$ [MPa]	E$_{HR}$ [MPa]
IS1	1076.8	3256.8	764.6	5398.5
IS2	1435	3844.5	3986.5	8558.7
IS3	1048.9	3022.6	1281.3	8270.6
Average	1186.9	3374.6	2010.8	7409.3
St. Dev	215.3	423.4	1730.4	1747.3
CV [%]	18.1	12.5	86.1	23.6

D. Foam Piece Measurements

Table D-1. Foam piece diameter measurements – Part A

Distance along hole [cm]	Hole Number					
	1	**2**	**3**	**4**	**5**	**6**
0	25.75	21.4	33.66	37.45	28.08	28.51
1	25.37	25.36	32.93	32.63	24.01	25.18
2	26.24	26.29	27.19	28.46	26.45	24.74
3	25.58	25.34	32.53	27.68	26.17	24.97
4	26.74	26.82	32.73	26.44	26.22	23.71
5	24.89	27.1	24.74	26.38	26.04	23.16
6	24.7	27.15	25.16	25.31	26.31	24.74
7	23.32	24.49	24	26.53	26.64	22.89
8	23.12	19.11	24.38	27.54	25.73	23.68
9	23.74	14.89	24.26	27.7	24.98	23.25
10	23.68		23.92	27.48	24.94	23.01
11	24.34		23.56	29.77	18.97	23.15
12	23.77		24.6	28.15	9.95	24.49
13	24.32		23.91	27.32	21.33	23.67
14	24.15		24.41	26.92	23.64	24.44
15	24.2	16.73	24.02	26.32	24.16	25.03
16	25.51	27.53	22.9	26.4	24.71	23.95
17	25.31	27.05	23.19	27.13	25.22	23.21
18	25.66	26.35	24.98	25.92	24.91	25.93
19	26.69	26.33	24.36	25.92	25.28	27.04
20	26.22	26.14	22.04	26.64	27.27	29.01
21	26.96	30.83	27.08	27.11	24.89	27.81
Average	25.01	25.25	25.93	27.78	25.05	24.80

Table D-2. Foam piece diameter measurements – Part B

Distance along hole [cm]	Hole Number					
	7	8	9	10	11	12
0	32.84	27.69	36.33	32.59	34.66	32.56
1	26.92	30.88	29.23	28.64	29.28	29.12
2	25.87	30.01	29.79	27.48	26.71	24.64
3	23.58	27.96	30.76	29.4	26.42	25.6
4	25.4	26.41	29.75	29.76	25.59	24.31
5	24.89	26.51	28.28	27.91	24.15	26.31
6	24.25	24.81	27.58	26.85	24.25	24.42
7	21.96	24.54	26.58	27.16	24.48	25.57
8	15.36	24.72	26.54	26.67	24.21	26.23
9	30.55	23.75	26.57	27.82	23.32	25.41
10	31.46	24.14	26.24	27.56	21.96	24.57
11	28.76	23.48	26.06	25.84	19.38	24.69
12	28.62	25.94	26.12	25.37	14.07	26.18
13	27.79	25.38	26.03	23.96	13.16	24.84
14	26.5	24.28	25.1	22.59	21.16	25
15	26.25	24.17	26.25	22.21	24.33	25.14
16	25.37	23.85	27.48	23.74	22.6	25.91
17	24.83	24.63	26.67	23.61	25.23	26.25
18	24.01	23.6	26.97	23.48	24.31	27.87
19	22.28	25.04	26.59	26.51	25.27	28.31
20	19.47	26.71	32.25	29.04	26.45	29.6
21	35.69	30.48	32.39	29.23	23.18	18.91
Average	26.54	25.86	28.16	26.70	24.85	25.97

E.   Irregular Wall Tube-jack Test Hole Measurements

Table E-1. Drilled hole diameters for the single tube-jack test in the irregular masonry wall

Hole #	Diameter [mm]							
	Front			Back			Front and Back	
	Vertical	Horizontal	Ave.	Vertical	Horizontal	Ave.	Total Ave.	Horizontal Ave.
1	34.0	27.5	30.75	23.0	25.5	24.25	27.50	26.50
2	26.0	26.0	26.00	20.0	22.0	21.00	23.50	24.00
3	27.5	26.5	27.00	23.0	20.0	21.50	24.25	23.25
4	36.0	25.5	30.75	22.0	19.5	20.75	25.75	22.50
5	29.5	26.0	27.75	21.0	22.0	21.50	24.63	24.00
6	25.5	23.0	24.25	20.5	22.5	21.50	22.88	22.75
7	29.5	26.0	27.75	24.5	24.5	24.50	26.13	25.25
8	23.0	27.5	25.25	22.5	24.0	23.25	24.25	25.75
9	28.0	26.0	27.00	21.0	22.0	21.50	24.25	24.00
10	37.0	28.0	32.50	20.0	25.0	22.50	27.50	26.50
11	29.0	27.5	28.25	21.5	22.5	22.00	25.13	25.00
12	28.0	27.5	27.75	22.0	26.0	24.00	25.88	26.75

Table E-2 Hole and tube-jack pressurization length for the single tube-jack test in the irregular masonry wall

Hole #	Hole Length [cm]	Tube Length [cm]	Length Difference [cm]	Ave. Horizontal Diameter [mm]	Hole Area [cm²]	Pressure Area [cm²]
1	18.0	18.0	0	26.50	47.700	47.700
2	18.5	17.5	1	24.00	44.400	42.000
3	17.0	18.0	0	23.25	39.525	39.525
4	15.0	17.5	0	22.50	33.750	33.750
5	16.5	17.5	0	24.00	39.600	39.600
6	17.0	17.5	0	22.75	38.675	38.675
7	16.5	17.5	0	25.25	41.663	41.663
8	18.5	17.5	1	25.75	47.638	45.063
9	18.5	17.5	1	24.00	44.400	42.000
10	17.5	17.5	0	26.50	46.375	46.375
11	17.0	17.5	0	25.00	42.500	42.500
12	18.0	17.5	0.5	26.75	48.150	46.813

Table E-3. Drilled hole diameters for the double tube-jack test in the irregular masonry wall

| Hole # | Diameter [mm] | | | | | | | |
| | Front | | | Back | | | Front and Back | |
	Vertical	Horizontal	Ave.	Vertical	Horizontal	Ave.	Total Ave.	Horizontal Ave.
13	28.5	31.5	30.00	23.0	23.0	23.00	26.50	27.25
14	28.0	28.5	28.25	24.0	25.0	24.50	26.38	26.75
15	28.5	28.0	28.25	23.0	24.5	23.75	26.00	26.25
16	26.5	27.0	26.75	26.5	24.0	25.25	26.00	25.50
17	27.0	26.5	26.75	26.0	28.5	27.25	27.00	27.50
18	28.5	29.0	28.75	24.0	25.0	24.50	26.63	27.00
19	28.5	28.5	28.50	22.5	26.0	24.25	26.38	27.25
20	27.5	26.0	26.75	22.5	26.0	24.25	25.50	26.00
21	28.0	27.5	27.75	22.5	24.0	23.25	25.50	25.75
22	25.5	26.0	25.75	24.5	23.0	23.75	24.75	24.50
23	27.0	26.0	26.50	24.0	24.5	24.25	25.38	25.25
24	32.0	26.5	29.25	26.0	25.5	25.75	27.50	26.00

Table E-4 Irregular masonry wall double tube-jack test top equivalent jack hole measurements

Hole #	Hole Length	Tube Length	Ave. Hole Width	Pressure Area
	[cm]	[cm]	[mm]	[m²]
13	17.5	17.5	27.25	0.00477
14	16.0	17.5	26.75	0.00428
15	16.0	17.5	26.25	0.00420
16	15.0	17.5	25.50	0.00383
17	16.5	17.5	27.50	0.00454
18	15.5	17.5	27.00	0.00419
19	14.5	17.5	27.25	0.00395
20	15.5	17.5	26.00	0.00403
21	16.5	17.5	25.75	0.00425
22	15.5	17.5	24.50	0.00380
23	15.5	17.5	25.25	0.00391
24	15.0	17.5	26.00	0.00390

F.   Numerical analysis of strains and stresses in the regular wall

F.1   Single Tube-jack Test - Analysis of Vertical Strains

A vertical strain contour plot of the masonry wall shows that the strain is limited almost entirely to the horizontal mortar joint where the holes have been created, see Figure F.1-1a. Zooming in to view the strains close to the holes, only a very small amount of strain is seen in the granite units above and below the holes, Figure F.1-1b. The small strains in the granite correspond to the dips in the displacements seen in Figure 6-22. Positive strains are seen above and below each hole as the mortar expands into the area of the removed mortar. Negative strains are seen to the right and left of each hole as the mortar contracts under the load of the masonry above. As pressure is applied radially to the edges of the holes, the strain reduces to nearly zero. Continuing to apply pressure beyond the restoring pressure, the tube-jacks push the masonry apart resulting in positive strains in the joint.
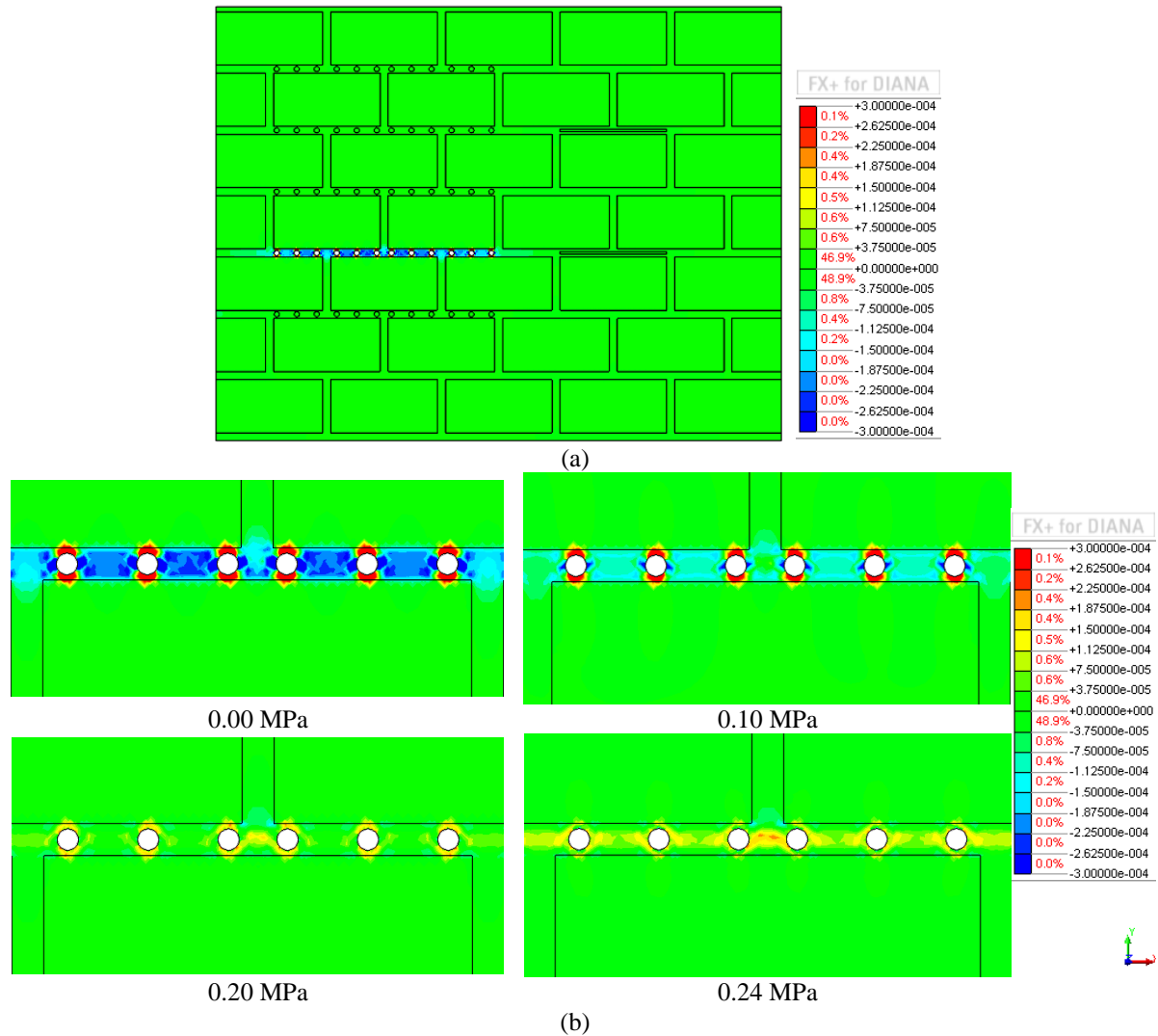
(a)

Figure F.1-1 Contour plots of the masonry vertical strain: (a) after creating the holes; and (b) at various applied pressure values

F.2 Single Tube-jack Test - Analysis of Horizontal Strains

The horizontal strains during the single tube-jack test are almost entirely contained to the mortar joints, just as the vertical strains were. Contour plots of the horizontal strains at various applied pressure values are shown in Figure F.2-1. After the holes are drilled, the mortar between the holes, and in the nearby vertical joints, expands. As pressure is applied radially to the edges of the holes, the mortar between the holes is compressed and the horizontal strains decrease. The horizontal strains in the horizontal joint are returned to zero at an applied pressure of approximately 0.04 MPa, 20% of the restoring pressure. Increasing the applied pressure to 0.10 MPa and 0.20 MPa further decreases the horizontal strains in the horizontal mortar joint between the holes, as the mortar contracts under the applied pressure.
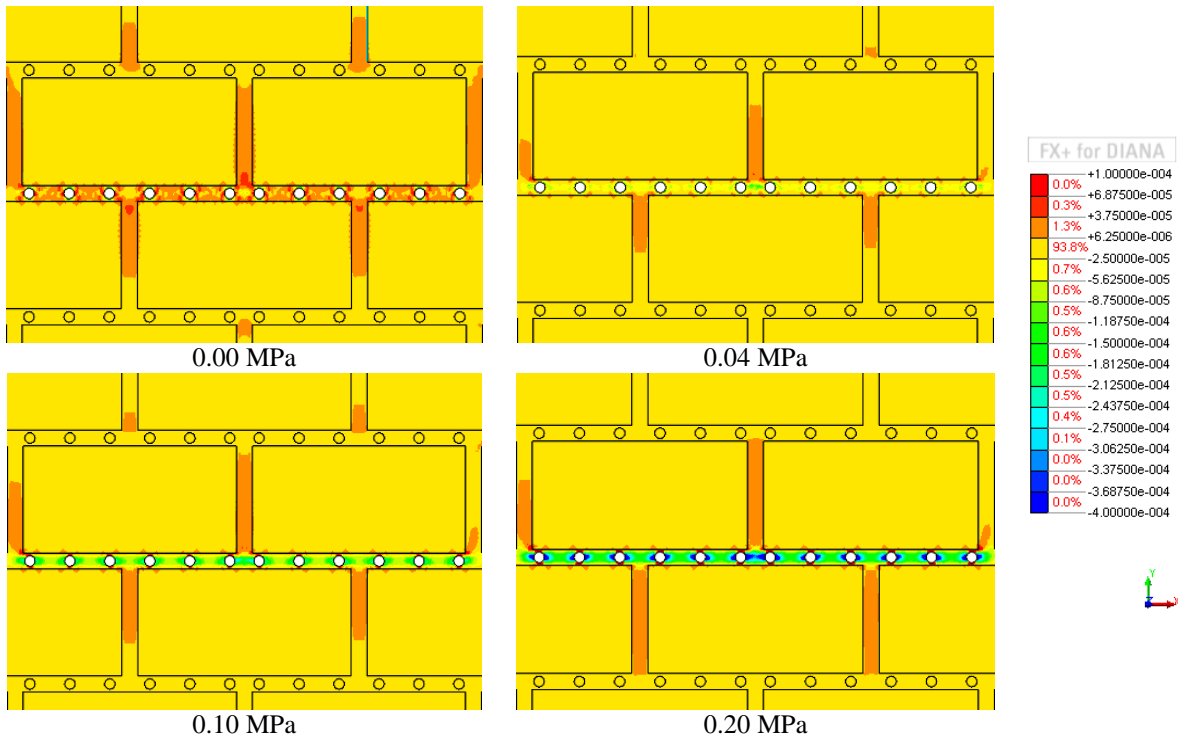
Figure F.2-1 Contour plots of the masonry horizontal strain at various applied pressure values

F.3   Single Tube-jack Test - Analysis of Horizontal Stresses

The contour plots of the horizontal stresses near the 3rd horizontal joint at various applied pressures are shown in Figure F.3-1. Before the holes are created, there exists some horizontal compressive stress in the mortar joint due to the load applied to the top of the wall. The mortar wants to deform horizontally due to the Poisson effect. Since the mortar is more deformable than the granite, the mortar wants to deform more than the granite under the same vertical load. However, the granite blocks above and below the joint are connected to the mortar and confine it. The horizontal confinement results in horizontal compressive stresses developing within the joint. At the ends of the wall and to a lesser extent at each of the vertical mortar joints, the mortar is able to expand horizontally, reducing or eliminating the horizontal compressive stresses.

When the holes are created in the joint, Figure 6-23 shows that the vertical stress increases between the holes. Since the vertical stress increases, the horizontal compressive stress also increases due to the same horizontal confinement (Figure F.3-1). Very close to either side of each hole, the horizontal stress is relieved and the mortar can expand into the hole, as shown by the negative horizontal strains in Figure F.2-1.

As pressure is applied to the edges of the holes, the compressive stresses in the mortar increase, with the greatest compressive stresses closest to the application of the pressure. The horizontal components of the radially applied pressure compress the mortar between the holes and increase the size of the holes horizontally. The size increase of the holes was seen in Figure 6-20. The horizontal movement away from the center of each hole creates tensile stresses above and below each hole, as seen in the bottom contour plots of Figure F.3-1.
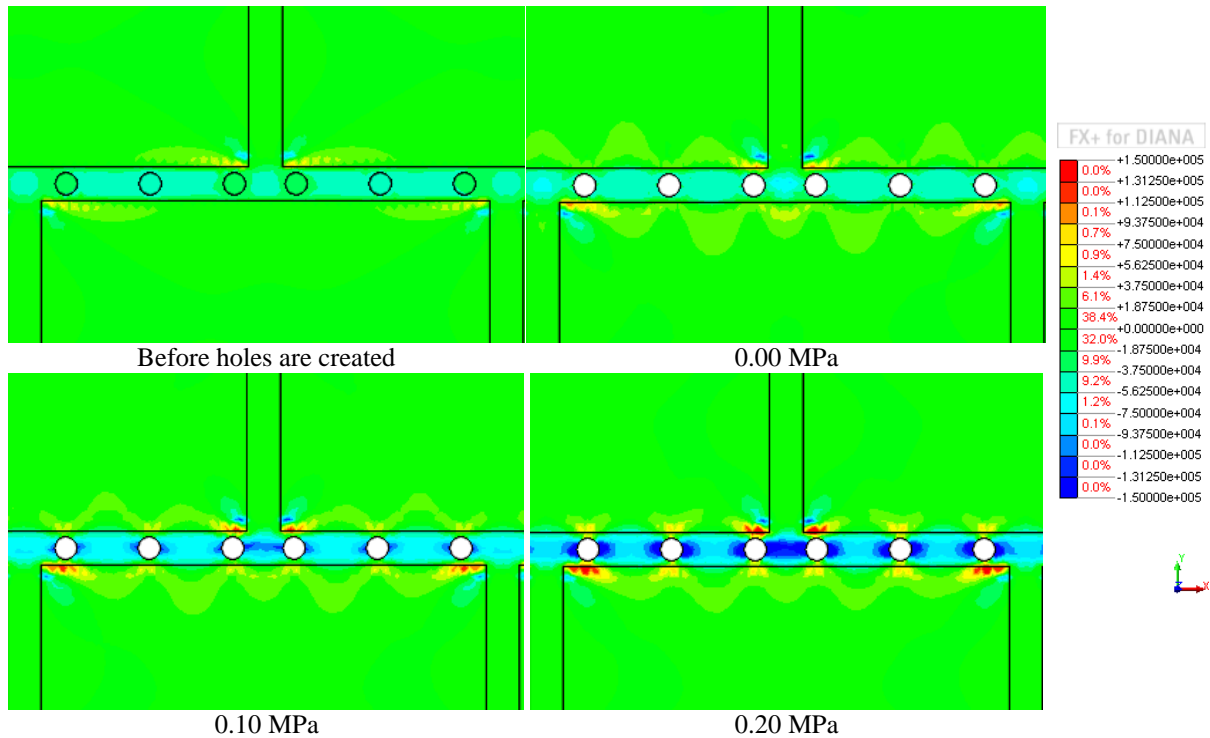
Figure F.3-1 Contour plots of the masonry horizontal stress at various applied pressure values [Pa]

F.4 Single Flat-jack - Analysis of Vertical Strains

A contour plot of the vertical strain in the masonry over the entire wall, Figure F.4-1, shows that the strain is almost entirely contained within the mortar joints, just as it was in the single tube-jack test. Two differences with the flat-jack test are that the strains are much larger and that the strains are seen in horizontal mortar joints above and below the joint that is being tested. In the single tube-jack test, strains were only visible in the contour plot in the joint being tested, see Figure F.4-1
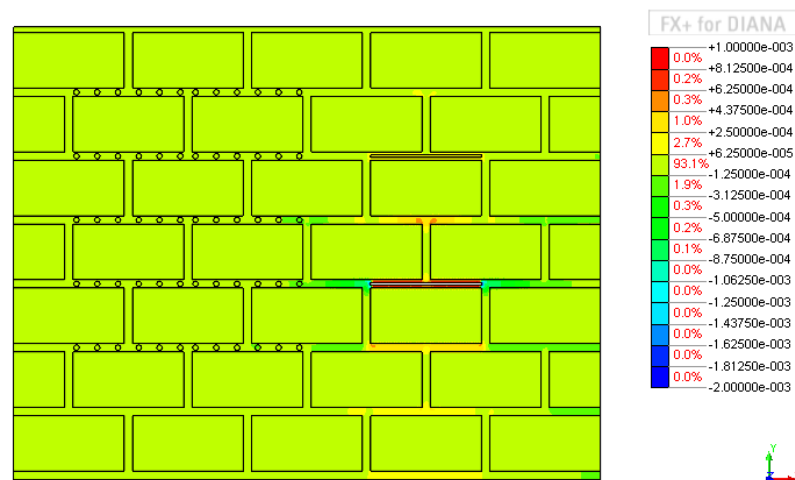

Figure F.4-1 Contour plot of the vertical strain of the regular masonry wall after opening the slot

Contour plots of the vertical strain near the flat-jack slot are shown in Figure F.4-2. Positive strains occur in the mortar above and below the slot just after the elements in the slot have been deactivated, as the mortar expands into the slot. Positive strains are also seen in the horizontal joints above and below the joint where the flat-jack test takes place. This is due to the units

above and below the slot moving together toward the slot. The load of the masonry and the applied load on the top of the wall is redistributed to either side of the slot, increasing the stress level resulting in negative strains. As pressure is applied vertically to the upper and lower edges of the slot, the magnitudes of the strains are reduced. At 0.2 MPa nearly all of the strains are zero. Only slightly negative strains are seen above the slot and just below the vertical joint. This effect was also seen in the single tube-jack test where there were vertical joints, and was noted in the analysis of the vertical displacements.
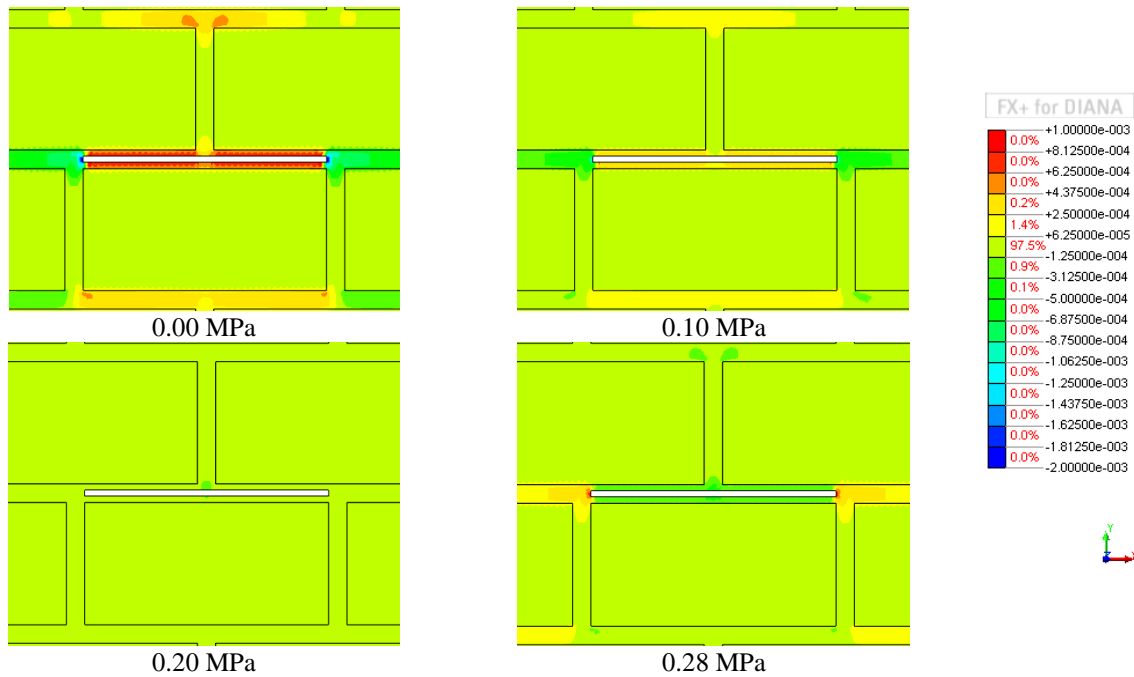

Figure F.4-2 Contour plots of the masonry vertical strain near the flat-jack slot at various applied pressure values

F.5 Single Flat-jack - Analysis of Horizontal Strains and Stresses

In the single flat-jack test, most of the movement of the masonry is in the vertical direction. The flat-jack and slot are very thin and the flat-jack does not apply pressure horizontally. Thus, only small horizontal strains and stresses are expected in the masonry surrounding the flat-jack test. As shown in the contour plot in Figure F.5-1, horizontal strains are located in the vertical joints, especially the vertical joint directly above the center of the flat-jack slot. The distribution of horizontal strains from positive at the bottom of the joint to negative at the top of the joint indicate the rotation of the two granite units downward toward the center of the flat-jack slot.
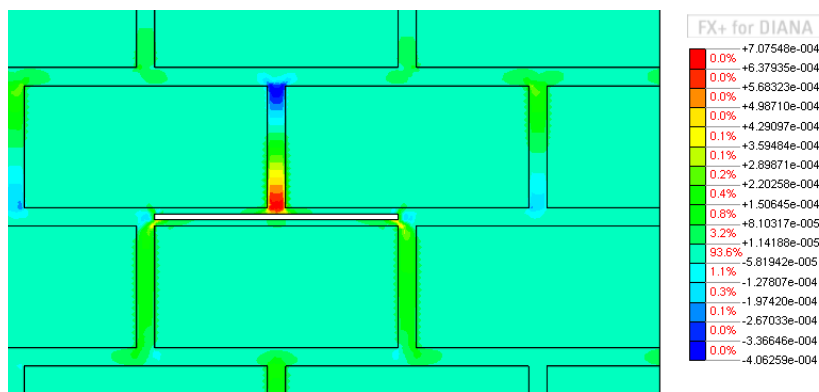

Figure F.5-1 Horizontal strains resulting from opening the flat-jack slot

However, significant horizontal stresses do occur in the granite units surrounding the flat-jack slot as a result of opening the slot. This is in contrast to the single tube-jack test where only small tensile stresses were seen in the units above and below the joint and most of the horizontal stresses were seen within the joint during the pressurization process (see Figure F.3-1). The horizontal stresses in the masonry during the flat-jack test are shown in the contour plots in Figure F.5-2.
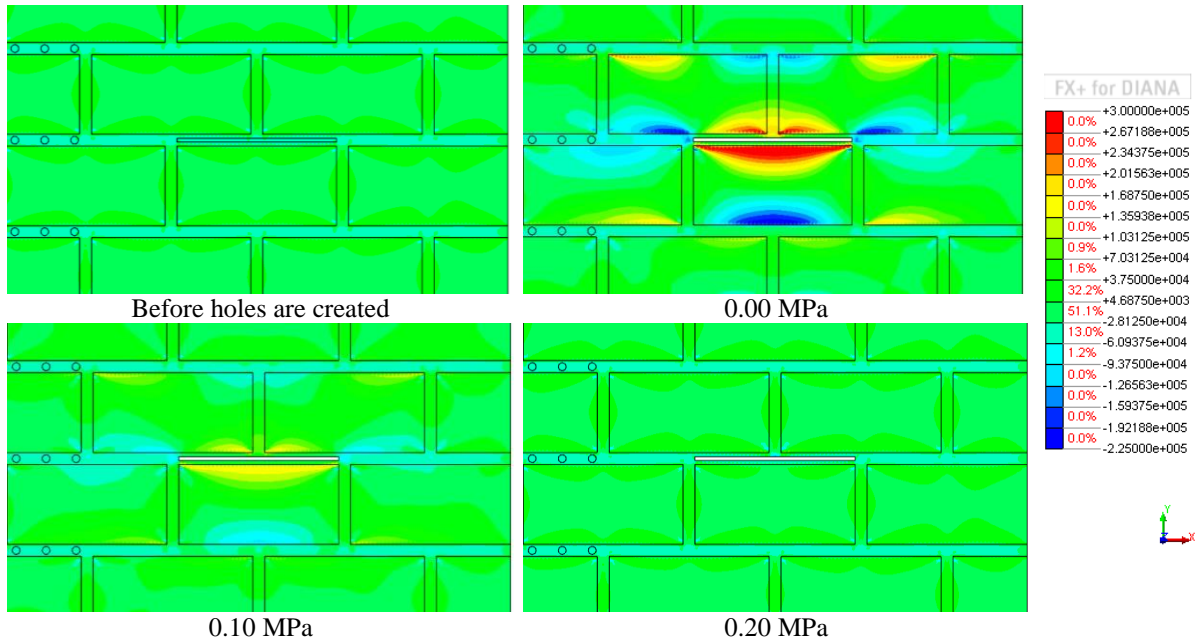

Figure F.5-2 Contour plots of the masonry horizontal stress during the simulated flat-jack test at various applied pressure values

When the slot is opened in the single flat-jack test, tensile stresses as high as 0.3 MPa, 50% larger than the average vertical compressive stress level in the wall, occur in the granite units above and below the slot. Horizontal compressive stresses also result from opening the flat-jack slot. Compressive stresses occur to the right and left of the slot and in the opposite ends of the granite units under horizontal tensile stresses. As the flat-jack applies pressure to the surrounding masonry, the horizontal stresses and strains return to the levels and distributions seen before the slot was opened.

F.6 Double Tube-jack - Analysis of Vertical Strains

Contour plots of the vertical strains are shown in Figure F.6-1. In these plots, the deformed shape of the masonry is not shown. The first phase of the analysis included the deactivation of the holes and was the initial condition for the second phase of the test. Thus, no displacements or strains were calculated for the creation of the holes. The localized displacements and strains due to the creation of the holes would be similar to those shown for the single tube-jack tests.
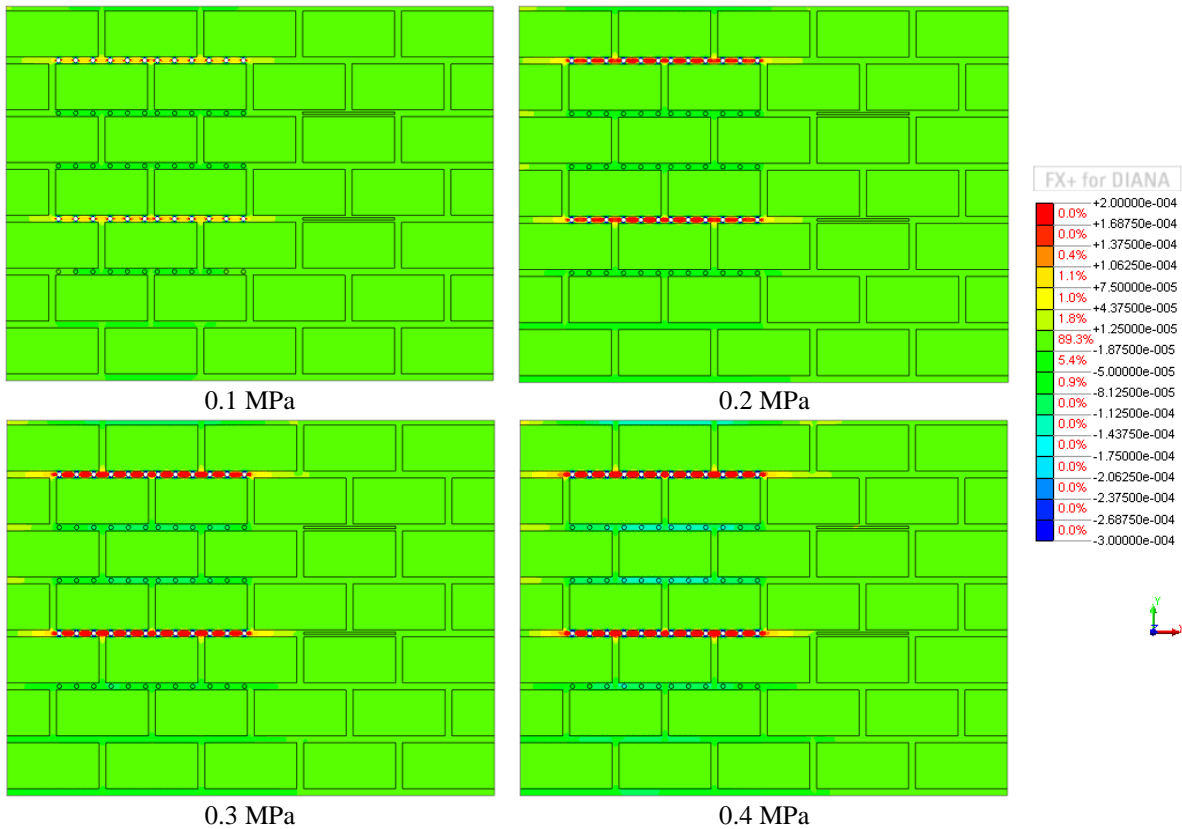
Figure F.6-1 Contour plots of the masonry vertical strains during the double tube-jack test simulation

Just as in the single tube-jack test, the vertical strains are contained almost entirely within the mortar joints. Initially at applied pressures of 0.1 MPa and 0.2 MPa, positive strains are seen mainly in the 3rd and 6th joints from the base of the wall, the joints where the tube-jacks are applying pressure radially. As the applied pressure is increased to 0.3 MPa and 0.4 MPa, the contour plots reveal negative strains in the horizontal joints between the two equivalent flat-jacks, indicating contraction of the masonry. Negative strains are also evident to a lesser extent in the horizontal joints below the lower equivalent flat-jack and above the upper equivalent flat-jack. This shows that the masonry above and below the separated specimen is also being influenced by the test.

F.7   Double Tube-jack - Analysis of Horizontal Strains and Stresses

The horizontal strains between the two equivalent flat-jacks due to the applied pressure are very small. This was shown in the applied pressure versus strain graph for the horizontal virtual LVDT in Figure 6-41. A contour plot at an applied pressure of 0.5 MPa is shown in Figure F.7-1 for a very small range of strain values. Again, values outside of the range shown in the legend are shown as the maximum or minimum contour colors. The horizontal strains between the equivalent flat-jacks are mainly in the vertical mortar joints and are greatest toward the center of the masonry separated by the two equivalent flat-jacks. However, even larger horizontal strains are seen in the vertical joints above the upper equivalent flat-jack and below the lower equivalent flat-jack. To see the distribution of the horizontal strains in more detail around the holes, see the contour plots for the single tube-jack test in Figure F.2-1.
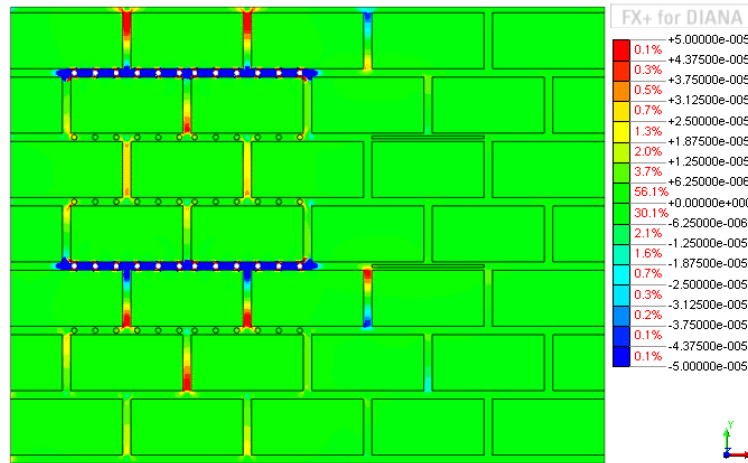
270

Figure F.7-1 Contour plot of the horizontal strains in the masonry at an applied pressure of 0.5 MPa during the double tube-jack test simulation

Very little change in the horizontal stresses occurs between the two equivalent flat-jacks during the double tube-jack test. The contours at zero applied pressure and at 0.5 MPa applied pressure are shown in Figure F.7-2. Slightly larger areas of tensile stresses can be seen at the center of the center unit between the two equivalent flat-jacks. Other than that area, the contours show most of the changes in horizontal stresses occurring right around the line of holes. The horizontal stresses around the holes were analyzed in section F.3 and shown in Figure F.3-1
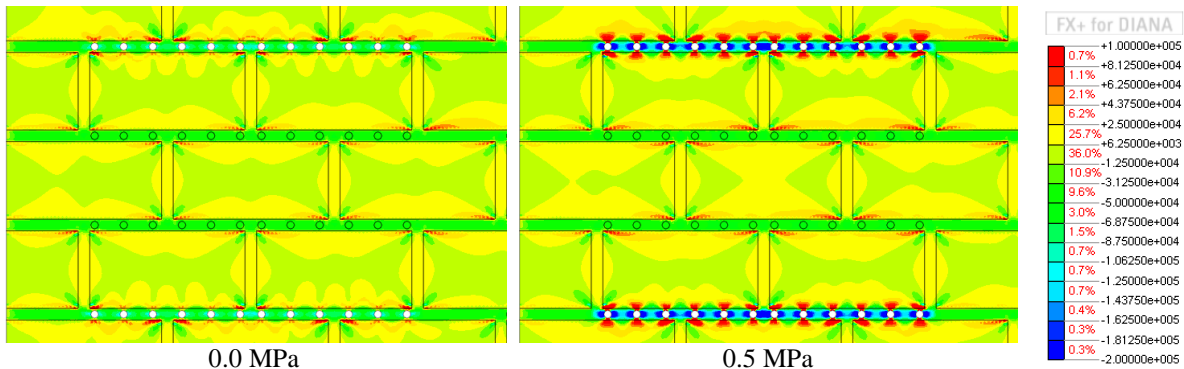

| 0.0 MPa | 0.5 MPa |

Figure F.7-2 Contour plots of the masonry horizontal stresses during the double tube-jack test simulation

F.8   Double Flat-jack - Analysis of Vertical Strains

Contour plots of the vertical strains are shown in Figure F.8-1. In these plots, the deformed shape of the masonry is not shown. As in the previous tests, the vertical strains are contained almost entirely within the mortar joints. Negative strains are seen above and below the slots in the same mortar joint as the slot and in the horizontal joints above and below the flat-jacks. Positive strains are only seen on either end of each of the flat-jacks where the pressurization is pulling the joint apart. In the double tube-jack test, there were more areas of positive strain in between each of the holes as the pressure from the tube-jacks caused the separation of the mortar. As the applied pressure is increased in the flat-jacks, the area of influence increases vertically to the joints above and below the test area but does not increase much horizontally.
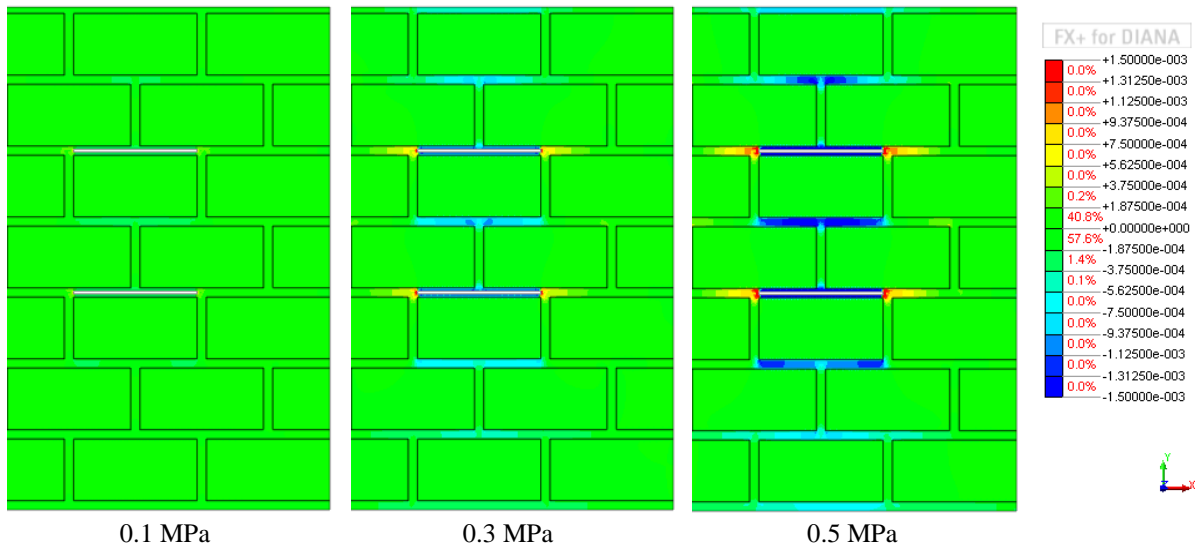
0.1 MPa	0.3 MPa	0.5 MPa

Figure F.8-1 Contour plots of the masonry vertical strains during the double flat-jack test simulation

F.9 Double Flat-jack - Analysis of Horizontal Strains and Stresses

A contour plot is shown in Figure F.9-1 of the horizontal strains in the regular masonry wall during the double flat-jack test at an applied pressure of 0.5 MPa. As in the double tube-jack test, the horizontal strains are mainly in the vertical joints. It is clear that the horizontal strains are due to the rotation of the granite units, which causes contraction and expansion in opposite ends of the vertical joints.
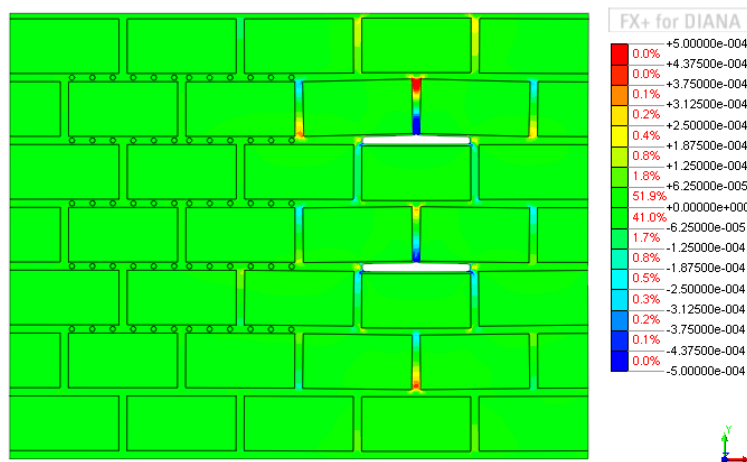
Figure F.9-1 Contour plot of the horizontal strains in the masonry at an applied pressure of 0.5 MPa during the double flat-jack test simulation (200 times actual deformation)

Contour plots of the horizontal stress throughout the wall during the double flat-jack test are shown in Figure F.9-2. Larger areas of horizontal stress occur during the double flat-jack test than during the double tube-jack test. When the slots are created, horizontal tensile stresses occur in the units above and below each slot. In some areas the tensile stress is nearly 0.2 MPa. Between the slots, near the center of the separated specimen, horizontal compressive stresses occur in the granite. Alternating compressive and tensile stresses throughout the area balance out the redistribution of stresses due to the slot openings.

When the restoring pressure of 0.2 MPa is applied in the slots, the horizontal stresses reduce to nearly zero everywhere in the wall. Continuing to apply pressure to the slots to 0.4 MPa and

0.5 MPa reverses the compressive and tensile stresses seen in the 0 MPa contour plot. Horizontal compressive stresses occur at each flat-jack slot and tensile stresses occur near the center of the separated specimen.
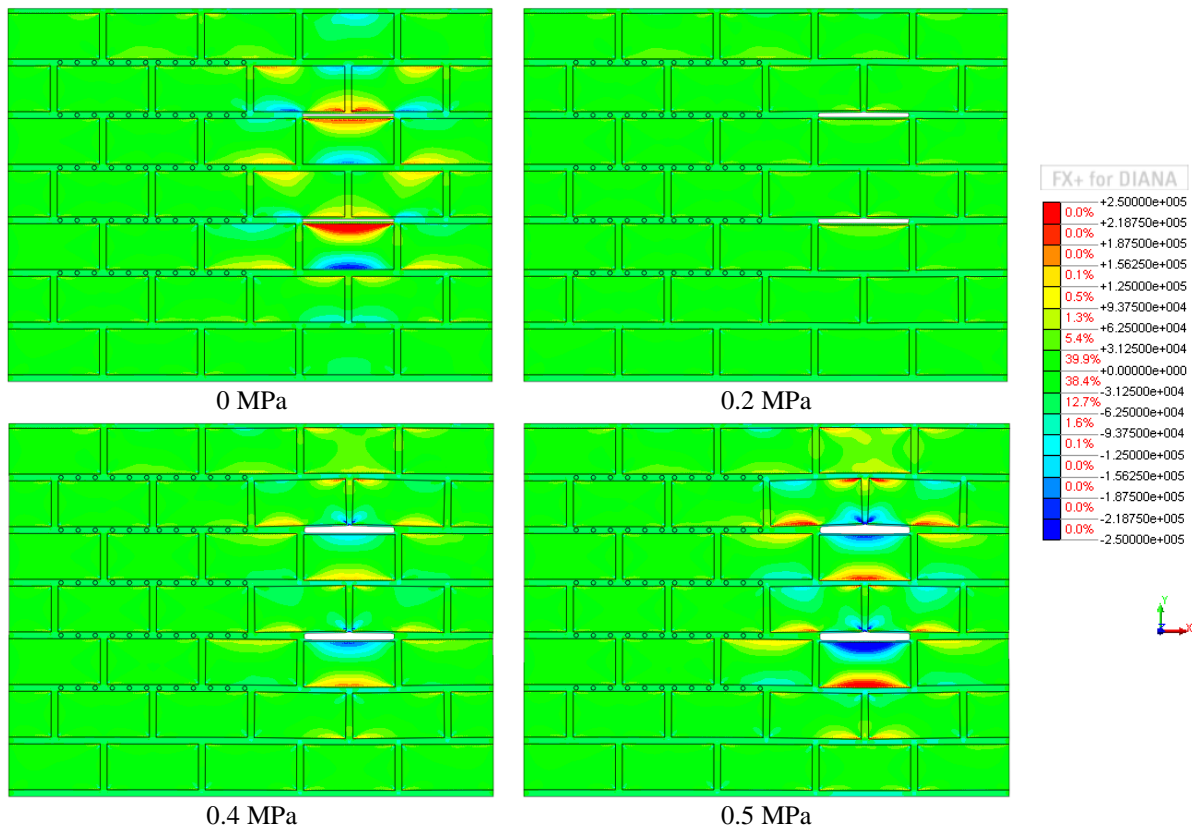
Figure F.9-2 Contour plots of the masonry horizontal stresses during the double flat-jack test simulation

G. Semi-Irregular Wall Measurement Distances

Table G-1 Locations of the virtual LVDTs in the semi-irregular wall model for the single tube-jack test

Virtual LVDT	Vertical Distance Between Nodes	Distance from Bottom of Wall to Bottom Node	Horizontal Distance from Bottom Left Corner of Wall to Bottom Node
	[m]	[m]	[m]
1	0.07856	0.57950	0.225
2	0.08142	0.58007	0.375
3	0.07993	0.58058	0.525
4	0.08188	0.57992	0.75
5	0.07839	0.58091	0.975

Table G-2 Virtual DEMEC and LVDT node locations in the semi-irregular wall model for the single flat-jack test

Virtual DEMEC or LVDT	Vertical Distance Between Nodes	Distance from Bottom of Wall to Bottom Node	Horizontal Distance from Bottom Left Corner of Wall to Bottom Node
	[m]	[m]	[m]
DEMEC 1	0.1991	0.4936	1.245
DEMEC 2	0.2016	0.6033	1.315
DEMEC 3	0.2014	0.5458	1.405
DEMEC 4	0.2001	0.5465	1.550
LVDT 1	0.0988	0.5863	1.220
LVDT 2	0.1987	0.4952	1.320
LVDT 3	0.0685	0.6283	1.420
LVDT 4	0.1012	0.5959	1.520

Table G-3 Locations of the vertical virtual LVDTs in the semi-irregular wall model for the double tube-jack test

Virtual LVDT	Vertical Distance Between Nodes	Distance from Bottom of Wall to Bottom Node	Horizontal Distance from Bottom Left Corner of Wall to Bottom Node
	[m]	[m]	[m]
1	0.3034	0.7753	0.395
2	0.3131	0.7686	0.605
3	0.3515	0.6998	0.850

Table G-4 Location of the horizontal virtual LVDT in the semi-irregular wall model for the double tube-jack test

Virtual LVDT	Horizontal Distance Between Nodes	Distance from Bottom of Wall to Left Node	Horizontal Distance from Bottom Left Corner of Wall to Left Node
	[m]	[m]	[m]
4	0.6012	0.934	0.335

Table G-5 Locations of the vertical virtual LVDTs in the semi-irregular wall model for the double flat-jack test

Virtual LVDT	Vertical Distance Between Nodes	Distance from Bottom of Wall to Bottom Node	Horizontal Distance from Bottom Left Corner of Wall to Bottom Node
	[m]	[m]	[m]
1	0.4860	0.7061	1.20
2	0.4542	0.6941	1.30
3	0.3721	0.7780	1.42
4	0.3737	0.7779	1.52

Table G-6 Location of the horizontal virtual LVDT in the semi-irregular wall model for the double flat-jack test

Virtual LVDT	Horizontal Distance Between Nodes	Distance from Bottom of Wall to Left Node	Horizontal Distance from Bottom Left Corner of Wall to Left Node
	[m]	[m]	[m]
5	0.6039	0.9495	1.07

H. Irregular Wall Measurement Distances

Table H-1 Locations of the virtual LVDTs in the irregular wall model for the single tube-jack test

Virtual LVDT	Vertical Distance Between Nodes	Distance from Bottom of Wall to Bottom Node	Horizontal Distance from Bottom Left Corner of Wall to Bottom Node
	[m]	[m]	[m]
1	0.096	0.417	0.939
2	0.396	0.388	0.784
3	0.105	0.369	0.714
4	0.097	0.420	0.559
5	0.353	0.429	0.484
6	0.103	0.440	0.335

Table H-2 Virtual DEMEC and LVDT node locations in the irregular wall model for the single flat-jack test

Virtual DEMEC or LVDT	Vertical Distance Between Nodes	Distance from Bottom of Wall to Bottom Node	Horizontal Distance from Bottom Left Corner of Wall to Bottom Node
	[m]	[m]	[m]
DEMEC 1	0.197	0.631	1.518
DEMEC 2	0.199	0.627	1.303
LVDT 1	0.148	0.655	1.543
LVDT 2	0.201	0.644	1.338
LVDT 3	0.149	0.656	1.253

Table H-3 Locations of the vertical virtual LVDTs in the irregular wall model for the double tube-jack test

Virtual LVDT	Vertical Distance Between Nodes	Distance from Bottom of Wall to Bottom Node	Horizontal Distance from Bottom Left Corner of Wall to Bottom Node
	[m]	[m]	[m]
1	0.347	0.662	0.854
2	0.309	0.652	0.644
3	0.302	0.649	0.414

Table H-4 Location of the horizontal virtual LVDT in the irregular wall model for the double tube-jack test

Virtual LVDT	Horizontal Distance Between Nodes	Distance from Bottom of Wall to Left Node	Horizontal Distance from Bottom Left Corner of Wall to Left Node
	[m]	[m]	[m]
4	0.583	0.310	0.804

Table H-5 Locations of the vertical virtual LVDTs in the irregular wall model for the double flat-jack test

Virtual LVDT	Vertical Distance Between Nodes	Distance from Bottom of Wall to Bottom Node	Horizontal Distance from Bottom Left Corner of Wall to Bottom Node
	[m]	[m]	[m]
1	0.301	0.800	1.493
2	0.292	0.845	1.339
3	0.305	0.801	1.224

Table H-6 Location of the horizontal virtual LVDT in the irregular wall model for the double flat-jack test

Virtual LVDT	Horizontal Distance Between Nodes	Distance from Bottom of Wall to Left Node	Horizontal Distance from Bottom Left Corner of Wall to Left Node
	[m]	[m]	[m]
4	0.602	1.049	0.956

I.   San Francisco Convent Testing

Table I-1. San Francisco Convent single tube-jack test hole measurements

Hole	Vertical distance from base of the wall	Horizontal distance from center of H1 to center of hole	Depth of hole	Diameter
	[cm]	[cm]	[cm]	[mm]
H1	62.7	0.0	23.0	22.41
H2	58.7	13.0	26.0	25.71
H3	60.1	26.5	22.0	22.40
H4	62.4	35.5	24.5	22.89
H5	60.5	45.0	23.5	23.58
H6	60.7	54.5	21.0	22.69
H7	61.0	64.5	27.0	23.82
H8	60.2	73.0	24.0	24.28
H9	60.7	83.0	27.0	23.29
H10	59.3	91.0	23.5	23.95

Table I-2. San Francisco Convent single flat-jack test pressure readings and DEMEC point measurements at various time points throughout the test

Time	Oil Pressure	Applied Pressure	Relative Displacement [mm]			
[sec]	[MPa]	[MPa]	L1	L2	L3	Average of L1-L3
-1260	0	0	0	0	0	0
-240	0	0	-0.363	-0.128	-0.250	-0.247
0	0	0	-0.363	-0.128	-0.250	-0.247
425	0.126	0.0448	-0.260	-0.152	-0.245	-0.219
650	0.126	0.0448	-0.260	-0.152	-0.245	-0.219
750	0.2	0.0711	-0.225	-0.097	-0.219	-0.180
910	0.2	0.0711	-0.225	-0.097	-0.219	-0.180
1020	0.4	0.1423	-0.207	-0.083	-0.219	-0.170
1180	0.4	0.1423	-0.207	-0.083	-0.219	-0.170
1300	0.6	0.2134	-0.076	0.124	-0.031	0.006
1520	0.6	0.2134	-0.076	0.124	-0.031	0.006
1620	0.8	0.2846	0.009	0.211	0.098	0.106
1860	0.8	0.2846	0.009	0.211	0.098	0.106
1950	1	0.3557	0.058	0.237	0.230	0.175
2120	1	0.3557	0.058	0.237	0.230	0.175

Table I-3. San Francisco Convent double tube-jack test hole measurements for the upper row of holes

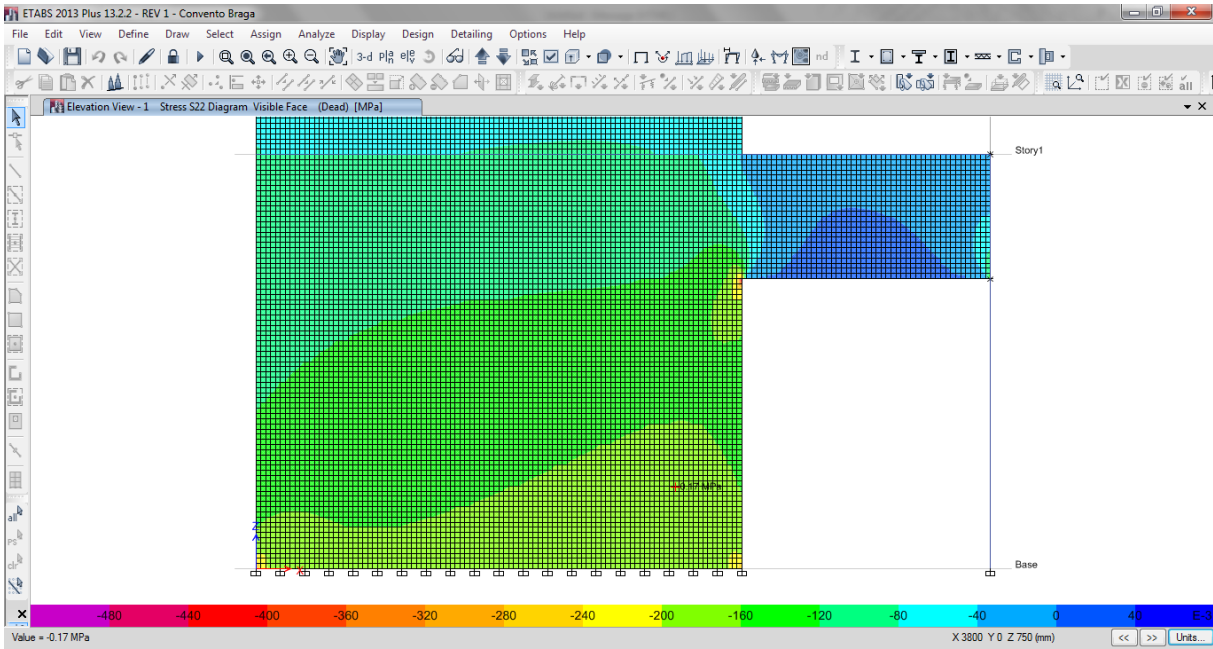| Hole	Vertical distance from base of the wall	Horizontal distance from center of H11 to center of hole	Depth of hole	Diameter
	[cm]	[cm]	[cm]	[mm]
H11	142.0	0.0	23.5	26.38
H12	137.5	10.0	23.5	25.63
H13	144.0	18.0	20.0	24.10
H14	140.3	28.5	20.5	25.70
H15	139.5	39.5	19.0	26.20
H16	140.2	51.0	23.0	26.80
H17	132.7	59.0	26.0	26.28
H18	135.1	67.0	21.0	25.78
H19	139.3	79.5	20.5	25.36
H20	142.5	88.0	20.5	25.62

Figure I-1 Stress distribution in the wall and stress level in the location of the single flat-jack test for a masonry density of 2200 kg/m^3
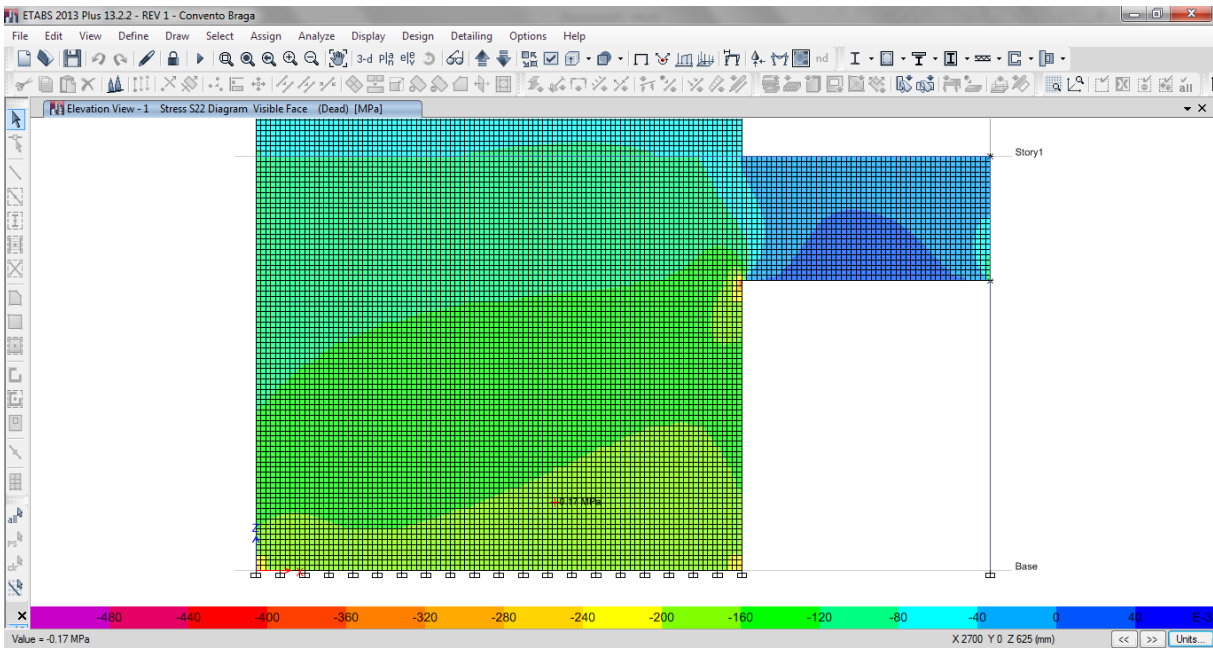

Figure I-2 Stress distribution in the wall and stress level in the location of the single tube-jack test for a masonry density of 2200 kg/m^3
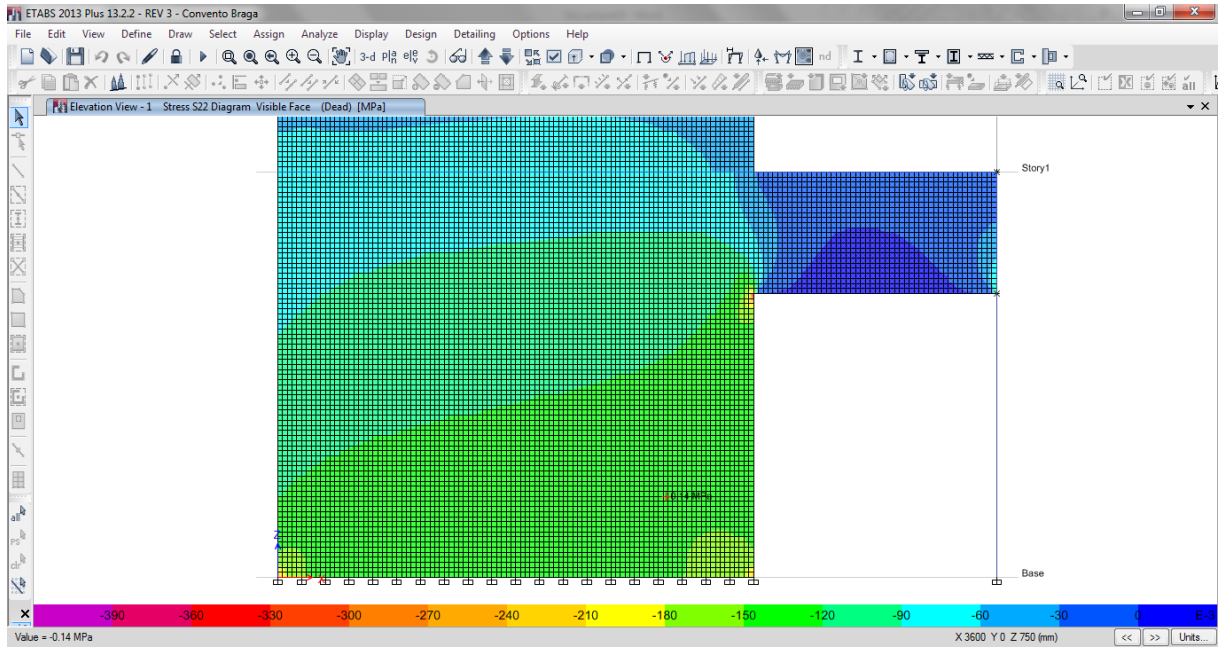
Figure I-3 Stress distribution in the wall and stress level in the location of the single flat-jack test for a masonry density of 1800 kg/m^3
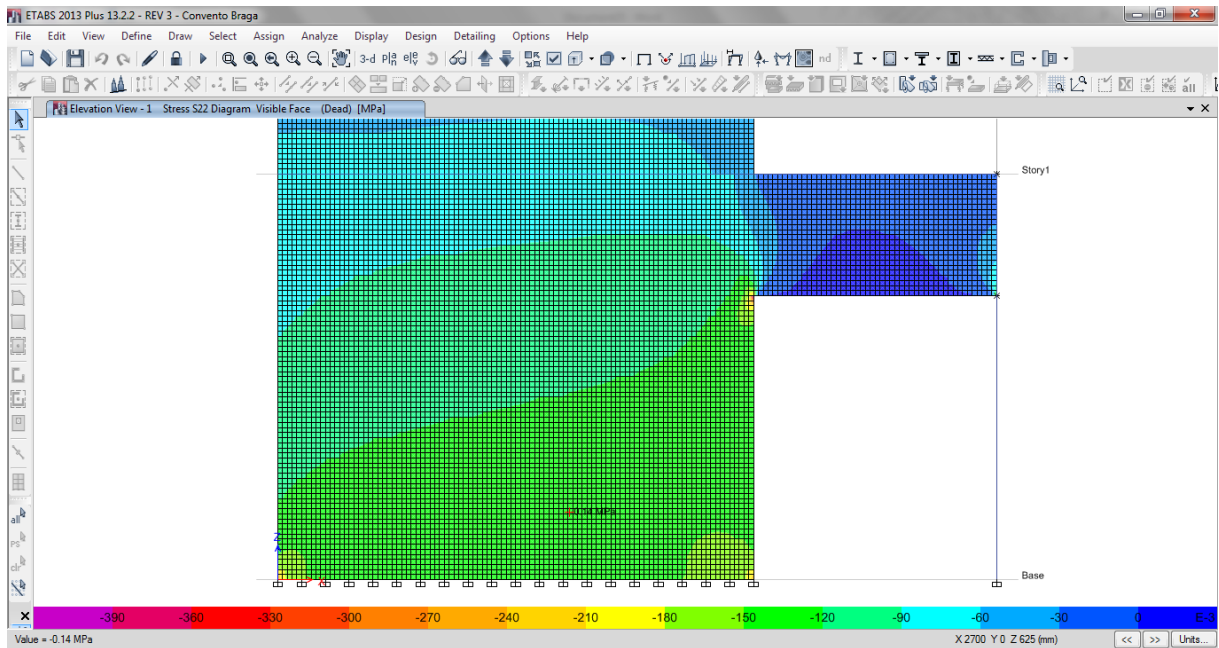

Figure I-4 Stress distribution in the wall and stress level in the location of the single tube-jack test for a masonry density of 1800 kg/m^3